

CUR

151/1997



# Derivation of fatality probability functions for occupants of buildings subject to blast loads

Phase 4

Prepared by

**W S Atkins Science & Technology**  
for the Health and Safety Executive

**FOR  
REFERENCE ONLY**

CONTRACT RESEARCH REPORT

151/1997



# Derivation of fatality probability functions for occupants of buildings subject to blast loads

Phase 4

R M Jeffries, L Gould,  
D Anastasiou & R Pottrill  
W S Atkins Safety & Technology  
Woodcote Grove  
Ashley Road  
Epsom  
Surrey KT18 5BW

The UK Health and Safety Executive (HSE) are consulted by local planning authorities on the safety aspects of proposed developments in the vicinity of major hazard installations and on the siting of new plant with major hazard potential. A quantified risk assessment approach may be used, which may include consideration of the effects of explosions with the potential to cause injury to people through direct effects on the body, secondary effects such as the impact of fragments or partial/total building collapse of buildings, or tertiary body translation effects. To date the likelihood of fatalities has been predicted using a probit based on World War II bomb data. The HSE has therefore initiated a research project to provide a more rational basis for assessing the vulnerability of the occupants of a building subject to vapour cloud explosions. A methodology has been developed for deriving generic fatality probability functions for different building types based on the primary structural characteristics of the building. This report details Phase 4 of the project in which the methodology developed in Phases 1 to 3 was applied to a number of generic building types in order to derive fatality probability functions in the form of pressure-impulse curves. Results for the buildings are presented in this report, together with a comparison of the results against historical data.

This report and the work it describes were funded by the Health and Safety Executive. Its contents, including any opinions and/or conclusions expressed, are those of the authors alone and do not necessarily reflect HSE policy.

© Crown copyright 1997

Applications for reproduction should be made in writing to:  
Copyright Unit, Her Majesty's Stationery Office,  
St Clements House, 2-16 Colegate, Norwich NR3 1BQ .

First published 1997

ISBN 0 7176 1451 4

All rights reserved. No part of this publication may be reproduced, stored in a retrieval system, or transmitted in any form or by any means (electronic, mechanical, photocopying, recording or otherwise) without the prior written permission of the copyright owner.

## ACKNOWLEDGEMENTS

Grateful acknowledgement is made to the following for permission to reproduce material used in creating figures in this report.

### Figures 2.2, 2.3 and 2.4

*The breakage of glass windows by gas explosions*  
Mainstone R J, Building Research Station Current Paper, CP 26/71, September 1971. Copyright © BRE, 1971. Reproduced by kind permission of BRE.

### Figure 2.10

Department of the Army Technical Manual TM 5-855-1  
*Fundamentals of protective design for conventional weapons* 3 November 1986.

### Figures 2.14, 2.21 and 2.27

*Explosion hazards and evaluation* Baker W E, Cox P A, Westine P S, Kulesz J J and Strehlow R A, Elsevier Science - NL, 1983. Copyright ©, Elsevier Science - NL, 1983. Pages 481, 519 and 290, reprinted with kind permission of Elsevier Science - NL, Sara Burgerhartstraat 25, 1055 KV Amsterdam, The Netherlands.

# CONTENTS

Glossary .....	v
List of Tables .....	vii
List of Figures .....	viii
<b>1. INTRODUCTION .....</b>	<b>1</b>
1.1 SUMMARY OF PHASE 1 .....	1
1.2 SUMMARY OF PHASES 2 AND 3 .....	2
1.3 OBJECTIVES OF PHASE 4 .....	3
<b>2. METHODOLOGY FOR CALCULATING FATALITY PROBABILITIES .....</b>	<b>6</b>
2.1 BLAST WAVE CHARACTERISTICS .....	6
2.2 BUILDING CHARACTERISTICS .....	7
2.2.1 <i>Global characteristics</i> .....	7
2.2.2 <i>Component Behaviour</i> .....	8
2.3 STRUCTURAL RESPONSE TO OVERPRESSURE .....	11
2.3.1 <i>Building Orientation</i> .....	11
2.3.2 <i>Front Face Pressure</i> .....	11
2.3.3 <i>Rear Face Pressure</i> .....	13
2.3.4 <i>Internal Pressure</i> .....	13
2.3.5 <i>Resultant Force on the Structure</i> .....	14
2.3.6 <i>Dynamic Response</i> .....	15
2.3.7 <i>Failure Sequence</i> .....	15
2.4 FRAGMENT GENERATION .....	16
2.4.1 <i>Glazing Fragments</i> .....	16
2.4.2 <i>Cladding Fragments</i> .....	18
2.5 FATALITY PROBABILITY .....	20
2.5.1 <i>Fatality probability due to glazing</i> .....	20
2.5.2 <i>Probability of fatality arising from cladding impact</i> .....	22
2.5.3 <i>Probability of fatality arising from building collapse</i> .....	23
2.5.4 <i>Overall fatality probability of building occupants</i> .....	24
2.5.5 <i>P-I diagrams</i> .....	26
2.6 CONCLUSIONS .....	27
<b>3. GENERIC BUILDING CALCULATIONS .....</b>	<b>54</b>
3.1 BUILDING TYPE B1: PORTACABINS .....	54
3.2 BUILDING TYPE B2: BRICK BUILDINGS .....	56
3.3 BUILDING TYPE B3: CONCRETE FRAMED BUILDINGS .....	57
3.4 BUILDING TYPE B4: STEEL FRAMED BUILDINGS .....	57
3.5 BUILDING TYPE B5: HARDENED STRUCTURE .....	59
3.6 BUILDING TYPE T: TALL BUILDINGS .....	60
3.7 BUILDING TYPE L: LONG SPAN BUILDINGS .....	61
3.8 P-I DIAGRAMS - GUIDANCE FOR USE .....	62
3.9 CONCLUSIONS .....	65
<b>4. COMPARISONS .....</b>	<b>80</b>
4.1 COMPARISON OF STRUCTURAL PREDICTIONS AGAINST EXPLOSIVES SAFETY DISTANCES .....	80
4.2 COMPARISON OF FATALITY PROBABILITY PREDICTIONS AGAINST HISTORICAL EXPLOSION DATA .....	82
4.3 COMPARISON OF MODEL AGAINST DATA FROM THE FLIXBOROUGH EVENT .....	83
4.4 COMPARISON OF EFFECTS FROM TNT EXPLOSION AND VCE .....	85
4.5 CONCLUSIONS .....	86

**CONTENTS (cont'd)**

**5. CONCLUSIONS .....99**

**6. FURTHER WORK ..... 103**

**7. REFERENCES ..... 106**

**APPENDIX A: GENERIC BUILDING CALCULATION RESULTS**

**APPENDIX B: WORKED EXAMPLE**

## GLOSSARY

$a_0$	speed of sound at atmospheric pressure (m/s)
$A_F$	frontal area of fragment (m <sup>2</sup> )
$A_m$	mean presented area of fragment (m <sup>2</sup> )
$A_0$	area of opening in the front face of a structure (m <sup>2</sup> )
$B$	maximum width of building (m)
$c$	damping (kg/s)
$C_D$	drag coefficient for a structure
$C_{DF}$	drag coefficient for a fragment
$C_L$	leakage pressure coefficient
$d_f$	distance factor
$E$	combustion energy (J)
$f_{injb}$	fraction of glazing fragments exceeding criterion for skin penetration
$f_{injh}$	fraction of glazing fragments exceeding criterion for skull fracture
$F(t)$	force as a function of time (N)
$H$	maximum height of building (m)
$I$	non-dimensional impulse
$I_s$	incident specific impulse (Ns/m <sup>2</sup> )
$k(x)$	stiffness as a function of displacement (N/m)
$K$	constant for calculation of $I$
$L$	maximum length of building (m)
$m$	mass (kg)
$m_f$	mass of fragment (kg)
$N_{fb}$	number of glazing fragments hitting body
$N_{fh}$	number of glazing fragments hitting head
$N_{injb}$	number of potentially injurious fragments hitting body
$N_{injh}$	number of potentially injurious fragments hitting head
$p_c$	probability of fatality arising from building collapse
$p_d$	probability of fatality arising from cladding failure
$p_{fatb}$	probability of fatality due to glazing fragments hitting the body
$p_{fath}$	probability of fatality due to glazing fragments hitting the head
$p_{fb}$	probability of a skin penetration injury leading to a fatality
$p_{fh}$	probability of a skull fracture leading to a fatality
$p_g$	probability of fatality arising from glazing failure
$p_{igb}$	probability of glazing fragment causing a skin penetration injury
$p_{igh}$	probability of glazing fragment causing a skull fracture
$p_{total}$	total fatality probability for a structure
$P_0$	atmospheric pressure (Pa)
$P_{eff}$	effective pressure across a structural component (i.e. the difference between the pressure on one side and that on the other side at any time) (Pa)
$P_{front}(t)$	pressure on the front face of structure as a function of time (Pa)
$P_i$	internal pressure in a building (Pa)
$P_r$	peak reflected overpressure (Pa)
$P_{rear}(t)$	pressure on the rear face of structure as a function of time (Pa)
$P_s$	peak side-on pressure (Pa)
$P$	non-dimensional pressure
$Q$	dynamic pressure (pa)

## GLOSSARY (cont'd)

$Q_D$	dynamic pressure on a surface (Pa)
R	distance from centre of explosion (m)
$R_0$	radius of source (m)
$\bar{R}$	energy scaled distance
S	building dimension equal to the small of B/2 and H(m)
$S_F$	Shape Factor
t	time (s)
$t_p$	positive phase pulse duration (s)
$\bar{t}_p$	scaled positive phase pulse duration
$t_2$	time taken for pressure at a finite reflective surface to reduce from the reflected value to the incident pressure plus the dynamic pressure (s)
T	natural period of structure (s)
U	velocity of wave front (m/s)
v	velocity of fragment (m/s)
$\bar{v}$	non-dimensional velocity
$V_0$	volume of a structure (m <sup>3</sup> )
w	minimum width of fragment (m)
x	displacement (m)
X	distance from front of fragment to the location of its largest cross-sectional area (m)
$\gamma$	ratio of the specific heat at constant pressure to the specific heat at constant volume
$\rho$	density of air (kg/m <sup>3</sup> )

## LIST OF TABLES

<b>Table 2.1:</b>	Overpressure for 1te, 3te and 10te Propane Equivalent
2.2:	Available Data for Alternative Glazing Types
2.3:	Typical Failure Pressures for Cladding [1]
3.1:	Generic Building Types
4.1:	Parameters for 1000lb TNT Explosion Comparison
4.2:	Comparison of Building Damage Predictions against Existing Explosives Safety Distances
4.3:	Parameters for Comparison from Hewkin [21]
4.4:	Overpressure-Pulse duration pairs derived for Flixborough explosion
4.5:	Comparison of Predictions against Flixborough Experience
4.6:	Comparison of VCE and TNT predictions for Building Type B2/2
4.7:	Comparison of VCE and TNT predictions for Building Type B3/1



## LIST OF FIGURES

- Figure 1.1: General Procedure**
- 2.1: Schematic Progression of Pulse Shape [3]
  - 2.2: Failure Pressures for Single Glazing [4]
  - 2.3: Variation of Flexural Strength of Glass with Duration of Loading [4]
  - 2.4: Failure Pressures for Double Glazing [4]
  - 2.5: Elasto-Plastic Stiffness
  - 2.6: Comparison of Calculations for Dynamic Pressure
  - 2.7: Schematic Representation of the Pressure - Time Diagram for a Finite Reflective Surface
  - 2.8: Rear Face Pressure Load: Shock
  - 2.9: Rear Face Pressure Load: Pressure Pulse
  - 2.10: Leakage Pressure Coefficient as a Function of the Differential Pressure across the Opening
  - 2.11: Pressure Relief on External Walls from Glazing/Cladding Failure
  - 2.12: Effect of Front Face Glazing/Cladding Failure
  - 2.13: Curve Fit to Mass Distribution Data
  - 2.14: Non-dimensional Object Velocity as a Function of Non-dimensional Pressure and Non-dimensional Impulse
  - 2.15: Criterion for 50% Probability of Skull Fracture
  - 2.16: Criterion for 10% Probability of Skin Penetration
  - 2.17: Methodology for Calculation of Probability of Fatality due to Glazing Fragment Impact
  - 2.18: Calculation of the Percentage of Potentially Injurious Glazing Fragments
  - 2.19: Glazing Fatality Probability Curves
  - 2.20: Methodology for Calculating the Probability of Fatality due to Cladding Impact
  - 2.21: Criterion for Non-Penetrating Fragment Impact
  - 2.22: Brickwork Fatality Probability Curve
  - 2.23: Methodology for Calculating the Probability of Fatality due to Building Collapse
  - 2.24: Illustration of Glazing Fatality Probability Calculation
  - 2.25: Methodology for Global Building Fatality Probability Calculation
  - 2.26: Sample Building Fatality Probability Curves
  - 2.27: P-I Diagrams for Masonry Building Damage
  - 2.28: Methodology for Deriving P-I Diagrams
- 
- 3.1: Possible Configurations for Core/Shear Walls in Tall Buildings
  - 3.2: P-I Diagram: B1, Shock Pulse, Comparison of 1% Fatality Probability Curves
  - 3.3: P-I Diagram: B1, Pressure Pulse, Comparison of 1% Fatality Probability Curves
  - 3.4: P-I Diagram: B2, Shock Pulse, Comparison of 1% Fatality Probability Curves
  - 3.5: P-I Diagram: B2, Pressure Pulse, Comparison of 1% Fatality Probability Curves
  - 3.6: P-I Diagram: B3, Shock Pulse, Comparison of 1% Fatality Probability Curves
  - 3.7: P-I Diagram: B3, Pressure Pulse, Comparison of 1% Fatality Probability Curves
  - 3.8: P-I Diagram: B4, Shock Pulse, Comparison of 1% Fatality Probability Curves

### **LIST OF FIGURES (cont'd)**

- 3.9: P-I Diagram: B4, Pressure Pulse, Comparison of 1% Fatality Probability Curves
- 3.10: P-I Diagram: Shock Pulse, Comparison of 1% Fatality Probability Curves
- 3.11: P-I Diagram: Pressure Pulse, Comparison of 1% Fatality Probability Curves
  
- 4.1: Fatality Probability Predictions for 1000lb TNT Explosion
- 4.2: Comparison of Fatality Probability Predictions against Data from Hewkin [21]
- 4.3: Comparison of VCE and TNT Predictions for Building Type B2/2
- 4.4: Comparison of VCE and TNT Predictions for Building Type B3/1

## 1. INTRODUCTION

Estimates of the probability of fatality of the occupants of buildings subject to explosions are a key aspect of risk assessment in the context of layout planning of hazardous installations. At present such fatalities are predicted based on a probit derived from World War II bomb data. Such data, while useful, cannot be directly correlated to the effects of a vapour cloud explosion (VCE) as the pulse shapes and peak overpressures arising from a VCE may be quite different from those arising from high explosives. Consequently there is a need for a comprehensive study of the effects of VCEs, both close to the source and at a distance from it, corresponding in industrial terms to on- and off- site.

Assessing fatality probabilities requires the determination of the failure sequence of a building subject to increasing blast loads and assessment of the consequential effect on people within the building. Risk to the building occupants arises from either debris generated by the blast load or partial/total collapse of the load bearing structure. In the work reported herein, the structural loads arising from an explosion, and the response of the structure to those loads have been assessed. Methods for predicting debris generation have also been derived, and a model has been assembled which predicts the collapse sequence for the structure based on its constructional characteristics subject to a specified pressure pulse. The differing hazards of glazing, debris and collapse have been assessed, and the collapse sequence has been used in conjunction with fatality probability criteria in order to calculate an overall occupant fatality probability for the building.

The majority of the work to develop and refine the methodology has been performed in phases, with the majority of the development being conducted in Phases 1 to 3 [1,2]. This report presents the conclusions from Phase 4, in which the methodology has been finalised and applied to a series of generic building examples. For completeness, a summary of Phases 1 to 3 is presented below.

### 1.1 Summary of Phase 1

In Phase 1 a general procedure was developed to obtain fatality probability functions for particular buildings and the individual functions for glazing failure, cladding failure and building collapse were determined. It included a comprehensive literature search, and indeed the search for useful information has been an ongoing part of the project.

The procedure is summarised in Figure 1.1. Factors considered included:

- **Building types**

Generic building types were defined, concentrating in particular on types typical of urban residential and commercial areas, with potentially high occupancy rates. Housing, offices, retail and leisure developments, schools and hospitals were all considered in order to identify a range of generic building types and geometries.

- **Pressure loads**  
Maximum overpressures, pulse shapes and durations were considered to identify those of most relevance to a VCE scenario.
- **Structural loads**  
The structural loads generated by the incident overpressure were considered.
- **Dynamic response**  
The response of the building to the dynamic input was considered using a non-linear single degree of freedom elasto-plastic model to predict maximum displacements under prescribed pressure loads.
- **Structural capacity**  
The capacities of various structural components under dynamic loading were calculated and compared against historical and experimental data where available.
- **Fatality Probability**  
Finally, considering the overall building response and the failure capacities of various components, the probability of fatality of the building occupants was assessed, based on the effects of the individual components such as glazing and cladding together with building collapse.

Phase 1 is reported in detail in [1].

## 1.2 Summary of Phases 2 and 3

Having derived the general procedure in Phase 1, Phases 2 and 3 involved assessing the sensitivity of the response of the structure and the corresponding occupant fatality probability to variations in the loading and structural models. The aim was to examine the importance of different aspects of the loading and structural characteristics.

In particular, the following areas were studied:

- the effects of the shape of the pressure pulse on the overall structural response of the building, using representative building sizes.
- the effects of pressure relief due to failure of the windows and wall cladding on the overall response of the building.
- the effects of pressure on the rear of the buildings.
- the effects of the negative phase of the blast pulse on the global response of the building and its importance for the assessment of occupant fatality probability.
- the structural characteristics of particular generic building types using historical, experimental and analytical data. The differences between the various approaches were reviewed, considering the possible effect of infill wall, etc.

- how the predictions of the model compared against others in the literature, based on historical data.
- the likelihood of fatality as a result of impact by glass and other debris.

In Phase 3, the methodology was applied to two specific building types in order to compare the results against experience. The building types selected were a typical brick-built semi-detached house and a reinforced concrete framed office building. For each type, two different typical construction techniques were assessed in order to investigate the range of possible capacities. Occupant fatality probabilities were then calculated for the two building types. The response to different pulse shapes was shown to be highly dependent on the rate of pressure build up on the inside and outside of the building which in turn is dependent on the building dimensions, glazing characteristics and orientation. It is thus necessary to consider all possible orientations in order to derive the fatality probabilities for a specific building type.

The calculated fatality probability curves were also compared against other predictions. A preliminary comparison against the models of Jarrett and Hewkin was sufficiently good to provide some confidence in the methodology developed.

Phases 2 and 3 are reported in detail in [2].

### **1.3 Objectives of Phase 4**

The primary objective of Phase 4 is to finalise the methodology and to extend its use to derive fatality probability curves for a range of generic building types. In order to do this, a detailed statement of the finalised methodology has been produced. This is contained in Section 2 of this document. Structural calculations have then been performed for each of seven different building types, based on typical building dimensions and construction details. In this way, component failure pressures have been generated for each of the components of interest in the structure. These are compared against historical and experimental data where appropriate in order to corroborate the values used. Fatality probability curves have been produced in the form of pressure-impulse diagrams for each building type: 4 such curves have been produced for each building, corresponding to fatality probabilities for two different orientations of the building under two different pulse shapes. The curves for each building are reproduced in Appendix A of this document, and a description of the buildings and results is contained in Section 3. Guidance for use of the P-I diagrams and the methodology are also given in Section 3.

Finally, validation studies have been performed in which the curves have been compared against historical data. The studies performed have included:

- Comparison of the structural predictions against the British explosives safety distances, using TNT explosion data [20]
- Comparison of the fatality probability predictions against historical explosion data [21]

- Comparison of the curves for a VCE against historical data from an actual accidental explosion, namely Flixborough [22,23]
- Comparison of the predictions of fatality probability arising from a VCE and an equivalent TNT explosion

The validation studies are described in more detail in Section 4.

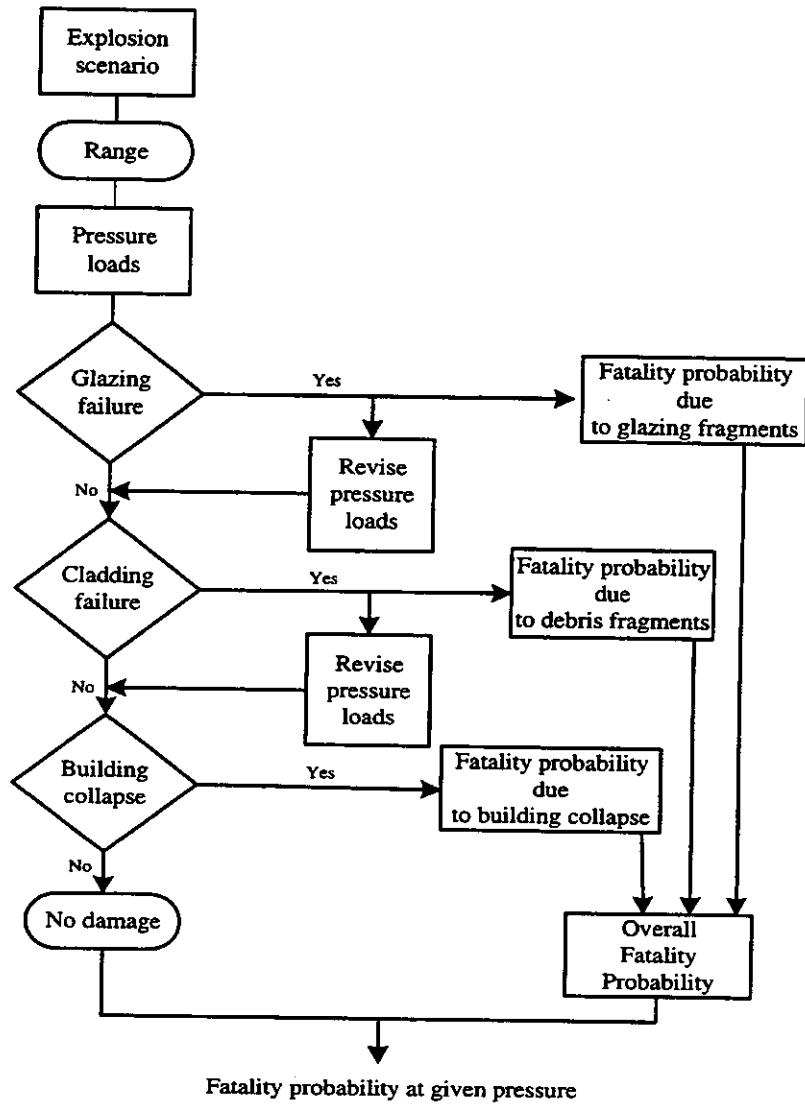


**Figure 1.1: General Procedure**

## 2. METHODOLOGY FOR CALCULATING FATALITY PROBABILITIES

This section summarises the derived methodology for assessing the vulnerability of occupants of different types of buildings subject to overpressures arising from vapour cloud explosions.

### 2.1 Blast Wave Characteristics

The pulse shape resulting from a VCE can be approximated by a triangular shape, varying in form as the distance from the centre of the blast increases. The shape can be characterised by a shape factor, equal to the ratio of rise time to pulse duration, and it is assumed that the shape factor changes with distance from the source as:

$$\text{Shape Factor}(SF) = \frac{\text{rise time}}{\text{pulse duration}} = \max(0.65(1 - 1.25d_f), 0) \quad (1)$$

where  $d_f$  is a distance factor related to the source radius,  $R_0$ , the peak pressure,  $P_s$  and the distance from the centre of the explosion,  $R$ , by the following equation:

$$d_f = \frac{R}{R_0} \left( \frac{P_s}{P_0} \right)^2 \quad (2)$$

where  $P_0$  is atmospheric pressure. The equations are taken from [3], and are based on experimental results. The shape resulting from this equation is shown in Figure 2.1; close to the centre, the pulse is similar to a pressure pulse (rise time = decay time =  $t_p/2$ ), whereas far from the source, the shape is that of a shock pulse (rise time = 0, decay time =  $t_p$ ).

The range of pressure magnitudes and pulse durations of interest have been taken from the TNO Multi-Energy Method Curve 7 [19], using a range of combustion energies from  $4.65 \times 10^{10}$ J to  $4.65 \times 10^{11}$ J, corresponding approximately to a range from 1te to 10te propane. This method has been used only to identify the range of pressures and impulses of interest and the model is not inextricably linked to the Multi-Energy Method. The range of energy scaled distances considered is between 0.3 and 30, where the energy scaled distance,  $\bar{R}$ , is defined by:

$$\bar{R} = R \left( \frac{P_0}{E} \right)^{1/3} \quad (3)$$

where  $E$  is the combustion energy. The scaled positive phase duration is defined by:

$$\text{Scaled Duration, } \bar{t}_p = t_p a_0 \left( \frac{P_0}{E} \right)^{1/3} \quad (4)$$

where  $a_0$  is the speed of sound at atmospheric pressure.



Given values for the energy scaled distance, the published curves can be used to identify the scaled duration together with the dimensionless maximum scaled side-on overpressure and dynamic overpressure: hence the corresponding actual duration,  $t_p$ , maximum side-on static overpressure and dynamic pressure can be calculated.

Examples of the overpressure - distance, dynamic pressure - distance and positive phase duration - distance values obtained for three different combustion energies are given in Table 2.1, at the end of this section.

The real shape of the pressure pulse includes a negative phase following on from the positive phase, in which the pressure falls below atmospheric pressure, reaches a minimum and slowly returns to the atmospheric value. It is usual practice to ignore this part of the pulse as its effects on the response of the building are generally unimportant in comparison with the positive phase. In Phase 3 [2] it was shown that this is generally the case, although for low values of the building aspect ratio ( $B/L < 1$ ) inclusion of the negative phase can lead to a small increase in the global building displacement. However, the effects of the negative phase on the building occupants are likely to be small, as local effects cause a suction force on the external glazing/cladding which, while it may cause the cladding to fail (cladding is designed for lower suction forces than pressure forces and the fixings may be preferentially stronger in one direction), will not result in any hazard to the occupants inside the building. It should perhaps be noted though that while our principal interest is in building occupants, for structures such as shopping centres or leisure complexes, the fatality probability of people outside the building may be important. Although the increase in building response implies that the building may collapse at a slightly lower pressure, the uncertainties in the analysis, and the uncertainties in characterisation of the negative phase are such that inclusion of the negative phase will not necessarily lead to a better estimate of the building failure pressure. Consequently for this assessment the negative phase will not be included although it is anticipated that as more data become available the analysis could be refined.

## **2.2 Building Characteristics**

Buildings need to be defined in terms of their fundamental structural characteristics in order for the structural response and expected failure sequence to be predicted. The fundamental structural characteristics are defined in terms of the global characteristics of the structure and the more specific details of the structural components. In addition the dimensions and failure pressures of the external cladding and glazing have to be defined in order for the vulnerability of the building occupants to be assessed.

### **2.2.1 Global characteristics**

A table of generic building types has been developed (Section 3), in which the buildings are categorised according to the construction type, i.e. Portacabin/timber building, Brick building, Concrete framed building, Steel framed building, or one of a number of special types e.g., long span, tall building or hardened structure. Within these categorisations, the

following characteristics need to be specified in order to assess the vulnerability of the occupants.

- Glazing total area, area of individual windows and window panes, thickness and type of glass (plain, toughened, laminated, etc.)
- Construction method of load-bearing frame, frame dimensions and spacing, section sizes and material specification, details of connections
- Dimensions and type of any floor slabs supported by the frame, dimensions and construction details of roof structure
- External wall cladding type, material specification, thickness, dimensions and connection details
- Overall dimensions of building.

For the purposes of these calculations, the internal layout of the structures has been assumed to be less definable and typical layouts have been considered wherever possible. The consideration of internal layout is very much dependent on the individual building type and purpose.

The generic building types considered are outlined in Section 3, and described in detail in Appendix A.

### **2.2.2 Component Behaviour**

In addition to the overall dimensions and constructional characteristics of the structure, it is necessary to assess the failure characteristics of the structural components.

#### **Glazing**

The failure pressure of the glazing is calculated from the charts presented in Mainstone [4]. The values specified are dependent on the area and aspect ratio of the window, together with the thickness of the glass. The charts for single glazing are reproduced in Figure 2.2.

These data are based on explosions inside a building and the pressures measured internally. Thus the rate of increase of pressure is gradual and in this sense is similar to a VCE pressure pulse. However, a comparison has been made of the Mainstone predictions against experimental data, and the results have been found to be good, even for shock pulses [2]. Consequently, the failure pressures predicted by the charts have been used irrespective of the shape of the pulse.

The failure pressures correspond to a pulse duration of 1 sec. Figure 2.3 shows the experimental relationship of failure pressure to pulse duration [4], and it shows that a reduction in duration by a factor of 10, i.e. to a duration of 0.1 sec, results in an increase in failure pressure by a factor of 1.25. These data do not appear to depend on the size of

the window, although the scatter of the data points on the figure is large. However, in the absence of any other data, factors from the graph are used in order to take into account the shorter pulse durations of interest.

Special glazing types are assessed on the basis of the available data, and the most realistic values assumed. For double glazed units of ordinary glass, values are also given in Mainstone, as shown in Figure 2.4. For alternative types of glazing, such as polycarbonate, tempered and laminated glass, the data available are outlined in Table 2.2.

### **Cladding**

The failure pressure of wall cladding is based on a combination of analytical calculations and historical/experimental data. Structural calculations have been primarily used as the basis of the assessment of structural strengths, with validation based on a comparison with historical and/or experimental data where available. For external cladding, the static load capacity is determined from the appropriate design code, using partial safety factors for loads and materials of 1.0. For ultimate limit state calculations partial safety factors which typically range from 1.05 to 1.7 are found, and material factors are defined according to the variability in the material properties. These factors represent the uncertainty with which the loads and material properties can be defined, and are intended to ensure that the structural design is 'safe': using factors of 1.0 implies that there are no factors of safety included in the calculation, i.e. that the actual structural capacity is being calculated, rather than a 'safe' design value.

The codes appropriate for assessing the static strength are as follows:

External cladding	BS 8200 [32]
Aluminium corrugated and trough	CP 143: Part 1: 1958 [33]
Galvanised corrugated steel	CP 143: Part 10: 1973 [34]
Corrugated asbestos cement	BS 5247: Part 14: 1973 [35]
Precast concrete	BS 8297: 1995 [36]

For the purposes of these calculations it is important to obtain the most realistic estimate of strength, rather than a conservatively low design value. Having established a static load capacity, the capacity of the cladding to carry dynamic loads, such as a blast load, can be assessed. The static collapse load is increased by a material factor and a dynamic strain rate factor. The material factor represents the difference between the actual value of a material property and the lower bound or minimum guaranteed value assumed in conventional design. The dynamic strain rate factor represents the increase in yield strength with increasing strain rate, which is a well-documented effect for typical structural components such as steel and concrete. The calculated capacity for dynamic loads is assumed to be the point at which the cladding will start to deform plastically, i.e. the elastic limit of the cladding.

The ductility of the structure is also assessed. This is the ratio of the deformation at failure to the deformation at yield (i.e. at the elastic limit) and is a measure of the post-yield capacity of the structure. It is used to calculate the pressure at which the component will actually fail. With a knowledge of the yield strength, the ductility and the pulse shape, the limiting overpressure can be calculated by solving the equation of motion for an elasto-plastic single degree of freedom system, i.e.:

$$m\ddot{x} + c\dot{x} + k(x)x = F(t) \quad (5)$$

where  $m$  is the mass of the system,  $c$  is the material damping and  $k(x)$  is the stiffness.  $F(t)$  is the applied pulse shape as a function of time. This equation is solved for the displacement,  $x$ , as a function of time. The displacement is assumed to be elastic up to a certain value (the elastic limit), and is proportional to the force applied: it returns to zero if the force is removed. Above this limit, the displacement is plastic and increases a large amount for only a small increase in force: removing the force will reduce the displacement, but there may be a small amount of permanent irreversible deformation remaining. This behaviour is represented by a bi-linear stiffness,  $k(x)$  as shown in Figure 2.5. The detail of this approach is described in Biggs [5].

The failure pressures calculated are dependent on the type of cladding used and the overall dimensions of the panels. As such, the failure pressure is specific to the building under consideration. Typical values, calculated in Phase 1 [1] are given in Table 2.3.

### Load-bearing frame

Failure of the load-bearing frame under a blast pulse is highly dependent on the load which the frame actually experiences i.e. if the cladding fails, it can no longer transmit load to the frame and the load on the frame is reduced. Conversely, if the cladding remains intact under the loading, the frame will be exposed to the full force of the blast. In order to calculate a limiting overpressure, it is necessary first to calculate a limiting load on the section, and then to consider whether the area on which the blast pressure is acting corresponds to the frame area alone, or to the frame plus a significant proportion of the cladding. The first failure pressure will be significantly higher than the second.

As detailed above for the cladding, there are a number of design codes which give details for assessing the static strength of a structure. For the different frame types, these include:

Concrete	BS8110 [37]
Steel	BS5950 [38]
Brick/Block	BS5628 [39]
Timber	BS5268 [40]

A similar technique is used for the structural frame as for the cladding, in that the static failure load is calculated and this is then modified by including a material factor and the dynamic strain rate effects. The limiting overpressure can then be calculated using

Equation 5, using a force function corresponding to the load that the frame will actually experience. The details of this calculation are outlined in Section 2.4, below.

### **Internal walls**

The internal walls are assumed not to contribute to the internal debris, and consequently their failure pressures are not considered here. This is because, for the majority of structures considered, all of the rooms have at least one external wall and the conservatism inherent in the calculations of the effects of debris from the external walls makes the inclusion of internal debris unnecessary. In addition, for frame structures, the internal partition walls tend to be quite lightweight, and it is considered that they do not present a significant fatality mechanism.

The internal walls are used, where appropriate, as a barrier to the increase of internal pressure or as a barrier to the travel of debris from the external walls, in the calculation of the probability of fatality, as outlined in Section 2.5.

## **2.3 Structural response to overpressure**

Having calculated the failure loads of the individual structural components, it is necessary to consider how the blast pulse interacts with the structure, and in what order the different structural components fail under the applied load.

The load experienced by the structure will be dependent on a great number of factors, such as the building orientation, the building dimensions, the distance from the source of the explosion, etc. It is necessary to simplify the problem in order to make it manageable. The assumptions made are outlined below:

### **2.3.1 Building Orientation**

The buildings are assumed to be symmetrical in shape, and orientated with either the short side or the long side perpendicular to the direction of the incoming blast. This greatly simplifies the calculations for the way in which the pulse travels around the structure and interacts with it. In particular, it means that only the pressure on the front and rear of the structure affect the global motion of the structure, as pressure on opposite sides will be equal and will cancel out. The calculations of the probability of fatality of the building occupants for the two different orientations are assumed to form bounding cases for the generic building fatality probabilities.

### **2.3.2 Front Face Pressure**

The method for assessing the pressure loading on a structure is based on [6]. The pressure experienced at the front face of a building is dependent on the shape of the blast pulse and the building dimensions. At a finite reflective surface, an incident pulse will be reflected such that the peak pressure experienced at the surface is higher than the peak incident overpressure. The measure of how much the reflected overpressure exceeds the incident overpressure is the reflection coefficient, which is dependent on the angle of incidence of the wave front, the peak incident overpressure and the wave type. As we are

considering only a structure which is orientated perpendicular to an incoming wave, the reflected pressure for a shock pulse can be expressed by the following equation [6]:

$$P_r = 2P_s + \frac{(\gamma + 1)P_s^2}{(\gamma - 1)P_s + 2\gamma P_0} \quad (6)$$

where  $P_r$  is the peak reflected overpressure,  $P_s$  is the peak incident overpressure, and  $P_0$  is atmospheric pressure.  $\gamma$  is the ratio of the specific heat at constant pressure to that at constant volume, and is equal to 1.4 for air at fairly low pressures. This value has been assumed to be valid over the range of pressures of interest.

In addition to the reflection effects, there is a dynamic pressure to be considered which arises from displacement of air in the direction of the blast wave, and gives rise to an additional increase in pressure at the structure. The dynamic pressure on a surface can be calculated from [6]:

$$Q_D = \frac{5}{2} \frac{P_s^2}{\gamma P_0 + P_s} C_D \quad (7)$$

where  $C_D$  is a drag coefficient, dependent on the shape of the structure. The typical value used for  $C_D$  for the structural calculations is 1.05, corresponding to a wave incident on one face of a cube [6]. This equation, however, is non-conservative close to the source of a blast in comparison with the value predicted by using the Multi-Energy Method. Figure 2.6 illustrates this difference. It is thus considered appropriate to use Equation 7 to calculate the dynamic pressure associated with a shock pulse, i.e. in the region which corresponds to a scaled distance greater than 1.0, and to use the Multi-Energy Method to calculate dynamic pressures associated with a pressure pulse.

For an incident shock pulse, the initial pressure experienced at the front face of a structure is equal to the peak reflected pressure. For an infinite reflecting surface, this pressure would decay linearly over the pulse duration to zero, giving rise to a triangular pressure pulse similar to the incident pulse but greater in magnitude. However, the finite length of the reflecting surface gives rise to a disturbance of the pressure at the edges of the surface, the consequence of which is to cause the pressure to decay at a more rapid rate down to a value equal to the sum of the incident pressure at that time plus the dynamic pressure (Figure 2.7). The time over which this initial decay occurs is approximately equal to:

$$t_2 = \frac{3S}{U} \quad (8)$$

where  $S$  is a building dimension equal to half the width or the height, whichever is the smaller, and  $U$  is the velocity of the wave front, given by the following expression:

$$U = a_0 \sqrt{1 + \frac{6 \cdot P_s}{7 \cdot P_0}} \quad (9)$$

Once the pressure has decayed to this point, it decays further until it reaches zero when the incident pulse reaches zero at the front face ( $t_p$ ).

For an incident pressure pulse the finite nature of the reflecting surface together with the gradual rise time of the incident pulse combine to negate the reflection effects such that the peak overpressure reached at the front face is simply equal to the sum of the incident plus the dynamic overpressure, and the time scale of the front face overpressure is the same as that of the incident pulse, i.e. rise time =  $t_p/2$ .

### 2.3.3 Rear Face Pressure

The pressure at the rear face is based on the methodology in [6], with a slight modification to account for large buildings where the maximum pressure might not be achieved at the rear face before the blast pulse has passed the building. The incident pulse travels along the length of the building until it reaches the rear face in a time equal to  $L/U$ , where  $L$  is the building length. If the incident pulse is a shock pulse, pressure at the rear face then builds up over a time of  $4S/U$ , at which time it reaches its peak. The average pressure falls to zero once the pulse has passed the rear face, i.e. at a time of  $L/U+t_p$ . If the time taken to reach the peak is greater than the time taken for the pulse to pass the rear face, i.e.  $4S/U > t_p$ , it is assumed that the pressure at the rear face does not reach the maximum value, but falls to zero when the pulse passes. This is illustrated in Figure 2.8.

For an incident pressure pulse, the calculation is similar, except that the pressure is assumed to reach its peak after a time of  $4S/U + t_p/2$ , i.e. the rise time of the incident peak is included. Again the average pressure falls to zero at a time  $L/U+t_p$ , but the same cut-off constraint has been imposed. In this case, the constraint corresponds to  $4S/U > t_p/2$ , so it is more likely that the peak average pressure on the rear face will not be achieved for a pressure pulse than for a shock pulse with the same duration. This is illustrated in Figure 2.9.

### 2.3.4 Internal Pressure

In addition to the pressure on the front and rear of the building, there is a component of pressure acting in the direction of travel arising from the pressure inside the building, which will rise if either the front face glazing or cladding fails. For simplification, it is assumed that failure of rear face glazing or cladding does not affect the internal pressure or the net force on the structure. This is a reasonable assumption, as the effects of an opening in the rear of the building will include opposing contributions from the internal and the external pressure, and the resultant change in pressure is likely to be secondary to that arising from an opening in the front face where the pressure increase is on only one side of the opening.

If the external pressure is sufficient to fail the glazing or the cladding, based on the failure pressures derived in Section 2.3.2 above, the increase in the average pressure inside the structure is calculated using the approach outlined in [7]. Interior pressures immediately adjacent to the opening will be higher than average, but it is assumed to be not necessary, within the accuracy of this methodology, to take local effects into account.

The change in internal pressure  $-P_i$  within a time interval  $-t$  is a function of the pressure difference at the opening, and the ratio of open area to structural volume, i.e.

$$\Delta P_i = C_L \left( 0.3048 \frac{A_0}{V_0} \right) \Delta t \quad (10)$$

where  $A_0$  is the area of the opening,  $V_0$  is the volume of the structure and  $C_L$  is a leakage pressure coefficient and is a function of the pressure difference at the opening, as illustrated in Figure 2.10. The initial pressure difference at the opening is assumed to be equal to the incident side-on overpressure. This equation is used iteratively in order to determine the change in average pressure inside the structure. The limitations of this method are that strictly it only applies to small values of the opening area to volume ratio (although 'small' is undefined) and that it only applies up to pressures of  $\sim 150$  psi (10 bar).

For the purposes of these calculations, it has been assumed that if the front face pressure is sufficiently high to fail the glazing, the area of the opening is equal to the total area of glazing on the front face. However, if the pressure is high enough that the cladding fails, the area of the opening is assumed to be  $0.8BH$  where  $B$  and  $H$  are the breadth and height of the building. The factor of 0.8 is an estimate to represent the fact that if the cladding fails, there will be a certain amount of material remaining which may partially block the opening and that the structural frame itself will present some obstacle to the pressure rise.

The method is illustrated in Figure 2.11.

### 2.3.5 Resultant Force on the Structure

Having calculated the pressure on the front face of the structure, the pressure on the rear face and the average internal pressure, it is necessary to combine these, together with the areas on which they act, in order to produce a net resultant force on the structure. If there is no glazing failure at the front face, the pressure on the front face,  $P_{front}(t)$  gives rise to a force acting in the direction of motion of the blast pulse equal to  $P_{front}(t)BH$  where  $B$  and  $H$  are the breadth and height of the building. Similarly, the pressure on the rear face,  $P_{rear}(t)$ , gives rise to a force acting in the opposite direction of  $P_{rear}(t)BH$ . Consequently, the resultant force is given by:

$$F(t) = [P_{front}(t) - P_{rear}(t)]. B.H \quad (11)$$

If however, the front face pressure is sufficient to fail the glazing or the cladding at the front face, the resultant force is given by:

$$F(t) = P_{front}(t)(BH - A_0) - P_{rear}(t)BH + P_i(t)A_0 \quad (12)$$

where  $A_0$  is the area of the opening at the front face and  $P_i(t)$  is the internal pressure. The derivation of this equation is illustrated in Figure 2.12.



### 2.3.6 Dynamic Response

The dynamic response of the structure is approximated by the behaviour of a single degree of freedom elasto-plastic system. The equation of motion, Equation 5, is solved for the complete structure, using the appropriate mass, ( $m$ ), stiffness, ( $k(x)$ ) and damping, ( $c$ ) and the appropriate force from Equations 11 and 12 above.

The mass of the structure is estimated from the structural dimensions and construction materials, making allowance for the presence of additional items such as internal partitions, live loads, etc. For example, in the brick building example of Phase 3, the mass was assumed to be 50% higher than the mass of the exterior brickwork alone, thus encompassing the internal walls and roof structure in the total mass.

The stiffness of the structure is defined in two parts for an elasto-plastic system, as described earlier (Figure 2.5). For the elastic part of the curve, the stiffness can be estimated from the mass,  $m$ , and the natural period,  $T$ , of the structure from the equation:

$$k = \frac{m}{\left(\frac{T}{2\pi}\right)^2} \quad (13)$$

The natural period of the structure is estimated from the empirical formula given by Lees [8], i.e.

$$T \approx 0.09 \left( \frac{H}{\sqrt{B}} \right) \quad (14)$$

Above the elastic limit,  $k(x)$  is effectively zero: failure occurs when the displacement is equal to the elastic limit multiplied by a ductility factor defined for the structural frame. The failure load calculated for the structural frame is used in conjunction with the stiffness to define the displacement at the elastic limit - this is multiplied by the ductility to give the displacement at failure.

The structural damping,  $c$ , depends on the structure under consideration. It is conservative to assume that it is zero, as this maximises the displacement of the structure.

By using these parameters and solving the equation of motion for the applied force (Equation 5), the global displacement of the structure is derived as a function of time. If the displacement exceeds the failure value, the structure is assumed to have collapsed. In this way, a collapse pressure for the structure can be calculated.

### 2.3.7 Failure Sequence

The sequence of failure of the building depends on the failure pressures of the individual structural components, the magnitude of the pressure on each face of the building, the internal pressure and the global failure pressure. It is usual for the glazing on the front face of the building to be the first structural component to fail: normally the glazing is the

weakest component, and at the front face it is subject to the full force of the blast. It is possible that the front face cladding may fail at the same time if the peak pressure at the front face is high enough.

As the blast pulse travels around the building, the pressure builds up on the sides and finally the rear face. Opposing this, the pressure may build up inside the building. Once the differential pressure across the component exceeds the failure pressure, the component is assumed to have failed: in real terms this will happen on the side walls first, followed finally by the rear wall, although for the purposes of these calculations it is assumed that the pressure build-up on the rear and sides occurs at the same time, opposing the internal pressure increase which is assumed to be uniform throughout the structure.

If the structure under consideration is a framed structure, failure of the glazing and cladding will relieve the load on the structural frame and the pressure required to collapse the frame itself will be very high. Conversely, if the cladding doesn't fail, the frame will be subject to much higher loads and will collapse at a much lower pressure. Thus the sequence of failure is highly dependent on the failure pressures of the individual components.

## **2.4 Fragment Generation**

In the structural calculations above the failure pressures of the different structural components are estimated, but it is important to know what happens to the windows, walls etc. after they have failed. In order to assess the vulnerability of the building occupants, it is first necessary to estimate the size, velocity and range of glazing and cladding fragments generated by the interaction of the blast with the external cladding.

### **2.4.1 Glazing Fragments**

Failure of a window under a blast load will result in a large number of small glazing fragments with a wide range of frontal area, mass and velocity. For the purposes of estimating the effects on the building occupants, it is necessary to calculate the mean fragment mass and velocity arising from the window failure, together with the number of fragments generated. The methodology for performing these calculations is based on experimental work performed by Fletcher et al [9,10,11] and Nowee [12] and is summarised to a large extent in Baker et al [13].

The fragment mean area and hence the mass distribution has been estimated from a curve fit to experimental data reported in [9,10]. The curve fit presented in those papers did not include all the available data, and appeared to underestimate the average fragment mass significantly at low pressures; hence a new curve has been fitted to all the available data. The curve used corresponds to the following equation:

$$\text{Mean Fragment Area} = 834.16 \times 10^{-4} (100P_{eff})^{-1.1772} m^2 \quad (15)$$

where  $P_{eff}$  is the effective pressure on the window in Pa i.e. the resultant pressure across the window arising from the difference between the external pressure and the internal pressure.

The experimental data and the resultant curve fit are shown graphically in Figure 2.13.

The mean fragment spatial density is also based on experimental data from [9,10]. The corresponding equation is as follows:

$$\text{Fragment Spatial Density} = (e^{(3.1037+0.05857\frac{P_{eff}}{1000})} - 22.28)4.910e^{-501.2t} \text{ fragments / m}^2 \quad (16)$$

where  $t$  is the thickness of the glazing in m. This equation is based on experiments using plain glass of thickness 2.0mm - 6.7mm, and can thus only be assumed to be valid for these types of glass. For other types, such as laminated or tempered glass, alternative sources of data would have to be found, or experiments performed, in order to determine the spatial density of the fragments.

This is used, in conjunction with the area of the head ( $0.031\text{m}^2$  [14]) and the area of the body ( $0.359\text{m}^2$  [14]) to calculate the number of fragments hitting the head or body. For double glazed windows, it is assumed that the fragment spatial density is double this value.

The mean fragment initial velocity is also derived from the experimental work performed by Fletcher et al. The equation given in Baker et al [13] is as follows:

$$\text{Mean initial velocity} = [0.2539 + 1.826.10^{-4}(t - 7.62.10^{-4})^{-0.928}] [0.3443P_{eff}^{0.547}] \text{ m / s} \quad (17)$$

This has been increased by a factor of 1.5, in order to bring the mean initial fragment velocities into line with the upper bound of values observed in the experimental data [11]. It should be noted that this equation is based on measurements taken by measuring the indentation of fragments impacting on a witness plate located behind the window. In Phase 3 [2], it was shown that at the time the fragment hits the witness plate, the fragment may still be accelerating under the blast, and may not have been subjected to the full blast load. This is a direct consequence of the long pulse duration used in the experiment (250msec), and implies that the fragments may have achieved higher velocities if the witness plate had been located further away from the window. Consequently, this equation may not be conservative. However, increasing the predicted mean values by a factor of 1.5 is considered to be sufficient to take any non-conservatism into account.

The subsequent velocities and the range of the fragments has been assessed by calculating the time it takes for the fragments to fall below a height of 0.5m above the floor (based on the initial height) and then calculating the velocity resulting from the initial velocity and the reduction due to drag forces. The drag force on an object moving with a velocity,  $v$  is [15]:

$$\text{Drag Force, } D = \frac{1}{2} \rho v^2 C_{DF} A_F \quad (18)$$

where  $\rho$  is the density of the medium through which the object is travelling (in this case air),  $C_{DF}$  is the drag coefficient and  $A_F$  is the frontal area of the object. This force acts in a direction opposite to the direction of travel and causes a deceleration of the object. For the glazing fragments considered here, the drag coefficient is assumed to be 1.2, based on an average of possible values for different fragment shapes [13]. The frontal area is assumed to be the minimum cross-sectional area of the average fragment size i.e. the fragment is assumed to travel either edge-on or side-on, dependent on which is the minimum dimension.

Having calculated the time that the fragment takes to fall below the 0.5m limit (below which level the fragments are assumed to be no longer hazardous), and the change in velocity with time, the maximum range of the fragment from the window can be calculated, together with its velocity at any distance from the window.

#### 2.4.2 Cladding Fragments

The methodology for calculating the mass and velocity of cladding fragments is highly dependent on the individual wall construction type. There is very little information available concerning the modes of failure of the different cladding types, or more particularly the size and velocity of the fragments produced on failure of the cladding. Consequently, the calculation of the mass and velocity of fragments generated requires a degree of engineering judgement to ensure that appropriate values are derived.

The mass of a cladding fragment is a case in point. For a brick wall, the smallest likely fragment size is that of a single brick, as experiments have shown that failure of a brick wall occurs primarily in the mortar, rather than the bricks themselves. By comparison, for aluminium cladding, failure is likely to occur at connection details, and large sections of cladding may come off in one piece. It is necessary to assess, for each individual construction type, the size of the most hazardous fragment likely to be generated by a blast load.

An approach has been derived for calculating the cladding fragment velocity which has been validated against the glazing velocity calculation [2]. The initial velocity of the fragment is assumed to arise from two components, firstly the velocity of the panel at the time of failure, and secondly the effect of the remainder of the pulse after failure on the unconstrained fragment. For the first component, the method used to extract the limiting overpressure for the panel is also used to derive the failure velocity: the wall is modelled as a single degree of freedom elasto-plastic system, with an appropriate mass, stiffness and damping and with the elastic limit, i.e. the displacement at yield, defined from the calculated dynamic failure pressure. Support conditions are taken from the actual characteristics of the panel i.e. it may be appropriate to assume that the panel acts as a simply supported plate or as a clamped beam, depending on whether it is designed to span one way or two ways and on the connection details. The equation of motion (Equation 5) is solved to calculate the displacement of the panel subject to the blast load

as time progresses. From this calculation, the time at which the displacement is equal to the elastic limit multiplied by the ductility can be identified, and this is assumed to be the point at which the panel fails. The velocity at the failure time can be extracted from this calculation, by calculating the gradient of the displacement-time curve at the time of failure. While this calculation does not take into account the strain energy stored in the panel, it was found in Phase 3 that this approach produced the better agreement with the experimental results for glazing [2].

For the second component of velocity, it is assumed that the remainder of the blast pulse, after the failure time, acts on an effectively unconstrained fragment. Baker et al [13] gives a methodology for calculating the velocity of an unconstrained fragment subject to a blast load, and this method is used to calculate the remaining component of the initial velocity. In Baker's method, two non-dimensional parameters are calculated,  $\bar{P}$  and  $\bar{I}$  from the following equations.

$$\bar{P} = \frac{P_s}{P_0} \quad (19)$$

and

$$\bar{I} = \frac{C_D I_s a_0}{P_s (Kw + X)} \quad (20)$$

where  $P_s$  is the peak incident side-on overpressure,  $P_0$  is atmospheric pressure,  $I_s$  is the incident specific impulse,  $a_0$  is the velocity of sound in air,  $K$  is a constant equal to 2 if the object is in the air,  $w$  is the minimum width of the object and  $X$  is the distance from the front of the object to the location of its largest cross-sectional area. Using these two parameters, a third parameter,  $\bar{v}$ , can be calculated from a graph (Figure 2.14), and the corresponding unconstrained fragment velocity can be calculated from:

$$\text{Unconstrained fragment velocity} = \frac{\bar{v} P_0 A_m (Kw + X)}{m_f a_0} \quad (21)$$

where  $A_m$  is the mean presented area of the object and  $m_f$  is its mass.

The initial velocity of the cladding is then calculated from the sum of the velocity at failure and the unconstrained fragment velocity. This approach is used for all panel types, even though for panels which fail in a ductile manner this leads to very high initial velocities. In these cases, the velocities have been assessed and if they are unrealistically high, either the fragment size has been reduced or the contribution from the blast pulse after failure has been reduced to ensure that the velocity remains appropriate. For steel cladding in particular, the velocities at failure calculated using this approach are very high, and do not appear to be realistic. In this case failure is more likely to occur at the connections of the panel to the supporting frame, which has not been taken into account

due to lack of data. This is one area where further development of the methodology would be worthwhile.

Subsequent velocities at a distance from the wall are calculated in the same way as for the glazing fragments, by calculating the velocity resulting from the initial velocity and the reduction due to drag forces. The change in velocity with time is used together with the time taken for the fragment to fall below a level of 0.5m above the floor to calculate the maximum range of the fragment.

Having calculated the mass and velocity of the glazing and cladding fragments, it is possible to calculate the vulnerability of the personnel to the fragments and hence the overall probability of fatality within the building.

## **2.5 Fatality probability**

There is considerable uncertainty in the prediction of human response to different types of trauma, and hence the calculation of the effects of an explosion is difficult. The area of human response is the subject of a further literature search which is currently being performed in order to try and gain a more specific understanding of the probability of a fatality occurring as the result of a particular injury.

The fatality probability calculations can conveniently be split into four sections: the probability of fatality due to a) glazing fragments, b) cladding, c) building collapse and finally, d) calculation of the overall fatality probability associated with the building. In addition it is useful to present the information in terms of P-I diagrams and the method for doing this is outlined at the end of this section.

### **2.5.1 Fatality probability due to glazing**

The probability of human fatality due to impact from fragments of glazing is assessed on the basis of hits on the head causing skull fracture and hits on the body causing penetration injuries. The criteria for injury are based on the critical velocity a fragment of a given mass needs in order to cause the injury of interest. The curve used for skull fracture is from Fletcher et al [11], and gives the velocity required for a given fragment mass to have a 50% probability of causing skull fracture, based on experimental tests on sheep and dogs. This curve is presented in Figure 2.15. A similar criterion is used for penetration injuries; in this case, data from Feinstein [14] is used. This is a collation of data from a wide range of different sources, and gives mass/velocity values for a 10%, 50% and 90% probability of skin penetration. The curve for 10% probability of skin penetration is shown on Figure 2.16.

A flow chart illustrating the methodology for calculating the fatality probability as a function of pressure is given in Figure 2.17. The steps are as follows:

For a given value of effective pressure:

- (a) Calculate the fragment spatial density and hence the number of fragments hitting a head or a body. The equations are given in Section 2.4.1 above for plain glass of thickness varying between 2.0 and 6.7mm.
- (b) Calculate the average fragment mass and initial velocity (Section 2.4.1).
- (c) The typical range of fragment masses and initial velocities corresponding to the average values at that pressure are then calculated. The heaviest, slowest fragments are assumed to have 10 times the average mass and 0.6 x 1.5 times the average initial velocity: conversely, the lightest, quickest fragments are assumed to have a tenth of the average mass and 1/0.6 x 1.5 times the average initial velocity. These assumptions are based on the upper bound of the spread of fragment masses and velocities observed in the experiments described in Fletcher et al [9,10,11].
- (d) From the initial velocities for each of the three mass-velocity pairs, and the height of the window, calculate the velocity as a function of distance from the window, and the time taken for the fragment to fall below a height of 0.5m above the floor. Once a fragment falls below this level, it is deemed to be no longer likely to cause a fatality.
- (e) A uniform distribution of fragment masses and velocities is assumed between the heaviest, slowest fragment and the lightest, quickest fragment at the given pressure. The proportion of fragments whose mass and velocity exceed the relevant criterion at that pressure is then calculated for a range of distances from the window. Physically, this is calculated by plotting the criterion on a mass-velocity graph, adding the points for the heaviest, slowest fragment and the lightest, quickest fragment at a particular distance, drawing a line between these two points and calculating the proportion of the line lying above the criterion, and the proportion lying below. The proportion above the criterion is assumed to correspond to the proportion of potentially injurious fragments at that distance from the window. This is illustrated in Figure 2.18.
- (f) Calculate the number of potentially injurious fragments from the number hitting the head or the body and the percentage of potentially injurious fragments i.e.

For skull fracture:

$$\begin{aligned}
 f_{inj h} &= \% \text{fragments exceeding criterion} \\
 N_{fh} &= \text{Number of fragments hitting head} \\
 N_{inj h} &= f_{inj h} \cdot N_{fh} = \text{Number of potentially injurious fragments}
 \end{aligned}
 \tag{22}$$

A similar equation applies for the number of potentially injurious fragments hitting the body,  $N_{inj b}$ .

- (g) Each potentially injurious fragment hit only has a certain probability of causing that injury, i.e. 50% for skull fracture and 10% for skin penetration ( $p_{igh}$  and  $p_{igb}$ ).

In addition, each injury only has a certain probability of causing fatality. This has been assumed to be 10% for skull fracture and 50% for penetration ( $p_{fh}$  and  $p_{fb}$ ). The probability of fatality arising from a skull fracture is assumed to be lower than that for a penetration injury as skull fracture does not necessarily lead to a brain injury, and it is the injury to the brain which is the cause of fatality, not just the fractured skull. By comparison, if a fragment is travelling sufficiently quickly to penetrate the skin, then it is assumed to be likely to travel a reasonable way into the body, and is therefore likely to cause a serious injury. These values are subjective, however, and may be subject to revision as more data become available.

- (h) Calculate the overall probability of fatality for a given pressure and a given distance from the window from:

For skull fracture

$$\text{Probability of Fatality, } p_{fath} = 1 - (1 - p_{igh} \cdot p_{fh})^{N_{inj}} \quad (23)$$

- (i) A similar equation is used for the probability of fatality due to skin penetration,  $P_{fatb}$ . The two probabilities are then combined to give a total fatality probability for glazing at a given pressure and a given distance from the window:

$$P_{fatality} = P_{fath} + P_{fatb} - P_{fath} \cdot P_{fatb} \quad (24)$$

This equation takes into account the fact that people cannot be ‘killed twice’. The calculation can then be repeated for a range of pressures and a range of distances to calculate the fatality probability with distance from the window at a given pressure. This calculation is continuous, i.e. the fatality probability varies continuously with distance. In order to make use of these values to calculate overall building fatality probability, it is useful to derive a series of ‘fatality probability contours’ with distance from the window, for the different incident pressures.

A typical glazing fatality probability graph, showing the probability of fatality as a function of pressure and distance from the window, is given in Figure 2.19. The curves show the change between domination by skull fracture effects and domination by skin penetration effects. Above 50%, the curves are dominated by skin penetration, and below 50% the curves are dominated by skull fracture: at 50%, there is a change in gradient in the line which reveals the point at which the primary cause of fatality changes from skin penetration to skull fracture as the speed of the fragment slows with distance from the window.

### 2.5.2 Probability of fatality arising from cladding impact

The calculation of the probability of fatalities arising from cladding impact is based on the criterion for the probability of fatality from non-penetrating fragment impact presented in Baker et al [13]. This case is slightly more straightforward than the glazing case above, partly because it is assumed that the fragment size does not change with



increasing pressure, and partly because only one criterion is used to calculate the fatality probability. The methodology is illustrated in Figure 2.20.

The criterion is shown in Figure 2.21. Given the mass of the fragment, which is specified according to the type of cladding considered (Section 2.4.2), there is a range of critical velocities given corresponding to the threshold for serious injury and 10%, 50% and 90% probability of fatality. The calculation of fatality probability involves first calculating the cladding velocities with distance from the wall (Section 2.4.2). The velocity is then compared against the different critical velocities in order to determine the fatality probability at different distances. The probability of fatality is divided into ranges, i.e. < 10%, 10% - 50%, 50% - 90% and >90%. These ranges can be used to derive the 'fatality probability contours' required for the calculation of the fatality probability for the whole building.

In addition to this calculation, for brick walls there is the added criterion that if wall failure occurs, directly behind it there is an area within which personnel are liable to be buried under a collapsed wall. In this case their fatality probability is assumed to be 60%. This area extends to a distance behind the wall equal to the height of the wall.

A typical cladding fatality probability curve is illustrated, for a brick wall, height 2.6m, in Figure 2.22.

### **2.5.3 Probability of fatality arising from building collapse**

The effect of building collapse on the building occupants is strongly dependent on the type of building and the behaviour of the structure on collapse. For a brick building, it is assumed that failure of the external walls signifies collapse of the structure, as the external walls effectively form the load-bearing frame of the structure. The collapse of a brick structure will result in large amounts of rubble and dust, and will give rise to hazards from suffocation in addition to those associated with the weight of the building materials. By comparison, for most framed structures, failure of the walls reduces the load on the load-bearing frame, and renders the structure less likely to collapse. When it does collapse it is likely to fail progressively, with those bays nearest the blast failing first, and the effects of floor slabs collapsing through the structure may be severe.

The criterion for calculating the probability of fatality due to building collapse is based on experience from earthquakes, although it has to be remembered that rescue times are likely to be quicker in a blast situation, which may reduce the probability of fatality post-collapse. This is because in a VCE event, damage would be relatively localised to an area around the explosion, whereas in an earthquake, damage could be far more widespread, hindering the rescue services. The data available indicate that, for masonry structures, where it is assumed that complete collapse occurs on failure of the external walls, a value of 60% is appropriate. For framed structures, where the collapse may be localised, it is assumed that 80% fatality occurs within the collapsed area, based on the assumption that local collapse of such a structure would lead to the collapse of roof and floor slabs, which are likely to be very heavy, in the affected area [1]. For single-storey framed structures, therefore, where collapse of the slabs is not an issue, 60% fatality probability has been assumed in line with the masonry structures. For wooden structures, such as

Portacabins, the fatality probability due to collapse is assumed to be negligible, as the walls and roof are lightweight such that collapse is assumed to not present a significant fatality mechanism.

The methodology for calculating the probability of fatality due to building collapse is shown in Figure 2.23.

#### **2.5.4 Overall fatality probability of building occupants**

The above individual vulnerabilities to glazing, cladding and building collapse are combined to calculate the overall building fatality probability, based on a knowledge of the building internal layout. In order to complete this calculation, it is necessary to make some assumptions concerning the layout and the occupancy of the building. First it is assumed that there is uniform occupancy, i.e. it is possible for any occupant to be in any room at any time. It is then necessary to define the dimensions of each room within the structure, and the behaviour of the internal partitions: for solid internal walls, it is assumed that the internal walls present a boundary to the travel of glazing or cladding from the external walls, while flexible partitions may be assumed to be effectively non-existent for the purposes of this calculation. In addition, it is necessary to define how the internal partitions affect the increase of pressure build-up within the structure: in general, they are assumed to present no obstacle, although for some structures, with a solid central wall obstructing flow through the structure (e.g. semi-detached housing), it may be assumed that only half the volume is available for increases in internal pressure.

Having defined the structural limits, the calculation proceeds as follows:

For a given incident pulse:

- (a) Calculate the pressure on the front face (Section 2.3.2), the pressure on the rear face (Section 2.3.3) and the internal pressure in the building (Section 2.3.4). From these pressure profiles, calculate the maximum differential pressure across the front and rear faces and the sides, assuming that the internal pressure build up is uniform throughout the structure and that the pressure on the sides of the structure is the same as that on the rear face.

It is possible, that in calculating the differential pressure, the internal pressure will be greater than the external pressure on the rear face. In this case, it is assumed that if the differential pressure is high enough to cause failure, then the windows or walls will fail, but the ensuing fragments will be blown out of the building and will present no hazard to the building occupants. This effect has been observed in experiments, but further study is required to verify that the model predictions are conservative [27].

- (b) For each window in the building calculate the contribution to the glazing fatality probability. This is done by first using the peak resultant pressure across the glazing in conjunction with the pressure-distance curve to identify the fatality probability contours within each room. It is assumed that the glazing does not spread out on failure, i.e. that only the region directly behind the window is

affected, and any constraints on movement of the glazing (i.e. internal walls or the opposite external walls) are taken into account. From the fatality probability contours and the width of the window, the area corresponding to each level of fatality probability is identified. The percentage fatalities within a given zone is the average of the percentage fatalities at one edge of the zone and the percentage fatalities at the other edge i.e. between the 90% and 50% contours, the fatality probability is assumed to be 70%. The contribution to the overall glazing fatality probability arising from that window is then calculated from the affected area divided by the overall floor area of the building and multiplied by the percentage fatalities within that affected area. The total fatality probability to glazing is then assumed to be the sum of the contributions from all the affected areas, i.e.

$$p_g = \sum_{\text{affected areas}} \frac{\text{Length}_{\text{affected area}} \cdot \text{Width}_{\text{window}} \cdot \% \text{probability of fatality in affected area}}{\text{Floor Area}} \quad (25)$$

This is shown schematically in Figure 2.24.

By performing the calculation in this way, it is assumed that each storey of the building is the same as the one below. If it were necessary to differentiate one storey from another, the calculation would include a factor equal to the volume of the storey divided by the volume of the building, and the sum of the values for each storey would be calculated.

In areas which are exposed to glazing fragments from more than one source, it may be necessary to calculate the overlapping areas and the resultant fatality probability in those areas (taking into account the fact that people cannot be killed twice) and then sum the contributions from all the affected areas in a similar manner to that shown above. For buildings with small areas of glazing, the overlap is likely to be small and has been conservatively ignored. For buildings with a high percentage of glazing, the overlapping areas have been assessed and where necessary it has been assumed that, for two overlapping regions, with corresponding fatality probabilities  $p_1$  and  $p_2$ , the combined value, taking the overlap into account, is:

$$\text{Fatality probability} = p_1 + p_2 - p_1 \cdot p_2 \quad (26)$$

- (c) For each room in the building, calculate the fatality probability due to cladding impact. This is a similar calculation to that performed for the glazing above. First the affected areas are worked out from the length of cladding in the walls. The effective pressure across the walls is then used in conjunction with the cladding fatality probability pressure-distance curves to estimate the fatality probability in the affected regions. If the internal pressure is greater than the external pressure, the net force on the wall is directed outwards and it is possible that the walls may be blown outwards, thus not presenting a hazard to the building occupants. As for the glazing, the fatality probability in all the affected areas is summed to give

an overall cladding fatality probability for the building, taking into account any overlapping regions.

- (d) Assess whether or not the structural frame of the building has partially or totally collapsed. If it has, the collapse fatality probability is calculated from either 80% of the ratio of the collapsed volume of the building to the total volume (frame buildings), or a constant value of 60% (masonry buildings).
- (e) Calculate the overall building fatality probability from the individual contributions from glazing,  $p_g$ , cladding,  $p_d$  and building collapse,  $p_c$ , according to the following expression:

$$P_{total} = p_g + p_d + p_c - p_g \cdot p_d - p_g \cdot p_c - p_d \cdot p_c + p_g \cdot p_d \cdot p_c \quad (27)$$

This equation takes into account the fact that the building occupants cannot be 'killed twice'.

The methodology is illustrated schematically in Figure 2.25.

By repeating the above process over a range of pressures, a building curve can be built up, showing the fatality probability as a function of pressure. A sample curve is given in Figure 2.26. This shows the individual contributions of glazing, cladding and building collapse together with the combined overall fatality probability curve. For the long side of the building facing the blast, the debris curve shows a drop in the fatality probability at a peak incident overpressure of approximately 650mbar. This is the point at which the internal pressure exceeds the external pressure to such an extent that the cladding starts to be blown out of the building on the sides and rear face, hence reducing the risk to the occupants.

This process is repeated for different orientations of the building and different proportions of external glazing in order to derive generic curves for a specific building type.

### 2.5.5 P-I diagrams

In order to be able to use the data generated for specific buildings in typical land use planning scenarios, it is useful to present the data in a slightly different format, i.e. in the form of Pressure - Impulse diagrams. These show the probability of fatality corresponding to different values of pressure and impulse. The form is similar to that shown in Figure 2.27, except that contours of fatality probability replace the contours of building damage shown on the figure.

To produce these curves, it is necessary to perform the above analysis for a range of pressure-impulse pairs and to identify the values which correspond to the required level of fatality probability. For the purposes of this project, 5 analyses have been performed for each building type, and each pulse type, i.e. shock pulse and pressure pulse, 3 using a varying pressure with a constant duration, designed to cross the fatality probability contours on the curved section of the contour. Of the remaining two, one uses a constant

pressure and varying duration, designed to intersect one end of the contours: the other has a constant impulse but a varying pressure, designed to intersect the other end. With these 5 points for each fatality probability level, the contours can be defined. This is illustrated in Figure 2.28.

## **2.6 Conclusions**

A methodology has been presented for estimating the fatality probability of building occupants to an explosion outside the building. It is based on an analysis of the structural behaviour under blast loading and the subsequent hazard to the occupants from failed structural components or the collapse of the building itself. While there are several aspects of the methodology which are worthy of a deeper investigation, the methodology as it stands is sufficiently developed to be applicable to any building, provided sufficient engineering information is available.

This methodology is applied to a range of generic building types as described in subsequent sections of this report in order to derive generic building fatality probability curves.

Overpressures for 1 te propane equivalent ( $4.65 \times 10^{10}$ J)							
Scaled Distance, R	Distance (m)	Scaled Pressure	Side-on Overpressure (kPa)	Scaled Dynamic Pressure	Dynamic Pressure (kPa)	Scaled Positive Phase Duration	Positive Phase Duration (ms)
0.3	23.14	1.0	101.325	0.595	60.29	0.368	83.57
0.5	38.57	0.941	95.30	0.380	38.50	0.285	64.68
1.0	77.13	0.454	46.02	0.060	6.08	0.305	69.21
3.0	231.40	0.094	9.54	0.003	0.278	0.401	90.95
5.0	385.67	0.051	5.188	0.0	0.0	0.434	98.473
8.0	617.07	0.030	3.056	0.0	0.0	0.461	104.59
10.0	771.34	0.023	2.378	0.0	0.0	0.473	107.35
30.0	2314.02	0.007	0.690	0.0	0.0	0.531	120.43

Overpressures for 3 te propane equivalent ( $1.395 \times 10^{11}$ J)							
Scaled Distance, R	Distance (m)	Scaled Pressure	Side-on Overpressure (kPa)	Scaled Dynamic Pressure	Dynamic Pressure (kPa)	Scaled Positive Phase Duration	Positive Phase Duration (ms)
0.3	33.37	1.0	101.325	0.595	60.29	0.368	120.52
0.5	55.62	0.941	95.30	0.380	38.50	0.285	93.29
1.0	111.25	0.454	46.02	0.060	6.08	0.305	99.82
3.0	333.74	0.094	9.54	0.003	0.278	0.401	131.17
5.0	556.23	0.051	5.188	0.0	0.0	0.434	142.02
8.0	889.97	0.030	3.056	0.0	0.0	0.461	150.85
10.0	1112.46	0.023	2.378	0.0	0.0	0.473	154.83
30.0	3337.39	0.007	0.690	0.0	0.0	0.531	173.69

Overpressures for 10 te propane equivalent ( $4.65 \times 10^{11}$ J)							
Scaled Distance, R	Distance (m)	Scaled Pressure	Side-on Overpressure (kPa)	Scaled Dynamic Pressure	Dynamic Pressure (kPa)	Scaled Positive Phase Duration	Positive Phase Duration (ms)
0.3	49.85	1.0	101.325	0.595	60.29	0.368	180.04
0.5	83.09	0.941	95.30	0.380	38.50	0.285	139.35
1.0	166.18	0.454	46.02	0.060	6.08	0.305	149.11
3.0	498.54	0.094	9.54	0.003	0.278	0.401	195.94
5.0	830.90	0.051	5.188	0.0	0.0	0.434	212.15
8.0	1329.44	0.030	3.056	0.0	0.0	0.461	225.34
10.0	1661.80	0.023	2.378	0.0	0.0	0.473	231.29
30.0	4985.40	0.007	0.690	0.0	0.0	0.531	259.46

**Table 2.1: Overpressures for 1te, 3te and 10te Propane Equivalent**

Type of Glazing	Reference	Data Available
Polycarbonate	[16]	Design parameters and peak blast pressures for various thicknesses of polycarbonate glazing
Tempered Glass	[17]	Design parameters and peak blast pressures for various thicknesses of tempered glass
Laminated, thermally tempered glass	[18]	Peak overpressure capacities for laminated, thermally tempered glass (design values)

**Table 2.2: Available Data for Alternative Glazing Types**

Type of Cladding	Static Failure Pressure (mbar)	Dynamic Failure Pressure (mbar)
Hardboard - 12.5mm thick	37	58 - 102
Aluminium corrugated sheet	24	70 - 108
Galvanised corrugated steel sheet	31-62	48 - 150
Corrugated asbestos cement sheet	15	14 - 40
Non-loadbearing pre-cast concrete panels	46	66 - 68
Brickwork	138	168 - 184

**Table 2.3: Typical Failure Pressures for Cladding [1]**

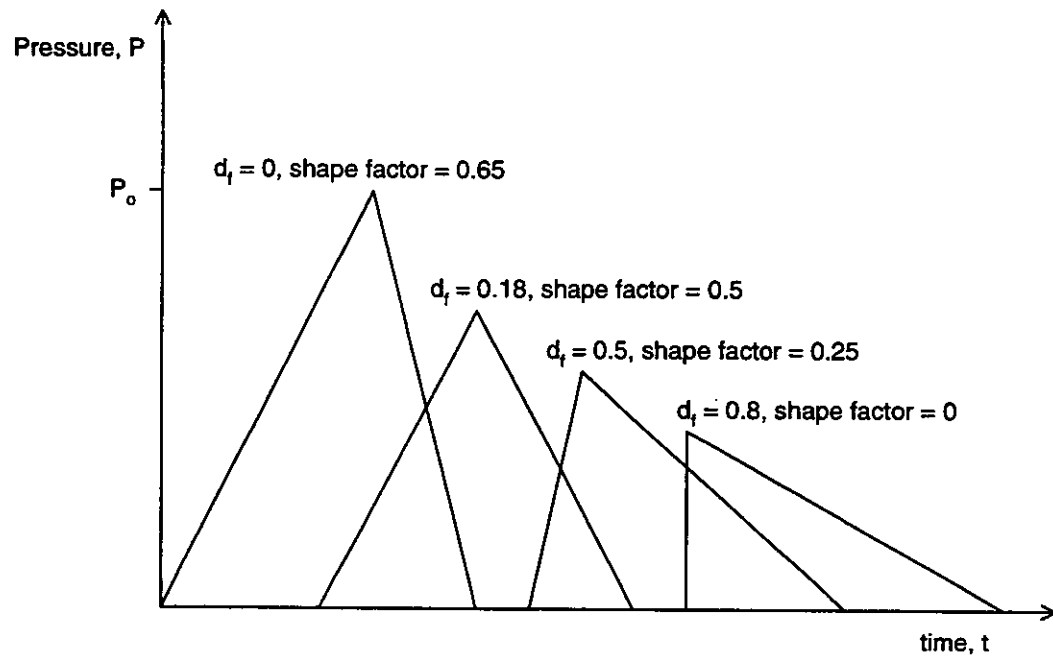


**Figure 2.1: Schematic Progression of Pulse Shape [3]**



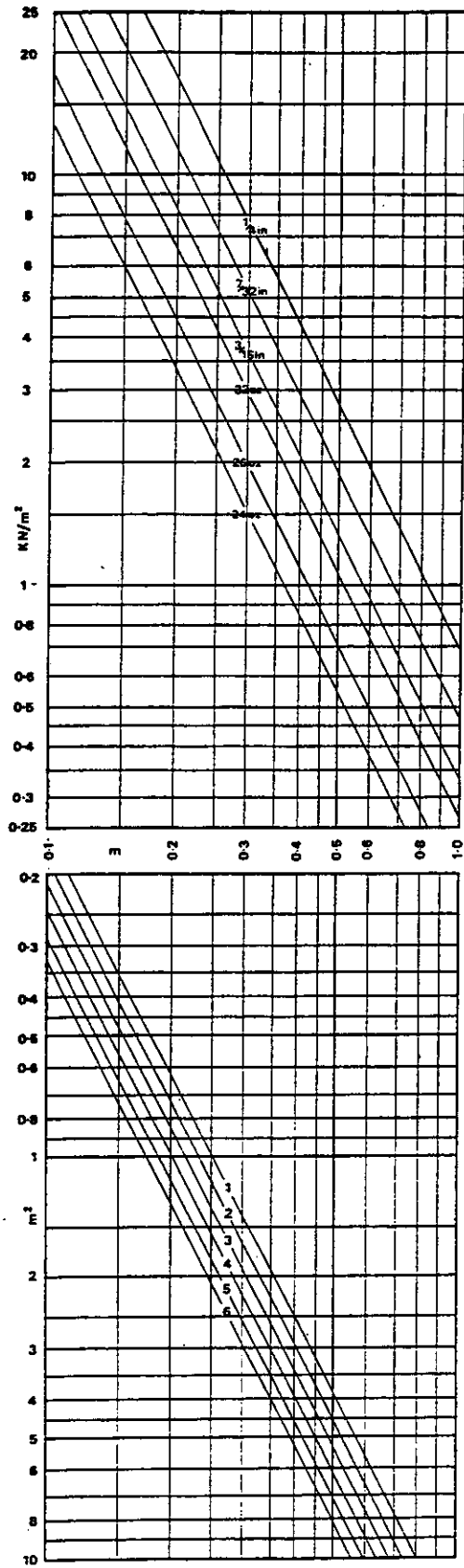
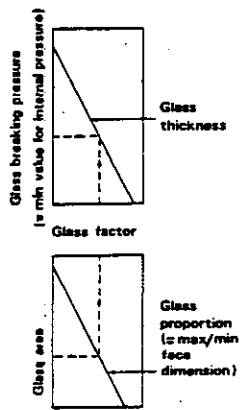


Figure 2.2: Failure Pressures for Single Glazing [4]

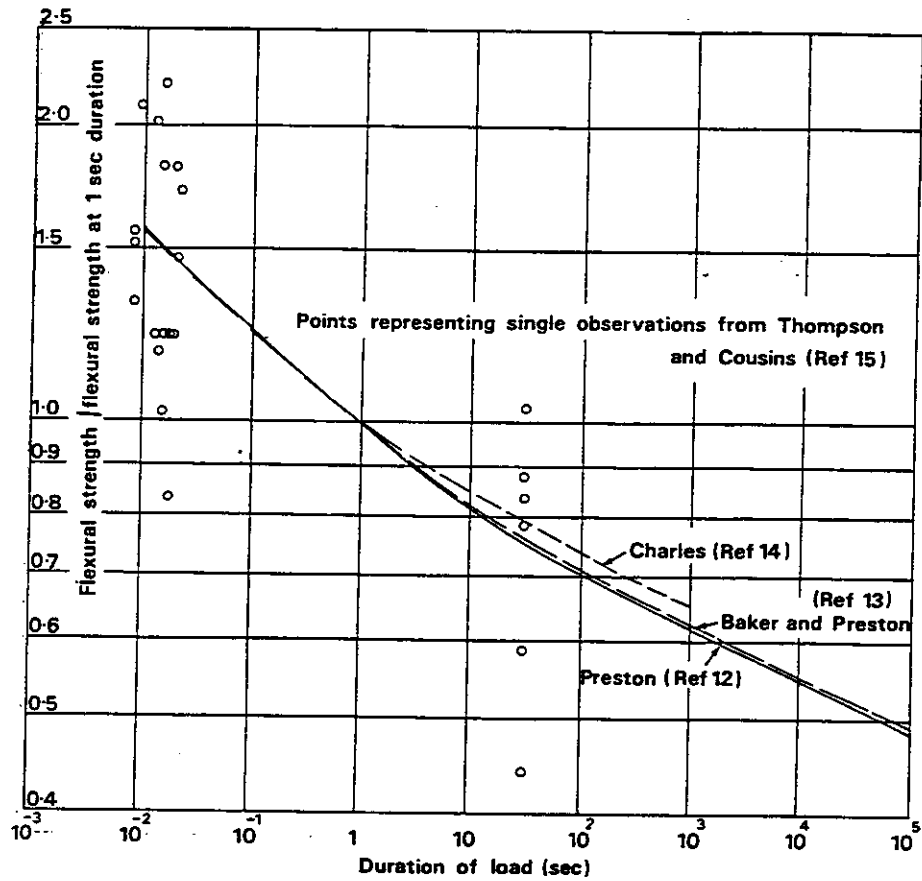


Figure 2.3: Variation of Flexural Strength of Glass with Duration of Loading [4]

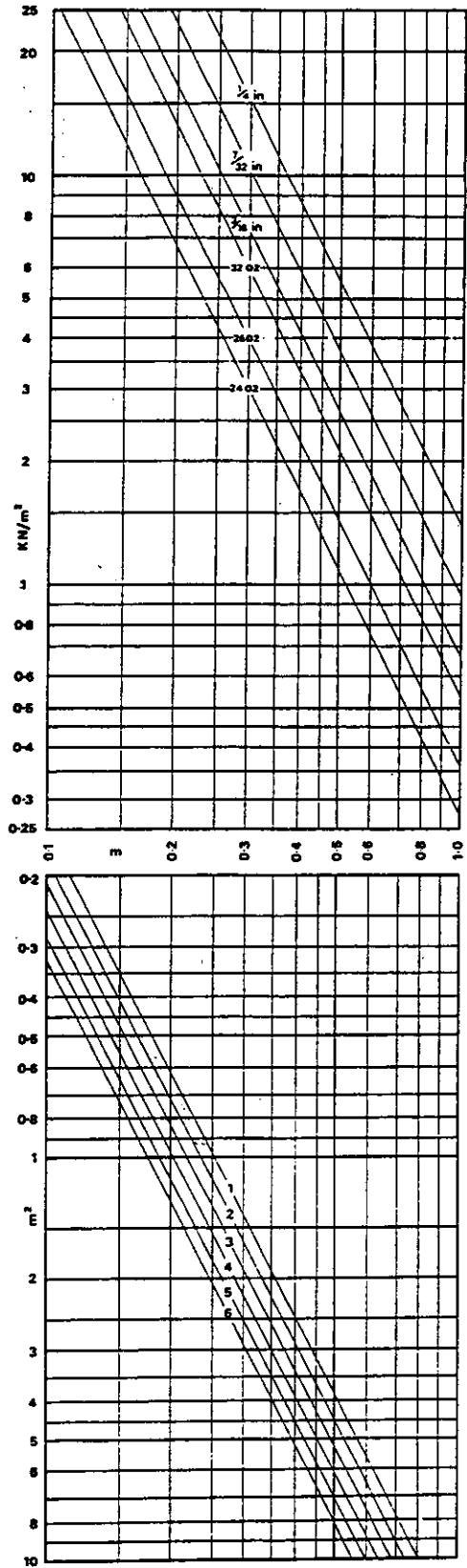
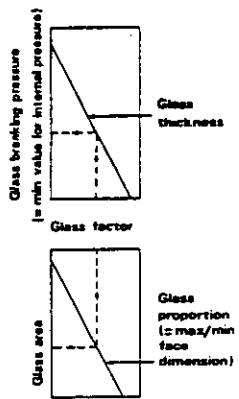
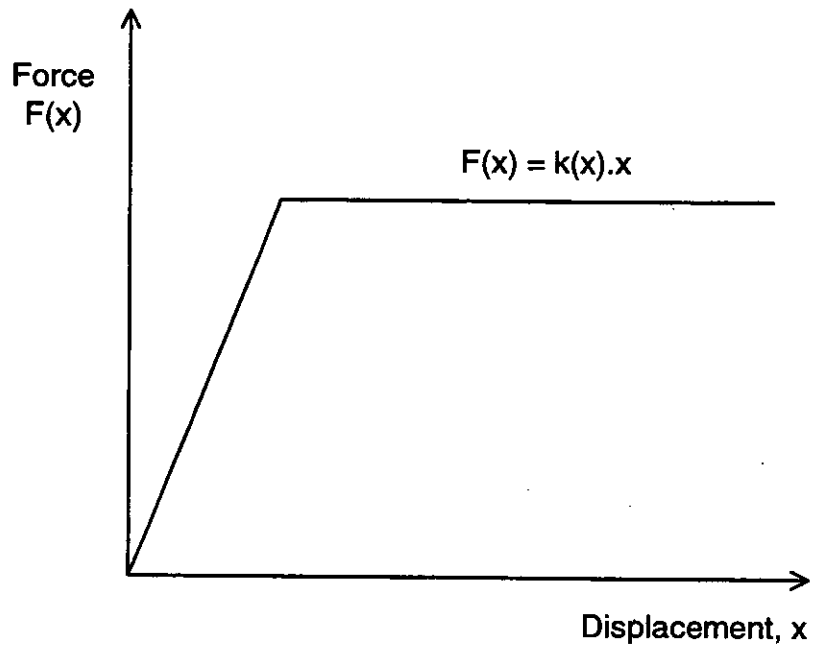
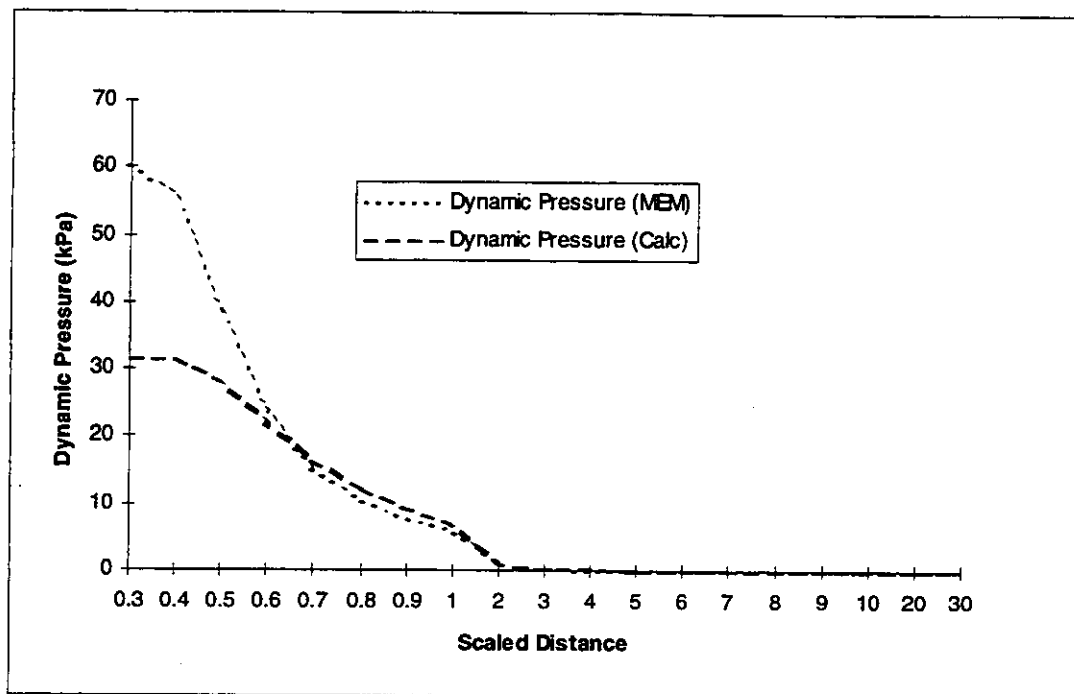


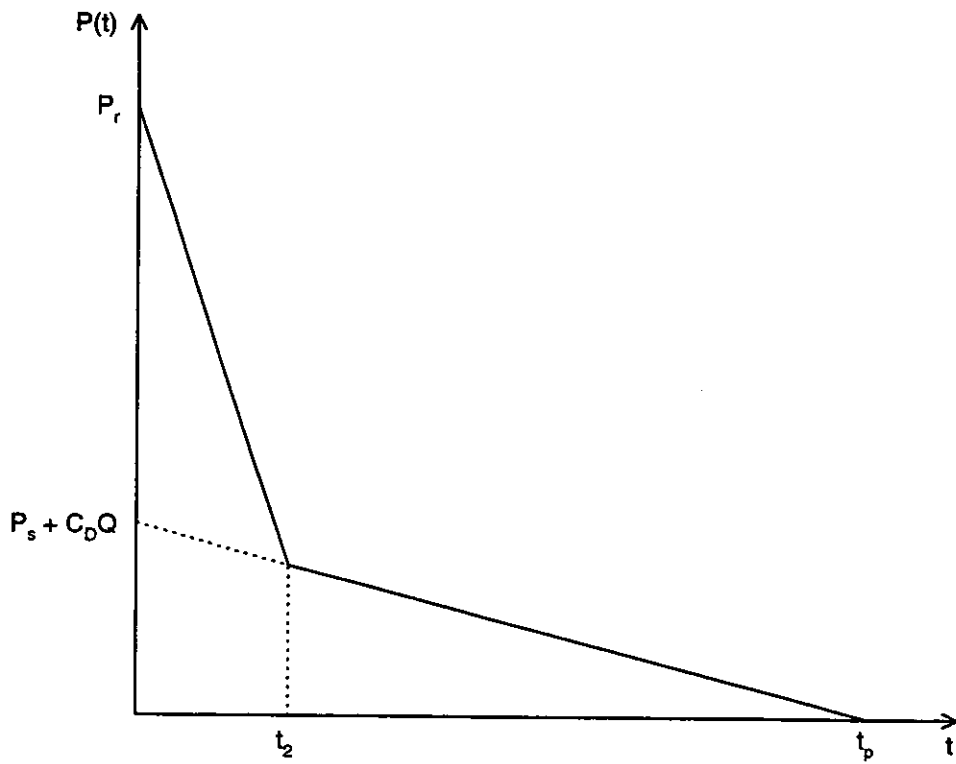
Figure 2.4: Failure Pressures for Double Glazing [4]



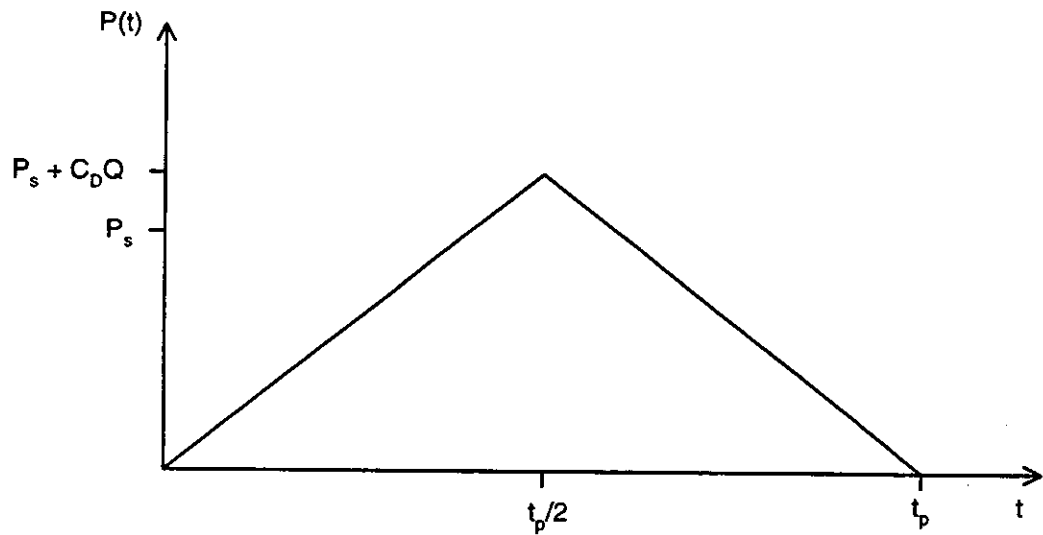
**Figure 2.5: Elasto-Plastic Stiffness**



**Figure 2.6: Comparison of Calculations for Dynamic Pressure**



a) Shock Pulse



b) Pressure Pulse

**Figure 2.7: Schematic Representation of the Pressure - Time Diagram for a Finite Reflective Surface**

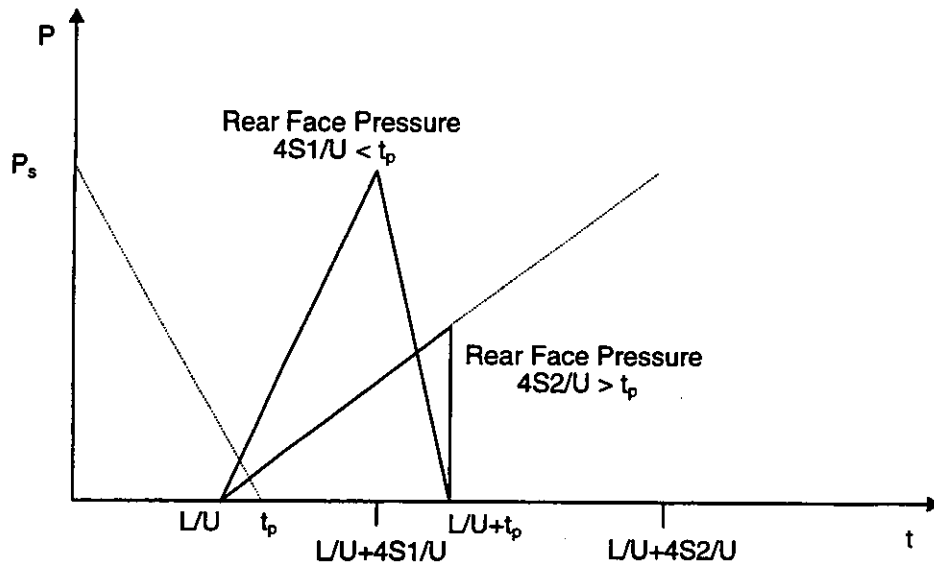


**Figure 2.8: Rear Face Pressure Load: Shock**

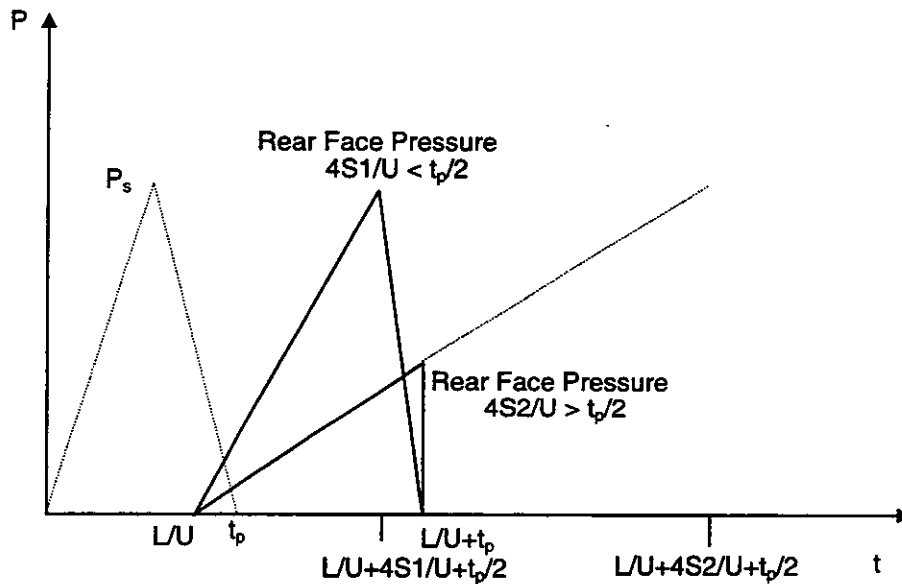


**Figure 2.9: Rear Face Pressure Load: Pressure Pulse**

Key:  
 L = Building Length  
 U = wave speed  
 Po = Incident Pressure  
 S1 = Building Dimension (= smaller of breadth/2 or height) for full rear face load  
 S2 = Building Dimension (= smaller of breadth/2 or height) for partial rear face load  
 tp = incident pulse duration

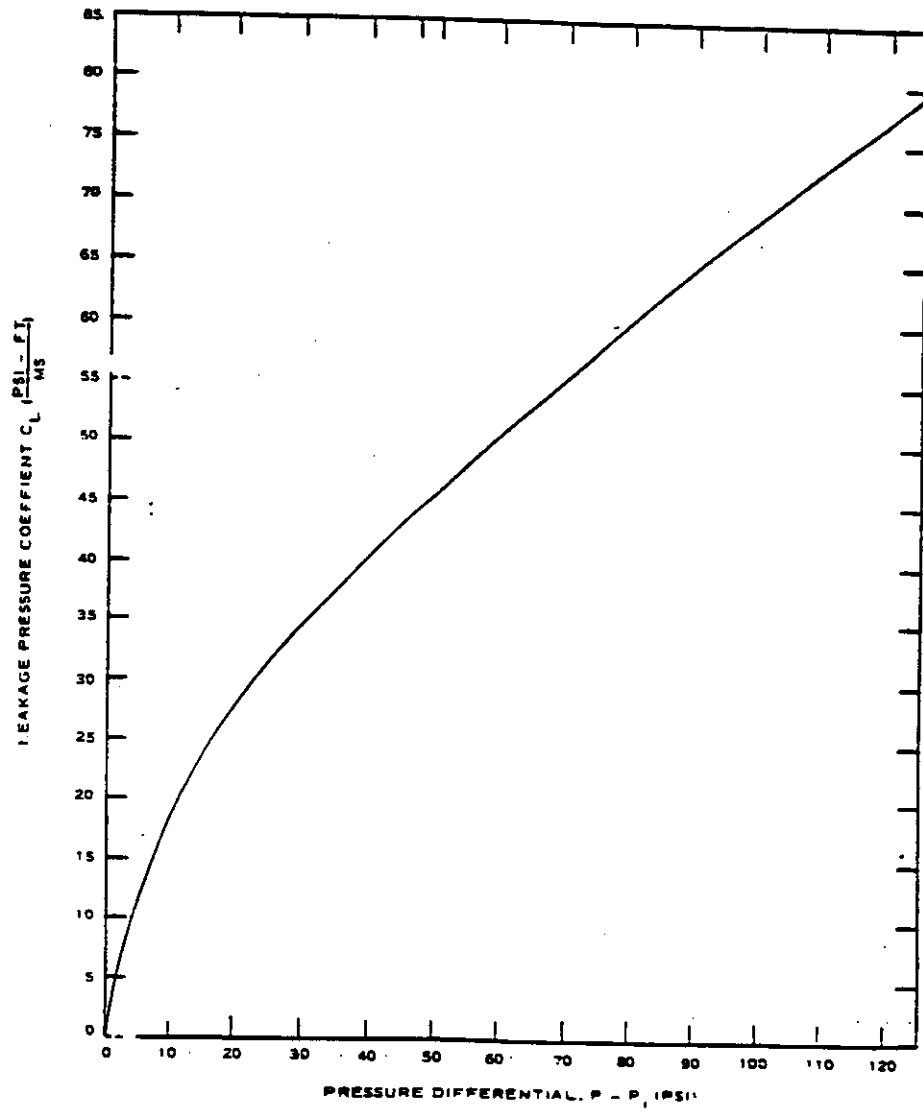
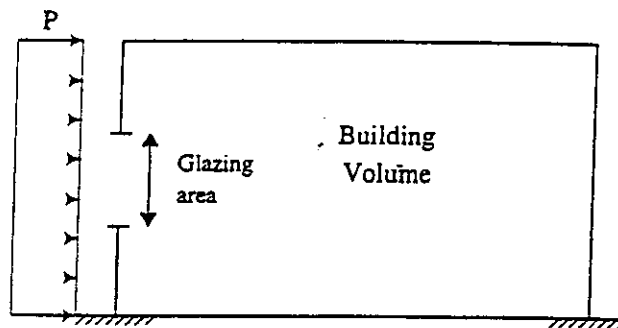


**Figure 2.10: Leakage Pressure Coefficient as a Function of the Differential Pressure across the Opening**





Pressure relief is dependent upon:

- Pressure in building
- Time to develop pressure within building

Average pressure increases within a structure are given by:

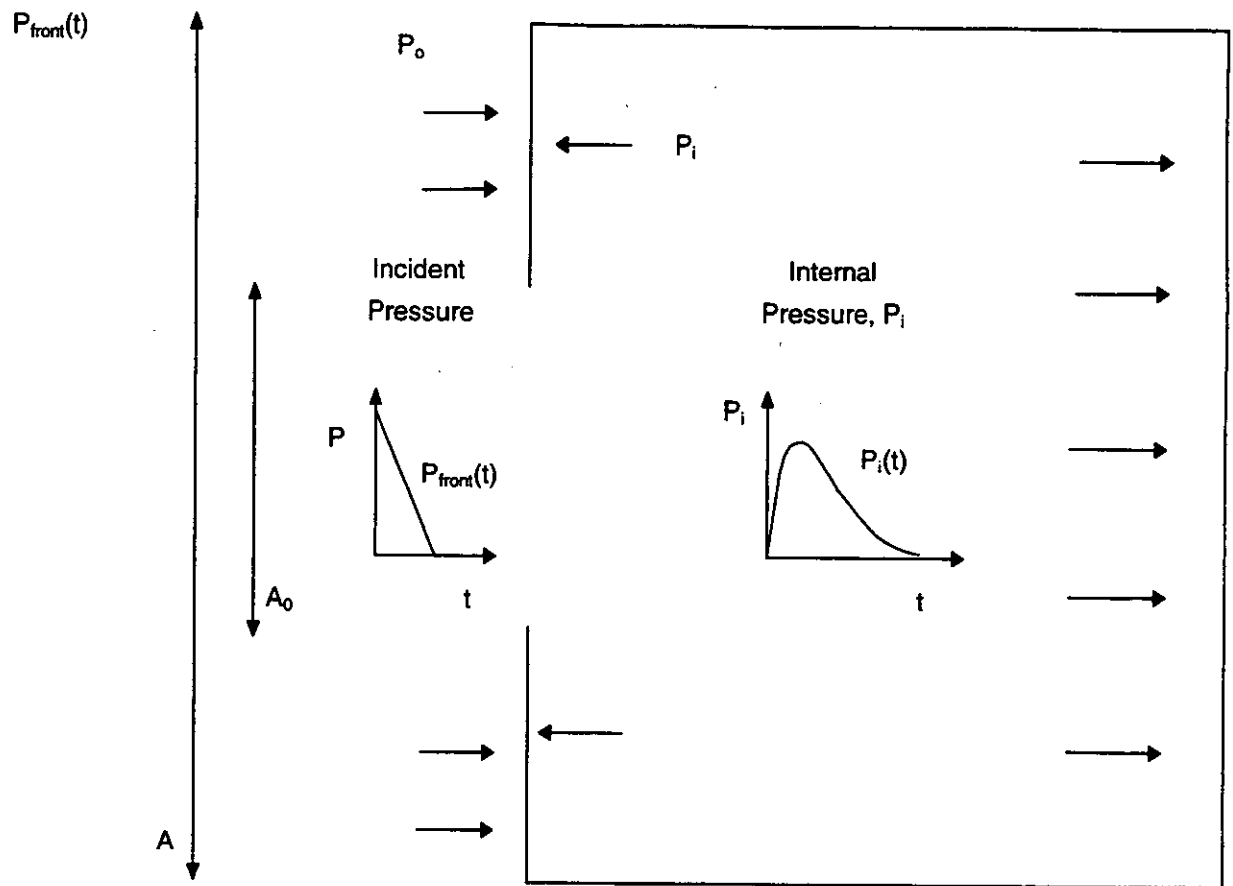
$$\Delta P_i = C_L \frac{A_0}{V_0} \Delta t$$

where:

$\Delta P_i$	=	internal pressure increment, psi
$C_L$	=	leakage pressure coefficient (function of pressure difference, $P - P_i$ )
$A_0$	=	area of openings, $\text{ft}^2$
$V_0$	=	volume of structure, $\text{ft}^3$
$\Delta t$	=	time increment, ms

Limitations: small area of opening / volume ratios applied  
 Pressure < 150 psi

**Figure 2.11: Pressure Relief on External Walls from Glazing/Cladding Failure**



Area of Front Face =  $A$

Area of Glazing =  $A_0$

$$\text{Horizontal Force on Building} = P_{front}(t)(A-A_0) - P_i(t)(A-A_0) + P_i(t)A \quad (\text{Eqn 1})$$

$$= P_{front}(t)(A-A_0) + P_i(t)A_0 \quad (\text{Eqn 2})$$

**Figure 2.12: Effect of Front Face Glazing/Cladding Failure**

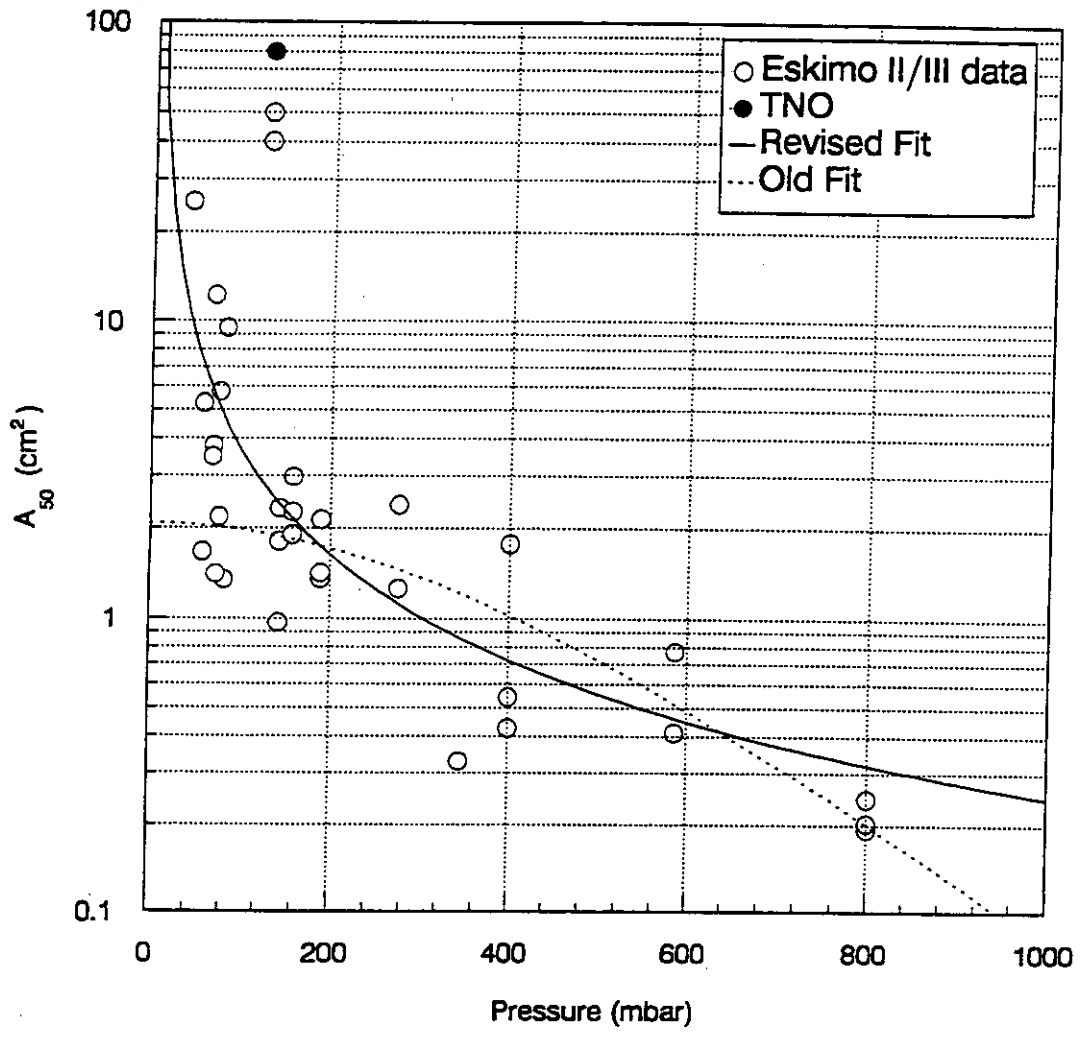


**Figure 2.13: Curve Fit to Mass Distribution Data**

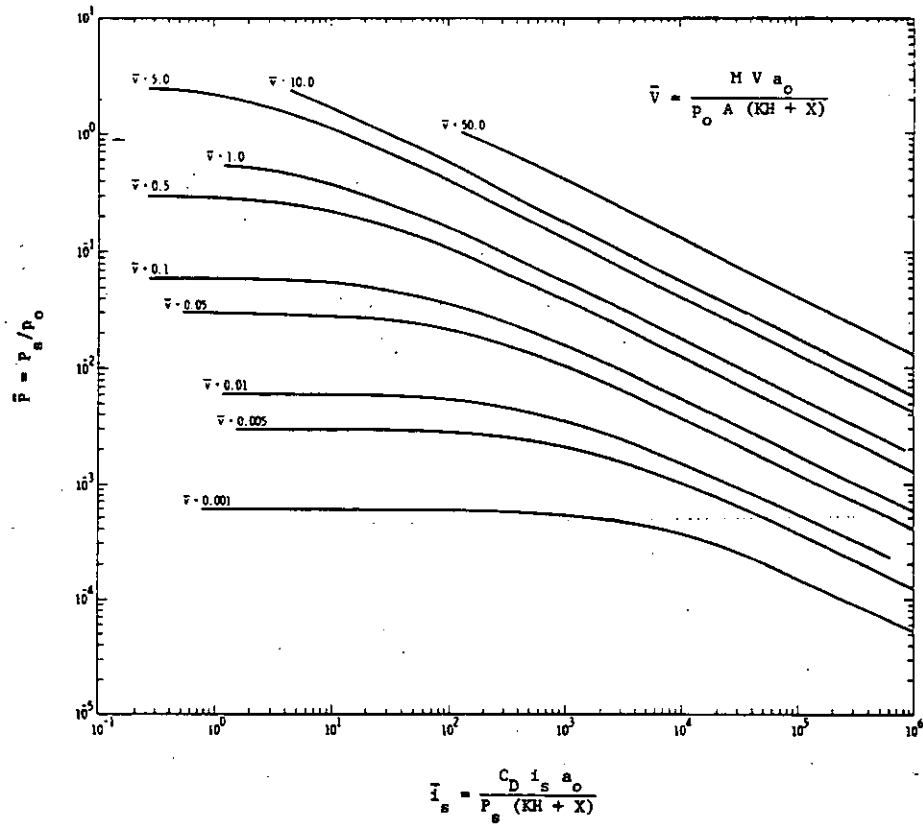


**Figure 2.14: Non-dimensional Object Velocity as a Function of Non-dimensional Pressure and Non-dimensional Impulse**

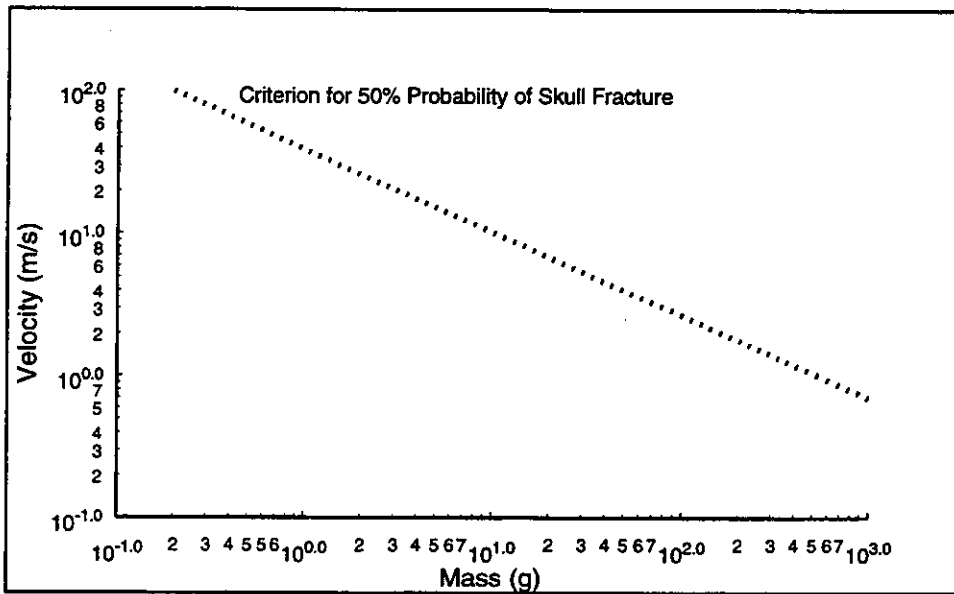


Figure 2.15: Criterion for 50% Probability of Skull Fracture

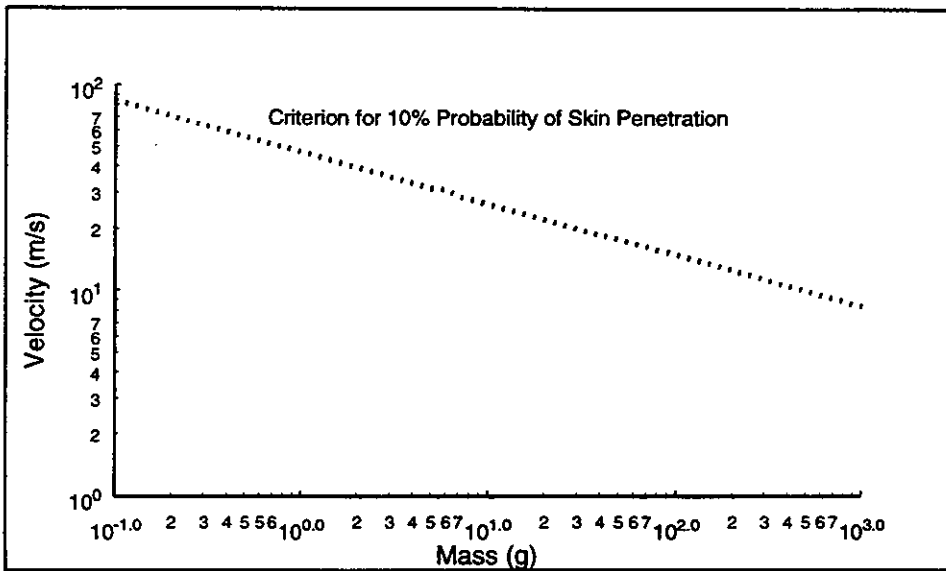


Figure 2.16: Criterion for 10% Probability of Skin Penetration

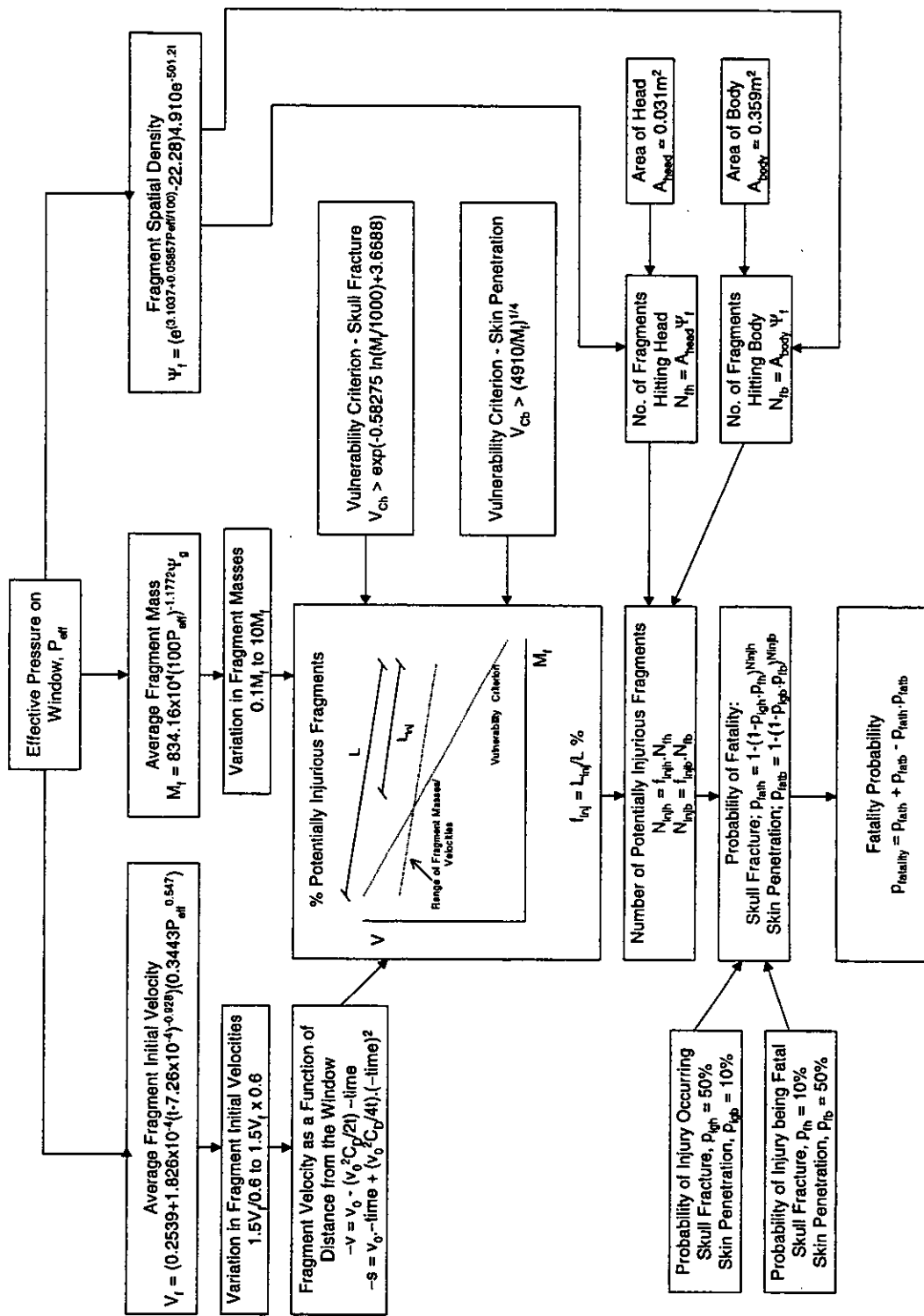
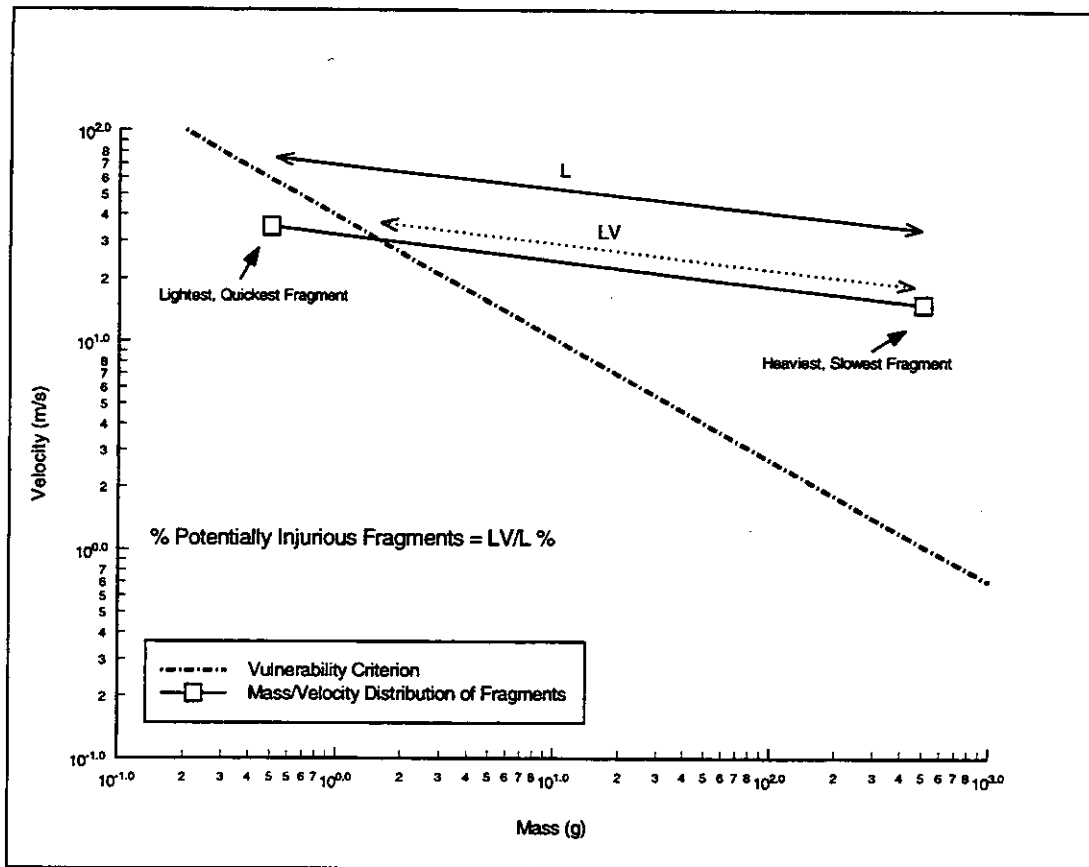
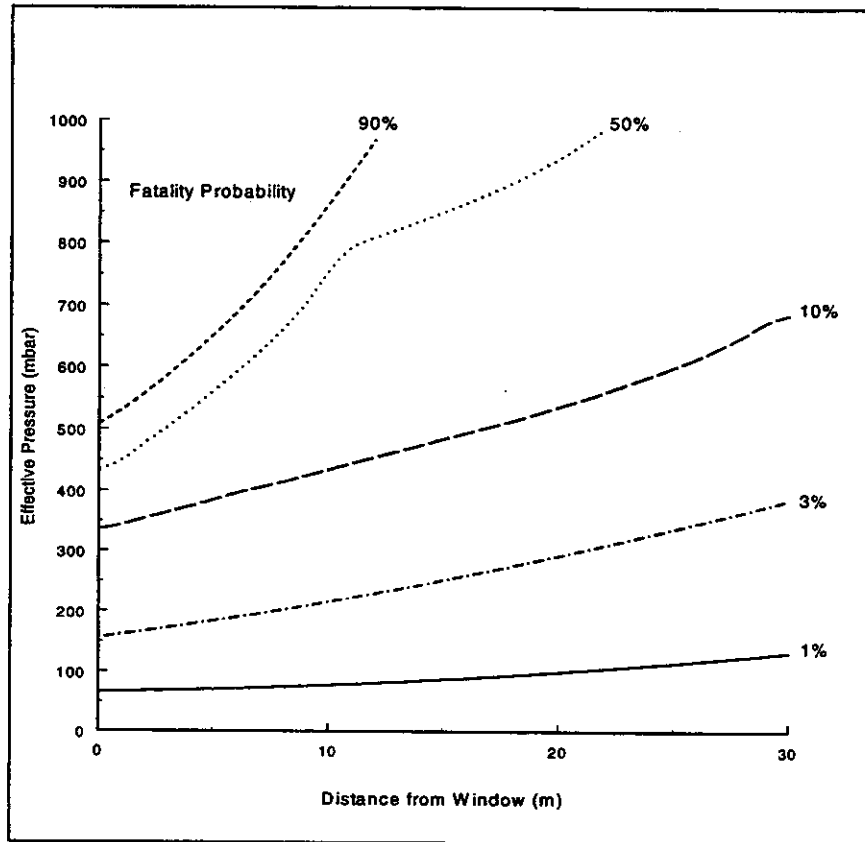


Figure 2.17: Methodology for Calculation of Probability of Fatality due to Glazing Fragment Impact



**Figure 2.18: Calculation of the Percentage of Potentially Injurious Glazing Fragments**



**Figure 2.19: Glazing Fatality Probability Curves**



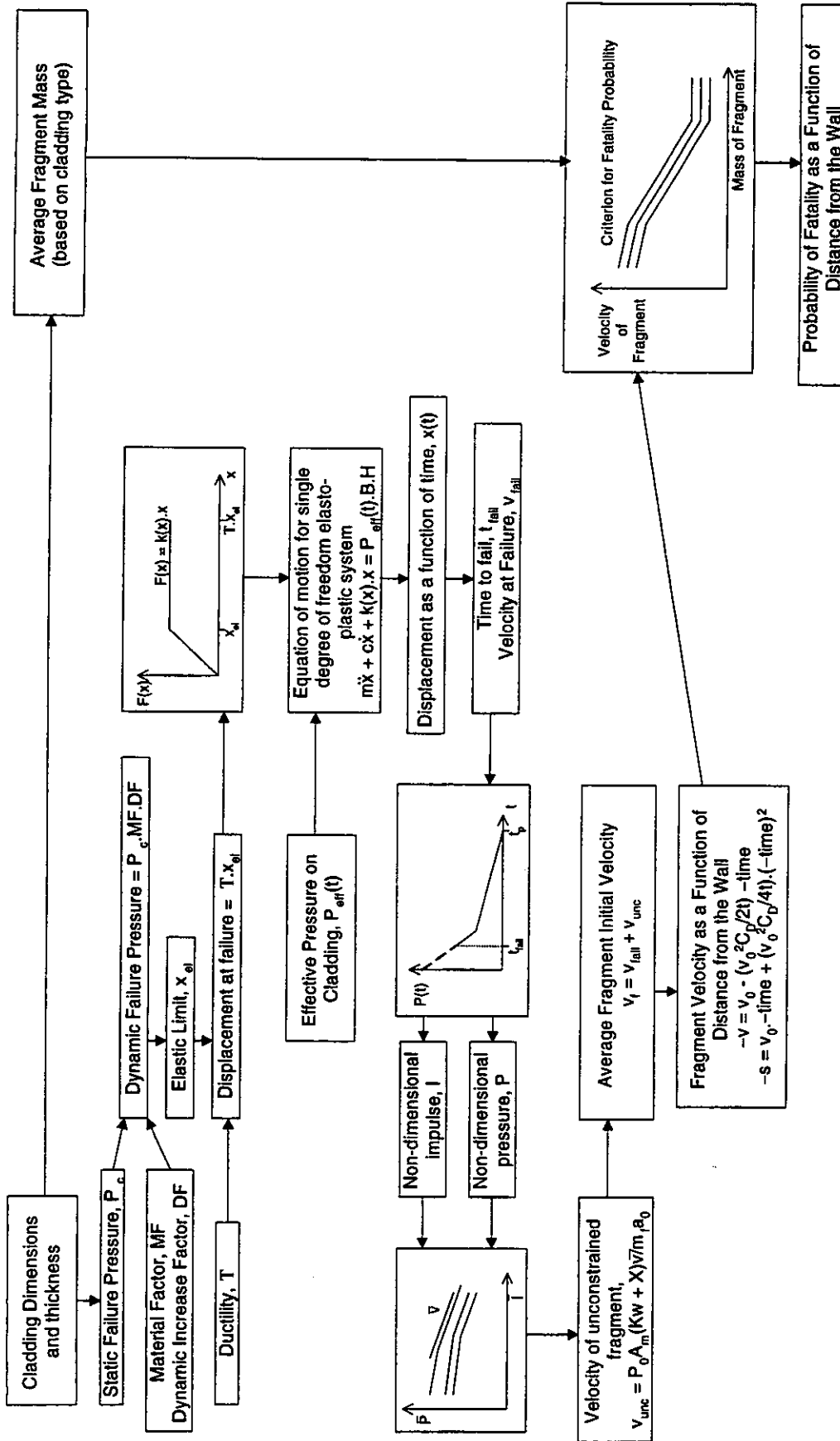
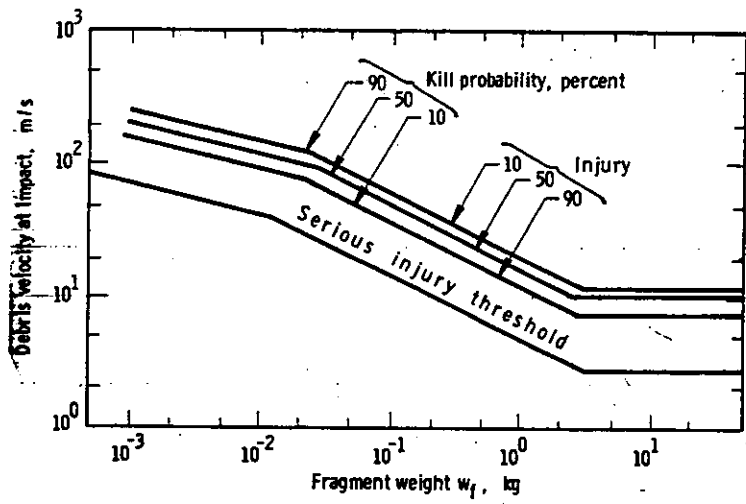
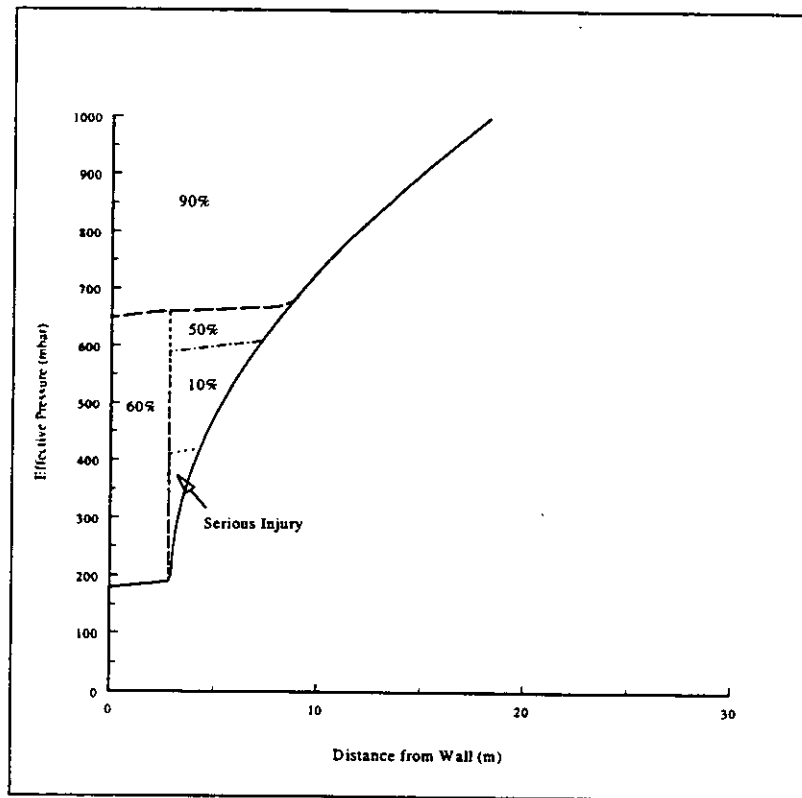


Figure 2.20: Methodology for Calculation of Probability of Fatality due to Cladding Impact



**Figure 2.21: Criterion for Non-Penetrating Fragment Impact**



**Figure 2.22: Brickwork Fatality Probability Curve**

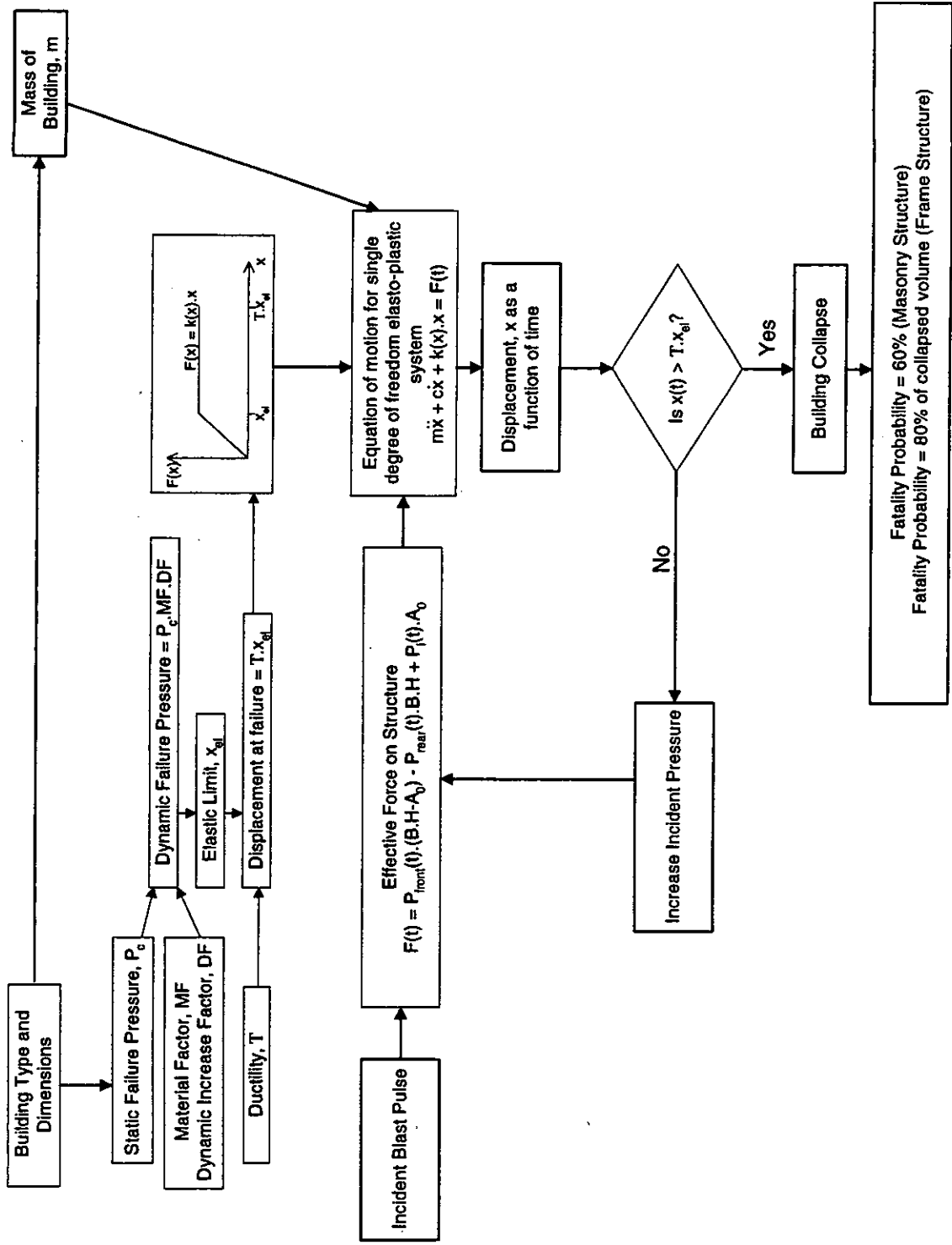
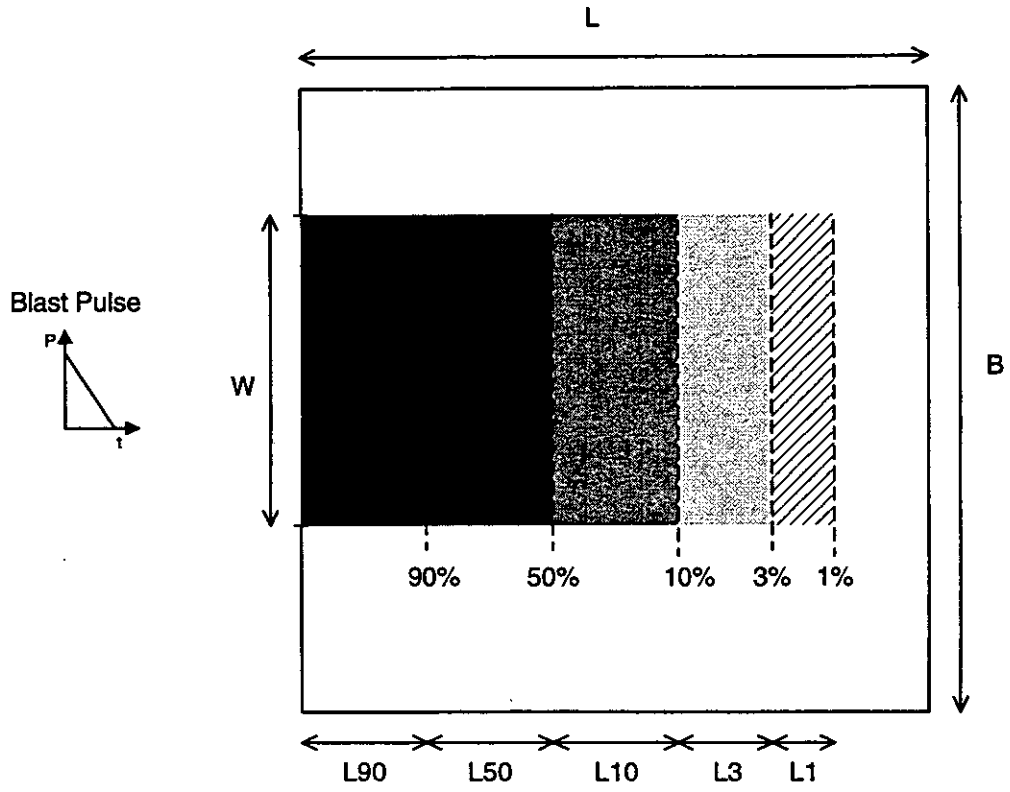


Figure 2.23: Methodology for Calculating the Probability of Fatality due to Building Collapse



**Figure 2.24: Illustration of Glazing Fatality Probability Calculation**

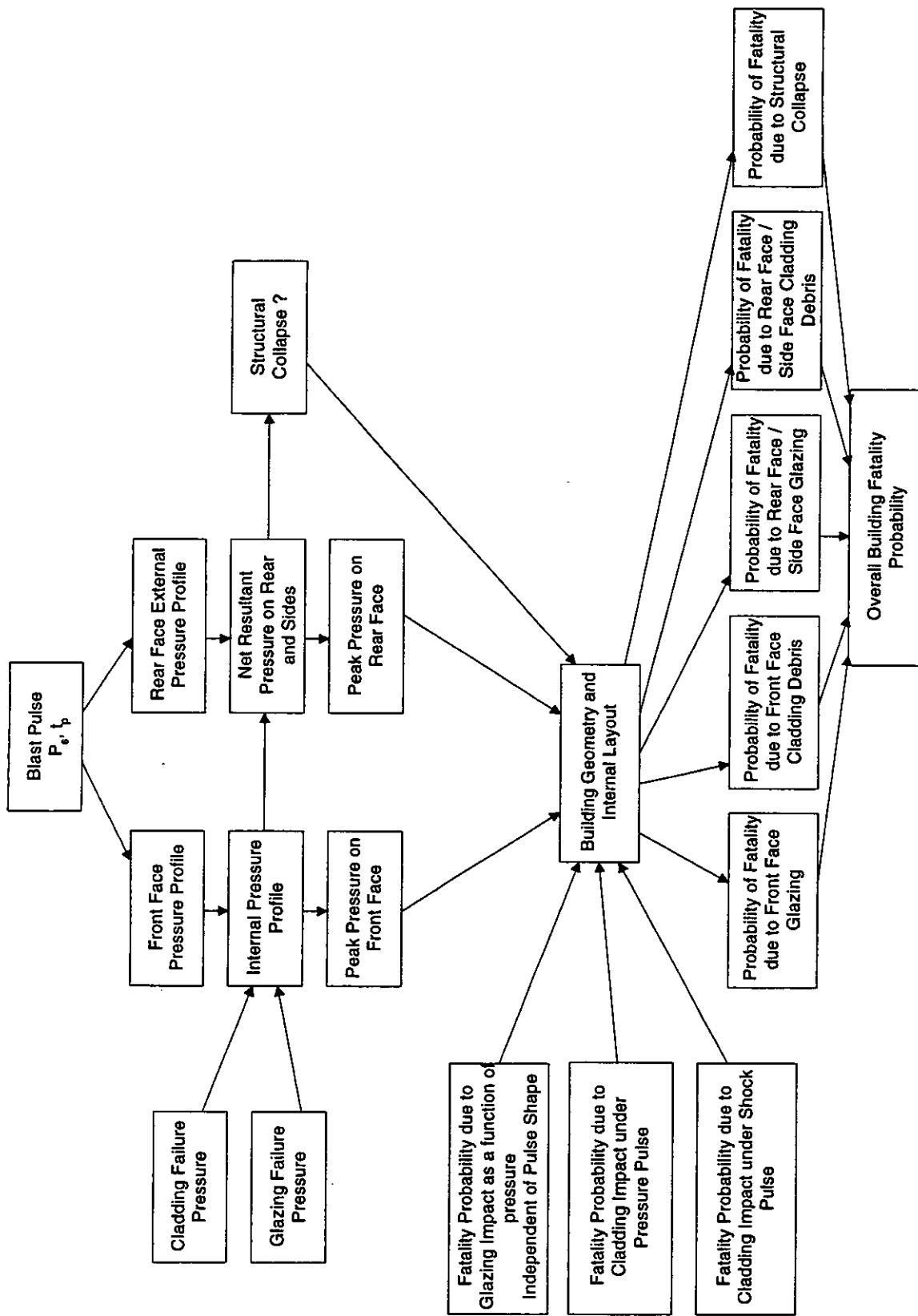


Figure 2.25: Methodology for Global Building Fatality Probability Calculation

B2/2 Shock Pulse 100ms

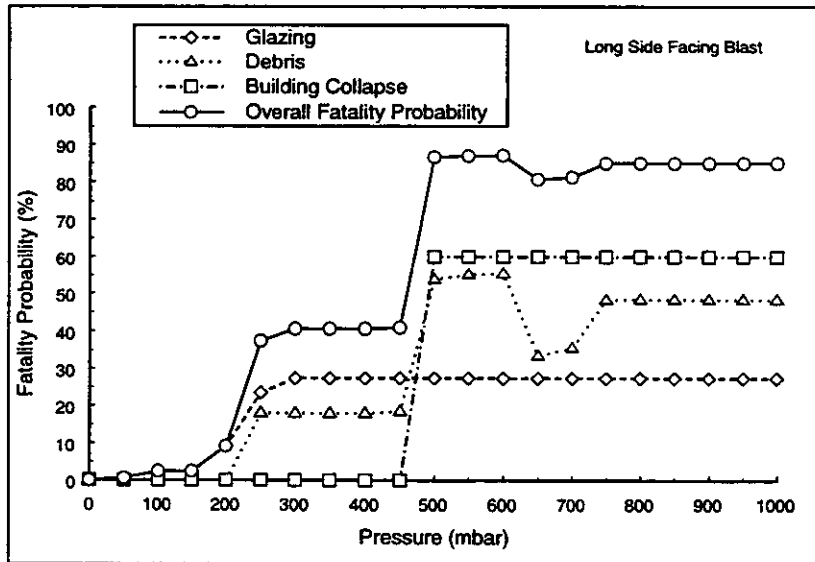
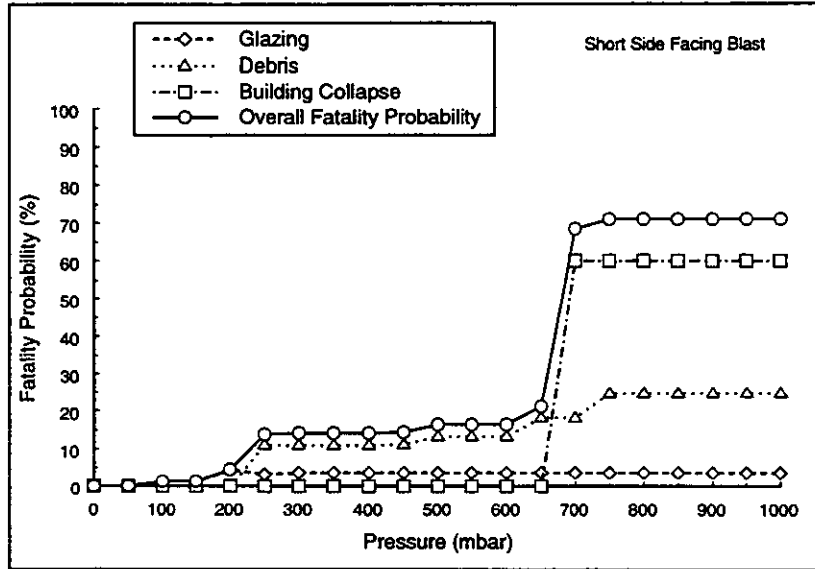


Figure 2.26: Sample Building Fatality Probability Curves

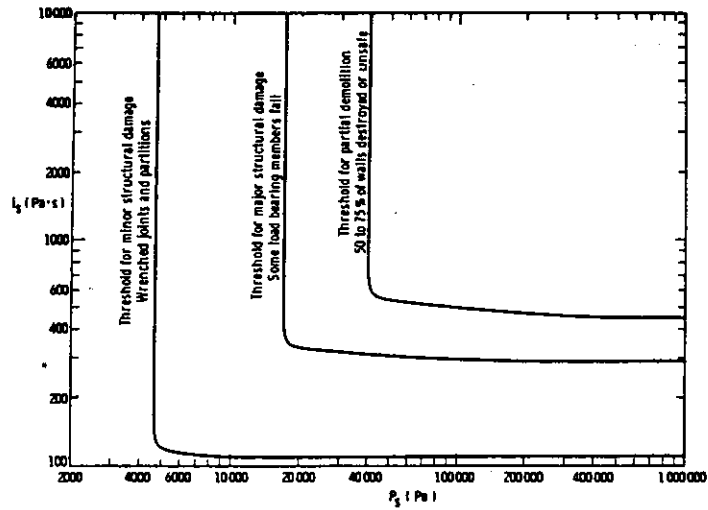


Figure 2.27: P-I Diagrams for Masonry Building Damage

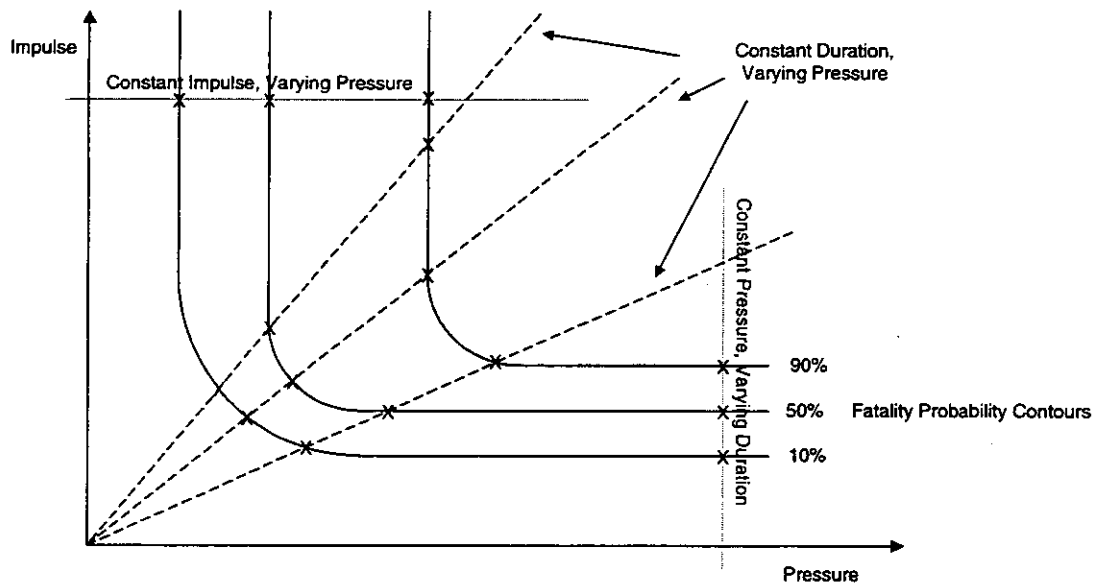


Figure 2.28: Methodology for Deriving P-I Diagrams

### 3. GENERIC BUILDING CALCULATIONS

Seven different categories of buildings have been identified, as outlined in Table 3.1, ranging from temporary Portacabin structures to 20 storey high rise buildings. For each of these generic buildings, structural calculations have been performed in order to assess the failure pressures for the different structural components and the collapse pressures for the overall structure. The calculations have been based on a design calculations using partial safety factors for loads and materials of 1.0, and the results have been compared against historical and experimental data where available in order to ensure that the appropriate values for failure are being used.

Construction characteristics and aspect ratios for the different building types are detailed in Table 3.1, together with maximum and minimum glazing percentages. The quantity of glazing has been shown to be significant in previous calculations, both from the point of view of the actual structural response, and also with respect to occupant vulnerability. The percentages given represent the percentage of the building perimeter which is glazed, based on observation, and the range is assumed to be the feasible range for the different building types. For most of the generic buildings, however, the variation is much more limited than is indicated in the table, and an average representative value has been used.

There are several points to note concerning the general assumptions and limitations of the methodology used to assess the different building types. First, no account has been taken of the internal components of the structure except where applicable as a barrier to travel of debris. The hazards associated with the failure of internal ducting, for example, have not been taken into account. In addition, the results are fairly sensitive to the assumed internal layout: where possible, an internal layout which is fairly open plan has been used in order to ensure that the results are conservative. No account, however, has been taken of a non-uniform distribution of building occupants throughout the building, and it has been assumed that all floor areas have an equal probability of being occupied. This may not be the case for structures such as the tall buildings where the central core of the structure houses services such as lifts, staircases etc., and is unlikely to be significantly occupied at any time. It should also be noted that no account has been taken of surrounding structures in calculating the pressure load on each of the buildings. This could significantly affect the structural loading in a typical urban environment.

The structural characteristics of each of the building types are described in this section, and the results of the calculations, together with detailed descriptions of the building geometries and layouts used in the assessment, are presented separately in Appendix A.

#### 3.1 Building Type B1: Portacabins

Portacabin type buildings are typically used on industrial sites and in schools where temporary accommodation is required. They are usually constructed from a number of factory made modules which can be fixed together side by side or end to end, on site, to form buildings of various shapes and sizes. Typical module dimensions are 2.9m wide with 7.2m, 9.6m or 12.0m internal spans. The modules can be used to form single storey buildings with, typically, 3.0m internal height, or two storey buildings with both ground



and first storey heights of 3.0m. In this study a typical 5.9m by 12.4m single storey (B1/1) and a 12.4m by 14.7m two storey building (B1/2) have been assessed.

Portacabin type buildings in general have a structural steel framework. Hot rolled rectangular hollow section columns are located external to the building envelope at each corner of the module. Cold-formed lipped channel section beams span longitudinally across the module at both roof and floor level. These are bolted to the columns via an angle bracket fully welded into the end of the beam, thus providing a full moment connection. The joists are cold formed channel sections at 407mm centres spanning transversely between the longitudinal beams. At the side to side junction of two modules the columns butt together to form a two column cluster. Similarly where modules are linked end to end (ie double span) the columns from the four adjacent units come together to form a four column cluster.

The floor decking is typically structural board fixed to a steel floor frame using pneumatically fired nails. Walls are usually one-piece sandwich panels, typically of Plastisol coated steel bonded by a rigid polymer core to an internal lining of gypsum board. Similarly, the ceiling/roof panel is a structural one piece insulated sandwich panel. The roof panels are supported below the lipped channel beams using bolts and spacer tubes to create the roof fall. The structural and fire behaviour of this form of construction and its connection to the main steel frame has been extensively researched and tested over the years.

Vertical dead and imposed loads are transferred from the floor decking into the floor beams via the joists and directly from the roof deck panel into the roof beams. The ground floor beams transfer their load directly into the foundations which are usually pad footings or occasionally strip footings. Some moment sharing between the ends of the beam and the columns occurs and this is catered for in the design. The composite first floor beams and the roof beams transfer their load through the moment connections into the columns and from there to the foundations. Wind loads are resisted in the longitudinal direction by the portal frame action of the "rigidly" connected steel beams and columns forming the frame. The frame is stable under the action of full design imposed and wind loads with the roof and first floor (when applicable) acting as diaphragms taking horizontal loads back to the longitudinal walls, thus ensuring the overall stiffness and stability of the building. In the transverse direction, wind loads are resisted by the short walls of the module acting together. For certain arrangements in the double span configuration, additional wind bracing is provided at the intermediate column positions.

The specific details of the examples assessed are given in Section A.1 of Appendix A. The assessment of the portacabins involved a study of the likely failure mode of the wall panels. In reality, experience has shown that the panels are likely to fail at the connections, leaving the frame essentially intact. It is unlikely that all four sides of the panel would fail simultaneously, and hence the panel is more likely to swing than to remain perpendicular to the applied load. In addition it seems likely that the panels would not be able to travel far before being stopped by impacting against obstacles, and also that panels would not fail simultaneously but one or two would fail first possible

relieving the pressure on the remaining panels. There are thus a number of factors which would be expected to reduce the hazard arising from failure of these panels. The method for calculating debris fragment velocities leads to unacceptably high values if a panel the full size of the wall panel is used. An investigation of this effect showed that, for panels up to  $1\text{m}^2$  in size, the velocity is approximately constant; above this size the velocity increases dramatically. This is due to the unconstrained fragment approach which is used to calculate part of the initial velocity based on the frontal area of the fragment. Given that the panel is unlikely to remain perpendicular to the applied blast, and consequently that a smaller proportion of the load will be transmitted directly to the panel, it seems appropriate to reduce the frontal area of the fragment to take this into account. A debris size of  $1\text{m}^2$  was thus used in the fatality probability assessment.

In addition to the standard structural assessment calculations, the pressures required to cause portacabin sliding and overturning were calculated. However, these were deemed not to be a significant fatality mechanism, and were not included in the fatality probability calculations.

### **3.2 Building Type B2: Brick Buildings**

Building type B2 encompasses one of the most important building types from the point of view of this assessment, namely residential housing. The range of possibilities within this type is broad, and there is a wide variation in the possible constructional characteristics. The primary difference between the different types, with the exception of the overall geometrical details, are the type of wall construction, i.e. solid brick or brick/block cavity wall.

Three of the examples of this building type are typical, fairly recent construction examples, where the brick walls form the load-bearing frame of the structure. For two of the three, the walls have been considered to be solid 215mm thick brick walls, with internal load bearing partitions of 100mm blockwork. The remaining example has 280mm thick external cavity walls with a facing brick outer leaf and a 100mm lightweight block inner leaf with cavity insulation. The floor construction for all examples is timber boarding on timber joists, either built into the masonry or supported on twist hangers. The roof construction is typically tiles and battens on timber trussed rafters, supported on wall plates on the front and rear walls, or on the inner leaf of the front and rear walls. It has been assumed that the roof is adequately braced to act as a rigid diaphragm to resist horizontal loads and that the floors and roof are adequately fixed to the masonry with connections capable of providing at least simple resistance to lateral movement.

Building type B2/1 is slightly different from the other three examples of this type, in that it is a single storey structure with a timber frame. Thus for this example, the brick panels do not form the load-bearing frame of the structure. Instead, the cladding cavity wall panels span between the timber frame and the frame is of a modular construction, acting compositely with the external cladding envelope. The roof structure is assumed to be

adequately braced to act as a rigid diaphragm to resist all horizontal loads; all horizontal and vertical loading at roof level is transferred via the frame to the foundations.

The specific details of the examples assessed are given in Section A.2 of Appendix A. As described in Section 2, a fatality probability due to building collapse of 60% has been assumed for these buildings. For all of the brick buildings, except B2/1 which has a timber frame, it has been assumed that, if all the walls fail, the structure has effectively collapsed, and a 60% fatality probability is applicable. For building type B2/1, a 60% fatality probability due to building collapse has been assumed, but as the walls are supported by a timber frame, i.e. the walls themselves do not form the load-bearing frame of the structure, failure of all of the walls does not necessarily imply that the structure has collapsed. In this case, it is necessary for the timber frame to collapse before there is any probability of fatality due to collapse.

### **3.3 Building Type B3: Concrete Framed Buildings**

Concrete framed structures can form the basis of buildings for a wide range of uses, but are typically used for office or commercial purposes. It has been assumed that the buildings assessed in this section are in fact office buildings, with fairly open plan interior layouts.

Two types of frame have been considered. The first is a moment resisting frame. The columns are designed to transfer all horizontal and vertical loading to the foundations in accordance with BS8110 [37]. The floors are likewise designed as monolithic beam and slab construction with solid slabs spanning one way and supported on secondary beams which in turn are carried by main beams framing into the columns. Two types of wall construction have been considered, brick/block and concrete panels, but they are similar in that continuous glazing is assumed, with the wall panels spanning horizontally above and below the glazing between the columns.

The second frame type is a 4 storey braced frame, with similar floor and column design. The primary difference is that the external wind loading in the transverse direction is resisted by end shear walls, while in the longitudinal direction, resistance is provided by shear panels in the end bays together with the staircases. This has implications for the collapse pressures calculated for these structures, and means that global collapse is unlikely. In addition, for B3/3 the wall panels have been assumed to be simply supported brick/block panels with openings for the glazing. For B3/4, the concrete wall panels are assumed to span vertically between the floors, again with openings for the glazing.

The specific details of the examples assessed are given in Section A.3 of Appendix A.

### **3.4 Building Type B4: Steel Framed Buildings**

Steel framed buildings encompass a wide range of building types, from small office developments, to hypermarkets and factory buildings. In order to satisfy this range of potential uses the possible construction characteristics of the buildings are quite varied. The common factor for building type B4 is a load bearing steel frame, the size and shape of which may be varied to generate the single, two and four storey buildings considered.

The other characteristics differentiating the possible building types are the amount of glazing and the type of wall construction.

Three generic building geometries have been analysed, single and two storey buildings, with aspect ratios of 5:1, and a four storey building of length twice its breadth. The single storey buildings have the simplest construction, B4/1 using a single bay moment resisting frame, and B4/2 double bay braced frames, spaced at 5m intervals along the length of the building. The cladding is assumed to be 0.6mm thick corrugated steel sheeting, attached to rails running between the frames. B4/2 has only a single area of double glazing on the short side of the building, while B4/1 has no glazing at all. For both B4/1 and B4/2, failure of the cladding is assumed to occur at the failure pressure of the supporting sheeting rails. This takes into account the fact that failure is most likely to occur at the panel connections rather than as a brittle failure of the panel itself, and that connection failure is likely to occur as the sheeting rails deform. However, this leads to unrealistically high velocities if the initial fragment velocity plus the velocity of an unconstrained fragment are both included. As for the portacabin wall panels, there are two factors which may mitigate the effect of the blast load. Firstly, it is unlikely that all four sides of the panels will fail at once, and consequently it is unlikely that the panel will travel perpendicular to the blast load. In addition, it is unlikely that all panels will fail at the same time, and hence there may well be some form of pressure relief on the majority of the panels arising from the initial failure of one or two panels. Consequently it has been assumed that the load on the panel does not include a significant portion of the blast load once the cladding has failed. This ensures that the velocities achieved are reasonable. This is one area of the methodology which would be worthy of further investigation.

Buildings B4/3 - B4/6 represent a small office development. The steel structure in each case has a load bearing slab at ground level which carries the weight of the steel structure and the precast concrete floors suspended below the cross beams. The frames are spaced at 4.0m intervals along the length of the buildings, and have the appropriate bracing and load bearing beams between them. Lateral stability is provided by a combination of the floor slab diaphragm action and the staircase blocks. The staircase blocks are enclosed in 225mm of brick or blockwork, and placed at either the two rear corners of the four storey buildings, or are evenly spaced along the rear wall of the two storey structure. The roof of the two storey building is a sloped tiled roof, supported by timber rafters spanning between steel purlins, which transfer the load to the steel columns. A flat roof, made of asphalt on lightweight screed laid to falls on precast concrete units, is assumed for the generic four storey building.

The typical window pattern for the office style buildings is continuous double glazing, 1.5m high on all external walls, except within the staircase blocks, on every floor. Above and below the windows is the cladding, of which two types were considered for each building geometry. Buildings B4/3 and B4/5 have brick/block cavity walls, 280mm thick, which are made up of standard bricks on the external face and less dense internal blocks, with an insulating gap between them. B4/4 and B4/6 have 180mm thick precast concrete panels as cladding. Failure of the brick/block cavity wall was modelled by representing the section of wall on each floor between portals as a panel simply

supported along all four edges, whereas the concrete panels were represented by horizontal simply supported beams, 1.5m high and 4.0m long, the largest area of concrete either side of the windows. The debris assumed to be generated by failure of these two cladding types were standard clay bricks and 125 x 250 x 40mm fragments of concrete respectively.

The specific details of the examples assessed are given in Section A.4 of Appendix A.

### 3.5 Building Type B5: Hardened Structure

Hardened structures are typically used on-site as control buildings for chemical or oil industry process plants. Consequently, they are usually designed to Chemical Industries Association guidelines or compatible procedures established by the interested parties. According to such guidelines, for the maximum release considered, i.e. in excess of 15 tonnes flammable material, the basis for the design is that the control building will survive one incident arising from an explosion which is at or near ground level [28].

The CIA guidelines specify that a control building should be designed to withstand the following blast pressures:

- I Peak overpressure =  $70\text{kN/m}^2$  duration 20ms (+ve), zero rise time
- II Peak overpressure =  $20\text{kN/m}^2$  duration 100ms (+ve), rise time equal to half the pulse duration

In addition, the structure should be checked for adequate resistance to a peak incident overpressure of  $100\text{kN/m}^2$  with a positive phase blast duration of 30 msec and zero rise time.

The structural characteristics of a hardened structure or control building are typically as follows:

- They are single storey framed structures with the frame supporting the roof independently of the side wall cladding.
- The column layout results in a 1:1 or 2:1 aspect ratio
- The typical construction is a reinforced concrete roof with structural steel braced or moment resisting load bearing framework and reinforced concrete wall cladding.
- The roof may typically be a 150mm thick or greater RC slab on permanent steel shuttering. The ground slab is ground bearing and the frame is carried on pad foundations or piles dependent on the ground conditions.
- The precast reinforced concrete cladding panels are typically between 150mm and 225mm thick and are retained at the base by a deep chase in the foundation slab (or ground beam) and at the head by bolting the precast unit to the in-situ roof slab. As

the cladding panels span from top to bottom of the building, load is transferred into the frame at ground and at roof level.

- There are usually no windows in these buildings.

The specific details of the example assessed are given in Section A.5 of Appendix A. The example generally conforms with the above typical details in that there is no glazing and the concrete panels span vertically between the foundation slab and roof slab. The fatality probabilities arising from the interaction of this structure with the blast have been found to be primarily due to structural collapse: few fatalities are expected up to a relatively high pressure, but once the structure collapses, the fatality probability is expected to be high.

In addition to the risk to the building occupants, if such a structure is used as a control building on an industrial site, it is of interest to estimate the effects of the blast on equipment within the building. Failure of this equipment could potentially affect the ability to control the plant safely in the event of an explosion; this could lead to an increase of the risks both on- and off-site. The way in which the structure responds to a blast indicates that the greatest levels of acceleration are experienced in the wall panels, particularly in the wall facing the blast. Equipment located on the floor of the structure or attached to the structural frame is less likely to be subjected to a high level of acceleration, as the building as a whole has a greater inertia to be overcome by the blast load than the individual wall panels. The levels of acceleration in the walls are potentially high enough to cause some damage to equipment situated on the walls unless that equipment is sufficiently well shock-mounted. The level of shock-mounting required is dependent on the nature of the equipment and the design blast loads.

### **3.6 Building Type T: Tall Buildings**

A change in the structural design of tall buildings has occurred in the last 15 to 20 years, mainly in the way the structural framing is strengthened to resist predominantly the lateral loading. In effect the design has changed from using moment-resisting frames to using flexible frames with stiff shear resisting walls. The result is a generic type of shear wall buildings which are commonly of 10 to 30 storeys. In general their structural behaviour is influenced by the shape and plan position of the shear walls present.

In this assessment, three aspect ratios are considered assuming a shear wall building frame of up to 20 storeys.

The plan distribution of shear walls is such that the building is torsionally, as well as flexurally stiff. In rectangular plan buildings, shear walls are often placed at the extremities of the building in order to resist load on the wider face of the building. In the other orthogonal direction, frame action is utilised.

Monolithic shear walls are usually classified as short, squat or cantilever according to their height to depth ratio. The walls are either planar, flanged or core in shape. In many cases, the walls are pierced by openings and therefore the behaviour of the individual

wall section is coupled to a degree, depending on the wall section and the connecting beams. Shear cores usually comprise channel sections coupled by beams or slabs.

Wind resisting cores rather than pierced shear walls are usually preferred internally within buildings. Office buildings often comprise a single central service core surrounded by a flexible frame. Different configurations of shear and core walls are illustrated in Figure 3.1. In this assessment the buildings under consideration are assumed to have this central core type of configuration. It has also been assumed that overall instability of the building due to shear wall failure is unlikely for the off-site pressures under consideration.

The specific details of the examples assessed are given in Section A.6 of Appendix A. It has been assumed that, within the central core of the building, there is no hazard from glazing or debris. However, it should be noted that the central core usually contains services such as lifts, staircases etc., and it is unlikely that many people will be in the central core at the time of an explosion, unless prior warning has been received. In this case, the assumption of uniform occupancy over the entire floor area of the building may not be strictly applicable. It has also been assumed that local collapse of the flexible frame is not likely to give rise a significant risk of fatality. This is primarily because the floor slabs will be supported both by the frame and at the central core, and damage to the central core would probably have to be sustained before the slabs would collapse. While this assumption perhaps loses some of the conservatism inherent in the model, it should be noted that, if it is assumed that local collapse leads to fatality on the basis of 80% of the collapsed area, this implies that the entire height of the building is involved in that local collapse. Historical evidence has tended to suggest that this is not the case, and that local collapse does not extend over more than a few floors of the building, provided that the building has been adequately designed. Consequently an assumption of this nature would be highly over-conservative.

### **3.7 Building Type L: Long Span Buildings**

The long span structures considered here are assumed to be used where it is important to have a large uninterrupted covered space. Typical examples include supermarkets and sports halls/swimming pools. Consequently the internal layout of the building tends to be very much open plan. They are steel framed structures, and both examples used here are assumed to be steel clad, with steel insulated panels on purlins or side sheeting rails.

The first example, building L/1, is assumed to have 30m span steel portal frames spaced at 6.0m centres. The structural calculations have assumed that the structure has been designed plastically in accordance with BS 5950 [38], and that member sizes have been optimised for economy. The portal frame is assumed to be haunched at the eaves of the frame, and plastic hinges are assumed to occur at the bottom of the eaves haunch in the leg and at the first or second purlin point below the ridge in the rafter at failure. The rafter portion of the haunch remains elastic.

The second example is assumed to have a 20m span. The frames consist of columns pinned at the top and fixed at the base support, spaced at 5.0m centres. Stability is

provided by the column fixity at the base and by bracing in both directions (simple stanchion and truss frame).

For both of these examples, as for the two steel-clad steel framed buildings, B4/1 and B4/2, failure of the cladding is assumed to occur at the failure pressure of the supporting structure, taking into account the fact that failure is most likely to occur at the panel connections rather than as a brittle failure of the panel itself, and that connection failure is likely to occur as the sheeting rails deform. However, as described in Section 3.4, this leads to unrealistically high velocities if the action of the blast pulse after failure is also taken into account and it has again been assumed that the time to fail is sufficiently long that the blast pulse plays no effect once the cladding has failed.

The specific details of the examples assessed are given in Section A.7 of Appendix A.

### **3.8 P-I Diagrams - Guidance for Use**

The results of the studies are presented in Appendix A in the form of Pressure-Impulse (P-I) diagrams for the different buildings. Results are presented for two different orientations of the buildings and two different pulse shapes. In order to create these plots, 5 different runs for each of the buildings have been performed, with the following variations:

- Constant pulse duration (100msec), varying peak incident overpressure
- Constant pulse duration (300msec), varying peak incident overpressure
- Constant pulse duration (10msec), varying peak incident overpressure
- Constant peak incident overpressure (1000mbar), varying pulse duration
- Constant impulse, varying peak incident overpressure and pulse duration

Each of these runs gives rise to a set of points on the P-I diagram corresponding to 1%, 10%, 50% and 90% fatality probability. Bounding curves have been plotted through the points to represent the lines of constant fatality probability for each particular building orientation and pulse shape. These curves have been drawn around the outermost data points (i.e. those closest to the origin) for a given level of fatality, and are therefore conservative.

As can be seen from the plots, there is a some degree of scatter in the points which makes plotting the contours a matter of some judgement. One major source of scatter is the variations in response of the structure under different pulse durations, which can give rise to different levels of hazard to the building occupants. For example, if the pulse duration is very short, the internal pressure rise may be negligible, which means that all the glazing and/or cladding will be blown into the building presenting a risk to the occupants. By comparison, for a longer duration pulse, the internal pressure rise may be significant leading to relief of the load on the rear face and sides of the structure and



possibly even causing the glazing and or cladding to be blown out of the structure, presenting no hazard to the building occupants.

In addition to the structural response aspects of the model, there are also numerical aspects of the model which may lead to scatter in the results. In particular, the failure pressure of the glazing is based on the method given in Mainstone [4] which gives a dependence of the failure pressure on pulse duration equivalent to a factor of  $\sim 1.5$  for a pulse duration of 10msec when compared with the failure pressure under 1 sec pulse duration i.e. if the failure pressure for a pulse duration of 1 sec is 65mbar, the corresponding failure pressure under 10msec would be 97.5mbar. Data for this approach are only available for pulse durations greater than 10msec, so if the pulse duration is shorter than this, the curve has to be extrapolated. For the constant pressure case used here i.e. a constant pressure of 1000mbar, with a varying pulse duration, the extrapolation indicates that the glazing fails for all of the pulse durations used, and consequently there is always a finite probability of fatality. In addition the glazing mass and velocity curves used in this assessment are dependent only on peak overpressure and do not take into account the pulse duration. For some of the buildings, the calculated fatality probability for the shortest pulse duration used is in excess of 1%, in which case the point representing 1% on the P-I diagram is calculated based on an extrapolation of the results. While this extrapolation seems to lead to sensible results in the majority of cases, this is one area where additional experimental data might lead to a refinement of the approach.

The curves plotted through the data points for 1, 10, 50% etc. have been fitted in such a way that they bound the calculated points. This is a conservative approach. For the majority of the buildings, the curves are fairly well spaced, but for some of the examples, one or more of the lines are quite close together. The spacing of the lines indicates the rate of rise of fatality probability with increased loading: for closely spaced lines the rate of rise is high, whereas for widely spaced lines the rate of rise is slower. As an example of this, the closeness of the curves for the control building B5/1, indicate that a fairly high rate of increase of fatality probability is expected. This is in line with the expected behaviour of the control building; fatalities are low until the building collapses, at which point a very high level of fatality is to be expected. In areas where the curves are close together, care must be taken when using the P-I diagrams to assess fatality probabilities; it would be necessary, in these areas, to perform a more accurate assessment of the specific building details in order to assess the fatality probability.

It is important to note that although curves for an incident pressure pulse have been calculated, for the majority of distances from the source of a blast, the pulse shape shows some degree of 'shocking up'. In this case, there may be reflection at the front face of the building, increasing the front face load. In the work performed here, it has been assumed that no reflection occurs for an incident pressure pulse, and hence if the incident pulse is partially shocked it would not necessarily be conservative to use the P-I diagrams for an incident pressure pulse to predict the fatality probability. It may be over-conservative to use the diagrams for an incident shock pulse, but this would be a better approach. The characterisation of the partially shocked pulse with distance from a blast,

and its interaction with a structure, is a problem which, at the time of writing, has not been assessed to a level which can be incorporated into this methodology.

The variability in the results for the different building orientations, and for the different buildings within a generic type, mean that it is not valid to combine the curves for each generic building type. As an example, Figures 3.2 to 3.9 show the 1% fatality probability curves for the portacabins (B1), brick buildings (B2), concrete framed buildings (B3) and steel framed buildings (B4), subject to an incident shock pulse and pressure pulse respectively. As can be seen, there is a significant amount of variation between the different buildings and the different building orientations. If the 10% lines were to be plotted on the same graphs, there would be a considerable amount of overlap between the 1% and 10% fatality probabilities for the different examples. Since there is such a variation, it is not felt to be appropriate to try to derive a single set of curves for each generic building type.

Also for comparison purposes, the curves for 1% fatality probability for one example of each of the generic building types have been plotted on Figures 3.10 and 3.11. It should be stressed that this is just for illustrative purposes and it is not suggested that the examples chosen are particularly representative of their type. Indeed, the examples chosen are those which seem to exhibit 1% fatality probability at the lowest pressures, namely B1/1, B2/2, B3/1 and B4/3. The control building, B5/1 has also been included for comparison. The figures serve to illustrate that the variation between the different building types is similar to the variation between different buildings within a generic type. Buildings which are similar in dimensions, glazing characteristics and internal layout may exhibit similar fatality probabilities even if technically they belong to different generic types. This reinforces the suggestion that it may not be appropriate to try and derive a single set of fatality probability curves for each generic type using this methodology.

It is important to note that the internal layout of the building can affect the derived fatality probabilities significantly, and may lead to different results for buildings which have similar external dimensions and construction details. As an example, building type B1/2 (portacabin) shows quite different results for the two different orientations owing to the presence of internal walls which are assumed to stop the travel of glass and debris. This dependency is largely due to the high glazing and cladding velocities at failure predicted using this methodology which are contrary to the commonly held 'safe breaking pressure' concept. These high velocities imply that the range for glazing and cladding is very important, and hence that the internal layout of the building is important, but this may be an artefact of the velocity profiles used. It would thus be extremely unwise to attempt to use these curves to predict fatality probabilities for any building which is significantly different from the examples studied.

However, the P-I diagrams do represent a conservative assessment of the specific building geometries selected within each generic group, and could potentially be used to assess the fatality probabilities for structures which correspond closely to the overall layout and construction characteristics of one of these typical buildings. It is anticipated that the curves could be used as a first approach to identify whether or not a specific

building in a specific location may be unsafe. For the reasons noted above, buildings which do not correspond closely with one of those given in Appendix A would have to be assessed individually, using the methodology described in Section 2.

It is envisaged that the methodology and the curves produced would normally be used within the context of a study of the risks to the building occupants. This would therefore encompass a consideration of the magnitude of any explosion that could occur and the likelihood of such an explosion occurring in addition to estimating the fatality probability for the building occupants. In the case of studies examining the location of buildings on a site handling materials which could give rise to a VCE, guidance has been produced by the American Institute of Chemical Engineers Center for Chemical Process Safety (CCPS) [30]. The methodology presented in this report could be used within the framework described by CCPS for carrying out studies of this type. In the UK, the Chemical Industries Association are in the process of preparing similar guidance [31].

It is not expected that the methodology should be used as a design tool. The methodology is based largely on engineering judgement concerning the way in which given buildings are expected to behave. It uses a simple representation of the structure which cannot be expected to replace a more detailed structural assessment of a building design. However, given a building design, the methodology could be used to calculate a conservative estimate of the risks to the building occupants, as outlined above.

### **3.9 Conclusions**

Appendix A includes more detailed descriptions and illustrations of all of the building types assessed, together with P-I diagrams showing the fatality probabilities for the different buildings for the two different orientations and subject to both a shock load and a pressure pulse load. A comparison of the results shows that similar buildings show similar properties, governed more by the overall geometry of the building and the internal layout than the specific details of glazing and cladding failure pressures. The dependency on the internal layout is in part due to the very high velocity profiles for the glazing and cladding which are predicted on failure, and which imply that as soon as the glazing or cladding has failed a quantity of it travels a significant distance into the room. Further refinement of the models for glazing and cladding failure may reduce this dependency and render the internal layout less important.

With the exception of the control building B5/1, the behaviour of all of the buildings in this assessment is dominated by the assumed internal layout, with lowest fatality probabilities achieved in the buildings which have the greatest internal area inaccessible from the outer surface of the building. The tall buildings in particular illustrate this, with the central core assumed impregnable to debris but forming a reasonably large proportion of the internal area, leading to fairly low fatality probabilities due to glazing. However, this does not take into account the fact that the occupancy of the central core is likely to be lower than the rest of the building as it houses essential building services such as lifts and staircases. This sensitivity to the internal layout means that it is not possible to draw any conclusions from this study concerning which generic type of building is the safest from the point of view of an incident blast. It is possible, however, to assess specific

buildings using the methodology given, and in this manner to make a judgement concerning the relative merits of different specific buildings.

The variability in the results and dependency on the internal layout means that it would be extremely unwise to attempt to use the P-I diagrams given to predict fatality probabilities for a building which is significantly different from the examples given. Buildings which do not correspond closely to the examples would have to be assessed individually, using the methodology outlined in Section 2.

Building type	Building use	No. of storeys	Aspect ratio	Frame type	Floor construction (elevated)	Roof construction	Wall construction	Glazing type	Glazing Percentage	Page Reference Appendix A
Portacabin (B1)	SC/TE/FBE	1	2:1	Timber/steel	-	Timber	Timber panels	Single	40 - 80%	A.2 - A.8
	SC/TE/FBE	2	1:1	Timber/steel	Timber	Timber	Timber panels	Single	40 - 80%	A.9 - A.14
Brick Built (B2)	RH/SC	1	2:1	Timber/steel	-	Timber	Brick/block	Single	50 - 80%	A.15 - A.21
	RH/SC	2	2:1	Brick/block	Timber	Timber	Brick/block	Single	50 - 80%	A.22 - A.27
	RH/SC	3	2:1	Brick/block	Timber	Timber	Brick/block	Single	50 - 80%	A.28 - A.33
	RH/SC/HO/RF	3	3:1	Brick/block	Concrete	Timber	Brick/block	Double	50 - 80%	A.34 - A.39
Concrete frame (B3)	RF/RH/HO/SC/CO	2	4:1	MRF	Concrete	Concrete	Brick/block	Double	25 - 90%	A.40 - A.46
	RF/RH/HO/SC/CO	2	4:1	MRF	Concrete	Concrete	Concrete panels	Double	25 - 90%	A.41 A.47 - A.51
	RF/HO/CO	4	4:1	Braced frame	Concrete	Concrete	Brick/block	Double	25 - 90%	A.52 - A.57
	RF/HO/CO	4	4:1	Braced frame	Concrete	Concrete	Concrete Panels	Double	25 - 90%	A.58 - A.63

**BUILDING USE CODE**

RH: Residential Housing

RF: Residential

SC: School

CO:

CI:

LB:

Commercial/Office

Commercial/Industrial

Leisure Building

FBO:

FBN:

TE:

Factory Building Old

Factory Building New

Temporary Building

HO:

RE:

FBE:

Hospital

Retail/Hypermarket

Factory Building Ext

**Table 3.1: Generic building types**

Building type	Building use	No. of storeys	Aspect ratio	Frame type	Floor construction (elevated)	Roof construction	Wall construction	Glazing type	Glazing Percentage	Page Reference Appendix A
Steel frame (B4)	C/RE/LB/FBN	1	5:1	MRF	-	Clad	Clad	Double	10 - 90%	A.64 - A.70
	C/RE/LB/FBN	1	5:1	Braced	-	Clad	Clad	Double	10 - 90%	A.71 - A.76
	CO/CJ/RE/LB	2	5:1	Braced	PC units	Tiles	Brick/block	Double	10 - 90%	A.77 - A.82
	CO/CJ/RE/LB	2	5:1	Braced	PC units	Clad	Concrete panels	Double	10 - 90%	A.77 A.83 - A.87
	CO	4	2:1	Braced	PC units	PC units	Brick/block	Double	50 - 90%	A.88 - A.93
	CO	4	2:1	Braced	PC units	PC units	Concrete panels	Double	50 - 90%	A.88 A.94 - A.98
Special hardened structure (B5)	CI	1	2:1	Braced steel	Concrete	Concrete	Concrete panels	None	0%	A.99 - A.105
Special: Tall building (T)	RF/CO	5-20	1:1	Coupled shear walls	Concrete	Concrete	Concrete panels	Double	40 - 90%	A.106 - A.112
	RF/CO	5-20	2:1	Coupled shear walls	Concrete	Concrete	Concrete panels	Double	40 - 90%	A.113 - A.118
	CO	5-20	3:1	Coupled shear walls	Concrete	Concrete	Curtain walling	Double	90%	A.119 - A.124
Special long span (L)	LB	1	2:1	Braced steel	-	Clad	Clad	Double	10 - 90%	A.125 - A.131
	LB	1	3:1	Braced steel	-	Clad	Clad	Double	10 - 90%	A.132 - A.137

**BUILDING USE CODE**

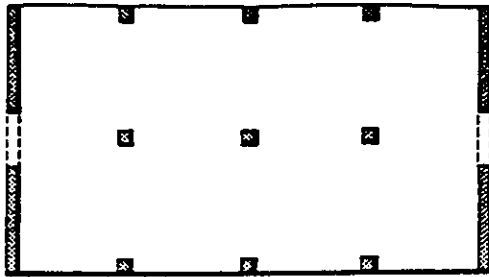
RH: Residential Housing  
RF: Residential  
SC: School

CO: Commercial/Office  
CI: Commercial/Industrial  
LB: Leisure Building

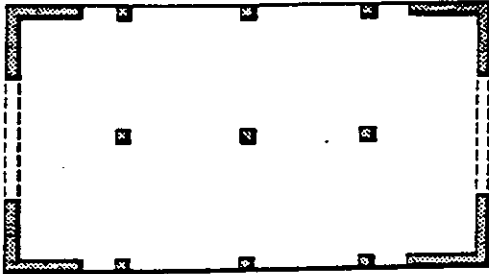
FBO: Factory Building Old  
FBN: Factory Building New  
TE: Temporary Building

HO: Hospital  
RE: Retail/Hypermarket  
FBE: Factory Building Ext

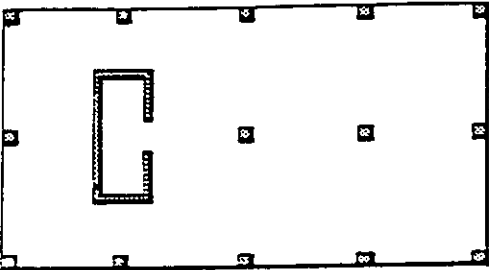
**Table 3.1: Generic building types**



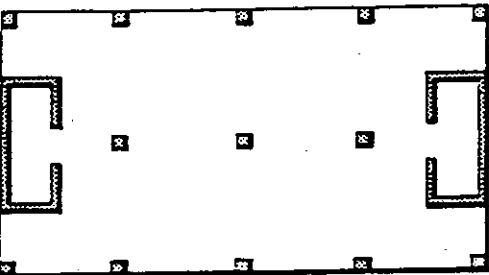
(i) Walls resist bending in one plane. Frame action in other plane.  
Good torsional stiffness.



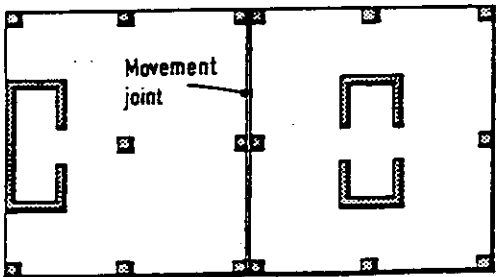
(ii) Walls resist bending in both planes.  
Good torsional stiffness.



(iii) Core resists bending in both planes. Poor torsional behaviour due to eccentricity.



(iv) Cores resist bending in both planes.  
Good torsional stiffness.



(v) Cores resist bending on each section of the building independently. Relative shear displacement at movement joint.

**Figure 3.1: Possible Configurations for Core/Shear Walls in Tall Buildings**

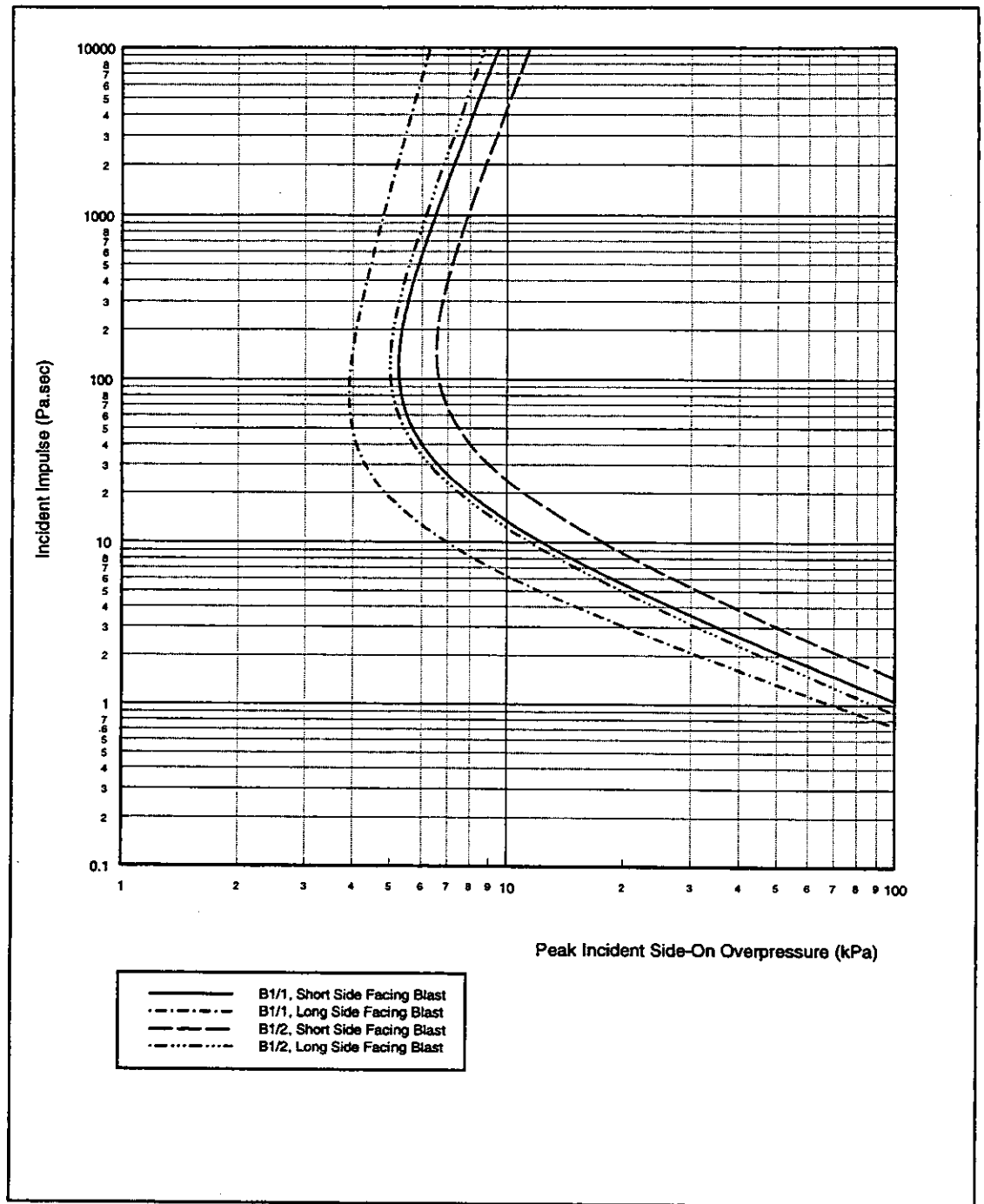


Figure 3.2: P-I Diagram: B1, Shock Pulse, Comparison of 1% Fatality Probability Curves



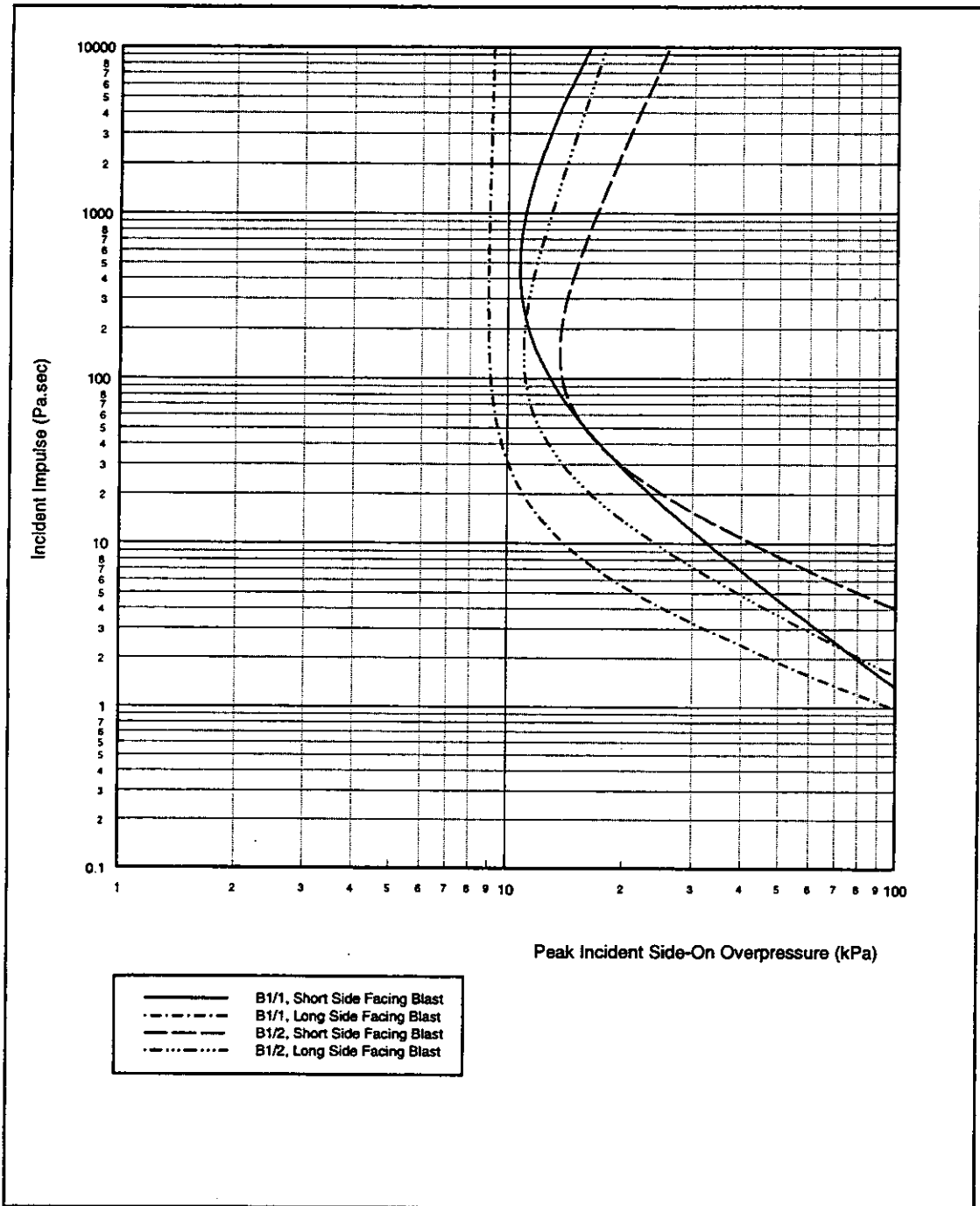


Figure 3.3: P-I Diagram: B1, Pressure Pulse, Comparison of 1% Fatality Probability Curves

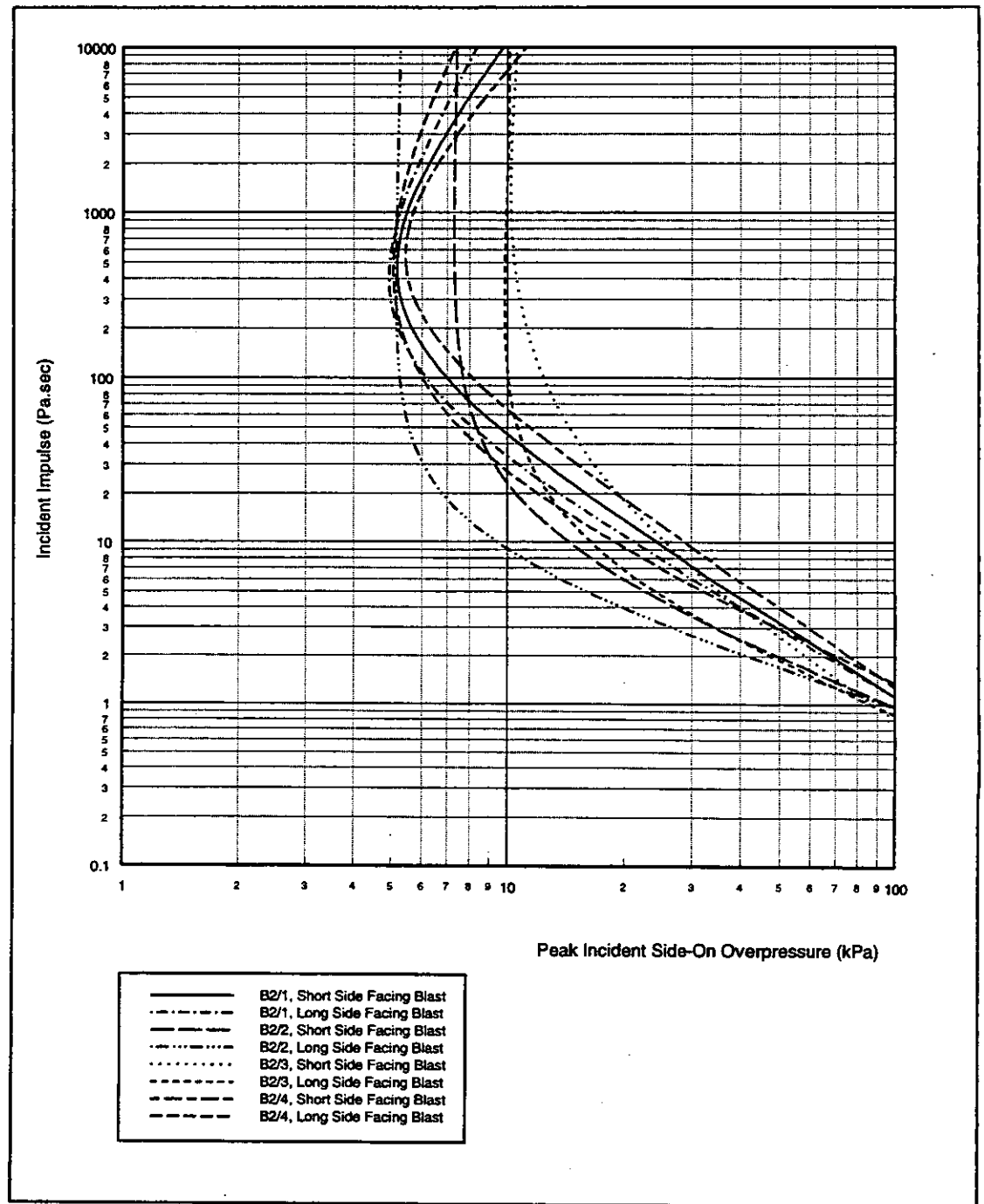


Figure 3.4: P-I Diagram: B2, Shock Pulse, Comparison of 1% Fatality Probability Curves

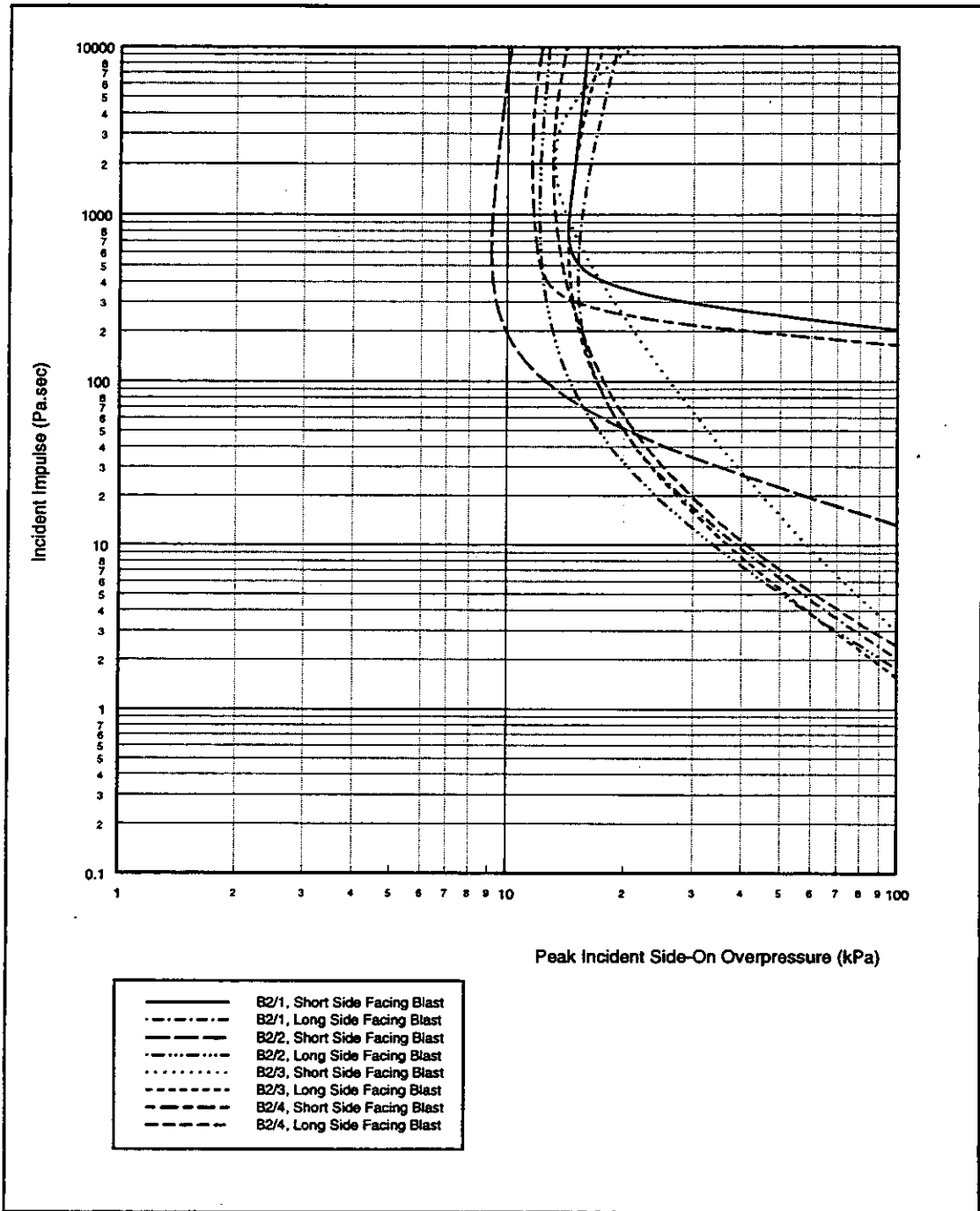


Figure 3.5: P-I Diagram: B2, Pressure Pulse, Comparison of 1% Fatality Probability Curves

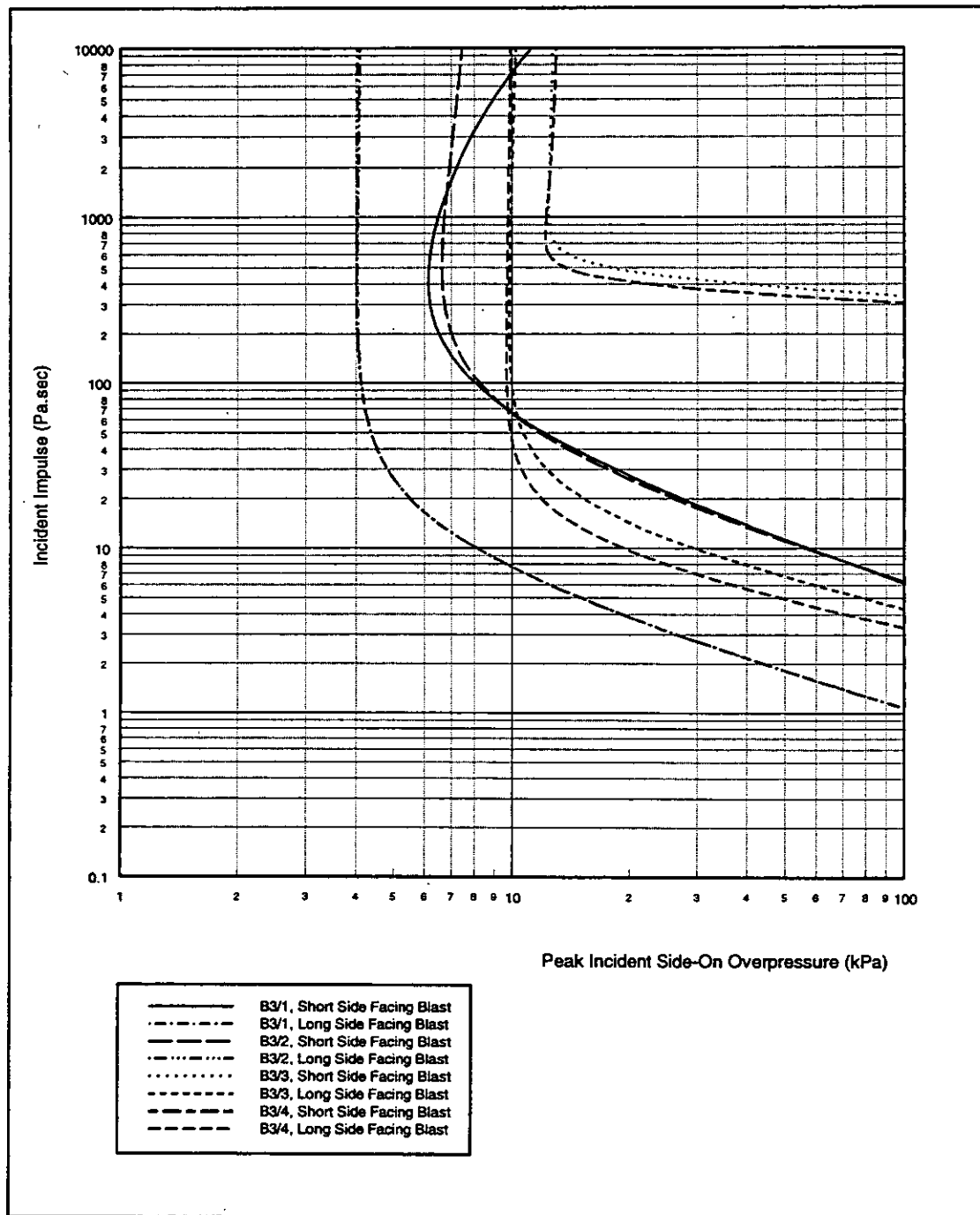


Figure 3.6: P-I Diagram: B3, Shock Pulse, Comparison of 1% Fatality Probability Curves

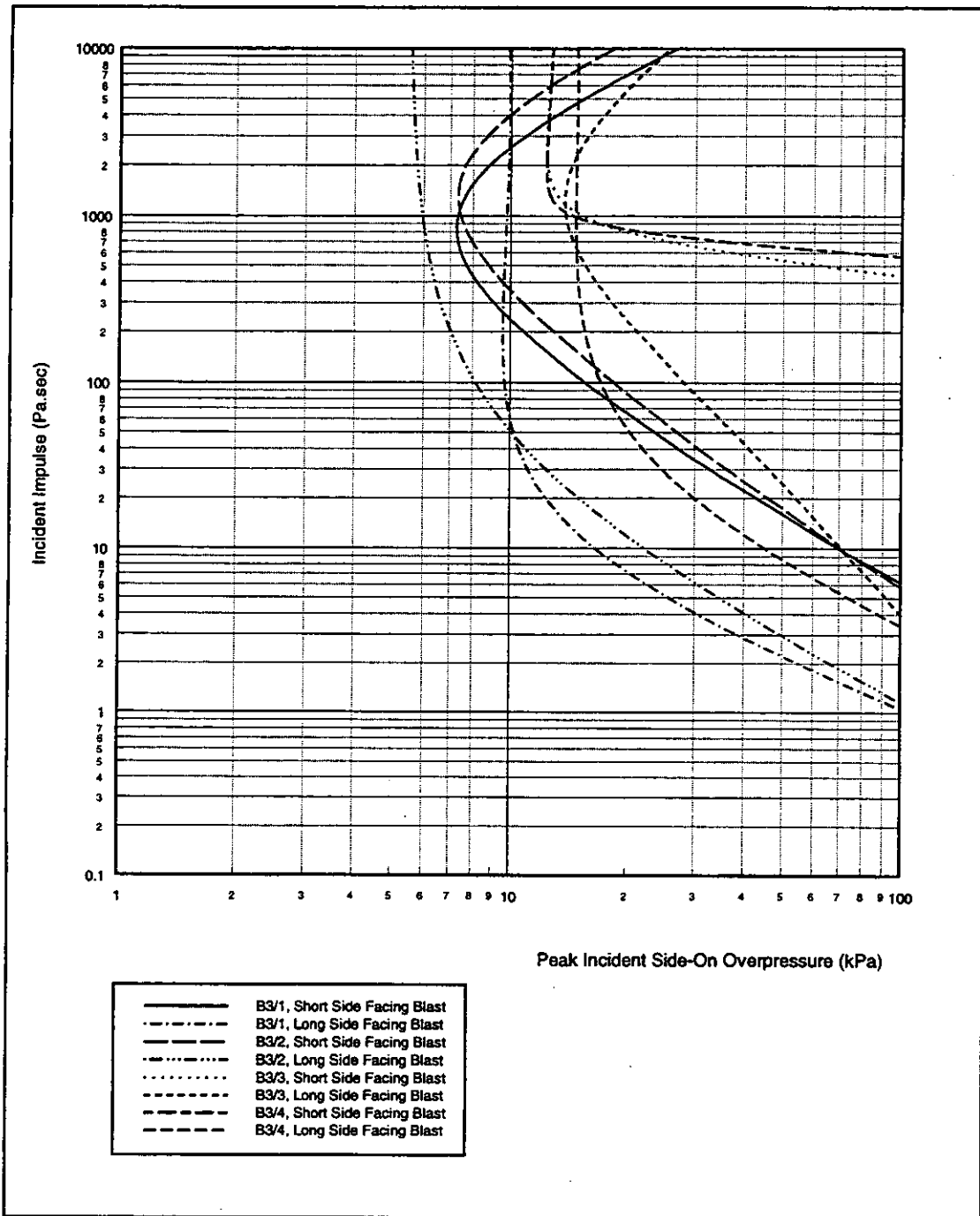


Figure 3.7: P-I Diagram: B3, Pressure Pulse, Comparison of 1% Fatality Probability Curves

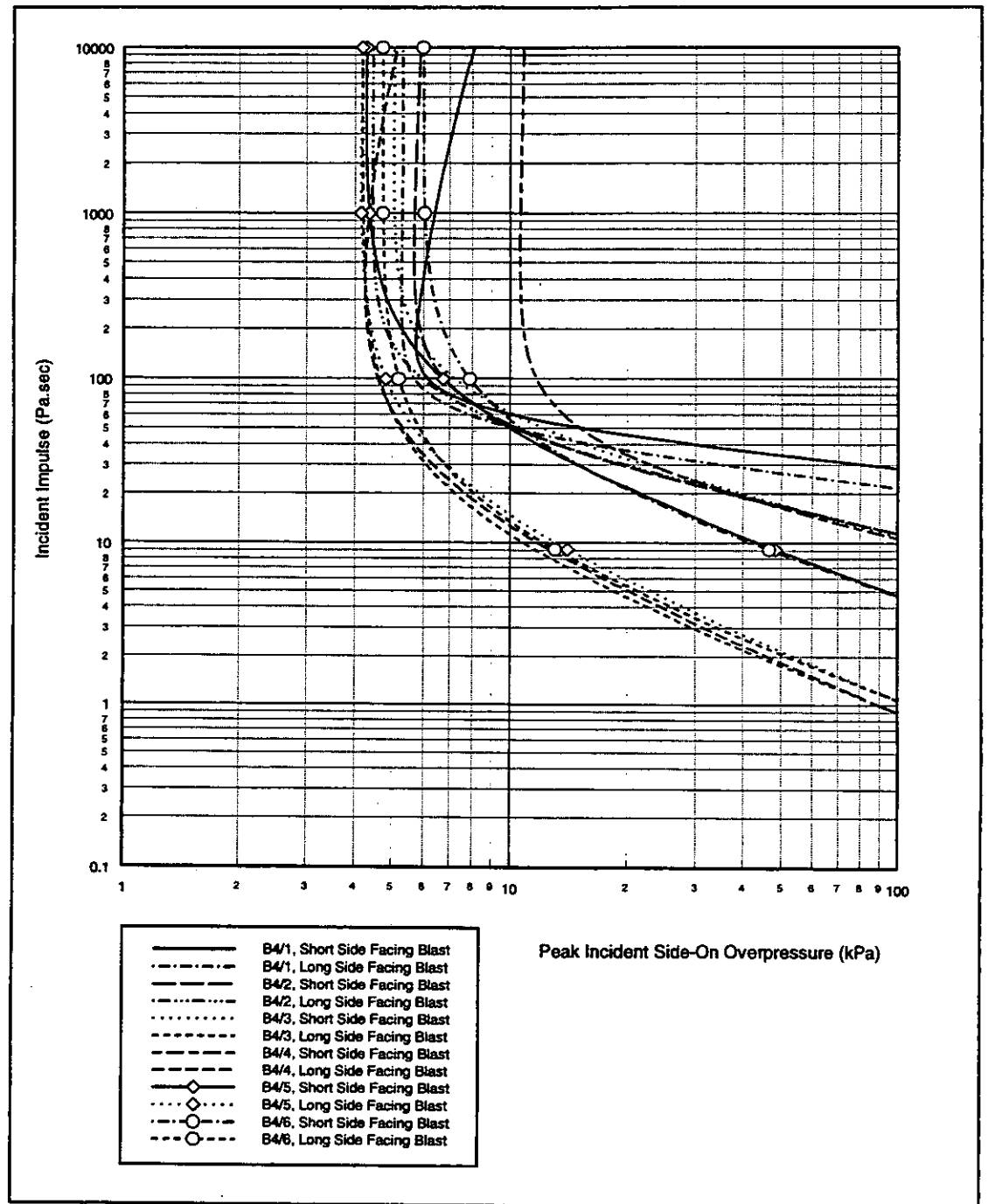


Figure 3.8: P-I Diagram: B4, Shock Pulse, Comparison of 1% Fatality Probability Curves

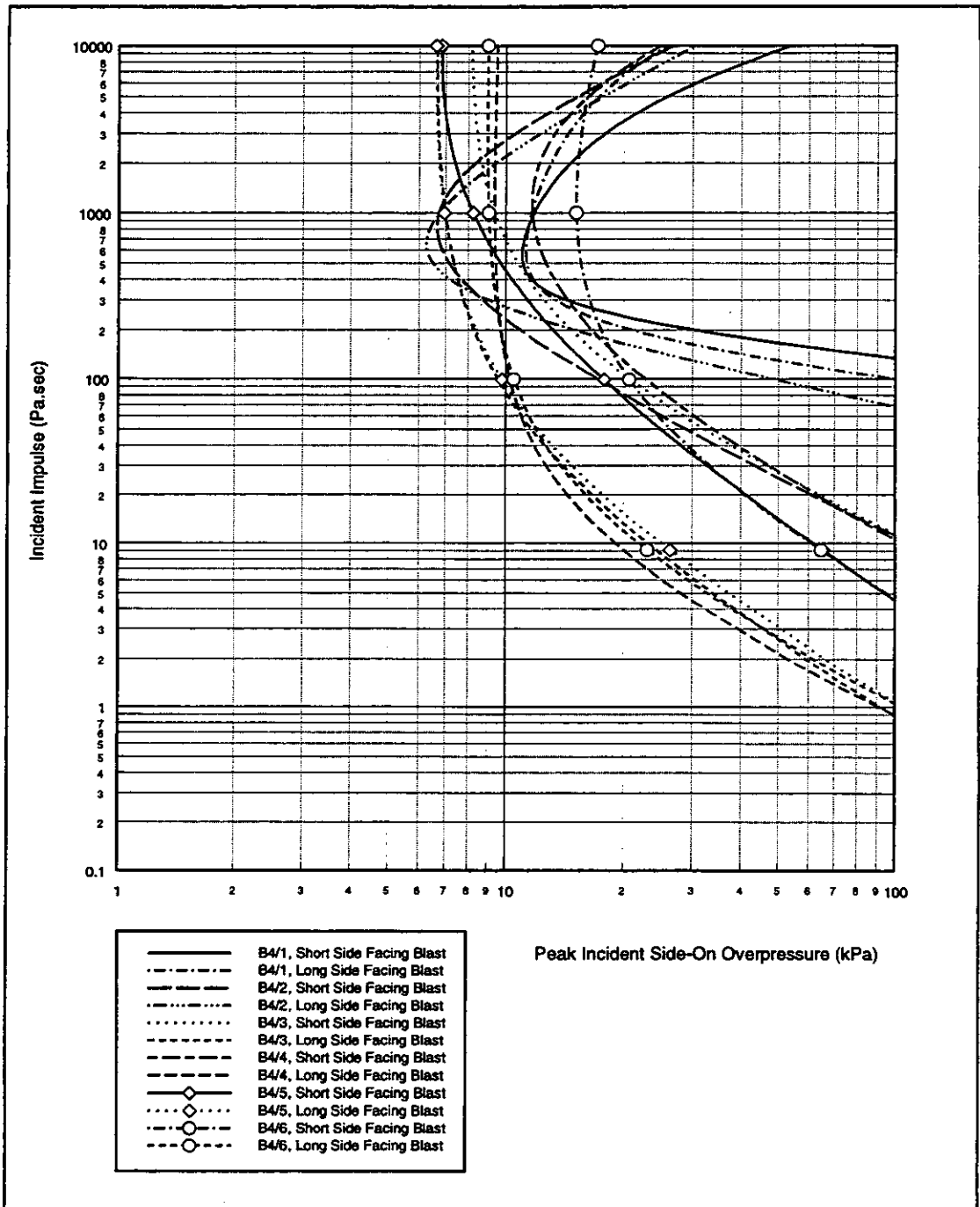


Figure 3.9: P-I Diagram: B4, Pressure Pulse, Comparison of 1% Fatality Probability Curves

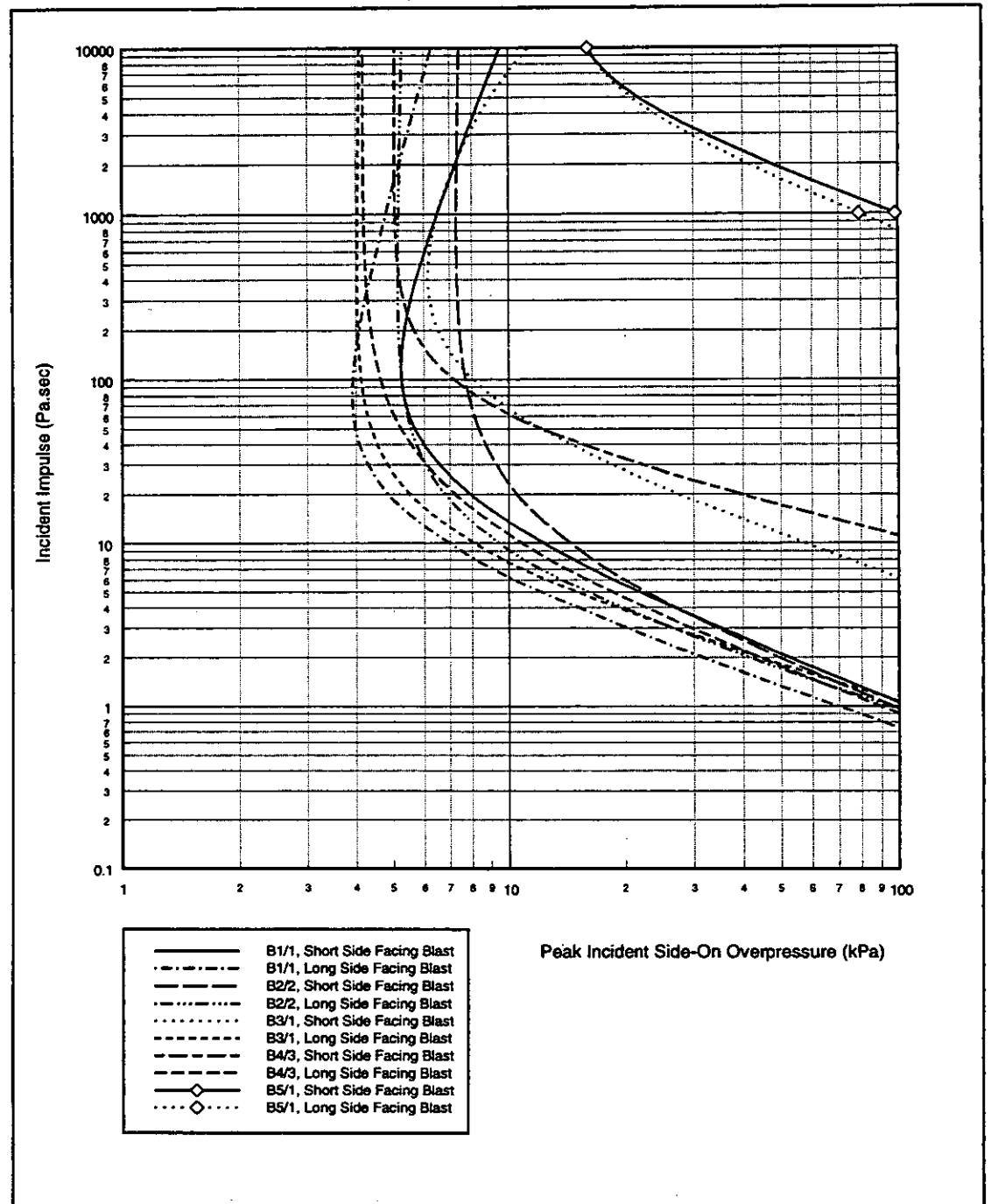


Figure 3.10: P-I Diagram: Shock Pulse, Comparison of 1% Fatality Probability Curves



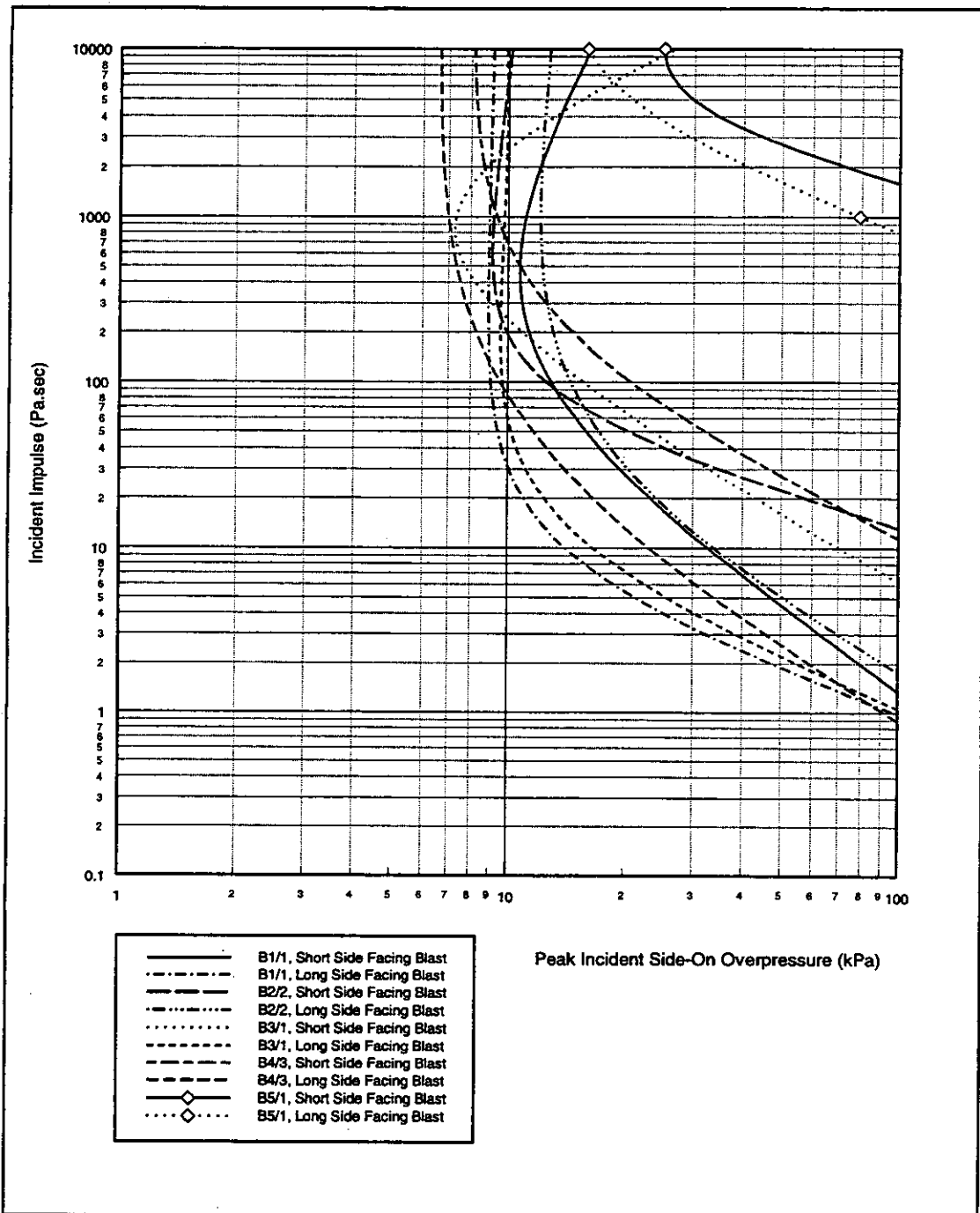


Figure 3.11: P-I Diagram: Pressure Pulse, Comparison of 1% Fatality Probability Curves

## 4. COMPARISONS

An important aspect of developing a tool of this nature is the validation of the tool against existing historical and/or experimental data. Rigorous validation of the methodology is difficult due to the scarcity of data. However, some comparison with the available data and other methods used is possible. As already mentioned, to date the majority of explosion predictions have been based on observations of the damage caused by high explosive, in particular World War II bomb damage. In addition there are reports from accidental industrial explosions which may be used to check the approach.

### 4.1 Comparison of Structural Predictions against Explosives Safety Distances

Clearly it is easier to validate the predictions of structural damage than fatality probability predictions. One standard against which it is useful to compare the predictions of the model is the British Explosives Safety distances, derived by Jarrett [20] and used to determine the location for safe storage of explosives. The criterion accepted for public distance is that an explosion should not cause serious structural damage to a standard dwelling house although minor damage such as broken windows, fallen ceilings or loosened slates is acceptable. Based on an analysis of damage from 24 well documented explosions together with experience of World War bombings, the distance at which various classes of damage would be sustained by an average British dwelling was found to be closely approximated by the formula:

$$R = \frac{kW^{1/3}}{\left[1 + \left(\frac{7000}{W}\right)^2\right]^{1/6}}$$

where R is the distance from an explosion of W lb explosive.

The classes into which damage is divided are as follows:

A	(k = 9.5)	almost complete demolition
B	(k = 14)	50 - 75% external brickwork destroyed or rendered unsafe and requiring demolition
Cb	(k = 24)	houses uninhabitable - partial or total collapse of roof, partial demolition of one to two external walls, severe damage to load-bearing partitions requiring replacement
Ca	(k = 70)	not exceeding minor structural damage, partitions and joinery wrenched from fixings
D	(k = 140)	remaining inhabitable after repair - some damage to ceilings and tiling, more than 10% window glass broken.

Other workers have noted that a series of earlier methodologies have generated wide differences of interpretation of the same bomb damage data.

The above criteria are for a TNT type explosion. For a given weight of TNT, it is possible to calculate the radius at which the above levels of damage occur, and hence, by using the

charts given in Baker et al [13], to calculate the peak overpressures and pulse durations of the blast pulses at those distances. For an explosion equivalent to 1000lb TNT, the parameters are given in Table 4.1 at the end of this section.

For a TNT explosion, the characteristic blast pulse shape corresponds to a short duration shock pulse (i.e. zero rise time). Using a shock pulse, with peak overpressures and pulse durations as given above, two of the generic building types have been assessed and the predicted damage levels have been extracted. The two buildings assessed were B2/2, a typical brick built semi-detached house, and B3/1, a 2-storey structure with a concrete moment resisting frame and brick/block wall panels. The results of the structural assessment are shown in Table 4.2. For the brick house, B2/2, the agreement is quite good. The exception to this is that for damage class D, our calculations do not predict any window breakage. For this particular building, the failure pressure of the glazing is calculated from Mainstone [4] as 74mbar for a 0.043 sec pulse duration. Hence a peak incident overpressure of 28mbar, even if fully reflected at the front face of the building, is not sufficiently high to fail the glazing. The failure pressure of the glazing is dependent on the pane size and thickness, and a slightly different choice of glazing configuration for this building would give better agreement with the expected damage level.

It is also of interest to calculate the fatality probabilities associated with these damage levels for these two building types subject to this TNT explosion. The fatality probabilities for the two building types for these damage classes are shown in Figure 4.1. For the brick house, the calculations predict that damage classes A and B lead to greater than 80% fatality probability, irrespective of the orientation of the building. Given the level of damage, this seems to be a not unreasonable result. For damage classes Ca and D, the predicted fatality probabilities are less than 1%, irrespective of the building orientation. Again, this seems to be reasonable. For damage class Cb, depending on the building orientation, fatality probabilities of between 14 and 40% are predicted. It is interesting that this middle case, which is probably the hardest case to predict accurately, gives rise to the greatest range in fatality probability, and is the most dependent on the building orientation and internal layout.

The damage classes are based on damage to a typical dwelling. Consequently we would not necessarily expect good agreement for building type B3/1, the concrete framed office type building. Table 4.2 shows that the damage to this building type is similar to that for B2/2, with the exception that structural collapse does not occur except in the case where the long side of the building is facing the blast. This is a feature of the modelled behaviour of the framed structures, in that the windows and wall panels tend to fail first in these types of structures, thus relieving the load on the frame and reducing the probability of frame collapse. The corresponding fatality probabilities are significantly lower if the short side of the building faces the blast, but are similar or higher if the long side is facing. This reflects the fact that the area in which the occupants are vulnerable to glazing and cladding debris is much greater when the blast hits the long face of the building than it is if the blast hits the short face, due primarily to the high aspect ratio of the structure.

#### 4.2 Comparison of Fatality Probability Predictions against Historical Explosion Data

Another useful source of data for comparison purposes is the work by Hewkin [21], which looks at accidental and military explosions and their consequences for building occupants. In the paper, data from a number of sources are drawn together and a possible blast lethality probability relationship is proposed, which bounds the majority of the historical data. The data sources include UK military explosions and three large scale industrial accidents, including a civil manufacturing incident at Silvertown, East London in 1917, an underground accident at Fauld near Burton on Trent in 1944 and an accident at Port Chicago in 1944. In all three of these latter accidents, no fatalities occurred beyond Scaled Distance 6, corresponding approximately to Category B damage in the Jarrett classifications. This implies that our calculated fatality probabilities for category Cb above might be over-conservative.

In order to compare our calculations against the historical data and the relationship proposed by Hewkin, it is necessary to convert the specified scaled distances into peak overpressure - pulse duration pairs. While the peak overpressure is relatively straightforward to extract, by using blast scaling charts such as those reproduced in Baker et al [13], the same charts give only a scaled pulse duration,  $t_p/W^{1/3}$ . In order to make use of this, it is therefore necessary to assume a mass of explosive,  $W$ . By comparison with the data within the paper for parachute mines and rocket bombs, a mass of 1000lb has been used. This leads to pulse durations of the order of 0.02 seconds, which are similar to the corresponding values for the historical data. However, it is important to note that assumption of a larger mass of explosive would lead to a longer pulse duration at the same scaled distance which would have a corresponding effect on the structural response and hence the fatality probabilities predicted.

The data points extracted from Hewkin are shown in Table 4.3.

As for the comparison with Jarrett, two building types have been assessed, namely the brick building, B2/2 and the concrete framed building, B3/1, assuming a shock pulse with parameters as defined in Table 4.3. The results are shown graphically in Figure 4.2.

The first point which stands out is that our calculations are more conservative than the curve proposed by Hewkin at the low fatality probability level, and less conservative at the high fatality probability level. In our calculations, the fatality probability at the low level is dominated by the risk from flying glass, and the comparison would seem to suggest that our assumptions are slightly overconservative. The assumptions which are most open to question in the assessment of glazing hazard are the assumed probabilities of a single hit causing a fatality. As described in Section 2, these have been assumed to be 10% for skull fracture and 50% for skin penetration. It is possible that further validation work might lead to a reduction in these values, although at present it is sufficient to note that they are probably conservative.

At the high fatality probability levels, the fatality probability for the brick building is dominated by building collapse. The fatality probability associated with collapse has been assumed to be 60% based on assessments of historical earthquake data. Although this leads to a value for fatality probability which is lower than the value proposed by

Hewkin at this scaled distance, a comparison of the actual historical data presented in Hewkin shows that the derived total fatality probability of 86% for the brick building at a scaled distance of 3 is in line with experience. The fatality probability values for the concrete framed building reflect the fact that the structural frame does not collapse under this loading.

#### **4.3 Comparison of Model against Data from the Flixborough Event**

One well known example of an accidental explosion is that at the Nypro (UK) Ltd. Plant at Flixborough in Lincolnshire on the 1<sup>st</sup> June 1974. As a consequence of pipe rupture at the plant, a large amount (probably more than 30 tons) of cyclohexane was released. The combustible chemical quickly mixed with air and was ignited shortly after. This explosion resulted in the deaths of 28 employees and injuries to others working at the plant, together with severe structural damage. No fatalities were recorded off site, although there was widespread low level damage to housing in the vicinity of the site.

There have been several studies of the damage caused by the blast. Van den Berg [23] has assessed the damage using the Multi -Energy Method (MEM), and concludes that a fairly consistent picture can be constructed if it is assumed that only about 10 tons of the cyclohexane were involved in the explosive combustion. This part generated a high strength blast, while the rest burned in the open, producing a minor strength blast. Van den Berg concludes that using the MEM curve 7 gives overpressure-pulse duration parameters which are consistent with the level of damage observed. Using curve 7 in conjunction with the description of damage given in Sadee et al [22], Table 4.4 has been derived. This table shows a selection of the buildings on and off site, for which damage levels have been recorded, and the corresponding overpressure - pulse duration pairs derived using Curve 7.

In order to compare the P-I diagrams derived in this report against the data arising from the Flixborough explosion, it has been necessary to select for each actual building the generic building type to which it corresponds most closely. For the majority of the housing, B2/2 appears to be the most appropriate choice, being a two storey brick built semi-detached house. The exception to this is the row of bungalows in Flixborough which are better represented by B2/1. On site there is a wider variation. The control building is described in Marshall [27] as constructed with a reinforced concrete frame, brick panels and a considerable window area. It was 2.5 storeys high in the middle section, and was part of a complex of buildings 160m long, orientated with its long axis at right angles to the blast. The control room is best represented by Building type B3/1. The offices are probably best represented by B2/2, although it is noted that the wall thickness in the actual building is considerably greater than that in our generic building. Consequently we might expect a prediction of damage using B2/2 to be over-conservative. The switch house is a reinforced concrete single storey structure with brick walls; this will be most accurately represented by B3/1. Finally, the Simon-Carves workshop and the stores/ workshop/ office block are both steel-framed structures and are most appropriately modelled by B4/1 and B4/3 respectively.

The results of a comparison of the actual damage and fatality levels against the levels predicted using the methodology proposed in this document are shown in Table 4.5. Fatality probabilities in the table are values calculated on site for a pulse duration of 100msec and off site for a pulse duration of 300msec, as values of 100msec and 300msec have been used to derive the P-I diagrams and variation in fatality probability between 100 and 300msec tends to be small. Damage levels have also been extracted for the 100msec pulse duration on site and 300msec off site calculations for the same reason. For the buildings on site, values for damage and fatality probability have been given for both a shock pulse and a pressure pulse, as the pressure wave is likely to be partially shocked at this distance from the explosion centre. Off site, however it has been assumed that the buildings are far enough away from the source of the blast that the pulse has 'shocked up' and consequently that a shock pulse is the appropriate shape to use. This agrees with the calculations by Puttock [3], described in Section 2.1 of this report.

The results show a generally acceptable level of agreement between the historical evidence and the predictions of the model, although there are one or two points arising which are worthy of discussion. Firstly, with the exception of the control building and the offices, the fatality probabilities on site seem to be high when compared against the level of damage actually observed. In particular, the model predicts very similar levels of damage and fatality probability for the Simon Carves workshop and the nearby stores/workshop, both of which are steel-framed structures. It has already been noted by Sadee et al [22] that the damage to the Simon Carves workshop is much less than that to the stores, indicating the possibility of a local explosion in the stores. However, our model agrees better with the damage observed at the stores rather than in the Simon Carves workshop, possibly indicating that our model is over conservative.

The predictions of fatality and damage for the control building are rather lower than observed. There are many possible reasons for this: the model does not predict structural collapse at this level of overpressure, primarily because the windows and walls fail and the load on the structure is relieved. If the walls had a higher failure pressure, a greater proportion of the load would be transmitted into the frame and the frame would fail at a lower pressure. Indeed if B3/2 is used for this comparison, under a shock pulse the concrete walls fail at a higher pressure and the structure collapses with a peak incident overpressure of approximately 600mbar, leading to a fatality probability at 800mbar in excess of 90%. B3/2 does not collapse under a pressure pulse, however. Alternatively, if the frame itself were weaker than assumed for building type B3/1, it would also fail at a lower pressure. In addition, the effects of surrounding structures on the control room have not been taken into account. Marshall [29] describes the damage to the control room in more detail than Sadee et al [23]. It appears that in addition to the blast itself, three adjacent pipe bridges fell onto the control room, one onto the south face of the building and the other two onto the ends of the building. Marshall [29] states that 'exactly what contribution the collapsing pipe bridges made to the catastrophic collapse of the control building can only be conjectured'. In addition to causing damage, however, the presence of the ruptured pipes made rescue impossible, which may or may not have contributed to the fatalities of the occupants. In the methodology used here, structural

collapse, arising from whatever cause, would lead to a fatality probability in excess of 80% for B3/1.

Off site, the agreement with the historical evidence is reasonable. A small level of fatality probability is predicted, due almost entirely to the glazing hazard. Fortunately no fatalities occurred off site, although no data are available concerning building occupancy at the time of the explosion. At the furthest distance from the blast, our model does not predict any damage to the buildings in question. However, it should be noted that only 2 possible glazing types have been considered off site, namely those used in B2/1 and B2/2, and that at these low pressures the results are very sensitive to the assumed failure pressure of the glass.. It is consequently quite possible that the failure pressure assumed for these two buildings is too high to be totally representative in these particular cases.

#### **4.4 Comparison of Effects from TNT explosion and VCE**

It is useful to compare the differences between the results achieved by using a TNT equivalent mass and a VCE in deriving fatality probabilities using the P-I diagrams. In order to make this comparison, a scenario has been proposed in which 10te of propane in a flammable cloud explodes. This has been treated in two ways: first the TNT equivalent mass has been calculated using a TNT equivalence factor of 0.42 for the full amount of propane. This gives an equivalent mass of 4.2te TNT. For this equivalent mass, the peak incident overpressure, the positive phase pulse duration and the impulse versus distance have been calculated using the charts reproduced in Baker et al [13]. From the P-I diagrams for B2/2 and B3/1, fatality probabilities corresponding to these values of pressure and impulse have been derived.

The second approach is to assume that 30% of the cloud will be confined/congested and to calculate the peak incident overpressure and positive phase pulse duration with distance using the Multi Energy Method (MEM) approach. The assumption of 30% confinement is deliberate in that it leads to a similar pressure distance profile for the VCE compared with the TNT explosion. For 3te propane, the derived values are given in Table 2.1 of this document, or in more detail in Table 7.2 of [1]. As above, the fatality probabilities can then be estimated by using the P-I diagrams for B2/2 and B3/1. Assuming that the explosion corresponds to Curve 7 of the MEM, the pulse shape is always partially shocked. In this case there will be some form of reflection at the front face of the structure, and it is conservative to use the shock pulse P-I diagrams to derive the fatality probabilities, rather than the pressure pulse P-I diagrams for which it has been assumed that no reflection occurs. However, this may overestimate the response for scaled distances less than 5.

The results are given in Tables 4.6 and 4.7 for B2/2 and B3/1 respectively, and are shown graphically in Figures 4.3 and 4.4. The principal difference between the TNT and VCE pulse profiles with distance from the source is that the pulse duration for the VCE is much longer, leading to a much greater impulse. This is reflected in the fatality probabilities with distance from the source, as the fatality probability is higher for the VCE, particularly in the mid-range, i.e. between 80 and 450m.

This comparison indicates that if a VCE is treated entirely like a TNT explosion for the purposes of predicting damage or fatality probability levels, the calculations would result in a serious under-prediction. This raises questions over the validity of using TNT-derived pressure-damage tables to predict damage from VCEs.

#### 4.5 Conclusions

The analyses described above have served to compare the predictions of building damage and the associated fatality probability with experience from historical events and with predictions made using existing techniques. With regard to structural damage it appears that the predictions are in reasonable agreement with experience. This gives us confidence that the methodology is appropriate for use in risk assessment. It should be noted, however, that for an incident pressure pulse, damage predictions are generally lower than for an incident shock pulse. This is primarily due to the assumption that full reflection occurs for a shock pulse incident on the front face of the building, whereas for an incident pressure pulse it has been assumed that there are no reflection effects. For a partially shocked pressure pulse, it is thus necessary to use the P-I diagrams derived for a shock pulse in order to ensure that the fatality probabilities predicted are conservative.

With regard to occupant fatality probability, the comparison exercises have confirmed that the methodology developed during this project is conservative, particularly for low levels of peak overpressure. It has also served to highlight a number of areas where the conservatism could be reduced as a result of further comparative work. The two areas which stand out as being suitable for further investigation include:

- The fatality probabilities associated with the glazing hazard. It appears from the comparison with Hewkin [21] that at very low pressures the derived fatalities are too high. The factors affecting fatality probabilities at low pressures are the failure pressure of the glazing, the velocity of the glazing fragments and the fatalities associated with the flying glass. From comparison with experience it appears that the failure pressures used for the glazing are reasonable, and hence it appears that either the fragment velocity or the probability of fatality associated with being hit by flying glass is too high. This is not surprising as the velocities are high immediately the window fails, and the fatality probabilities are based on estimates of the probability of a single hit causing fatality which are subject to a high level of uncertainty.
- The debris velocity and associated hazard. In our model there is no allowance for partial failure of the cladding: for a particular face of the building either all of the cladding fails or none of it fails. In the Flixborough experience, however, particularly for the steel clad buildings, it is quite clear that only some of the steel panels became detached from the structure. This has implications for the associated risk to the building occupants in that if there is less debris, the risk must be reduced.

As a general conclusion, it is reassuring that the comparisons do show a reasonable level of agreement, with the predictions erring on the conservative side. Considering that the comparison with the Flixborough experience was based, not on an accurate reproduction of the specific building geometries and internal layouts, or a consideration of the local



site layouts, but on a comparison of buildings which are assumed to be typical of that particular generic type, i.e. steel-framed, brick, concrete framed etc., it is encouraging to find that the comparisons hold reasonably well and are conservative, particularly for the off-site cases.

Finally, it has been shown that it may be unconservative to treat a VCE entirely like a TNT explosion for the purposes of predicting damage or fatality probability levels. The methodology presented herein may therefore represent a viable alternative for predicting the effects of an accidental explosion.

Damage Class	Distance (m)	Peak Overpressure (mbar)	Pulse Duration (s)
A	15	1825	0.015
B	22	849	0.018
Cb	38	325	0.025
Ca	111	66	0.035
D	222	28	0.043

**Table 4.1: Parameters for 1000lb TNT Explosion Comparison**

Jarrett Classification [20]	Description of damage [20]	1000lb TNT Peak Incident Overpressure (mbar)	1000lb TNT Positive Phase Pulse Duration (sec)	Predicted Damage to Brick House (B2/2)	Predicted Damage to Concrete Framed Building (B3/1)
A	'Almost complete demolition'	1824	0.015	All glazing broken All walls demolished - collapse	All glazing broken Front wall failed Complete global collapse occurs if long side of building faces blast.
B	'50 - 75% external brickwork destroyed or rendered unsafe and requiring demolition'	849	0.018	All glazing broken All walls demolished - collapse	All glazing broken Front wall failed No collapse
C <sub>b</sub>	'Houses uninhabitable - partial or total collapse of roof, partial demolition of one to two external walls, severe damage to load-bearing partitions requiring replacement'	325	0.025	All glazing broken Front wall failed No collapse	All glazing broken Front wall failed No collapse
C <sub>a</sub>	'Not exceeding minor structural damage and partitions and joinery wrenched from fixings'	66	0.035	Front face glazing broken No wall failure No collapse	Front face glazing broken No wall failure No collapse
D	'Remaining inhabitable after repair - some damage to ceilings and tiling, more than 10% window glass broken'	28	0.043	No glazing damage No wall failure No collapse	No glazing damage No wall failure No collapse

Table 4.2: Comparison of Building Damage Predictions against Existing Explosives Safety Distances

Fatality Probability (%)	Peak Incident Overpressure (mbar)	Pulse duration (sec)
1	211	0.026
10	344	0.024
50	568	0.020
90	725	0.020
100	825	0.018

**Table 4.3: Parameters for Comparison from Hewkin [21]**

<b>Building</b>	<b>Distance from assumed source centre (m)</b>	<b>Derived Peak Overpressure MEM Curve 7 (mbar)</b>	<b>Derived Positive Phase Pulse Duration MEM Curve 7 (sec)</b>
<b>On Site</b>			
Control Room	101	800	0.14
Offices Two storey load bearing brick building	120 - 160	780	0.14
Switch House Single storey RC frame building	220	289	0.16
Simon Carves Workshop Light steel frame building clad with corrugated sheeting	230 (front end)	251	0.17
Stores/workshop Steel frame building with 115mm brick infill panels and 115mm brick facing panels over frame	230	251	0.17
<b>Off site</b>			
Pair of cottages Flixborough Stather	335	149	0.187
Corner House, Flixborough Stather	400	117	0.201
Group of 6 pairs of Semi-detached houses	535	81	0.215
Amcotts village, houses near river bank	700	58	0.225
Flixborough, row of six 3-4 year old bungalows on hill with rear of bungalows facing plant	825	49	0.231
Rose Cottage	1340	27	0.244

**Table 4.4: Overpressure-Pulse duration pairs derived for Flixborough explosion**

Building	Peak Overpressure (mbar)	Impulse (kPa.s)	Damage Description	Building type used for comparison	Predicted Damage	Predicted Fatality Probability
<b>On Site</b>						
Control Room	800	5.60	Demolished	B3/1	Shock Pulse: Front and rear glazing and debris failed, frame intact Pressure Pulse: Front and rear glazing and debris failed, frame intact	Shock Pulse: 13 - 58% Pressure Pulse: 9 - 49%
Offices Two storey load bearing brick building	780	5.46	Walls severely damaged. Upper storey walls at front end collapsed	B2/2	Shock Pulse: Structure completely collapsed Pressure Pulse: Structure completely collapsed	Shock Pulse: 71 - 85% Pressure Pulse: 77 - 81%
Switch House Single storey RC frame building	289	2.31	End wall of 230mm brickwork 8.7m long and 3m high was demolished	B3/1	Shock Pulse: Front and rear glazing and debris failed, no structural collapse. Pressure Pulse: Front and rear glazing and debris failed, no structural collapse.	Shock Pulse: 17 - 48% Pressure Pulse: 12 - 18%
Simon Carves Workshop Light steel frame building clad with corrugated sheeting	251	2.13	General frame and roof distortion. Cladding broken away from end and side walls. A few roof cladding sheets dislodged at each end of building	B4/1	Shock Pulse: No glazing. Cladding failure on all sides, no structural collapse. Pressure Pulse: No glazing. Cladding failure on all sides, no structural collapse.	Shock Pulse: 20 - 55% Pressure Pulse: 8 - 12%
Stores/workshop Steel frame building with 115mm brick infill panels and 115mm brick facing panels over frame	251	2.13	Six out of 10 panels on one side had collapsed and 2 panels were badly dished. Roof cladding destroyed and roof beams badly buckled.	B4/3	Shock Pulse: Glazing and cladding failure on all sides, no structural collapse. Pressure Pulse: Glazing and cladding failure on all sides, no structural collapse.	Shock Pulse: 22 - 53% Pressure Pulse: 13 - 28%

**Table 4.5: Comparison of Predictions against Flixborough Experience [23]**

Building	Peak Overpressure (mbar)	Impulse (kPa.s)	Damage Description [23]	Building type used for comparison	Predicted Damage	Predicted Fatality Probability
<b>Off site</b>						
Pair of cottages Flixborough Stather	149	1.39	All front and side windows and some window frames broken. Rear windows 30% broken. Roof dished and all tiles displaced. Lower floor ceilings damaged. Internal brick partition wall badly cracked. Shear crack in external side wall	B2/2	Shock Pulse: Front and rear glazing failed. No debris hazard as walls fail at ~175mbar peak incident overpressure	Shock Pulse: 1.3 - 2.5%
Comer House, Flixborough Stather	117	1.18	All front windows and 75% of rear windows broken. Roof collapsed and upper part of chimney breast broken. Internal doors broken.	B2/2	Shock Pulse: Front and rear glazing failed. No wall failure or collapse.	Shock Pulse: 1.3 - 2.5%
Group of 6 pairs of Semi-detached houses	81	0.87	All front and most of rear windows broken. Wooden window frames damaged. Roof tiles displaced and 20% main rafters broken. All doors damaged. Ceilings collapsed and some vertical cracking in exterior walls near front corners.	B2/2	Shock Pulse: Front and rear glazing failed. No wall failure or collapse.	Shock Pulse: <1.3 - 1.8%
Amcotts village, houses near river	58	0.65	100% window breakage. Some tile damage to roofs	B2/2	Shock Pulse: Front glazing failure only. No wall failure or collapse.	Shock Pulse: < 1%
Flixborough, row of six 3-4 year old bungalows with rear facing plant	49	0.57	All rear windows and 75% of larger windows on front broken. 25% tiles on slope facing plant dislodged.	B2/1	Shock Pulse: Front glazing failure only. No wall failure or collapse.	Shock Pulse: < 1%
Rose Cottage	27	0.33	Slates dislodged in centre of roof. Facing windows broken but front door in porch apparently undamaged. 75% rear windows broken.	B2/2	Shock Pulse: No glazing failure, wall failure or collapse.	Shock Pulse: 0%

**Table 4.5: Comparison of Predictions against Flixborough Experience [23]**

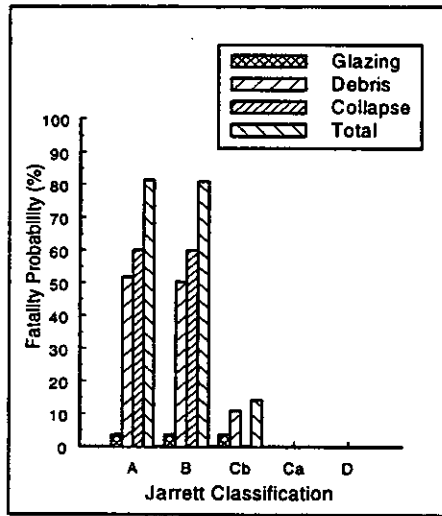
Distance (m)	Scaled Distance R	Peak Incident Overpressure Ps (kPa)	Positive Phase Pulse Duration tp (msec)	Impulse Is (Pa.sec)	Fatality Probability (%)		Scaled Distance Z (m/Kg <sup>1/3</sup> )	Peak Incident Overpressure Ps (kPa)	Positive Phase Pulse Duration tp (msec)	Impulse Is (Pa.sec)	Fatality Probability (%)	
					Short Side facing Blast	Long Side facing Blast					Short Side facing Blast	Long Side facing Blast
VCE												
33	0.3	101.3	120	6080	50 - 90%	50 - 90%	2.1	190.0	32	1613	> 90%?	> 90%?
45	0.4	101.3	106	5378	50 - 90%	50 - 90%	2.8	88.2	38	1242	50 - 90%	50 - 90%
56	0.5	95.3	93	4446	50 - 90%	50 - 90%	3.4	57.0	43	976	50 - 90%	50 - 90%
78	0.7	72.0	87	3125	50 - 90%	50 - 90%	4.8	32.0	49	713	10 - 50%	50 - 90%
89	0.8	61.7	92	2835	50 - 90%	50 - 90%	5.5	26.0	53	634	10 - 50%	10 - 50%
111	1.0	46.0	100	2295	10 - 50%	50 - 90%	6.9	17.8	59	508	1 - 10%	10 - 50%
223	2.0	16.6	121	1005	1 - 10%	10 - 50%	13.8	6.1	73	245	< 1%	1 - 10%
445	4.0	6.7	138	461	< 1%	1 - 10%	27.6	2.7	83	127	< 1%	< 1%
668	6.0	4.2	146	306	< 1%	< 1%	41.4	1.6	98	82	< 1%	< 1%
890	8.0	3.1	151	234	< 1%	< 1%	55.2	1.2	104	60	< 1%	< 1%
1113	10.0	2.4	155	186	< 1%	< 1%	69.0	0.9	115	46	< 1%	< 1%
TNT												

Table 4.6 Comparison of VCE and TNT predictions for Building Type B2/2

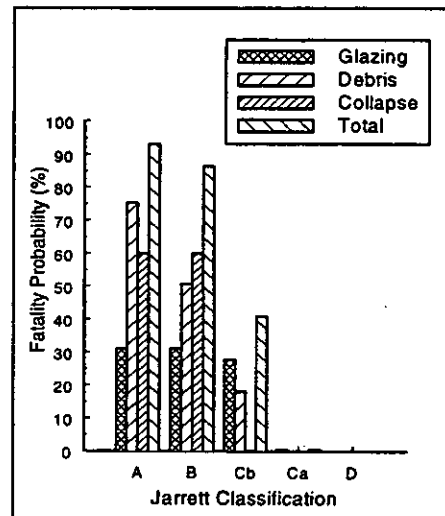


Distance (m)	VCE					TNT				
	Scaled Distance R	Peak Incident Overpressure Ps (kPa)	Positive Phase Pulse Duration tp (msec)	Impulse Is (Pa.sec)	Fatality Probability (%)	Scaled Distance Z (m/kg <sup>1/3</sup> )	Peak Incident Overpressure Ps (kPa)	Positive Phase Pulse Duration tp (msec)	Impulse Is (Pa.sec)	Fatality Probability (%)
33	0.3	101.3	120	6080	10 - 50%	2.1	190.0	32	1613	> 90%?
45	0.4	101.3	106	5378	10 - 50%	2.8	88.2	38	1242	10 - 50%
56	0.5	95.3	93	4446	10 - 50%	3.4	57.0	43	976	10 - 50%
78	0.7	72.0	87	3125	10 - 50%	4.8	32.0	49	713	10 - 50%
89	0.8	61.7	92	2835	10 - 50%	5.5	26.0	53	634	10 - 50%
111	1.0	46.0	100	2295	10 - 50%	6.9	17.8	59	508	10 - 50%
223	2.0	16.6	121	1005	10 - 50%	13.8	6.1	73	245	< 1%
445	4.0	6.7	138	461	1 - 10%	27.6	2.7	83	127	< 1%
668	6.0	4.2	146	306	< 1%	41.4	1.6	98	82	< 1%
890	8.0	3.1	151	234	< 1%	55.2	1.2	104	60	< 1%
1113	10.0	2.4	155	186	< 1%	69.0	0.9	115	46	< 1%

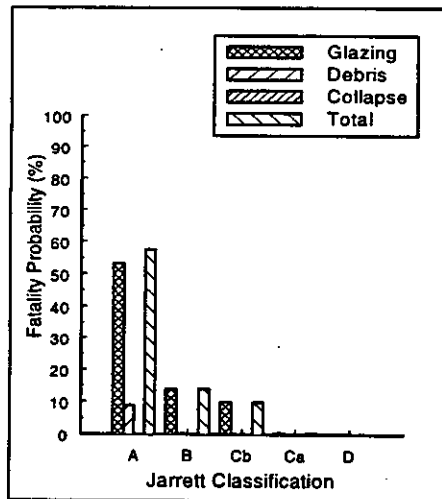
Table 4.7 Comparison of VCE and TNT predictions for Building Type B3/1



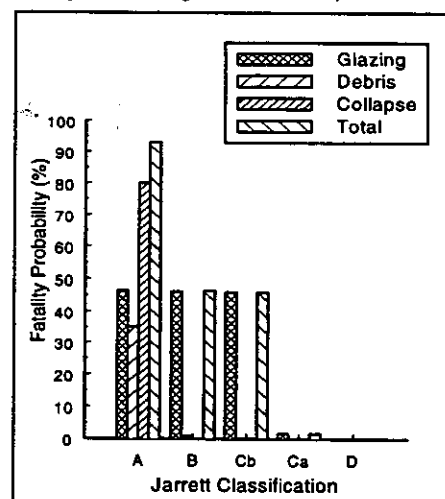
Building Type B2/2  
Short Side Facing 1000lb TNT Explosion



Building Type B2/2  
Long Side Facing 1000lb TNT Explosion



Building Type B3/1  
Short Side Facing 1000lb TNT Explosion



Building Type B3/1  
Long Side Facing 1000lb TNT Explosion

**Figure 4.1: Fatality Probability Predictions for 1000lb TNT Explosion**

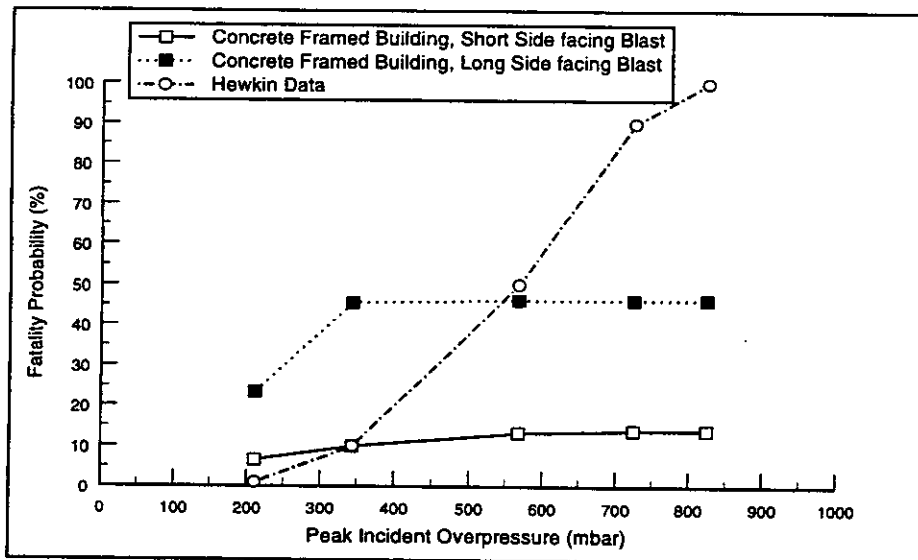
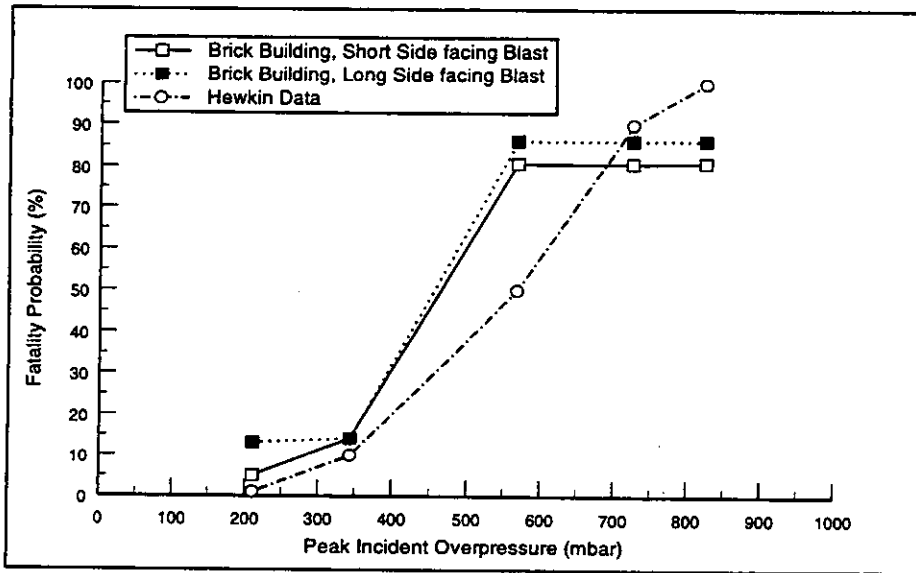


**Figure 4.2: Comparison of Fatality Probability Predictions against Data from Hewkin [21]**

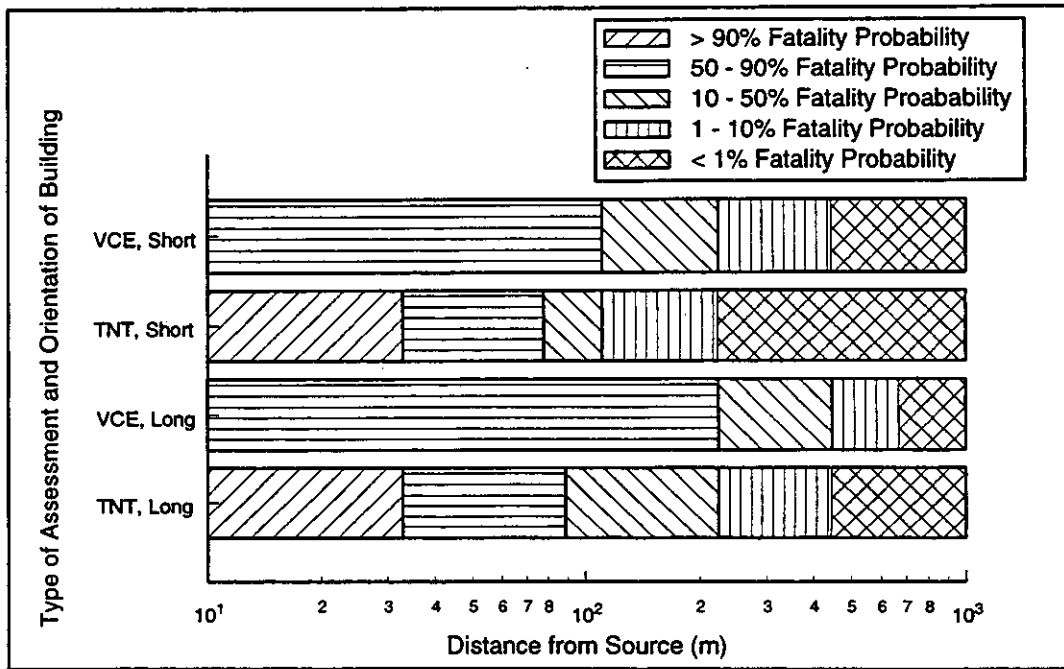


Figure 4.3: Comparison of VCE and TNT Predictions for Building Type B2/2

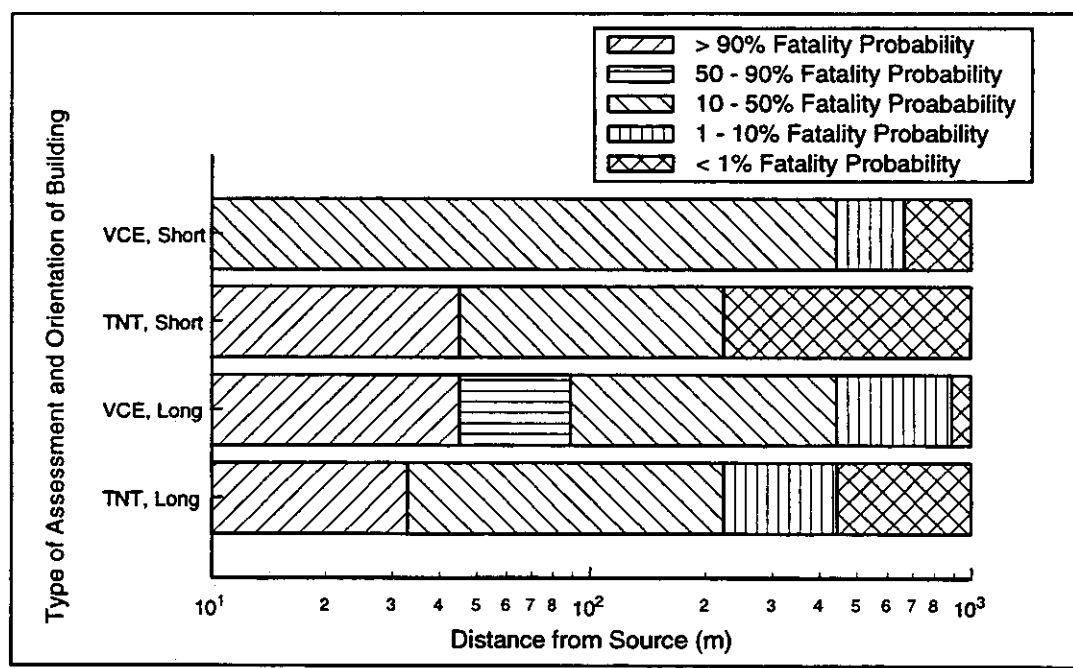


Figure 4.4: Comparison of VCE and TNT Predictions for Building Type B3/1

## 5. CONCLUSIONS

A workable methodology for predicting the effects of a blast on different building types and for predicting the corresponding probability of fatality of the building occupants has been developed. A considerable amount of data has been collected and gaps in the data have been noted. In addition, the sensitivity of the methodology to the different components has been investigated. A number of generic building types have been assessed and fatality probabilities have been produced in the form of pressure-impulse (P-I) diagrams.

A comprehensive literature search has been conducted. It was found that the historical and experimental data available in the public domain on the effects of explosions on structures and humans is limited. In terms of experimental data for structural components, the majority of references relate to work by Glasstone and Dolan [24] on the effects of nuclear explosions on structures. These data need to be treated with caution if the explosion under consideration is a Vapour Cloud Explosion (VCE), primarily because the durations associated with a nuclear explosion are far longer than those for a VCE. There are other sources of data available, notably Jarrett [20], Astbury et al [25] and Colwell and Crowhurst [26], but the data tends to be specific to particular explosion types and particular structural examples. Engineering judgement, based on a knowledge of the dynamics of the structures under consideration, needs to be applied in order to derive sensible failure pressures for the different structural components.

Other workers in the field have indicated that data of a restricted or confidential nature exist, particularly within defence related establishments. However, the difficulties inherent in obtaining these data and the need to construct a methodology that is transparent have meant that these data could not be used.

With regard to the effects of missile impact and blast effects on humans, the publicly available information is summarised in Baker et al [13] and little additional information has been discovered during the course of this project. Detailed documentation of accidental and terrorist explosions could provide a useful insight into the distribution of injuries and fatalities, but accident reports tend to focus on the numbers of casualties, rather than the causes of injury or fatality. Information relating to earthquakes is also of interest, although care must be taken to interpret the data taking into account the length of duration of the incident and the time taken for emergency services to respond to the incident, both of which may be quite different for an earthquake than for an explosion incident.

The methodology described in Section 2 of this document has been developed taking the available data into account, but supplementing these data with structural calculations and sensitivity studies to ensure that the approach used is representative of the actual structural behaviour. The factors affecting the building response are complex. Of primary importance are the shape of the blast pulse and the way in which the progressive failure of the different structural components affects the interaction of the structure with the remaining blast pulse. In particular, the extent to which the blast pulse is reflected as it hits the building is very important, as it can effectively double the load that the

building experiences; it would be useful to be able to quantify the reflection effects for partially shocked pulse shapes. The pressure rise within the structure is also important, particularly for the assessment of rear and side wall failure, which are both dependent on the differential pressure across the wall. If the internal pressure rise is similar to or greater than the external pressure rise, risk to the building occupants may be greatly reduced, as the rear and side glazing and walls either may not fail at all or may be blown outwards by the blast thus presenting no risk to the occupants.

The loading on the rear face of the building also plays an important part in the overall structural response, having a beneficial effect for smaller structures. This is because the rear face load on a small structure may significantly oppose the front face load if the time of travel of the blast to the rear face is short. For a large structure, or one with a high aspect ratio, the load on the front face will generally have finished by the time the load on the rear face starts to increase and the incident overpressure may have decayed significantly by the time the pulse reaches the rear face.

The sensitivity studies [2] also showed that the negative phase of a blast pulse is less important for predicting structural response and that ignoring its effects are likely to be conservative. Hence, for this phase of the work, the negative phase has not been included. However, certain structural components behave differently under pressure and suction, and it may be necessary in further studies to include the negative phase. This may be particularly important for buildings such as shopping centres and leisure centres where risks to people outside the structure may be important.

In addition to predicting the global response of the structure, it is important to be able to predict glazing and debris masses and velocities following component failure. These predictions fundamentally affect the predictions of fatality probability, as the criteria for fatality probability tend to be governed by the mass and velocity of the impacting fragment. In Phase 3 [2], the methods for estimating the variation of the mean glazing fragment mass and velocity with pressure were investigated. The equations given in Baker et al [13] appeared to represent a realistic prediction of velocity distribution, although it was clear that further experimental work would have to be performed to corroborate fully the use of this equation. Similarly, the equations given for mean glazing fragment mass in Baker et al [13] appeared to be reasonable, although, for incident pressures lower than those used to derive the equation, the predicted masses seemed to be too low. As a consequence, a new curve was fitted to the available experimental data to try and improve the approximation at low pressures. The new curve predicts slightly higher masses at low pressures, but some fragments observed in experiment are still considerably larger than even the new equation would predict. It should perhaps be noted that, for this particular project, the low pressure regime is very important, as it is important to try to identify the furthest distance from a blast source at which fatality is possible.

As a result of studies performed into the behaviour of the glazing, a methodology was developed for predicting cladding velocities as outlined in Section 2 of this document. This methodology is based on the velocity at which the cladding is travelling when it fails plus the velocity which it achieves due to the blast impulse received after failure.

From the building calculations performed in this phase, together with the validation work, it would appear that the method used may be appropriate for panels which are expected to fail in a fairly brittle manner, i.e. brick/block panels and precast concrete, but for more ductile materials, such as steel, it was found that the velocities achieved were unrealistically high. The combination of this over-prediction with the assumption that, if panel failure occurs, all the panels on that particular side of the building fail, means that very conservative results are achieved for steel clad structures. In addition, for structures such as portacabins, where experience would suggest that the wall panels would fail in a fairly brittle manner at the connections giving a debris size equal to the size of the whole panel, the approach used again gave unrealistically high velocities. Consequently, the panels were assumed to break up into smaller units, even though this is not consistent with experience. This is one area within the methodology where further refinement would be worthwhile, in particular if it were to be backed up by experimental evidence.

The development of the methodology has culminated in this final phase of the project in which a total of 22 different generic building types have been assessed for occupant fatality probabilities. The results for similar buildings show similar properties, governed more by building overall geometry and internal layout than by specific details of glazing and cladding failure pressures. As an example of this, building types B3/3 and B3/4, which are identical in geometry and internal layout but have different wall construction details, show similar results, the exception being that the 50% fatality probability line is visible for B3/4 at a lower pressure than B3/3 owing to a higher debris fatality probability arising from the concrete panels in B3/4. In addition the portacabin B1/1, which is completely open plan, shows very similar results irrespective of the building orientation, whereas building type B1/2, which again is a portacabin with very similar structural details to B1/1, shows quite different results for the two different orientations owing to the presence of internal walls which are assumed to stop the travel of glass and debris.

The validation work described in Section 4 indicates, from the comparison with Hewkin [21], that the derived fatalities are too high at very low pressures. The principal factors affecting fatality probabilities at low pressures are the failure pressure of the glazing, the velocity of the glazing fragments and the fatalities associated with the flying glass. From comparison with experience, it appears that the failure pressures used for the glazing are reasonable, and hence it appears that either the fragment velocity, or the corresponding probability of fatality associated with being hit by flying glass, are too high. This is not surprising as the mass and velocities of the glazing are subject to considerable uncertainty. In addition the fatality probabilities are based on estimates of the probability of a single hit causing fatality which are subject to a high level of uncertainty.

With the exception of the control building B5/1, the behaviour of all of the buildings is governed by the assumed internal layout, with lowest fatalities achieved in the buildings which have the greatest internal area inaccessible from the outer surface of the building. The tall buildings in particular illustrate this, with the central core assumed impregnable to debris but forming a reasonably large proportion of the internal area, leading to fairly low fatality probabilities due to glazing. This sensitivity to the internal layout means that it is not possible to draw any conclusions concerning which generic type of building is the safest from the point of view of an incident blast. While the P-I diagrams derived

here may only provide some guidance to the respective risk, with sufficient engineering knowledge, the derived methodology is suitable for application to any building. Existing or proposed buildings could therefore be assessed by using the approach described here in conjunction with specific building details.



## 6. FURTHER WORK

A number of areas have been highlighted where further work might be appropriate in order either to refine the methodology or to improve the data which are used as a basis for the methodology. The principal areas highlighted are outlined below in an approximate order of priority.

The 1% fatality probability pressure-impulse curve essentially marks the onset of fatalities for the occupants of a building subject to blast loading. The 1% line is largely governed by the glazing hazard, and there are a number of uncertainties associated with the approach used to model glazing which could justifiably be investigated. The points of particular interest are as follows:

- Conditional probabilities relating to glazing impact. At present, the probability of fatality arising as a result of a specific injury, either skull fracture or skin penetration, is based on judgement, given a highly limited amount of data. It would be useful to investigate this further, taking into account military and other medical experience, with the aim of producing a more representative set of conditional probabilities
- Failure pressures and fragment masses for additional types of glazing. The data used for failure pressures and fragment characteristics for glass is based largely on the paper by Mainstone [4]. This does not cover additional types of glazing such as toughened glass, which may be used in shop fronts and leisure buildings where there is a high risk to people if the glass breaks. Further data relating to this and other types of glazing would be useful.
- Glazing velocities. The glazing fragment velocity is at present based on a single equation from Baker et al [13], which again is based on data from one type of glass only and may not relate to toughened glass. In addition, the curve rises steeply at failure, such that if the glass breaks at all it immediately travels a considerable distance into the room i.e. the equation does not predict a 'safe' breaking pressure. Further data concerning velocity profiles, in particular at or near the breaking pressure, would be very useful.

Investigation of the glazing model is a high priority for further work.

Another top priority is the characterisation of the blast pulse itself. The pressure - impulse combinations are derived from the expected profile of the blast wave as it travels away from the source of the blast, and this itself is subject to a considerable amount of uncertainty. In particular, it appears that the blast wave shocks up progressively with increasing distance, such that at intermediate distances the pulse is only partially shocked. The characterisation of the pulse in its partially shocked state and the way in which such a pulse interacts with a structure is a primary source of uncertainty which is worth studying further.

Another important area where the uncertainty is high but which is marginally lower priority than the glazing model is the debris model. Data are scarce in most of the areas of interest, but particularly in the areas of cladding modes of failure together with

fragment sizes and velocities on failure. It would be very useful to obtain results of experimental tests on cladding panels together with detailed structural analysis in order to reduce the levels of uncertainty in this area of the methodology. At present the cladding debris sizes are based on engineering judgement and historical data. The velocities have been based on an approach which has been validated against the experimental data available for glazing. For certain types of cladding which fail in a more ductile manner, it appears that this approach may not be appropriate, as it can lead to very high fragment velocities. Refining the approach used for such cladding types would be worthwhile. Further data on the probability of human fatality due to cladding impact would also be very useful, either based on information from actual explosion events, or based on a more informed assessment of existing data.

Failure of glazing and cladding panels is governed by the differential pressure across the walls of the building, which in turn is determined by the external and the internal pressures. At present the approach used to determine the internal pressure is very crude, being based on the average pressure increase inside a void equal in size to the volume of the building. Clearly the presence of internal walls will disrupt the travel of the pulse into the building, and the use of such an averaging approach could lead to inaccuracies, particularly in the prediction of whether glazing/cladding is blown in or out of the structure. In order to improve the approach, it would be necessary to investigate the effect of the internal layout of the structure and the way in which the blast pulse travels through the structure.

Finally, there are a number of aspects which are of lower priority but which would be useful when considering the application of the approach to actual urban layouts. These are as follows:

- Development of the model to include the effects of the negative phase of the blast pulse. Although the sensitivity of the structural response to inclusion of the negative phase of the blast pulse was investigated in Phase 3, the sensitivity of the overall probability of fatality was not assessed. It would be useful to investigate the characteristics of the negative phase and to apply this to the model. In addition, the effects of the negative phase on structures such as shopping centres, where there may be significant numbers of people 'outside' the main body of the building, could be significant.
- Congestion between buildings. At present, the model is based on the assumption that the building experiences a load calculated assuming that it is isolated in an open space. Historical evidence suggests that the actual pressures experienced by buildings may be enhanced or reduced by the presence of other buildings in the vicinity. For the approach outlined here to be used for an urban assessment, it would be necessary to take this congestion effect into account. In addition, it would be useful to investigate the effects of local topography and vegetation on the blast wave form and the corresponding effect on the assessment.
- Model uncertainty. The development of the methodology has been very much based on assumptions, estimations and engineering judgement. Consequently there are

many parts of the methodology which are subject to uncertainty. There may be scope for developing the approach using probabilistic techniques to assess and incorporate the uncertainty in the predictions.

Although a wide range of buildings has been covered in this report, there will always be buildings which do not fit into any of the categories used here. In these cases, it would be necessary to assess buildings individually, based on their construction details and internal layouts. If this were regularly found to be the case, it would be useful to have a PC based tool for performing the assessment which is more user friendly than the methods used at present. It would be feasible to develop such a model to produce P-I diagrams based on a user input of building characteristics.

## 7. REFERENCES

1. 'Derivation of Fatality Probability Functions for Occupants of Buildings Subject to Blast Loads - Interim Report (Phase 1) WS Atkins Science & Technology, October 1995
2. 'Derivation of Fatality Probability Functions for Occupants of Buildings Subject to Blast Loads - Interim Report (Phases 2 and 3) WS Atkins Science & Technology, July 1996
3. Puttock, J.S. 'Fuel Gas Explosion Guidelines - the Congestion Assessment Method', IChemE Symposium Series No.139, 1995
4. 'The Breakage of Glass Windows by Gas Explosions', Mainstone, R.J., Building Research Station Current Paper, CP 26/71, September 1971
5. 'Introduction to Structural Dynamics', Biggs, J.M., McGraw Hill Book Company, New York, 1964
6. 'Methods for the Determination of Possible Damage', CPR 16E, TNO 1992
7. 'Fundamentals of Protective Design for Conventional Weapons', TM 5-855-1, Technical Manual, Headquarters, Department of the Army, November, 1986
8. 'Loss Prevention in the Process Industries. Volume 1', Lees, F.P., Butterworths, 1989
9. 'Airblast Effect on Windows in Buildings and Automobiles on the Eskimo II event', Fletcher, E.K., Richmond, D.R. and Jones, R.K., Minutes of the Department of Defence Explosives Safety Seminar (15th), 1973
10. 'Airblast Effect on Windows in Buildings and Automobiles on the Eskimo III event', Fletcher, E.K., Richmond, D.R. and Richmond, D.W., Minutes of the Department of Defence Explosives Safety Seminar (16th), September, 1974
11. 'Glass Fragment Hazard from Windows Broken by Airblast', Fletcher, Richmond and Yelverton, Lovelace Biomedical and Environmental Research Institute (1980)
12. 'Dynamic Failure Pressure and Fragmentation of Thermally Hardened Window Panes', Nowee, J., TNO Report No. PML 1985 - C - 103, 1985
13. 'Explosion Hazards and Evaluation', Baker, W.E., Cox, P.A., Westine, P.S., Kulesz, J.J. and Strehlow, R.A., Elsevier Scientific Publishing Company, Oxford, 1983.
14. 'Fragment Hazard Criteria', Feinstein, D.I., Minutes of the Department of Defence Explosives Safety Seminar, 1971
15. 'Physical Fluid Dynamics', Tritton, D.J., Oxford Science Publications, 1988

16. 'Interim Handbook for Security Glazing', Meyers, G.E. and Becker, R.P., DOE Technical Memorandum 5603 TM., Naval Civil Engineering Laboratory, Port Hueneme, California 93043, USA, September, 1987.
17. 'Interim Design Criteria and Acceptance Test Specifications for Blast Resistant Windows', Meyers, G.E., The Shock and Vibration Bulletin, Bulletin 56, Part 1, August, 1986
18. 'Security Design Criteria for Embassy Construction', Meyers, G.E., US Department of State Bureau of Diplomatic Security
19. 'Guidelines for Evaluating the Characteristics of Vapour Cloud Explosions, Flash Fires, and BLEVEs', Centre for Chemical Process Safety of the American Institute of Chemical Engineers, 1994.
20. 'Derivation of the British Explosives Safety Distances', Jarrett, D.E., Annals of the New York Academy of Sciences, 1968
21. 'Consequences of Pressure Blast - the probability of fatality inside buildings', Hewkin, D.J., US DoD Explosives Safety Seminar, Anaheim, CA, 18-20 August, 1992.
22. 'The Multi-Energy Method. A Framework for Vapour Cloud Explosion Blast Prediction', Van den Berg, A.C., Journal of Hazardous Materials, 1984
23. 'The Characteristics of the explosion of Cyclohexane at the Nypro (UK) Flixborough Plant on 1<sup>st</sup> June, 1974', Sadee, C., Samuels, D.E. and O'Brien, T.P., Journal of Occupational Accidents, 1 (1976/1977) 203-235
24. 'The Effects of Nuclear Weapons', Glasstone, S. and Dolan, P.J., 3<sup>rd</sup> Ed., 1977
25. 'Gas Explosions in Load-Bearing Brick Structures', Astbury, N.F., West, H.W.H., Hodgkinson, H.R., Cabbage, P.A. and Clare, R., Jan., 1971.
26. 'Development of Validated Predictive Methods so that the Response of Buildings and Structures Subjected to the Effects Arising from Vented Dust Explosions can be Assessed', Colwell, S. And Crowhurst, D., CREDIT Project Final Report, Contract No. EV5V-CT92-0082
27. 'Some Considerations on the Damage Criteria and Safety Distances for Industrial Explosions', Mercx, W.P.M., Weerheijm, J. And Verhagen, Th.L.A., IChemE Symposium Series No 124 pp 255 - 275
28. 'An approach to the Categorisation of Process Plant Hazard and Control Building Design', Prepared by Working Group 3 of the Major Hazards Steering Group, Issued by the Safety Committee of the Chemical Industry Safety and Health Council of the Chemical Industries Association
29. 'Major Chemical Hazards', Marshall, V.C., Chichester: Ellis Horwood, 1987

30. 'Guidelines for Evaluating Process Plant Buildings for External Explosions and Fires', AIChE/CCPS, 1996
31. 'Guidance for the location and design of occupied buildings on chemical manufacturing sites', Chemical Industries Association, to be published.
32. 'British Standard Code of Practice for Design of non-loadbearing external vertical enclosures of buildings', BS8200: 1985
33. 'British Standard Code of Practice for Sheet Roof and Wall Coverings Part 1: Aluminium, corrugated and troughed', CP 143: Part 1: 1958
34. 'British Standard Code of Practice for Sheet Roof and Wall Coverings Part 10: Galvanised corrugated steel. Metric units', CP 143: Part 10: 1973
35. 'British Standard Code of Practice for Sheet Roof and Wall Coverings Part 14: Corrugated asbestos-cement', BS 5247 Part 14: 1975
36. 'British Standard Code of Practice for Design and installation of non-loadbearing precast concrete cladding', BS 8297: 1995
37. 'British Standard Structural use of concrete Part 1: Code of practice for design and construction', BS 8110: Part 1: 1985
38. 'British Standard Structural use of steelwork in building Part 5: Code of practice for design of cold-formed structures', BS 5950: Part 5: 1987
39. 'British Standard Code of Practice for use of masonry Part 1: Structural use of unreinforced masonry', BS 5628: Part 1: 1992
40. 'British Standard Structural use of timber Part 2: Code of practice for permissible stress design, materials and workmanship', BS 5268: Part 2: 1991
41. 'Formulas for Natural Frequency and Mode Shape', Blevins, R.D., Van Nostrand Reinhold Company, 1979.

**APPENDIX A**  
**Generic Building Calculations**

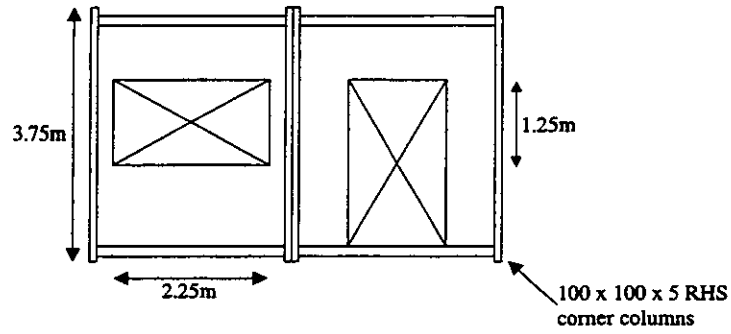
**CONTENTS**

<b>A.1. BUILDING TYPE B1: PORTACABINS .....</b>	<b>2</b>
<b>A.2. BUILDING TYPE B2: BRICK BUILDINGS.....</b>	<b>15</b>
<b>A.3. BUILDING TYPE B3: CONCRETE FRAMED BUILDINGS .....</b>	<b>40</b>
<b>A.4. BUILDING TYPE B4: STEEL FRAMED BUILDINGS.....</b>	<b>64</b>
<b>A.5. BUILDING TYPE B5: HARDENED STRUCTURE .....</b>	<b>99</b>
<b>A.6. BUILDING TYPE T: TALL BUILDINGS .....</b>	<b>106</b>
<b>A.7. BUILDING TYPE L: LONG SPAN BUILDINGS.....</b>	<b>125</b>

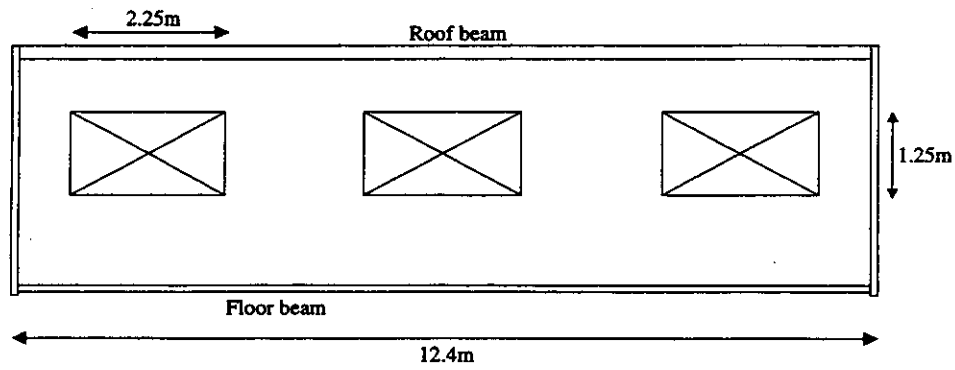
## **A.1. Building Type B1: Portacabins**



**Side elevation**



**Front elevation**



**Plan**

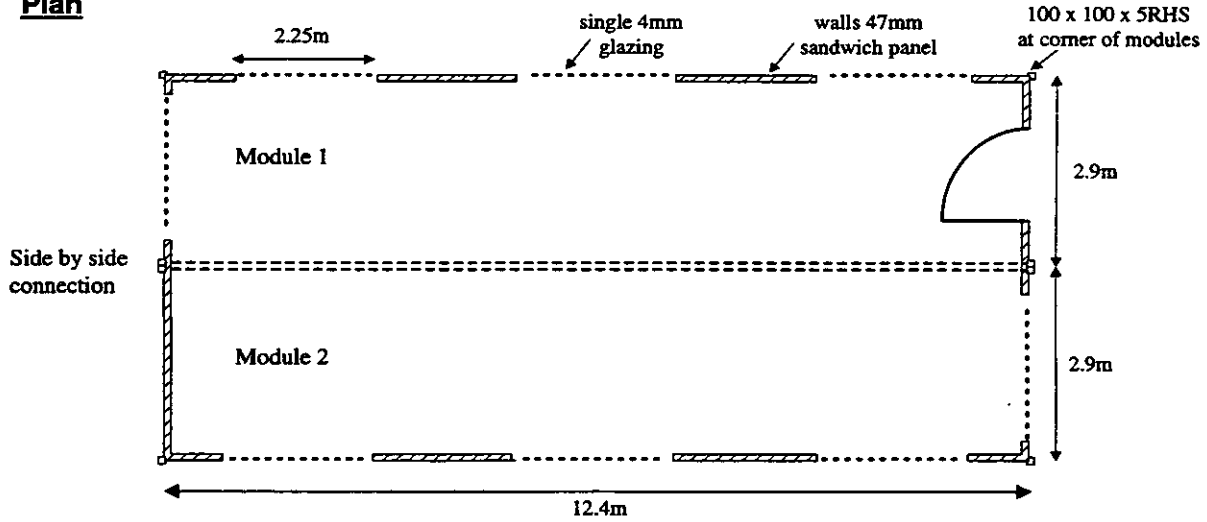
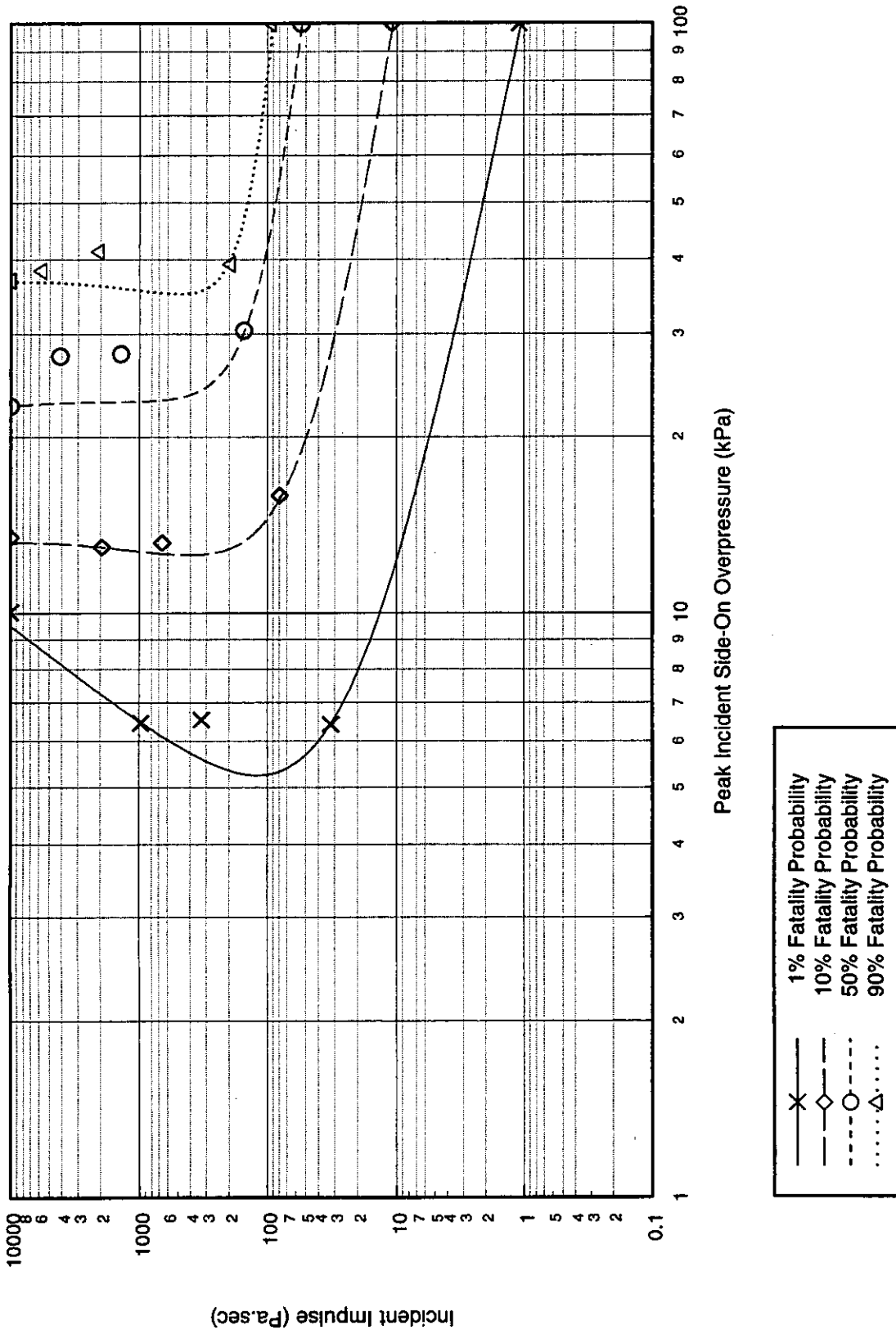


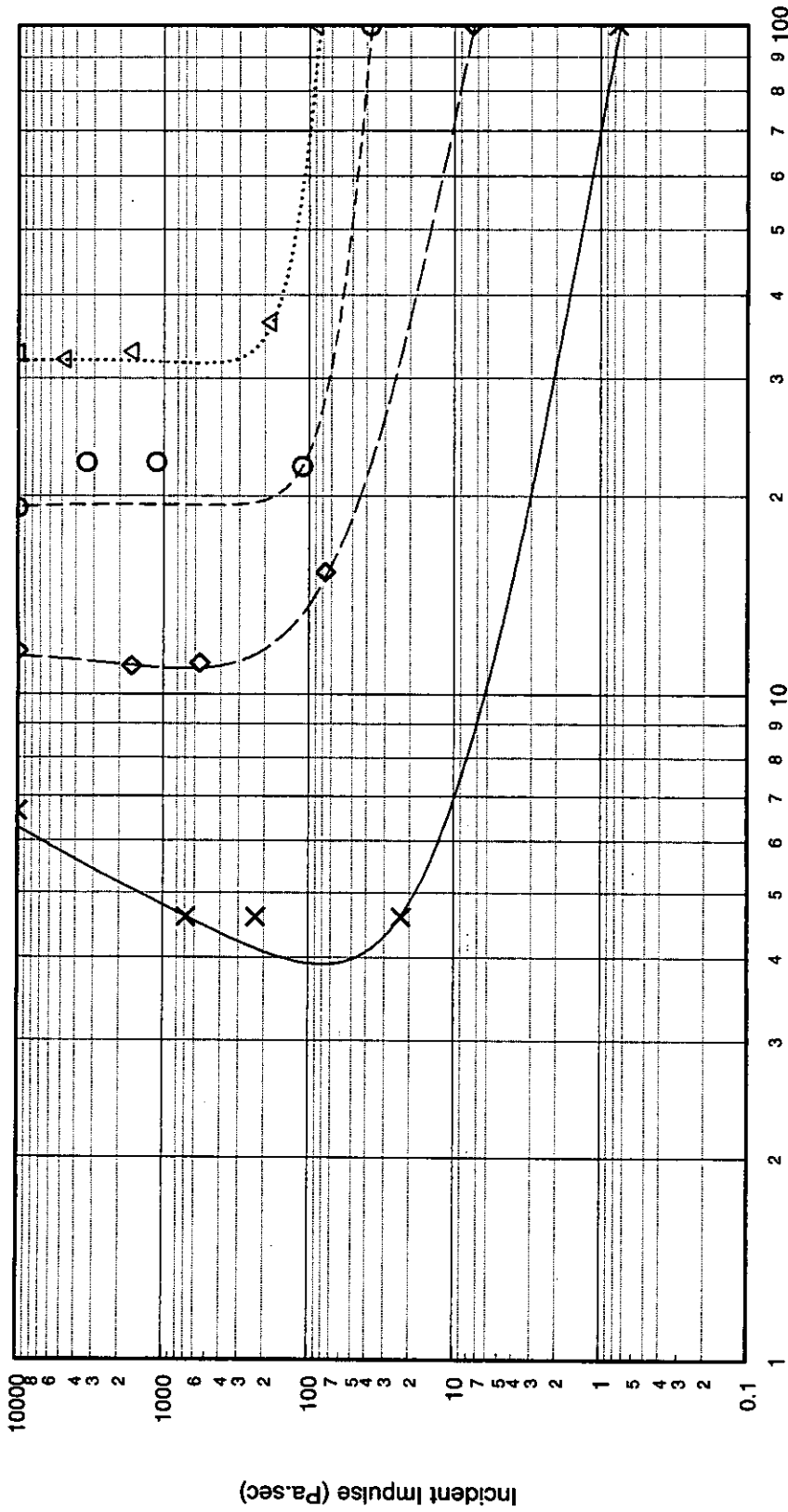
**Figure A.1: Illustration of Portacabin Type B1/1**

Quantity	Value	Comments
<b>Building Type: B1/1</b>		
Description	Portacabin Single storey, single span, 2 module unit Aspect ratio 2:1	Module sizes typical values taken from manufacturer's literature
<b>Global Dimensions</b>		
Breadth	5.9m	
Length	12.4m	
Height	3.75m	
<b>Glazing Characteristics</b>		
Thickness	4mm - single glazed	
Max. Pane dimensions	2.25 x 1.25m	
Failure Pressure (1 sec pulse duration)	30 mbar	Mainstone [4]
<b>Cladding/Wall Panel Characteristics</b>		
Thickness	47mm sandwich panel	Softwood frame, 12.5mm plasterboard internal skin, 0.6mm plastic coated steel sheet outer skin, insulating core
Panel Dimensions	2.9 x 3.75m	
Dynamic Failure Pressure	174 mbar	Failure of panels most likely to occur at connections, consequently failure pressure is assumed to correspond to the frame failure pressure. Experimental data gives a value of 65mbar at which 90% recovery from deformation occurs
Support Conditions	Simply supported on all 4 sides	
Ductility	2.5	
Debris Size	1.0 x 1.0 x 0.047m	Debris size has been chosen to be the largest size consistent with a realistic velocity: above this size, velocities increase dramatically according to the Baker unconstrained fragment approach.
<b>Frame Details</b>		
Frame Type	Steel RHS framework, 100x100x5 columns with channel section beams at roof and floor	
Dynamic Failure Pressure	174 mbar	Frame has been checked under combined axial and lateral loading
Ductility	5	
<b>Additional Information</b>		
Overturning and sliding of the modules have also been considered, but have been discounted as a primary mode of fatality primarily because glazing and panel failure is likely to occur first, relieving the load on the structure.		

P-I Diagram: B1/1, Shock Pulse, Short Side Facing Blast

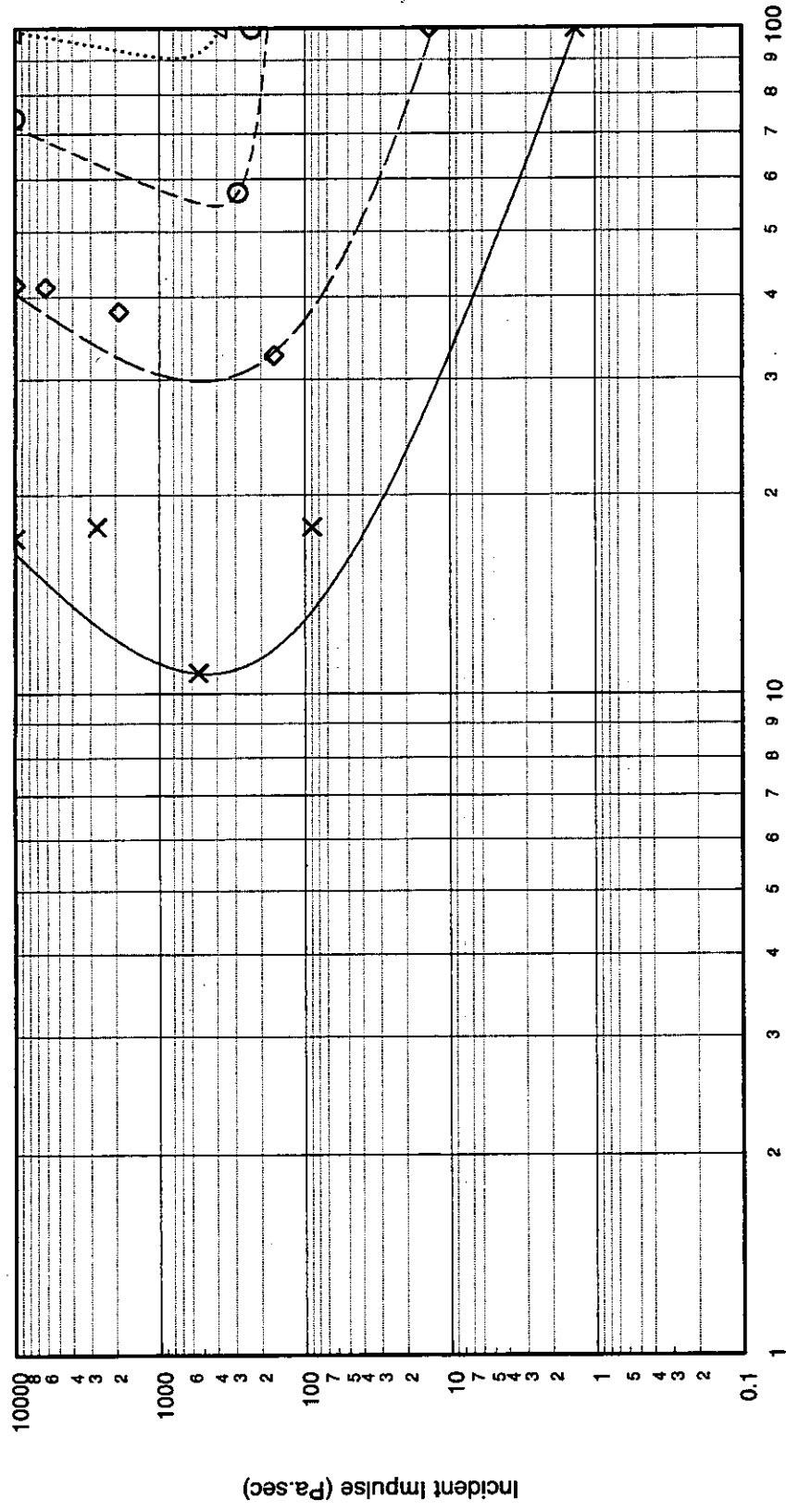


P-I Diagram: B1/1, Shock Pulse, Long Side Facing Blast



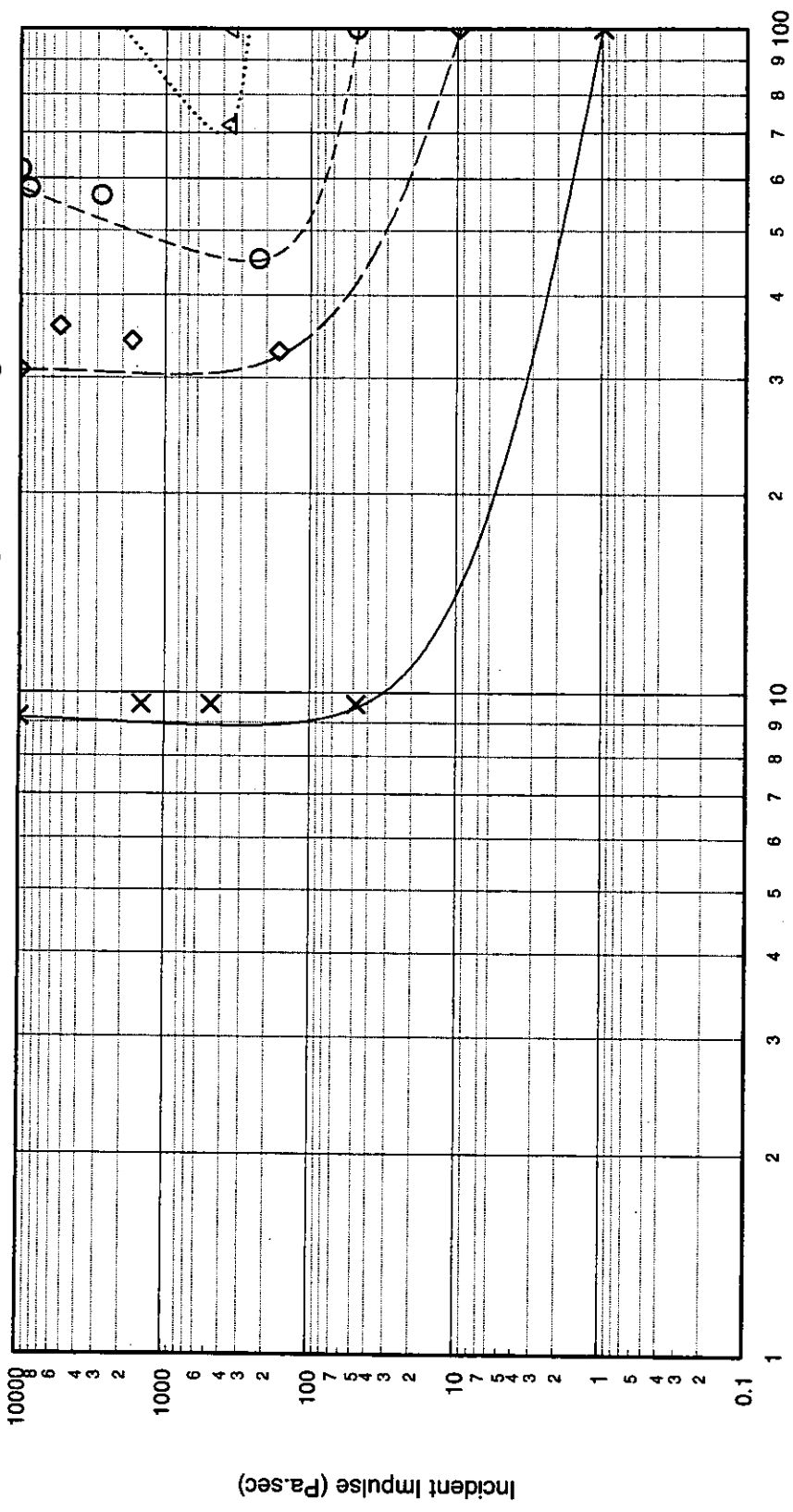
X — 1% Fatality Probability  
 —◇— 10% Fatality Probability  
 - - -○- - - 50% Fatality Probability  
 .....△..... 90% Fatality Probability

P-I Diagram: B1/1, Pressure Pulse, Short Side Facing Blast

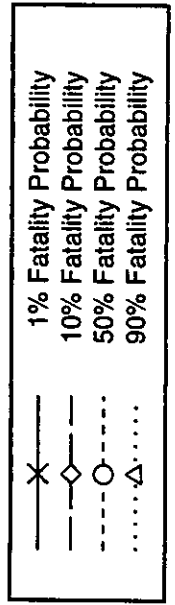


X — 1% Fatality Probability  
 —◇— 10% Fatality Probability  
 - - -○- - - 50% Fatality Probability  
 .....△..... 90% Fatality Probability

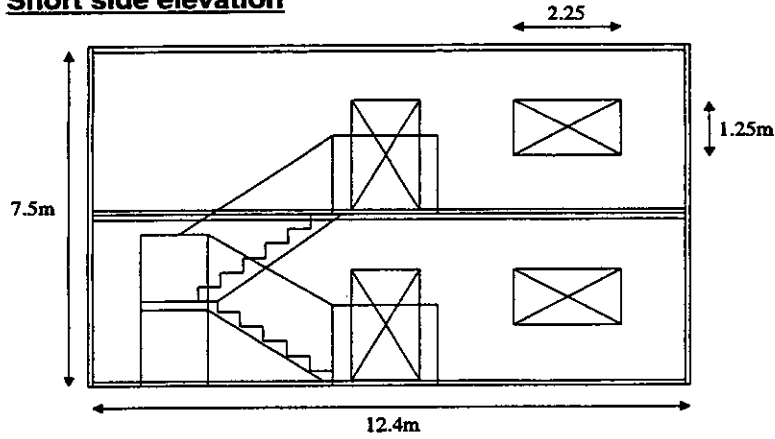
P-I Diagram: B1/1, Pressure Pulse, Long Side Facing Blast



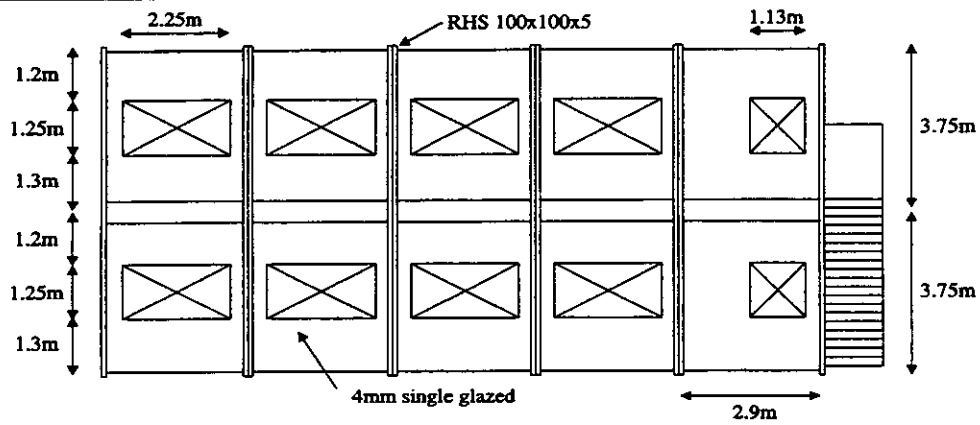
Peak Incident Side-On Overpressure (kPa)



**Short side elevation**



**Side elevation**



**Plan of ground floor**

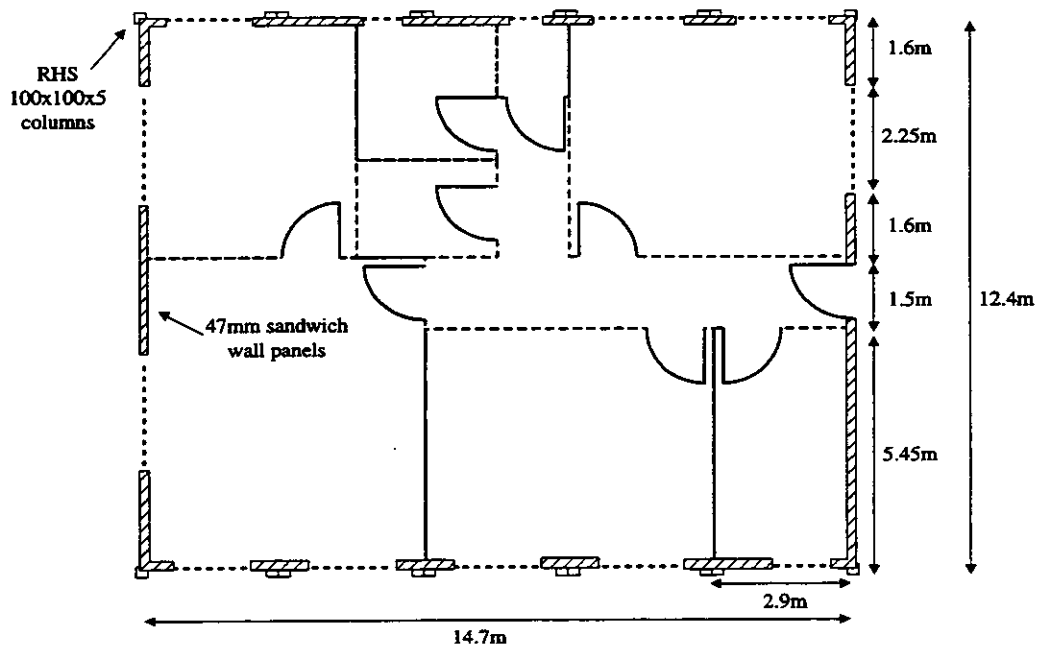
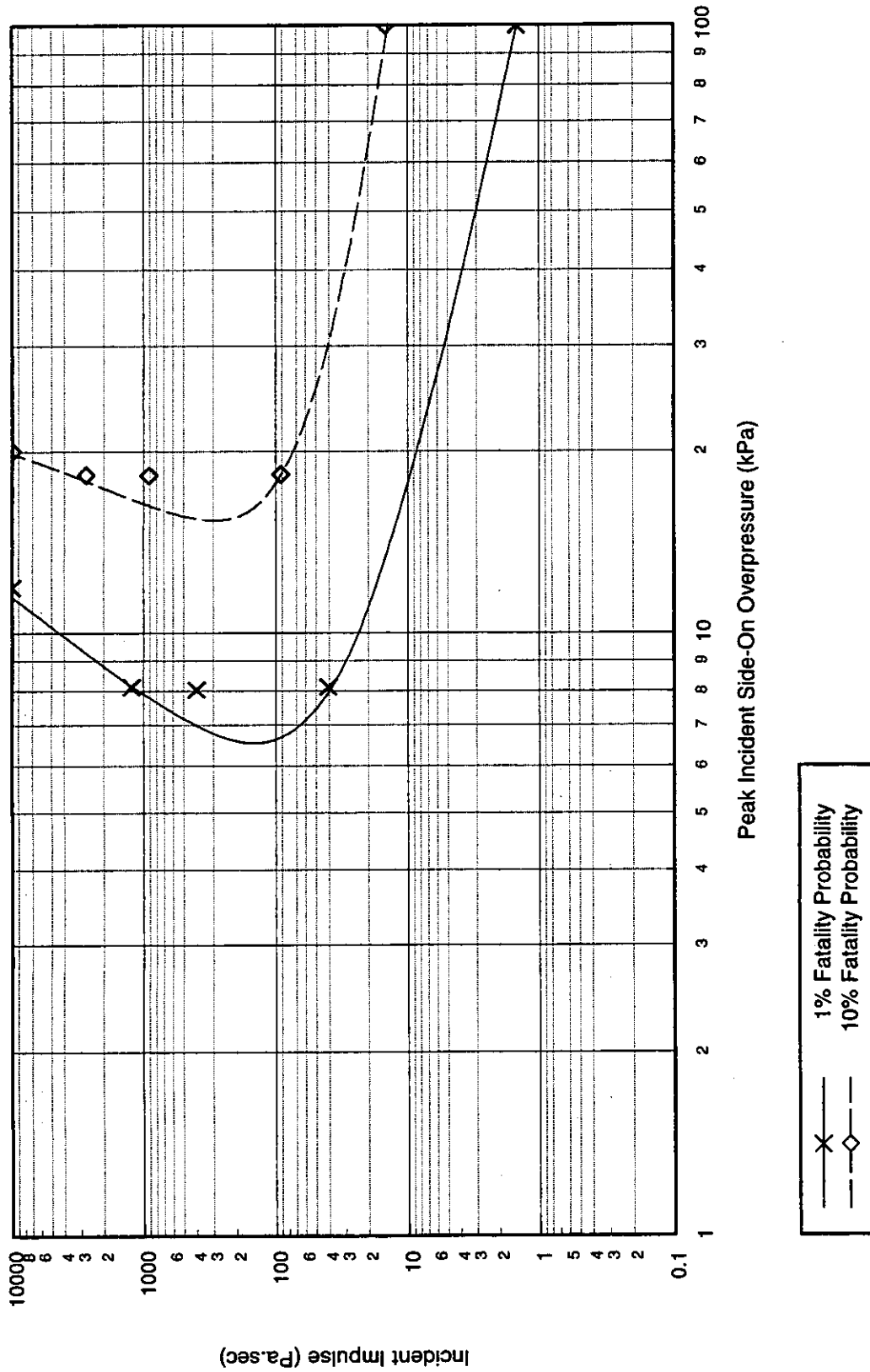


**Figure A.2: Illustration of Portacabin Type B1/2**

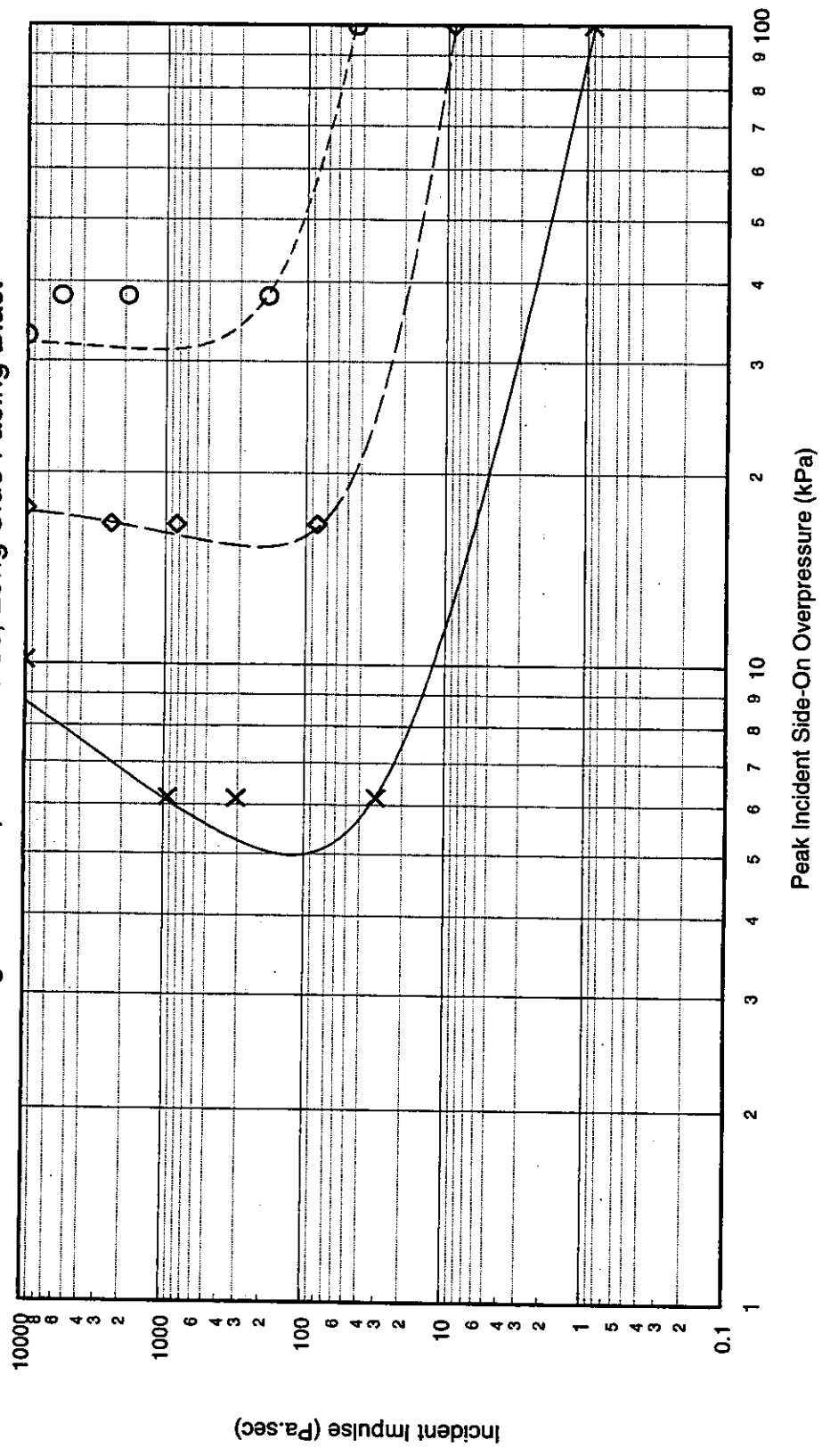
Quantity	Value	Comments
<b>Building Type: B1/2</b>		
Description	Portacabin Two storey structure constructed from 10 single span modules Aspect ratio 1:1	Module sizes typical values taken from manufacturer's literature
<b>Global Dimensions</b>		
Breadth	12.4m	
Length	14.7m	
Height	7.5m	
<b>Glazing Characteristics</b>		
Thickness	4mm - single glazed	
Max. Pane dimensions	2.25 x 1.25m	
Failure Pressure (1 sec pulse duration)	30 mbar	Mainstone [4]
<b>Cladding/Wall Panel Characteristics</b>		
Thickness	47mm sandwich panel	Softwood frame, 12.5mm plasterboard internal skin, 0.6mm plastic coated steel sheet outer skin, insulating core
Panel Dimensions	2.9 x 3.75m	
Dynamic Failure Pressure	92 mbar	Failure of panels most likely to occur at connections, consequently failure pressure is assumed to correspond to the frame failure pressure. Experimental data gives a value of 65mbar at which 90% recovery from deformation occurs
Support Conditions	Simply supported on all 4 sides	
Ductility	2.5	
Debris Size	1.0 x 1.0 x 0.047m	Debris size has been chosen to be the largest size consistent with a realistic velocity: above this size, velocities increase dramatically according to the Baker unconstrained fragment approach.
<b>Frame Details</b>		
Frame Type	Steel RHS framework, 100x100x5 columns with channel section beams at roof and floors	
Dynamic Failure Pressure	92 mbar	Frame has been checked under combined axial and lateral loading - failure is lower for B1/2 than B1/1 as there is greater compression in the columns
Ductility	5	
<b>Additional Information</b>		
Overturning and sliding of the modules have also been considered, but have been discounted as a primary mode of fatality primarily because glazing and panel failure is likely to occur first, relieving the load on the structure.		



P-I Diagram: B1/2, Shock Pulse, Short Side Facing Blast

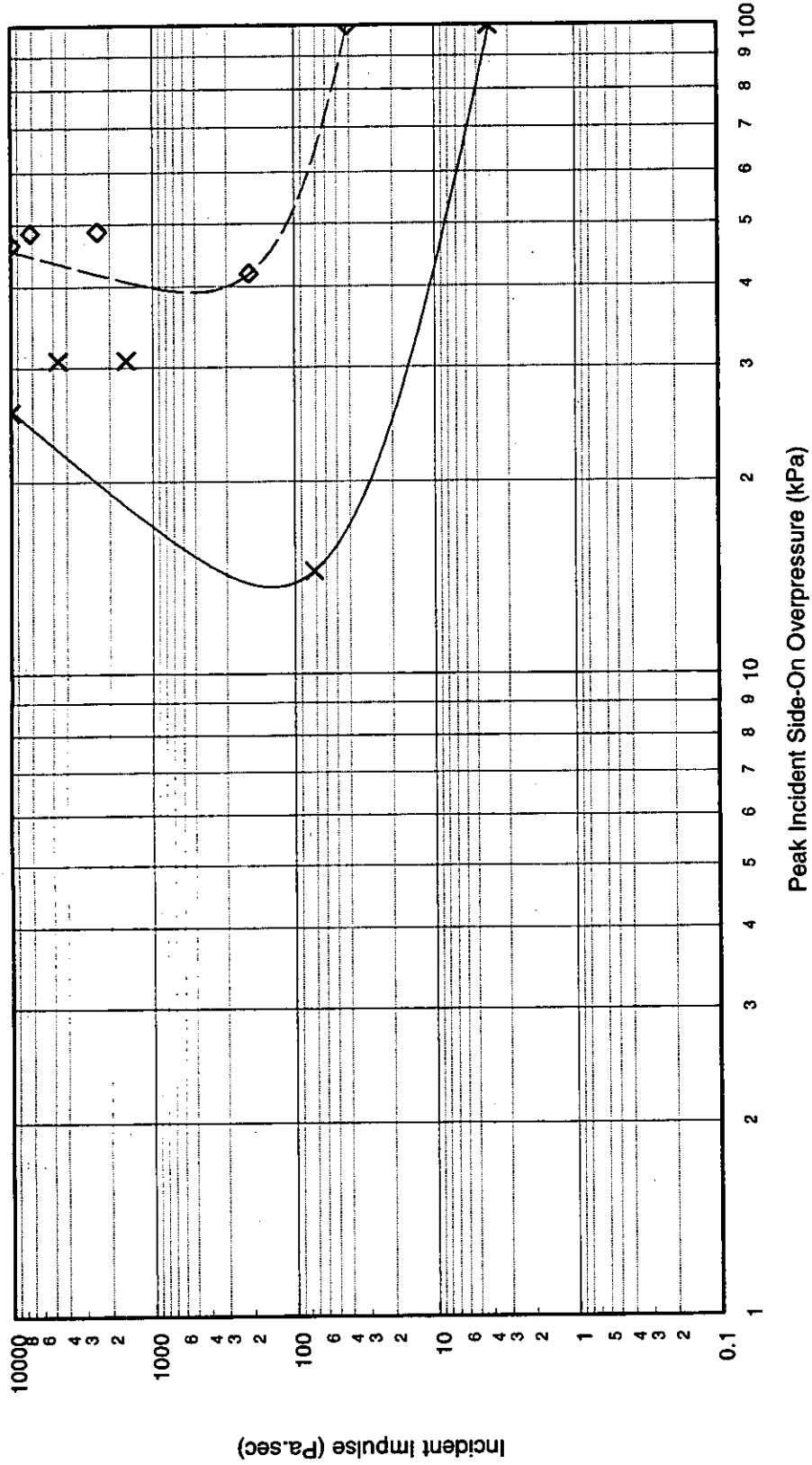


P-I Diagram: B1/2, Shock Pulse, Long Side Facing Blast



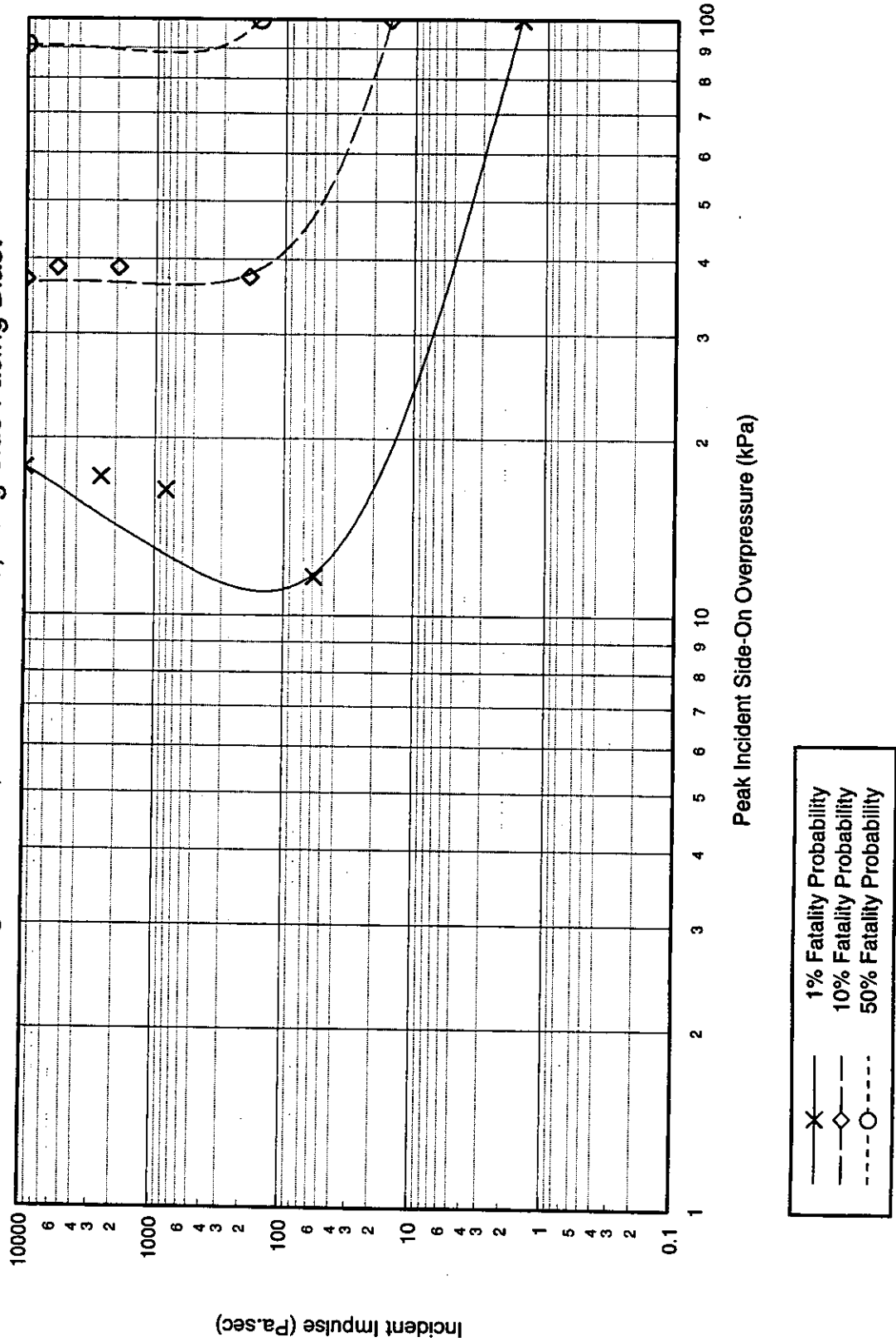
- X 1% Fatality Probability
- ◇ 10% Fatality Probability
- 50% Fatality Probability

P-I Diagram: B1/2, Pressure Pulse, Short Side Facing Blast



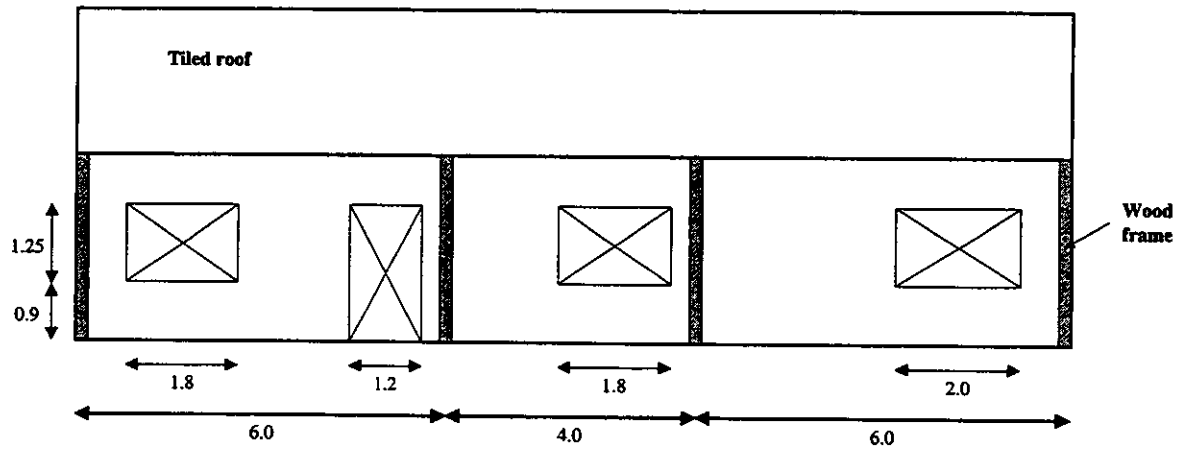
x ——— 1% Fatality Probability  
 ———◇—— 10% Fatality Probability

P-I Diagram: B1/2, Pressure Pulse, Long Side Facing Blast

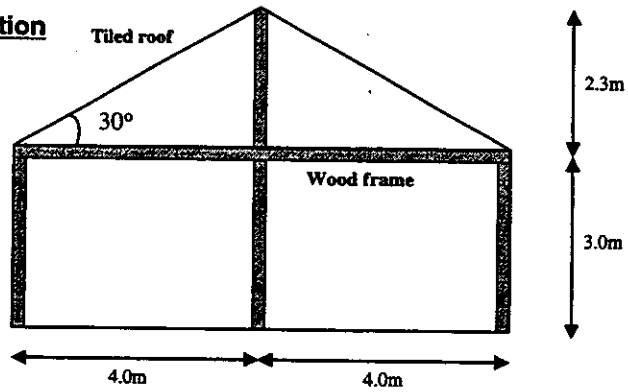


**A.2. Building Type B2: Brick Buildings**

**Front elevation**



**Side elevation**



**Plan**

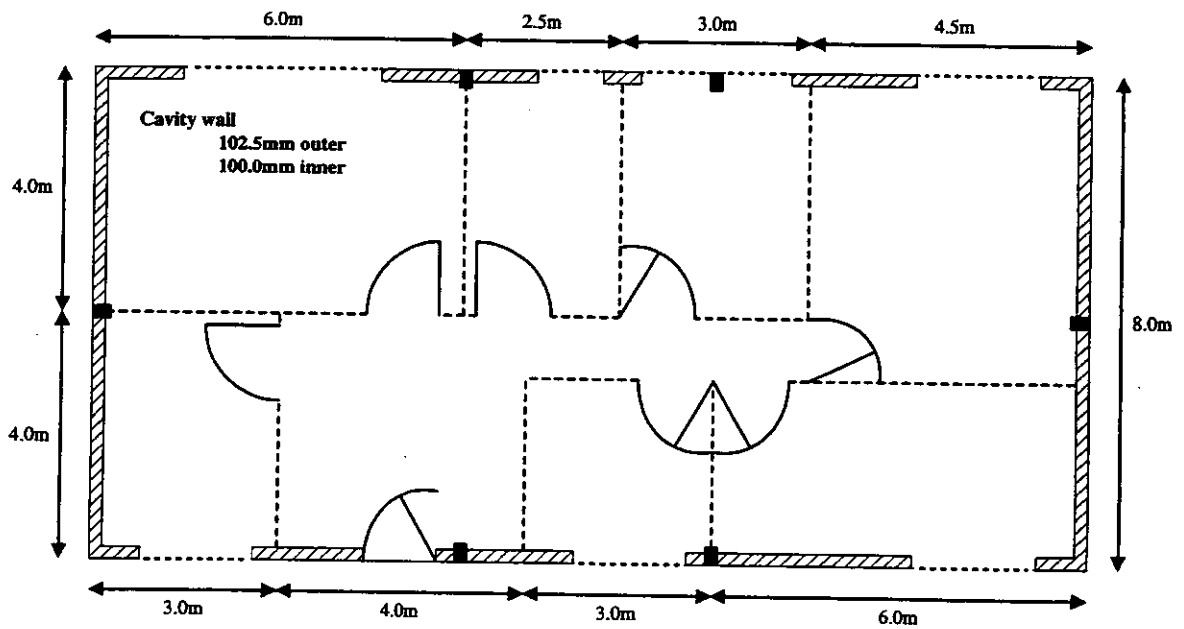
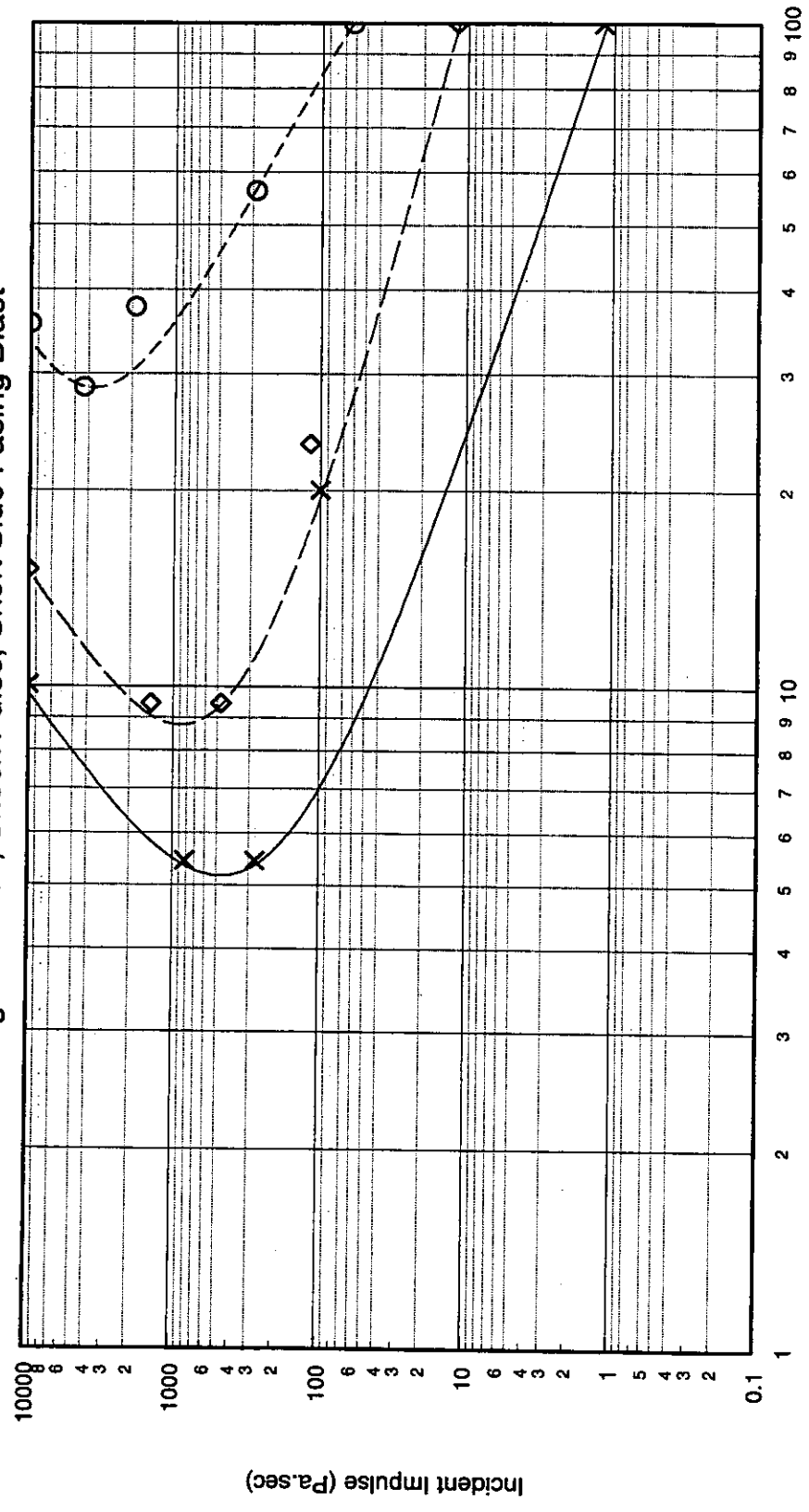


**Figure A.3: Illustration of Brick Building Type B2/1**

Quantity	Value	Comments
<b>Building Type: B2/1</b>		
Description	Brick bungalow Timber framed structure with brick/block walls Aspect ratio 2:1	
<b>Global Dimensions</b>		
Breadth	8.0m	
Length	16.0m	
Height	5.3m	
<b>Glazing Characteristics</b>		
Thickness	4mm - single glazed	
Max. Pane dimensions	0.7 x 1.25m	
Failure Pressure (1 sec pulse duration)	55 mbar	Mainstone [4]
<b>Cladding/Wall Panel Characteristics</b>		
Thickness	0.203m	Brick/block cavity wall panels, 102.5mm brick outer skin with 100mm blockwork inner
Panel Dimensions	4.0 x 3.0m	
Dynamic Failure Pressure	160 mbar	The failure pressure was originally calculated as 87mbar (load to initiate cracking). However a comparison with historical/experimental data [CREDIT] suggested that a value of 160mbar would be more appropriate - this is the pressure at which displacement of internal blockwork was observed.
Support Conditions	Simply supported on all 4 sides	
Ductility	5	
Debris Size	75 x 225 x 112.5 mm	This is approximately equivalent to the size of a single brick
<b>Frame Details</b>		
Frame Type	Timber frame	
Dynamic Failure Pressure	160 mbar	It is assumed that the frame has been designed to be capable of carrying the full capacity of the panels. Consequently the frame failure pressure has been assumed to be the same as that of the panels.
Ductility	10	
<b>Additional Information</b>		

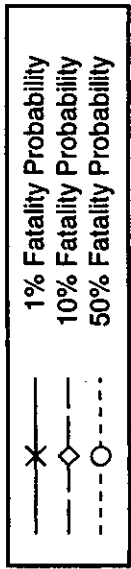
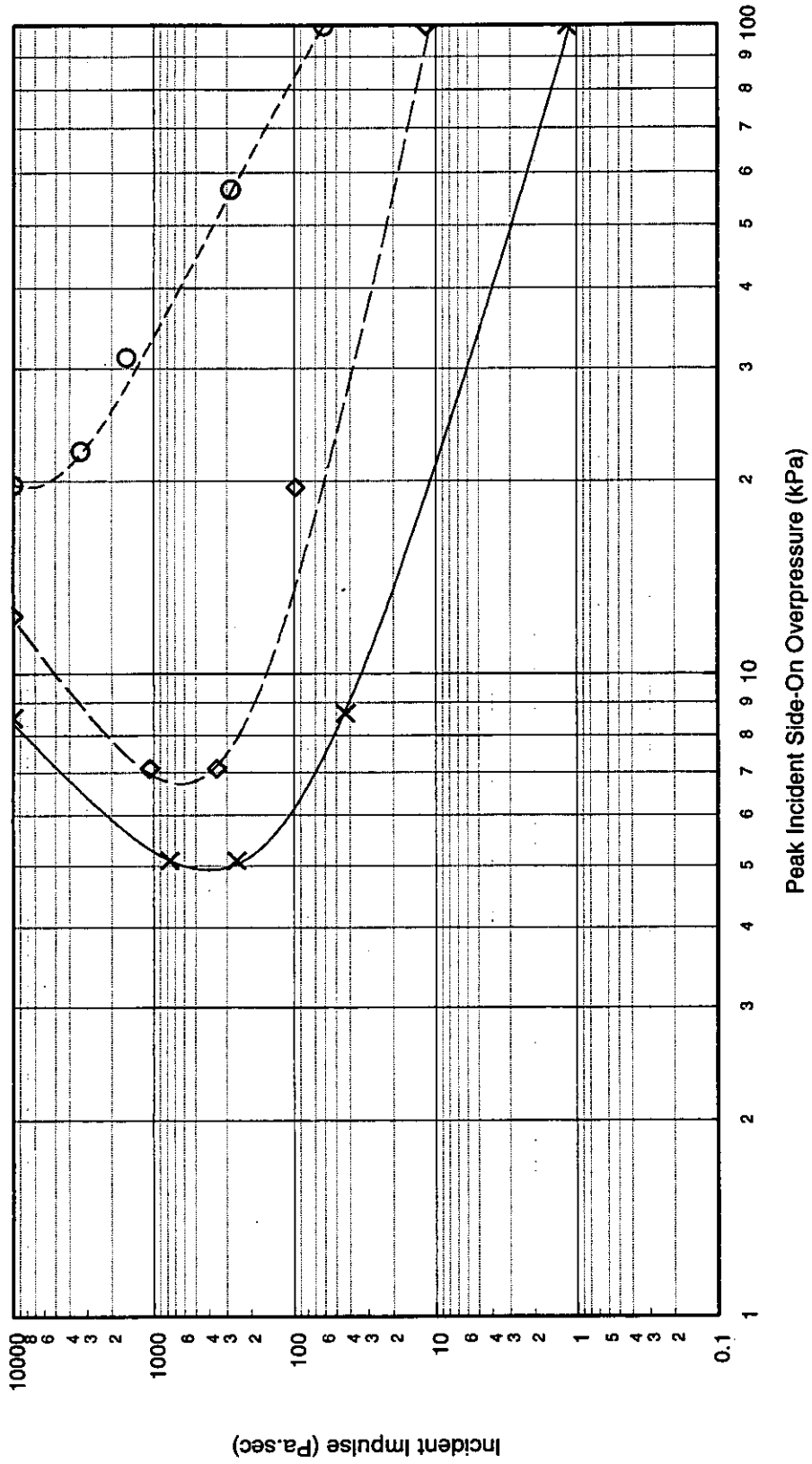
P-I Diagram: B2/1, Shock Pulse, Short Side Facing Blast



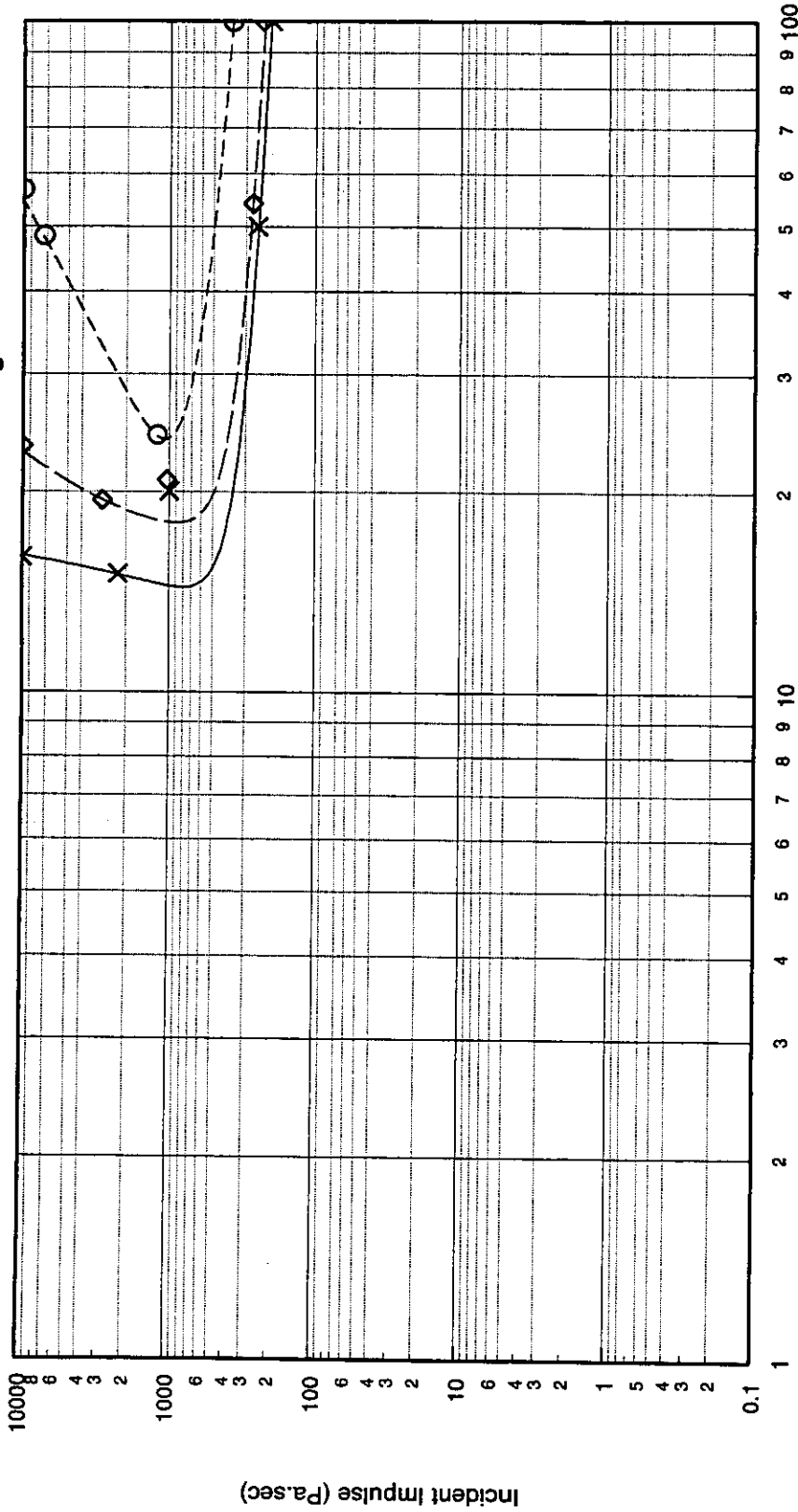
- x — 1% Fatality Probability
- - - ◊ - - 10% Fatality Probability
- · · · · ○ · · · · 50% Fatality Probability



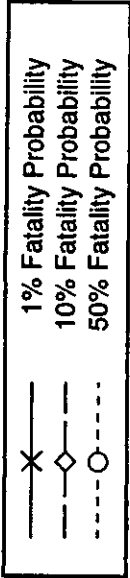
P-I Diagram: B2/1, Shock Pulse, Long Side Facing Blast



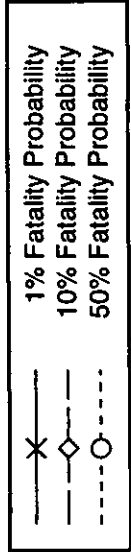
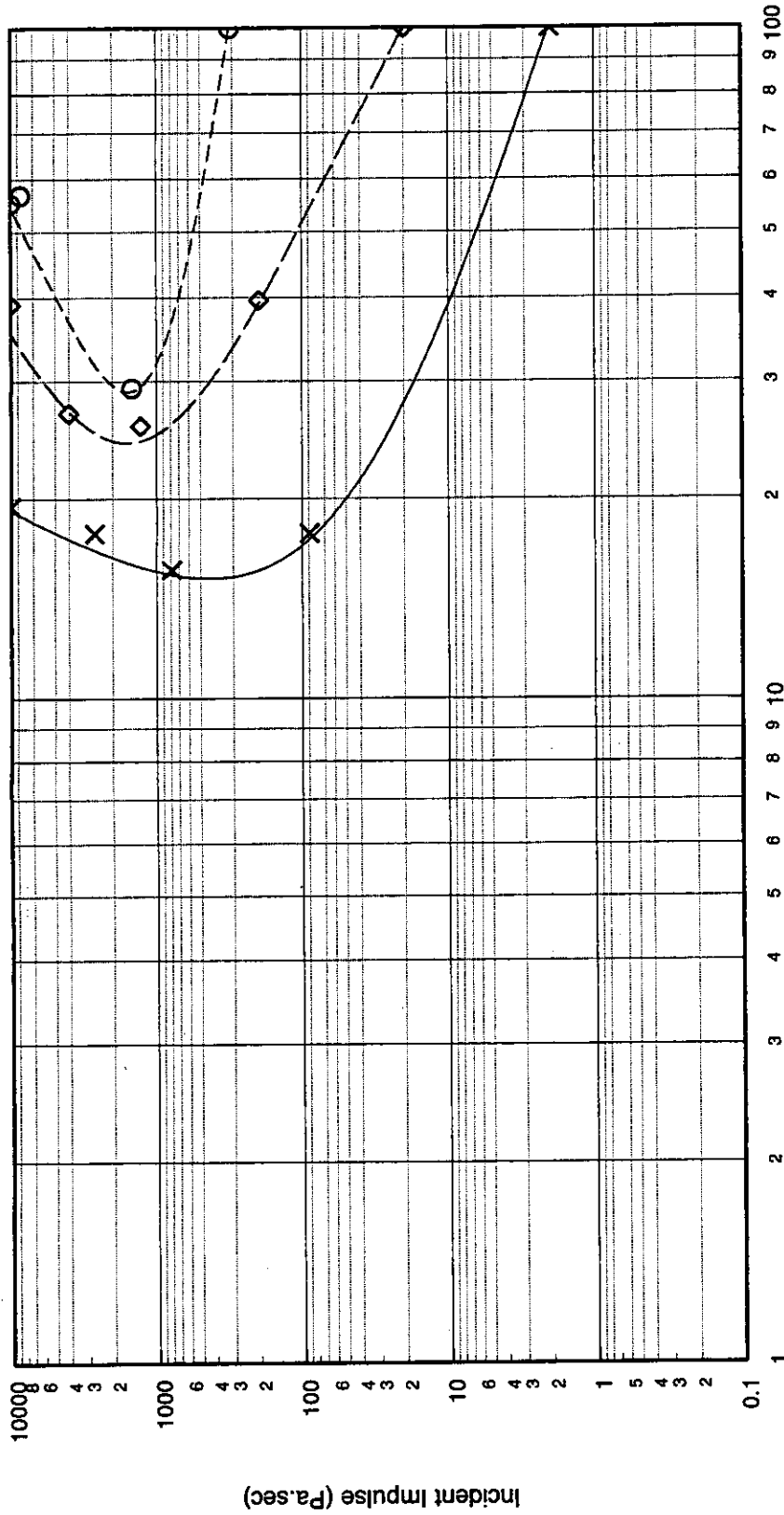
P-I Diagram: B2/1, Pressure Pulse, Short Side Facing Blast

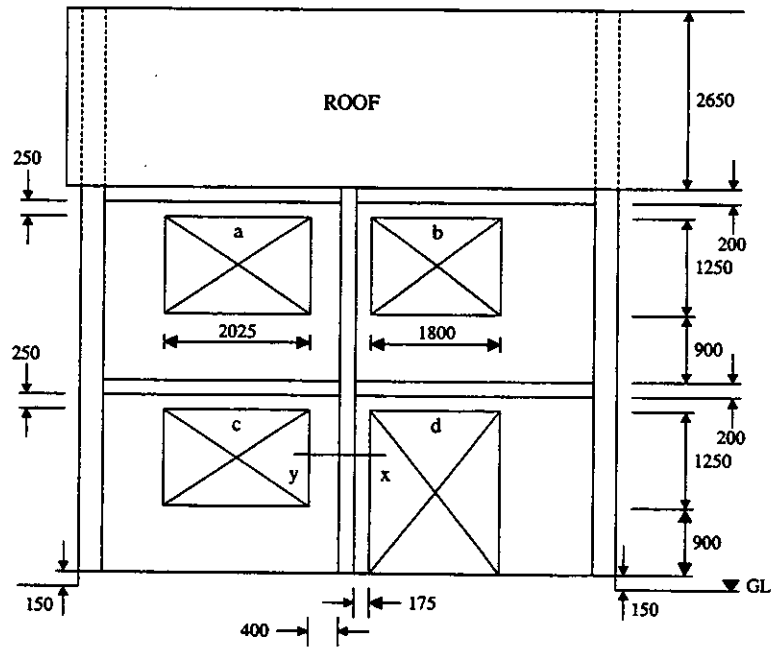


Peak Incident Side-On Overpressure (kPa)

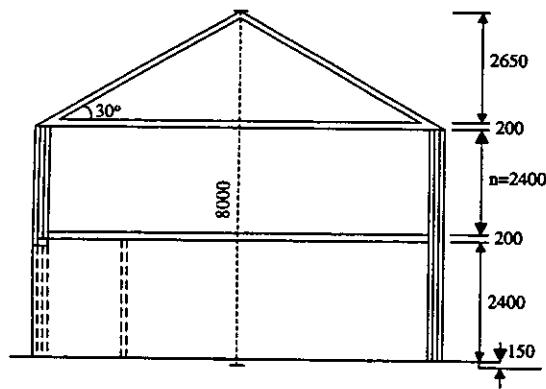


P-I Diagram: B2/1, Pressure Pulse, Long Side Facing Blast

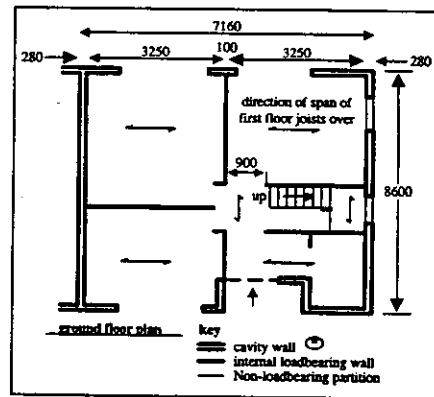




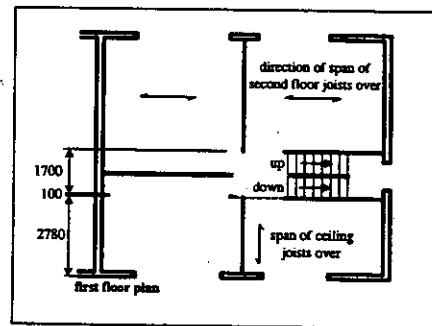
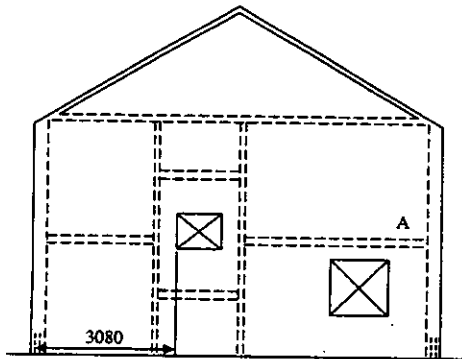
Side Elevation



Short Side Elevation



Recent construction  
 Solid wall for the older 1930's example (not shown)

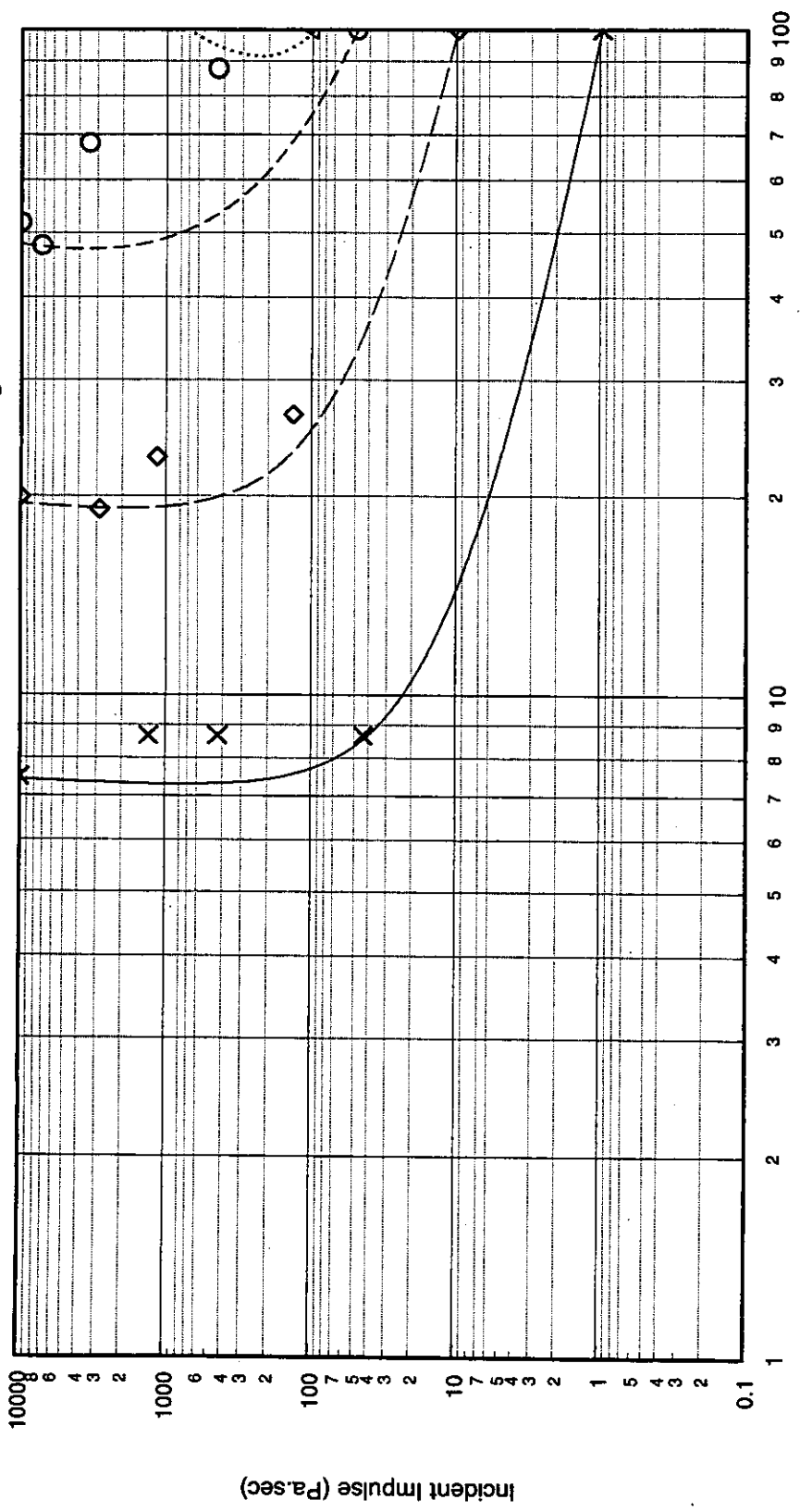


Roof  
 (Plan not shown)  
 Dual pitch trussed rafter spanning of roof front-to-back, ridge line at centre

Figure A.4: Illustration of Brick Building Type B2/2

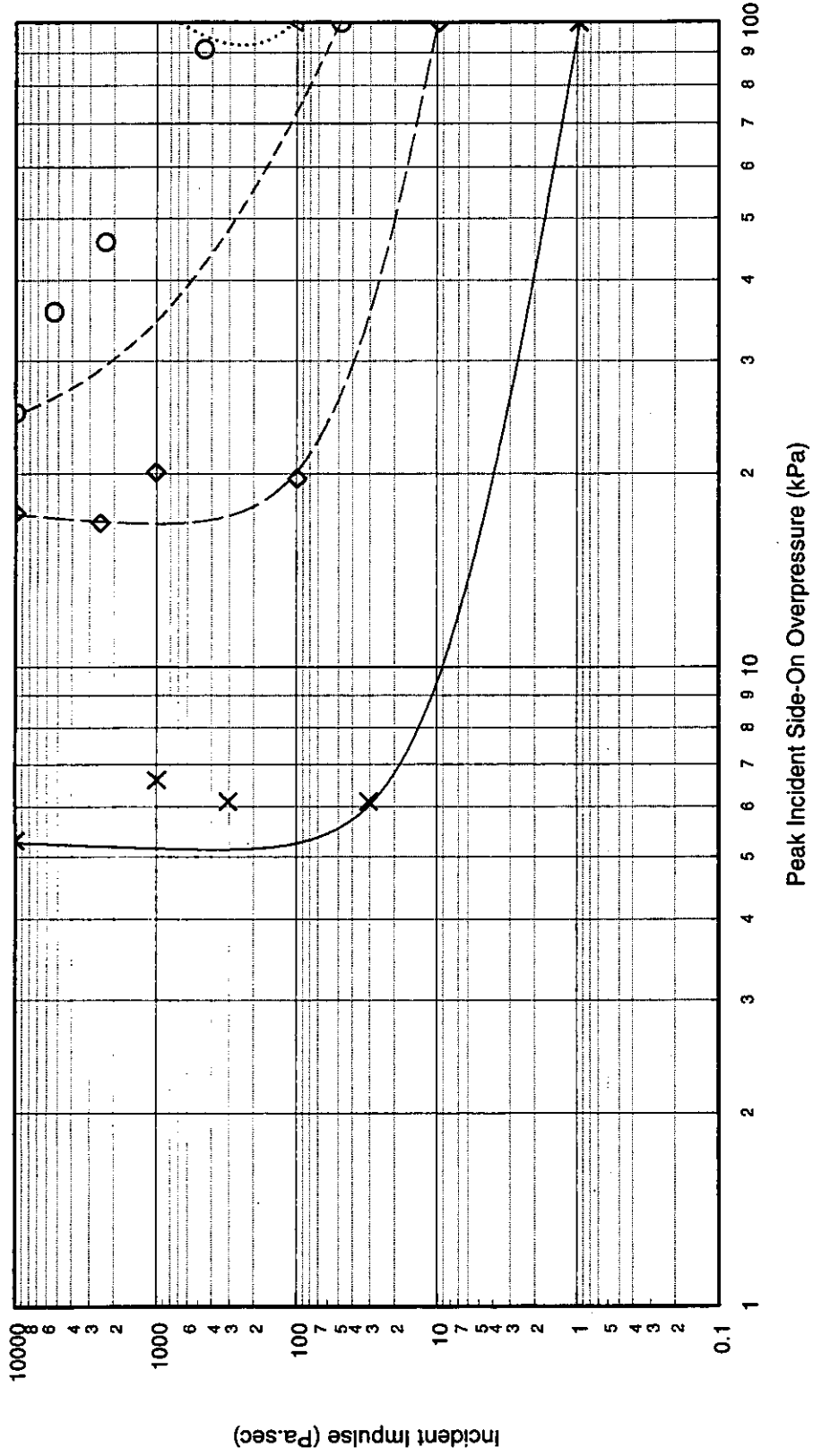
Quantity	Value	Comments
<b>Building Type: B2/2</b>		
Description	Brick House 2 storey, semi-detached house with solid brick walls and timber floors and roof. Aspect ratio 2:1	
<b>Global Dimensions</b>		
Breadth	8.6m	
Length	14.3m	
Height	8.0m	
<b>Glazing Characteristics</b>		
Thickness	3mm - single glazed	
Max. Pane dimensions	1.25 x 0.675m	
Failure Pressure (1 sec pulse duration)	55 mbar	Mainstone [4]
<b>Cladding/Wall Panel Characteristics</b>		
Thickness	215 mm	Solid brick walls
Panel Dimensions	2.6 x 3.85m	
Dynamic Failure Pressure	275 mbar	Calculated based on accidental wind loading design criteria, and comparable with the CREDIT experiments [26]
Support Conditions	Simply supported on all 4 sides	
Ductility	5	
Debris Size	75 x 225 x 112.5 mm	This is approximately equivalent to the size of a single brick
<b>Frame Details</b>		
Frame Type	Brick walls form loadbearing frame for structure	Failure of all four external walls is assumed to imply collapse
Dynamic Failure Pressure	275 mbar	
Ductility	5	
<b>Additional Information</b>		

P-I Diagram: B2/2, Shock Pulse, Short Side Facing Blast



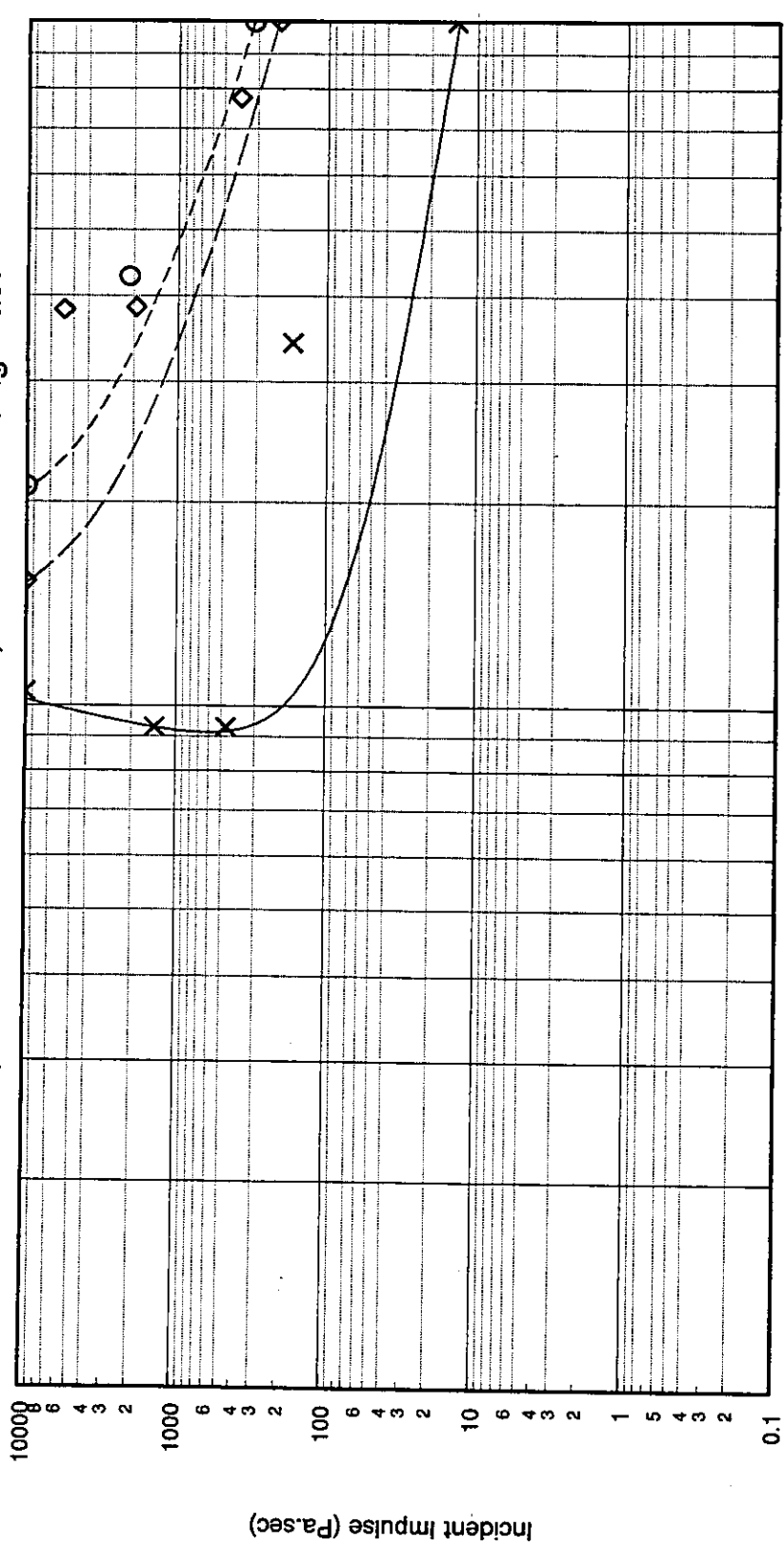
- x — 1% Fatality Probability
- - - ◊ - - 10% Fatality Probability
- ..... ○ ..... 50% Fatality Probability
- · - · - · △ · - · - · 90% Fatality Probability

P-I Diagram: B2/2, Shock Pulse, Long Side Facing Blast

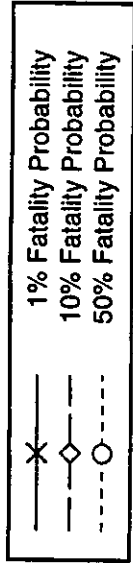


- X 1% Fatality Probability
- ◇ 10% Fatality Probability
- 50% Fatality Probability
- △ 90% Fatality Probability

P-I Diagram: B2/2, Pressure Pulse, Short Side Facing Blast

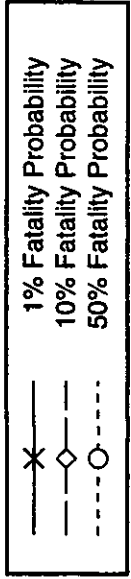
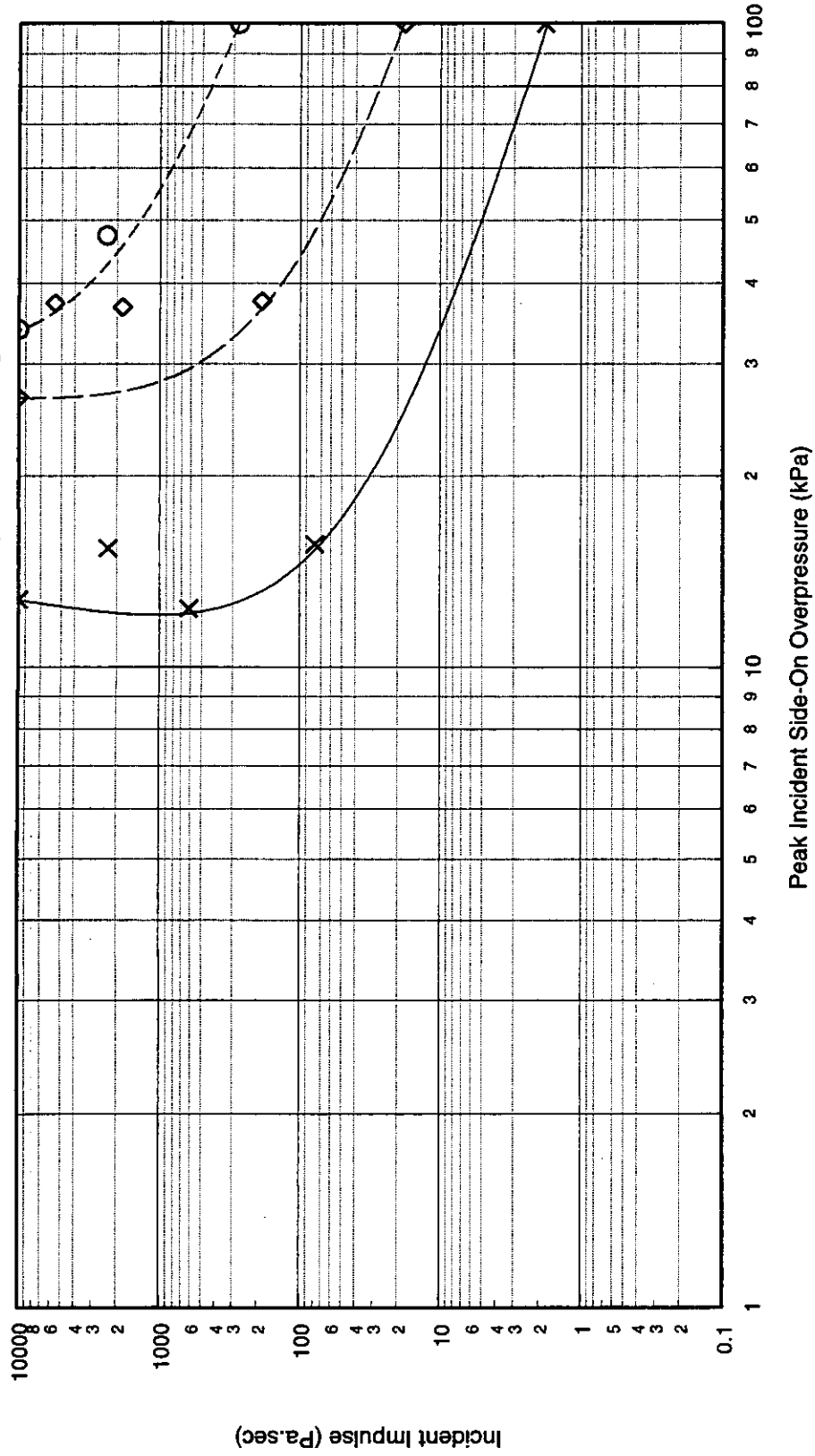


Peak Incident Side-On Overpressure (kPa)

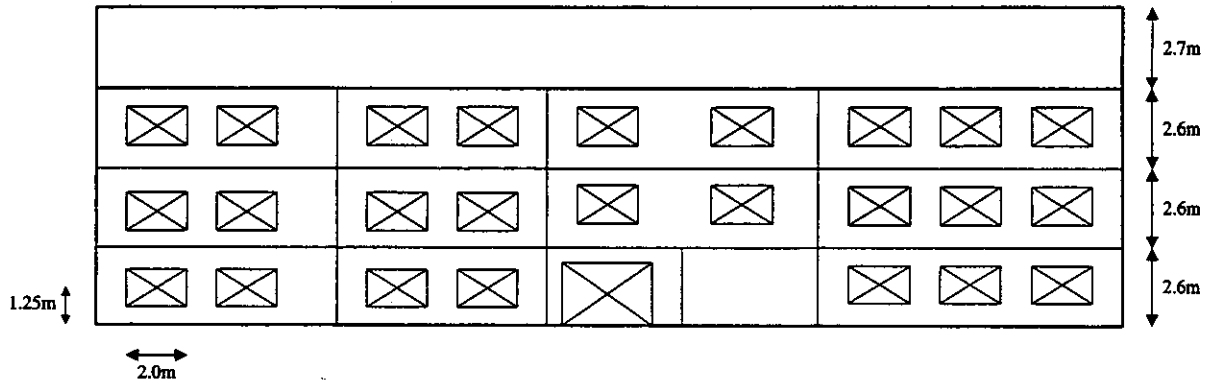




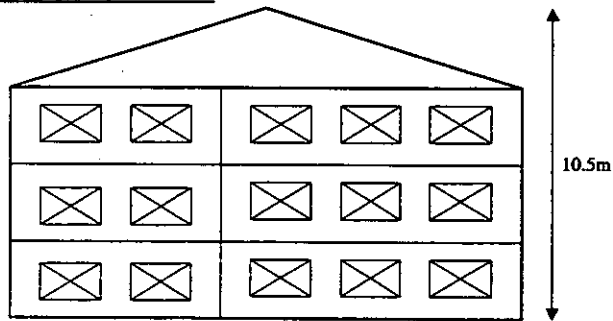
P-I Diagram: B2/2, Pressure Pulse, Long Side Facing Blast



**Elevation of side wall**



**Elevation of end wall**



**Plan of ground floor**

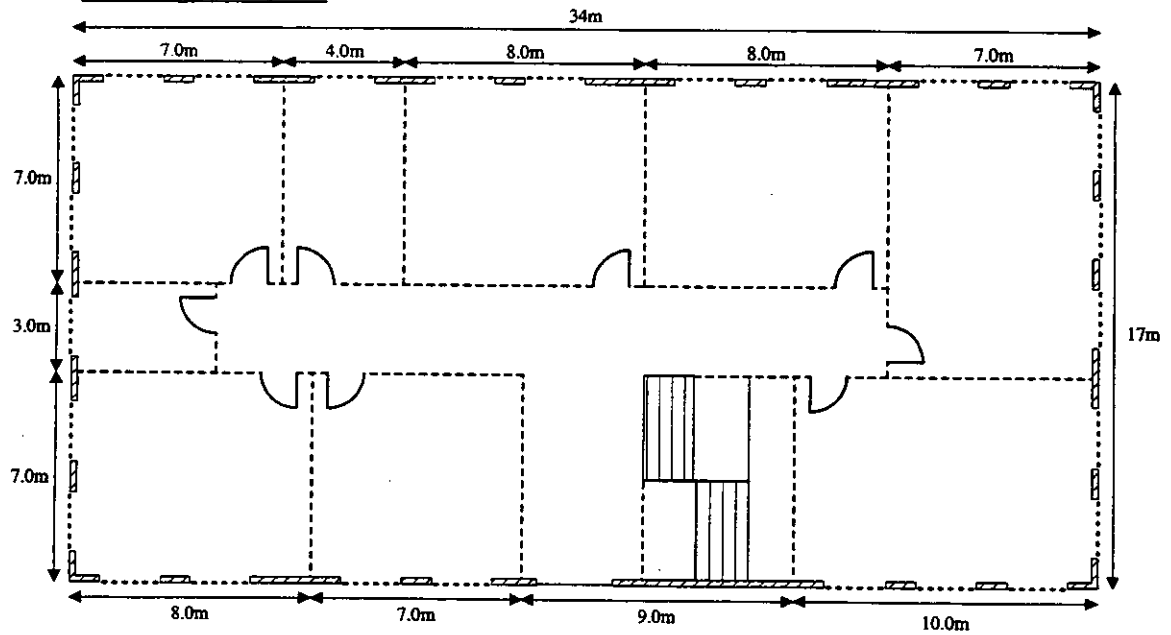
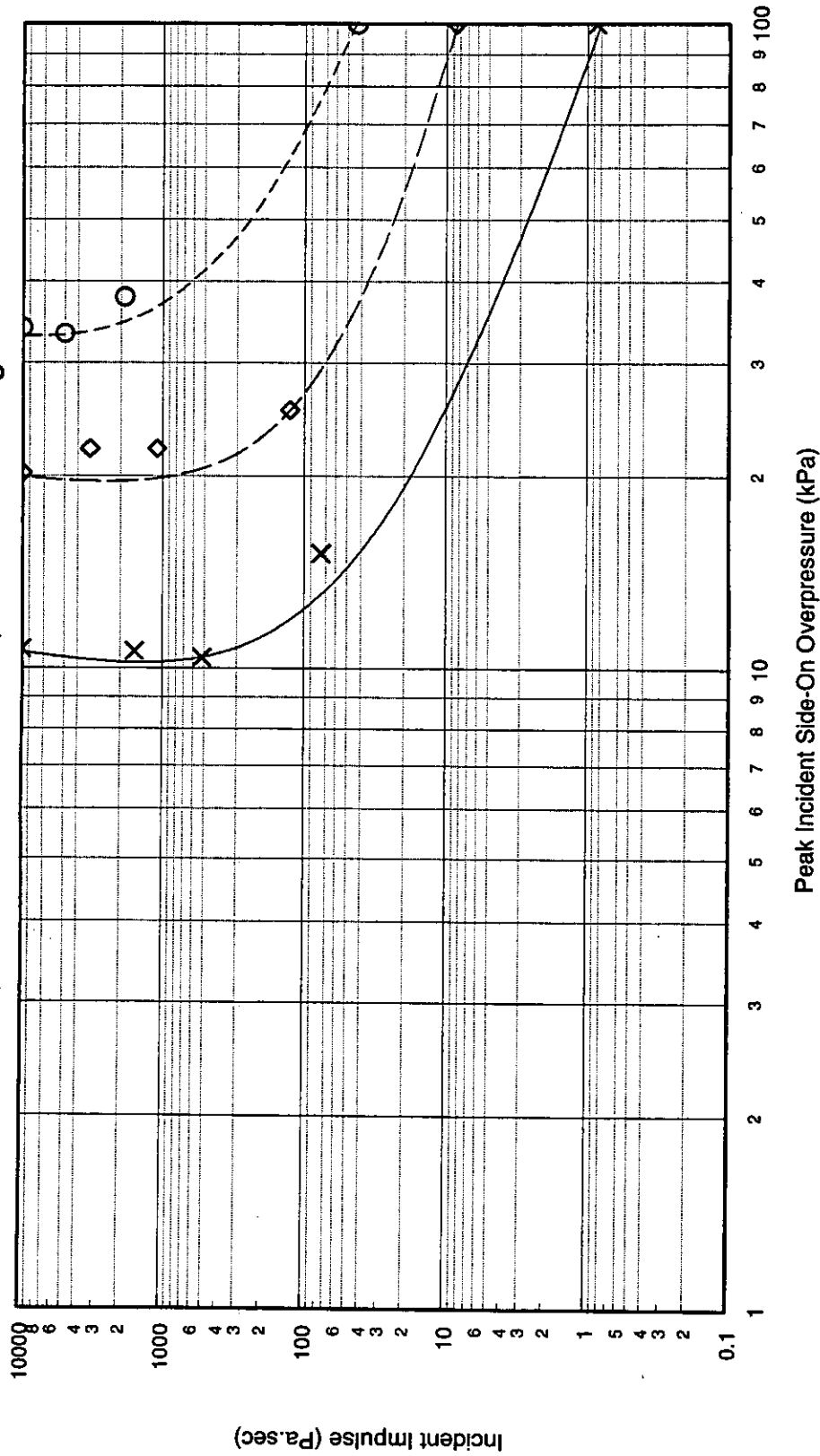


**Figure A.5: Illustration of Brick Building Type B2/3**

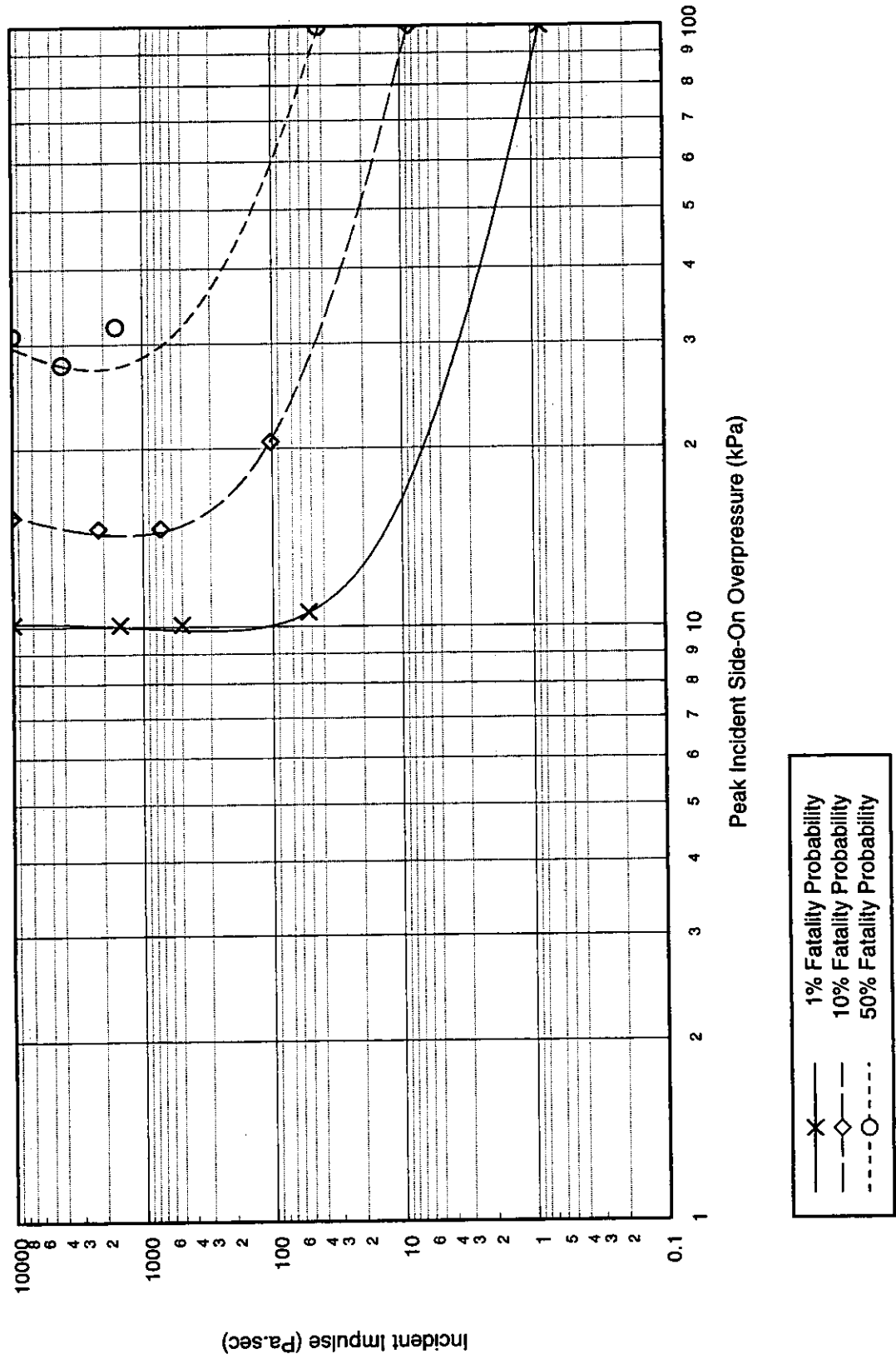
Quantity	Value	Comments
<b>Building Type: B2/3</b>		
Description	Brick Building 3 storeys, with solid brick walls and timber floors and roof. Aspect ratio 2:1	Typical school or office building
<b>Global Dimensions</b>		
Breadth	17.0m	
Length	34.0m	
Height	10.5m	
<b>Glazing Characteristics</b>		
Thickness	4mm - single glazed	
Max. Pane dimensions	1.25 x 0.65m	
Failure Pressure (1 sec pulse duration)	60 mbar	Mainstone [4]
<b>Cladding/Wall Panel Characteristics</b>		
Thickness	215 mm	Solid brick walls
Panel Dimensions	2.6 x 3.85m	
Dynamic Failure Pressure	275 mbar	Calculated based on accidental wind loading design criteria, and comparable with the CREDIT experiments [26]
Support Conditions	Simply supported on all 4 sides	
Ductility	5	
Debris Size	75 x 225 x 112.5 mm	This is approximately equivalent to the size of a single brick
<b>Frame Details</b>		
Frame Type	Brick walls form loadbearing frame for structure	Failure of all four external walls is assumed to imply collapse
Dynamic Failure Pressure	275 mbar	
Ductility	5	
<b>Additional Information</b>		

P-I Diagram: B2/3, Shock Pulse, Short Side Facing Blast

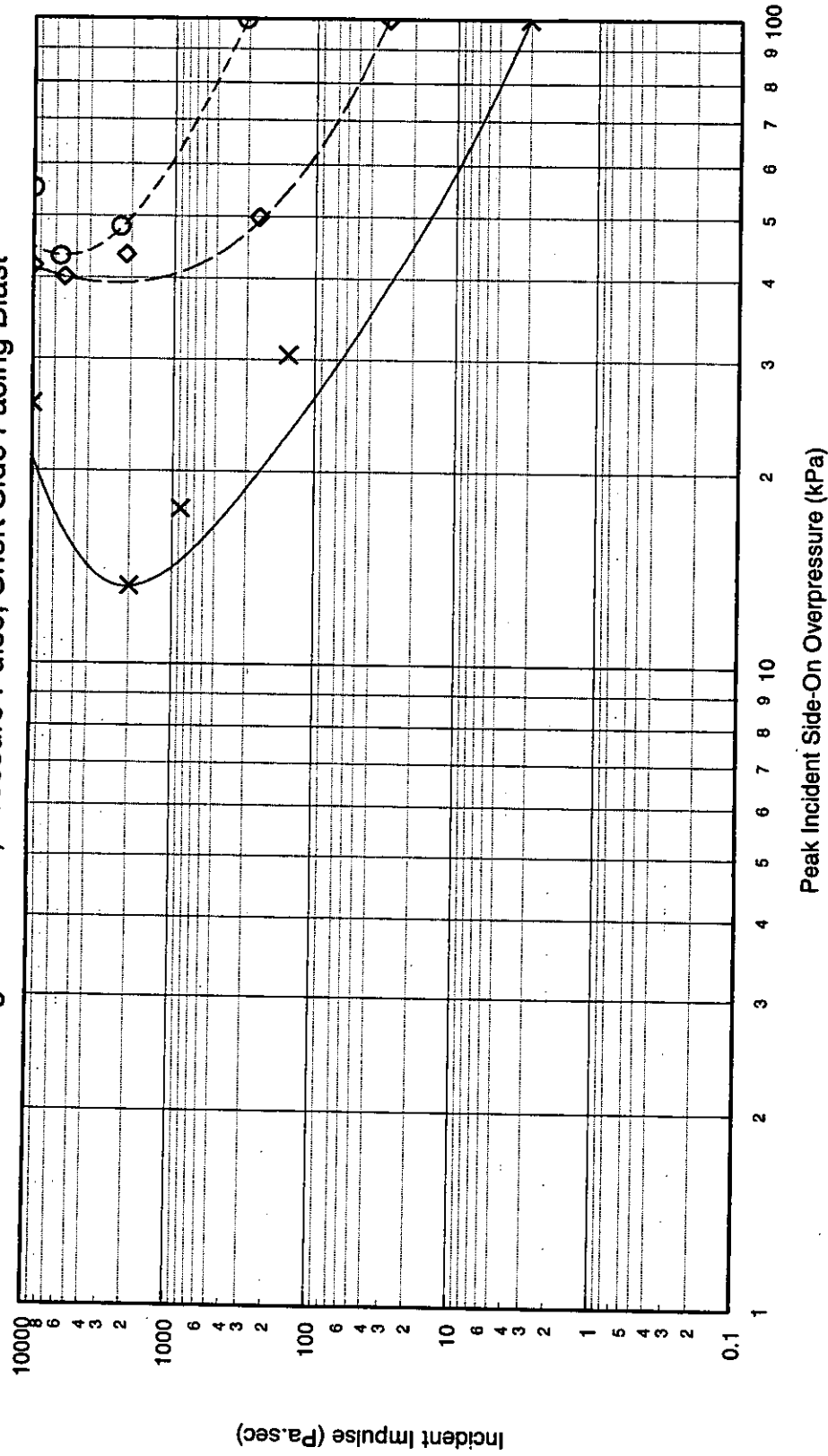


x — 1% Fatality Probability  
 ◇ — 10% Fatality Probability  
 ○ — 50% Fatality Probability

P-I Diagram: B2/3, Shock Pulse, Long Side Facing Blast

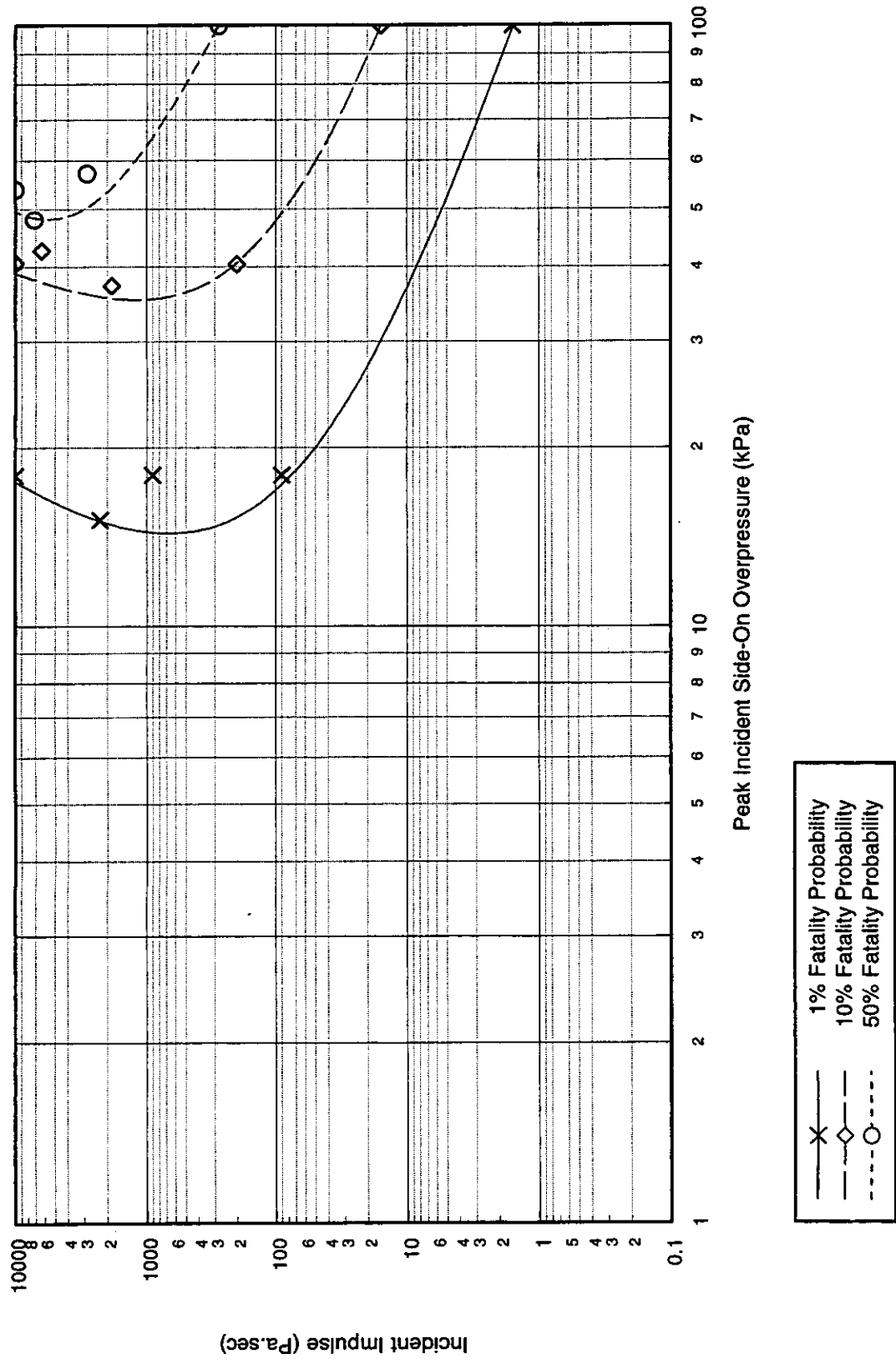


P-I Diagram: B2/3, Pressure Pulse, Short Side Facing Blast



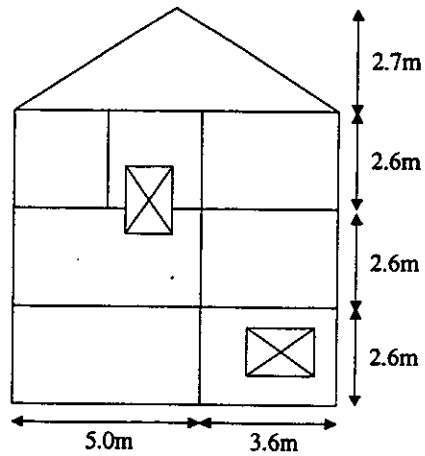
x — 1% Fatality Probability  
 ◇ — 10% Fatality Probability  
 ○ — 50% Fatality Probability

P-I Diagram: B2/3, Pressure Pulse, Long Side Facing Blast



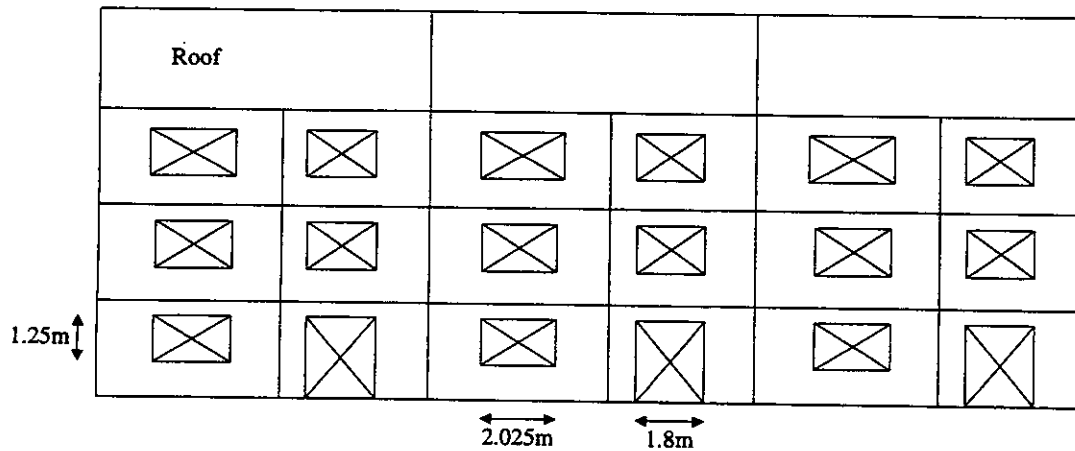
x — 1% Fatality Probability  
 —◇— 10% Fatality Probability  
 - - -○ - - - 50% Fatality Probability

**Elevation on end wall**



**Elevation on front**

(elevation on rear assumed the same)



**Plan of ground floor**

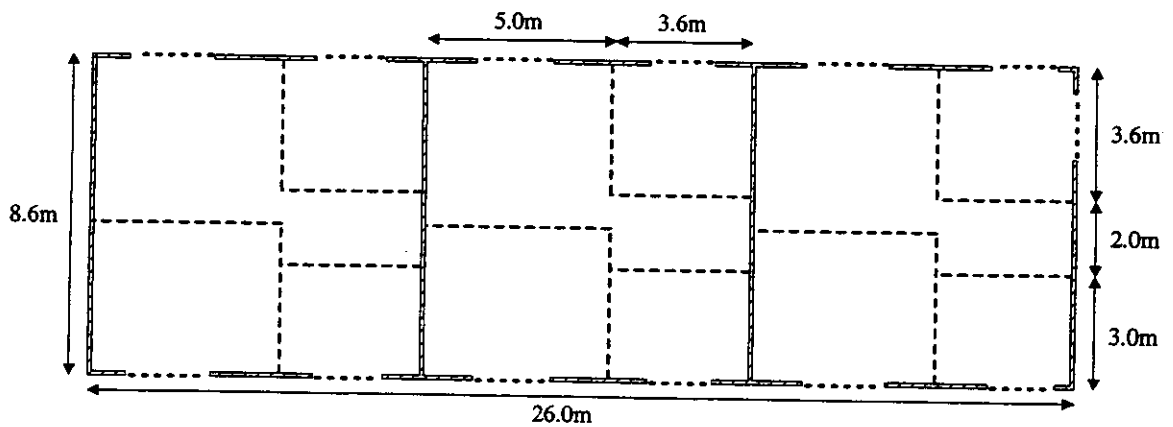
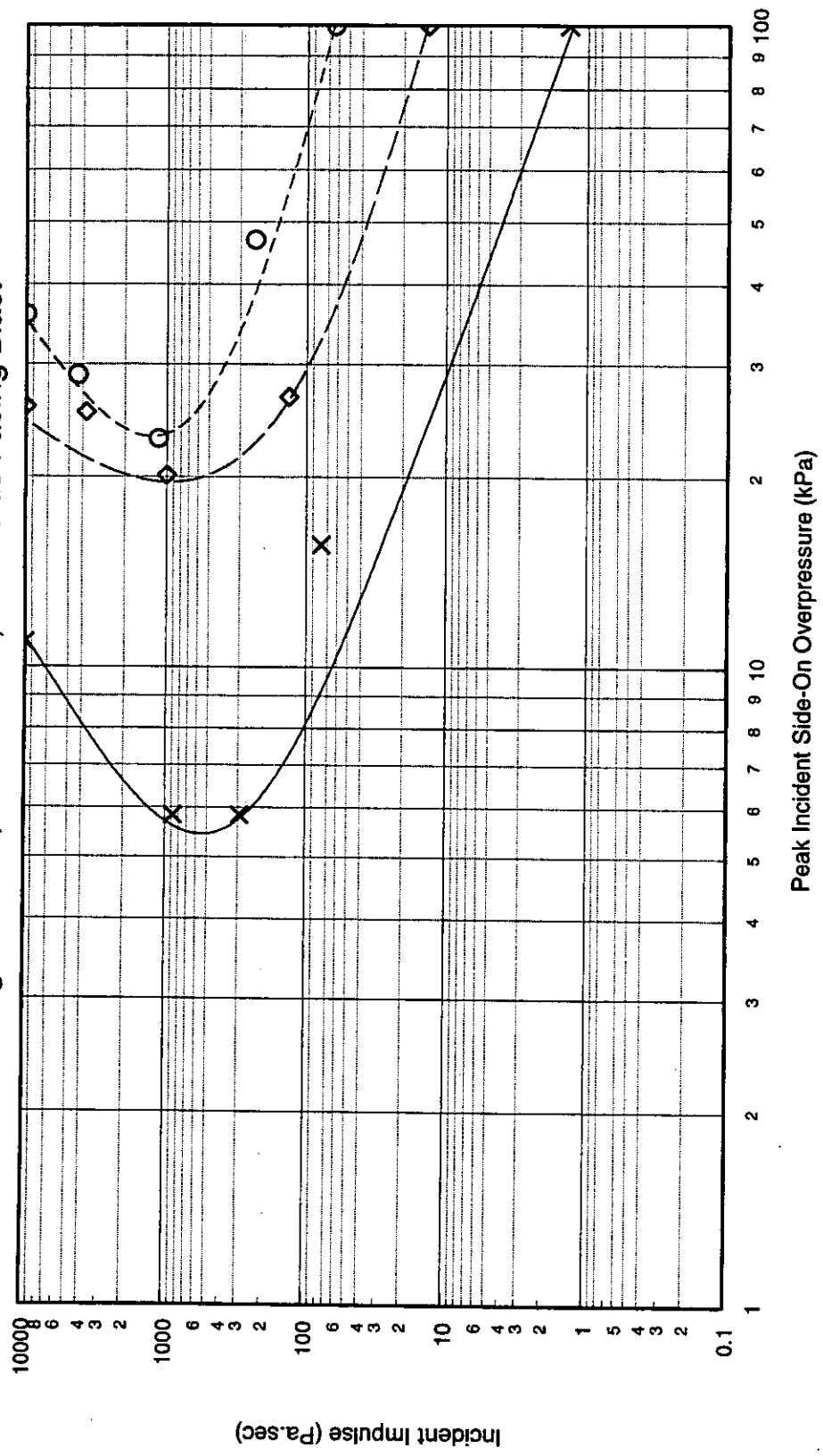


**Figure A.6: Illustration of Brick Building Type B2/4**



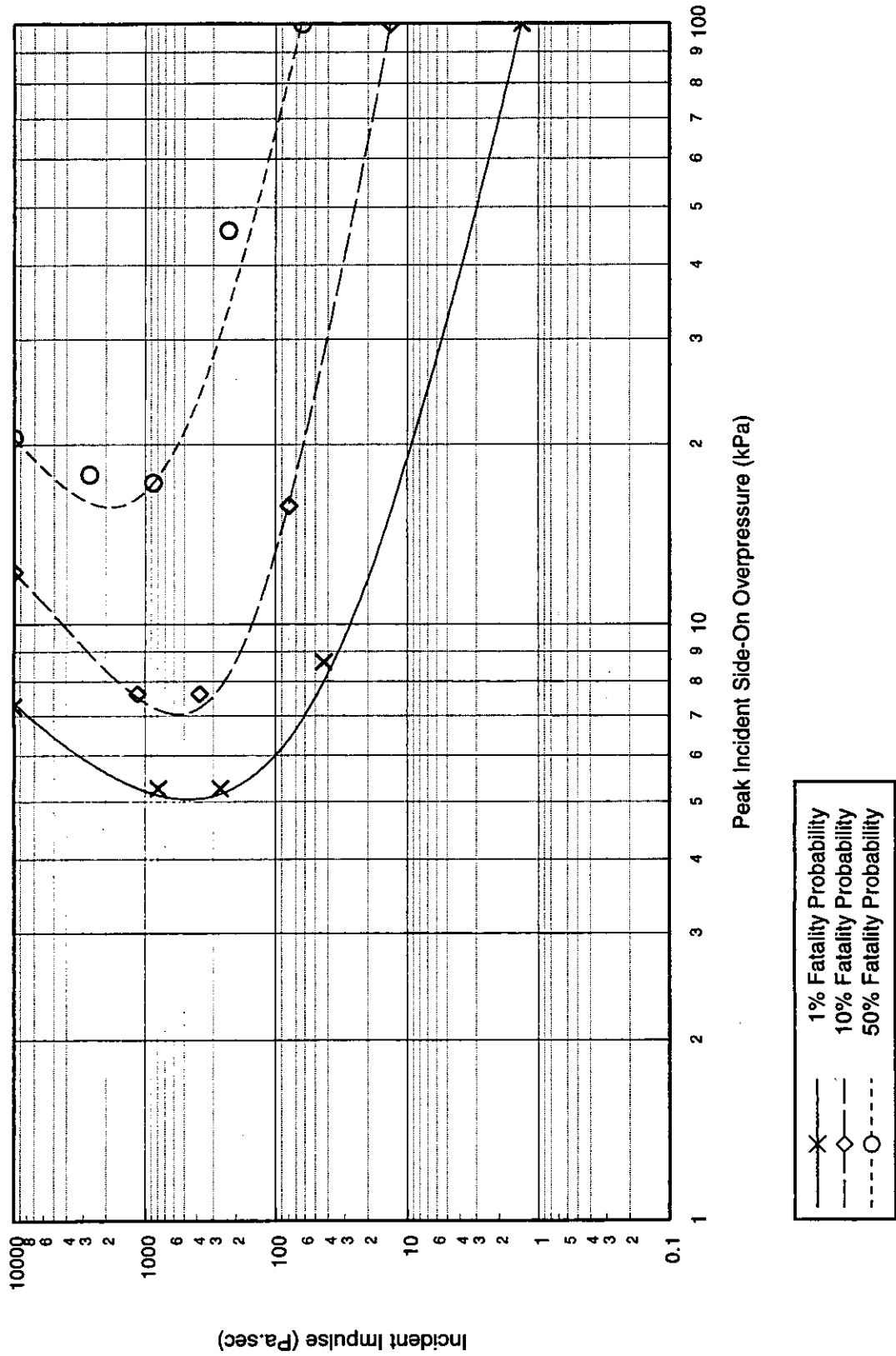
Quantity	Value	Comments
<b>Building Type: B2/4</b>		
Description	Brick Building 3 storey, brick/block walls, concrete floors and timber roof. Aspect ratio 3:1	Typical row of 3 houses - modern construction
<b>Global Dimensions</b>		
Breadth	8.6m	
Length	26.0m	
Height	10.5m	
<b>Glazing Characteristics</b>		
Thickness	4mm - double glazed	
Max. Pane dimensions	1.25 x 0.675m	
Failure Pressure (1 sec pulse duration)	110 mbar	Mainstone [4]
<b>Cladding/Wall Panel Characteristics</b>		
Thickness	215 mm	Solid brick walls
Panel Dimensions	2.6 x 3.85m	
Dynamic Failure Pressure	160 mbar	Calculated based on accidental wind loading design criteria, and comparable with the CREDIT experiments [??]
Support Conditions	Simply supported on all 4 sides	
Ductility	5	
Debris Size	75 x 225 x 112.5 mm	This is approximately equivalent to the size of a single brick
<b>Frame Details</b>		
Frame Type	Brick walls form loadbearing frame for structure	Failure of all four external walls is assumed to imply collapse
Dynamic Failure Pressure	160 mbar	
Ductility	5	
<b>Additional Information</b>		

P-I Diagram: B2/4, Shock Pulse, Short Side Facing Blast

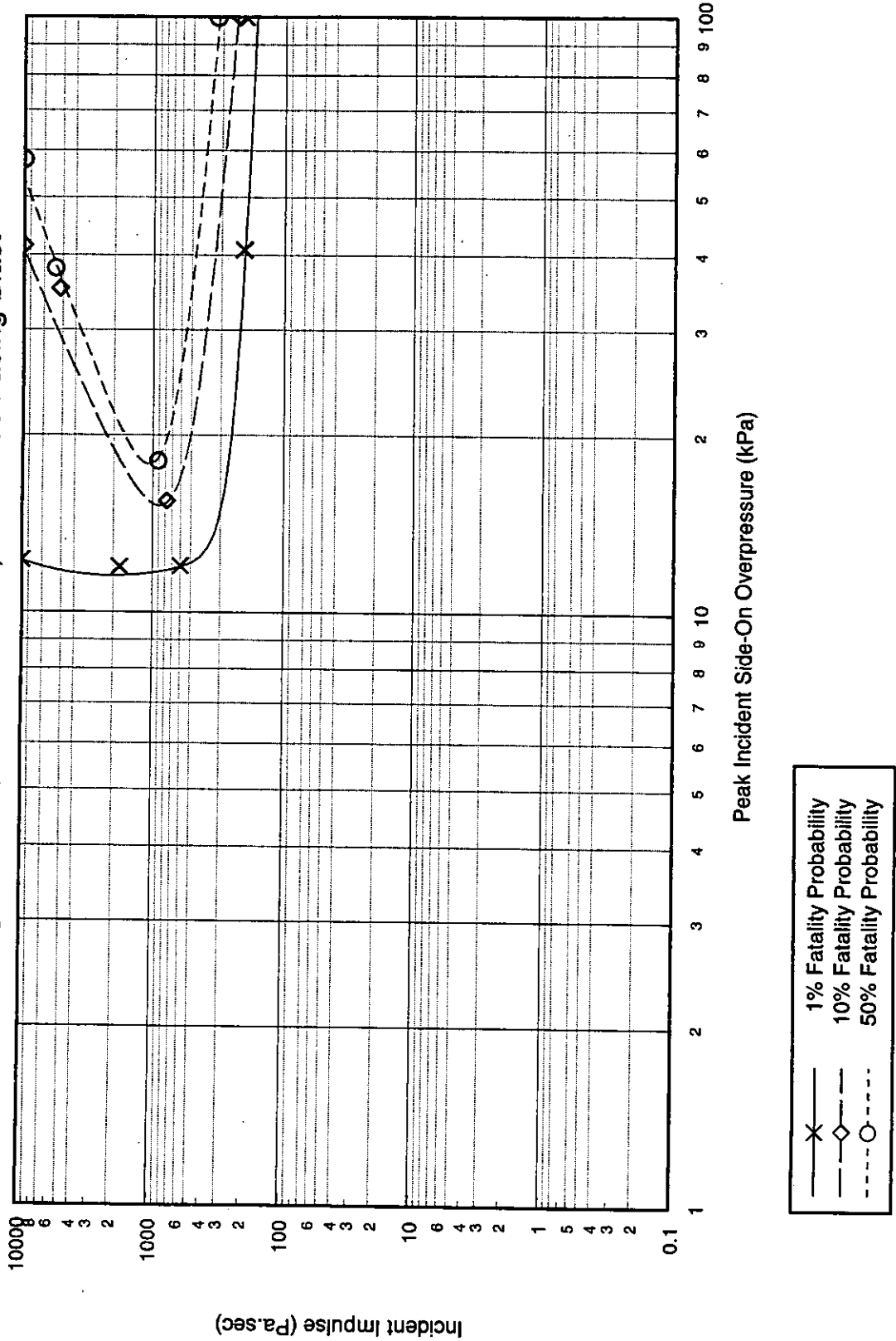


- X 1% Fatality Probability
- ◇ 10% Fatality Probability
- 50% Fatality Probability

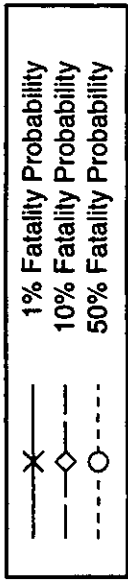
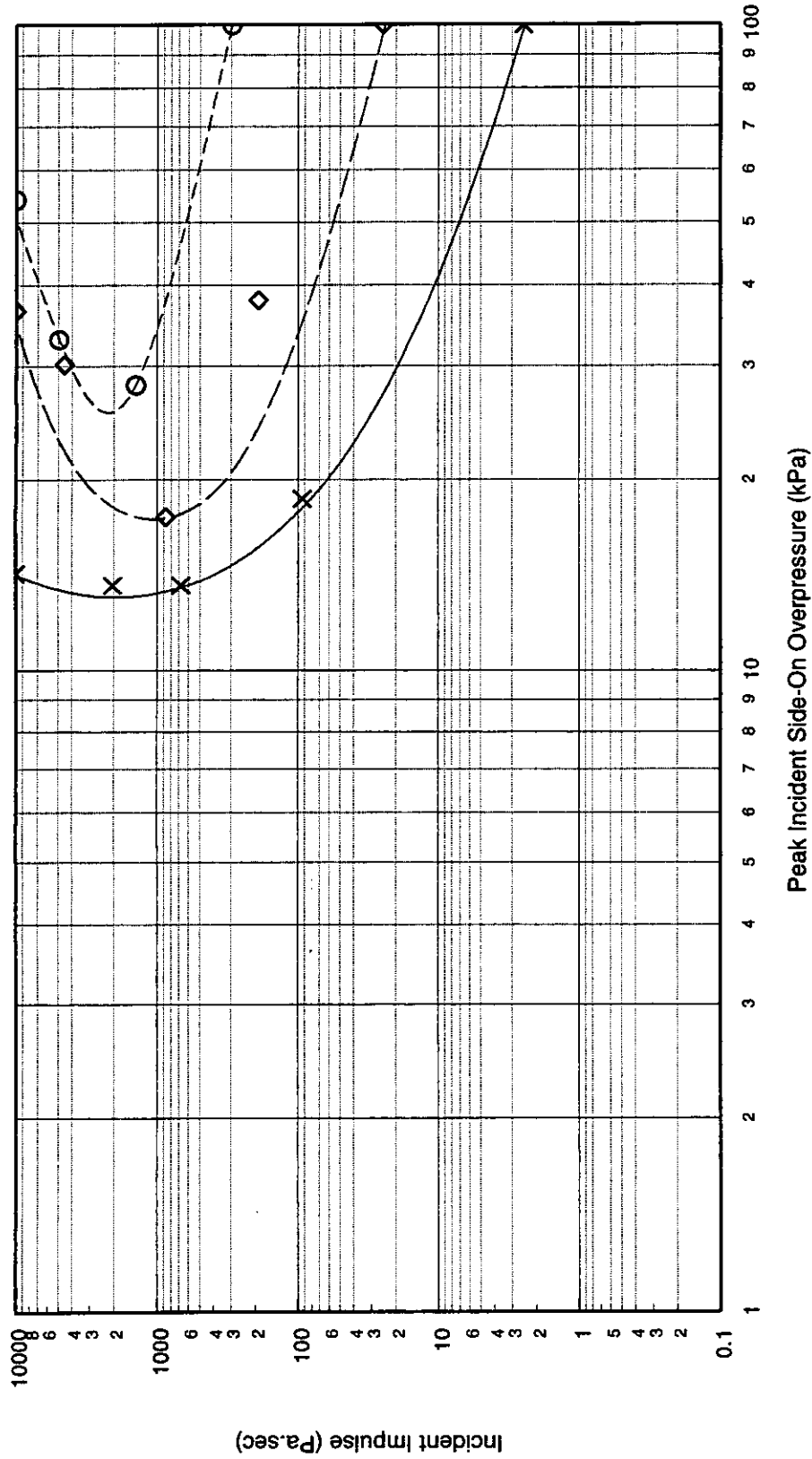
P-I Diagram: B2/4, Shock Pulse, Long Side Facing Blast



P-I Diagram: B2/4, Pressure Pulse, Short Side Facing Blast



P-I Diagram: B2/4, Pressure Pulse, Long Side Facing Blast



### **A.3. Building Type B3: Concrete Framed Buildings**

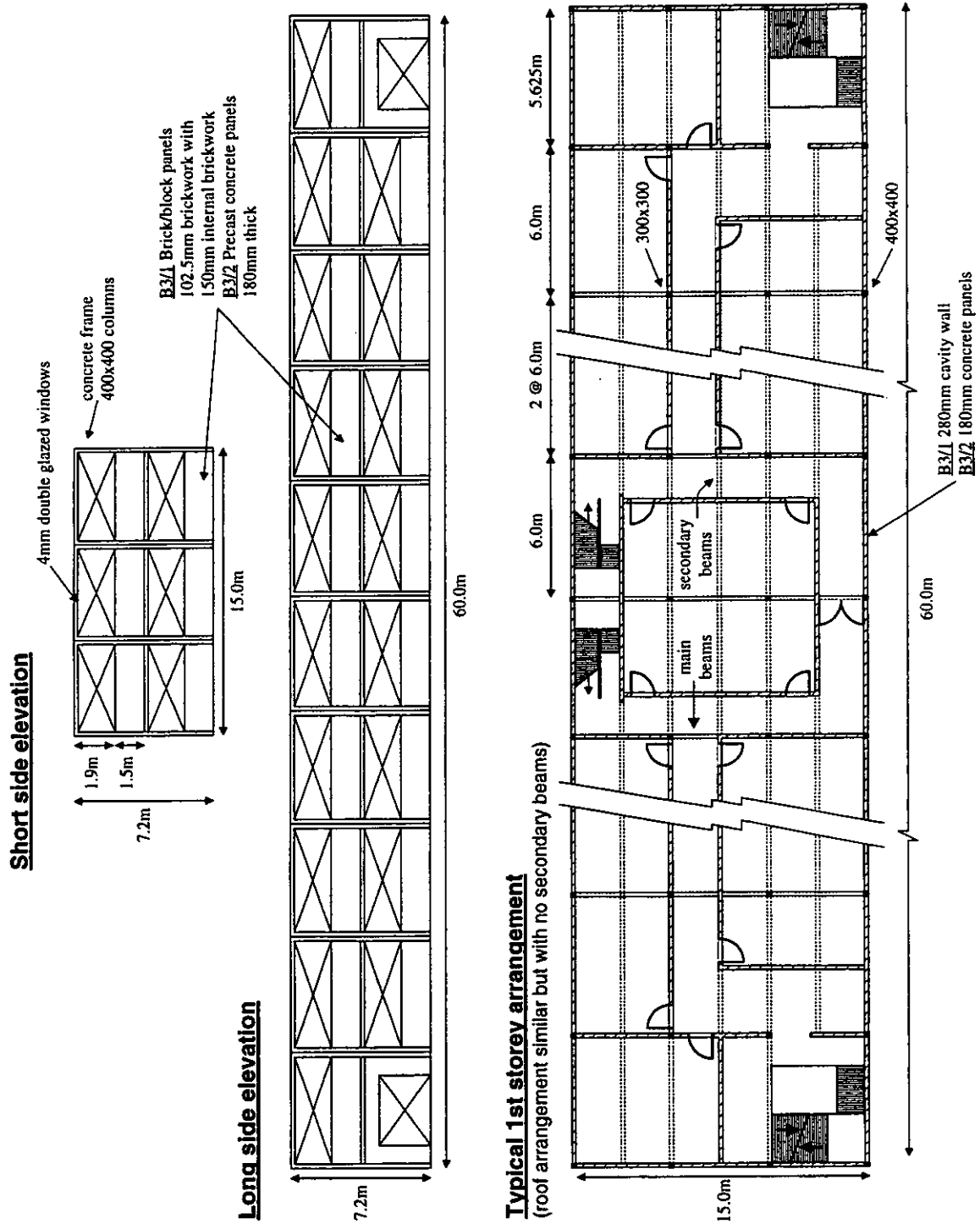
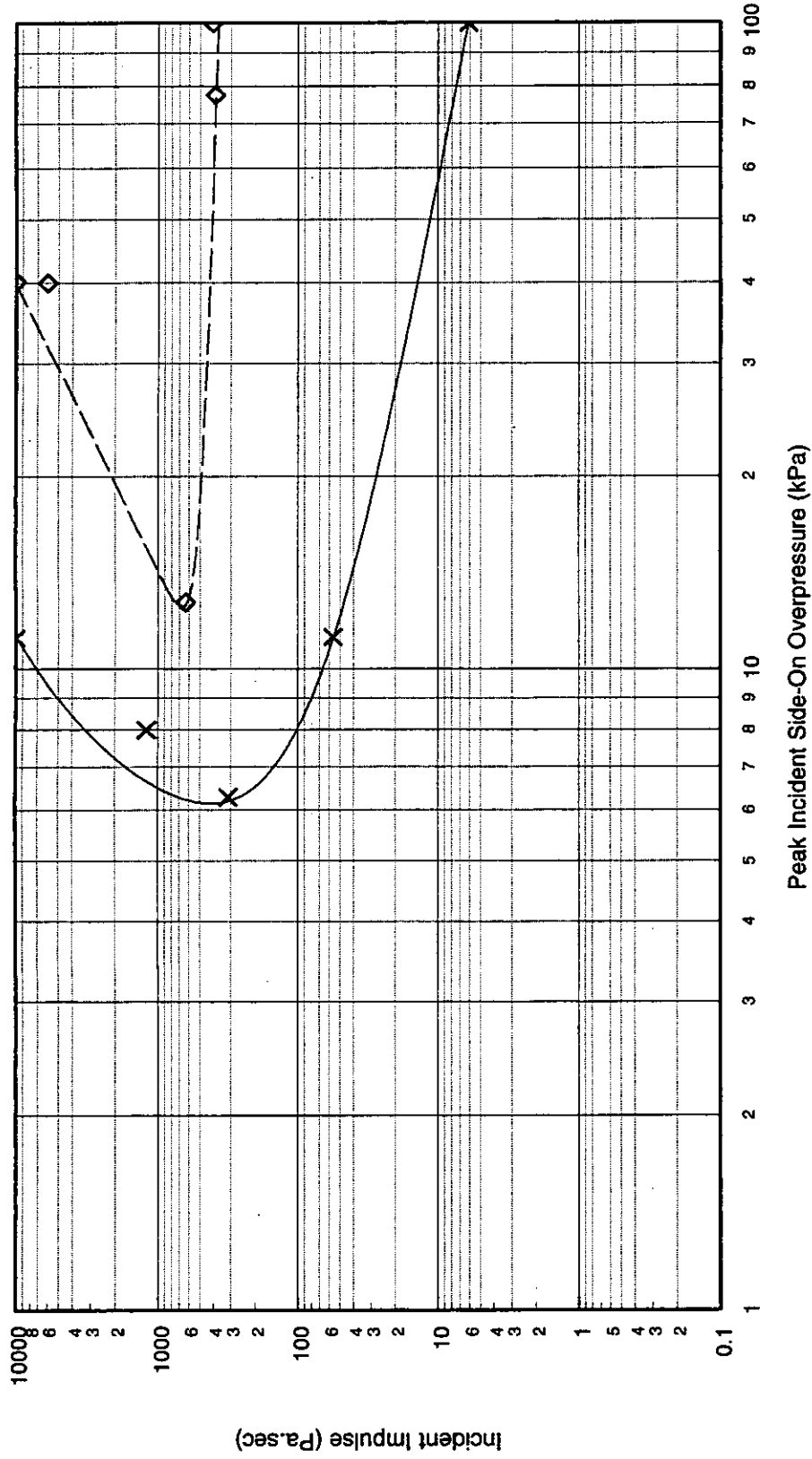


Figure A.7: Illustration of Concrete Framed Buildings Types B3/1 and B3/2

Quantity	Value	Comments
<b>Building Type: B3/1</b>		
Description	Concrete Framed Building 2 storey, reinforced concrete moment resisting frame, brick/block wall panels Aspect ratio 4:1	Typical office building - may have underground basement, but not considered here, as it is assumed that the risk from a blast load is much lower in the basement
<b>Global Dimensions</b>		
Breadth	15.0m	
Length	60.0m	
Height	7.2m	
<b>Glazing Characteristics</b>		
Thickness	4mm - double glazed	Continuous glazing
Max. Pane dimensions	1.9 x 1.5m	
Failure Pressure (1 sec pulse duration)	65 mbar	Mainstone [4]
<b>Cladding/Wall Panel Characteristics</b>		
Thickness	253 mm	Brick/block walls
Panel Dimensions	1.5 x 6.0m	
Dynamic Failure Pressure	90 mbar	Calculated as 40mbar, but increased to 90mbar based on a comparison with the CREDIT experiments [26] and previous calculations
Support Conditions	Horizontally spanning - assumed fully fixed at ends	
Ductility	5	
Debris Size	75 x 225 x 112.5 mm	This is approximately equivalent to the size of a single brick
<b>Frame Details</b>		
Frame Type	Reinforced concrete moment resisting frame	External columns 400x400mm Internal columns 300x300mm Main beams 600x200mm(roof) and 500x250mm(1st floor) Secondary beams, 400x200mm
Dynamic Failure Pressure	1535 mbar - global collapse, short side facing blast 557 mbar - global collapse, long side facing blast 655 mbar - local collapse, shock pulse 619 mbar - local collapse, pressure pulse	All collapse pressures are given for a 100msec pulse duration. Global collapse corresponds to failure of the entire building. Local collapse corresponds to failure of an external column due to hinge formation at its mid-height. All collapse pressures assume that the cladding is capable of transmitting this load into the frame
Ductility	1.5	
<b>Additional Information</b>		

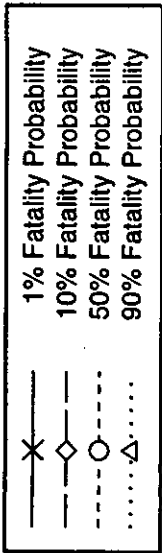
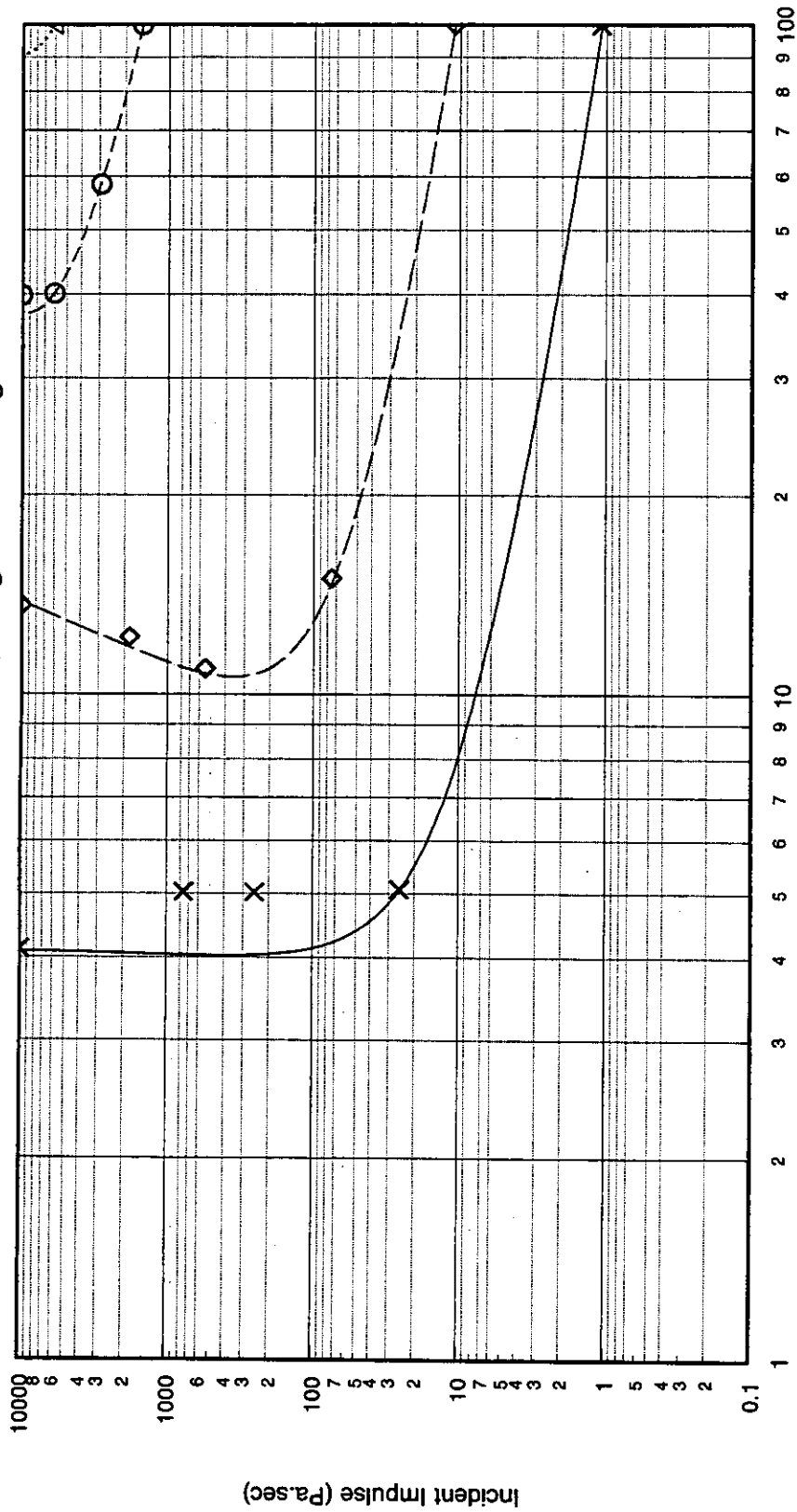


P-I Diagram: B3/1, Shock Pulse, Short Side Facing Blast

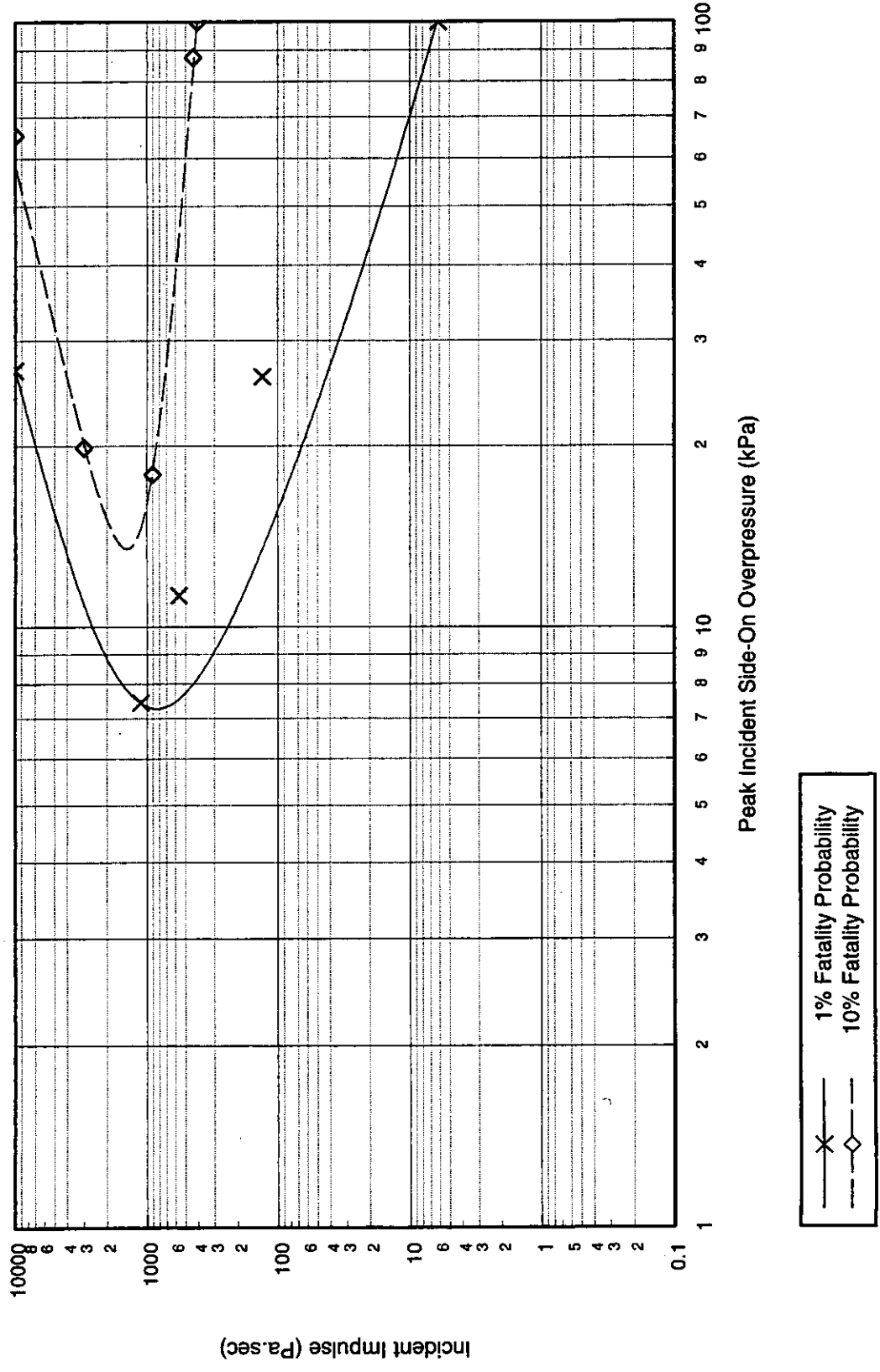


X ——— 1% Fatality Probability  
 ———◇——— 10% Fatality Probability

P-I Diagram: B3/1, Shock Pulse, Long Side Facing Blast

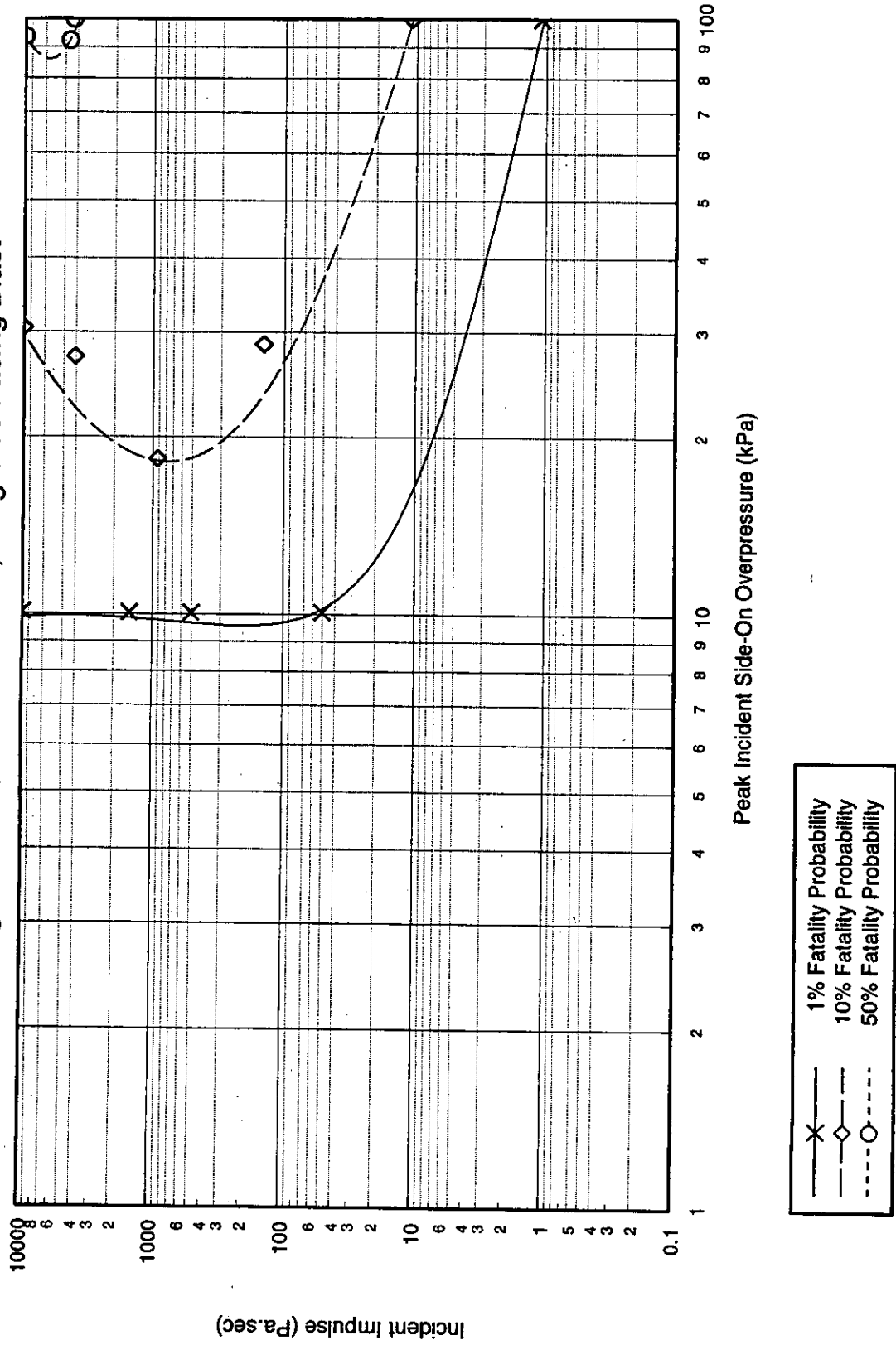


P-I Diagram: B3/1, Pressure Pulse, Short Side Facing Blast



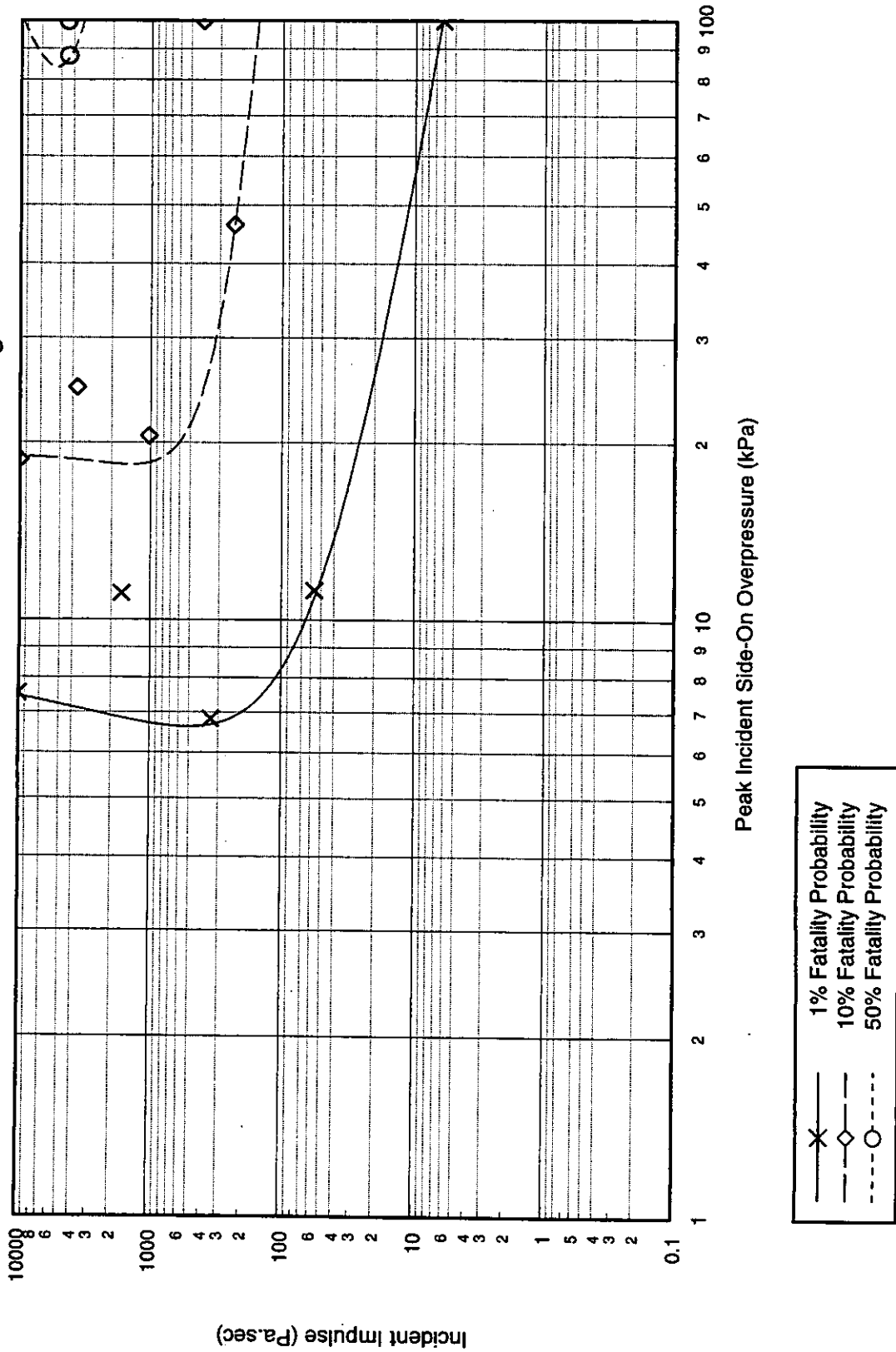
x — 1% Fatality Probability  
 —◇— 10% Fatality Probability

P-I Diagram: B3/1, Pressure Pulse, Long Side Facing Blast

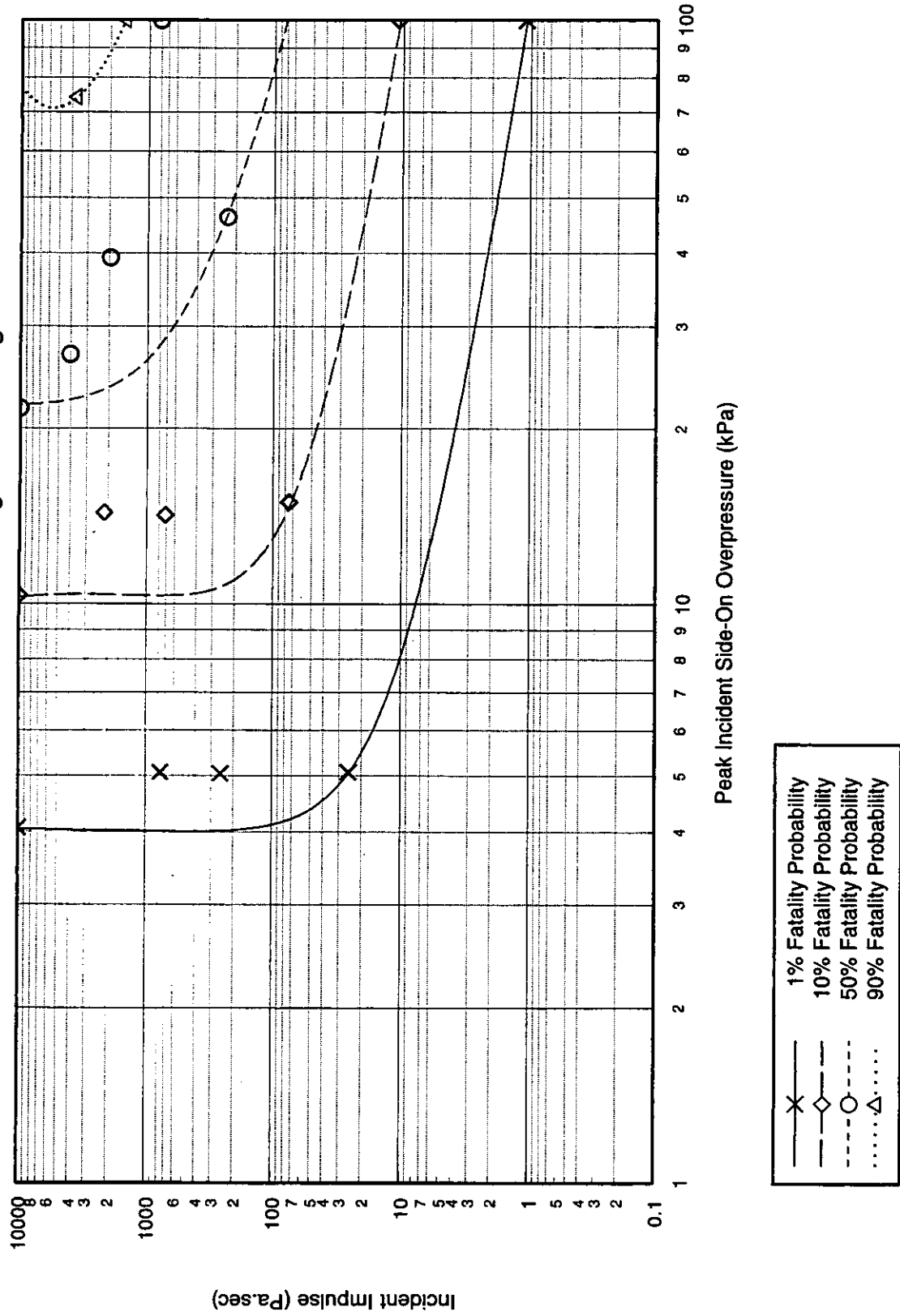


Quantity	Value	Comments
<b>Building Type: B3/2</b>		
Description	Concrete Framed Building 2 storey, reinforced concrete moment resisting frame, precast concrete wall panels Aspect ratio 4:1	Typical office building - identical to B3/1 except that wall panels are precast concrete instead of brick/block
<b>Global Dimensions</b>		
Breadth	15.0m	
Length	60.0m	
Height	7.2m	
<b>Glazing Characteristics</b>		
Thickness	4mm - double glazed	Continuous glazing
Max. Pane dimensions	1.9 x 1.5m	
Failure Pressure (1 sec pulse duration)	65 mbar	Mainstone [4]
<b>Cladding/Wall Panel Characteristics</b>		
Thickness	180 mm	Precast concrete panels
Panel Dimensions	1.5 x 6.0m	
Dynamic Failure Pressure	48.8 mbar	
Support Conditions	Horizontally spanning - assumed simply-supported at ends	
Ductility	10	
Debris Size	210 x 210 x 35 mm	This is a conservative assessment of the debris size based on the fatality probability criterion used
<b>Frame Details</b>		
Frame Type	Reinforced concrete moment resisting frame	External columns 400x400mm Internal columns 300x300mm Main beams 600x200mm(roof) and 500x250mm(1st floor) Secondary beams, 400x200mm
Dynamic Failure Pressure	1535 mbar - global collapse, short side facing blast 557 mbar - global collapse, long side facing blast 655 mbar - local collapse, shock pulse 619 mbar - local collapse, pressure pulse	All collapse pressures are given for a 100msec pulse duration. Global collapse corresponds to failure of the entire building. Local collapse corresponds to failure of an external column due to hinge formation at its mid-height. All collapse pressures assume that the cladding is capable of transmitting this load into the frame
Ductility	1.5	
<b>Additional Information</b>		

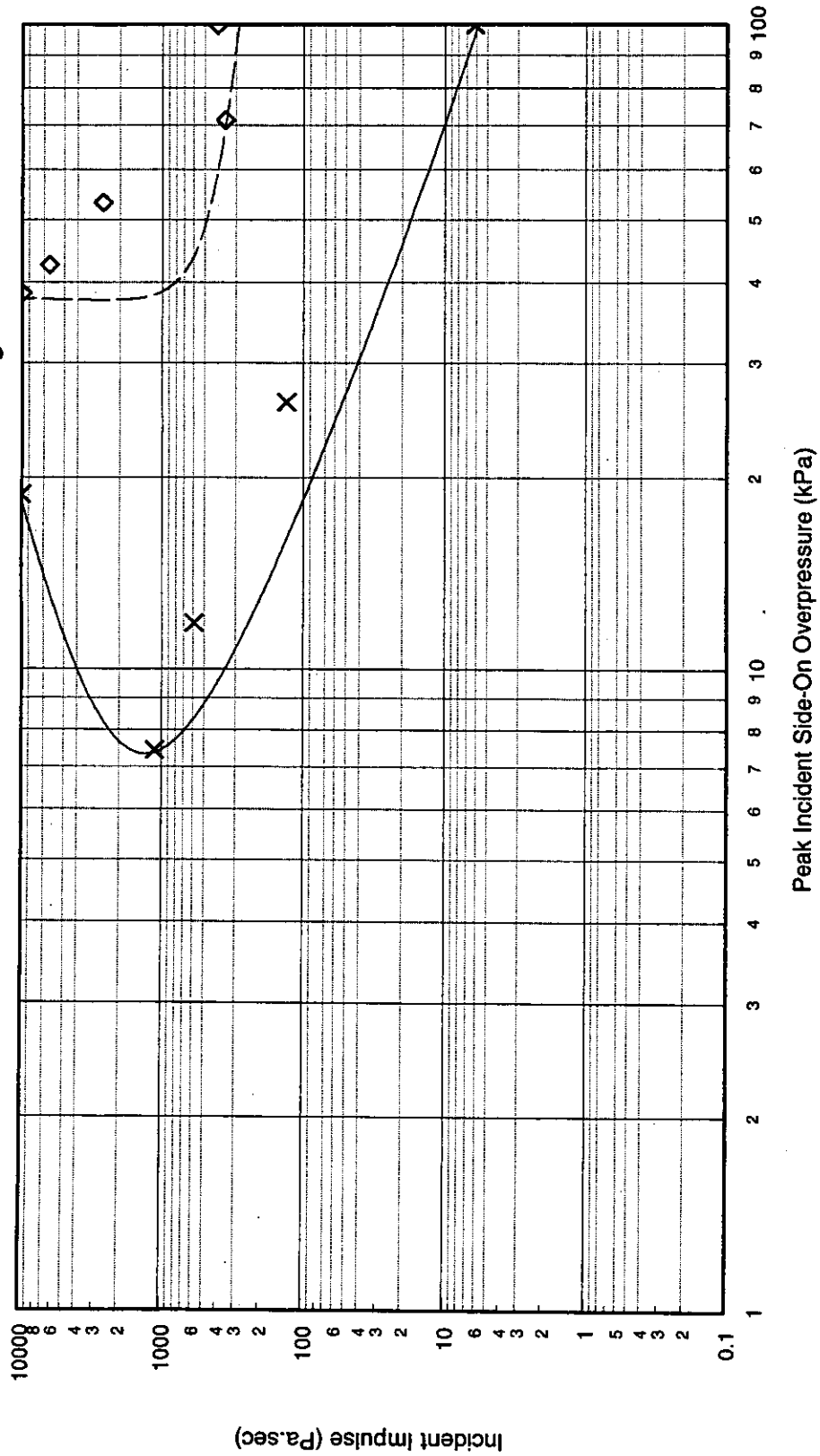
P-I Diagram: B3/2, Shock Pulse, Short Side Facing Blast



P-I Diagram: B3/2, Shock Pulse, Long Side Facing Blast



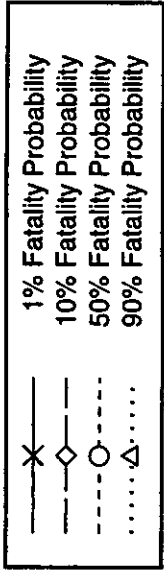
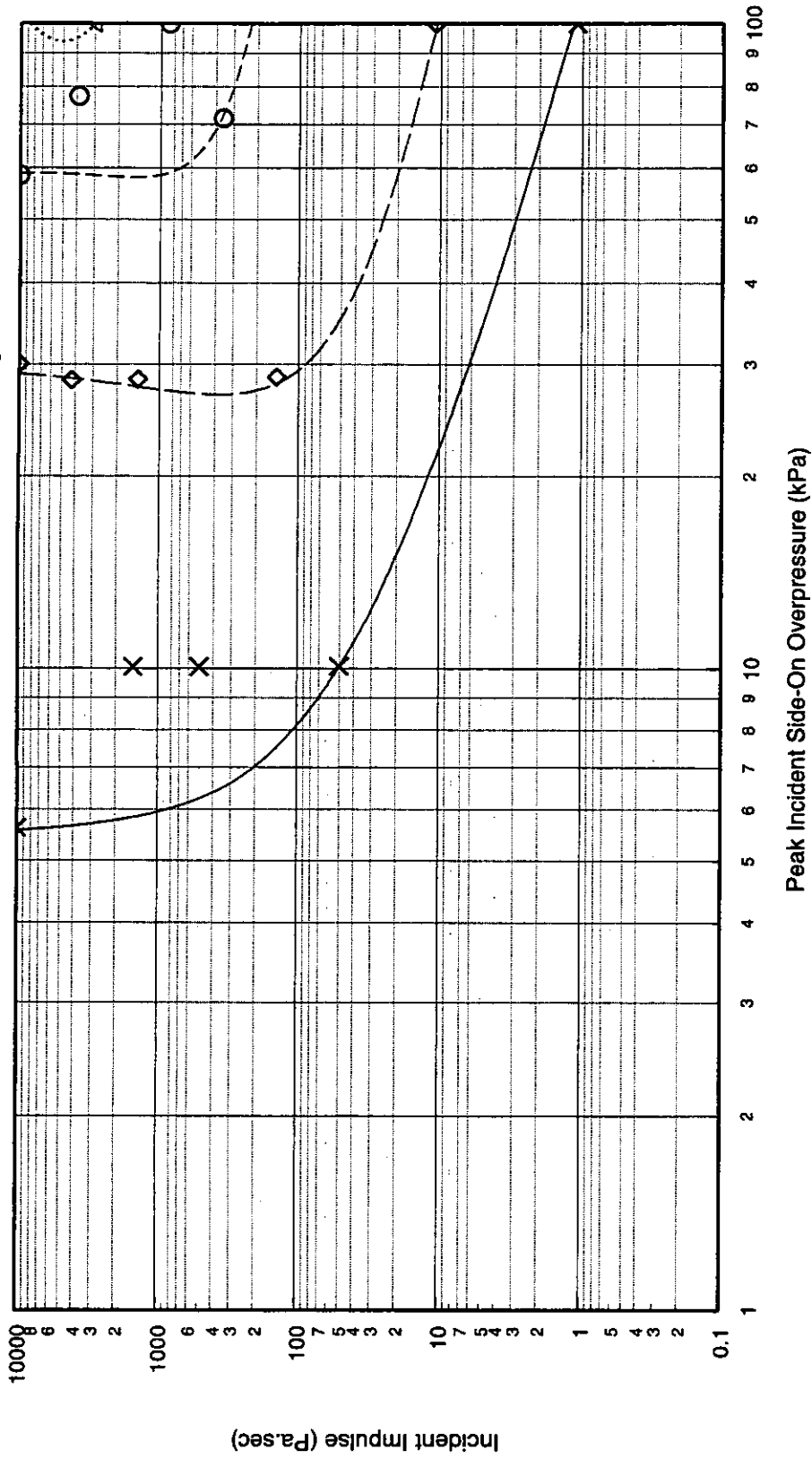
P-I Diagram: B3/2, Pressure Pulse, Short Side Facing Blast



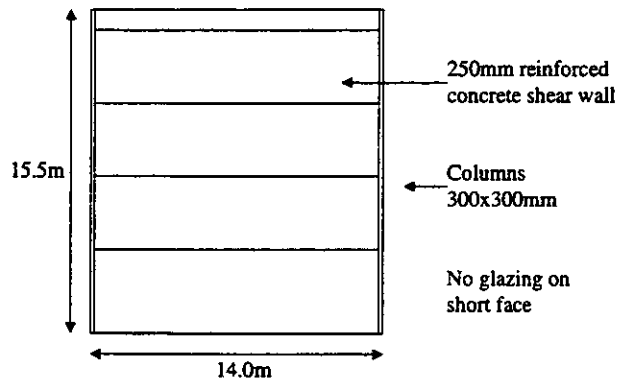
X ——— 1% Fatality Probability  
 ———◇—— 10% Fatality Probability



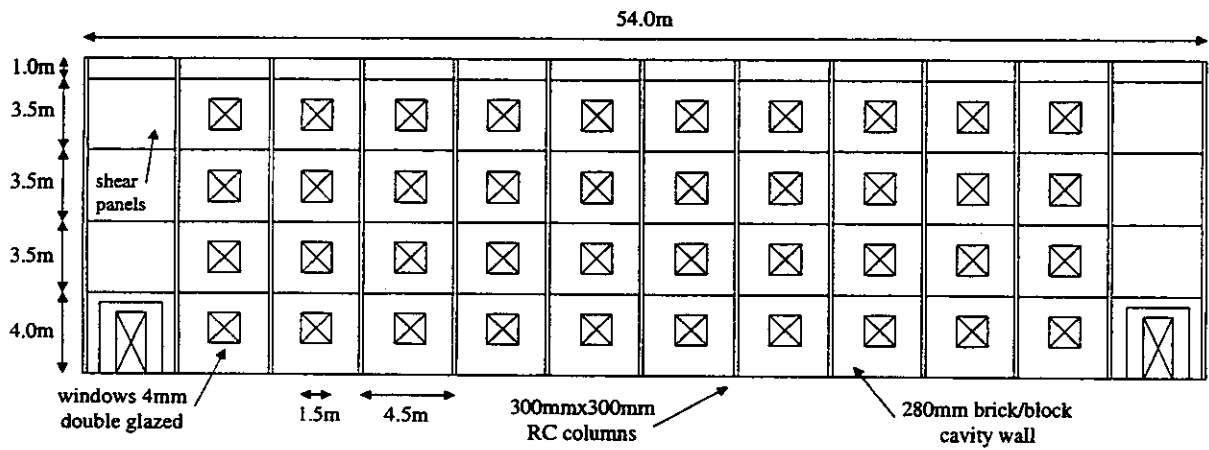
P-I Diagram: B3/2, Pressure Pulse, Long Side Facing Blast



**Short side elevation**



**Front elevation**



**Internal layout**

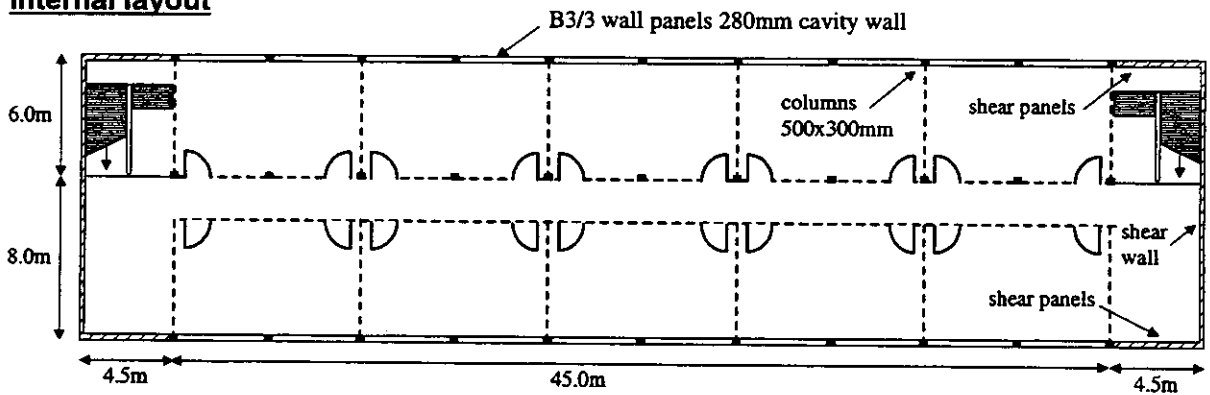
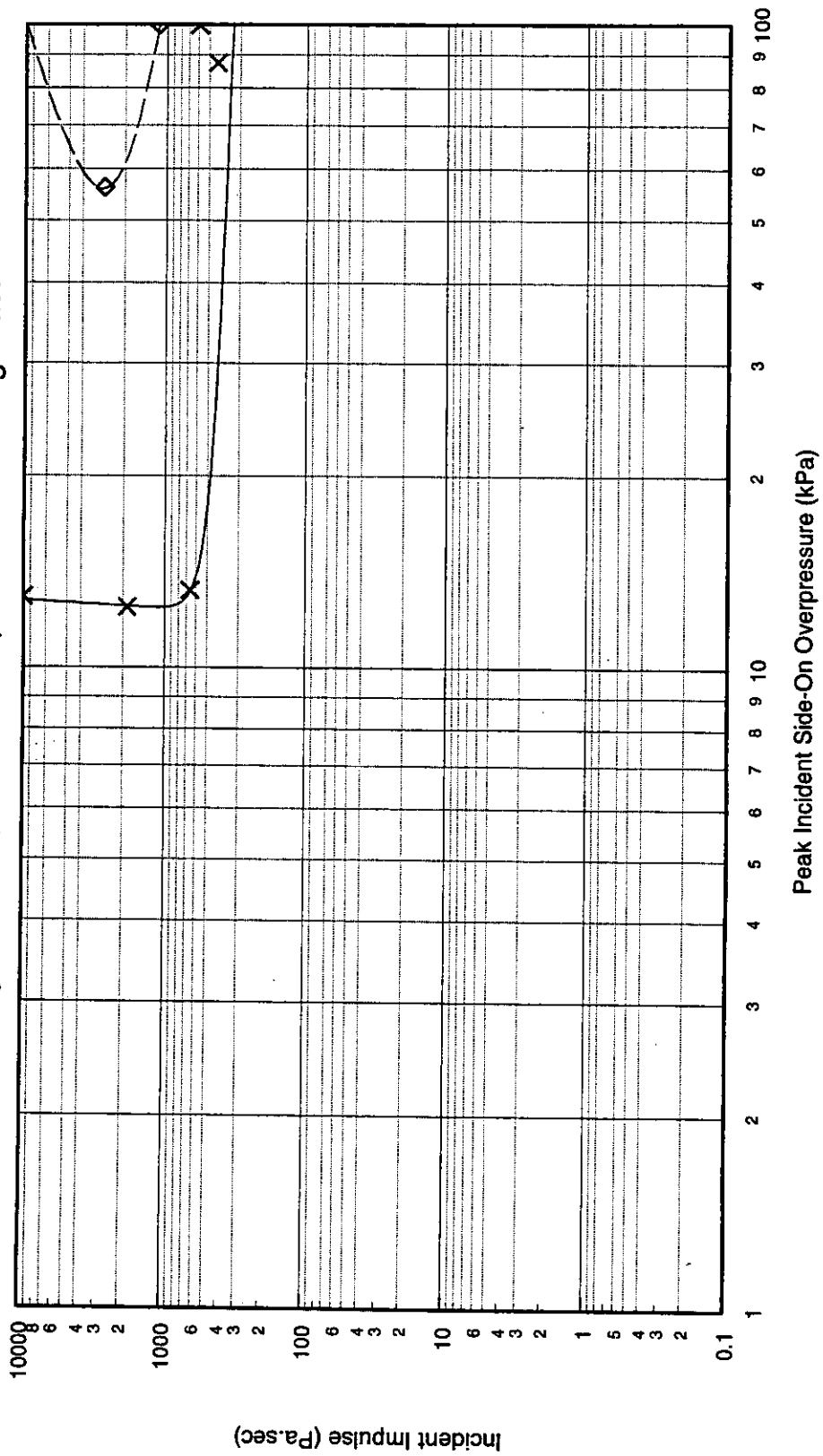


**Figure A.8: Illustration of Concrete Framed Building Type B3/3**

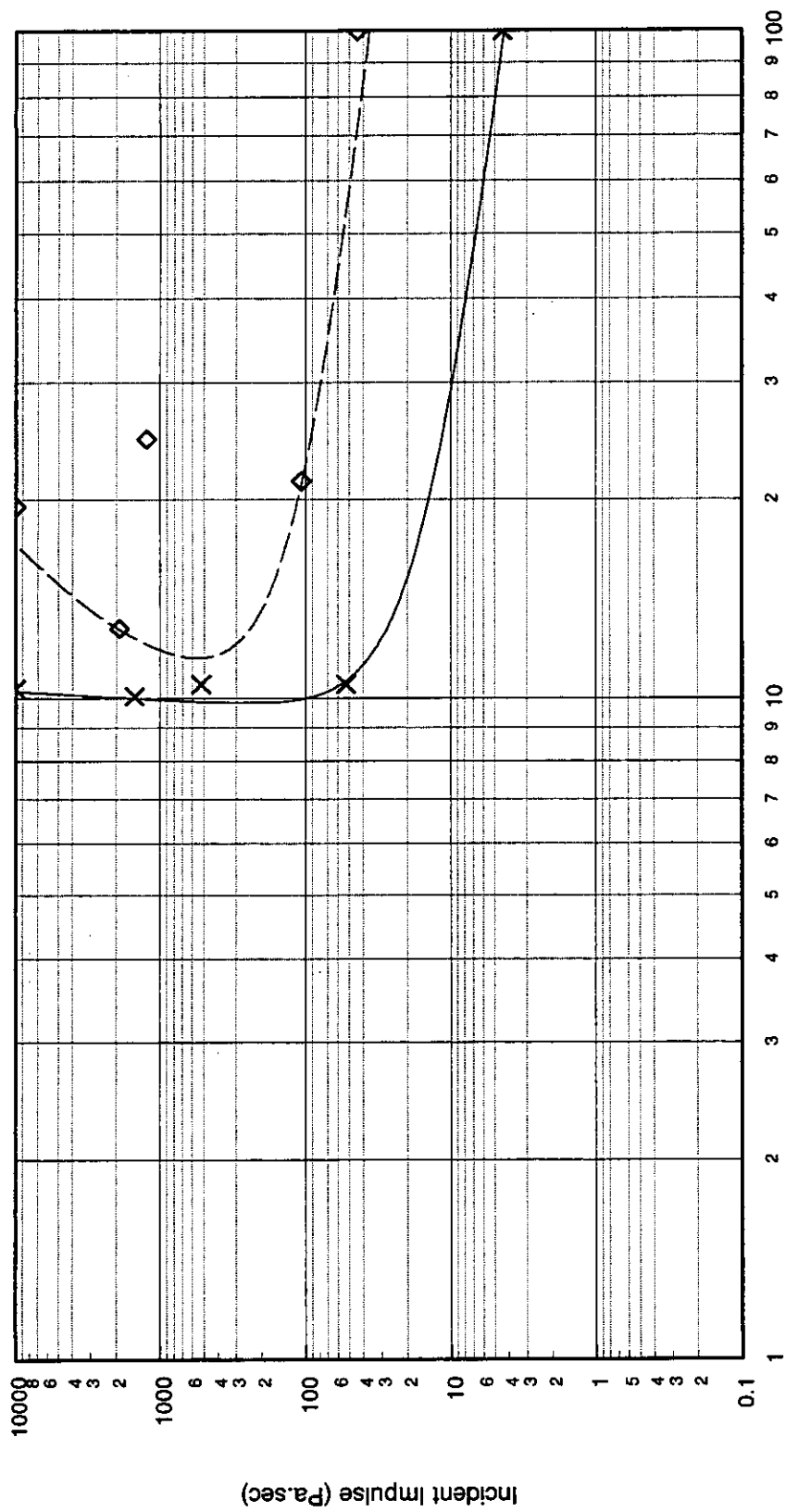
Quantity	Value	Comments
<b>Building Type: B3/3</b>		
Description	Concrete Framed Building 4 storey concrete braced frame, brick/block wall panels, end shear walls Aspect ratio 4:1	Typical office/school building
<b>Global Dimensions</b>		
Breadth	14.0m	
Length	60.0m	
Height	15.5m	
<b>Glazing Characteristics</b>		
Thickness	4mm - double glazed	Apertures in brick/block wall panels
Max. Pane dimensions	1.5 x 1.5m	
Failure Pressure (1 sec pulse duration)	82 mbar	Mainstone [4]
<b>Cladding/Wall Panel Characteristics</b>		
Thickness	242.5 mm	Brick/block panels
Panel Dimensions	3.5 x 4.0m	
Dynamic Failure Pressure	200 mbar	
Support Conditions	Simply-supported on all four sides	
Ductility	5	
Debris Size	225 x 102.5 x 75 mm	This is approximately equivalent in size to a single brick - a conservative assumption
<b>Frame Details</b>		
Frame Type	Reinforced concrete braced frame with shear walls at short sides and infill shear panels in first bay of long sides.	External and internal columns 300x300mm Main beams 500x300mm Secondary beams, 350x300mm Slabs 175mm thick
Dynamic Failure Pressure	952 mbar - global collapse, short side facing blast 6070 mbar - global collapse, long side facing blast 348 mbar - local collapse, shock pulse 317 mbar - local collapse, pressure pulse	All collapse pressures are given for a 100msec pulse duration. Global collapse corresponds to failure of the entire building, by failure of the shear walls. Local collapse corresponds to failure of an external column due to hinge formation at its mid-height. All collapse pressures assume that the cladding is capable of transmitting this load into the frame
Ductility	1.5	
<b>Additional Information</b>		

P-I Diagram: B3/3, Shock Pulse, Short Side Facing Blast



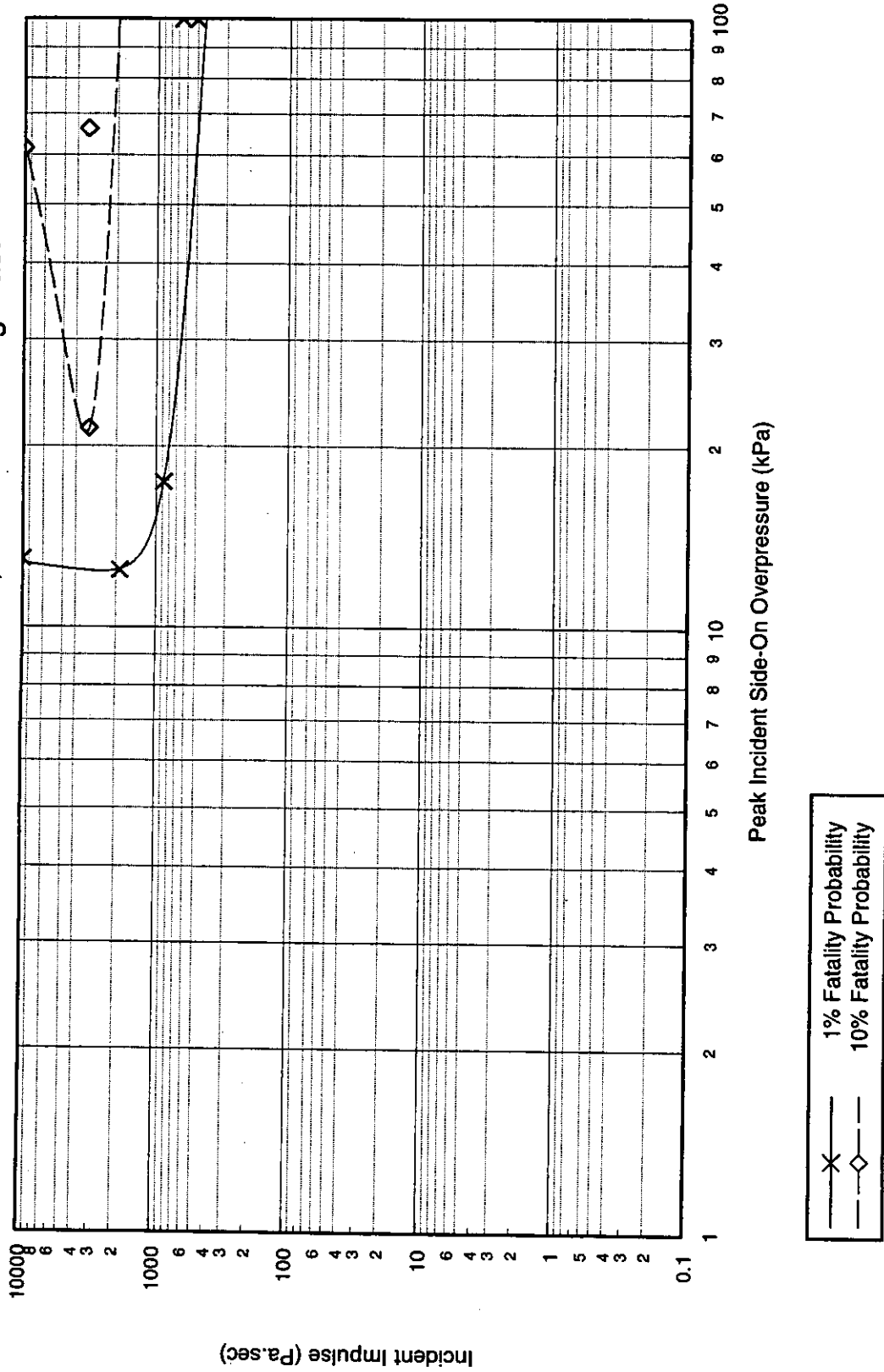
x ——— 1% Fatality Probability  
 o - - - 10% Fatality Probability

P-I Diagram: B3/3, Shock Pulse, Long Side Facing Blast

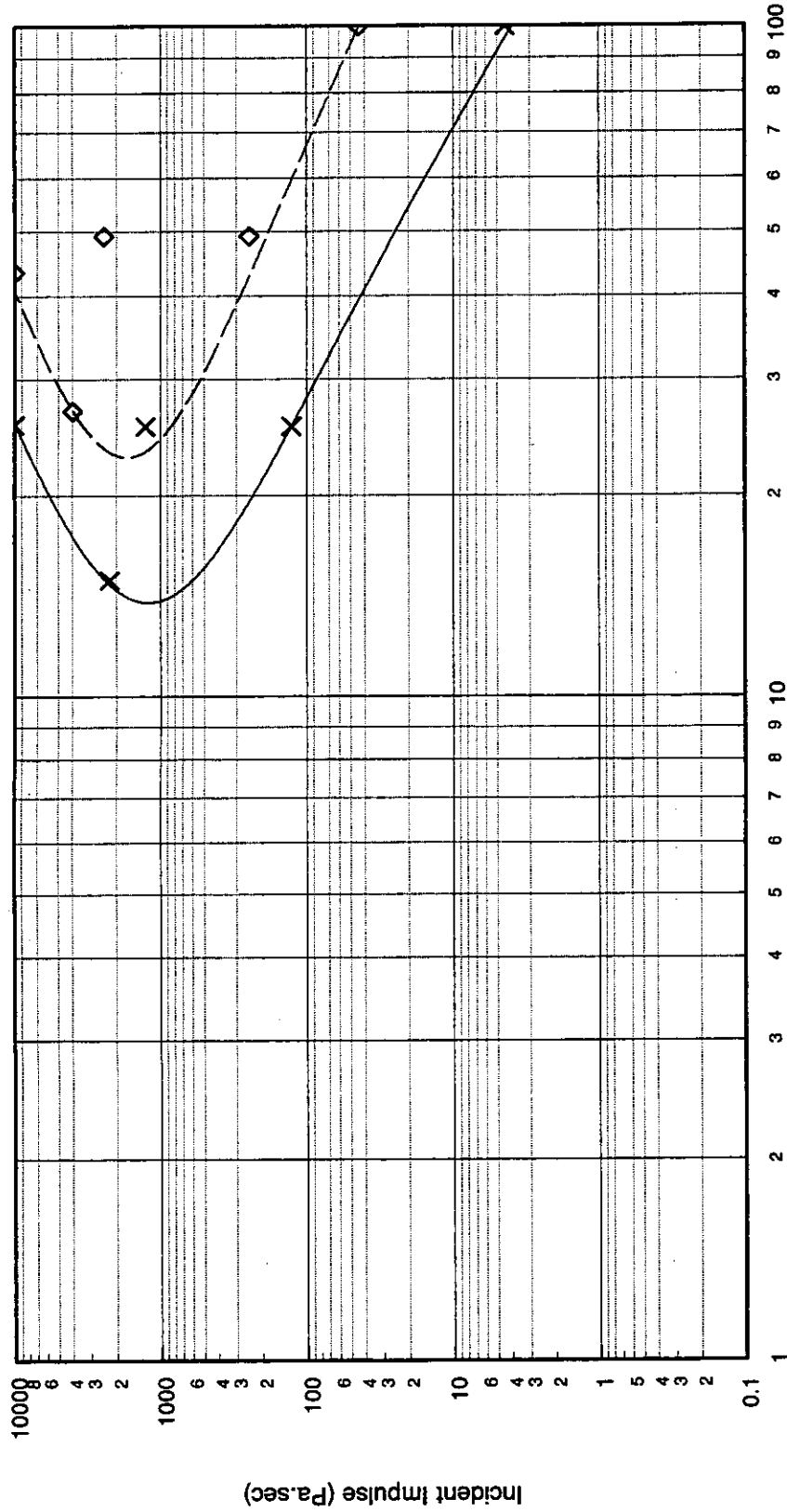


x ——— 1% Fatality Probability  
 ———◇—— 10% Fatality Probability

P-I Diagram: B3/3, Pressure Pulse, Short Side Facing Blast

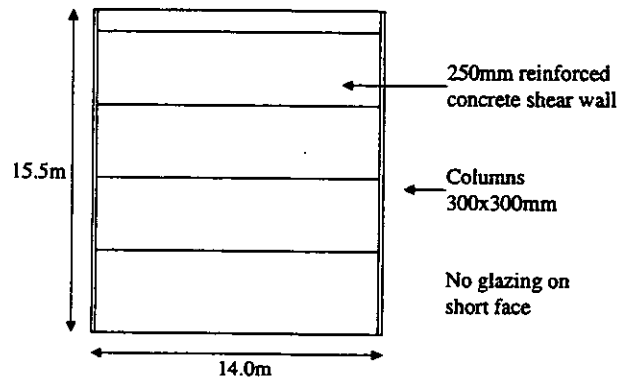


P-I Diagram: B3/3, Pressure Pulse, Long Side Facing Blast

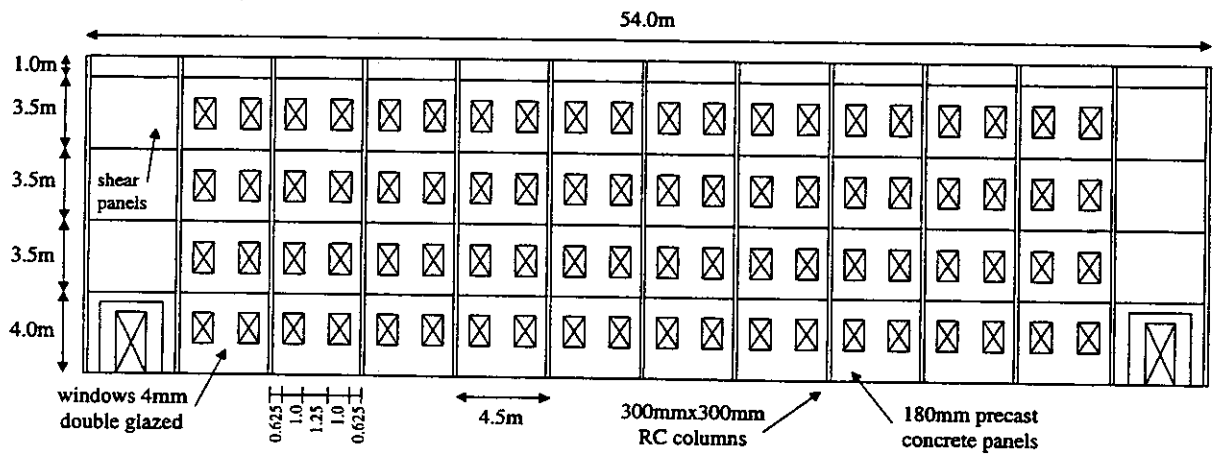


— x — 1% Fatality Probability  
 - - - ◊ - - - 10% Fatality Probability

**Short side elevation**



**Front elevation**



**Internal layout**

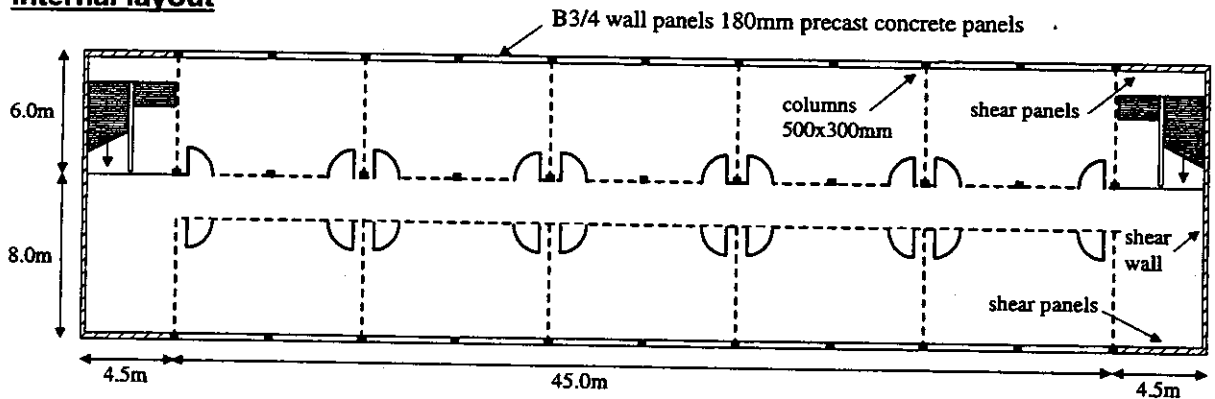
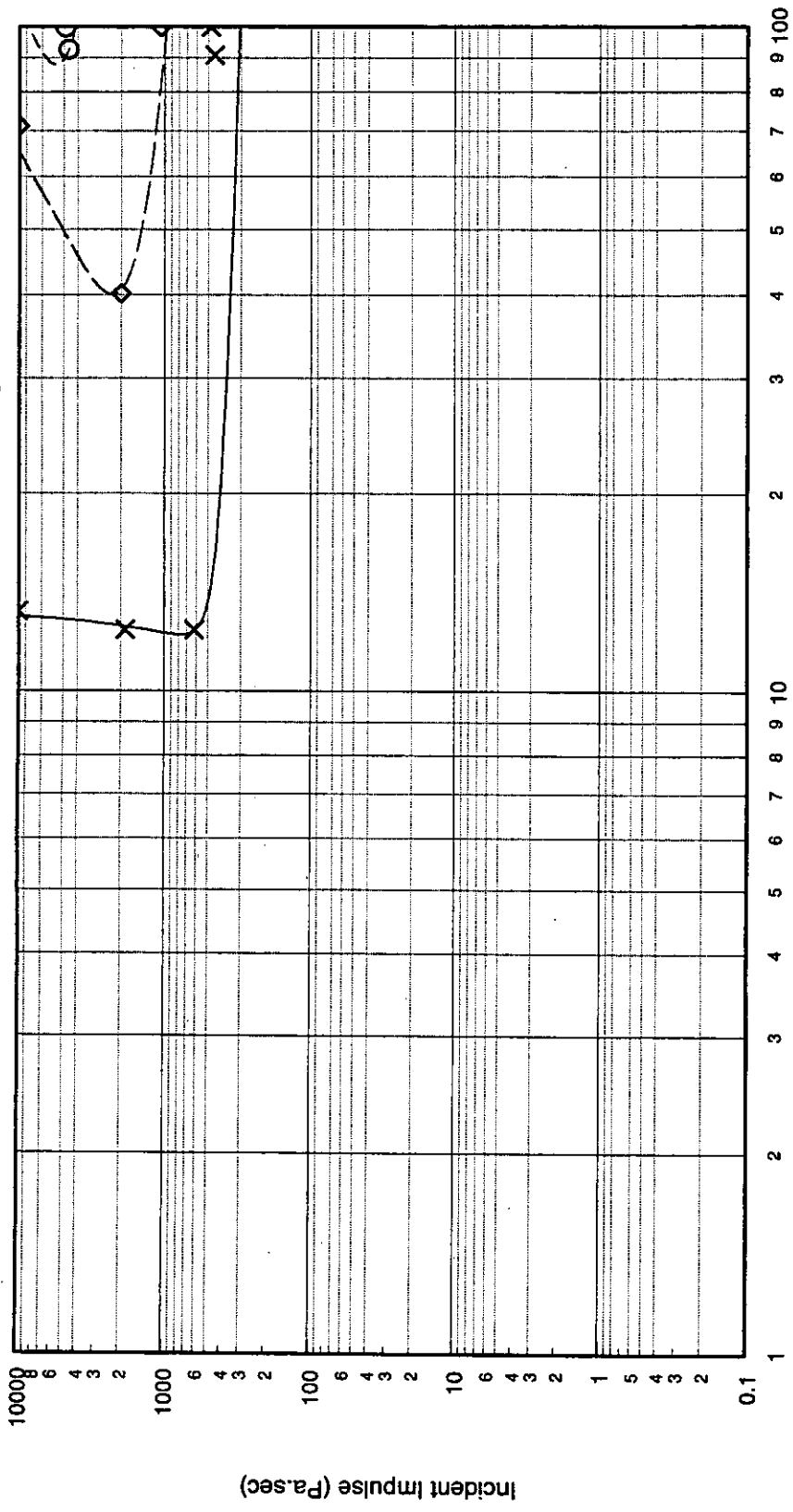


**Figure A.9: Illustration of Concrete Framed Building Type B3/4**



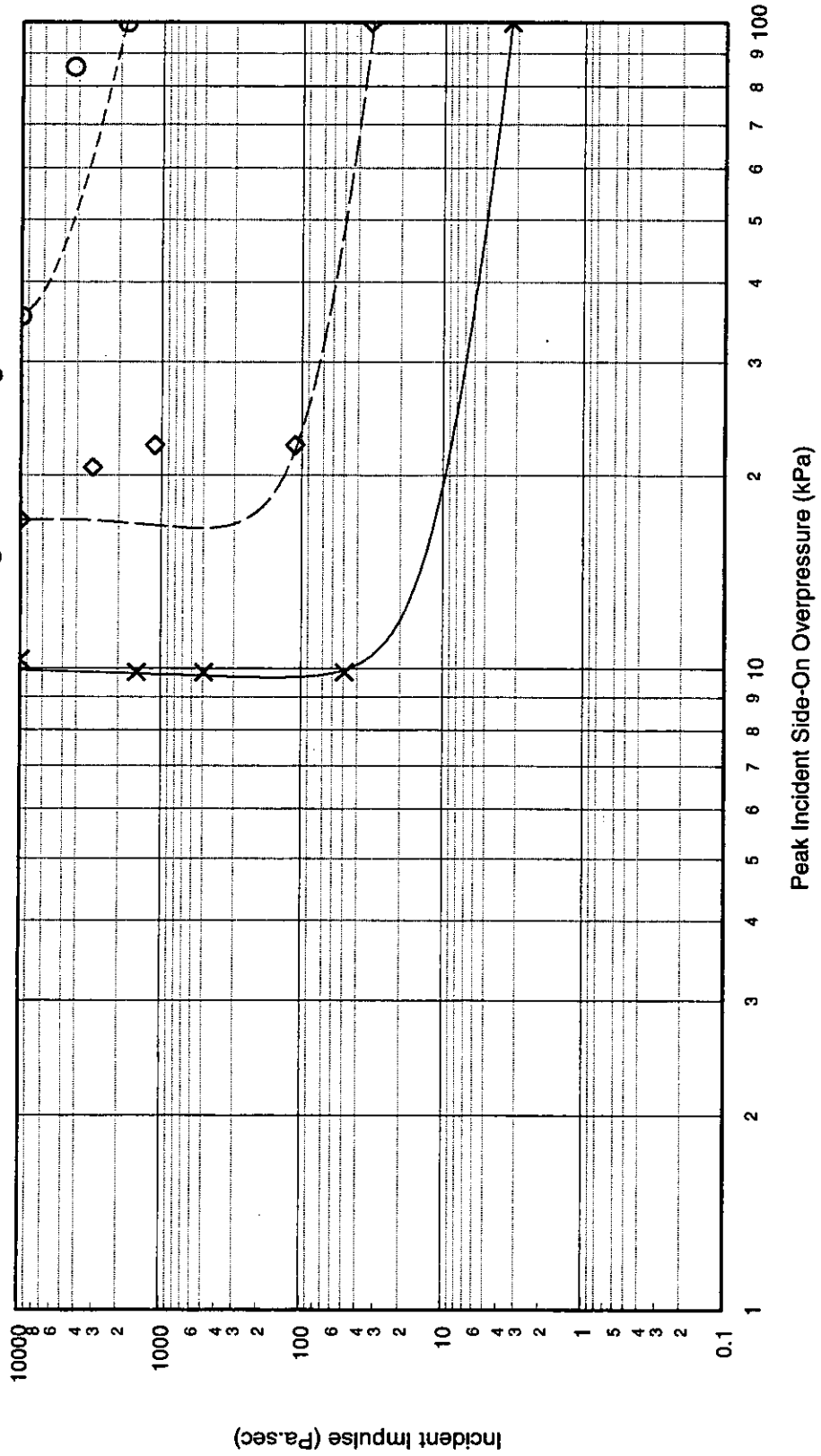
Quantity	Value	Comments
<b>Building Type: B3/4</b>		
Description	Concrete Framed Building 4 storey concrete braced frame, precast concrete wall panels, end shear walls Aspect ratio 4:1	Typical office/school building, similar to B3/3, except with precast concrete wall panels
<b>Global Dimensions</b>		
Breadth	14.0m	
Length	54.0m	
Height	15.0m	
<b>Glazing Characteristics</b>		
Thickness	4mm - double glazed	Apertures in precast concrete wall panels
Max. Pane dimensions	1.0 x 1.5m	
Failure Pressure (1 sec pulse duration)	110 mbar	Mainstone [4]
<b>Cladding/Wall Panel Characteristics</b>		
Thickness	180 mm	Precast concrete wall panels
Panel Dimensions	2.0 x 3.5m	
Dynamic Failure Pressure	215 mbar	
Support Conditions	Simply-supported on all four sides	
Ductility	10	
Debris Size	210 x 210 x 35 mm	This is a conservative assessment of the debris size based on the fatality probability criterion used
<b>Frame Details</b>		
Frame Type	Reinforced concrete braced frame with shear walls at short sides and infill shear panels in first bay of long sides.	External and internal columns 300x300mm Main beams 500x300mm Secondary beams, 350x300mm Slabs 175mm thick
Dynamic Failure Pressure	952 mbar - global collapse, short side facing blast 6070 mbar - global collapse, long side facing blast 348 mbar - local collapse, shock pulse 317 mbar - local collapse, pressure pulse	All collapse pressures are given for a 100msec pulse duration. Global collapse corresponds to failure of the entire building, by failure of the shear walls. Local collapse corresponds to failure of an external column due to hinge formation at its mid-height. All collapse pressures assume that the cladding is capable of transmitting this load into the frame
Ductility	1.5	
<b>Additional Information</b>		

P-I Diagram: B3/4, Shock Pulse, Short Side Facing Blast



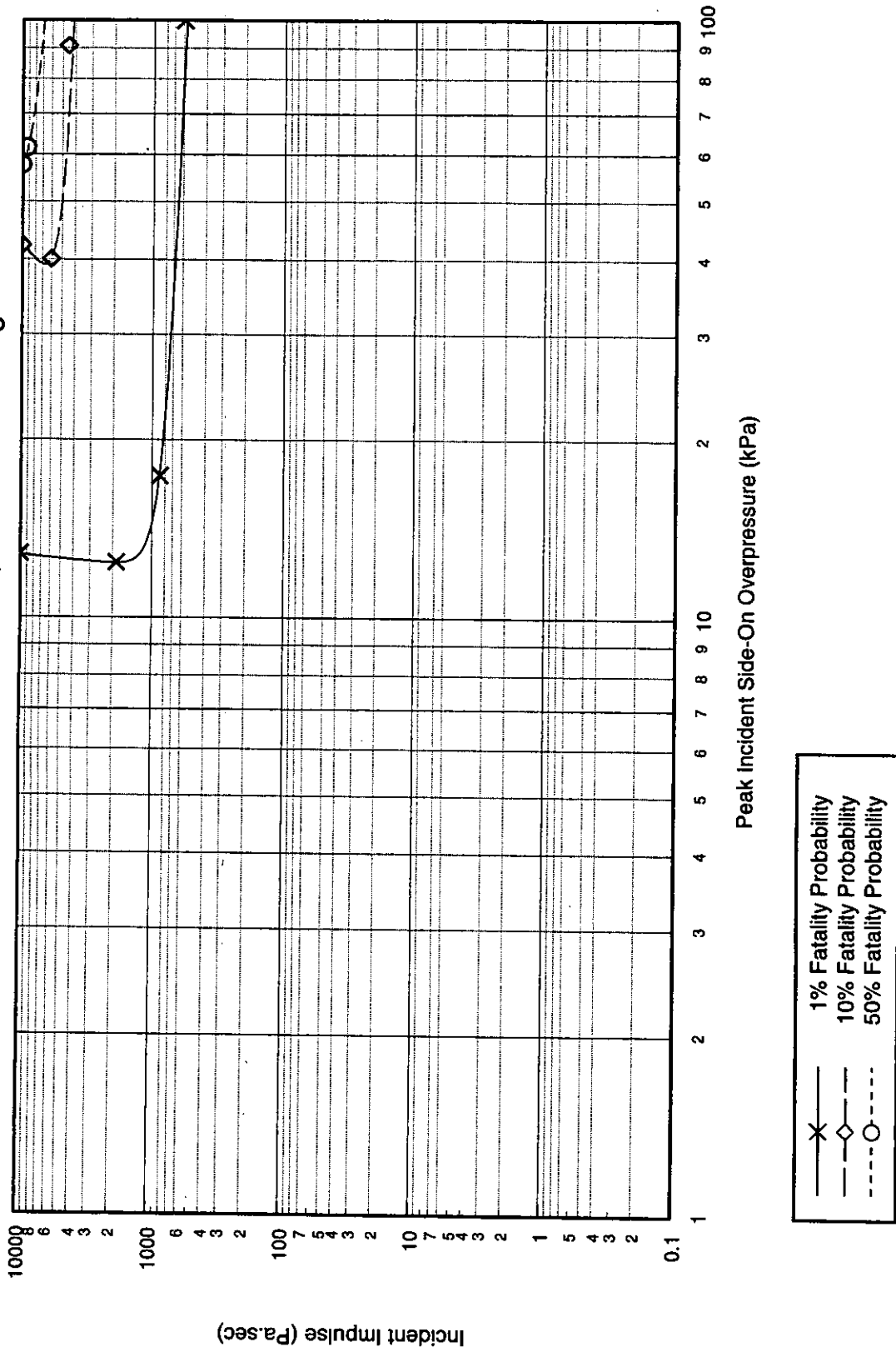
x 1% Fatality Probability  
 ◇ 10% Fatality Probability  
 ○ 50% Fatality Probability

P-I Diagram: B3/4, Shock Pulse, Long Side Facing Blast

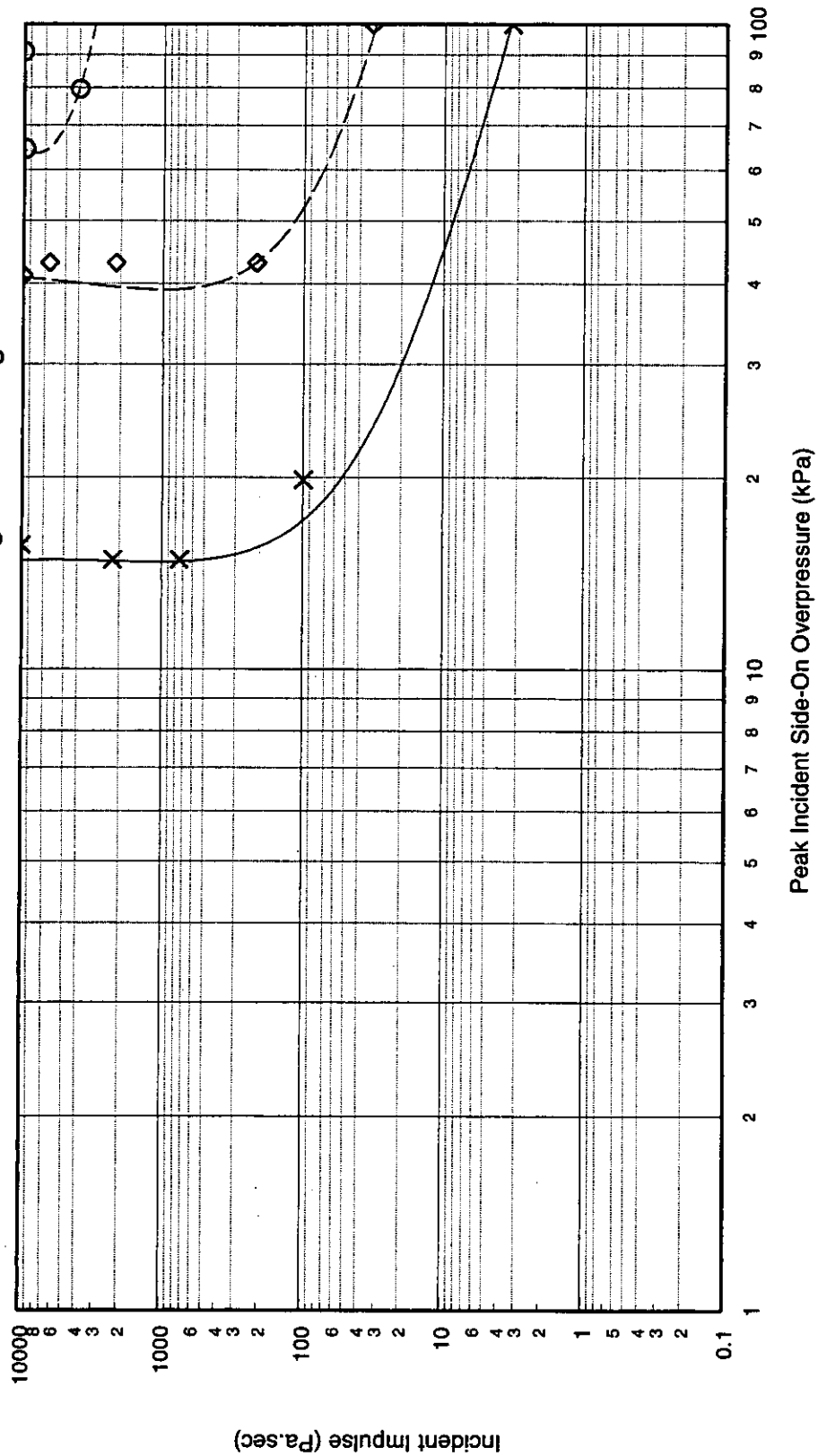


- x— 1% Fatality Probability
- ◇- 10% Fatality Probability
- 50% Fatality Probability

P-I Diagram: B3/4, Pressure Pulse, Short Side Facing Blast



P-I Diagram: B3/4, Pressure Pulse, Long Side Facing Blast



x — 1% Fatality Probability  
 ◇ — 10% Fatality Probability  
 ○ - - - 50% Fatality Probability

#### **A.4. Building Type B4: Steel Framed Buildings**

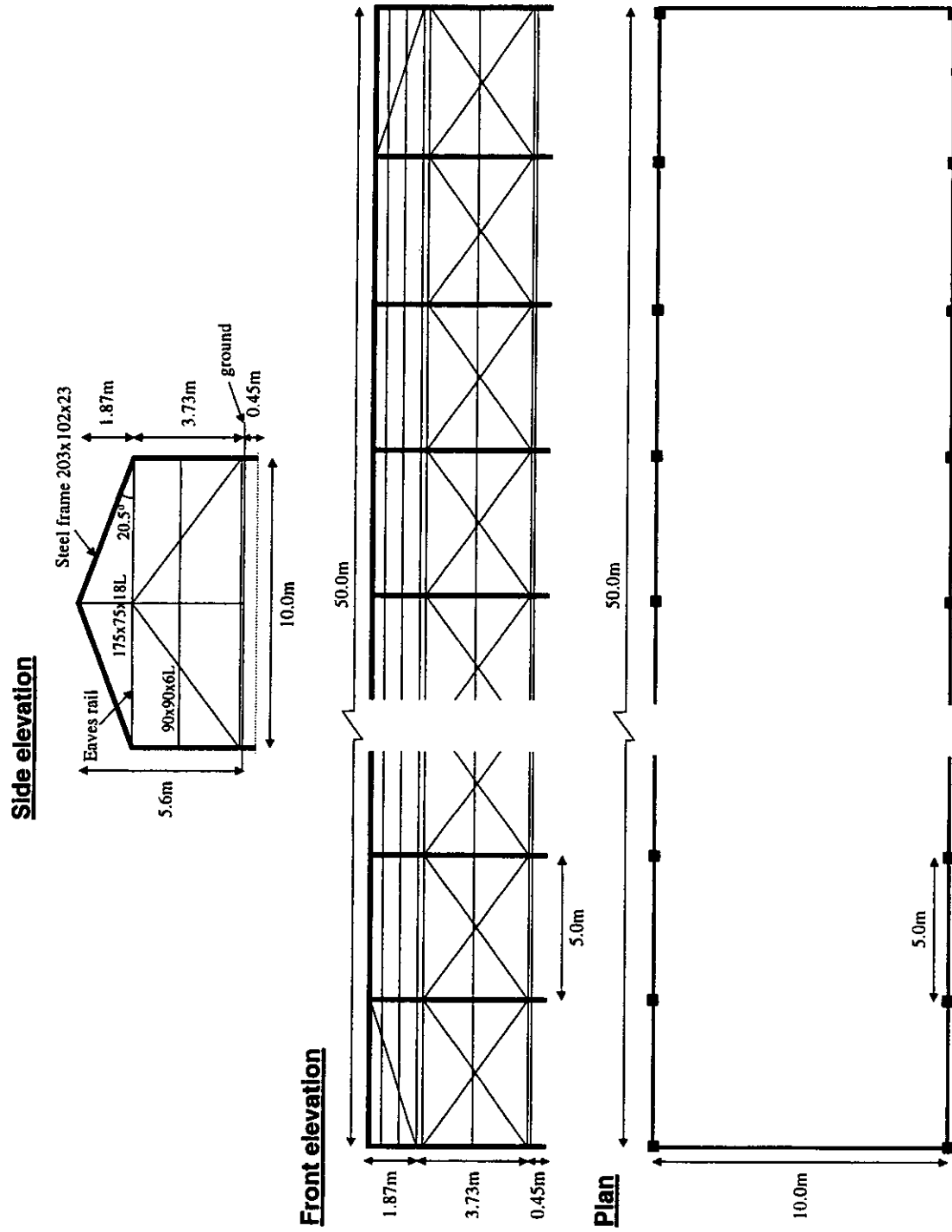
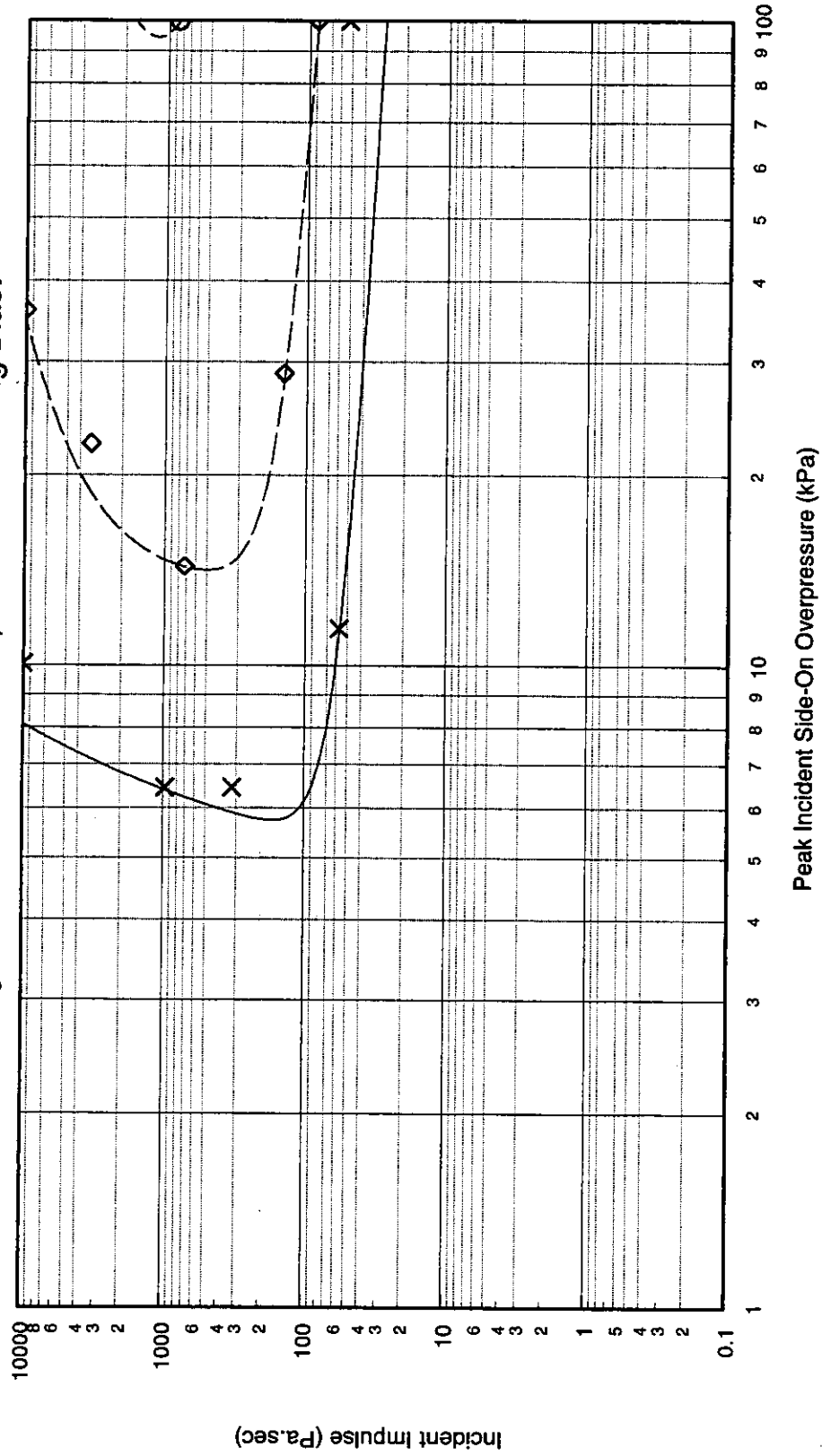


Figure A.10: Illustration of Steel Framed Building B4/1

Quantity	Value	Comments
<b>Building Type: B4/1</b>		
Description	Steel framed and clad, single storey, moment resisting single bay building. Aspect ratio 5:1	
<b>Global Dimensions</b>		
Breadth	10.0m	
Length	50.0m	
Height	5.6m	
<b>Glazing Characteristics</b>		
Thickness		No glazing
Max. Pane dimensions		
Failure Pressure (1 sec pulse duration)		
<b>Cladding/Wall Panel Characteristics</b>		
Thickness	0.6mm	Corrugated steel panel
Panel Dimensions	1.865 x 1.0m	
Dynamic Failure Pressure	92.5 mbar	Failure of panels is most likely to occur upon failure of supporting steel work, therefore failure pressure corresponds to the bracing failure pressure.
Support Conditions	Simply supported at both ends of bracing beam.	
Ductility	5	
Debris Size	1.865 x 1.0 x 0.0006m	Debris size has been chosen to be equivalent to a standard steel construction panel. The velocity of the panel is calculated for edge on separation from the frame, whereas the flight of the debris assumes perpendicular flight, producing acceptable velocities.
<b>Frame Details</b>		
Frame Type	Steel I-beam moment resisting framework, 203 x 102 x UB23 columns, as portal frame, with 90 x 90 x 6L rail bracing.	
Dynamic Failure Pressure	1158 mbar	Frame failure pressure calculated for collapse, based on all the panels having failed and transferring no load to the frame.
Ductility	5	
<b>Additional Information</b>		

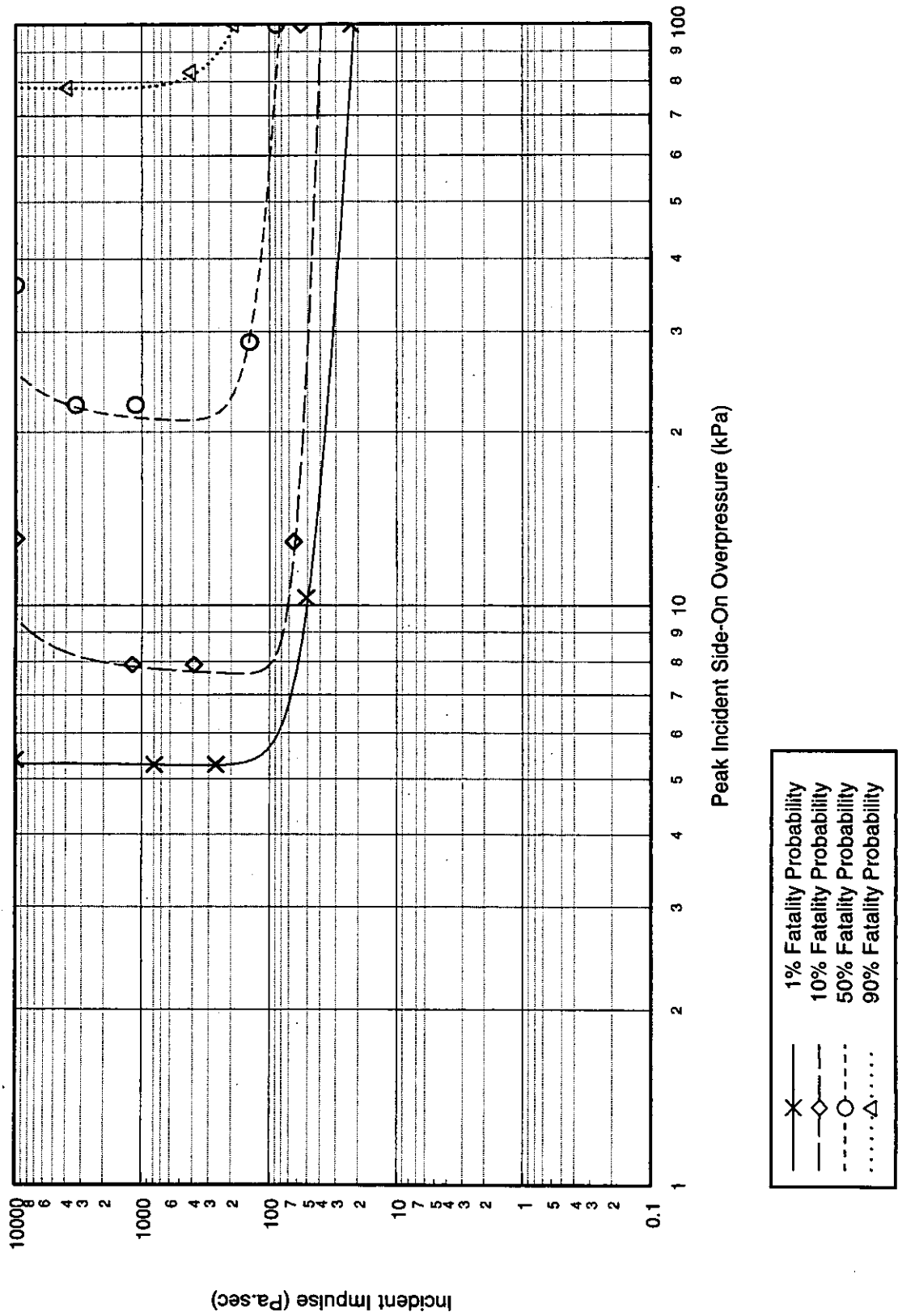


P-I Diagram: B4/1, Shock Pulse, Short Side Facing Blast

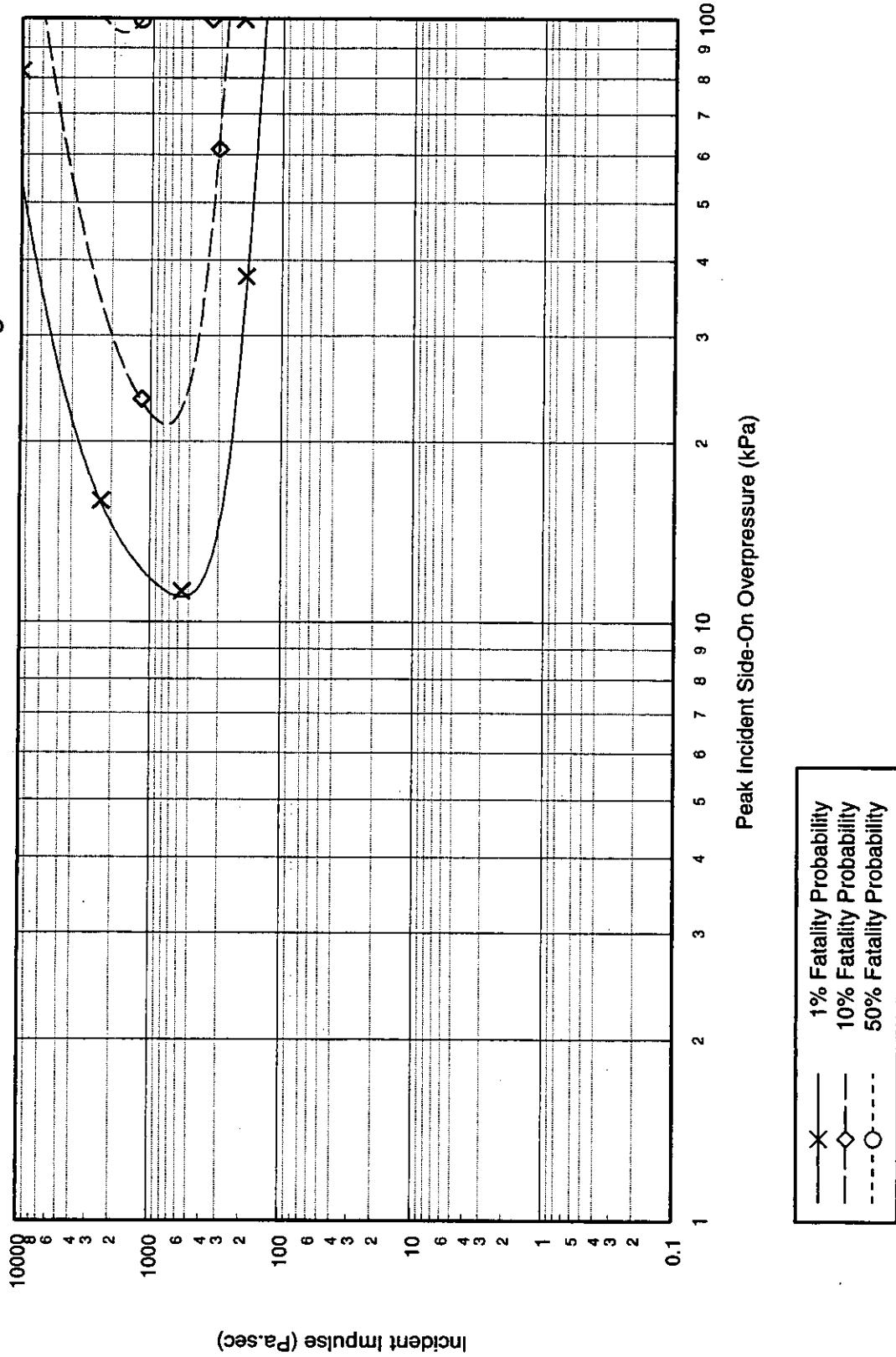


x 1% Fatality Probability  
 ◊ 10% Fatality Probability  
 ○ 50% Fatality Probability

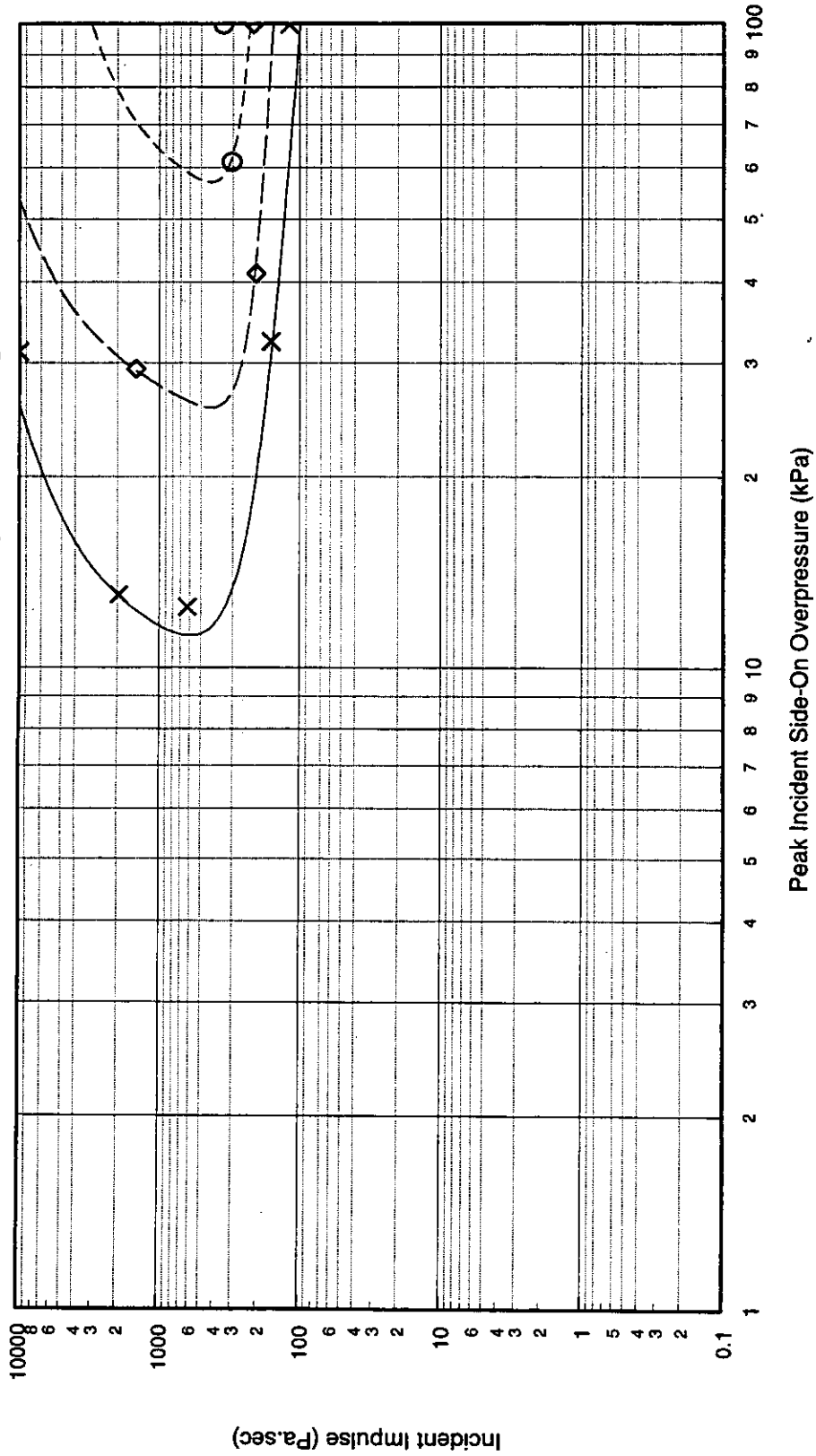
P-I Diagram: B4/1, Shock Pulse, Long Side Facing Blast



P-I Diagram: B4/1, Pressure Pulse, Short Side Facing Blast

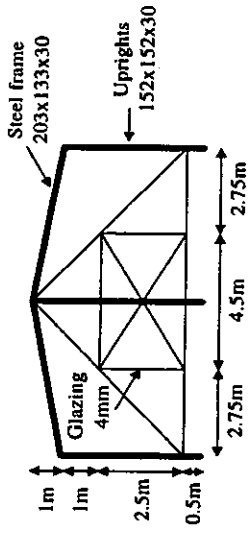


P-I Diagram: B4/1, Pressure Pulse, Long Side Facing Blast

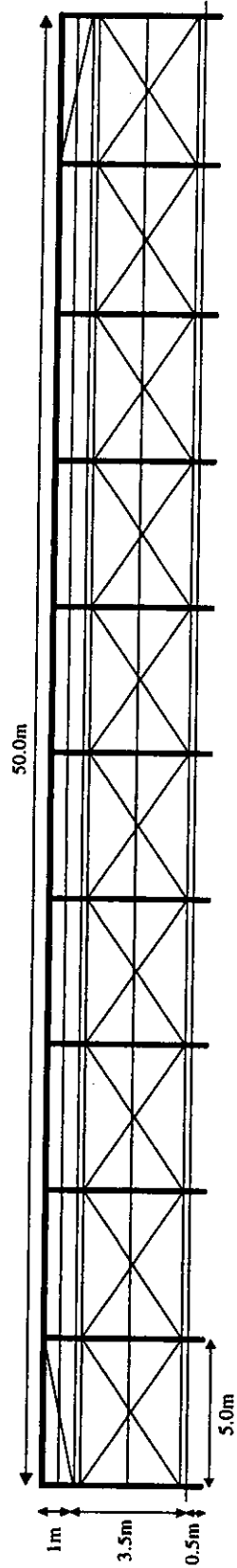


— x — 1% Fatality Probability  
 - - - ◊ - - 10% Fatality Probability  
 . . . ○ . . . 50% Fatality Probability

**Front elevation**



**Side elevation**



**Plan**

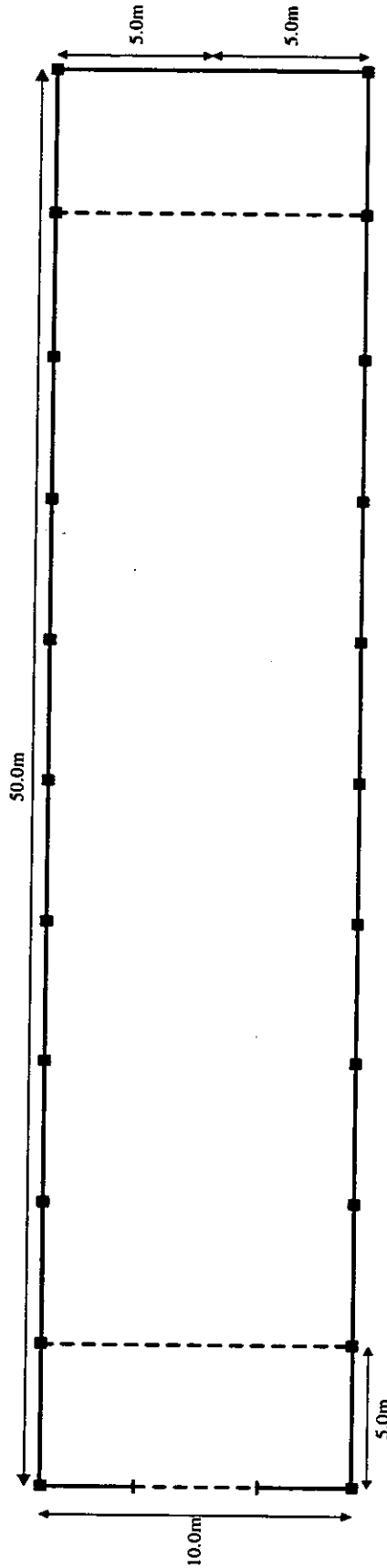
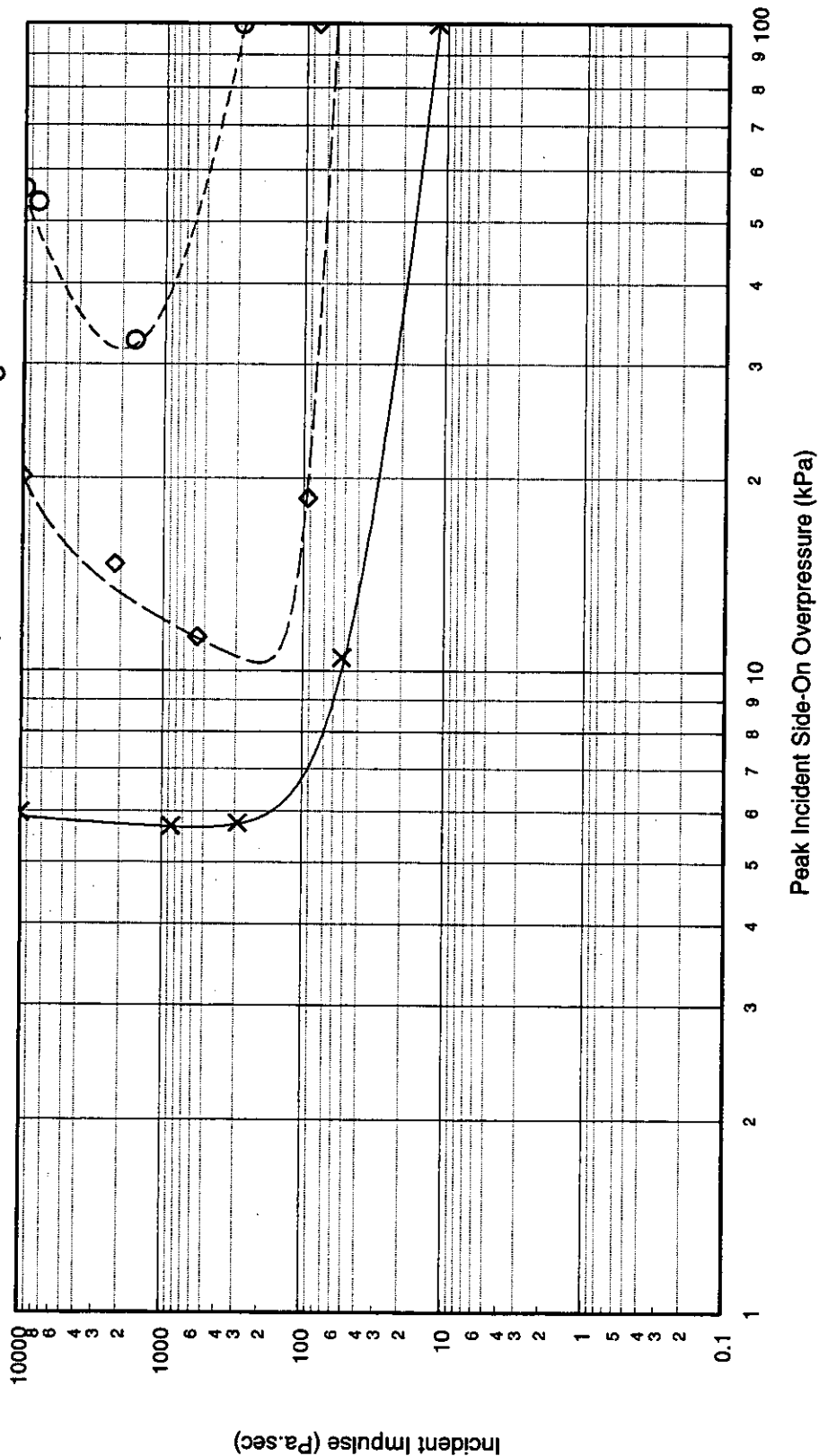


**Figure A.11: Illustration of Steel Framed Building Type B4/2**

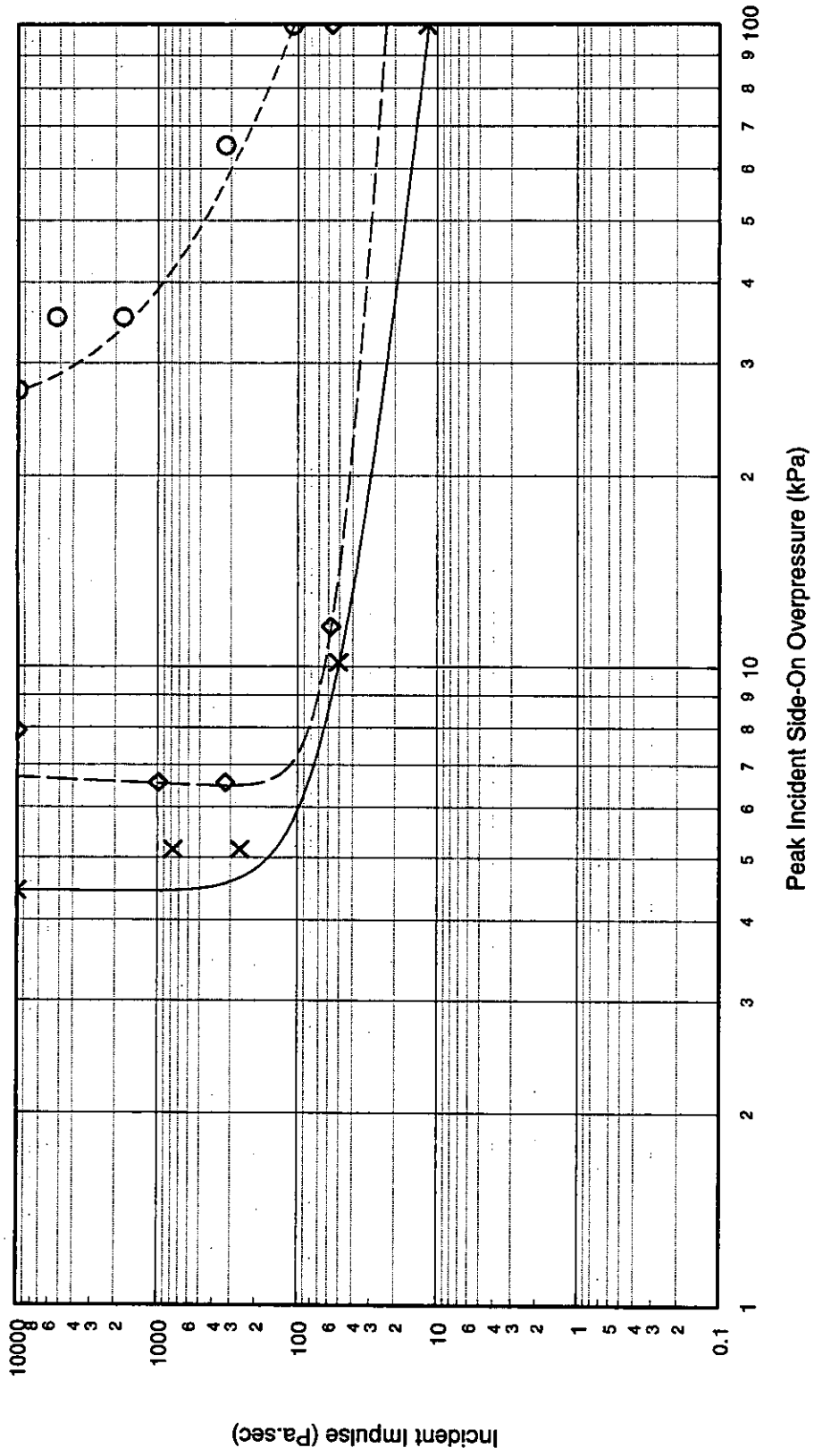
Quantity	Value	Comments
<b>Building Type: B4/2</b>		
Description	Steel framed and clad, double bay, single storey, braced frame building. Aspect ratio 5:1	
<b>Global Dimensions</b>		
Breadth	10.0m	
Length	50.0m	
Height	4.5m	
<b>Glazing Characteristics</b>		
Thickness	4mm - double glazed	
Max. Pane dimensions	1.25 x 0.75m	
Failure Pressure (1 sec pulse duration)	90 mbar	Mainstone [4]
<b>Cladding/Wall Panel Characteristics</b>		
Thickness	0.6mm	Corrugated steel panel
Panel Dimensions	1.75 x 1.0m	
Dynamic Failure Pressure	74.9 mbar	Failure of panels is most likely to occur upon failure of supporting steel work, therefore failure pressure corresponds to the bracing failure pressure.
Support Conditions	Simply supported at both ends of bracing beam.	
Ductility	5	
Debris Size	1.75 x 1.0 x 0.0006m	Debris size has been chosen to be equivalent to a standard steel construction panel. The velocity of the panel is calculated for edge on separation from the frame and perpendicular flight.
<b>Frame Details</b>		
Frame Type	Steel I-beam braced frame	125 x 125 x UC30 columns and 203 x 133 x UB30 roof supports as portal frame, with 100 x 100 x 8 L rail bracing.
Dynamic Failure Pressure (100msec pulse duration)	Global collapse :- 112.9 mbar - short side facing blast 100.2 mbar - long side facing blast Local collapse: - Shock pulse:- 92.2 mbar - short face 275 mbar - long face Pressure pulse:- 111 mbar - short face 326 mbar - long face	Global collapse corresponds to failure of the entire building. Local collapse corresponds to failure of an external column due to hinge formation at its mid-height. All collapse pressures assume that the cladding is capable of transmitting load into the frame, and are increased by a suitable multiplication factor if the panels fail before the columns
Ductility	5	
<b>Additional Information</b>		

P-I Diagram: B4/2, Shock Pulse, Short Side Facing Blast



— x — 1% Fatality Probability  
 - - - ◊ - - - 10% Fatality Probability  
 . . . ○ . . . 50% Fatality Probability

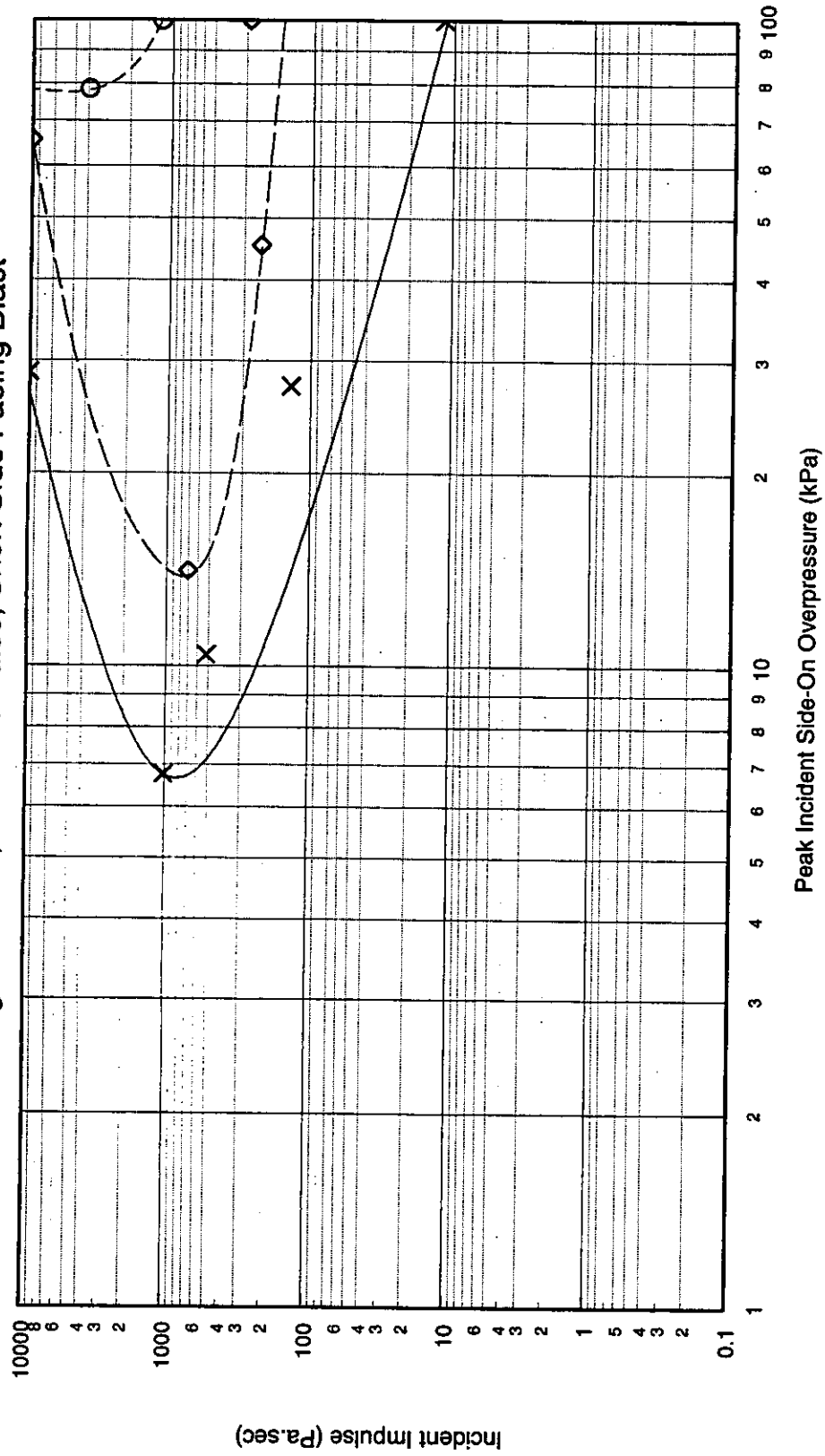
P-I Diagram: B4/2, Shock Pulse, Long Side Facing Blast



x — 1% Fatality Probability  
 —◇— 10% Fatality Probability  
 - - -○- - - 50% Fatality Probability

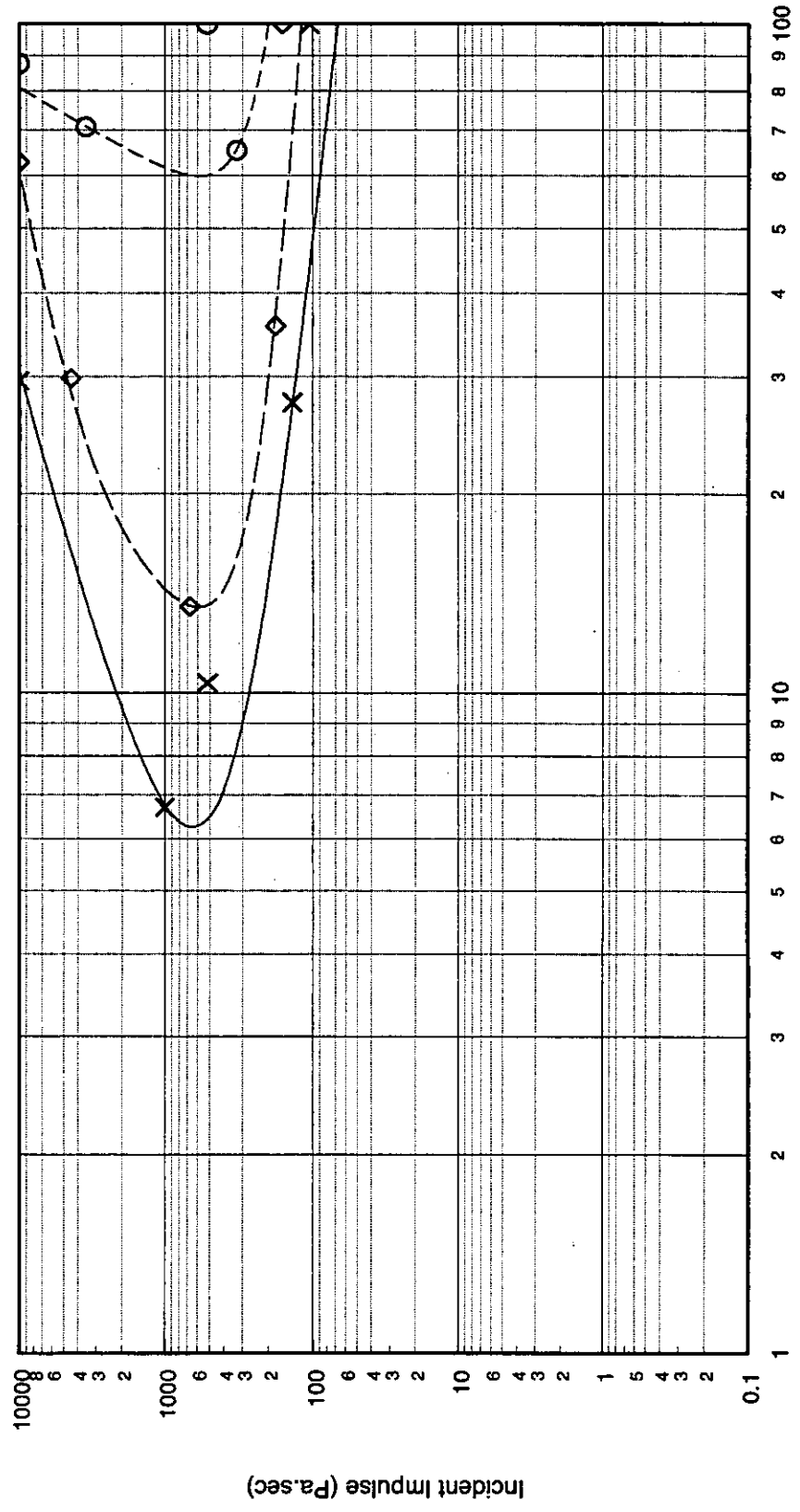


P-I Diagram: B4/2, Pressure Pulse, Short Side Facing Blast



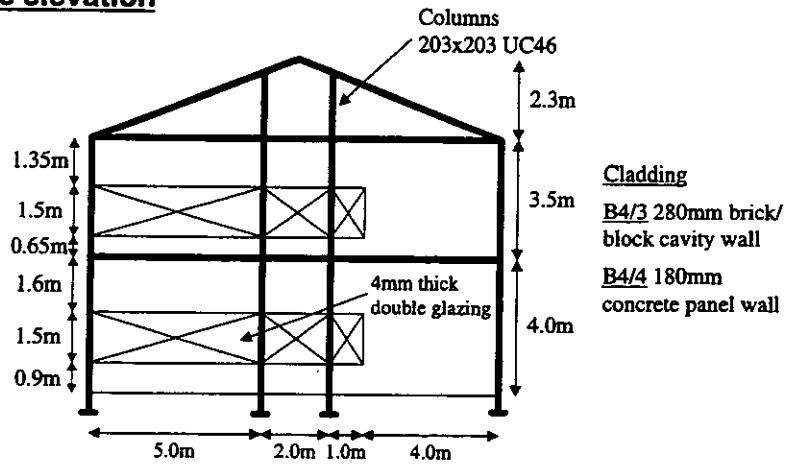
X — 1% Fatality Probability  
 —◇— 10% Fatality Probability  
 - - -○- - - 50% Fatality Probability

P-I Diagram: B4/2, Pressure Pulse, Long Side Facing Blast

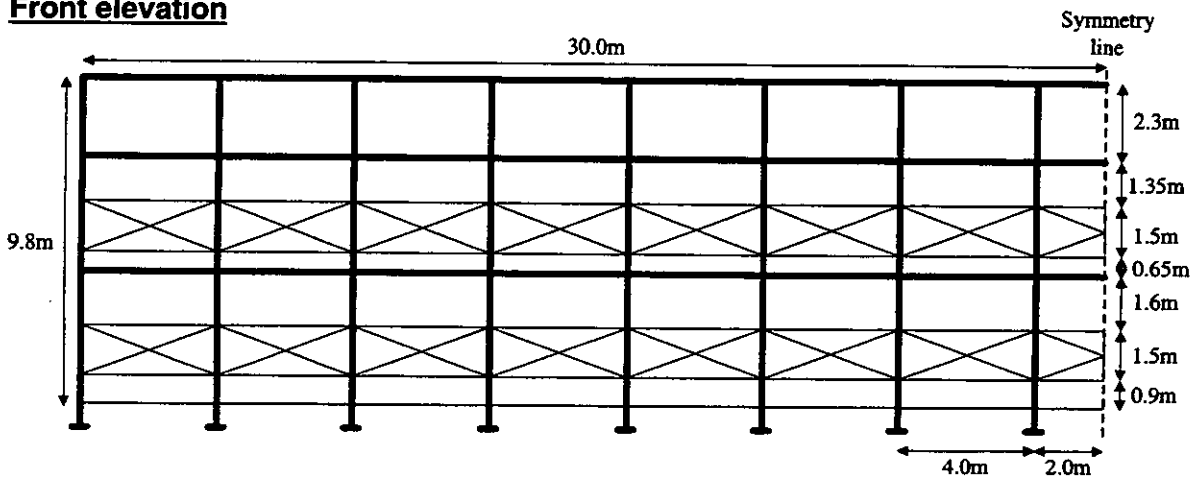


- x— 1% Fatality Probability
- ◇- 10% Fatality Probability
- 50% Fatality Probability

**Side elevation**



**Front elevation**



**Plan - floors ground and first**

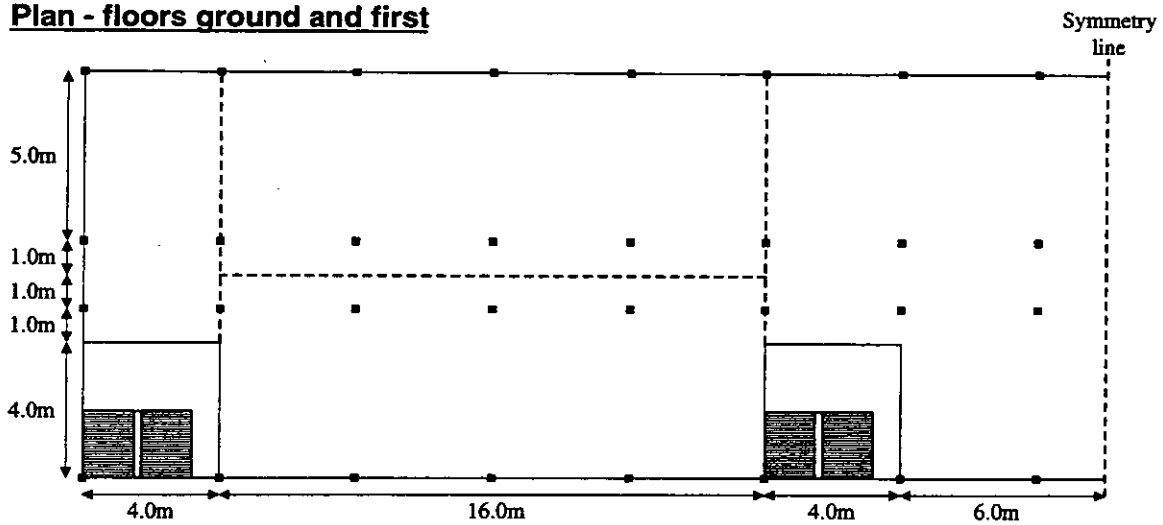
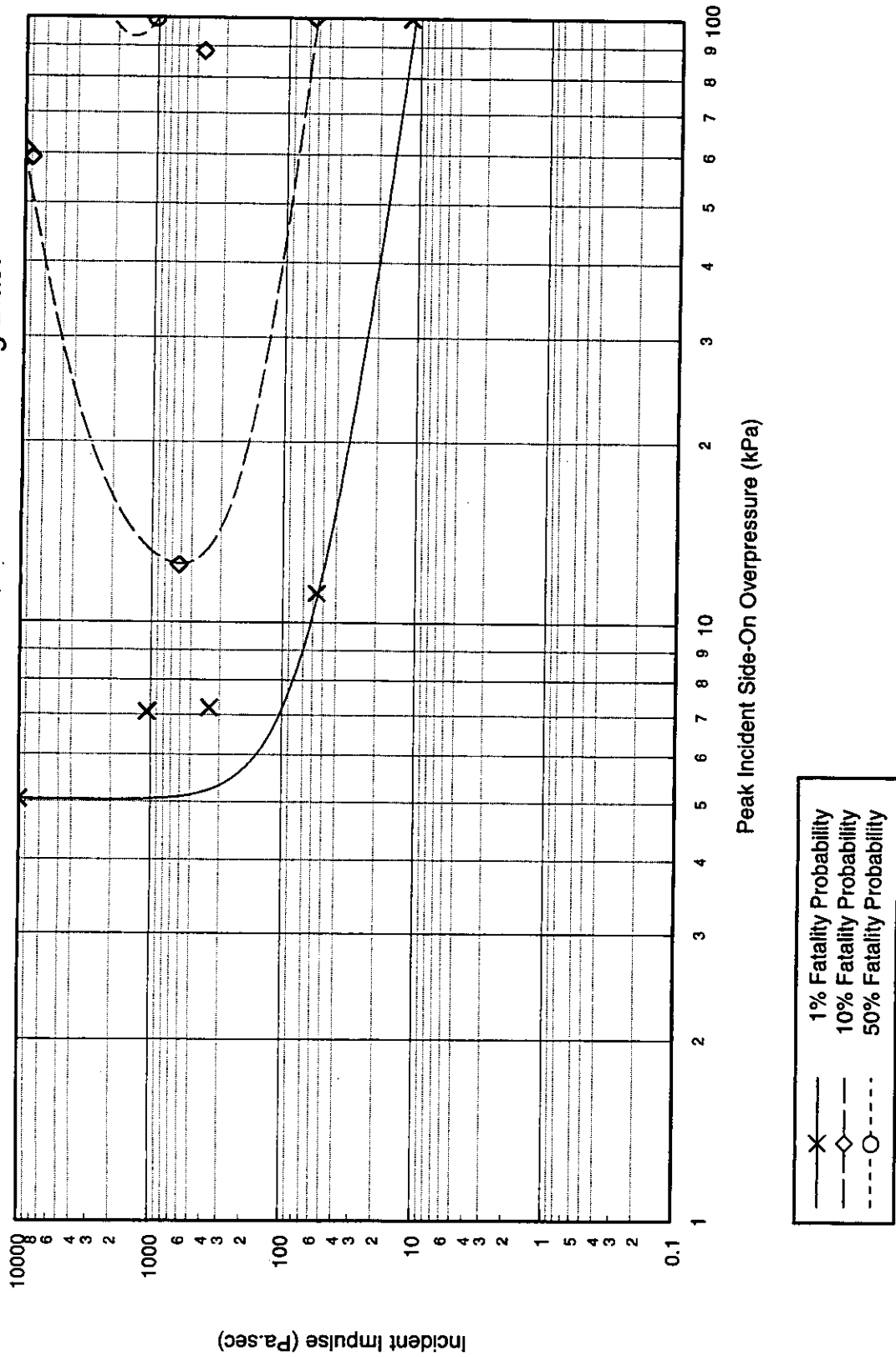


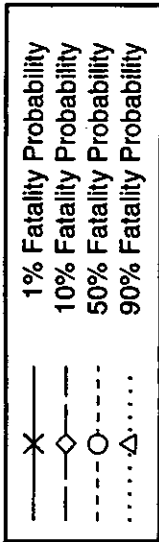
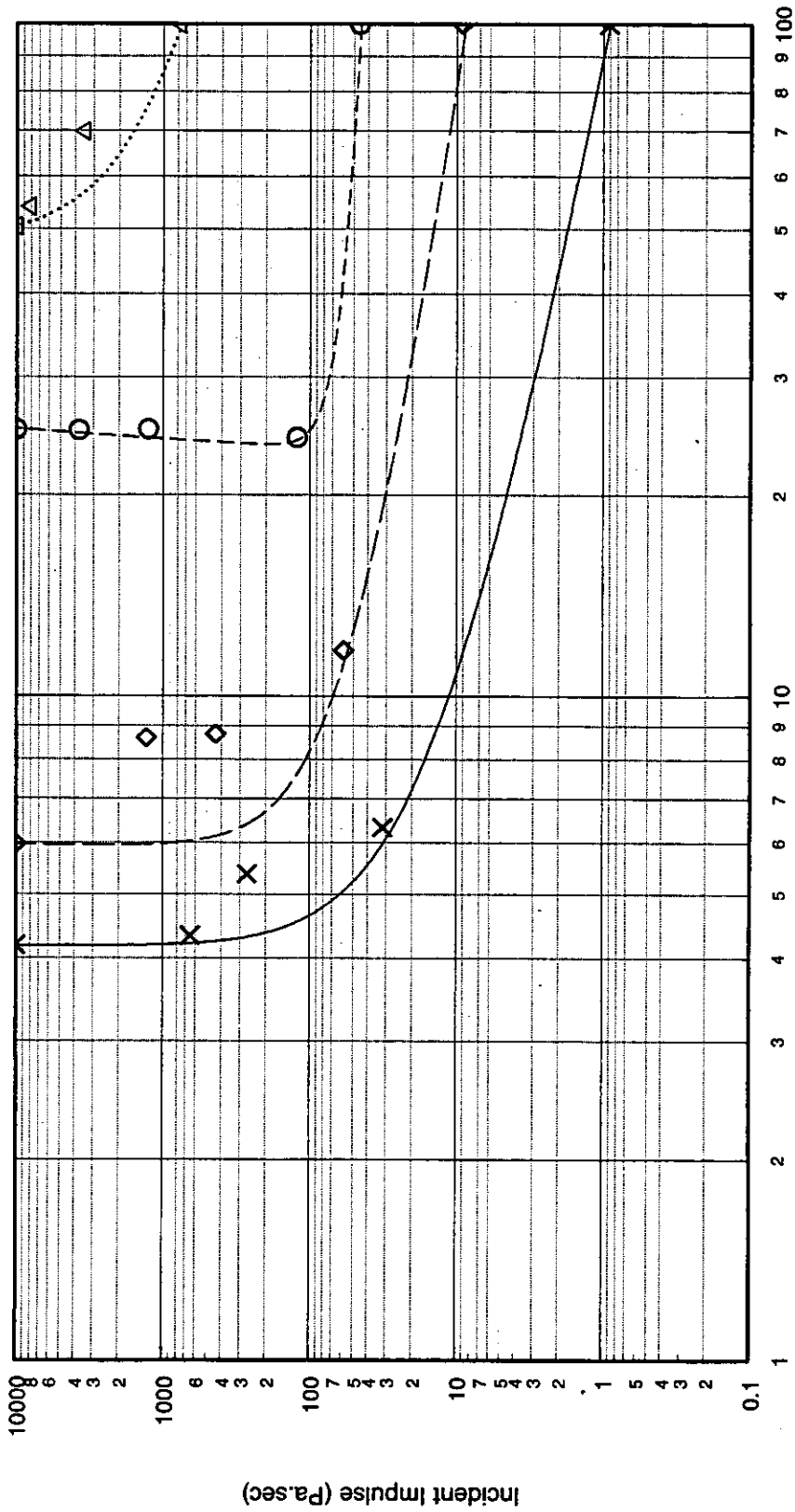
**Figure A.12: Illustration of Steel Framed Building Types B4/3 and B4/4**

Quantity	Value	Comments
<b>Building Type: B4/3</b>		
Description	Steel framed, brick/block clad, two storey, braced frame building. Aspect ratio 5:1	
<b>Global Dimensions</b>		
Breadth	12.0m	
Length	60.0m	
Height	9.8m	
<b>Glazing Characteristics</b>		
Thickness	4mm - Double glazed	Continuous glazing
Max. Pane dimensions	1.25 x 0.75m	
Failure Pressure (1 sec pulse duration)	90 mbar	Mainstone [4]
<b>Cladding/Wall Panel Characteristics</b>		
Thickness	280mm brick/block cavity wall	102.5 x 225 x 75mm bricks 100 x 400 x 200mm blocks
Panel Dimensions	3.5 x 4.0m	
Dynamic Failure Pressure	90 mbar	
Support Conditions	Simply supported along 4 edges of representative plate	
Ductility	5	
Debris Size	102.5 x 225 x 75mm	The debris is assumed to be made up of bricks only, and therefore the standard brick size was used.
<b>Frame Details</b>		
Frame Type	Steel I-beam braced frame of 203 x 203 x UC46 columns	Staircase blocks are enclosed in 225mm blockwork or brickwork, providing lateral stability and an area of no collapse.
Dynamic Failure Pressure	Global collapse :- 154.9 mbar - short side facing blast 72.9 mbar - long side facing blast Local collapse: - Shock pulse:- 337 mbar - short face 595 mbar - long face Pressure pulse:- 407.6 mbar - short face 711.1 mbar - long face	Global collapse corresponds to failure of the entire building. Local collapse corresponds to failure of an external column due to hinge formation at its mid-height. All collapse pressures assume that the cladding is capable of transmitting load into the frame, and are increased by a suitable multiplication factor if the panels fail before the columns
Ductility	5	
<b>Additional Information</b>		

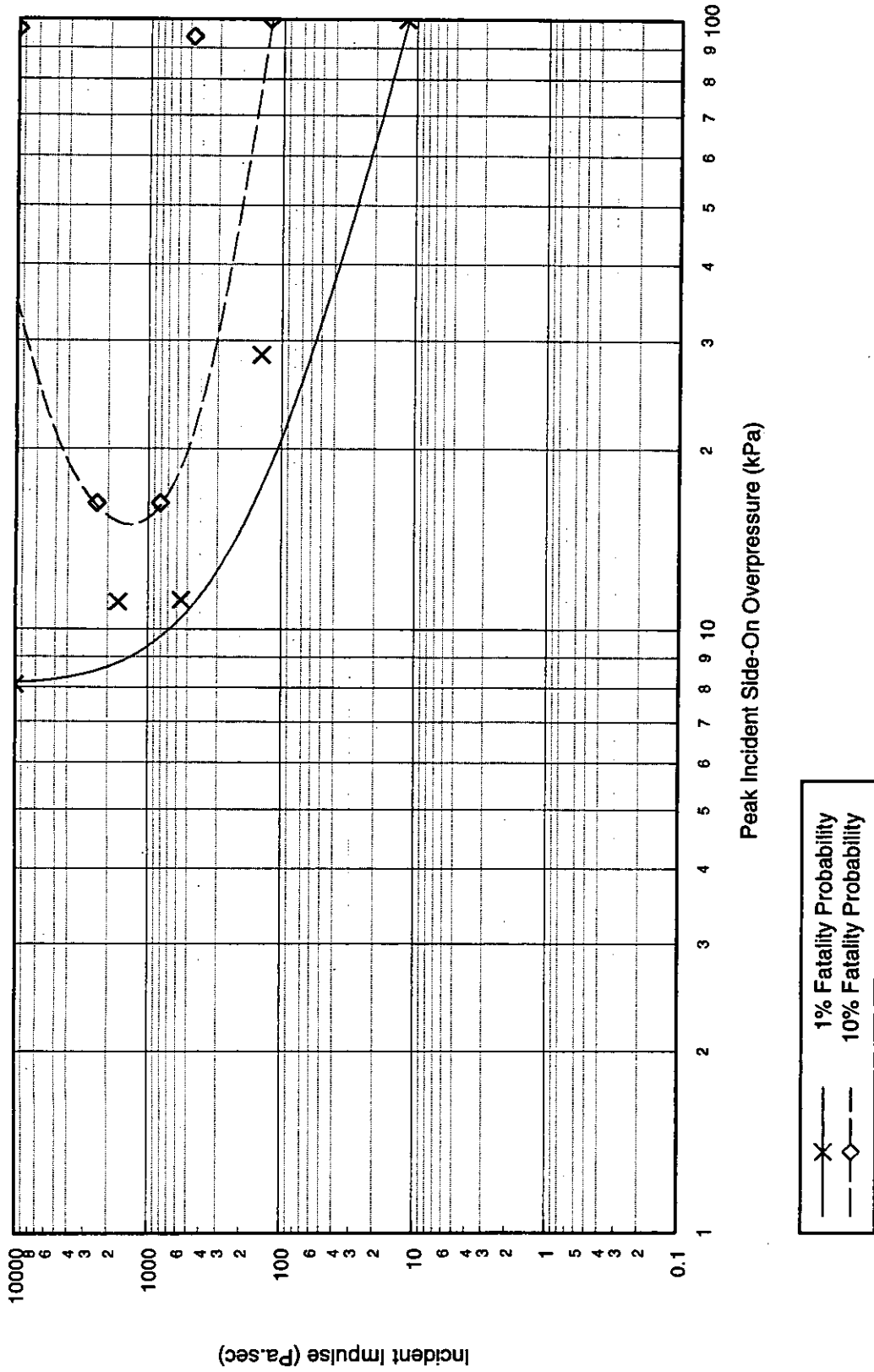
P-I Diagram: B4/3, Shock Pulse, Short Side Facing Blast



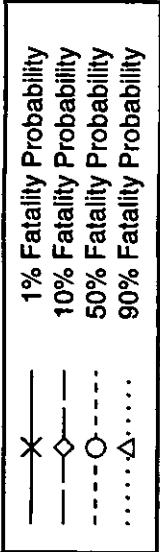
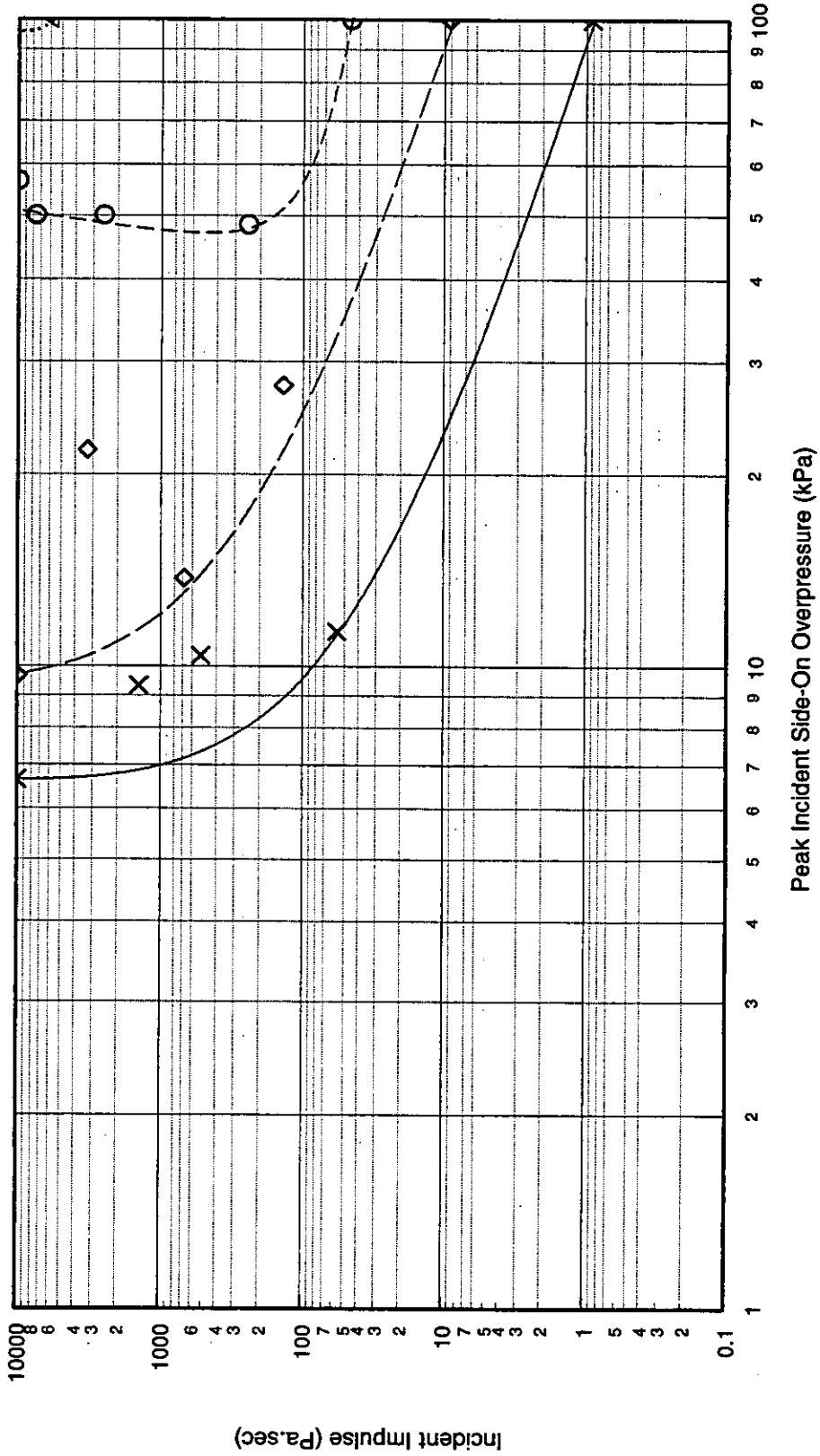
P-I Diagram: B4/3, Shock Pulse, Long Side Facing Blast



P-I Diagram: B4/3, Pressure Pulse, Short Side Facing Blast



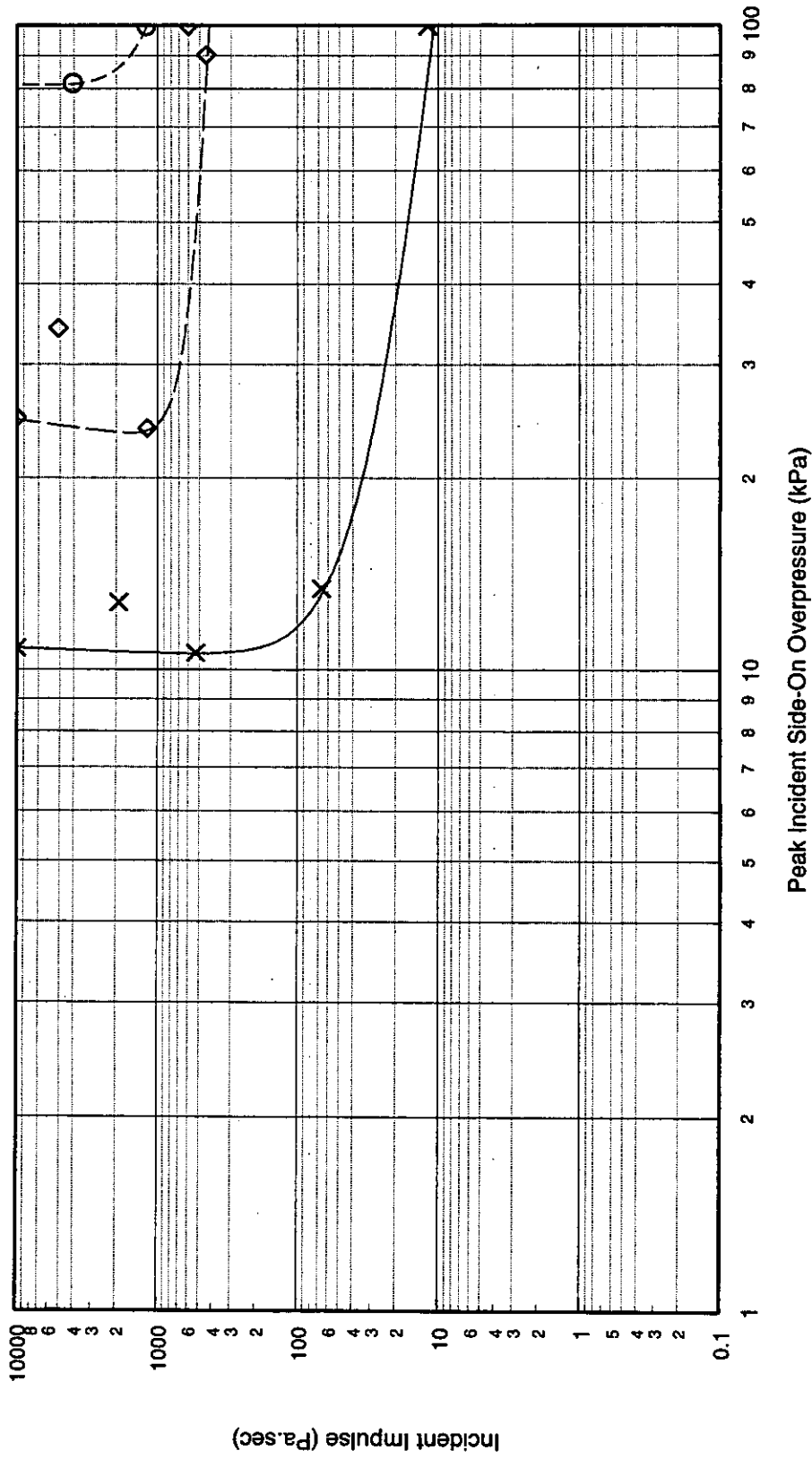
P-I Diagram: B4/3, Pressure Pulse, Long Side Facing Blast





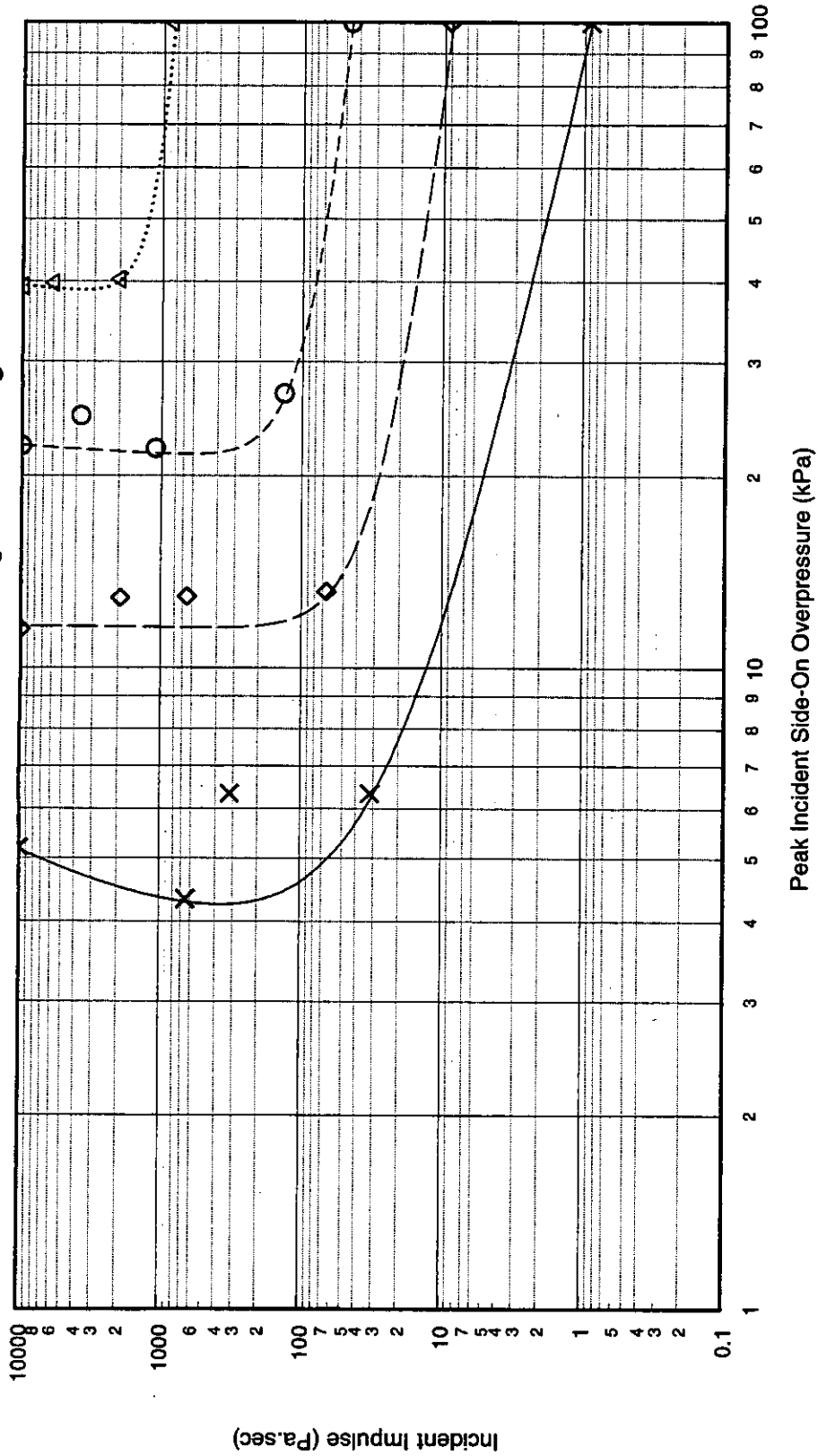
Quantity	Value	Comments
<b>Building Type: B4/4</b>		
Description	Steel framed, concrete panel clad, two storey, braced frame building. Aspect ratio 5:1	Typical office building - identical to B4/3 except that wall panels are precast concrete instead of brick/block
<b>Global Dimensions</b>		
Breadth	12.0m	
Length	60.0m	
Height	9.8m	
<b>Glazing Characteristics</b>		
Thickness	4mm - Double glazed	Continuous glazing
Max. Pane dimensions	1.25 * 0.75m	
Failure Pressure (1 sec pulse duration)	90 mbar	Mainstone [4]
<b>Cladding/Wall Panel Characteristics</b>		
Thickness	180mm	Precast concrete panels
Panel Dimensions	1.5 x 4.0m	
Dynamic Failure Pressure	100 mbar	
Support Conditions	Horizontally spanning - assumed simply-supported at ends	
Ductility	10	
Debris Size	125 x 250 x 40mm	This is a conservative assessment of the debris size based on the fatality probability criterion used
<b>Frame Details</b>		
Frame Type	Steel I-beam braced frame of 203 x 203 x UC46 columns	Staircase blocks are enclosed in 225mm blockwork or brickwork, providing lateral stability and an area of no collapse.
Dynamic Failure Pressure	Global collapse :- 154.9 mbar - short side facing blast 72.9 mbar - long side facing blast Local collapse: - Shock pulse:- 337 mbar - short face 595 mbar - long face Pressure pulse:- 407.6 mbar - short face 711.1 mbar - long face	Global collapse corresponds to failure of the entire building. Local collapse corresponds to failure of an external column due to hinge formation at its mid-height. All collapse pressures assume that the cladding is capable of transmitting load into the frame, and are increased by a suitable multiplication factor if the panels fail before the columns
Ductility	5	
<b>Additional Information</b>		

P-I Diagram: B4/4, Shock Pulse, Short Side Facing Blast



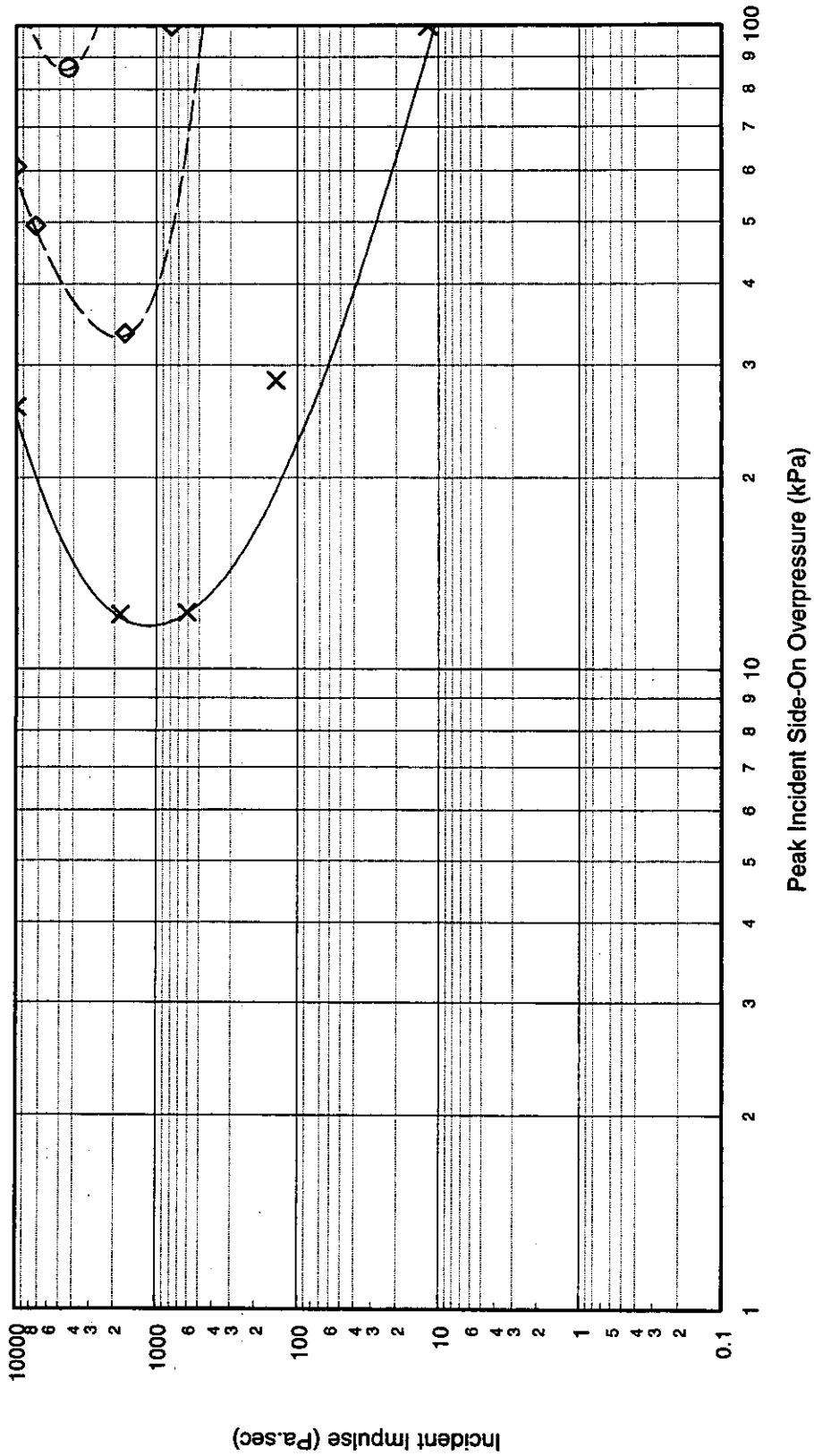
x — 1% Fatality Probability  
 ◇ — 10% Fatality Probability  
 ○ — 50% Fatality Probability

P-I Diagram: B4/4, Shock Pulse, Long Side Facing Blast



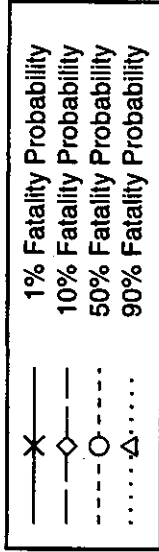
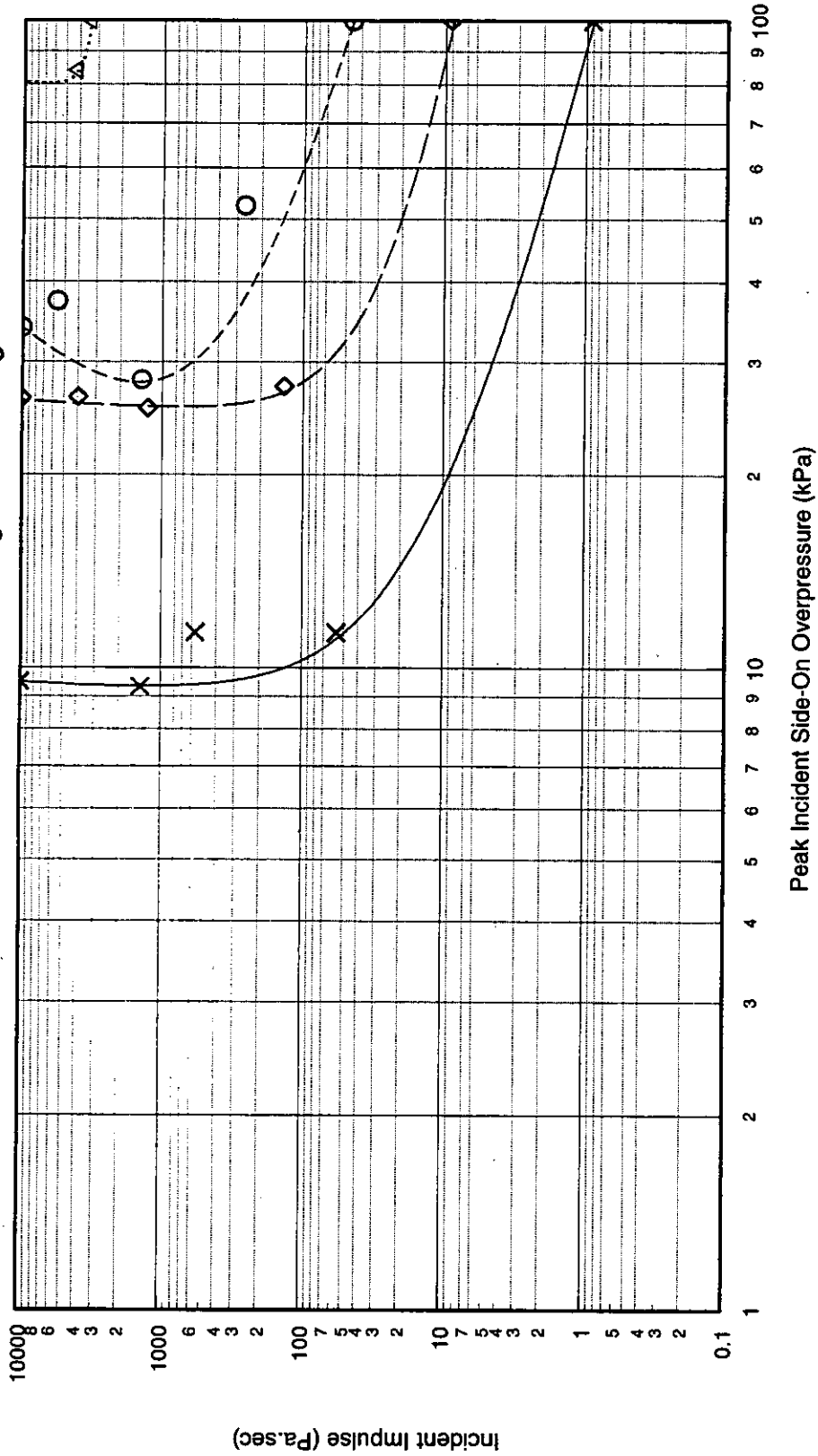
X — 1% Fatality Probability  
 ◊ — 10% Fatality Probability  
 ○ — 50% Fatality Probability  
 △ — 90% Fatality Probability

P-I Diagram: B4/4, Pressure Pulse, Short Side Facing Blast

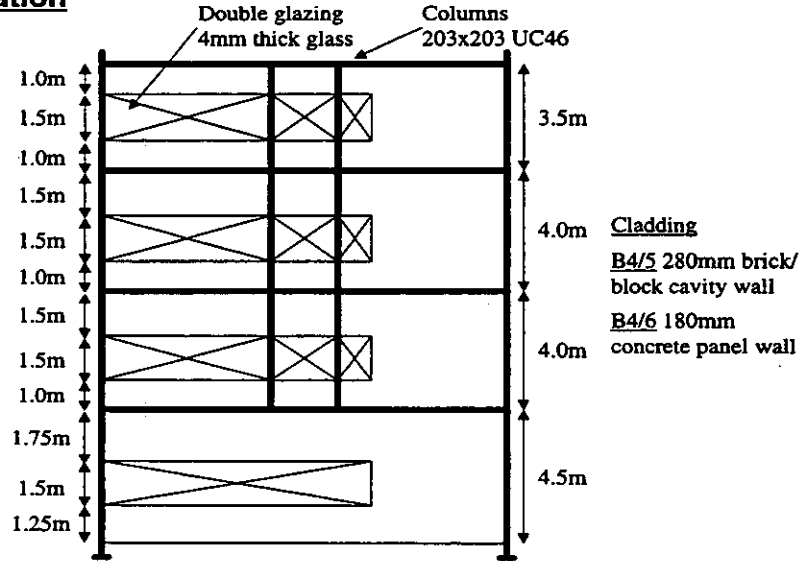


x 1% Fatality Probability  
 ◇ 10% Fatality Probability  
 ○ 50% Fatality Probability

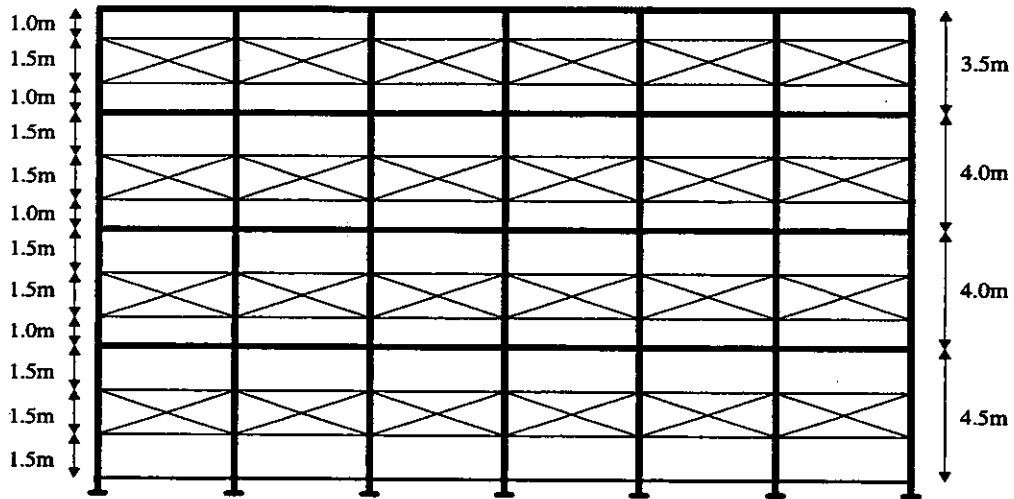
P-I Diagram: B4/4, Pressure Pulse, Long Side Facing Blast



**Side elevation**



**Front elevation**



**Plan - floors second and third**

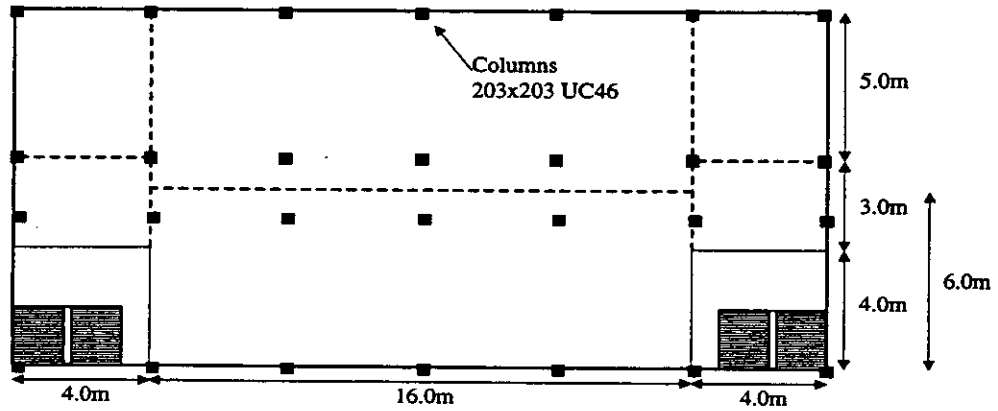
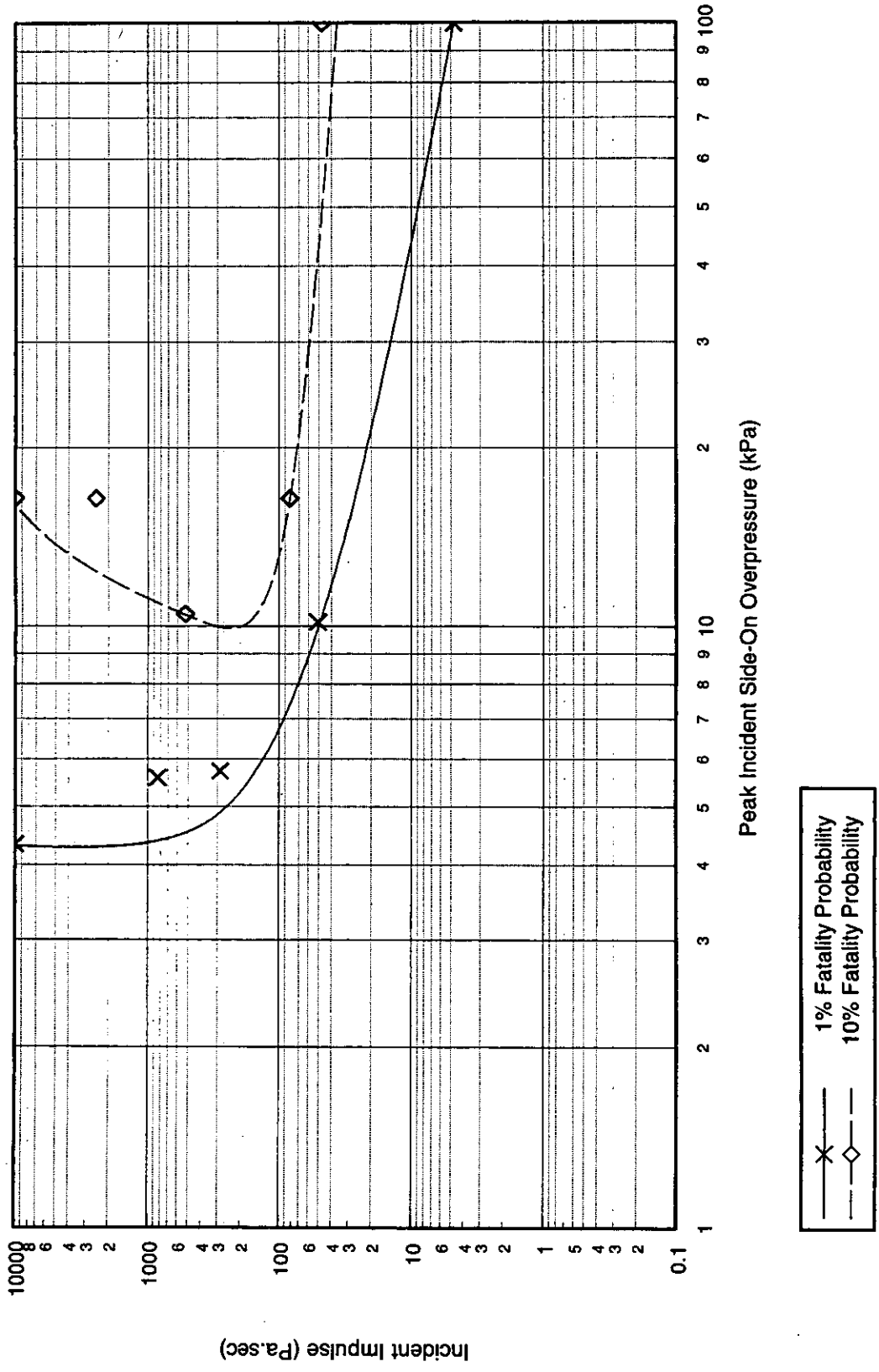


**Figure A.13: Illustration of Steel Framed Building Types B4/5 and B4/6**

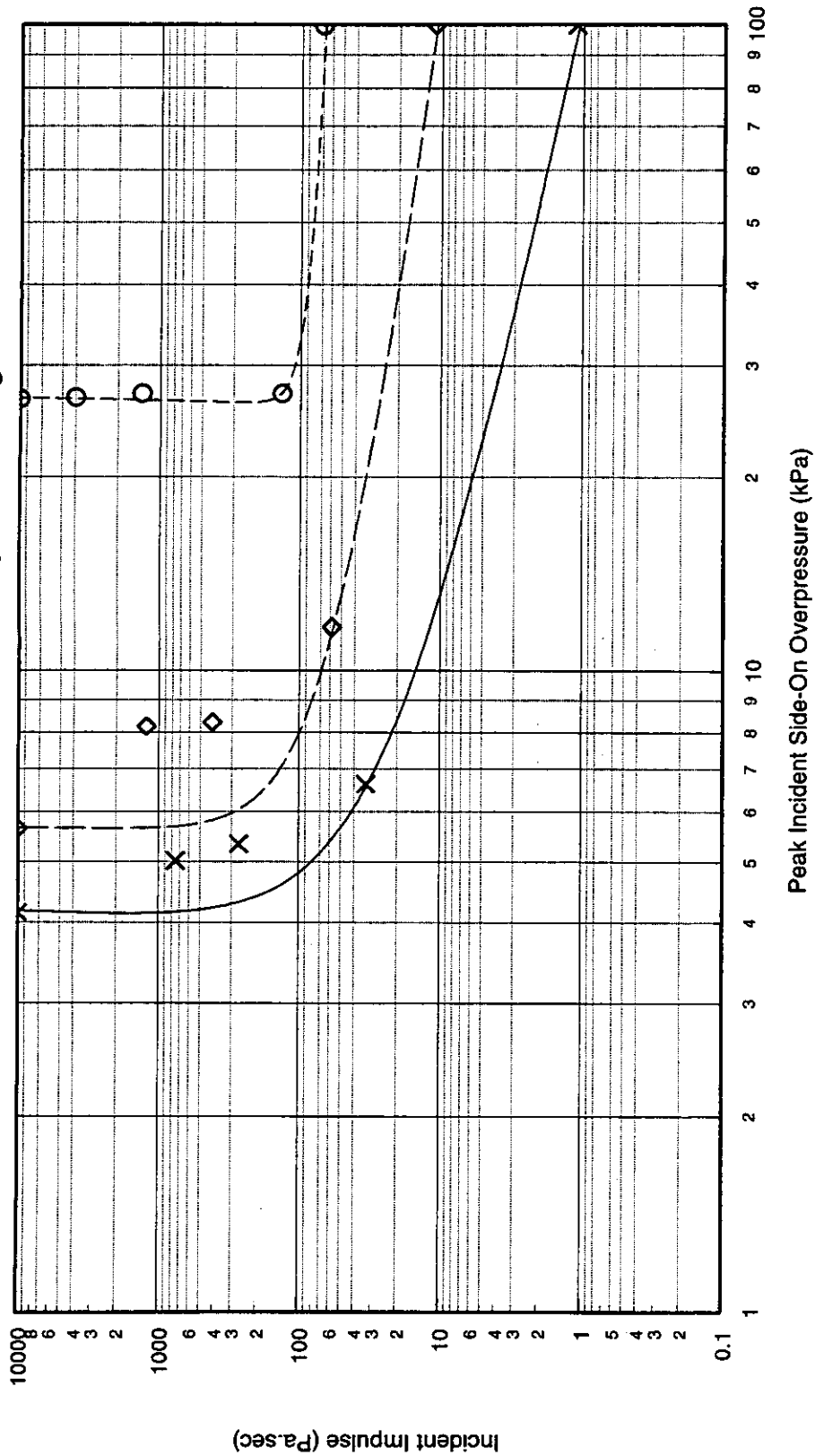
Quantity	Value	Comments
<b>Building Type: B4/5</b>		
Description	Steel framed, brick/block clad, four storey, braced frame building. Aspect ratio 2:1	
<b>Global Dimensions</b>		
Breadth	12.0m	
Length	24.0m	
Height	16.0m	
<b>Glazing Characteristics</b>		
Thickness	4mm - Double glazed	Continuous glazing
Max. Pane dimensions	1.25 x 0.75m	
Failure Pressure (1 sec pulse duration)	90 mbar	Mainstone [4]
<b>Cladding/Wall Panel Characteristics</b>		
Thickness	280mm brick/block cavity wall	102.5 x 225 x 75mm bricks 100 x 400 x 200mm blocks
Panel Dimensions	3.5 x 4.0m	
Dynamic Failure Pressure	90 mbar	
Support Conditions	Simply supported along 4 edges of representative plate	
Ductility	5	
Debris Size	102.5 x 225 x 75mm	The debris is assumed to be made up of bricks only, and therefore the standard brick size was used.
<b>Frame Details</b>		
Frame Type	Steel I-beam braced frame of 203 x 203 x UC46 columns (ground to 2nd floor external columns are 203 x 203 x UC86)	Staircase blocks are enclosed in 225mm blockwork or brickwork, providing lateral stability and an area of no collapse.
Dynamic Failure Pressure	It is assumed that there is no Global collapse. Local collapse: - Shock pulse:- 283.6 mbar - short face 522.9 mbar - long face Pressure pulse:- 363.1 mbar - short face 625 mbar - long face	Global collapse corresponds to failure of the entire building. Local collapse corresponds to failure of an external column due to hinge formation at its mid-height. All collapse pressures assume that the cladding is capable of transmitting load into the frame, and are increased by a suitable multiplication factor if the panels fail before the columns
Ductility	5	
<b>Additional Information</b>		

P-I Diagram: B4/5, Shock Pulse, Short Side Facing Blast



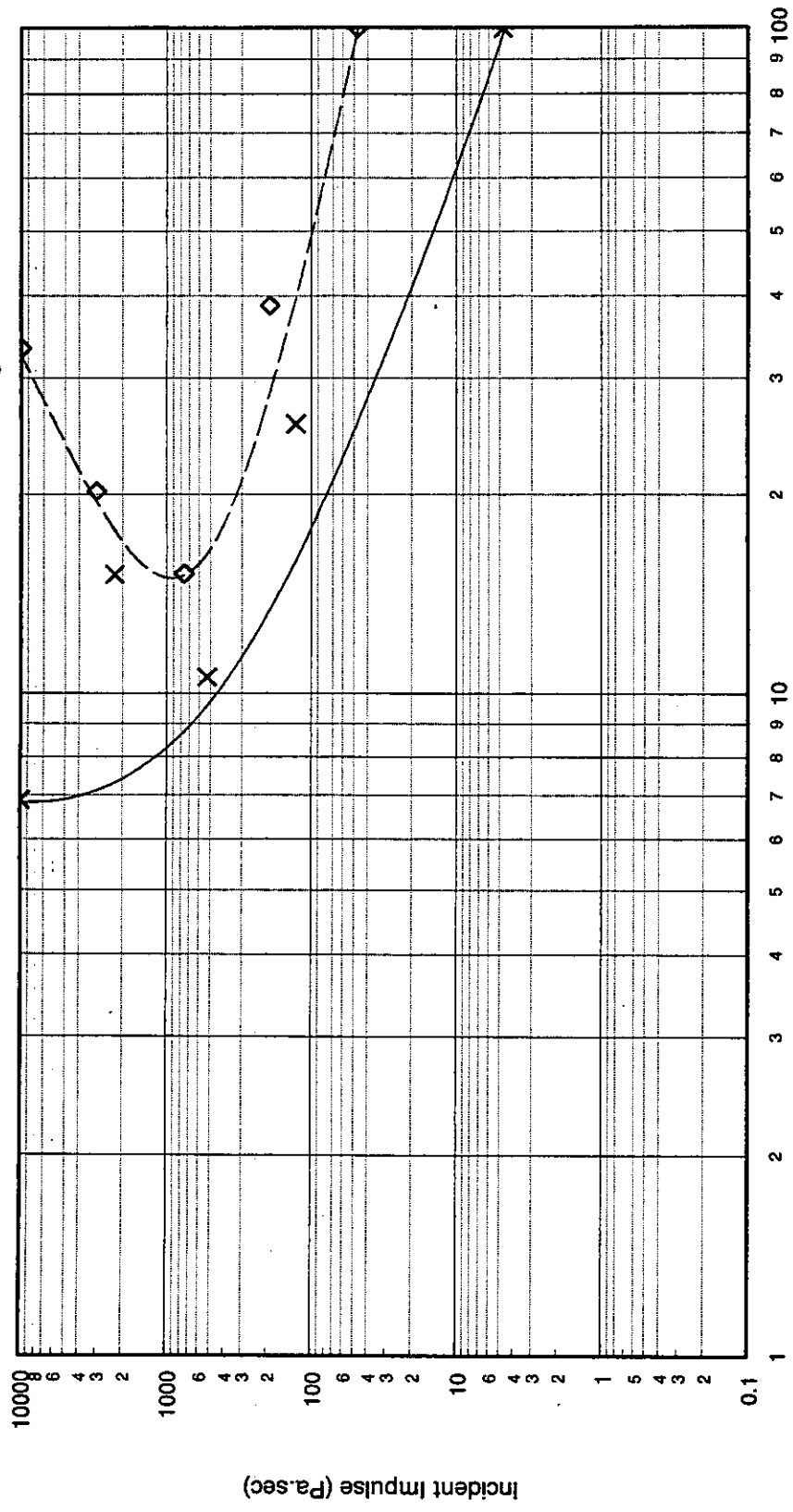


P-I Diagram: B4/5, Shock Pulse, Long Side Facing Blast



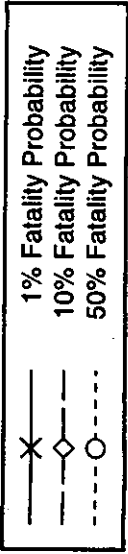
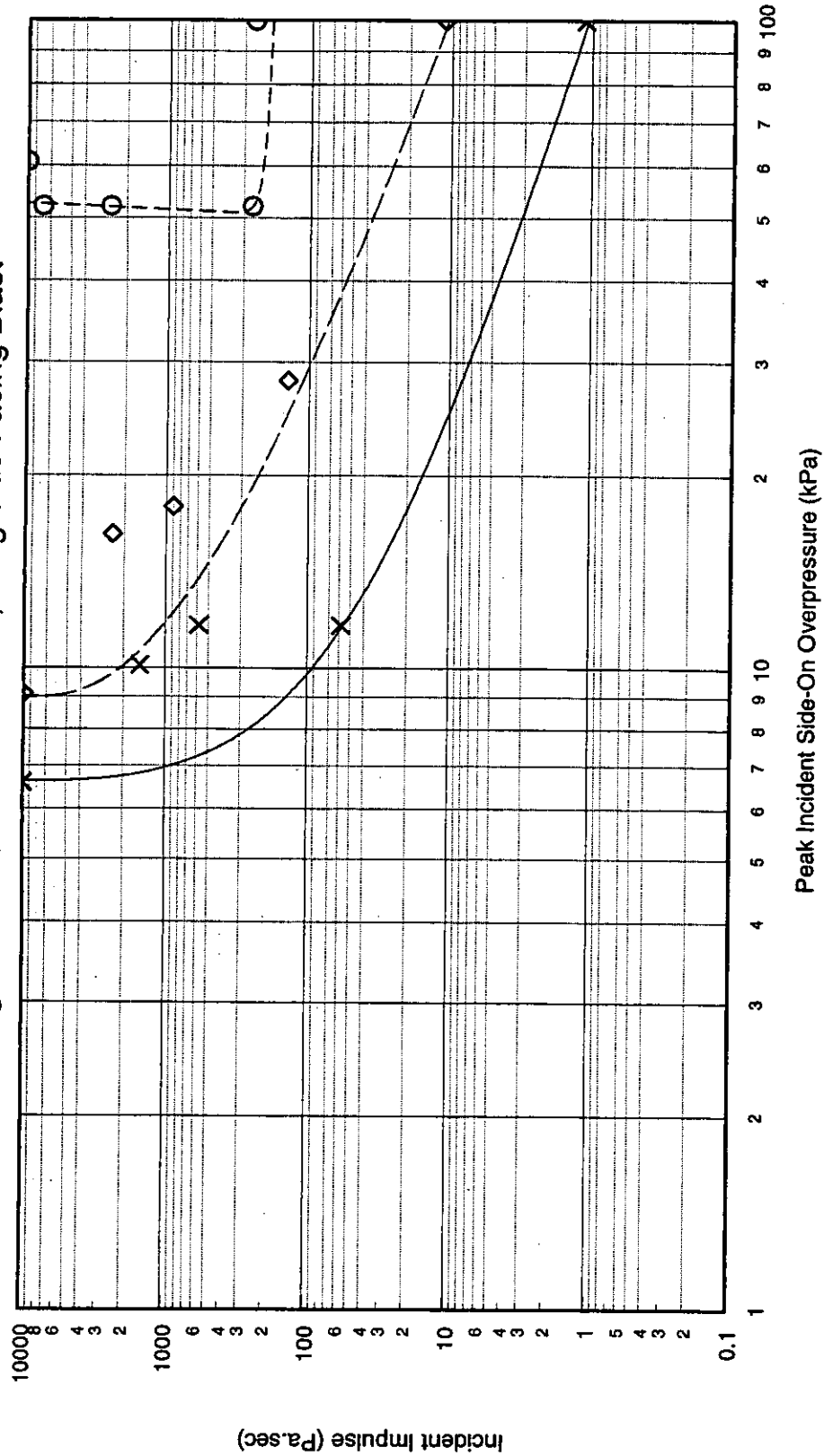
x 1% Fatality Probability  
 ◊ 10% Fatality Probability  
 ○ 50% Fatality Probability

P-I Diagram: B4/5, Pressure Pulse, Short Side Facing Blast



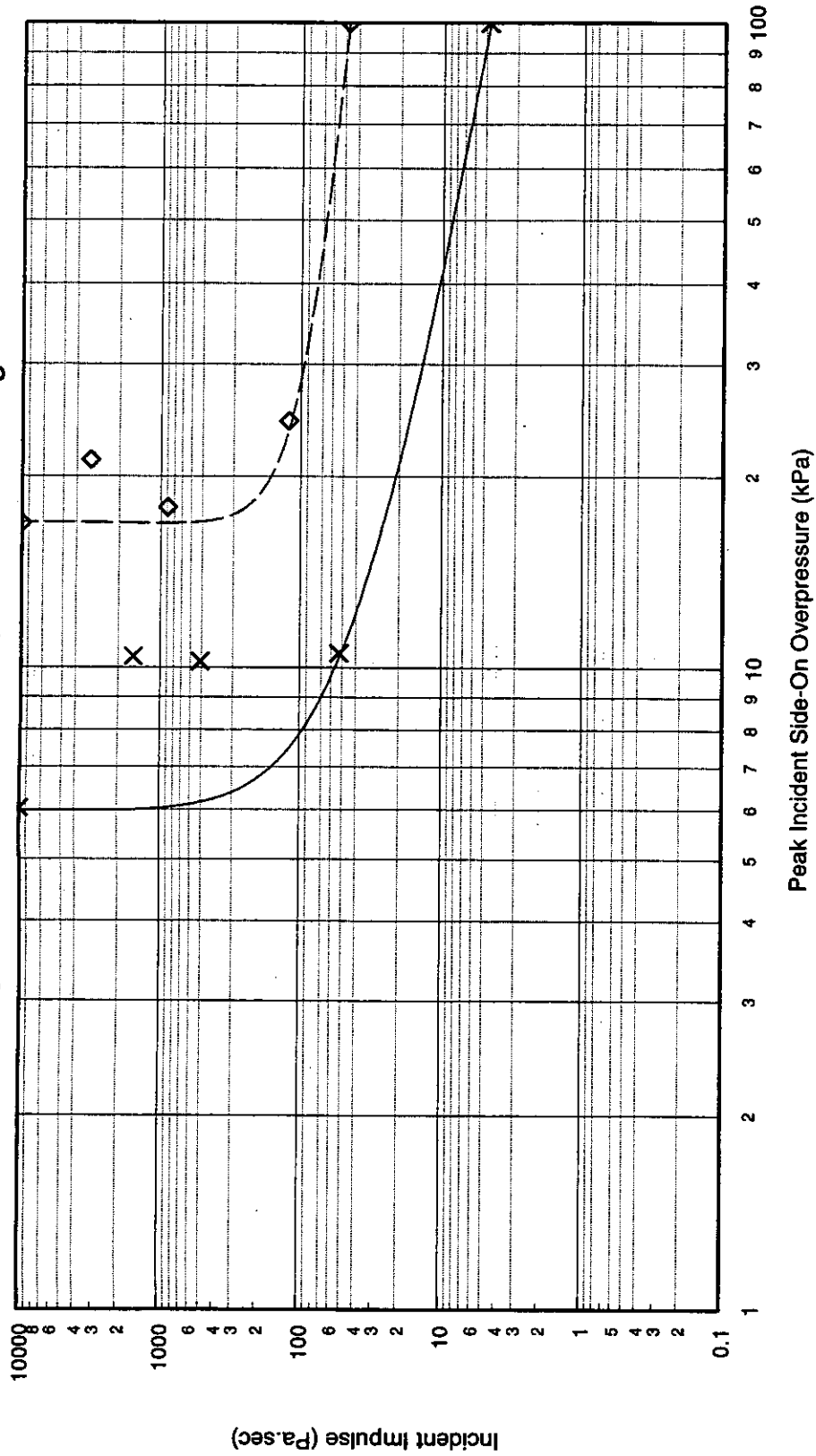
X ——— 1% Fatality Probability  
 ———◇—— 10% Fatality Probability

P-I Diagram: B4/5, Pressure Pulse, Long Side Facing Blast



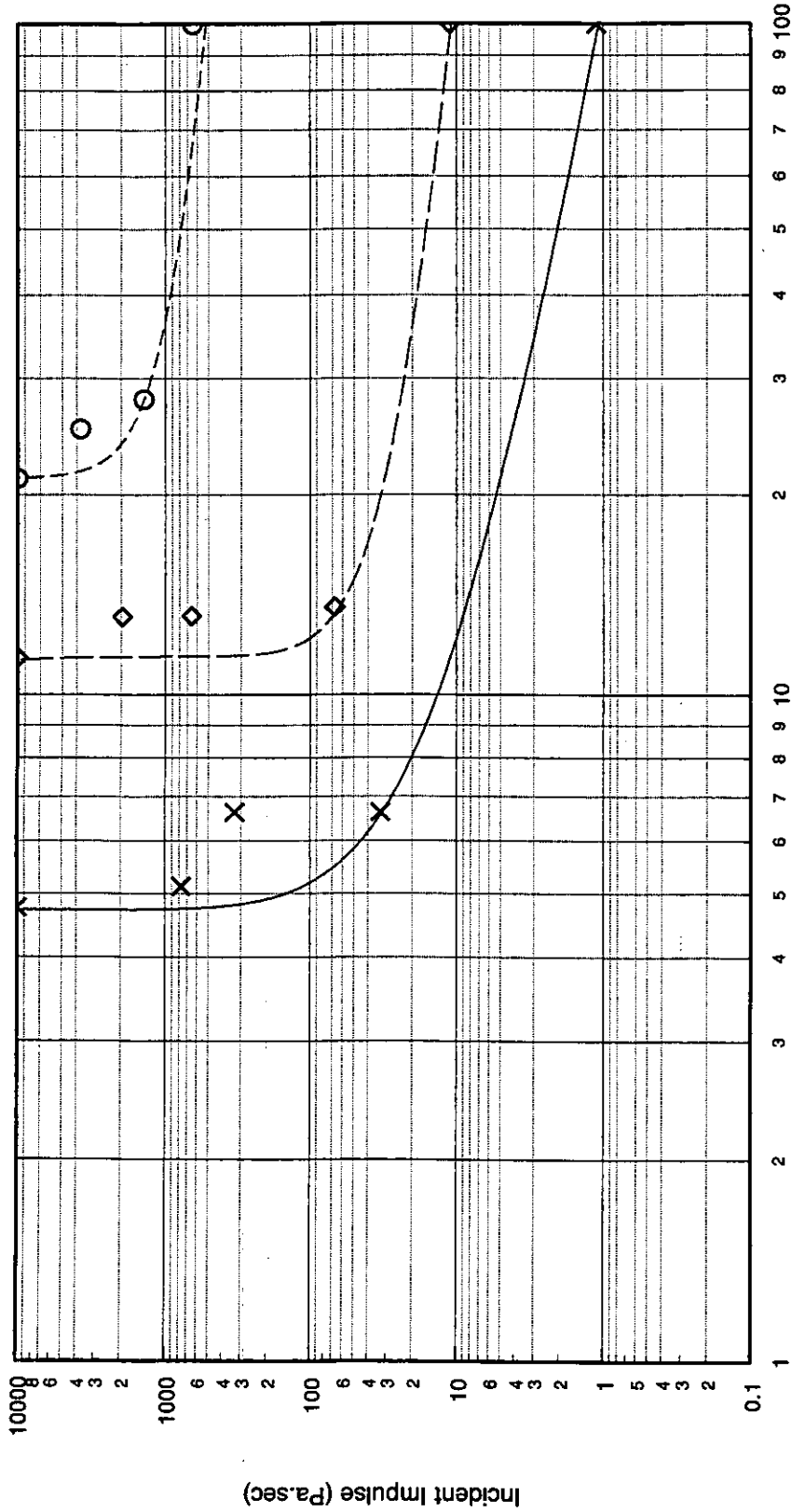
Quantity	Value	Comments
<b>Building Type: B4/6</b>		
Description	Steel framed, concrete panel clad, four storey, braced frame building. Aspect ratio 2:1	Typical office building - identical to B4/5 except that wall panels are precast concrete instead of brick/block
<b>Global Dimensions</b>		
Breadth	12.0m	
Length	24.0m	
Height	16.0m	
<b>Glazing Characteristics</b>		
Thickness	4mm - Double glazed	Continuous glazing
Max. Pane dimensions	1.25 * 0.75m	
Failure Pressure (1 sec pulse duration)	90 mbar	Mainstone [4]
<b>Cladding/Wall Panel Characteristics</b>		
Thickness	180mm	Precast concrete panels
Panel Dimensions	1.5 x 4.0m	
Dynamic Failure Pressure	100 mbar	
Support Conditions	Horizontally spanning - assumed simply-supported at ends	
Ductility	10	
Debris Size	125 x 250 x 40mm	This is a conservative assessment of the debris size based on the fatality probability criterion used
<b>Frame Details</b>		
Frame Type	Steel I-beam braced frame of 203 x 203 x UC46 columns (external columns ground to 2nd floor are 203 x 203 x UC86)	Staircase blocks are enclosed in 225mm blockwork or brickwork, providing lateral stability and an area of no collapse.
Dynamic Failure Pressure	It is assumed that there is no Global collapse. Local collapse: - Shock pulse:- 283.6 mbar - short face 522.9 mbar - long face Pressure pulse:- 363.1 mbar - short face 625 mbar - long face	Global collapse corresponds to failure of the entire building. Local collapse corresponds to failure of an external column due to hinge formation at its mid-height. All collapse pressures assume that the cladding is capable of transmitting load into the frame, and are increased by a suitable multiplication factor if the panels fail before the columns
Ductility	5	
<b>Additional Information</b>		

P-I Diagram: B4/6, Shock Pulse, Short Side Facing Blast



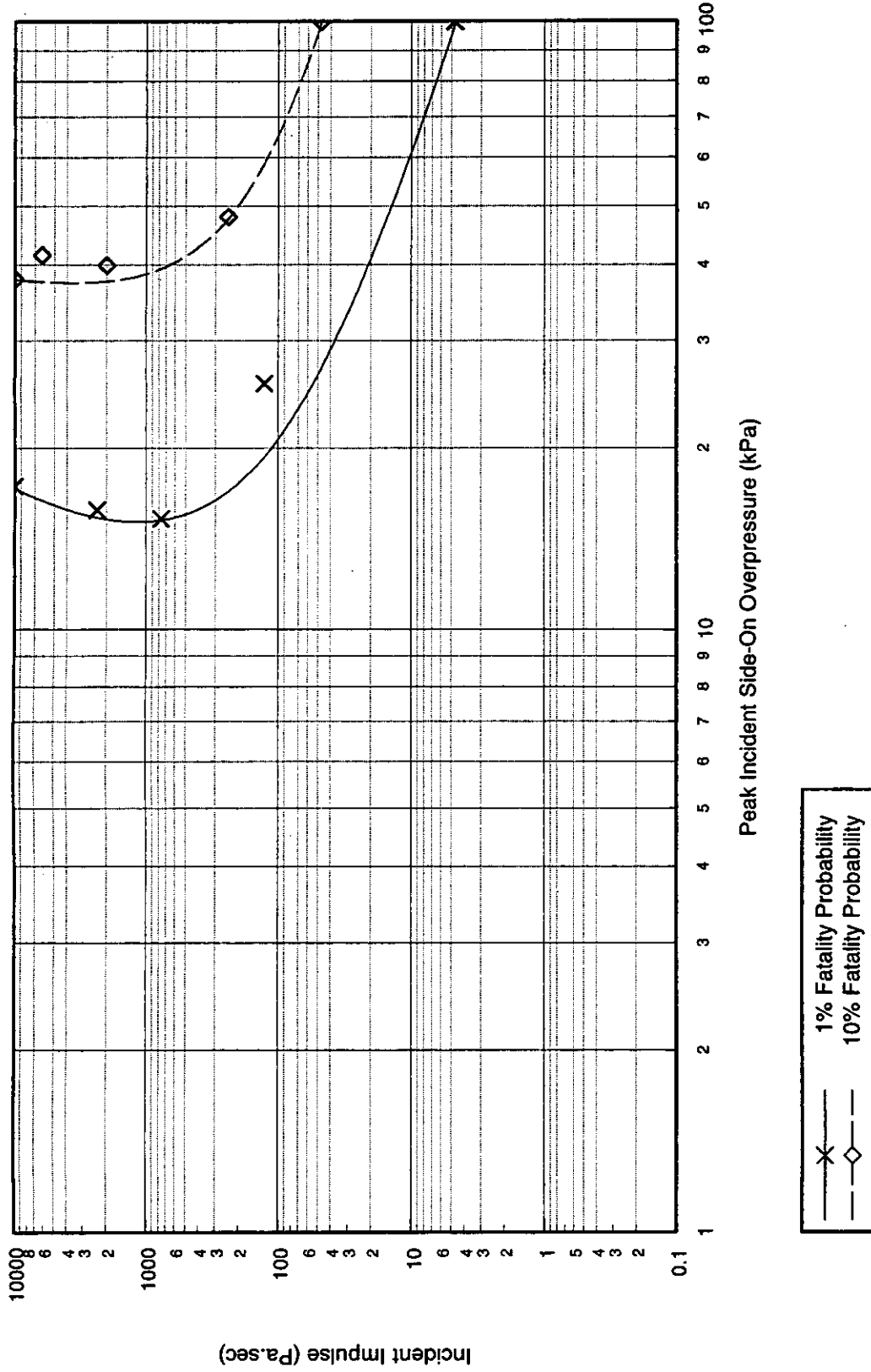
X ——— 1% Fatality Probability  
 ———◇—— 10% Fatality Probability

P-I Diagram: B4/6, Shock Pulse, Long Side Facing Blast

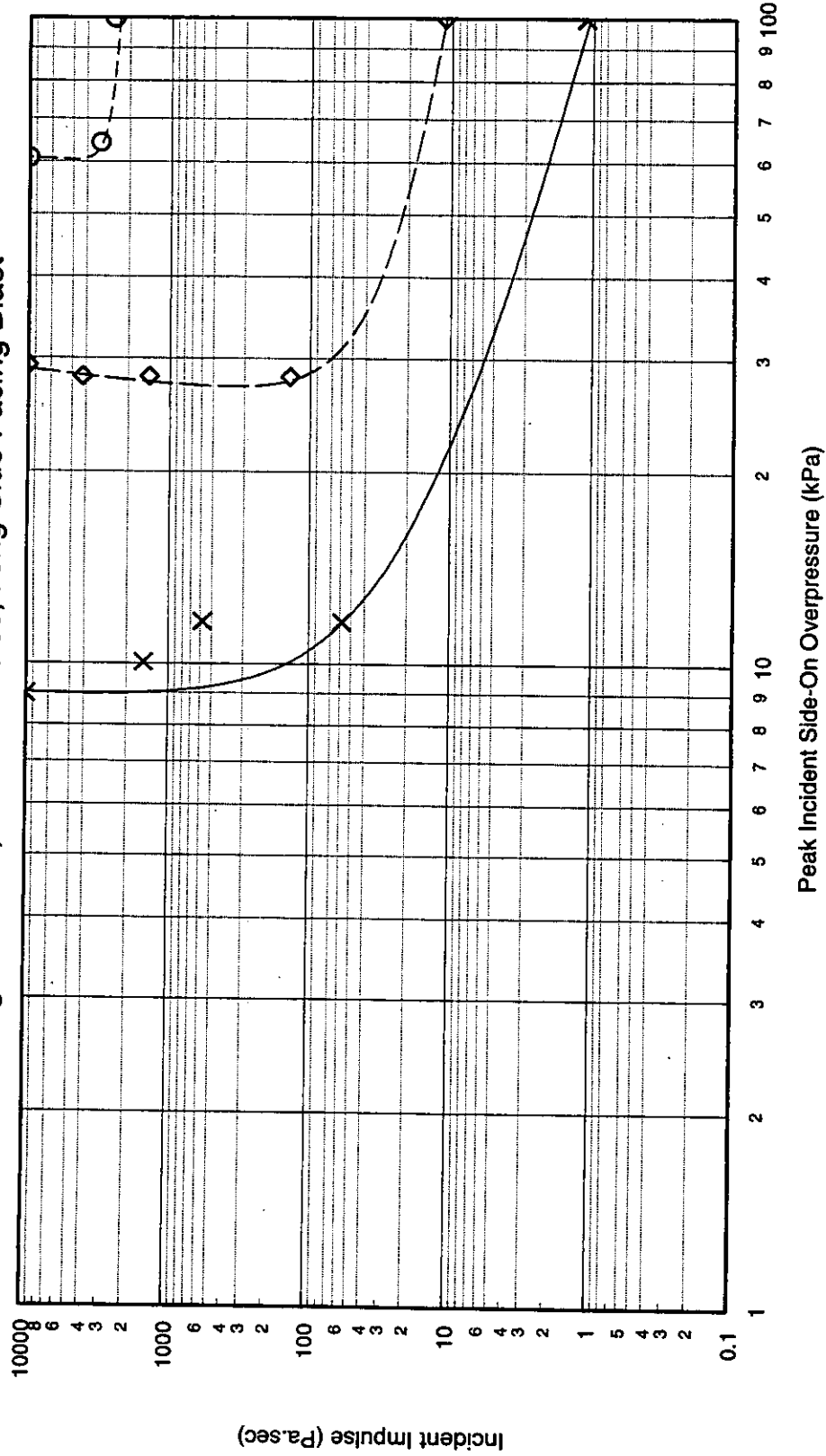


— x — 1% Fatality Probability  
 - - - ◊ - - - 10% Fatality Probability  
 ····· ◯ ····· 50% Fatality Probability

P-I Diagram: B4/6, Pressure Pulse, Short Side Facing Blast



P-I Diagram: B4/6, Pressure Pulse, Long Side Facing Blast



x 1% Fatality Probability  
 ◇ 10% Fatality Probability  
 ○ 50% Fatality Probability



**A.5. Building Type B5: Hardened Structure**

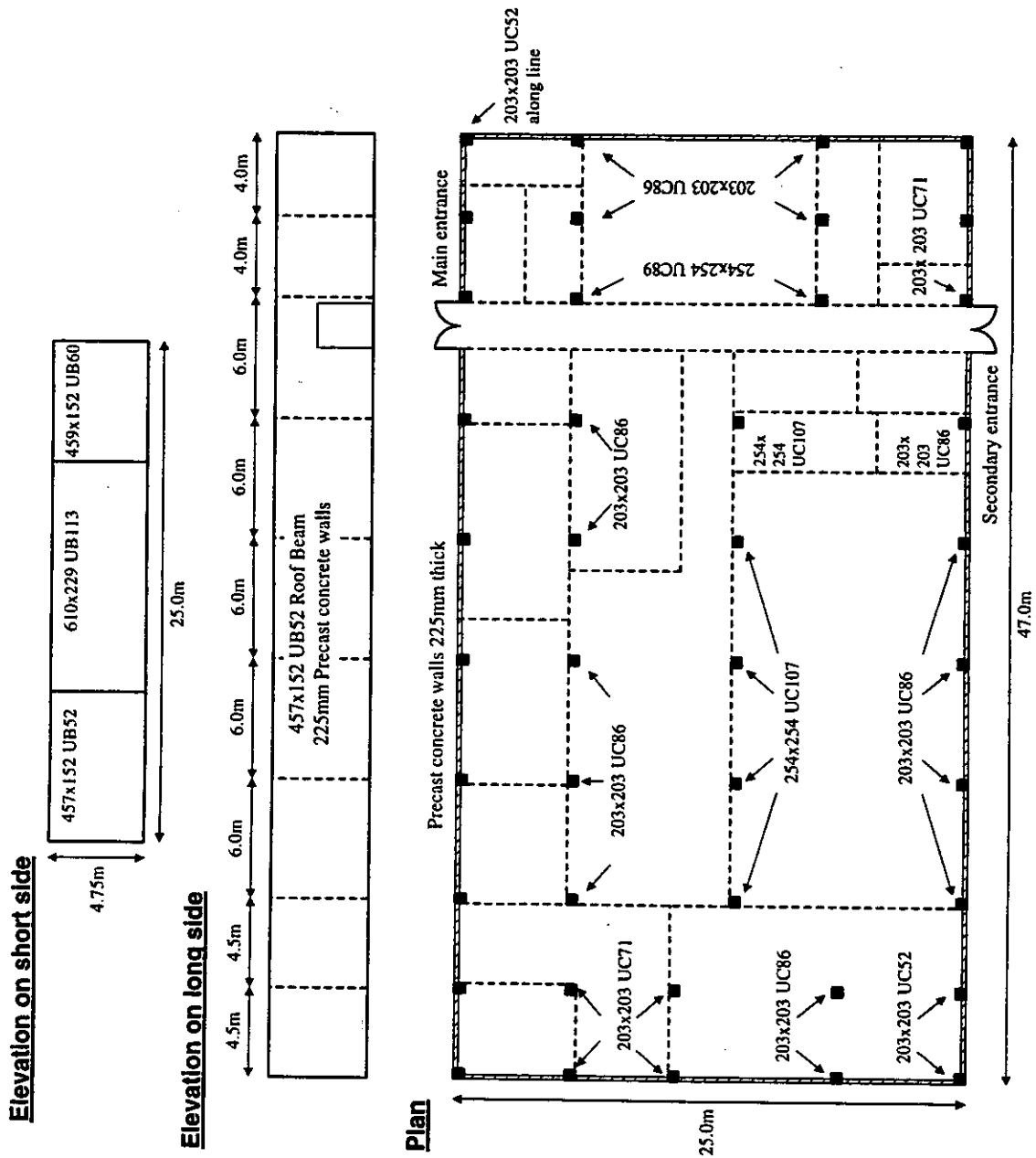
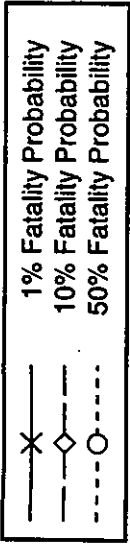
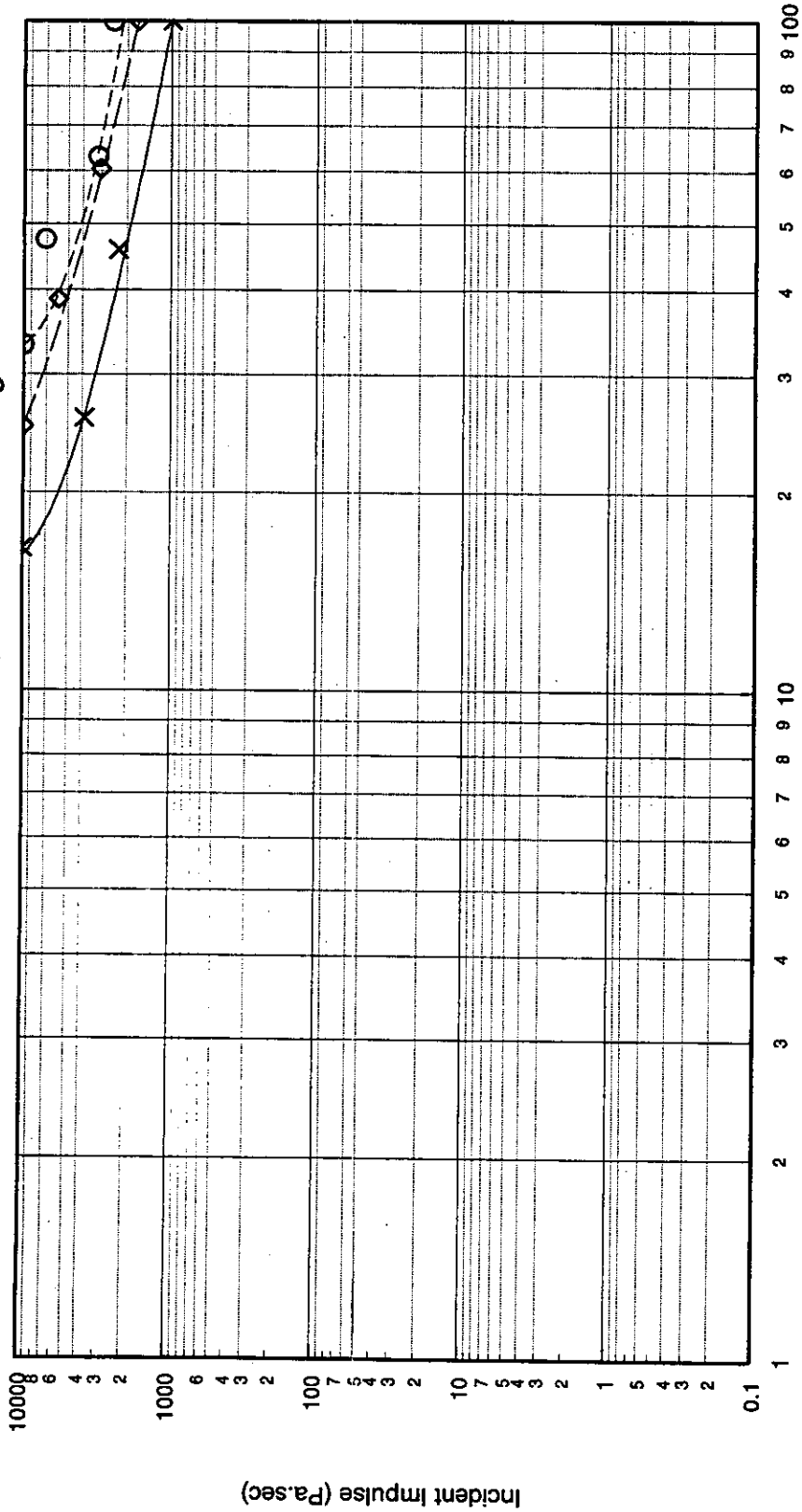


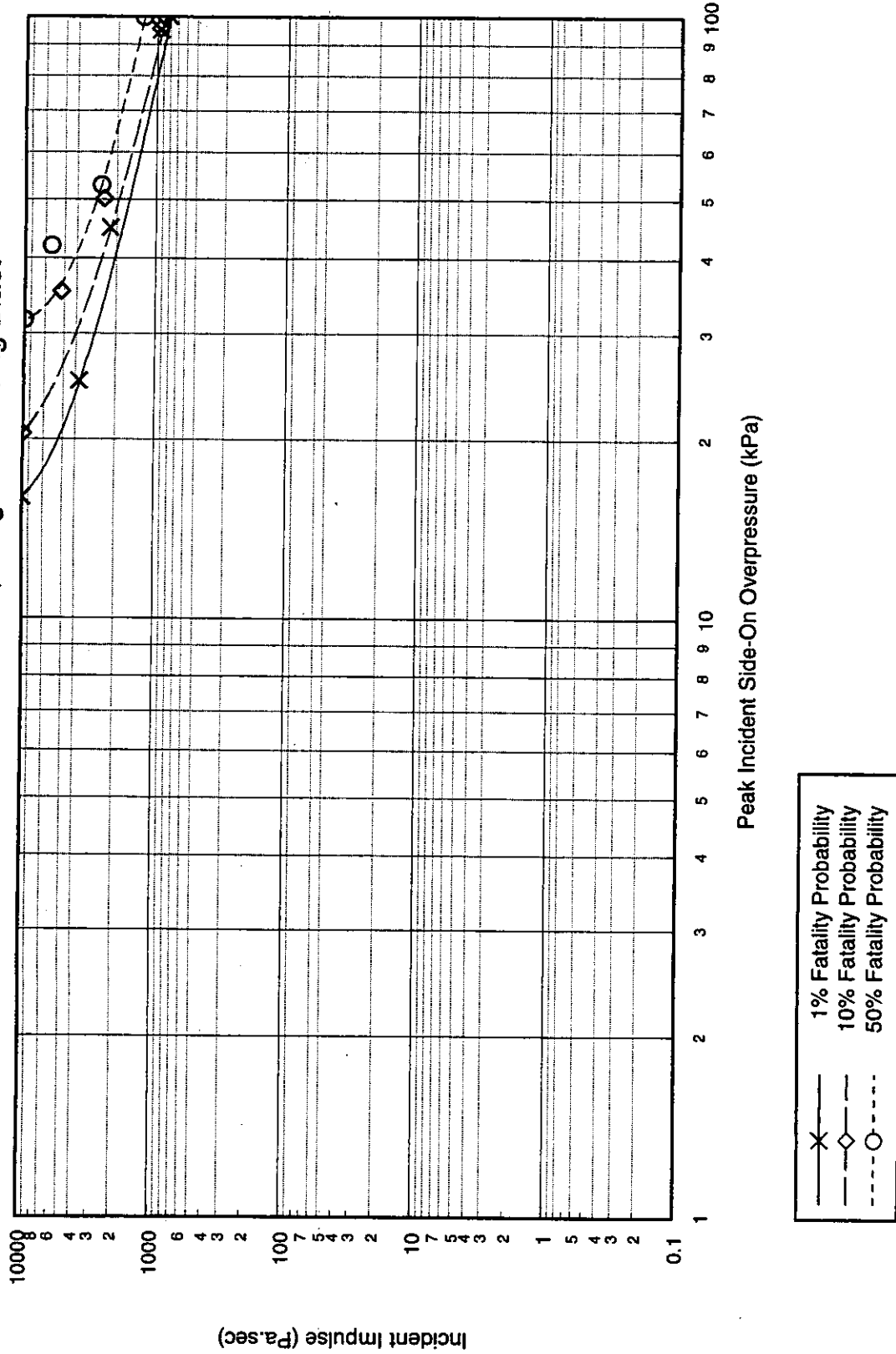
Figure A.14: Illustration of Control Building B5/1

Quantity	Value	Comments
<b>Building Type: B5/1</b>		
Description	Steel framed, concrete panel clad, single storey, building, designed to be blast resistant Aspect ratio 2:1	Typical control building for on site application
<b>Global Dimensions</b>		
Breadth	25.0m	
Length	47.0m	
Height	4.75m	
<b>Glazing Characteristics</b>		
Thickness	No glazing	
Max. Pane dimensions		
Failure Pressure (1 sec pulse duration)		
<b>Cladding/Wall Panel Characteristics</b>		
Thickness	225mm	Precast concrete panels
Panel Dimensions	1.2 x 4.5m	
Dynamic Failure Pressure	100 mbar	
Support Conditions	Vertically spanning - assumed simply-supported at ends	
Ductility	10	
Debris Size	100 x 250 x 40mm	This is a conservative assessment of the debris size based on the fatality probability criterion used
<b>Frame Details</b>		
Frame Type	Steel frame of 203 x 203 x UC86, 203 x 203 x UC71, 254 x 254 x UC107 and 203 x 203 x UC52 columns	
Dynamic Failure Pressure	Global collapse: - 468 mbar	It is assumed that there is no local collapse, as panels span vertically and cannot transmit load at mid height. Global collapse is calculated based on the average column capacity. The collapse pressures assume that the cladding is capable of transmitting load into the frame, and are increased by a suitable multiplication factor if the panels fail before the columns
Ductility	5	
<b>Additional Information</b>		
Control building is designed to withstand high pressures and hence has no glazing and a blast resistant structural design		

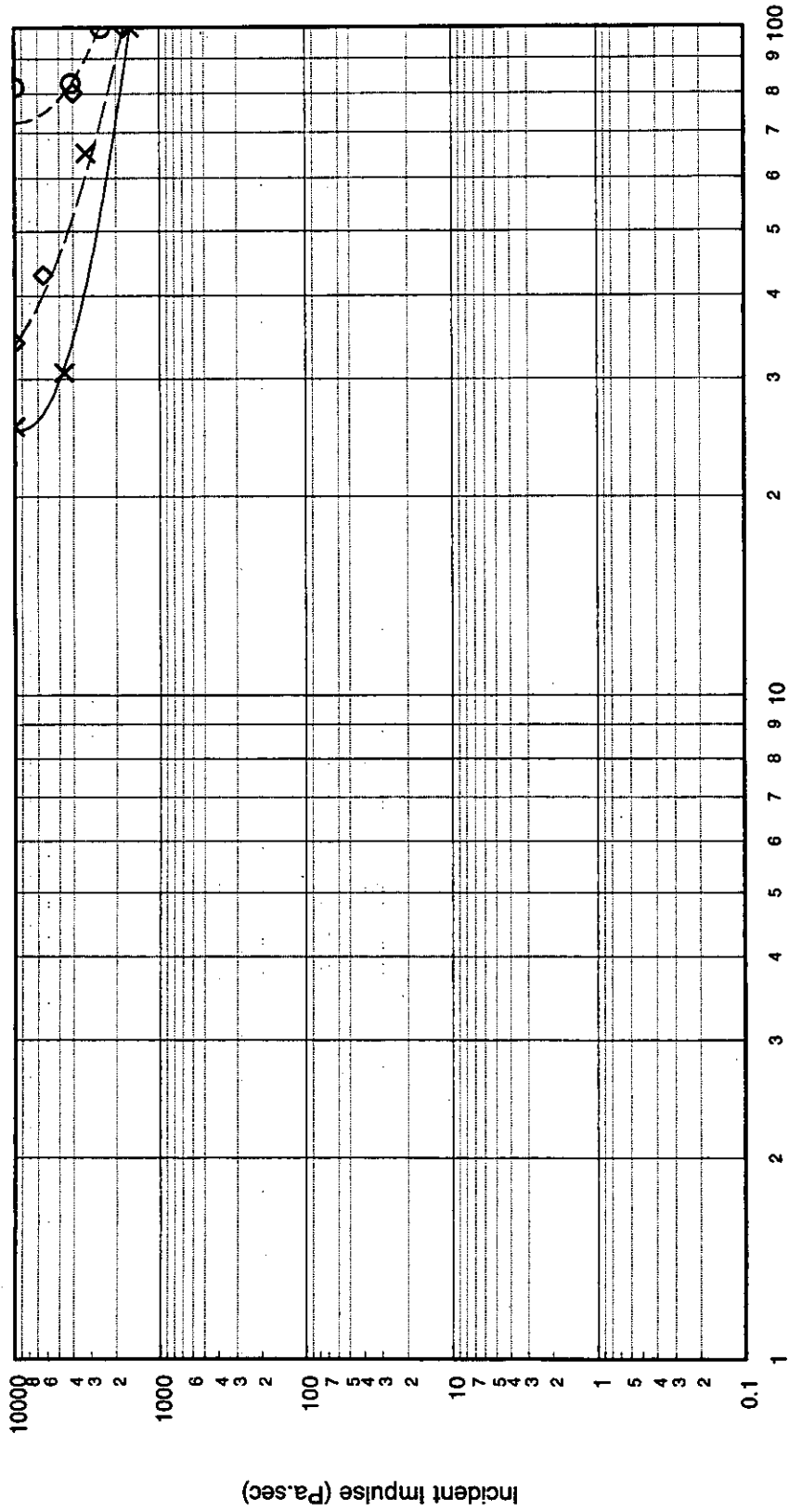
P-I Diagram: B5/1, Shock Pulse, Short Side Facing Blast



P-I Diagram: B5/1, Shock Pulse, Long Side Facing Blast

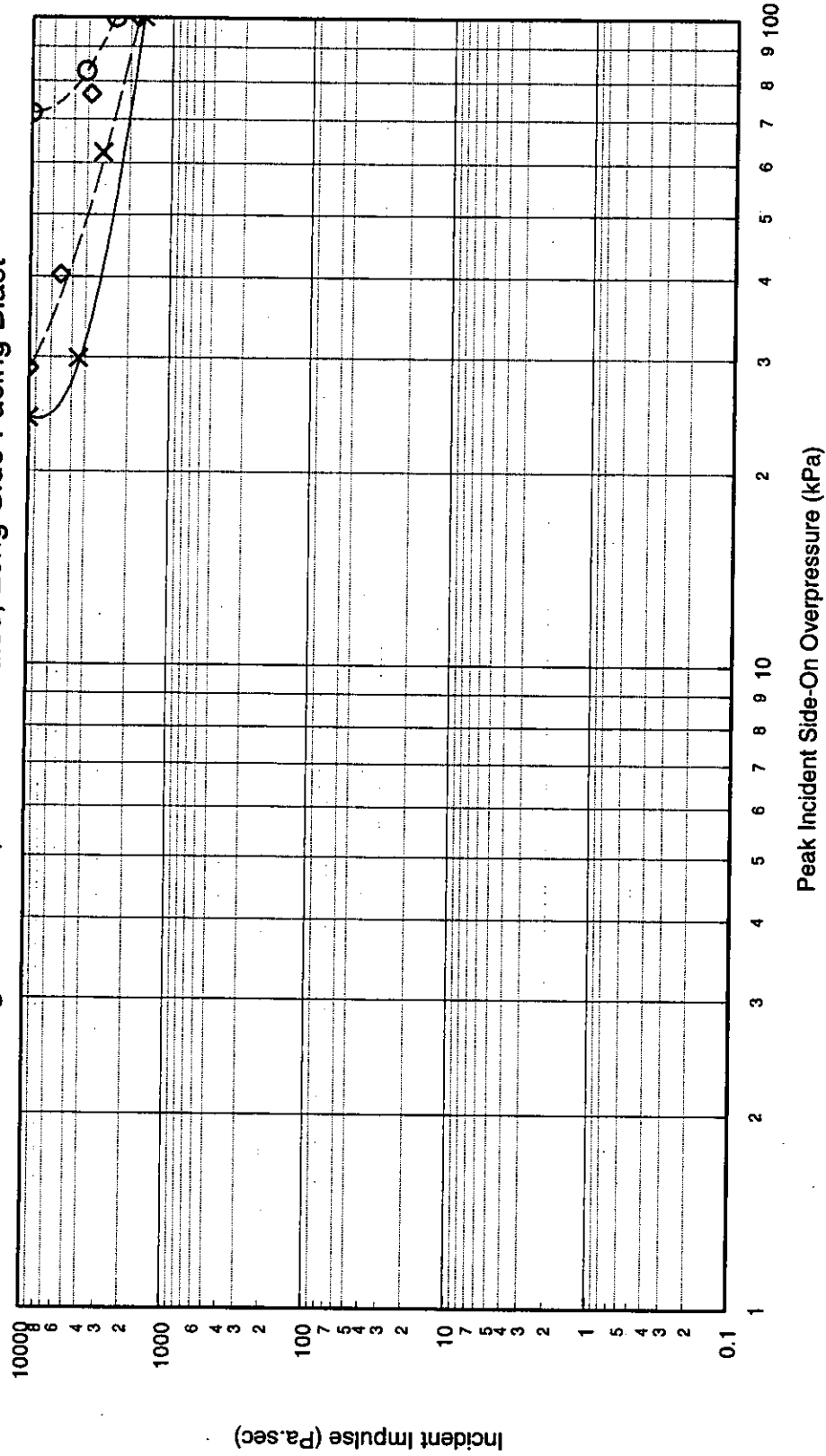


P-I Diagram: B5/1, Pressure Pulse, Short Side Facing Blast



— x — 1% Fatality Probability  
 - - - ◊ - - - 10% Fatality Probability  
 ····· ○ ····· 50% Fatality Probability

P-I Diagram: B5/1, Pressure Pulse, Long Side Facing Blast

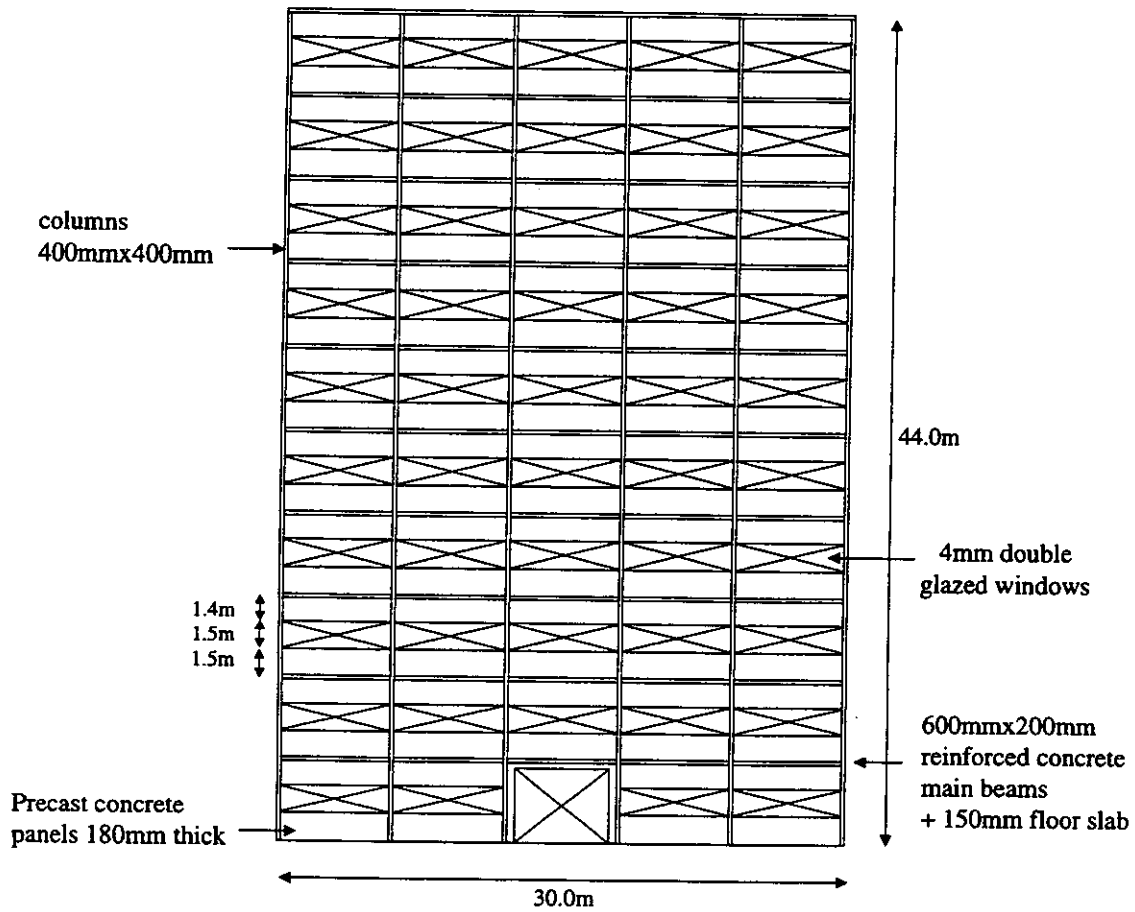


X ——— 1% Fatality Probability  
 —◇— 10% Fatality Probability  
 - - -○- - - 50% Fatality Probability

**A.6. Building Type T: Tall Buildings**



**Side elevation (same both sides)**



**Typical internal layout**

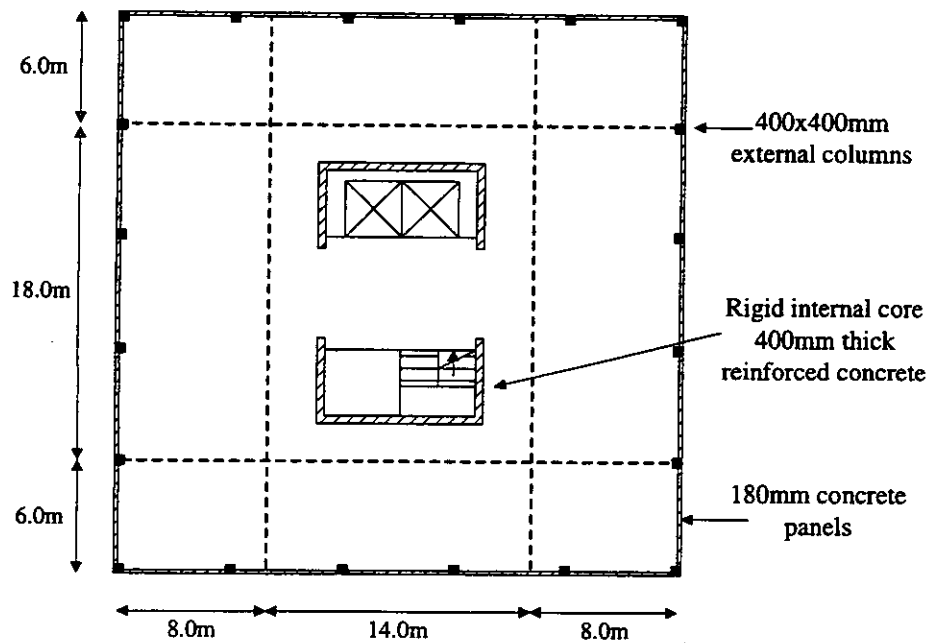
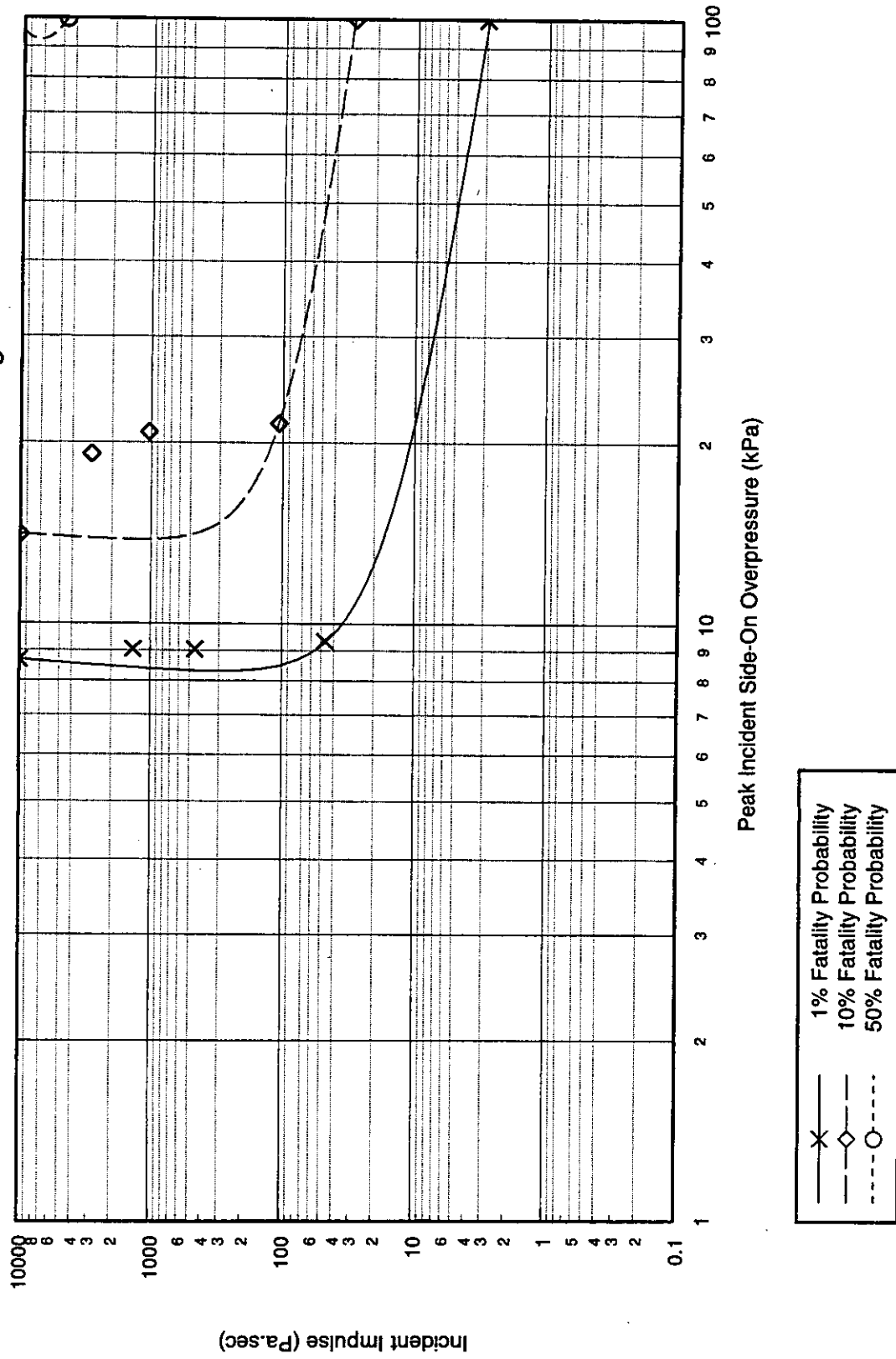


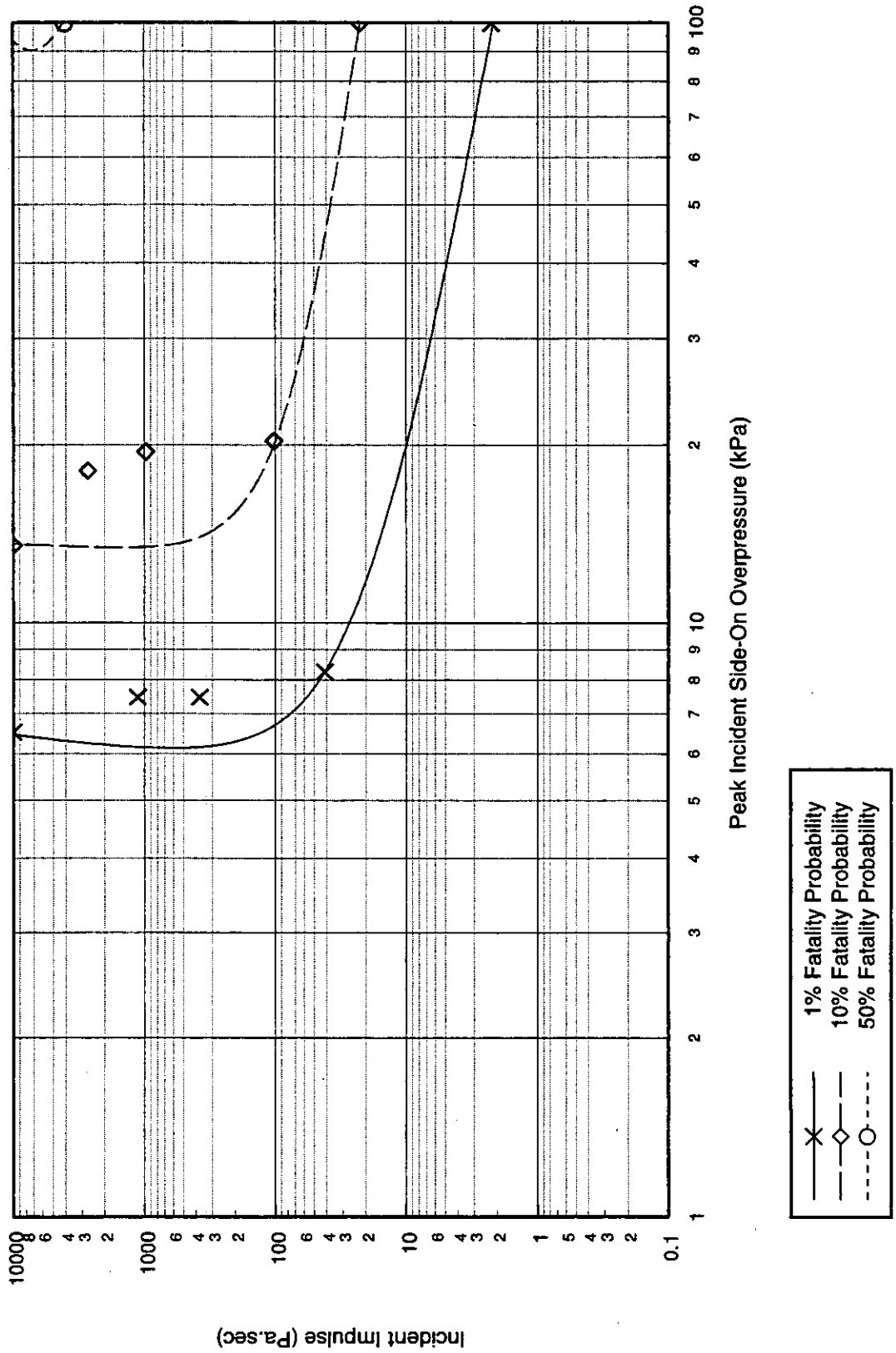
**Figure A.15: Illustration of Tall Building Type T/1**

Quantity	Value	Comments
<b>Building Type: T/1</b>		
Description	Ten storey tall building with rigid core at centre surrounded by relatively flexible frame constructed from reinforced concrete columns and beams, Aspect ratio 1:1	Typical high rise office building
<b>Global Dimensions</b>		
Breadth	30.0m	
Length	30.0m	
Height	44.0m	
<b>Glazing Characteristics</b>		
Thickness	4mm - Double glazed	Continuous glazing
Max. Pane dimensions	1.5 x 1.5m	
Failure Pressure (1 sec pulse duration)	80 mbar	Mainstone [4]
<b>Cladding/Wall Panel Characteristics</b>		
Thickness	180mm	Precast concrete panels
Panel Dimensions	1.5 x 6.0m	
Dynamic Failure Pressure	78 mbar	
Support Conditions	Horizontally spanning - assumed simply-supported at ends	
Ductility	10	
Debris Size	210 x 210 x 35mm	This is a conservative assessment of the debris size based on the fatality probability criterion used
<b>Frame Details</b>		
Frame Type	Rigid internal core surrounded by flexible outer structure - 400 x 400mm external columns	Internal core provides lateral stability
Dynamic Failure Pressure	Global collapse: - 2517 mbar	It has been assumed that local collapse does not lead to a significant fatality probability over the entire height of the structure. Global collapse corresponds to failure of the entire building. All collapse pressures assume that the cladding is capable of transmitting load into the frame, and are increased by a suitable multiplication factor if the panels fail before the columns
Ductility	1.5	
<b>Additional Information</b>		

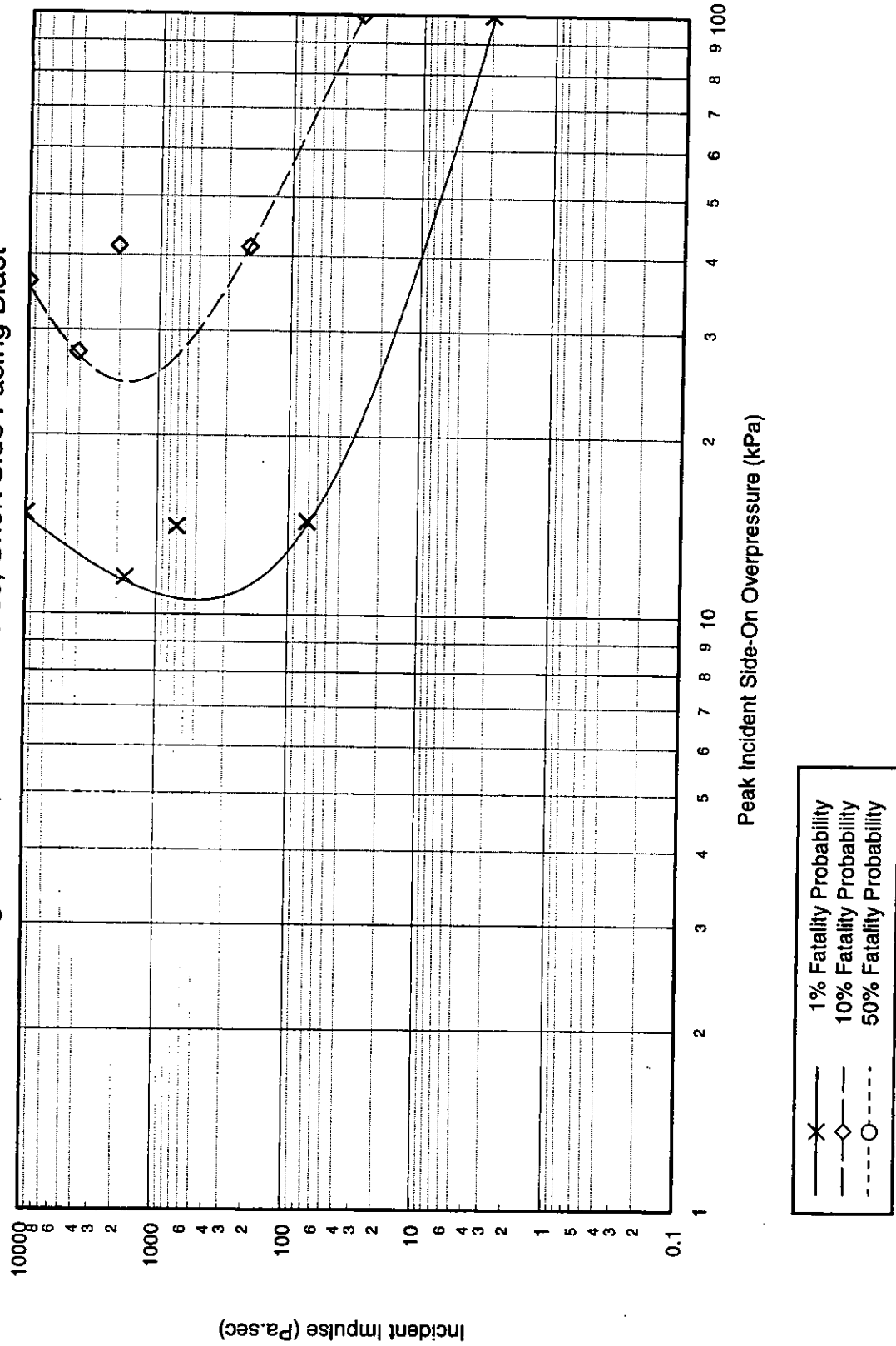
P-I Diagram: T1, Shock Pulse, Short Side Facing Blast



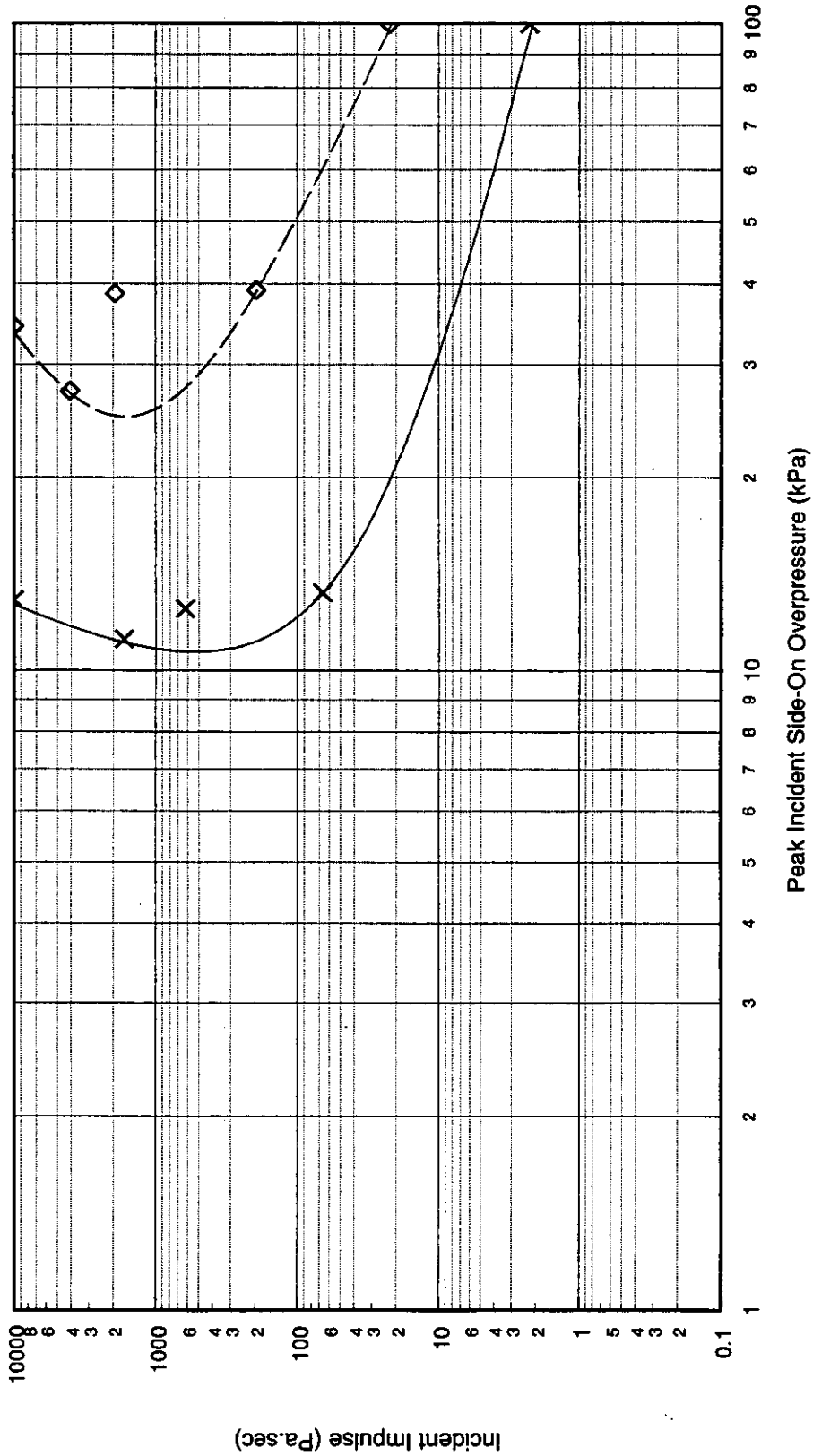
P-I Diagram: T1, Shock Pulse, Long Side Facing Blast



P-I Diagram: T1, Pressure Pulse, Short Side Facing Blast



P-I Diagram: T1, Pressure Pulse, Long Side Facing Blast



x — 1% Fatality Probability  
 ◇ — 10% Fatality Probability  
 ○ — 50% Fatality Probability

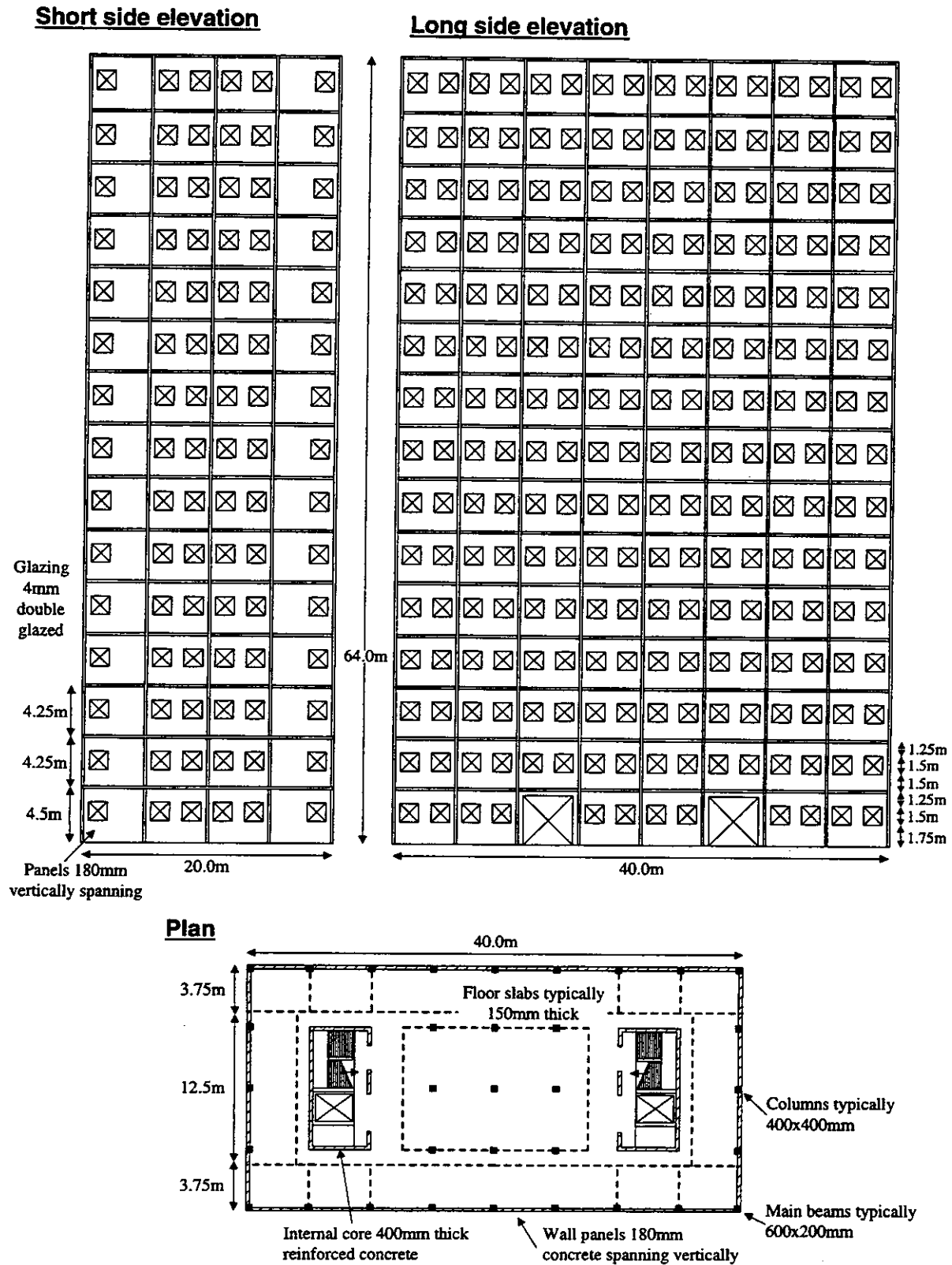
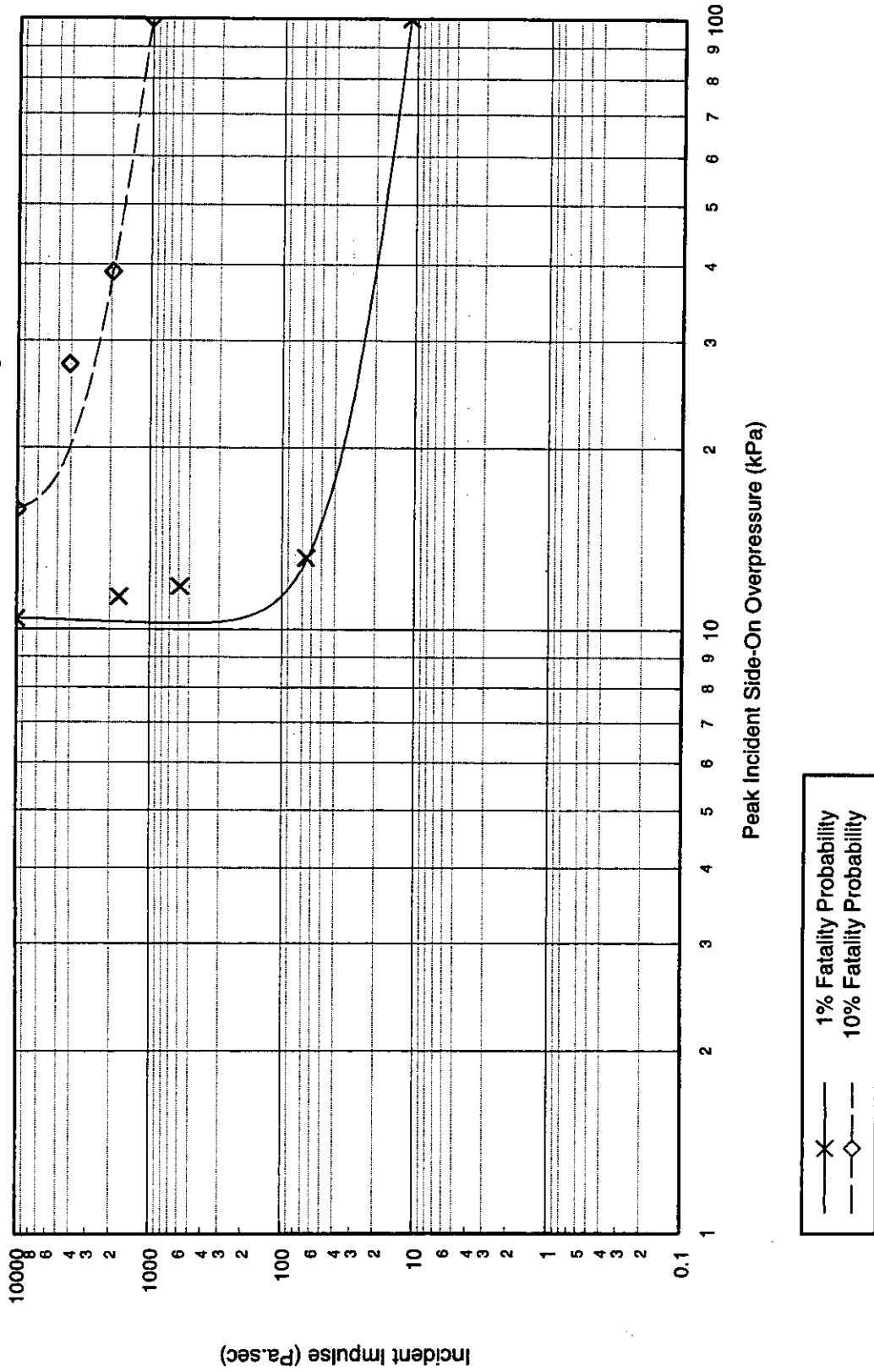


**Figure A.16: Illustration of Tall Building Type T/2**

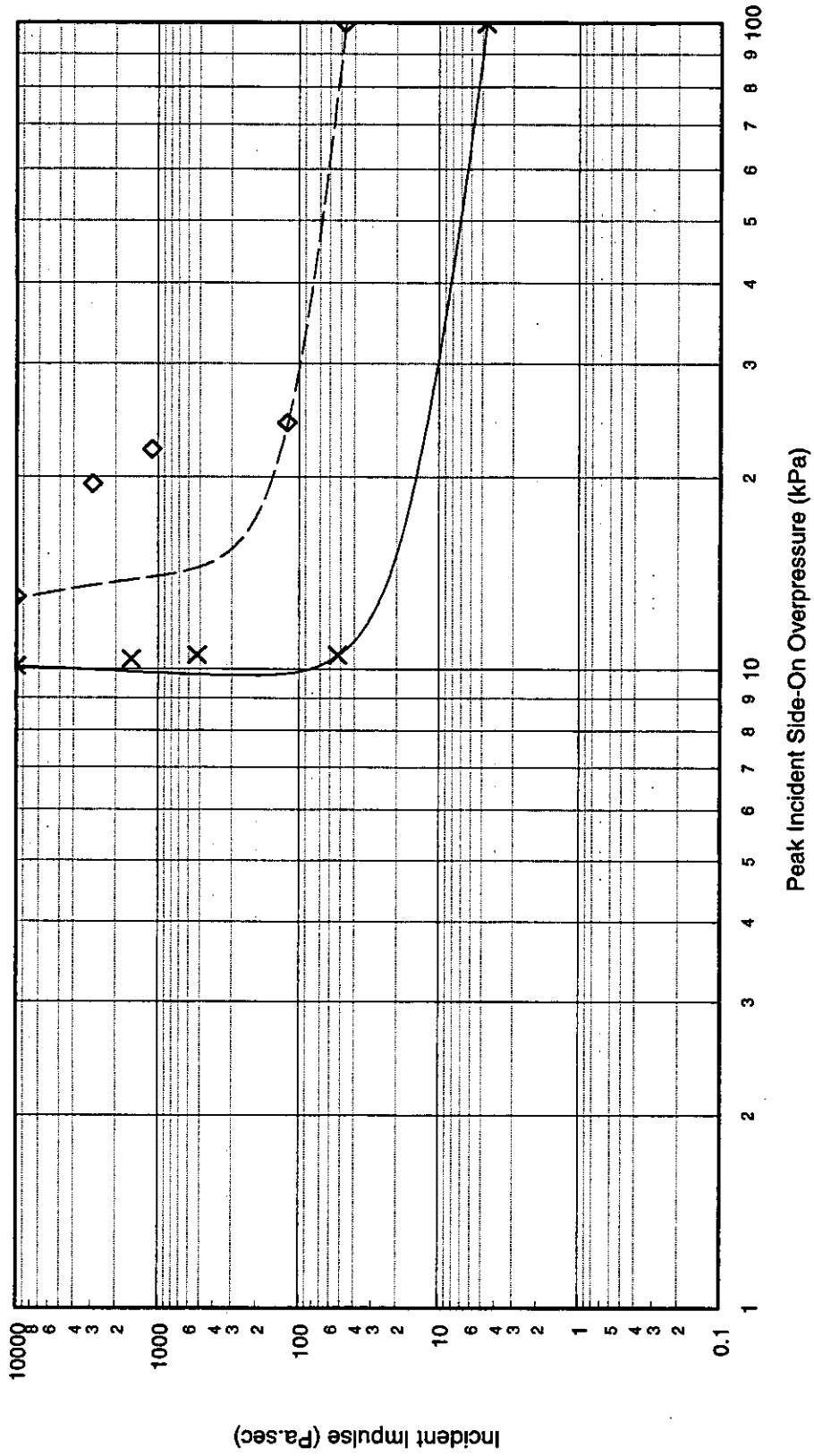
Quantity	Value	Comments
<b>Building Type: T/2</b>		
Description	15 storey tall building with rigid core at centre surrounded by relatively flexible frame constructed from reinforced concrete columns and beams, Aspect ratio 2:1	Typical high rise office building
<b>Global Dimensions</b>		
Breadth	20.0m	
Length	40.0m	
Height	64.0m	
<b>Glazing Characteristics</b>		
Thickness	4mm - Double glazed	Continuous glazing
Max. Pane dimensions	1.5 x 1.5m	
Failure Pressure (1 sec pulse duration)	80 mbar	Mainstone [4]
<b>Cladding/Wall Panel Characteristics</b>		
Thickness	180mm	Precast concrete panels
Panel Dimensions	2.3 x 3.5m	
Dynamic Failure Pressure	78 mbar	
Support Conditions	Vertically spanning - assumed simply-supported at ends	
Ductility	10	
Debris Size	210 x 210 x 35mm	This is a conservative assessment of the debris size based on the fatality probability criterion used
<b>Frame Details</b>		
Frame Type	Rigid internal core surrounded by flexible outer structure - 400 x 400mm external columns	Internal core provides lateral stability
Dynamic Failure Pressure	Global collapse: - Short side facing - 1185 mbar Long Side facing - 1730 mbar	It has been assumed that local collapse does not lead to a significant fatality probability over the entire height of the structure. Global collapse corresponds to failure of the entire building. All collapse pressures assume that the cladding is capable of transmitting load into the frame, and are increased by a suitable multiplication factor if the panels fail before the columns
Ductility	1.5	
<b>Additional Information</b>		



P-I Diagram: T2, Shock Pulse, Short Side Facing Blast

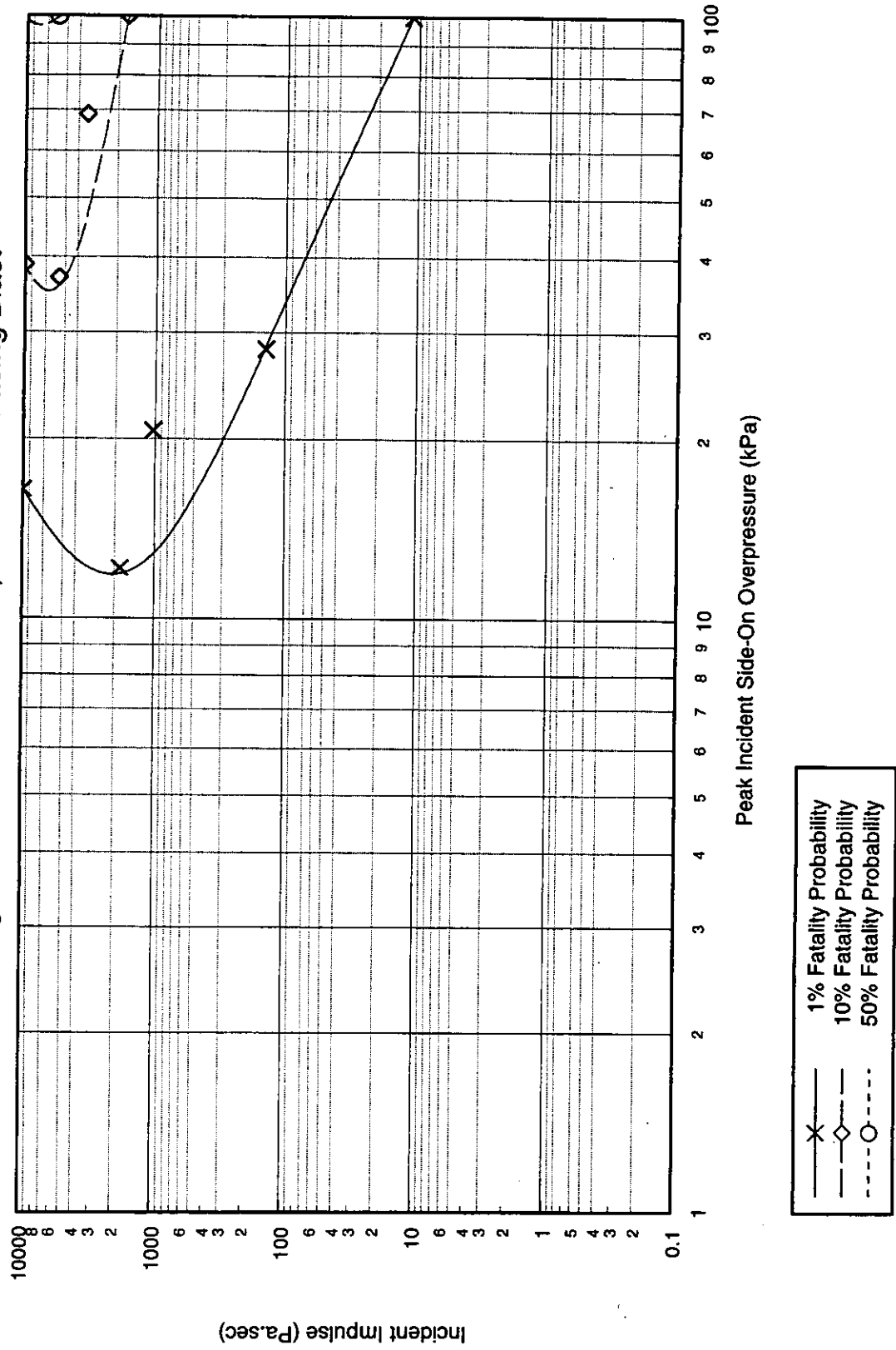


P-I Diagram: T2, Shock Pulse, Long Side Facing Blast

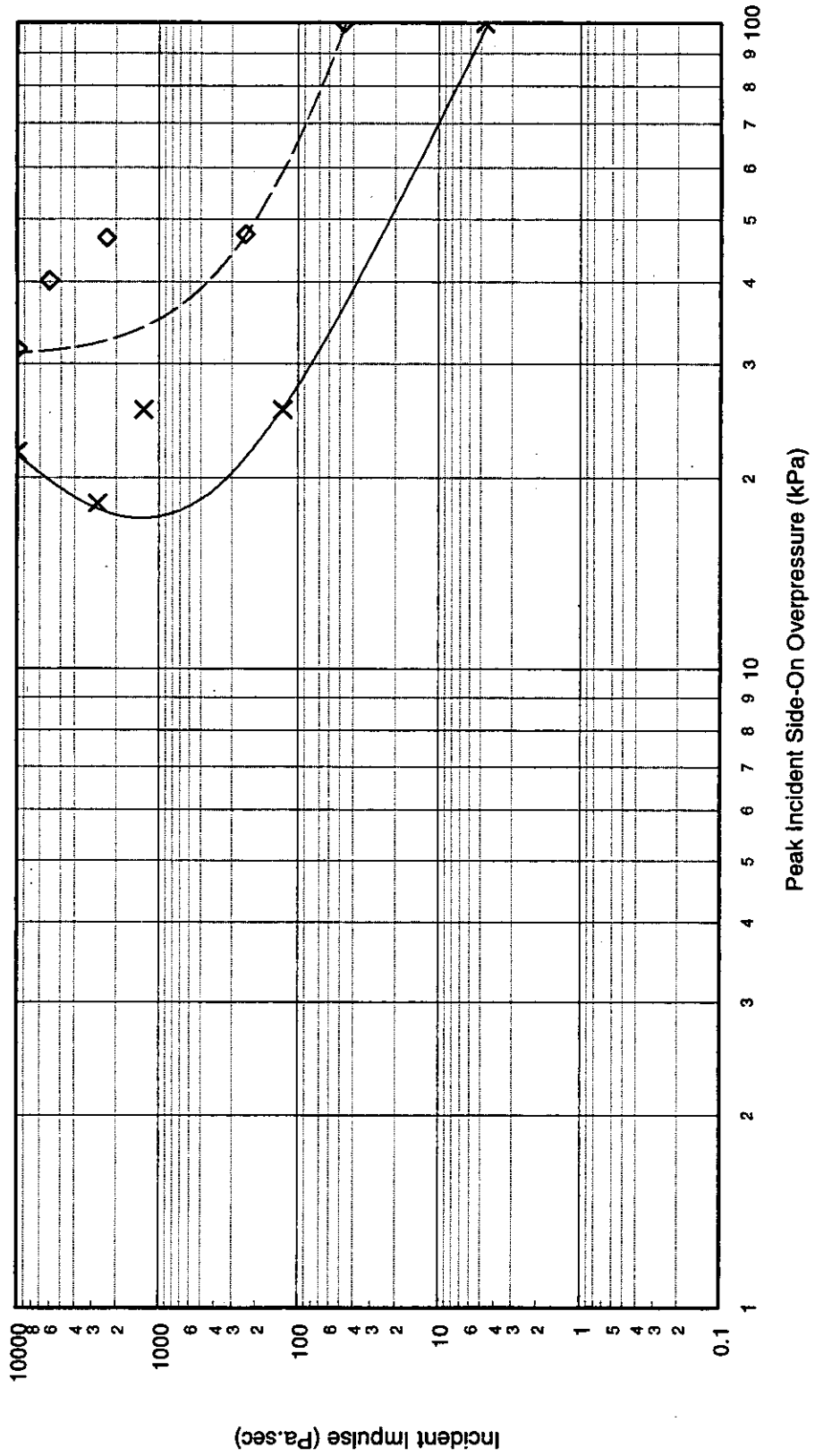


X ——— 1% Fatality Probability  
 ————◇——— 10% Fatality Probability

P-I Diagram: T2, Pressure Pulse, Short Side Facing Blast



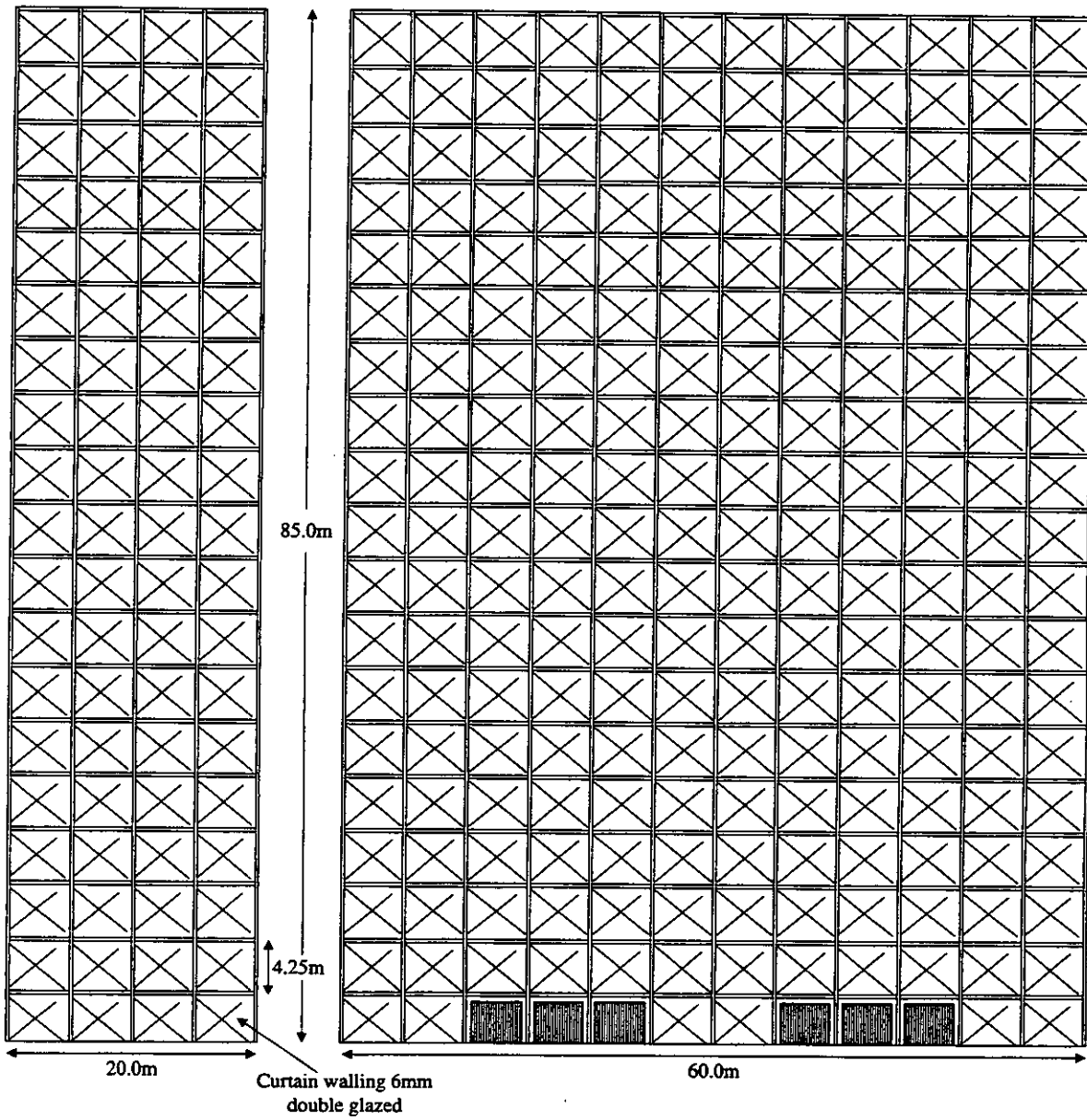
P-I Diagram: T2, Pressure Pulse, Long Side Facing Blast



x ——— 1% Fatality Probability  
 ———◇—— 10% Fatality Probability

**Short side elevation**

**Long side elevation**



**Plan**

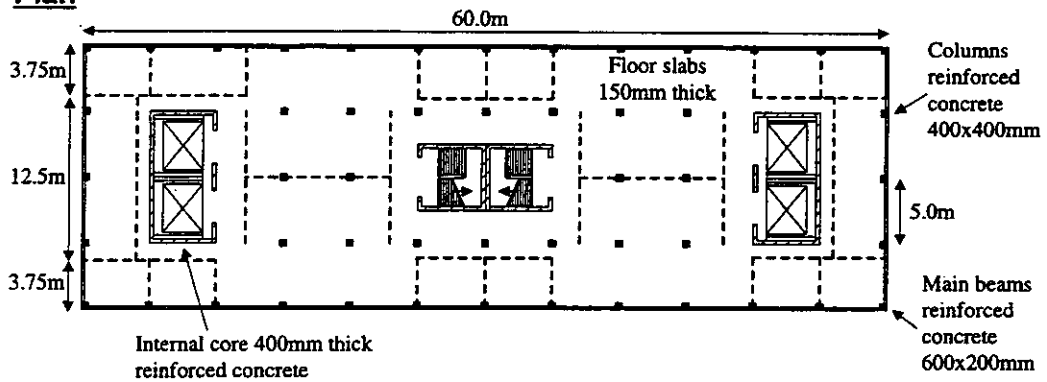
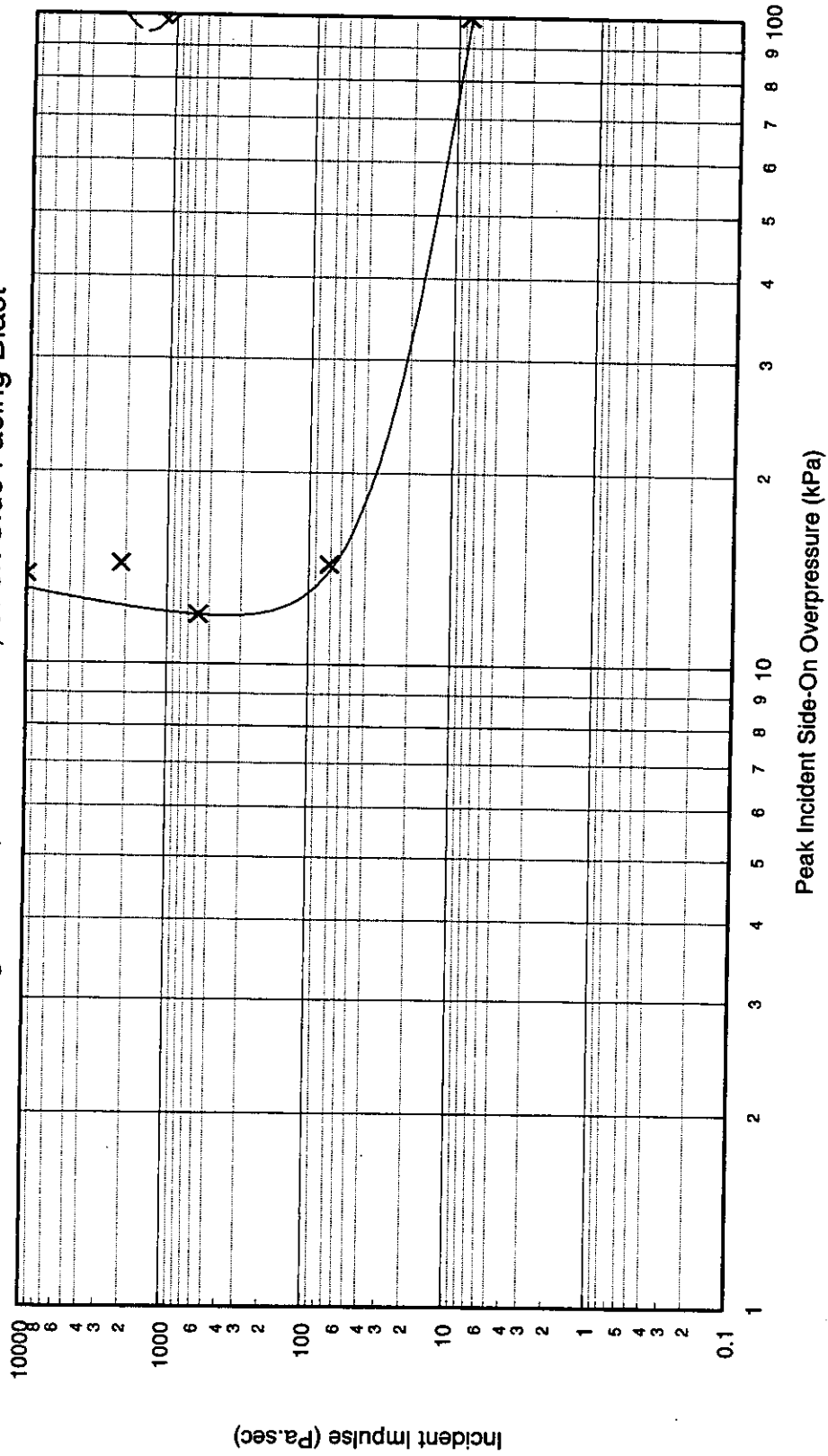


**Figure A.17: Illustration of Tall Building Type T/3**

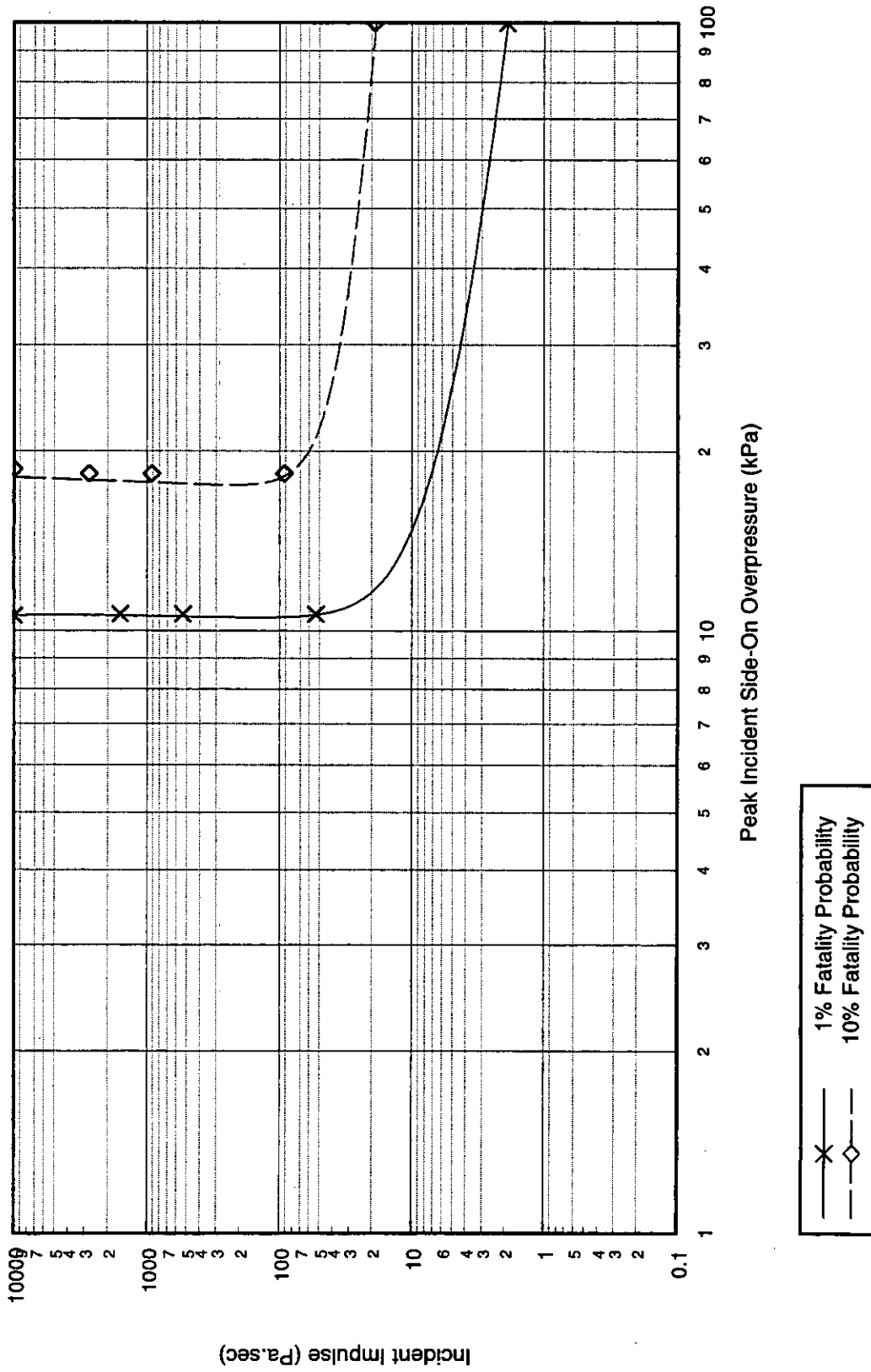
Quantity	Value	Comments
<b>Building Type: T/3</b>		
Description	20 storey tall building with rigid core at centre surrounded by relatively flexible frame constructed from reinforced concrete columns and beams, Aspect ratio 3:1	Typical high rise office building, completely clad in curtain wall glazing
<b>Global Dimensions</b>		
Breadth	20.0m	
Length	60.0m	
Height	85.0m	
<b>Glazing Characteristics</b>		
Thickness	6mm - Double glazed	Curtain walling
Max. Pane dimensions	5.0 x 4.0m	
Failure Pressure (1 sec pulse duration)	66 mbar	Manufacturer's literature - Mainstone [4] gives a value lower than 20mbar for 10m <sup>2</sup> pane area. The value of 66mbar used here is based on the manufacturer's data with the factors of safety removed, and is in line with the values for more usual glazing dimensions in the other building examples.
<b>Cladding/Wall Panel Characteristics</b>		
Thickness	No cladding	
Panel Dimensions		
Dynamic Failure Pressure		
Support Conditions		
Ductility		
Debris Size		
<b>Frame Details</b>		
Frame Type	Rigid internal core surrounded by flexible outer structure - 400 x 400mm external columns	Internal core provides lateral stability
Dynamic Failure Pressure	Global collapse: - Short side facing - 1320 mbar Long side facing - 1303 mbar	It has been assumed that local collapse does not lead to a significant fatality probability over the entire height of the structure. Global collapse corresponds to failure of the entire building. All collapse pressures assume that the cladding is capable of transmitting load into the frame, and are increased by a suitable multiplication factor if the panels fail before the columns
Ductility	1.5	
<b>Additional Information</b>		

P-I Diagram: T3, Shock Pulse, Short Side Facing Blast



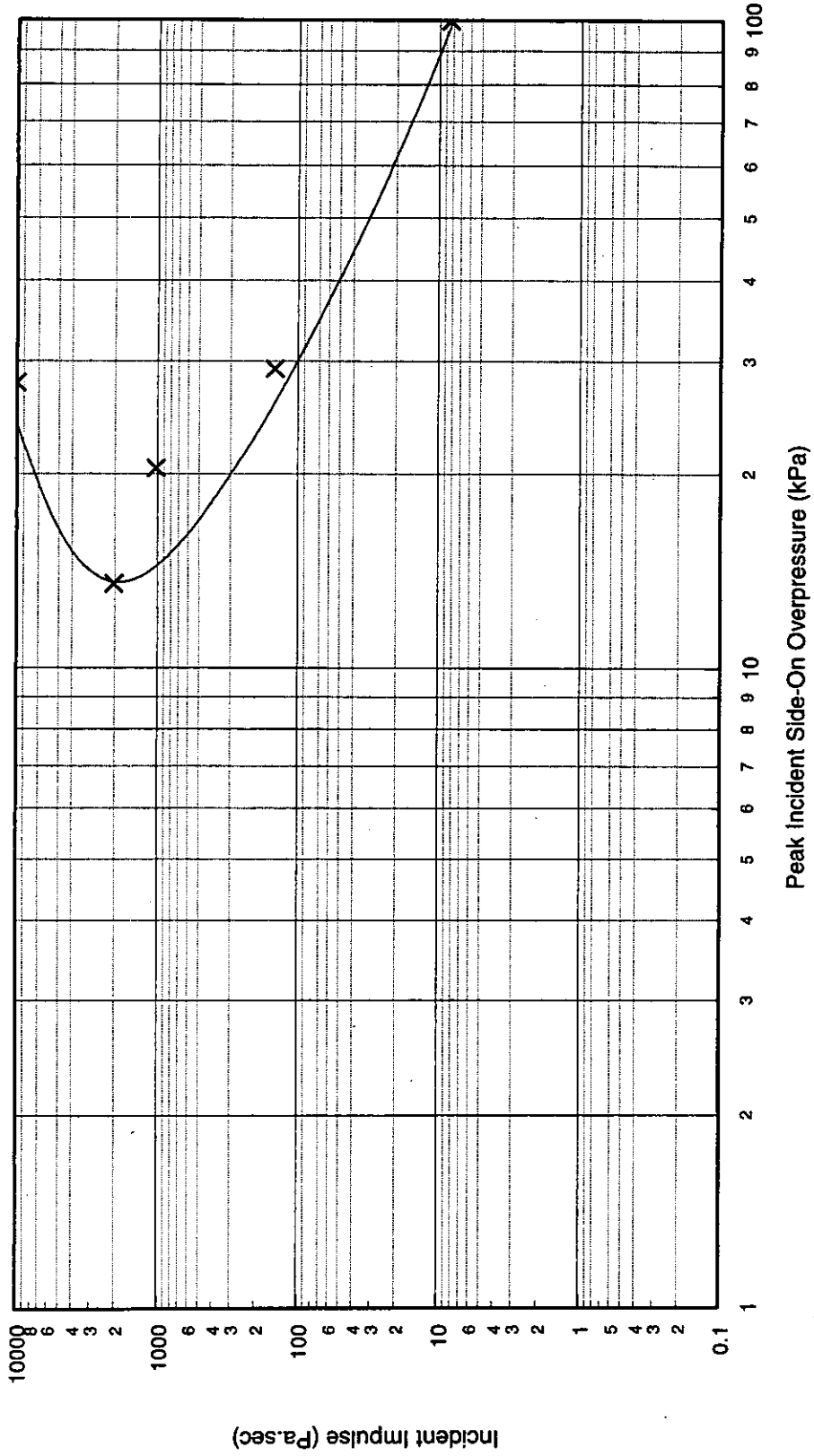
— X — 1% Fatality Probability
   
 - - - ◊ - - - 10% Fatality Probability

P-I Diagram: T3, Shock Pulse, Long Side Facing Blast



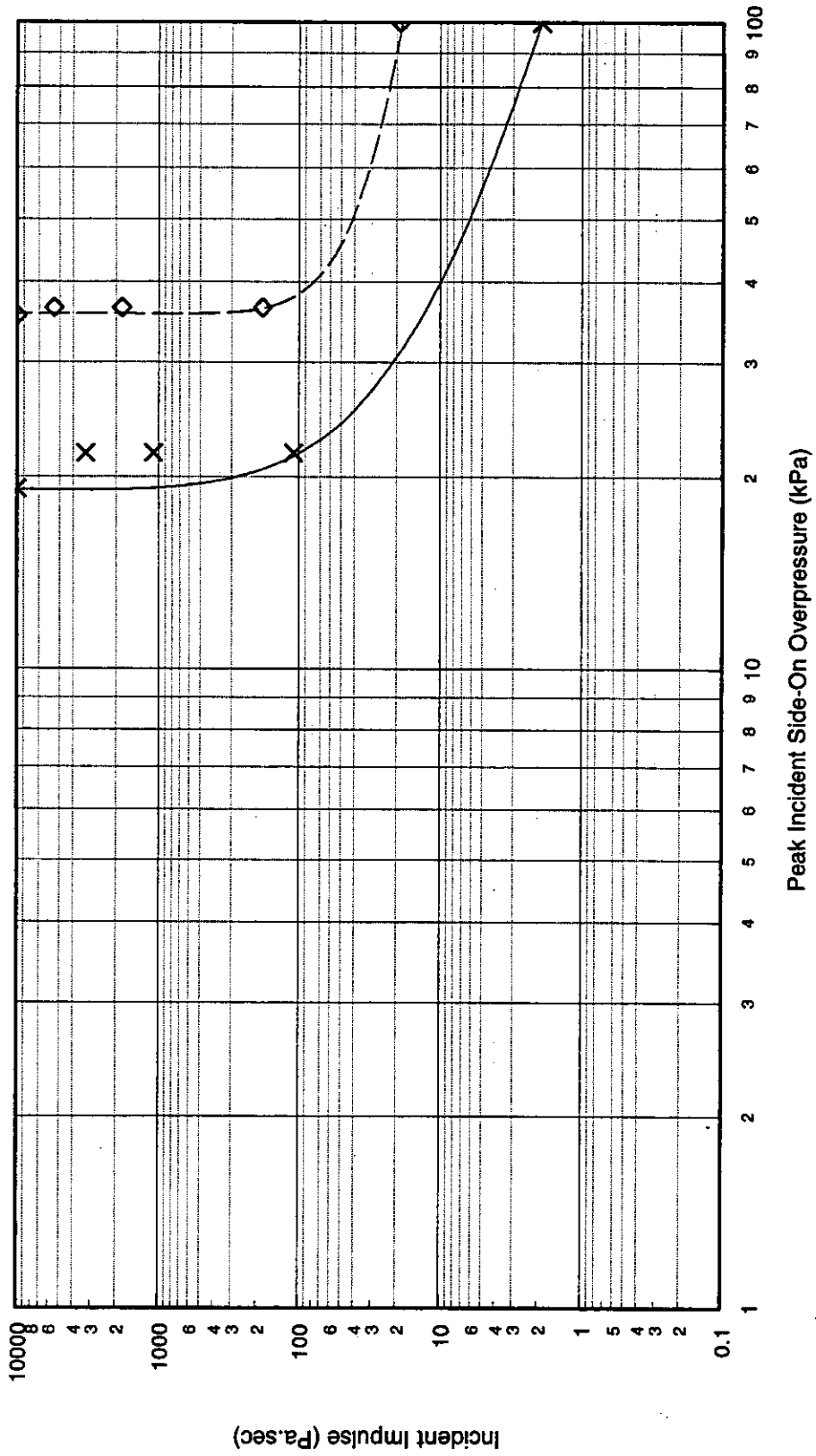


P-I Diagram: T3, Pressure Pulse, Short Side Facing Blast



X ——— 1% Fatality Probability

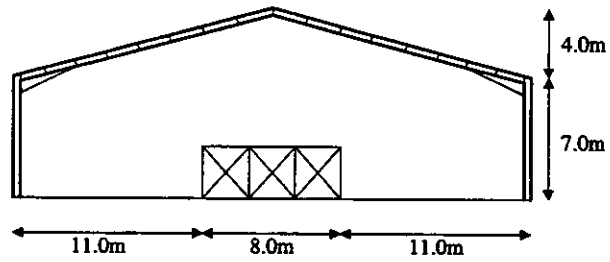
P-I Diagram: T3, Pressure Pulse, Long Side Facing Blast



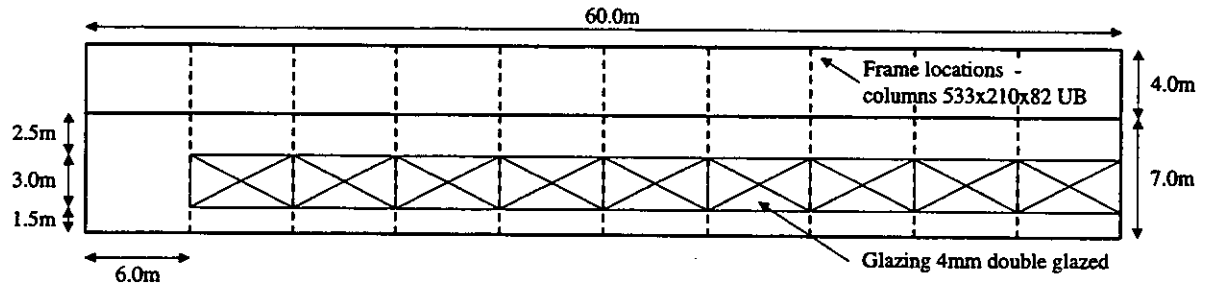
X ——— 1% Fatality Probability  
 ———◇—— 10% Fatality Probability

## **A.7. Building Type L: Long Span Buildings**

**Front elevation**



**Side elevation**



**Internal layout**

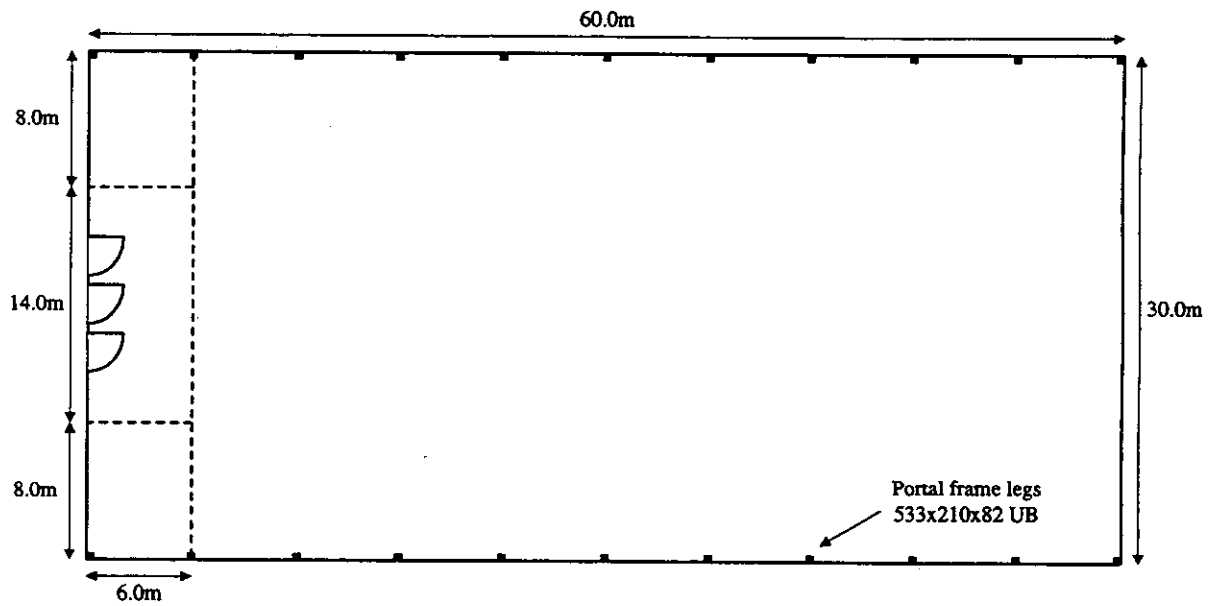
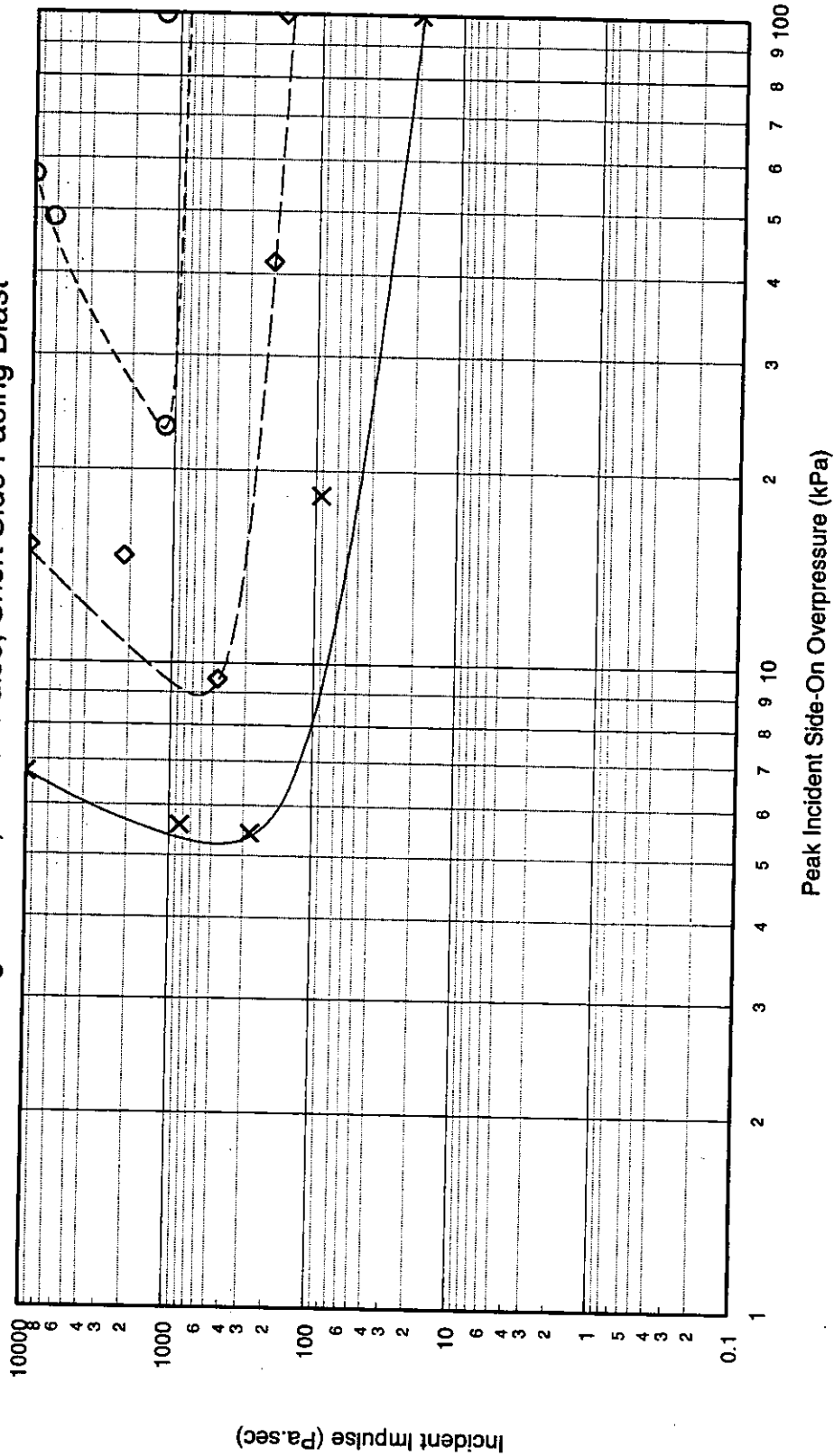


**Figure A.18: Illustration of Long Span Building Type L/1**

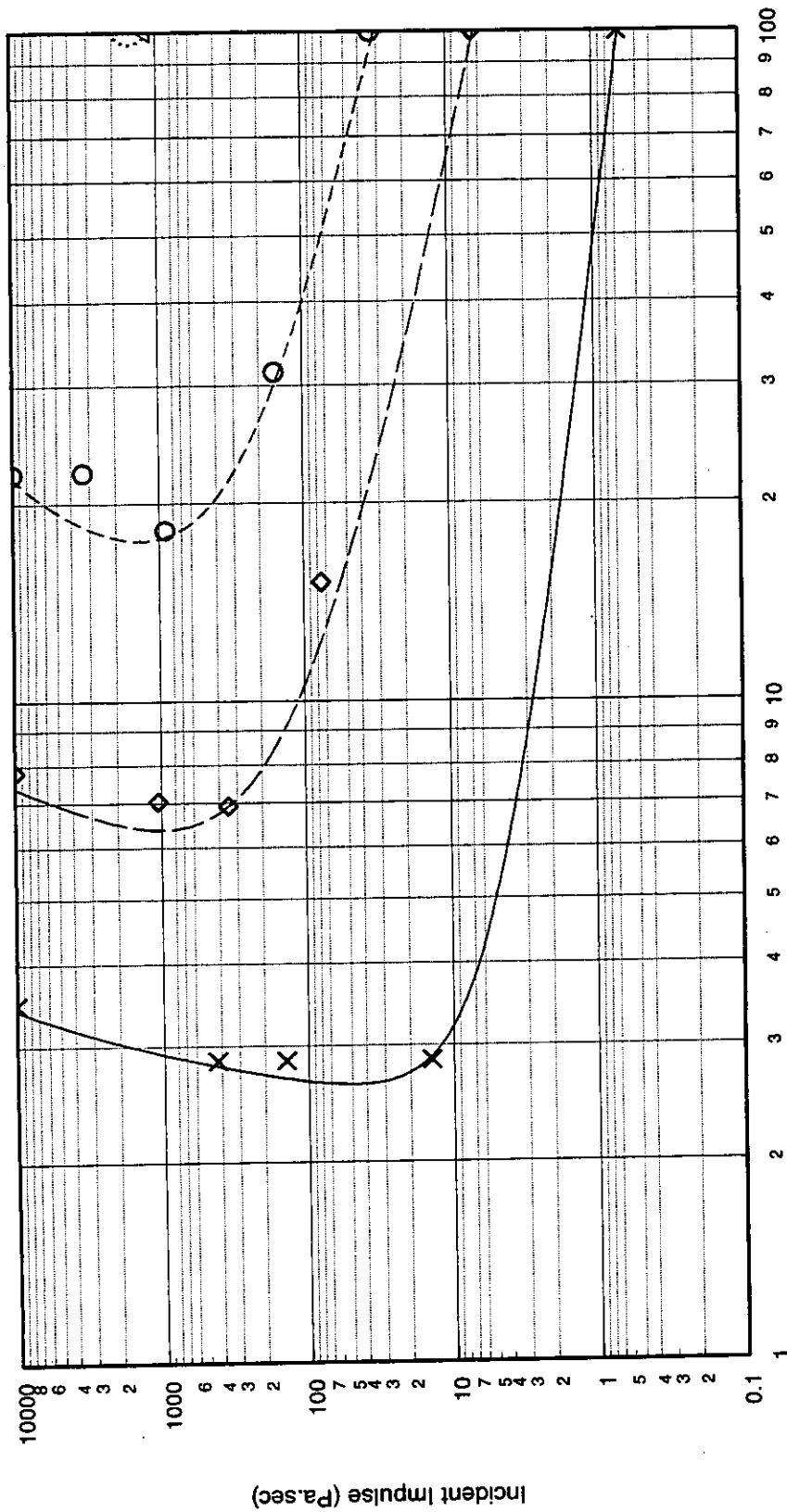
Quantity	Value	Comments
<b>Building Type: L/I</b>		
Description	Steel framed, long span structure with steel cladding. Aspect ratio 2:1	Typical supermarket or sports hall construction - open plan interior layout
<b>Global Dimensions</b>		
Breadth	30.0m	
Length	60.0m	
Height	11.0m	
<b>Glazing Characteristics</b>		
Thickness	4mm - Double glazed	Continuous glazing
Max. Pane dimensions	1.5 x 1.0m	
Failure Pressure (1 sec pulse duration)	60 mbar	Mainstone [4]
<b>Cladding/Wall Panel Characteristics</b>		
Thickness	0.6mm	Steel cladding panels
Panel Dimensions	1.5 x 6.0m	
Dynamic Failure Pressure	22.5 mbar	Calculated value
Support Conditions	Horizontally spanning - assumed simply-supported at ends	
Ductility	5	
Debris Size	1.5 x 1.0m	This is approximately equal to a single panel section
<b>Frame Details</b>		
Frame Type	Steel frame of 533 x 210 x 82UB columns	
Dynamic Failure Pressure	Global collapse. 133 mbar - short face 294 mbar - long face	Global collapse corresponds to failure of the entire building. All collapse pressures assume that the cladding is capable of transmitting load into the frame, and are increased by a suitable multiplication factor if the panels fail before the columns. For this building, the panels were found to fail before the columns in all cases
Ductility	5	
<b>Additional Information</b>		

P-I Diagram: L/1, Shock Pulse, Short Side Facing Blast

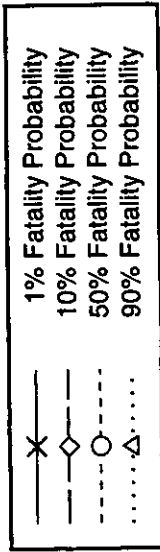


— x — 1% Fatality Probability  
 - - - ◊ - - - 10% Fatality Probability  
 . . . ○ . . . 50% Fatality Probability

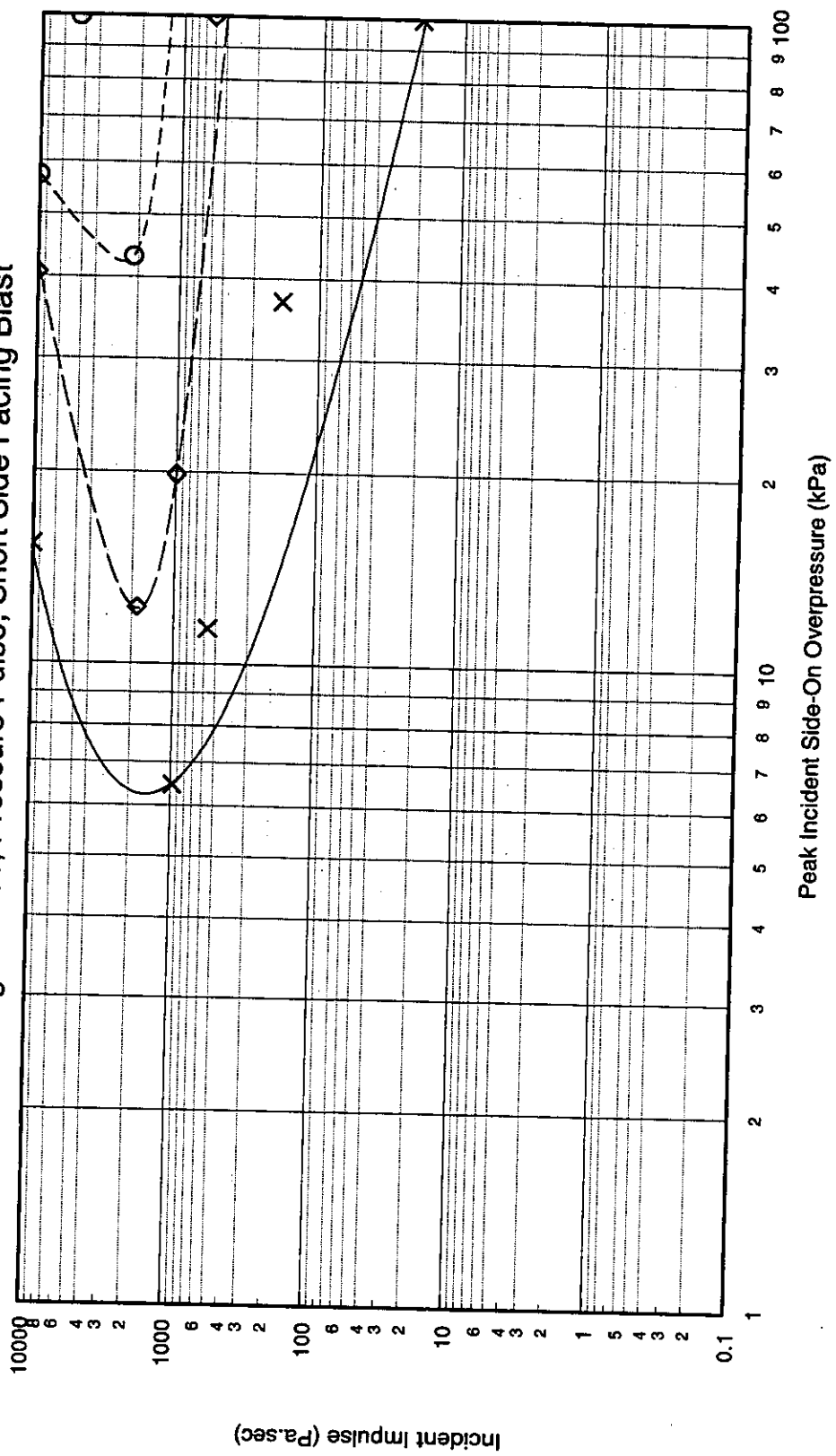
P-I Diagram: L/1, Shock Pulse, Long Side Facing Blast



Peak Incident Side-On Overpressure (kPa)



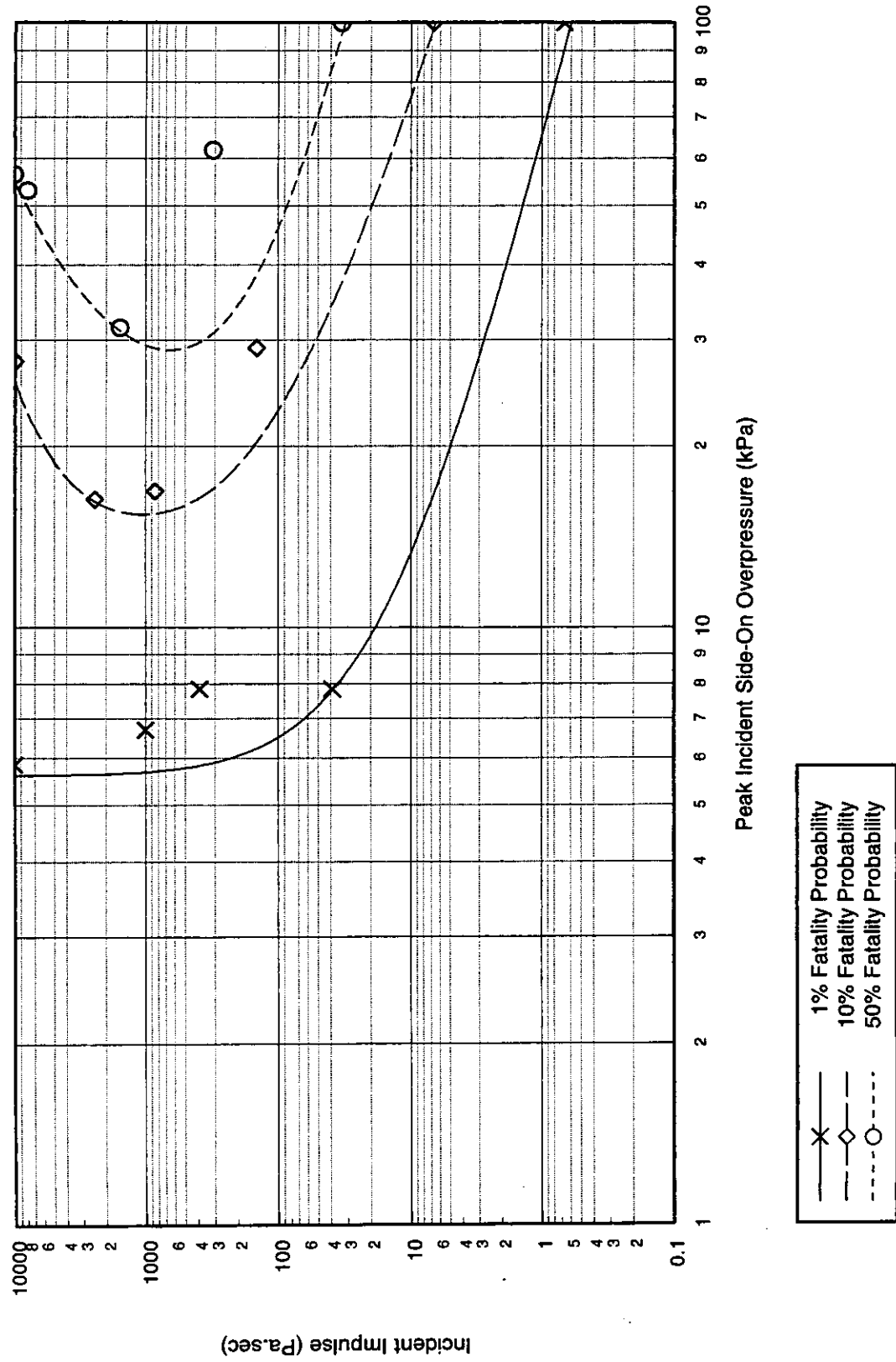
P-I Diagram: L/1, Pressure Pulse, Short Side Facing Blast



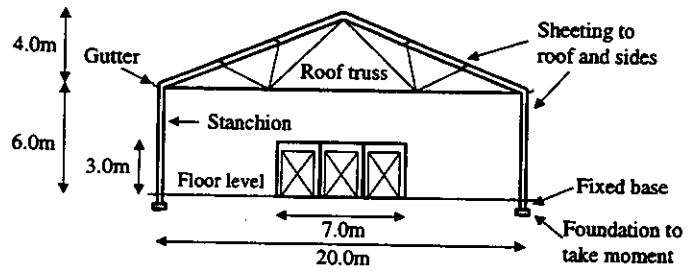
- x— 1% Fatality Probability
- - -o- 10% Fatality Probability
- ...o... 50% Fatality Probability



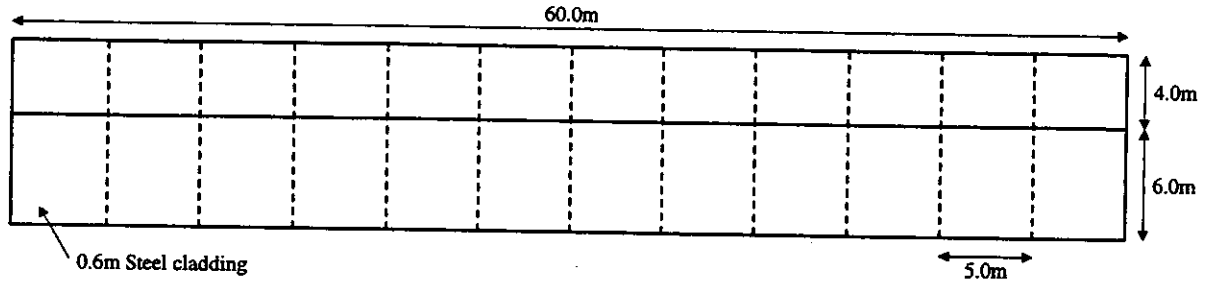
P-I Diagram: L/1, Pressure Pulse, Long Side Facing Blast



**End elevation**



**Side elevation**



**Internal plan (sports hall or supermarket)**

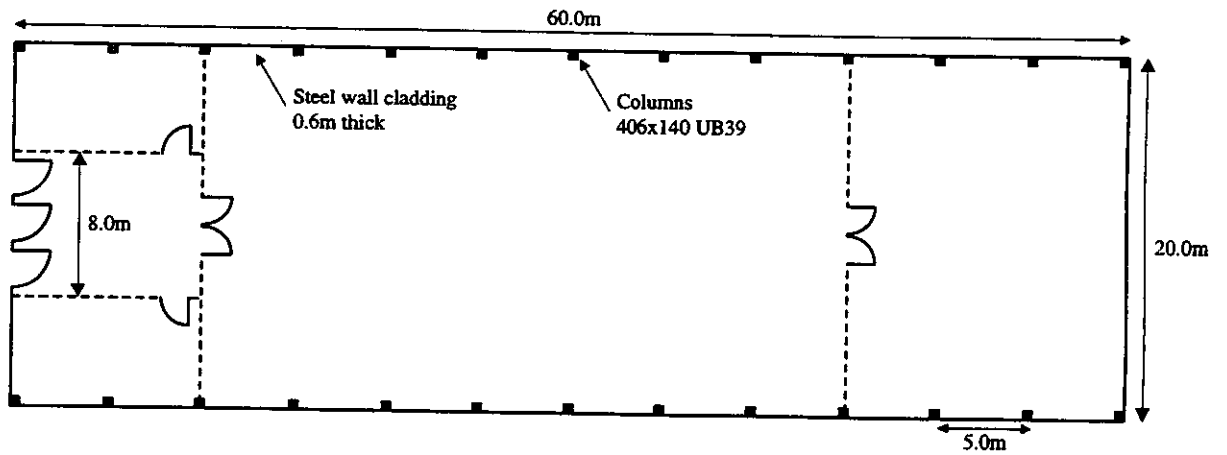
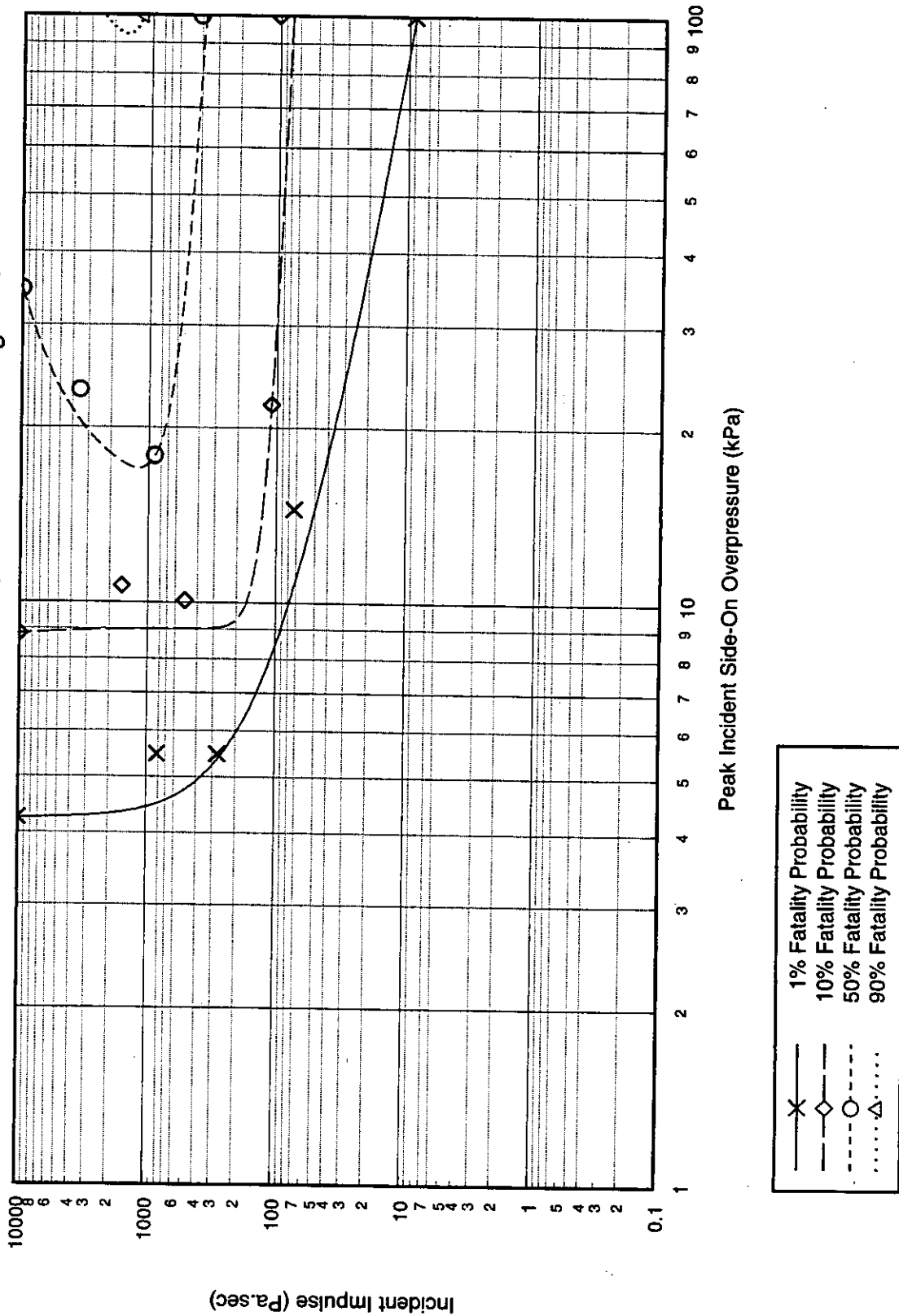


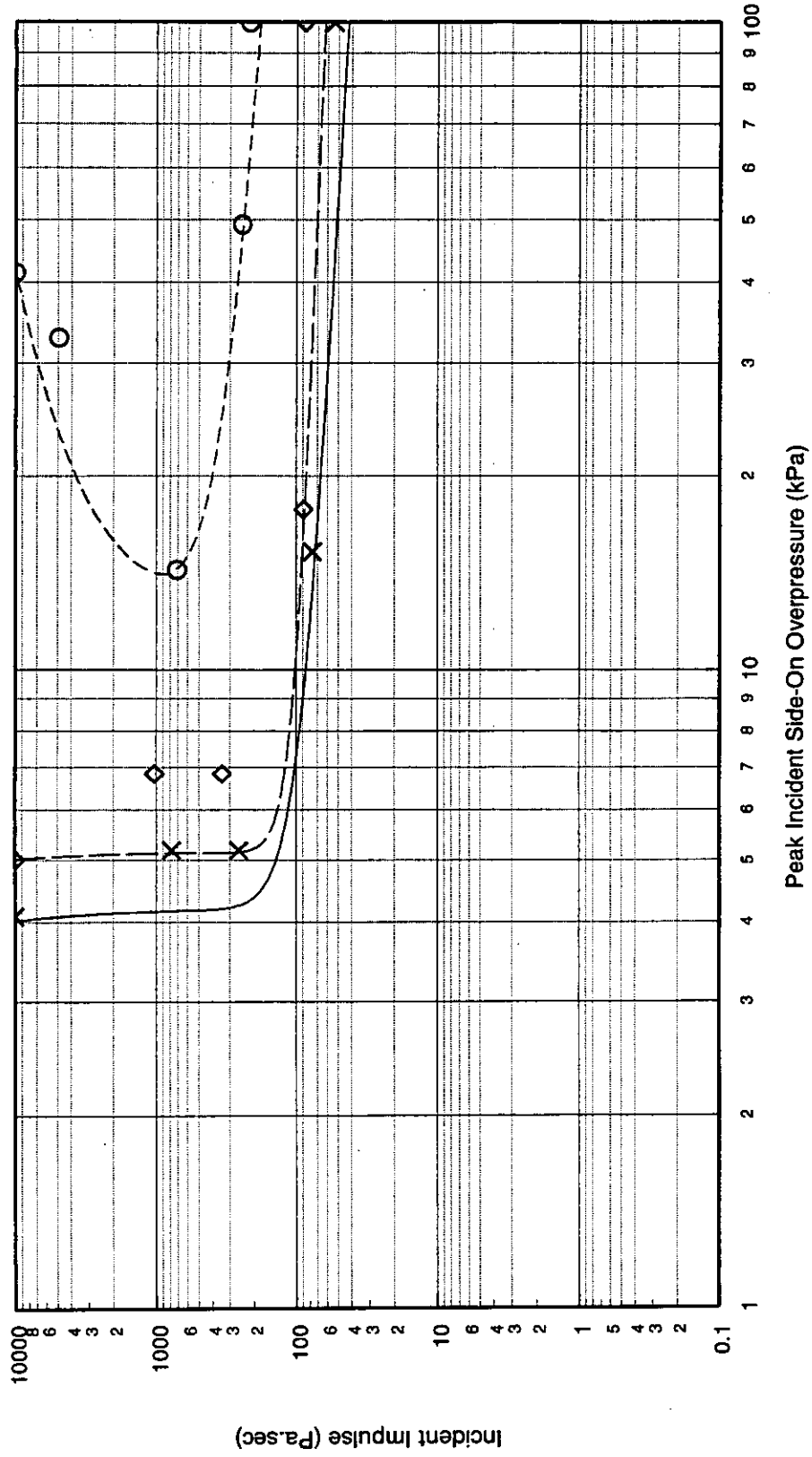
**Figure A.19: Illustration of Long Span Building Type L/2**

Quantity	Value	Comments
<b>Building Type: L/2</b>		
Description	Steel framed, long span structure with steel cladding and minimum glazing. Aspect ratio 3:1	Typical supermarket or sports hall construction - open plan interior layout
<b>Global Dimensions</b>		
Breadth	20.0m	
Length	60.0m	
Height	10.0m	
<b>Glazing Characteristics</b>		
Thickness	4mm - Double glazed	Continuous glazing
Max. Pane dimensions	1.125 x 1.25m	
Failure Pressure (1 sec pulse duration)	63 mbar	Mainstone [4]
<b>Cladding/Wall Panel Characteristics</b>		
Thickness	0.6mm	Steel cladding panels
Panel Dimensions	1.5 x 5.0m	
Dynamic Failure Pressure	22.3 mbar	Calculated value
Support Conditions	Horizontally spanning - assumed simply-supported at ends	
Ductility	5	
Debris Size	1.5 x 1.0m	This is approximately equal to a single panel section
<b>Frame Details</b>		
Frame Type	Steel frame of 406 x 140 x 39UB columns	
Dynamic Failure Pressure	Global collapse. 94 mbar - short face 167 mbar - long face	Global collapse corresponds to failure of the entire building. All collapse pressures assume that the cladding is capable of transmitting load into the frame, and are increased by a suitable multiplication factor if the panels fail before the columns. For this building, the panels were found to fail before the columns in all cases
Ductility	5	
<b>Additional Information</b>		

P-I Diagram: L/2, Shock Pulse, Short Side Facing Blast

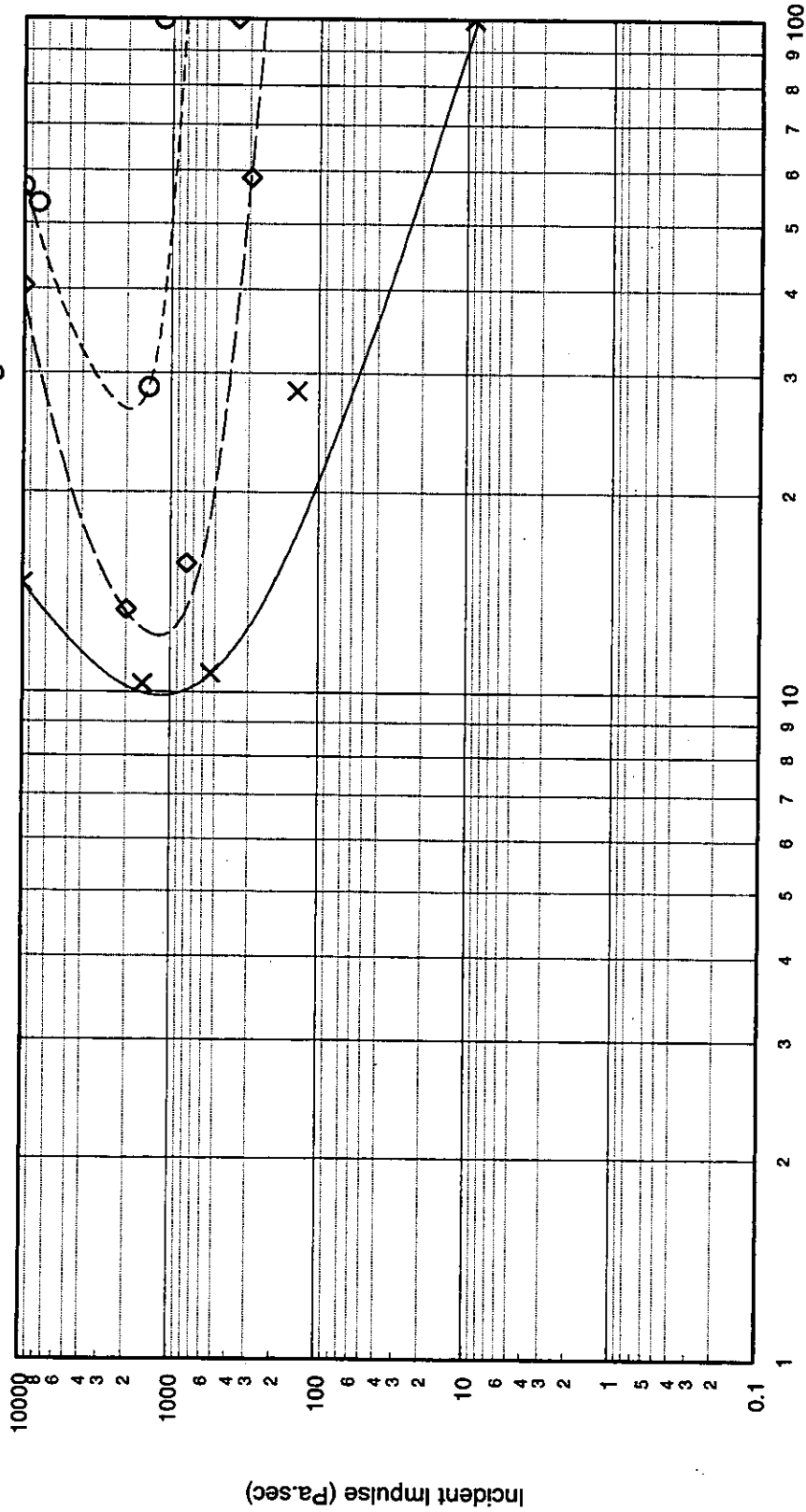


P-I Diagram: L/2, Shock Pulse, Long Side Facing Blast



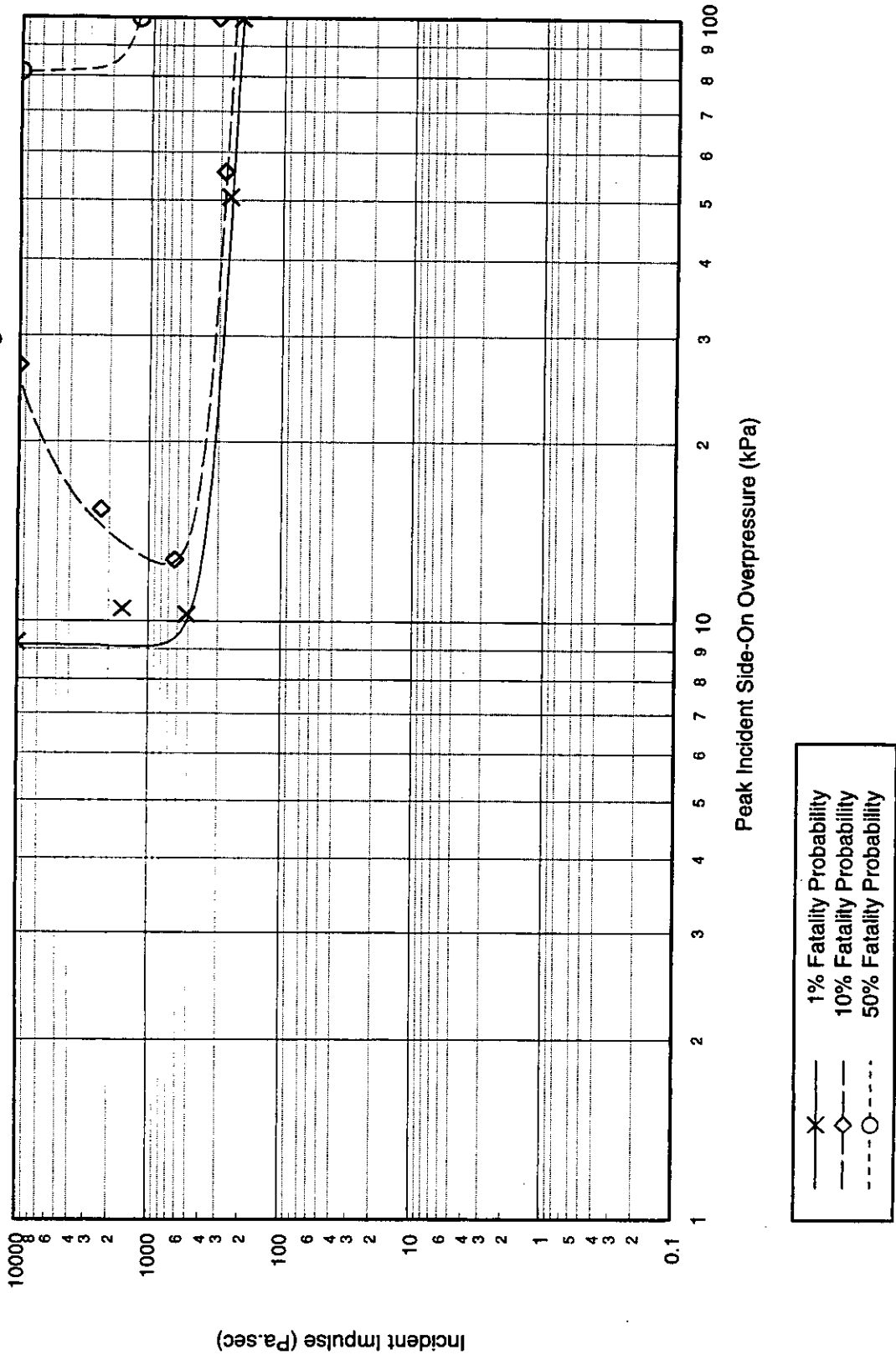
— x — 1% Fatality Probability  
 - - - ◊ - - - 10% Fatality Probability  
 - · - · - ○ - · - · 50% Fatality Probability

P-I Diagram: L/2, Pressure Pulse, Short Side Facing Blast



x — 1% Fatality Probability  
 ◇ — 10% Fatality Probability  
 ○ — 50% Fatality Probability

P-I Diagram: L/2, Pressure Pulse, Long Side Facing Blast



- x — 1% Fatality Probability
- - - ◊ - - 10% Fatality Probability
- ⋯ ○ ⋯ 50% Fatality Probability

## **APPENDIX B**

### **Worked Example**



## **Worked Example**

The following worked example presents the calculations for building type B2/2 subject to a 100msec duration shock and pressure pulse.

The calculations are presented in the following order:

1. Definition of building characteristics
2. Calculation of fatality probability due to glazing impact
3. Calculation of the impulse on a wall subjected to blast loading and the subsequent debris fragment velocity
4. Calculation of the fatality probability due to debris under blast loading
5. Calculation of the global structural response of the building (Shock Pulse)
6. Calculation of the global structural response of the building (Pressure Pulse)
7. Calculation of the fatality probability of the building occupants (Shock Pulse)
8. Calculation of the fatality probability of the building occupants (Pressure Pulse)

The calculations are explained in more detail in Section 2 of this report, and where possible, reference has been made within the calculations to the relevant equations and descriptions within that section.

## 1. Building characteristics

This Mathcad Sheet outlines all the data relating to the building characteristics including the glazing and cladding details and internal layout .

### Units definition

Pulse Duration - 100msec

$$\text{mbar} := 100 \cdot \text{Pa}$$

$$t_{p_0} := 0.1$$

### Building Characteristics

B2/2 - See Figure A.4

Type of building

*Typical brick-built house - two storey semi-detached: the building is symmetrical about its centre, with 5 rooms each side, and is assumed to have the same layout on both floors.*

Height of building

$$H := 8.0 \cdot \text{m}$$

Breadth of building (width)

$$B := 8.6 \cdot \text{m}$$

Length of building (front to back)

$$L := 14.3 \cdot \text{m}$$

Wall thickness

$$t_w := 0.215 \cdot \text{m}$$

### Internal Layout - Symmetrical about centre line

Number of different rooms

$$N_{\text{room}} := 5$$

Range of debris from short face

$$\text{maxr} := 3.72 \cdot \text{m}$$

Range of debris from long faces

Room 1

$$\text{maxr1} := 4.95 \cdot \text{m}$$

Room 2

$$\text{maxr2} := 3.85 \cdot \text{m}$$

Room 4

$$\text{maxr4} := 2.93 \cdot \text{m}$$

Room 5

$$\text{maxr5} := 3.65 \cdot \text{m}$$

Length: Room 1

$$L_{d1} := 3.43 \cdot \text{m}$$

Length: Room 3

$$L_{d3} := 1.82 \cdot \text{m}$$

Length: Room 5

$$L_{d5} := 3.43 \cdot \text{m}$$

This is the maximum range for glazing and debris assuming internal walls impede travel

This is the external perimeter length of the room which gives rise to debris

### Glazing Dimensions / Properties

Thickness of glass

$$t_{\text{win}} := 3 \cdot \text{mm}$$

Length: Room 1

$$L_{\text{win1}} := 2.025 \cdot \text{m}$$

Length: Room 2

Side

$$L_{\text{win2s}} := 2.025 \cdot \text{m}$$

Front

$$L_{\text{win2f}} := 1.275 \cdot \text{m}$$

Length: Room 4

$$L_{\text{win4}} := 2.025 \cdot \text{m}$$

Length: Room 5

$$L_{\text{win5}} := 2.025 \cdot \text{m}$$

Height of window	$H_{win} := 1.25 \cdot m$	
Width of glass pane	$B_{win} := 0.675 \cdot m$	
Failure Pressure (1 sec duration)	$G_{fail} := 55 \cdot mbar$	Mainstone [4]
Density of glazing	$\rho_g := 2500 \cdot kg \cdot m^{-3}$	
Elastic Modulus of Glass	$E_g := 80 \cdot 10^9 \cdot Pa$	
Poisson's Ratio	$\nu_g := 0.3$	
Maximum height of window	$maxh := 2.2 \cdot m$	

### Debris Dimensions

For the brick building, the size of the debris from the wall is assumed to correspond to a single brick. The size of the wall of interest is assumed to be that of the maximum room on the front face.

Height of wall	$H_{wall} := 2.6 \cdot m$
Breadth of wall (width)	$B_{wall} := 3.85 \cdot m$
Height of debris	$H_{deb} := 112.5 \cdot mm$
Width of debris	$B_{deb} := 225 \cdot mm$
Thickness of debris	$t_{deb} := 75 \cdot mm$
Failure Pressure of wall under dynamic load	$W_{fail} := 275 \cdot mbar$
Density of brickwork	$\rho_b := 2000 \cdot kg \cdot m^{-3}$
Elastic Modulus of Brick	$E_b := 900 \cdot 8.0 \cdot newton \cdot mm^{-2}$
Poisson's Ratio	$\nu_b := 0.3$

A file (b22) is output from this sheet and contains all the data necessary to run the following Mathcad sheets

## 2. Calculation of fatality probability due to glazing impact

The glazing hazard calculations are performed next. The description of the calculations is given in Section 2.4.1 and 2.5.1, and is illustrated in Figure 2.17.

### Definition of units

$$\text{mbar} := 100 \cdot \text{Pa}$$

$$\text{bar} := 1000 \cdot \text{mbar}$$

### Input variables

The characteristics of the building which are used in the glazing calculations are read in as a matrix from the previous Mathcad sheet, and are assigned variable names for use in this sheet only.

$$\text{gvar} := \text{READPRN}(\text{b22})$$

*Height of glass pane*

$$H := \text{gvar}_{6,1} \cdot \text{m}$$

$$H = 1.25 \cdot \text{m}$$

*Breadth of glass pane*

$$B := \text{gvar}_{7,1} \cdot \text{m}$$

$$B = 0.675 \cdot \text{m}$$

*Thickness of pane*

$$t_w := \text{gvar}_{0,1} \cdot \text{m}$$

$$t_w = 3 \cdot \text{mm}$$

*Density of glass*

$$\rho := \text{gvar}_{9,1} \cdot \text{kg} \cdot \text{m}^{-3}$$

$$\rho = 2.5 \cdot 10^3 \cdot \text{kg} \cdot \text{m}^{-3}$$

$\gamma$  for air

$$\gamma := 1.4$$

Density of air

$$\rho_{\text{air}} := 1.225 \cdot \text{kg} \cdot \text{m}^{-3}$$

Atmospheric pressure

$$p_0 := 1 \cdot 10^5 \cdot \text{Pa}$$

Coefficient of drag

$$C_D := 1.2$$

Speed of sound in the atmosphere

$$C_o := 340 \cdot \frac{\text{m}}{\text{sec}}$$

### Failure Pressure of Glazing

The failure pressure of the glazing is calculated from Mainstone [4], and increased to take into account the shorter duration of the blast load, in accordance with Section 2.2.2 of the report.

*Breaking pressure of pane (Mainstone)*

$$bp := \text{gvar}_{8,1} \cdot \text{mbar}$$

$$bp = 55 \cdot \text{mbar}$$

*Pulse duration*

$$t_p := \text{READPRN}(\text{pdur})_0$$

$$t_p = 0.1 \text{ (seconds)}$$

Factor on glazing failure calculation

$$\text{gfactor} := -0.141 \cdot \ln(t_p) + 0.104 \cdot t_p + 0.904$$

$$\text{gfactor} = 1.239$$

Increased glazing failure pressure

$$bp := \text{gfactor} \cdot bp$$

$$bp = 68.149 \cdot \text{mbar}$$

**Glazing Velocity Profile**

(The following equation is taken from Baker [13], page 492)

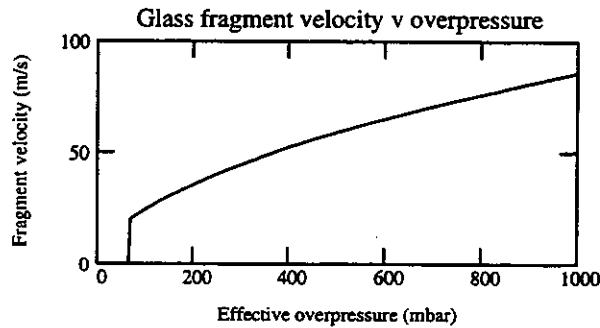
$$i := 0, 1..500$$

The average velocity has been increased by a factor of 1.5 to represent the upper bound of values shown on figure 5 in Fletcher et al, 1980, [11]

Effective Pressure  $P_{eff_i} := i \cdot 2 \cdot \text{mbar}$  (0 to 1000 mbar in steps of 2 mbar)

Initial velocity 
$$V_i := \left[ (0.2539) + (1.826 \cdot 10^{-4}) \cdot \left( \frac{tw}{m} - 7.62 \cdot 10^{-4} \right)^{-0.928} \right] \cdot \left[ 0.3443 \cdot \left( \frac{P_{eff_i}}{Pa} \right)^{0.547} \right] \cdot 1.$$

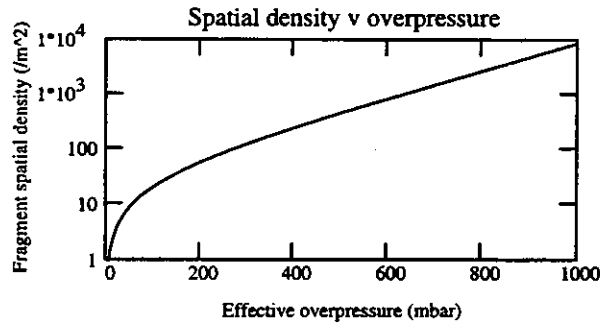
$V_i := \text{if}(P_{eff_i} \leq bp, 0, V_i)$



**Fragment Spatial Density**

The equation for the number of fragments per square metre is taken from the Eskimo II and III data, and the subsequent analysis in Fletcher et al (1980) [11]

Number of fragments per square metre 
$$pd_i := \left[ e^{\left( 3.1037 + 0.05857 \cdot \frac{P_{eff_i}}{1000 \cdot Pa} \right)} - 22.28 \right] \cdot 4.910 \cdot e^{-5.012 \cdot \frac{tw}{cm}}$$



In order to calculate the relative vulnerabilities to skin penetration and skull fracture, it is necessary to know the relative areas of the head and the body. These values are taken from Feinstein [14], and relate to the head and the whole body (i.e. not just the thorax area)

Area of Head  $A_{head} := 0.031 \cdot m^2$

Area of Body  $A_{body} := 0.359 \cdot m^2$

No of fragments hitting head  $N_{fh_i} := A_{head} \cdot pd_i \cdot \frac{1}{m^2}$

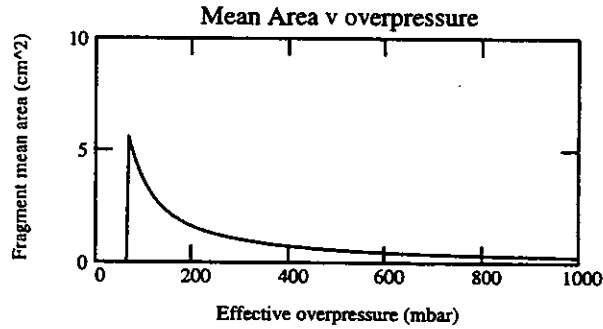
No of fragments hitting body  $N_{fb_i} := A_{body} \cdot pd_i \cdot \frac{1}{m^2}$

NB This doesn't take into account the fact that the height of the fragments is changing

**Fragment Area and Mass Distribution**

The fragment mean area is taken from a curve fit to the experimental data as presented in the Eskimo II and III papers and described in Section 2.4.1

Fragment mean area  $A_i := \text{if} \left[ \frac{\text{Peff}_i}{\text{mbar}} \geq \frac{\text{bp}}{\text{mbar}}, 834.16 \cdot \left( \frac{\text{Peff}_i}{\text{mbar}} \right)^{-1.1772} \cdot \text{cm}^2, 0 \cdot \text{cm}^2 \right]$  (15)



**Mass-Velocity pairs of interest**

The heaviest, slowest fragments are assumed to have 10 times the average mass and 0.6 times the average velocity, while the lightest, quickest fragments are assumed to have a tenth of the average mass and 1/0.6 times the average velocity, based on the upper bound in the spread of fragment masses and velocities observed by Fletcher et al [9,10,11]

10 x Area	$A10_i := A_i \cdot 10$
0.1 x Area	$A01_i := A_i \cdot 0.1$
Fragment Mass	$M_i := A_i \cdot t_w \cdot \rho$
10 x Mass	$M10_i := M_i \cdot 10$
Corresponding Velocity	$V10_i := V_i \cdot 0.6$
0.1 x Mass	$M01_i := M_i \cdot 0.1$
Corresponding Velocity	$V01_i := \frac{V_i}{0.6}$

**Calculation of total flight time**

The total flight time is based on the time taken for the fragment to fall below a height of 0.5m above the floor

Maximum initial height  $\text{height} := gvar_{12,1} \cdot m - 0.5 \cdot m$       height = 1.7•m

Flight time  $\text{time} := \sqrt{\frac{\text{height}}{0.5 \cdot g}}$       time = 0.589•sec

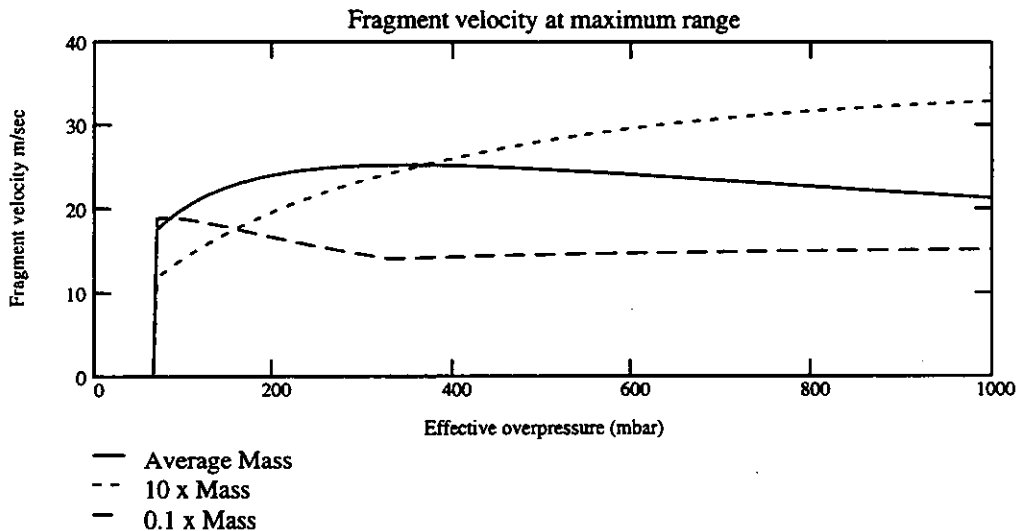
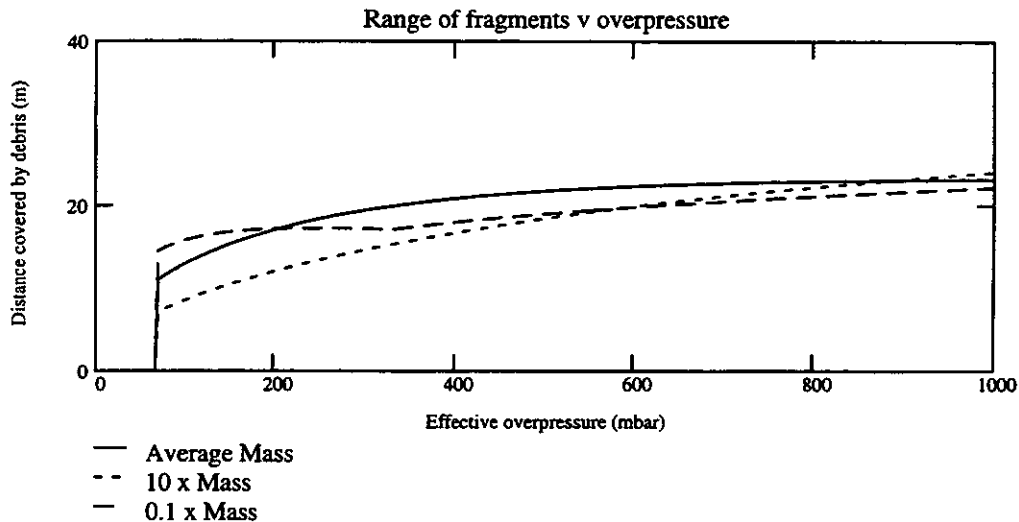
### Calculation of maximum range and velocities of fragments

The velocity and maximum range of the glass fragments is calculated using the method outlined below.

Firstly, the failure pressure of the glass pane is compared to the effective overpressure, to determine whether the glazing has failed. Then the orientation of the glass fragments is determined, based on the assumption that the fragments fly such that their frontal area is minimised, either by travelling edge-on or side-on. Finally, for each of the three fragment sizes considered, the distance and velocity of the fragments is calculated, based on the initial velocity, overpressure and drag (Equation 18) at 1.0m intervals up to a maximum of 30m, taking into account whether the fragment falls below 0.5m above the floor. This is an iterative calculation.

Thus for each of the effective overpressures considered, we now have a mass profile (M, M01 and M10) and a velocity profile (V, V01 and V10) with distance from the window.

### Maximum ranges and velocities    $i := 0..500$



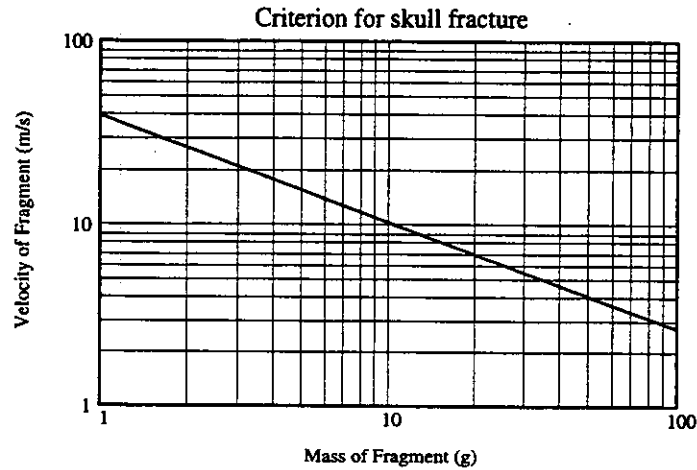
## Skull Fracture

### Calculation of critical velocities to cause a 50% chance of skull fracture

The criterion for injury due to skull fracture is based on Fletcher et al [11], and is reproduced below. If the fragment mass and velocity exceed the line shown on the graph, then a person hit on the head by that fragment will experience a 50% probability of skull fracture

$$y := 1..100$$

$$Avel(y) := e^{(-0.58275 \cdot \ln(y) + 3.6688)}$$



For the mass distributions given above, M, M10 and M01, it is necessary to identify the critical velocities above which a 50% fatality probability exists. This is done by comparing the fragment mass with the above curve and extracting the velocity corresponding to that mass.

Define mass values

$$y_i := \frac{M_i}{\text{gm}}$$

$$y_{10_i} := \frac{M_{10_i}}{\text{gm}}$$

$$y_{01_i} := \frac{M_{01_i}}{\text{gm}}$$

Extract velocities

Critical velocity for average fragment mass

$$P_{45crit_i} := \text{if}(y_i > 0, Avel(y_i) \cdot \text{m} \cdot \text{sec}^{-1}, 0)$$

Critical velocity for 10 x average fragment mass

$$P_{45crit10_i} := \text{if}(y_{10_i} > 0, Avel(y_{10_i}) \cdot \text{m} \cdot \text{sec}^{-1}, 0)$$

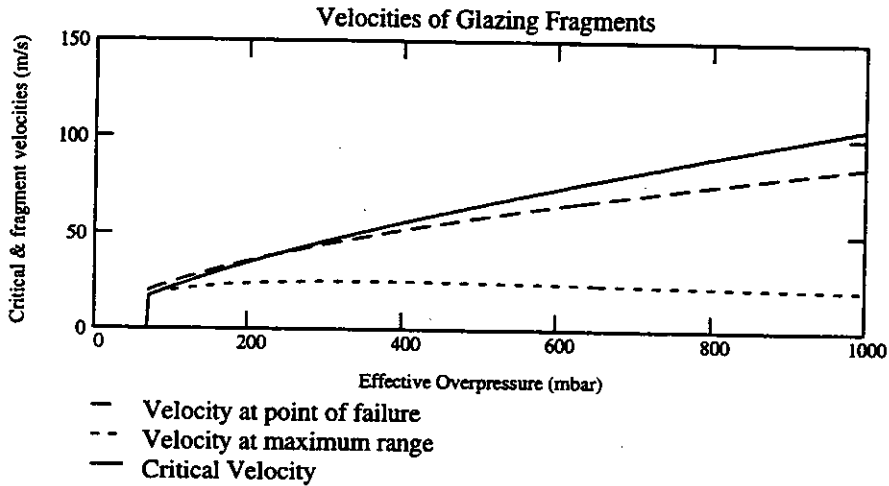
Critical velocity for 0.1 x average fragment mass

$$P_{45crit01_i} := \text{if}(y_{01_i} > 0, Avel(y_{01_i}) \cdot \text{m} \cdot \text{sec}^{-1}, 0)$$



**Comparison of Glazing Fragment Velocities (Average fragment mass)**

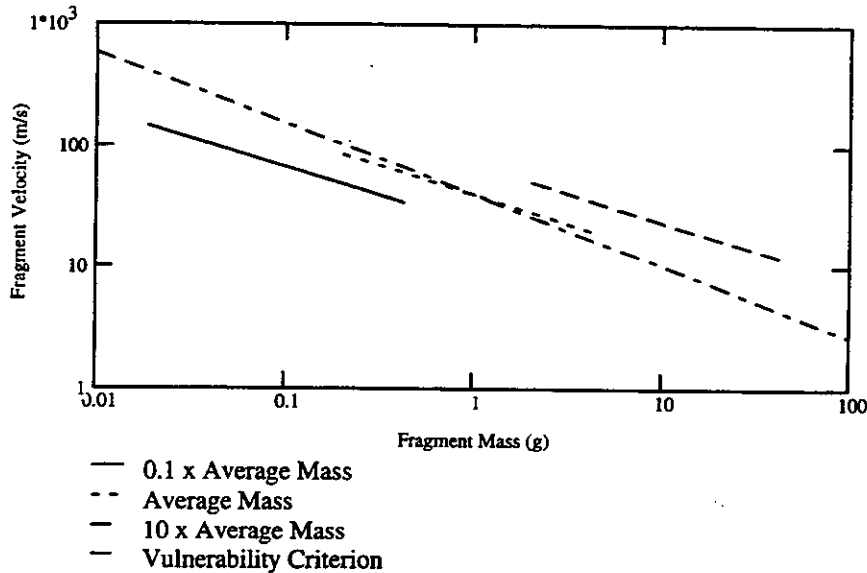
The following figure shows the initial velocity, the velocity at maximum range and the critical velocity for skull fracture for the average mass fragment, as a function of the effective overpressure



**Comparison of Mass-Velocity Profiles against Vulnerability Criterion**

It is necessary to calculate the proportion of the fragments which exceed the vulnerability criterion at each distance from the window. This process is explained in greater detail in Section 2.5.1(e) and is illustrated in Figure 2.18. Basically, for each distance from the window a figure can be drawn which is similar to the one below. At each distance from the window, there is a range of fragment masses and velocities corresponding to the effective overpressure considered. This is shown below for the point of failure, with lines drawn to represent the average mass, 0.1 times the average mass and 10 times the average mass. If a line is drawn between the corresponding pressure points for the 0.1 x mass curve and the 10 x mass curve, it intersects the criterion at some point (Figure 2.18). It has been assumed that the proportion of fragments exceeding the criterion corresponds to the proportion of this line which lies above the criterion.

```
ii := 35..500    j := 0, 1..30    mass := 0.01..100
avel(mass) := if(mass > 0, Avel(mass), 0)
```



The proportion of potentially injurious fragments is extracted for all distances and all effective overpressures as described on the previous page. This calculation results in a matrix, pig, which contains the percentage of fragments which exceed the criterion for any given distance (up to 30m), and any given effective pressure (up to 1000mbar)

Distance (m intervals up to 30m) ->

	22	23	24	25	26	27	28
29	0.06	0.054	0.047	0.041	0.036	0.03	0.025
30	0.06	0.053	0.047	0.041	0.036	0.03	0.025
31	0.06	0.053	0.047	0.041	0.035	0.03	0.025
32	0.059	0.053	0.047	0.041	0.035	0.03	0.025
33	0.059	0.053	0.047	0.041	0.035	0.03	0.024
34	0.059	0.053	0.046	0.04	0.035	0.029	0.024
35	0.059	0.052	0.046	0.04	0.035	0.029	0.024
36	0.059	0.052	0.046	0.04	0.034	0.029	0.024
37	0.058	0.052	0.046	0.04	0.034	0.029	0.024
38	0.058	0.052	0.045	0.04	0.034	0.029	0.023
39	0.058	0.051	0.045	0.039	0.034	0.028	0.023
40	0.058	0.051	0.045	0.039	0.033	0.028	0.023

Effective Pressure  
(2 mbar intervals,  
up to 1000mbar)



pig =

This sets the probability for the number of injurious fragments, Pinjh

$$k := 1..500$$

$$Pinjh_{k,j} := pig_{k,j}$$

#### Number of injurious fragments (skull fracture)

The number of injurious fragments is equal to the number of fragments multiplied the percentage of injurious fragments:

$$Ninjh_{k,j} := Pinjh_{k,j} \cdot Nfh_k$$

#### Probability of Fatality

It is necessary to define conditional probabilities for a single hit causing injury and for that injury causing a fatality.

Probability of single hit causing injury

$$Ptryg := 0.5$$

Probability of single injurious hit being fatal

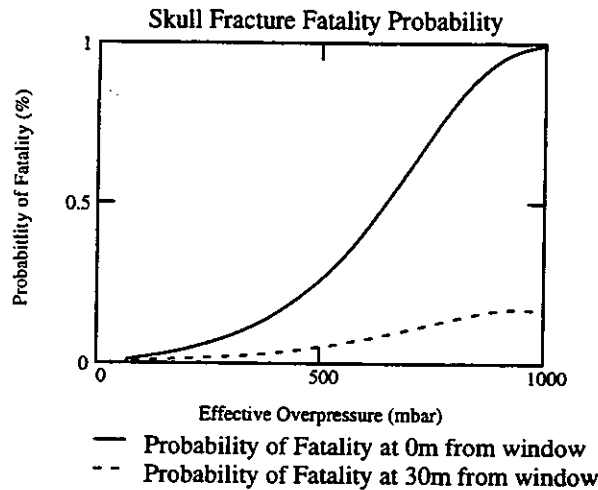
$$Pfh := 0.1$$

These conditional probabilities are combined with the number of injurious fragments to give a probability of fatality due to skull fracture!

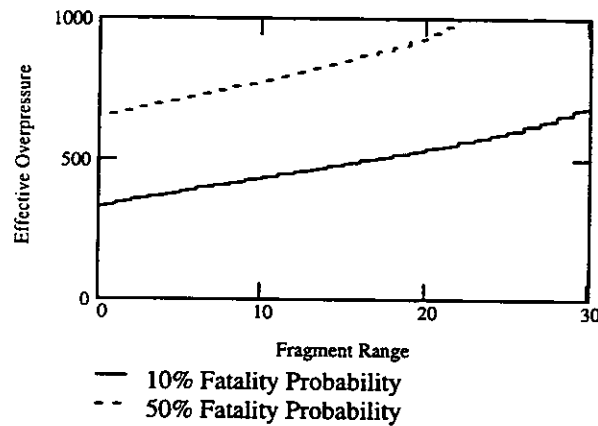
Probability of fatality

$$Pfath_{k,j} := 1 - (1 - Ptryg \cdot Pfh)^{Ninjh_{k,j}}$$

This gives the probability of fatality under pressure k at distance j



It is more convenient to view this as a plot of probability of fatality, for varying distance and effective overpressure. The plot below shows 10% fatality probability (solid line) and 50% fatality probability (dashed line) curves.



### Skin Penetration

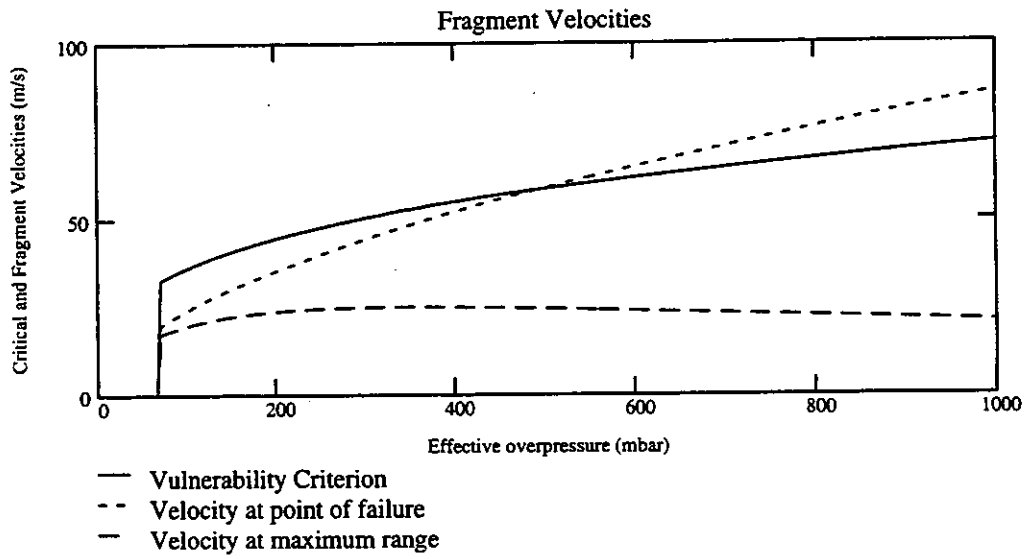
A similar calculation is performed for skin penetration, except a different vulnerability criterion is used. The skin penetration criterion is based on a relationship between the mass and the velocity<sup>4</sup>, based on Feinstein [14].

$$\text{Criterion} \quad C50 := (4.91 \cdot 10^3) \cdot \text{kg} \cdot \frac{\text{m}^4}{\text{sec}^4} \quad \text{const} := C50 \cdot \frac{1 \cdot \text{sec}^4}{\text{kg} \cdot \text{m}^4}$$

The above criterion defines a value equal to the mass of the fragment x (velocity of the fragment)<sup>4</sup>

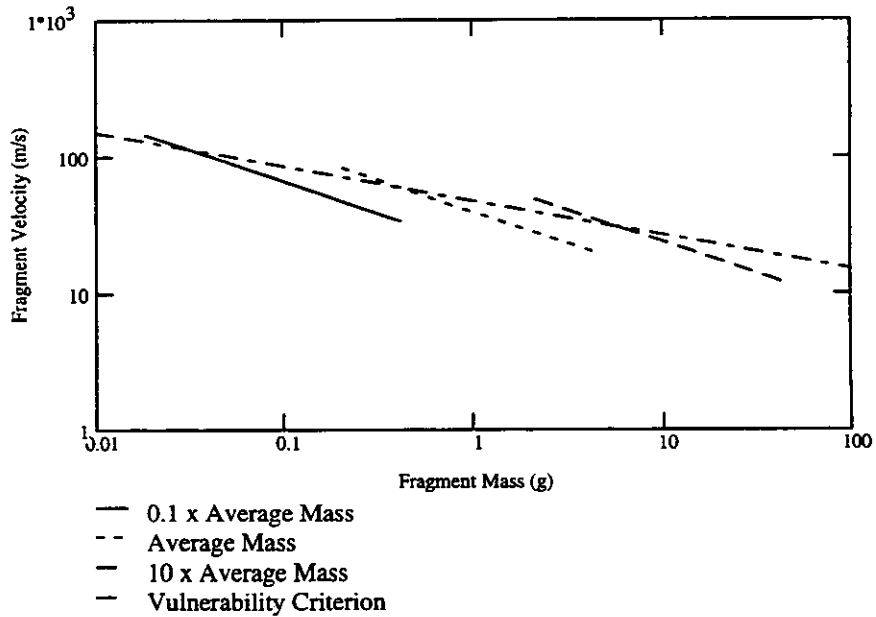
If the combination of mass and velocity values at a given pressure and distance from the window exceeds this value, a 10% probability of skin penetration is assumed.

$$\text{Critical velocity for skin penetration} \quad V_{try_i} := \text{if} \left[ M_i > 0, \left( \frac{C50}{M_i} \right)^{\frac{1}{4}}, 0 \right]$$



As for the skull fracture calculation, it is necessary to calculate the proportion of the fragments which exceed this criterion at each distance and each value of effective overpressure:

Criterion 
$$\text{skpf}(\text{mass}) := \text{if} \left[ \text{mass} > 0, \left( \frac{\text{const}}{\text{mass} \cdot 10^{-3}} \right)^{\frac{1}{4}}, 0 \right]$$



For each distance from the window, the proportion of injurious fragments with effective overpressure,  $\text{pig}_2$ , is calculated:

Distance (m intervals up to 30m) ->

	0	10	20	30	40	50
0	0.524	0.244	0.132	0.072	0.034	$7.88 \cdot 10^{-3}$
10	0.531	0.249	0.135	0.074	0.036	$9.291 \cdot 10^{-3}$
20	0.539	0.253	0.138	0.076	0.037	0.011
30	0.547	0.258	0.141	0.078	0.039	0.012
40	0.555	0.262	0.144	0.081	0.041	0.013
50	0.562	0.266	0.147	0.083	0.042	0.015
60	0.57	0.27	0.15	0.085	0.044	0.016
70	0.578	0.275	0.153	0.087	0.046	0.018
80	0.585	0.279	0.156	0.089	0.048	0.019
90	0.593	0.283	0.159	0.091	0.049	0.02
100	0.6	0.288	0.162	0.094	0.051	0.022
200	0.608	0.292	0.164	0.096	0.053	0.023

Effective Pressure  
(2 mbar intervals,  
up to 1000mbar)

This sets the probability for the number of injurious fragments,  $Pinjb$

$$Pinjb_{i,j} := pig2_{i,j}$$

#### Number of injurious fragments (skin penetration)

The number of injurious fragments is equal to the number of fragments multiplied the percentage of injurious fragments:

$$Ninjb_{i,j} := Pinjb_{i,j} \cdot Nfb_i$$

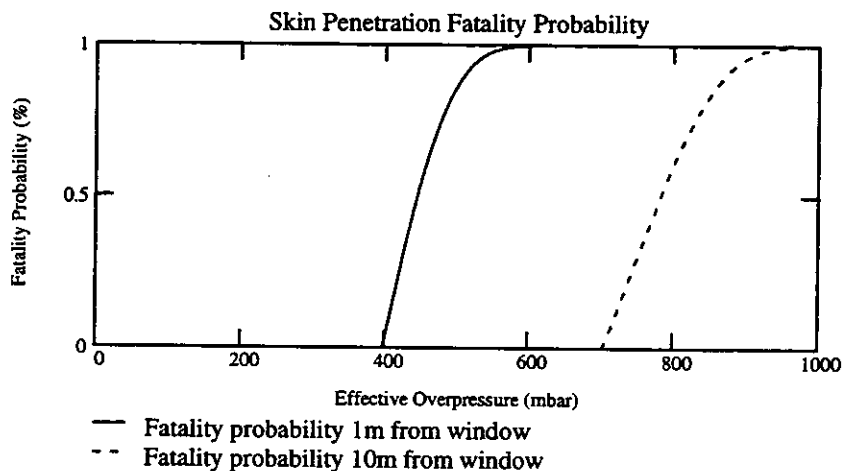
#### Probability of Fatality

As for the skull fracture case, it is necessary to define conditional probabilities:

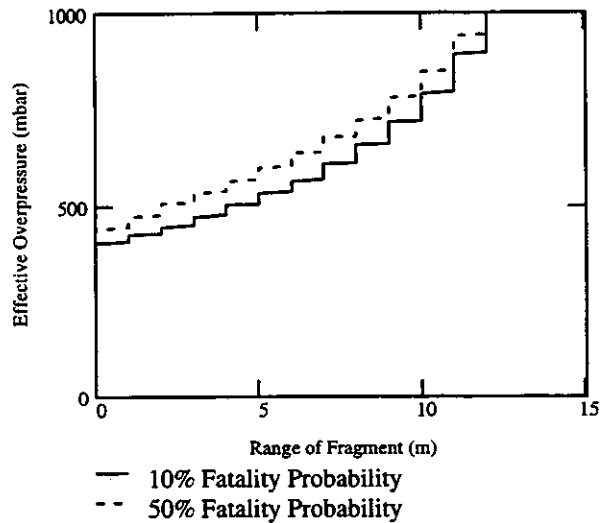
Probability of single hit causing injury  $Ptry := 0.1$

Probability of single injurious hit being fatal  $Pfb := 0.5$

Probability of fatality  $Pfatb_{i,j} := 1 - (1 - Ptry \cdot Pfb)^{Ninjb_{i,j}}$



It is more convenient to view this as a plot of probability of fatality, for varying distance and effective overpressure. The plot below shows 10% fatality probability (solid line) and 50% fatality probability (dashed line) curves.

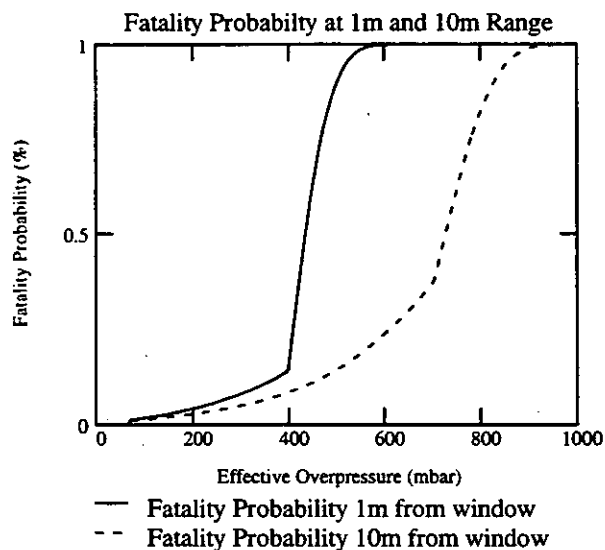


### Combined Fatality Probability

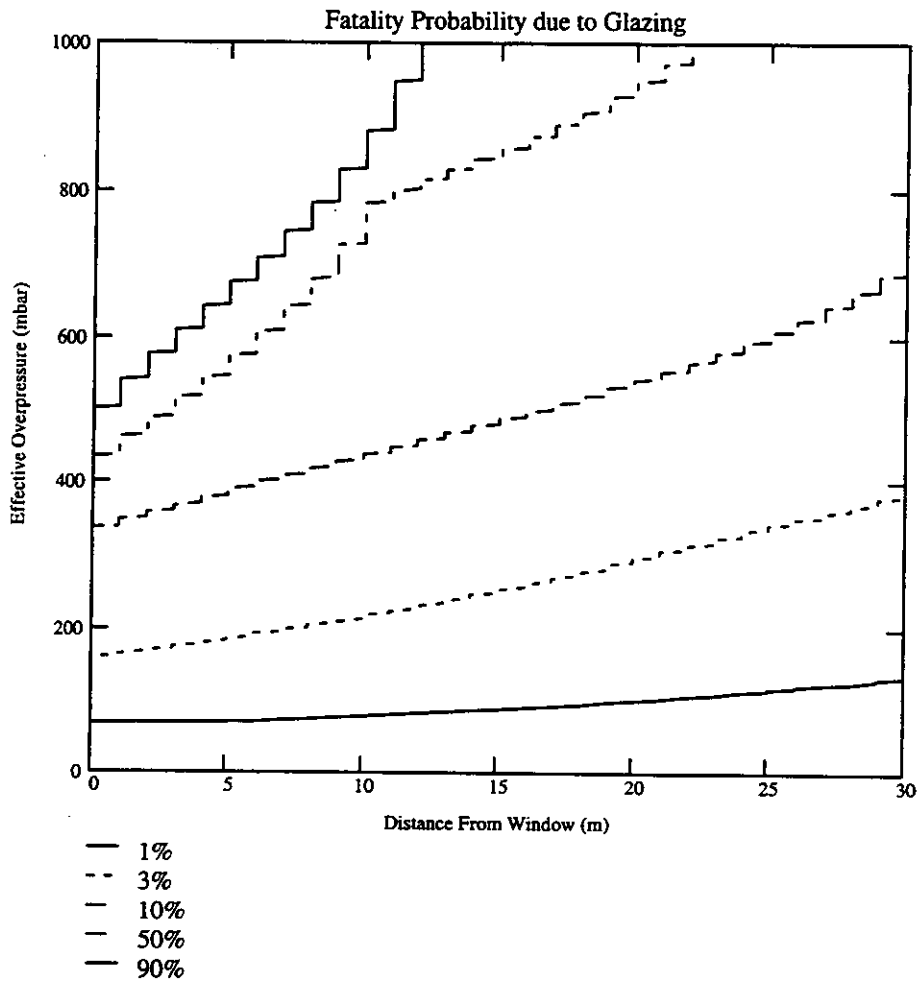
The probabilities for fatality due to skull fracture and skin penetration are combined to give an overall fatality probability

Combined Probability:

$$P_{fat_{i,j}} := P_{fath_{i,j}} + P_{fatb_{i,j}} - P_{fath_{i,j}} \cdot P_{fatb_{i,j}}$$



The two sets of curves above are combined to produce curves of constant fatality probability as it varies with effective overpressure and distance travelled by the glazing fragments.



This graph is written out to a file for input into the final Mathcad sheet where the building fatality probability curves are calculated.

### **3. Calculation of the impulse on a wall subjected to blast loading and subsequent debris fragment velocity**

In order to calculate the risk to the building occupants of debris from the walls, it is first necessary to calculate the dynamic pressure under which the cladding fails, and the subsequent velocity of the debris. These calculations are described in Section 2.4.2.

#### **Definition of units**

$$\text{mbar} := 100 \cdot \text{Pa}$$

#### **Input variables**

The characteristics of the building which are required for this set of calculations are read in as a matrix and assigned variable names for use in this sheet only:

	$\text{deb} := \text{READPRN}(\text{b22})$	
<i>Height of Building</i>	$H := \text{deb}_{0,0} \cdot \text{m}$	$H = 8 \cdot \text{m}$
<i>Breadth of Building</i>	$B := \text{deb}_{1,0} \cdot \text{m}$	$B = 8.6 \cdot \text{m}$
<i>Length of Building</i>	$L := \text{deb}_{2,0} \cdot \text{m}$	$L = 14.3 \cdot \text{m}$
<i>Height of wall</i>	$H_{\text{wall}} := \text{deb}_{0,2} \cdot \text{m}$	$H_{\text{wall}} = 2.6 \cdot \text{m}$
<i>Breadth of wall (width)</i>	$B_{\text{wall}} := \text{deb}_{1,2} \cdot \text{m}$	$B_{\text{wall}} = 3.85 \cdot \text{m}$
<i>Wall thickness</i>	$\text{tw} := \text{deb}_{3,0} \cdot \text{m}$	$\text{tw} = 0.215 \cdot \text{m}$
<i>Height of debris</i>	$H_{\text{deb}} := \text{deb}_{2,2} \cdot \text{m}$	$H_{\text{deb}} = 112.5 \cdot \text{mm}$
<i>Width of debris</i>	$B_{\text{deb}} := \text{deb}_{3,2} \cdot \text{m}$	$B_{\text{deb}} = 225 \cdot \text{mm}$
	$\text{tdeb} := \text{deb}_{4,2} \cdot \text{m}$	$\text{tdeb} = 75 \cdot \text{mm}$
$\gamma$ for air	$\gamma := 1.4$	
Atmospheric pressure	$p_0 := 1103 \cdot \text{mbar}$	
Coefficient of drag	$C_D := 1.05$	
Speed of sound in atmosphere	$C_0 := 340 \cdot \text{m} \cdot \text{sec}^{-1}$	



## Pulse Characteristics - Shock and Pressure Pulses

In this sheet, a series of iterative calculations for a range of peak incident overpressures are performed. It is first necessary to define the overpressures of interest:

	$i_{max} = 20$	$pit = 0..i_{max}$	$P_{pit} = pit \cdot 50$
Maximum overpressure	$P_s := P \cdot mbar$		20 values ranging from 0 to 1000mbar in 50mbar increments
Total shock wave duration	$t_p := READPRN(pdur)_0$		$t_p = 0.1$
Time step for calculations	$T1 := 0.0005$		
Total time for calculations	$t_{max} := 1.0$		
Total number of iterations	$it_{max} := \frac{t_{max}}{T1}$		$it_{max} = 2 \cdot 10^3$

### Applied pulse shape $i := 0..i_{max}$ $itt := 0..it_{max}$

Functions defining the shape of the blast pulse with time are defined:

#### Shock Pulse:

Pressure drop

$$p_{try_{i,itt}} := P_{s_i} - \left( \frac{P_{s_i}}{t_p} \cdot \frac{itt}{it_{max}} \right)$$

$$p_{try_{i,itt}} := \text{if}(p_{try_{i,itt}} \geq 0, p_{try_{i,itt}}, 0)$$

#### Pressure Pulse:

Pressure increase

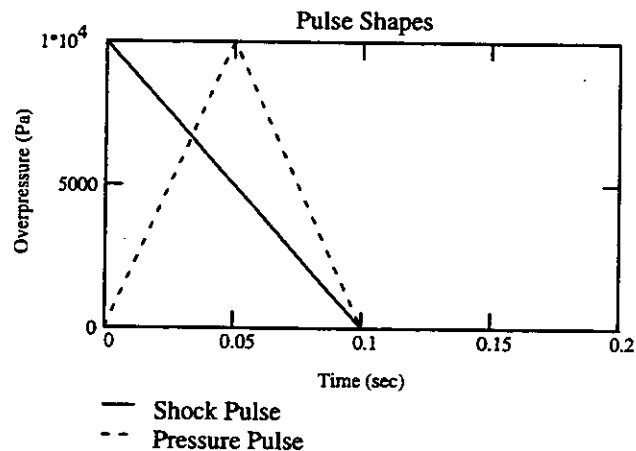
$$up_{i,itt} := \text{if} \left[ \left( \frac{itt}{it_{max}} \leq \frac{t_p}{2} \right), 2 \cdot P_{s_i} \cdot \frac{itt}{t_p \cdot it_{max}}, 0 \right]$$

Pressure drop

$$down_{i,itt} := \text{if} \left[ \left( \frac{itt}{it_{max}} > \frac{t_p}{2} \right) \cdot \left( \frac{itt}{it_{max}} < t_p \right), \left[ P_{s_i} - \left( \frac{P_{s_i}}{t_p} \cdot \frac{itt}{it_{max}} \right) \right] \cdot 2, 0 \right]$$

Combination

$$pt_{i,itt} := up_{i,itt} + down_{i,itt}$$



### Interaction of pulse with wall

Initially it is assumed that the short side of the building faces the blast. It is necessary to calculate how the pulse interacts with the building in order to determine the load on the wall. This is described further in Section 2.3.2. For an incident shock pulse, the pulse is reflected at the front face, and the subsequent load on the wall is calculated from the decay of the reflected pressure plus the incident pulse and the dynamic pressure. For a pressure pulse, zero reflection is assumed.

### Calculation of building dimension

S is the average distance from any wall section to the wall edge. It is conservative to assume  $S=B/2$  as this gives a higher impulse:

$$\text{Wall dimension} \quad S := \text{if} \left( \frac{B}{2} \geq H, H, \frac{B}{2} \right) \quad S = 4.3 \cdot \text{m}$$

### Calculation of perpendicularly reflected overpressure due to shock wave

$$Pr_i := 2 \cdot P_{s_i} + \frac{(\gamma + 1) \cdot (P_{s_i})^2}{[(\gamma - 1) \cdot P_{s_i}] + 2 \cdot \gamma \cdot p_o} \quad Pr_5 = 5.47 \cdot 10^4 \cdot \frac{\text{newton}}{\text{m}^2}$$

### Calculation of dynamic pressure Q

$$Qs_i := \frac{5}{2} \cdot \frac{(P_{s_i})^2}{7 \cdot p_o + P_{s_i}} \quad Qs_8 = 49.255 \cdot \text{mbar}$$

For pressure pulse use MEM - curve fit, as described in Section 2.3.2.

$$Qsp_i := \left[ 4.403 \cdot 10^{-13} \cdot \left( \frac{P_{s_i}}{\text{mbar}} \right)^5 + 0.09 \cdot \frac{P_{s_i}}{\text{mbar}} + 1.868 \cdot 10^{-4} \right] \cdot \text{mbar} \quad Qsp_8 = 40.509 \cdot \text{mbar}$$

### Dynamic pressure at front face

$$QD := C_D \cdot Qs \quad QD_5 = 2.058 \cdot 10^3 \cdot \frac{\text{newton}}{\text{m}^2}$$

### Velocity of wave front

$$U_i := C_o \cdot \sqrt{1 + \frac{6 \cdot P_{s_i}}{7 \cdot p_o}} \quad U_5 = 371.562 \cdot \frac{\text{m}}{\text{sec}}$$

### Time for pressure to reach incident plus dynamic (shock pulse only)

$$t_{s_i} := \frac{3 \cdot S}{U_i} \quad t_{s_5} = 0.035 \cdot \text{sec}$$

### Pressure Profiles

Typical pressure profiles on the wall are calculated here, corresponding to either a shock pulse on the front face of the building or an effective pressure pulse. The shock pulse results will be used for just the shock at the front face: the pressure pulse will be used for differential pressures on the other faces.

$$\text{Peak Stagnation pressure} \quad P_{tot_i} := P_{s_i} + (C_D \cdot Qs_i) \quad P_{eff_i} := P_{s_i}$$

**Shock Pulse:**

Decay of peak stagnation pressure to zero over pulse duration

$$p_{tryd_{i,itt}} := \frac{P_{tot_i}}{mbar} - \frac{\frac{P_{tot_i}}{mbar}}{t_p} \cdot \frac{itt}{itmax}$$

Pressure value at which reflected pressure has decayed to stagnation pressure

$$dtstry_{i,itt} := \frac{P_{tot_i}}{mbar} - \frac{\frac{P_{tot_i}}{mbar}}{t_p} \cdot \frac{t_{s_i}}{sec}$$

Decay of reflected pressure to stagnation pressure

$$c_{try_{i,itt}} := \frac{Pr_i}{mbar} - \left[ \frac{\frac{Pr_i}{mbar} - dtstry_{i,itt}}{\left(\frac{t_{s_i}}{sec}\right)} \cdot \frac{itt}{itmax} \right]$$

Contribution from pulse after reflected pressure has decayed to stagnation pressure value

$$e_{try_{i,itt}} := \text{if} \left[ \left( \frac{itt}{itmax} \geq \frac{t_{s_i}}{sec} \right) \cdot \left( \frac{itt}{itmax} < t_p \right), p_{tryd_{i,itt}}, 0 \right]$$

Contribution from pulse from reflected pressure

$$f_{try_{i,itt}} := \text{if} \left[ \left( \frac{itt}{itmax} \leq \frac{t_{s_i}}{sec} \right) \cdot (p_{tryd_{i,itt}} > 0), c_{try_{i,itt}}, 0 \right]$$

Combined pulse shape

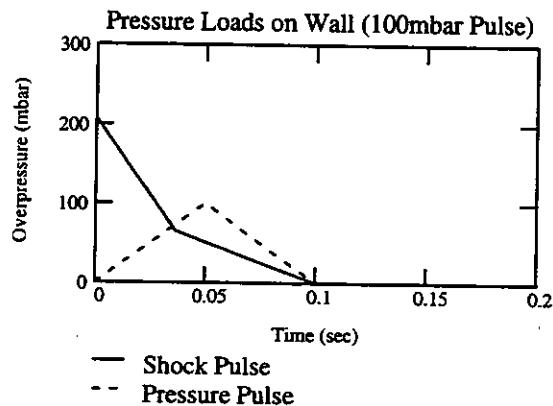
$$p_{front_{i,itt}} := e_{try_{i,itt}} + f_{try_{i,itt}}$$

**Pressure Pulse:**

Pulse shape

(Dynamic pressure is not considered here, as the results for this calculation are to be used for the differential pressures across the rear and sides of the building)

$$p_{frp} := \frac{pt}{mbar}$$



**Force on wall**

The force on the wall is calculated from the pressure profile and the area of the wall:

**Shock Pulse:**

$$F_t := p_{front} \cdot H_{wall} \cdot B_{wall} \cdot mbar$$

**Pressure Pulse:**

$$F_{pt} := p_{frp} \cdot H_{wall} \cdot B_{wall} \cdot mbar$$

## Structural Response

Having calculated the force on the plate, it is now necessary to calculate the resultant displacement: The wall is represented by a simply supported plate in order to use a single degree of freedom (SDOF) elasto-plastic model as described in Section 2.4.2.

### Mass of plate:

Density of brickwork

$$\rho_b := deb_{6,2} \cdot \text{kg} \cdot \text{m}^{-3}$$

$$\rho_b = 2 \cdot 10^3 \cdot \text{kg} \cdot \text{m}^{-3}$$

$$\text{Mass} := B_{\text{wall}} \cdot H_{\text{wall}} \cdot t_w \cdot \rho_b$$

$$\text{Mass} = 4.304 \cdot 10^3 \cdot \text{kg}$$

### Equivalent System for Simply Supported Plate

Assuming that the panel behaves as a simply supported plate, it can be modelled as a SDOF elasto-plastic system by using the approach set out in Biggs [5].

Elastic Modulus of Brick

$$E := deb_{7,2} \cdot \text{Pa}$$

$$E = 7.2 \cdot 10^9 \cdot \text{kg} \cdot \text{m}^{-1} \cdot \text{sec}^{-2}$$

Poisson's Ratio

$$\nu := deb_{8,2}$$

$$\nu = 0.3$$

Aspect ratio of plate

$$\beta := \frac{B_{\text{wall}}}{H_{\text{wall}}}$$

$$\beta = 1.481$$

Blevins [40] Table 11-4 Case 16 (Simply Supported)

$$\lambda_s := \left[ \pi^2 \cdot \left[ 1 + \left( \frac{B_{\text{wall}}}{H_{\text{wall}}} \right)^2 \right] \right]^{\frac{1}{2}}$$

$$\lambda_s^2 = 31.51$$

Natural Frequency of structure

$$f := \frac{\lambda_s^2}{2 \cdot \pi \cdot B_{\text{wall}}^2} \cdot \left[ \frac{E \cdot t_w^3}{12 \cdot \rho_b \cdot t_w \cdot (1 - \nu^2)} \right]^{0.5}$$

$$f = 41.767 \cdot \text{Hz}$$

Natural Period

$$T := \frac{1}{f}$$

$$T = 0.024 \cdot \text{sec}$$

Biggs [5] Chapter 5 - Table 5.4

$$\beta = 1.481$$

$$\frac{1}{\beta} = 0.675$$

We need to interpolate between the points to obtain the load and mass factors

$$\text{Int}_1 := 0.5 \quad \text{KL}_1 := 0.55 \quad \text{KM}_1 := 0.41 \quad \text{I}_1 := 201$$

$$\text{Int}_2 := 0.6 \quad \text{KL}_2 := 0.53 \quad \text{KM}_2 := 0.39 \quad \text{I}_2 := 197$$

$$\text{Int}_3 := 0.7 \quad \text{KL}_3 := 0.51 \quad \text{KM}_3 := 0.37 \quad \text{I}_3 := 201$$

$$\text{Int}_4 := 0.8 \quad \text{KL}_4 := 0.49 \quad \text{KM}_4 := 0.35 \quad \text{I}_4 := 212$$

$$\text{Int}_5 := 0.9 \quad \text{KL}_5 := 0.47 \quad \text{KM}_5 := 0.33 \quad \text{I}_5 := 230$$

$$\text{Int}_6 := 1.0 \quad \text{KL}_6 := 0.46 \quad \text{KM}_6 := 0.31 \quad \text{I}_6 := 252$$

$$N := \text{ceil} \left( \frac{\frac{1}{\beta} - 0.5}{0.1} \right) + 1$$

$$N = 3$$

Interpolating:

Load Factor

$$K_L := \frac{\text{KL}_N - \text{KL}_{(N-1)}}{\text{Int}_N - \text{Int}_{N-1}} \cdot \left( \frac{1}{\beta} \right) + \text{KL}_{N-1} - \left( \frac{\text{KL}_N - \text{KL}_{N-1}}{\text{Int}_N - \text{Int}_{N-1}} \right) \cdot \text{Int}_{N-1}$$

$$K_L = 0.515$$

Mass Factor 
$$K_M := \frac{KM_N - KM_{(N-1)}}{Int_N - Int_{N-1}} \cdot \left(\frac{1}{\beta}\right) + KM_{N-1} - \left(\frac{KM_N - KM_{N-1}}{Int_N - Int_{N-1}}\right) \cdot Int_{N-1}$$

$K_M = 0.375$

Stiffness Factor 
$$IF := \frac{I_N - I_{(N-1)}}{Int_N - Int_{N-1}} \cdot \left(\frac{1}{\beta}\right) + I_{N-1} - \left(\frac{I_N - I_{N-1}}{Int_N - Int_{N-1}}\right) \cdot Int_{N-1}$$

$IF = 200.013$

These factors are used to define equivalent properties for the SDOF elasto-plastic system:

Equivalent Mass  $M_e := K_M \cdot Mass$   $M_e = 1.614 \cdot 10^3 \cdot \text{kg}$

Equivalent Force

Shock Pulse  $Ft_e := K_L \cdot Ft$

Pressure Pulse  $Fpt_e := K_L \cdot Fpt$

Stiffness of plate: 
$$I_a := \frac{\frac{1}{12} \cdot H_{wall} \cdot t_w^3}{H_{wall}}$$

Stiffness 
$$:= \frac{IF \cdot E \cdot I_a}{H_{wall}^2}$$
  $Stiffness = 1.764 \cdot 10^8 \cdot \text{newton} \cdot \text{m}^{-1}$

Equivalent Stiffness  $K_e := Stiffness \cdot K_L$

Check: 
$$f_{check} := \frac{1}{2 \cdot \pi} \cdot \sqrt{\frac{K_e}{M_e}}$$
  $f_{check} = 37.762 \cdot \text{Hz}$

$f = 41.767 \cdot \text{Hz}$

### Elastic Limits of SDOF system

Calculated failure pressure  $W_{fail} := deb_{5,2} \cdot \text{mbar}$   $W_{fail} = 275 \cdot \text{mbar}$

Using this calculated failure pressure, we can define an effective positive yield value. This value corresponds to the change in gradient in the bi-linear stiffness (Figure 2.5)

Corresponding Force  $Posy := W_{fail} \cdot B_{wall} \cdot H_{wall}$   $Posy = 2.753 \cdot 10^5 \cdot \text{newton}$

Effective Positive yield  $R0 := \frac{Posy \cdot K_L}{\text{newton}}$   $R0 = 1.417 \cdot 10^5$

It is assumed that the panel behaves exactly the same in the negative direction (i.e. towards the source of the blast, and away from the room) as in the positive direction (into the room)

$Negy := Posy \cdot K_L \cdot -1$

Effective Negative yield  $R1 := \frac{Negy}{\text{newton}}$   $R1 = -1.417 \cdot 10^5$

Effective Elastic Limit  $y_{el} := \frac{Posy \cdot K_L}{K_e}$   $y_{el} = 1.56 \cdot \text{mm}$

In addition to the elastic limit, it is necessary to define the critical damping in the system and the ductility. The damping has been conservatively assumed to be zero, and the ductility is dependent on the material from which the panel is constructed - in this case, masonry.

% critical damping  $B_D := 0.0$

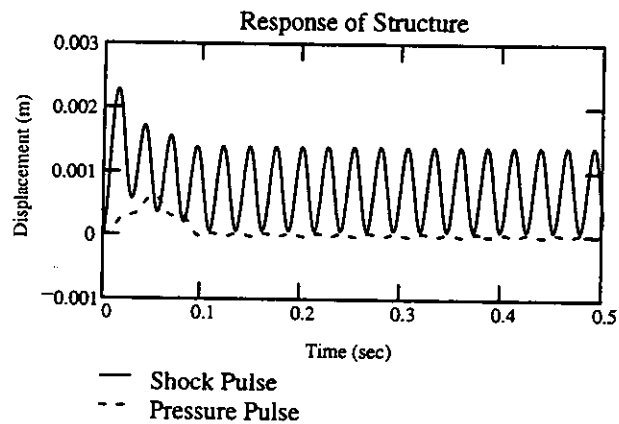
Ductility  $\mu := 5$

The displacement at failure is assumed to be equal to the elastic limit multiplied by the ductility

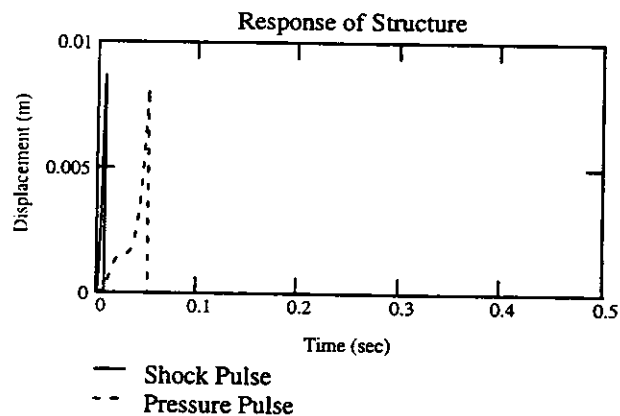
Displacement at failure  $fail := \frac{y_{el} \mu}{m}$   $fail = 7.801 \cdot 10^{-3}$  (mm)

The response of the system developed here is calculated in an iterative calculation for each of the incident pulses considered, by solving the equation of motion (Eqn 5), replacing  $F(t)$  with the functions  $F_t$  (shock) or  $F_{pt}$  (pressure), and using the equivalent mass and stiffness as calculated above. The panel is assumed to fail if the displacement exceeds the displacement at failure given above.

The response of the panel under a load which is not sufficient to cause it to fail (100mbar peak incident overpressure) is shown below for an incident shock pulse and an incident pressure pulse:



By comparison, the response under a greater pressure (500mbar peak incident overpressure) is shown below. The panel fails quickly.



In order to identify the pressure at which the panel fails, it is necessary to calculate the iteration for each pressure increment at which the displacement is zero:

Shock Pulse	Iteration
	0
Max iteration, bss	$2 \cdot 10^3$
bss =	$2 \cdot 10^3$
	30
	24
	21
	19
	17

Pressure Pulse	Iteration
	0
Max iteration, bps	$2 \cdot 10^3$
bps =	$2 \cdot 10^3$
	$2 \cdot 10^3$
	$2 \cdot 10^3$
	$2 \cdot 10^3$
	$2 \cdot 10^3$
	133

The time at which the panel fails is calculated from the iteration and the timestep:

**Shock Pulse**

Time to yield  $Ty_{ss_i} := \frac{bss_i}{itmax} \cdot sec$

0
0
1
1
1
0.015
0.012
0.011
$9.5 \cdot 10^{-3}$
$8.5 \cdot 10^{-3}$
$8 \cdot 10^{-3}$
$7.5 \cdot 10^{-3}$

$Ty_{ss} =$  **0.012** **·sec**

**Pressure Pulse**

$Ty_{ps_i} := \frac{bps_i}{itmax} \cdot sec$

0
0
1
1
1
1
1
1
0.067
0.058
0.053
0.051
0.047

$Ty_{ps} =$  **1** **·sec**

Panel will yield at  $t = Tyield$ . The initial velocity of fragment is assumed to be generated from the velocity at failure, while the remaining portion of the pressure pulse acts on the unconstrained fragment.

The failure pressure of the panel under the applied load is derived from the iteration at which the panel fails. This is denoted by  $fss$  (shock pulse) or  $fps$  (pressure pulse). The failure pressure is assumed to be the average of the pressure corresponding to that increment and the one before:

**Shock Pulse**

$fss = 4$

$P_{fail_1} := \frac{P_{fss} + P_{fss-1}}{2}$

$P_{fail_1} = 175$

**Pressure Pulse**

$fps = 7$

$P_{fail_2} := \frac{P_{fps} + P_{fps-1}}{2}$

$P_{fail_2} = 325$

$WRITEPRN(pfail) := P_{fail}$

**Velocity of Fragment from Panel Failure**

The velocity of the panel at failure for each value of pressure is calculated from the difference in the displacement over the last iteration before failure

Example: 500mbar Peak Incident Overpressure ( $P_{10}$ )

$P_{10} = 500$

**Shock Pulse:**

Set iteration parameters

$kss_i := if(bss_i > 0, bss_i - 1, 0)$

**Pressure Pulse:**

$kps_i := if(bps_i > 0, bps_i - 1, 0)$



**Shock Pulse:**

Iteration value at failure

$bss_{10} = 15$

Displacement at failure

$ass_{10, bss_{10}} = 8.692 \cdot 10^{-3}$

Iteration value immediately before failure

$kss_{10} = 14$

Displacement immediately prior to failure

$ass_{10, kss_{10}} = 7.662 \cdot 10^{-3}$

**Pressure Pulse:**

Iteration value at failure

$bps_{10} = 101$

Displacement at failure

$aps_{10, bps_{10}} = 8.197 \cdot 10^{-3}$

Iteration value immediately before failure

$kps_{10} = 100$

Displacement immediately prior to failure

$aps_{10, kps_{10}} = 7.779 \cdot 10^{-3}$

**Failure Velocity**

$$V_{ssf_i} := \frac{ass_{i, bss_i} - ass_{i, kss_i}}{T1} \cdot m \cdot sec^{-1}$$

$V_{ssf_{10}} = 2.062 \cdot m \cdot sec^{-1}$

$$V_{psf_i} := \frac{aps_{i, bps_i} - aps_{i, kps_i}}{T1} \cdot m \cdot sec^{-1}$$

$V_{psf_{10}} = 0.834 \cdot m \cdot sec^{-1}$

This velocity forms part of the initial velocity of the fragment. The remaining contribution is assumed to arise from the action of the remaining pulse on the unconstrained fragment:

**Velocity of Unconstrained Fragment**

The remainder of the blast pulse acts on the unconstrained fragment, as described in Section 2.4.2:

Mass of debris  $M_{deb} := B_{deb} \cdot H_{deb} \cdot \rho_b \cdot t_{deb}$

$M_{deb} = 3.797 \cdot kg$

Drag coefficient for debris  $C_{DF} := 1.17$

Calculation for Unconstrained Secondary Fragment from Baker et al [13]

The remaining impulse acting on the fragment is calculated:

NB this is specific aquired impulse -  $Ns/m^2$

**Shock:**

$$Imp_{ss_i} := \frac{\sum_{it=0}^{t_p \cdot itmax} p_{front_{i, it}} \cdot mbar \cdot T1 \cdot sec}{Ty_{ss_i} \cdot itmax} \cdot sec$$

**Pressure:**

$$Imp_{ps_i} := \frac{\sum_{it=0}^{t_p \cdot itmax} p_{frp_{i, it}} \cdot mbar \cdot T1 \cdot sec}{Ty_{ps_i} \cdot itmax} \cdot sec$$

0
0
0
0
904.72
$1.264 \cdot 10^3$
$1.61 \cdot 10^3$
$1.96 \cdot 10^3$
$2.337 \cdot 10^3$
$2.698 \cdot 10^3$
$3.076 \cdot 10^3$
$3.472 \cdot 10^3$

Impss =  $\cdot \text{kg} \cdot \text{m}^{-1} \cdot \text{sec}^{-1}$

0
0
0
0
0
0
0
0
398.65
731
983.475
$1.238 \cdot 10^3$
$1.574 \cdot 10^3$
$1.904 \cdot 10^3$
$2.223 \cdot 10^3$

Impps =  $\cdot \text{kg} \cdot \text{m}^{-1} \cdot \text{sec}^{-1}$

From I, the non dimensional value can be calculated

$$\text{ibarss}_i := \frac{C_{DF} \cdot \text{Impss}_i \cdot C_o}{P_{s_i} \cdot 2 \cdot H_{deb}}$$

0
0
0
0
79.977
89.368
94.865
99.01
103.307
106.019
108.783
111.6
114.471
117.396
118.432

ibarss =

$$\text{ibarps}_i := \frac{C_{DF} \cdot \text{Impps}_i \cdot C_o}{P_{s_i} \cdot 2 \cdot H_{deb}}$$

0
0
0
0
0
0
0
0
20.138
32.31
38.64
43.758
50.582
56.09
60.466
64.523

ibarps =

And the non-dimensional pressure term

NB This is the same for both shock and pressure pulses - it may be better to use  $P_r$  throughout for the shock pulse, but this isn't consistent with Baker

$$pbar_i := \frac{P_{s_i}}{p_0}$$

0
0
0.045
0.091
0.136
0.181
0.227
0.272
0.317
0.363
0.408
0.453
0.499
0.544
0.589
0.635

pbar =

**Calculation of the Non-dimensional Object Velocity, V, as a function of the Non-dimensional Pressure, pbar, and the Non-dimensional Impulse, ibar.**

The values of V are to be defined by approximating the P against I curves as two-piece linear logarithmic curves, separated by a straight logarithmic line, of gradient DIVG, and then interpolating between adjacent P-I curves.

The following vectors define the values of V, P and I on the dividing line, using values approximated from the V contour plot.

Pit :=	0.0006	Iit :=	6000	V :=	0.001
	0.002		1200		0.005
	0.005		700		0.01
	0.03		130		0.05
	0.06		80		0.1
	0.3		18		0.5
	0.6		9.75		1.0
	2.9		2.1		5.0
	4.5		1.4		10.0
	20.5		0.32		50.0

The dividing line can be described in terms of the logarithmic equation

$$\log(P) = \text{DIVG} \cdot \log(I) + \log(c) \text{ or } P = c \cdot I$$

Taking best fit points for the definition of DIVG, using i=2 and 6

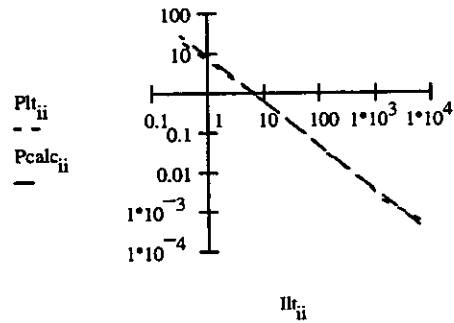
$$\text{DIVG} := \frac{\log\left(\frac{P_{i6}}{P_{i2}}\right)}{\log\left(\frac{I_{i6}}{I_{i2}}\right)} \quad \text{DIVG} = -1.12$$

and thus generating c

$$c := \frac{Plt_6}{(Ilt_6)^{DIVG}} \quad c = 7.692$$

Comparing the calculated line and the data points measured from the book.

$$ii := 0, 1..9 \quad Pcalc_{ii} := c \cdot (Ilt_{ii})^{DIVG}$$



0	
1	$4.506 \cdot 10^{-4}$
2	$2.734 \cdot 10^{-3}$
3	$5 \cdot 10^{-3}$
4	0.033
5	0.057
6	0.302
7	0.6
8	3.35
9	5.276
9	27.565

Now we have to calculate the gradient of the curves which occur to the right of the dividing line. This same gradient will be applied to all V contours.

$$\text{contourgrad} := \frac{\log\left(\frac{0.9}{0.0004}\right)}{\log\left(\frac{0.1}{1000000}\right)} \quad \text{contourgrad} = -0.479$$

and contour\_c is required to be defined for every contour, and therefore using the values of P and I above we calculate

$$\text{contour\_c}_{ii} := \frac{Plt_{ii}}{(Ilt_{ii})^{\text{contourgrad}}} \quad \text{contour\_c} =$$

0	
1	0.039
2	0.06
3	0.115
4	0.309
5	0.489
6	1.197
7	1.786
8	4.137
9	5.287
9	11.879

Now to calculate the V value corresponding to input I and P values.

FIRSTLY, we need the I and P values.

$$Iss_i := \text{ibarss}_i \quad Ips_i := \text{ibarps}_i \quad \text{Preq}_i := \text{pbar}_i$$

Secondly, a program is generated to determine which side of the dividing line that the P and I intersect occurs, and then the appropriate curves are interpolated between to generate an value for V.

A quick check to see which side of the dividing line the specified point lies.

$$Pconss_i := \text{if} [Iss_i > 0, \text{contour\_c}(Iss_i)^{\text{contourgrad}}, 0] \quad Pconps_i := \text{if} [Ips_i > 0, \text{contour\_c}(Ips_i)^{\text{contourgrad}}, 0]$$

$$Ptss_i := \text{if} [Iss_i > 0, c \cdot (Iss_i)^{\text{DIVG}}, 0] \quad Ptps_i := \text{if} [Ips_i > 0, c \cdot (Ips_i)^{\text{DIVG}}, 0]$$

$$Voutss_i := \text{if} [Iss_i > 0, \left[ \text{if} \left[ \text{Preq}_i \leq c \cdot (Iss_i)^{\text{DIVG}}, \text{interp}(Plt, V, \text{Preq}_i), \text{interp}(Pconss_i, V, \text{Preq}_i) \right] \right], 0]$$

$$Voutps_i := \text{if} [Ips_i > 0, \left[ \text{if} \left[ \text{Preq}_i \leq c \cdot (Ips_i)^{\text{DIVG}}, \text{interp}(Plt, V, \text{Preq}_i), \text{interp}(Pconps_i, V, \text{Preq}_i) \right] \right], 0]$$

	0
	0
	0
	0
	0
	0.739
Voutss =	1.278
	2.056
	2.837
	3.648
	4.438
	5.631
	7.746
	9.908
	12.955
	15.809

	0
	0
	0
	0
	0
	0
	0
	0
	0
	0
	0
	0.618
	1.221
	1.956
	2.672
	3.515
	4.328
	5.283
	7.31

NB. If the output value of Vout is greater than 50 then extrapolation has occurred, and therefore the accuracy of the result may be impaired.

Velocity of unconstrained fragment

$$V_{ssunc_i} := \frac{V_{outss_i} \cdot p_o \cdot B_{deb} \cdot H_{deb} \cdot 2 \cdot H_{deb}}{M_{deb} \cdot C_o}$$

0
0
0
0
0
0.359
0.622
1
1.38
1.775
2.16
2.74
3.769
4.821
6.304
7.693

V<sub>ssunc</sub> = •m•sec<sup>-1</sup>

$$V_{psunc_i} := \frac{V_{outps_i} \cdot p_o \cdot B_{deb} \cdot H_{deb} \cdot 2 \cdot H_{deb}}{M_{deb} \cdot C_o}$$

0
0
0
0
0
0
0
0
0
0.301
0.594
0.952
1.3
1.711
2.106
2.571
3.557

V<sub>psunc</sub> = •m•sec<sup>-1</sup>

**Fragment Velocity**

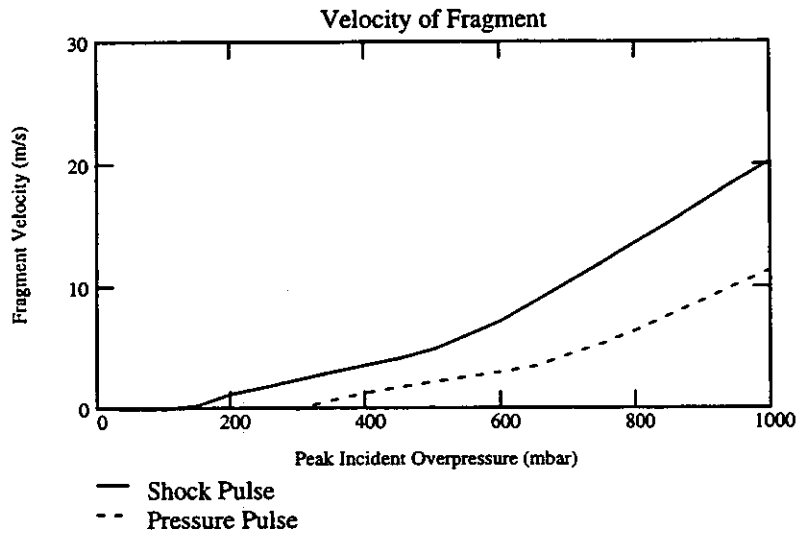
The fragment velocity due to the failure of the panel is assumed to be the sum of these two contributions, i.e.

**Shock Pulse:**

$$F_{ssvel_i} := V_{ssf_i} + V_{ssunc_i}$$

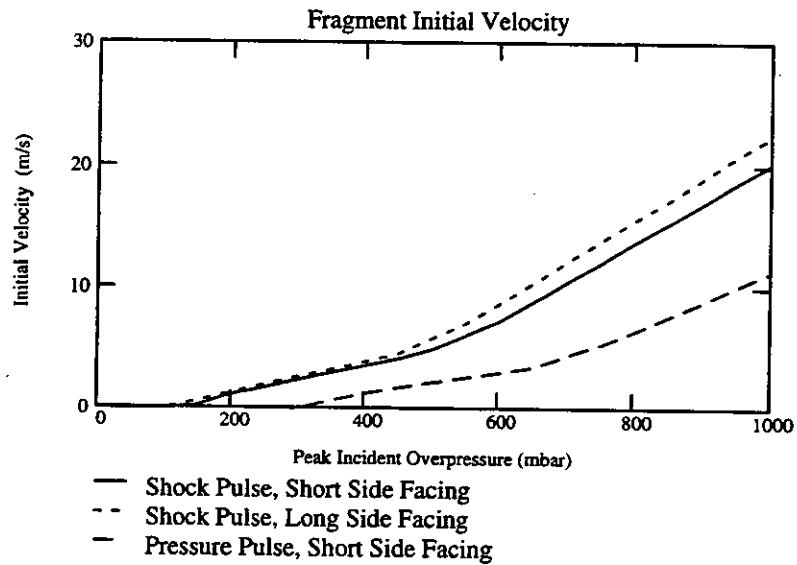
**Pressure Pulse:**

$$F_{psvel_i} := V_{psf_i} + V_{psunc_i}$$



## Repeat Calculations for Long Side Facing Blast

So far the calculations have assumed that the short side of the building faces the blast. The calculations are repeated for the opposite orientation of the building for an incident shock pulse, as the loading is slightly increased for this orientation:



These curves are written out for use in the next sheet which calculates the risk to the building occupants from the cladding debris.

#### 4. Calculation of vulnerability to debris under blast loading

Having calculated the initial velocity of the debris, it is necessary to calculate the velocity at a distance from the wall and the corresponding risk to the building occupants. These calculations are described in more detail in Section 2.5.2 and illustrated in Figure 2.20

##### Definition of units

mbar := 100·Pa

##### Input variables

The characteristics of the building and debris which are used in this sheet are read in as a matrix and assigned variable names for use in this sheet only:

	deb := READPRN(b22)	( Object = single brick )
Height of object	H := deb <sub>2,2</sub> ·m	H = 112.5·mm
Breadth of object (width)	B := deb <sub>3,2</sub> ·m	B = 225·mm
Length of object (front to back)	L := deb <sub>4,2</sub> ·m	L = 75·mm
Density of brickwork	$\rho_b := deb_{6,2} \cdot \text{kg} \cdot \text{m}^{-3}$	$\rho_b = 2 \cdot 10^3 \cdot \text{kg} \cdot \text{m}^{-3}$
Mass of object	M := H·B·L· $\rho_b$	M = 3.797·kg
Frontal area	A := H·B	A = 0.025·m <sup>2</sup>
$\gamma$ for air	$\gamma := 1.4$	
Density of air	$\rho_{\text{air}} := 1.225 \cdot \text{kg} \cdot \text{m}^{-3}$	
Atmospheric pressure	$p_o := 1 \cdot 10^5 \cdot \text{Pa}$	
Coefficient of drag	$C_D := 1.2$	
Speed of sound in atmosphere	$C_o := 340 \cdot \text{m} \cdot \text{sec}^{-1}$	

The failure pressures calculated in the previous sheet are read in for use in this sheet:

Failure pressures:

Shock Pulse	Pfails := READPRN(pfail) <sub>1</sub>	Pfails = 175
Pressure Pulse	Pfailp := READPRN(pfail) <sub>2</sub>	Pfailp = 325



## Shock Pulse

### Debris Velocity Profile

This has been calculated in the previous sheet for different orientations and different pulse shapes. The velocity is read in as a function of incident overpressure, but includes reflection effects.

It is necessary to fit a curve to the velocity profile in order to use it in subsequent calculations:

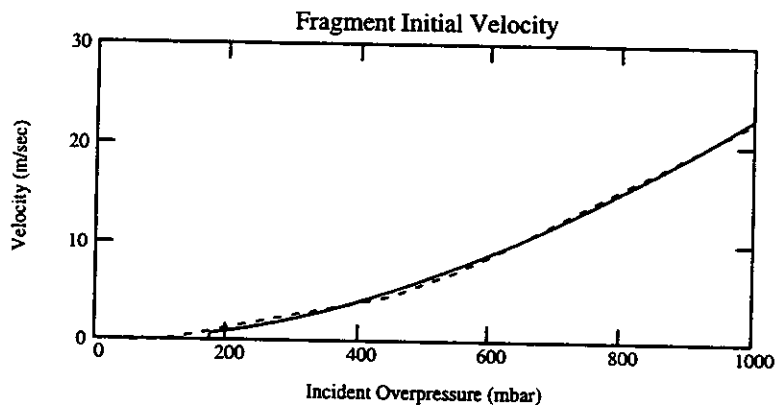
```
Shock Pulse:      ii := 0..20      vy := READPRN(bkvels)
                  vxii := ii·50
                  p := 1,2..1000
```

Fit a line to the velocity data:

$$F(p) := \begin{bmatrix} p \\ p^2 \\ p^3 \end{bmatrix} \quad G := \text{linfit}(vx, vy, F) \quad G = \begin{bmatrix} -1.338 \cdot 10^{-3} \\ 3.036 \cdot 10^{-5} \\ -6.338 \cdot 10^{-9} \end{bmatrix}$$

If the pressure is lower than that required to cause failure, the velocity is zero:

$$\text{Vel}(p) := \text{if}(p \leq P_{\text{fails}}, 0, G \cdot F(p))$$



```
i := 1,2..100
```

```
Vi := Vel(10·i)
```

Incident Pressure

```
Pinci := i·10·mbar
```

### Calculation of total flight time for debris

Maximum initial height of debris

$$\text{height} := \text{deb}_{9,2} \cdot \text{m} - 0.5 \cdot \text{m}$$

$$\text{height} = 2.1 \cdot \text{m}$$

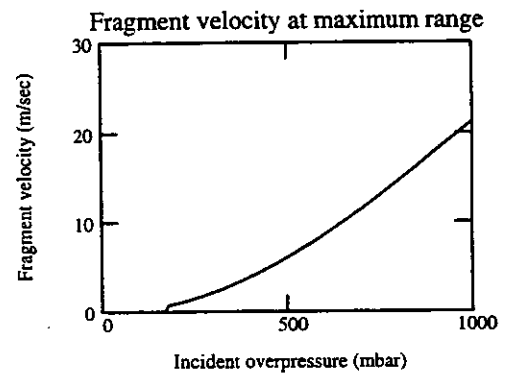
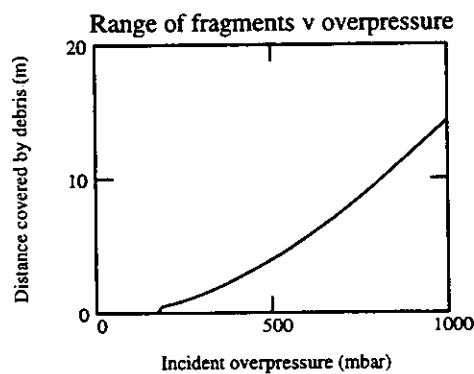
Flight time

$$\text{time} := \sqrt{\frac{\text{height}}{0.5 \cdot g}}$$

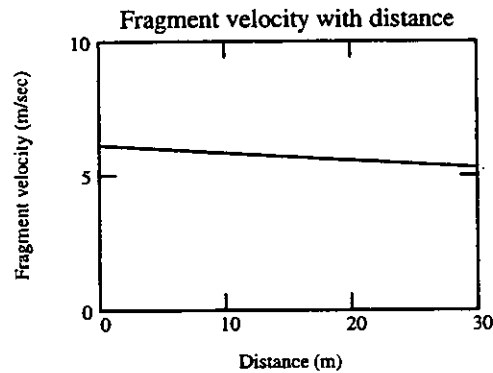
$$\text{time} = 0.654 \cdot \text{sec}$$

### Calculation of debris velocities with distance and maximum range

For the debris the distance and velocity of the fragments is calculated, based on the initial velocity, overpressure and drag (Equation 18), using an iterative calculation.



The velocities of the debris are calculated at 1m intervals up to a maximum range of 30m, for the range of peak incident overpressures considered. As an example, the fragment velocity for 500mbar peak incident overpressure is given below:



### Critical velocities to cause fatalities

The critical velocities at which a fragment of debris is assumed to give rise to a given level of fatality probability are dependent on the mass of the fragment and are obtained from Baker et al [13]

Mass of debris

$$M = 3.797 \cdot \text{kg}$$

Serious injury threshold

$$V_{\text{serious}} := 2.5 \cdot \text{m} \cdot \text{sec}^{-1}$$

10% fatality threshold

$$V_{10\%} := 6 \cdot \text{m} \cdot \text{sec}^{-1}$$

50% fatality threshold

$$V_{50\%} := 10 \cdot \text{m} \cdot \text{sec}^{-1}$$

90% fatality threshold

$$V_{90\%} := 12 \cdot \text{m} \cdot \text{sec}^{-1}$$

### **Range for Fatalities**

Having calculated the velocity profile of the fragment from the wall and specified the fragment critical velocities, it is necessary to compare one against the other to derive the distance from the wall at which the probability of fatality changes. This calculation results in 4 sets of distances corresponding to the probabilities of injury, 10% fatality, 50% fatality and 90% fatality, and are called injure, fatals\_10%, fatals\_50% and fatals\_90% respectively. In addition, the possibility of the wall toppling over and crushing people underneath needs to be taken into account:

### **60% fatality range (Wall height)**

Wall height  $WH := deb_{0,2} \cdot m$

Range for 60% fatality probability  $Wall_i := WH$   $WH = 2.6 \cdot m$

### **Choosing the limiting factor (range / velocity) for the maximum distance at which injuries could occur**

The range at which the velocity drops below the value necessary to cause injury is compared against the range at which the fragment falls below a height of 0.5m above the floor in order to determine the maximum range for injury.

$$serious_i := \text{if}(\text{injure}_i < hope3_{i,1} \cdot m, \text{injure}_i, hope3_{i,1} \cdot m)$$

### **Choosing the limiting factor (range / velocity) for the maximum distance at which 10% fatalities could occur**

As above, for 10% fatality probability

$$F10_i := \text{if}(\text{fatals}_{10\%}_i < hope3_{i,1} \cdot m, \text{fatals}_{10\%}_i, hope3_{i,1} \cdot m)$$

### **Choosing the limiting factor (range / velocity) for the maximum distance at which 50% fatalities could occur**

As above, for 50% fatality probability

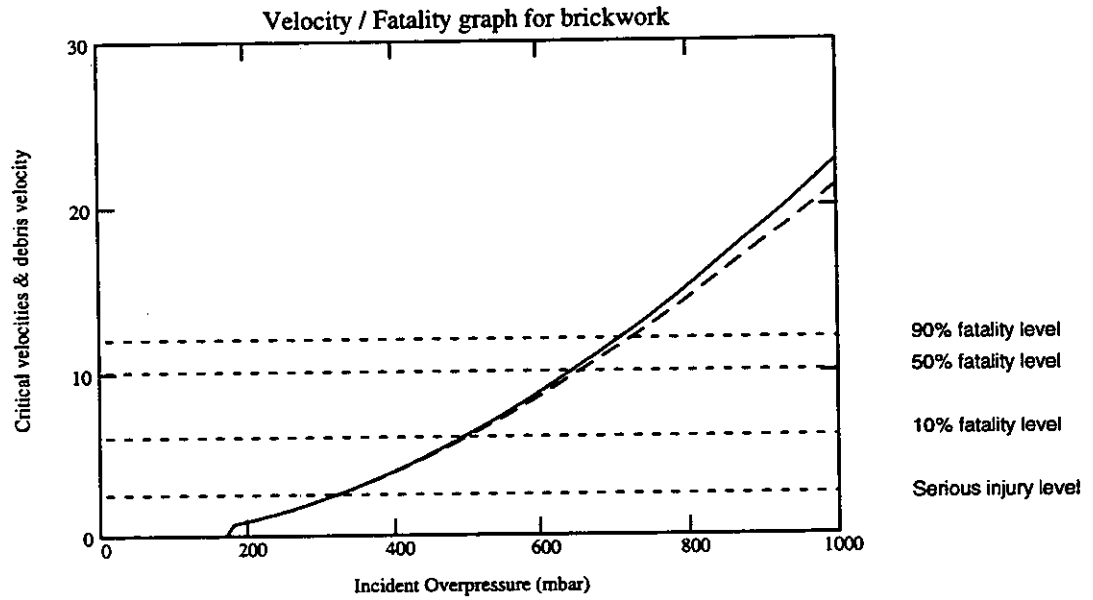
$$F50_i := \text{if}(\text{fatals}_{50\%}_i < hope3_{i,1} \cdot m, \text{fatals}_{50\%}_i, hope3_{i,1} \cdot m)$$

### **Choosing the limiting factor (range / velocity) for the maximum distance at which 90% fatalities could occur**

As above for 90% fatality probability

$$F90_i := \text{if}(\text{fatals}_{90\%}_i < hope3_{i,1} \cdot m, \text{fatals}_{90\%}_i, hope3_{i,1} \cdot m)$$

The following graph shows the initial velocity and velocity at maximum range as a function of pressure together with the criteria for different levels of fatality probability



**Final values calculation**

Finally the ranges for fatality probability are compared to identify overlapping regions and the maximum fatality probability in any region is taken:

$$V_i := 1-i \quad xx := 0, 0.1..5$$

$$60\% \text{ fatalities} \quad F60P_i := \text{if} \left( \frac{P_{inc_i}}{\text{mbar}} \geq P_{fails, WH}, 0 \right)$$

$$\text{Serious injuries} \quad FSERP_i := \text{if} \left[ \left( \text{serious}_i \leq WH \right) \cdot \left( \frac{P_{inc_i}}{\text{mbar}} \geq P_{fails} \right), F60P_i, \text{serious}_i \right]$$

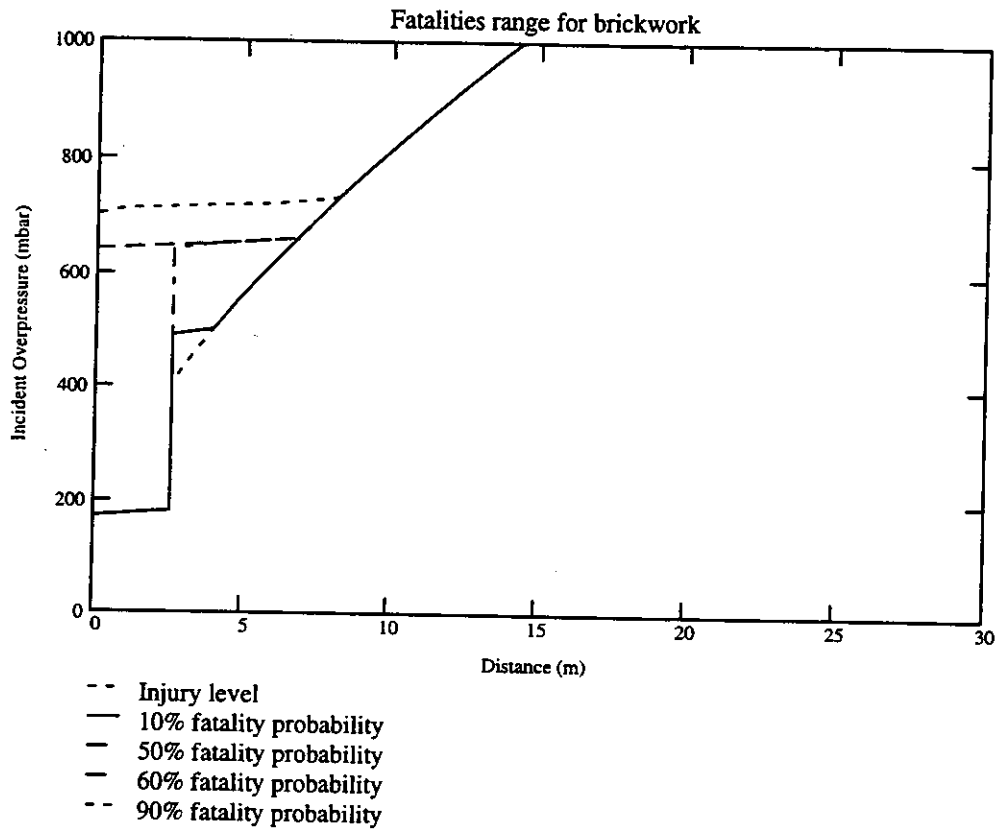
$$10\% \text{ fatalities} \quad F10P_i := \text{if} \left[ \left( F10_i \leq WH \right), F60P_i, F10_i \right]$$

$$50\% \text{ fatalities} \quad F50P_i := F50_i$$

$$90\% \text{ fatalities} \quad F90P_i := F90_i$$

$$F60P_i := \text{if} \left( F60P_i \geq F50P_i, F60P_i, F50P_i \right)$$

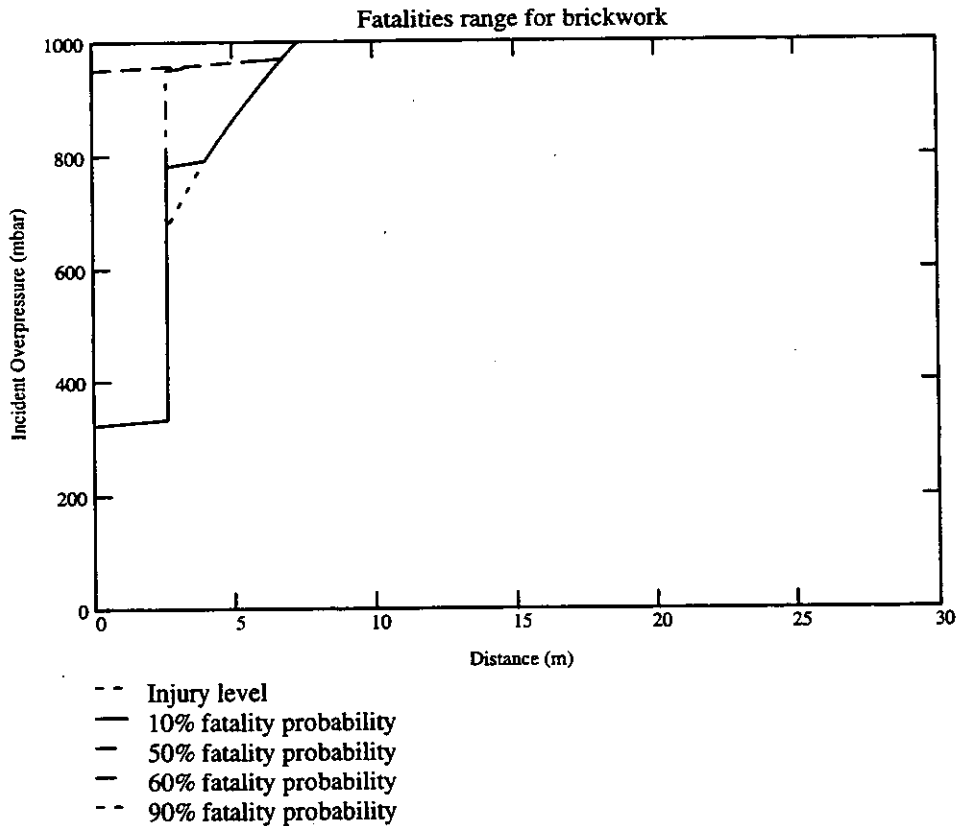
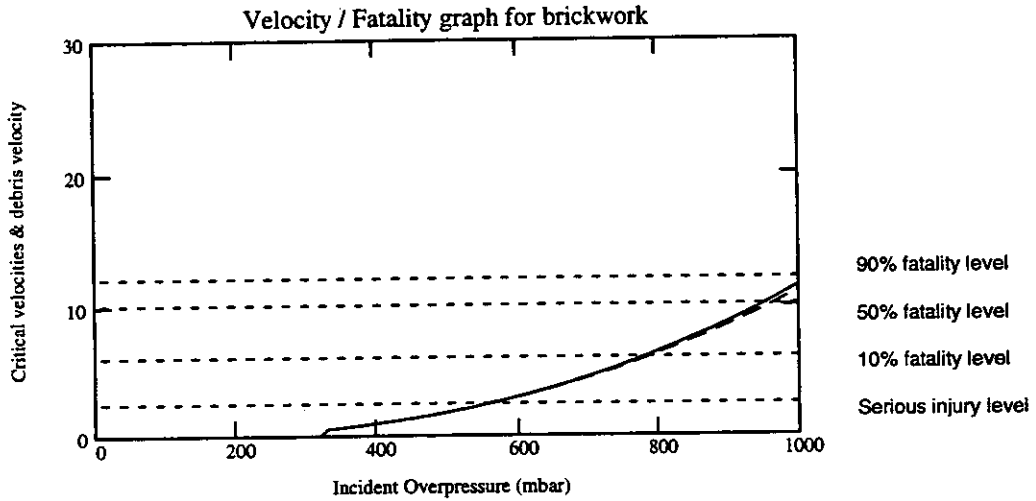
This calculation leads to a plot of fatality probability with distance from the wall under different levels of peak incident overpressure, as shown overleaf:



This graph is written out to a file for input into the final sheet where the building fatality probability curves are calculated.

## Repeat Calculation for Pressure Pulse

The calculations are repeated for an incident pressure pulse. In this case it should be noted that the overpressure is an effective overpressure across the wall. The following results are obtained:



Again, this graph is written out to a file for use in subsequent calculations.

## 5. Calculation of the global structural response of the building (Shock Pulse)

The overall load on the structure and its response to that load are calculated here. This encompasses the load on the front face, load on the rear face and internal pressure calculations, as described in detail in Section 2.3. The methodology is illustrated in Figure 2.23.

### Definition of units

$$\text{mbar} := 100 \cdot \text{Pa}$$

$$\text{zero} := 0 \cdot \frac{\text{newton}}{\text{m}^2}$$

### Input variables

The characteristics of the building which are required for this set of calculations are read in as a matrix and assigned variable names for use in this sheet only:

	$\text{build} := \text{READPRN}(\text{b22})$	
<i>Height of building</i>	$H := \text{build}_{0,0} \cdot \text{m}$	$H = 8 \cdot \text{m}$
<i>Breadth of building (width)</i>	$B := \text{build}_{1,0} \cdot \text{m}$	$B = 8.6 \cdot \text{m}$
<i>Length of building (front to back)</i>	$L := \text{build}_{2,0} \cdot \text{m}$	$L = 14.3 \cdot \text{m}$
<i>Wall thickness</i>	$\text{tw} := \text{build}_{3,0} \cdot \text{m}$	$\text{tw} = 0.215 \cdot \text{m}$
<i>Length of Glazing on Short Side</i>	$L2f := \text{build}_{3,1} \cdot \text{m}$	$L2f = 1.275 \cdot \text{m}$
<i>Height of Windows</i>	$\text{Hwin} := \text{build}_{6,1} \cdot \text{m}$	$\text{Hwin} = 1.25 \cdot \text{m}$
<i>Length of Glazing on Long Side</i>	$L1 := \text{build}_{1,1} \cdot \text{m}$	
	$L2s := \text{build}_{2,1} \cdot \text{m}$	
	$L4 := \text{build}_{4,1} \cdot \text{m}$	
	$L5 := \text{build}_{5,1} \cdot \text{m}$	
Select the larger glazing area	$\text{LG} := \text{if}((L1 + L2s) \geq (L4 + L5), (L1 + L2s), (L4 + L5))$	$\text{LG} = 4.05 \cdot \text{m}$
Area of glazing on short side (nominal glazing on side wall)	$A_f := L2f \cdot \text{Hwin} \cdot 2$	$A_f = 3.188 \cdot \text{m}^2$
Area of glazing on long face	$A_l := \text{LG} \cdot \text{Hwin} \cdot 2 \cdot 2$	$A_l = 20.25 \cdot \text{m}^2$
NB This assumes identical glazing on lower and upper floors		
$\gamma$ for air	$\gamma := 1.4$	
Atmospheric pressure	$p_o := 1103 \cdot \text{mbar}$	
Coefficient of drag	$C_D := 1.05$	
Speed of sound in atmosphere	$C_o := 340 \cdot \frac{\text{m}}{\text{sec}}$	

### Applied shock wave

In this sheet, a series of iterative calculations for a range of peak incident overpressures are performed. It is first necessary to define the overpressures of interest:

$$i_{\max} = 20 \quad p_{it} = 0..i_{\max} \quad P_{pit} = p_{it} \cdot 50$$

Maximum overpressure  $P_s := P \cdot \text{mbar}$  20 values ranging from 0 to 1000mbar in 50mbar increments

Total shock wave duration  $t_p := \text{READPRN}(p_{dur})_0 \quad t_p = 0.1$

Factor on glazing failure calculation  $g_{\text{factor}} := -0.141 \cdot \ln(t_p) + 0.104 \cdot t_p + 0.904$   
 $g_{\text{factor}} = 1.239$

Time division for calculations  $T1 := 0.0005$

Total time for calculations  $t_{\max} := 1.0$

Total number of iterations  $i_{\text{tmax}} := \frac{t_{\max}}{T1} \quad i_{\text{tmax}} = 2 \cdot 10^3$

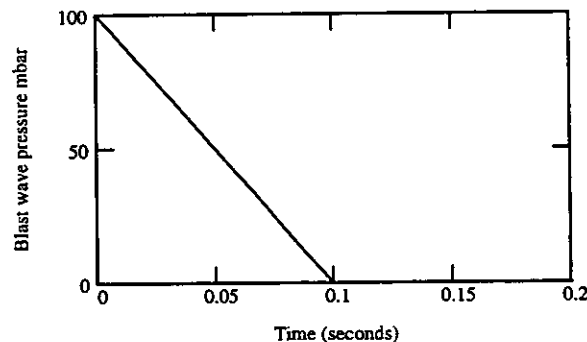
$i := 0..i_{\max} \quad itt := 0..i_{\text{tmax}}$

### Pulse shape

Pressure drop

$$p_{try_{i,itt}} := P_{s_i} - \left( \frac{P_{s_i}}{t_p} \cdot \frac{itt}{i_{\text{tmax}}} \cdot t_{\max} \right)$$

$$p_{try_{i,itt}} := \text{if}(p_{try_{i,itt}} \geq 0, p_{try_{i,itt}}, 0)$$



### Interaction of Pulse with Front Face

Initially it is assumed that the short side of the building faces the blast. It is necessary to calculate how the pulse interacts with the building in order to determine the load. This is described further in Section 2.3.2. For an incident shock pulse, the pulse is reflected at the front face, and the subsequent load on the wall is calculated from the decay of the reflected pressure plus the incident pulse and the dynamic pressure.

### Calculation of building dimension

S is the average distance from any wall section to the wall edge.

Wall dimension  $S := \text{if}\left(H \leq \frac{B}{2}, H, \frac{B}{2}\right) \quad S = 4.3 \cdot \text{m}$



Calculation of perpendicularly reflected overpressure due to shock wave (Equation 6)

$$Pr_i := 2 \cdot P_{s_i} + \frac{(\gamma + 1) \cdot (P_{s_i})^2}{[(\gamma - 1) \cdot P_{s_i}] + 2 \cdot \gamma \cdot p_o} \quad Pr_5 = 5.47 \cdot 10^4 \cdot \frac{\text{newton}}{\text{m}^2}$$

Calculation of pressure Q (Equation 7)

$$Q_{s_i} := \frac{5}{2} \cdot \frac{(P_{s_i})^2}{\gamma \cdot p_o + P_{s_i}} \quad Q_{s_5} = 1.96 \cdot 10^3 \cdot \frac{\text{newton}}{\text{m}^2}$$

Dynamic pressure at front face

$$Q_D := C_D \cdot Q_s \quad Q_{D_5} = 2.058 \cdot 10^3 \cdot \frac{\text{newton}}{\text{m}^2}$$

Velocity of wave front (Equation 9)

$$U_i := C_o \cdot \sqrt{1 + \frac{6 \cdot P_{s_i}}{7 \cdot p_o}} \quad U_5 = 371.562 \cdot \frac{\text{m}}{\text{sec}}$$

Time for pressure to reach incident plus dynamic (Equation 8)

$$t_{s_i} := \frac{3 \cdot S}{U_i} \quad t_{s_5} = 0.035 \cdot \text{sec}$$

Time required to reach the back face

$$t_{\text{back}_i} := \frac{L}{U_i} \quad t_{\text{back}_5} = 0.038 \cdot \text{sec}$$

Time to reach maximum pressure on back face (outside)

$$t_{\text{max}_i} := \frac{4 \cdot S}{U_i} \quad t_{\text{max}_5} = 0.046 \cdot \text{sec}$$

Maximum pressure on back face

$$pb := P_s \quad pb_5 = 250 \cdot \text{mbar}$$

**Pressure on Front Face**

Peak Stagnation pressure

$$P_{\text{tot}_i} := P_{s_i} + (C_D \cdot Q_{s_i})$$

Decay of peak stagnation pressure to zero over pulse duration

$$p_{\text{tryd}_{i,\text{itt}}} := \frac{P_{\text{tot}_i}}{\text{mbar}} - \frac{\frac{P_{\text{tot}_i}}{\text{mbar}}}{t_p} \cdot \frac{\text{itt}}{\text{itt}_{\text{max}}} \cdot t_{\text{max}}$$

Pressure value at which reflected pressure has decayed to stagnation pressure

$$dt_{\text{stry}_{i,\text{itt}}} := \frac{P_{\text{tot}_i}}{\text{mbar}} - \frac{\frac{P_{\text{tot}_i}}{\text{mbar}}}{t_p} \cdot \frac{t_{s_i}}{\text{sec}}$$

Decay of reflected pressure to stagnation pressure

$$c_{ry_{i,it}} := \frac{Pr_i}{mbar} \cdot \left[ \frac{\frac{Pr_i}{mbar} - dtstry_{i,it}}{\left(\frac{t_{s_i}}{sec}\right)} \cdot \frac{itt}{itmax} \cdot t_{max} \right]$$

Contribution from pulse after reflected pressure has decayed to stagnation pressure

$$e_{ry_{i,it}} := \text{if} \left[ \left( \frac{itt}{itmax} \cdot t_{max} \geq \frac{t_{s_i}}{sec} \right) \cdot \left( \frac{itt}{itmax} \cdot t_{max} < t_p \right), ptryd_{i,it}, 0 \right]$$

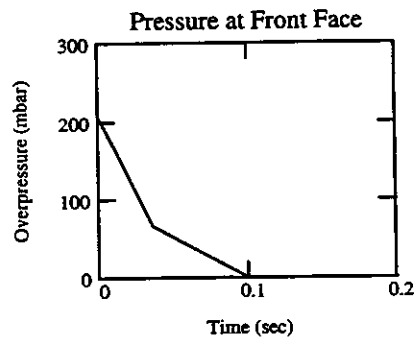
Contribution from reflected pressure

$$f_{ry_{i,it}} := \text{if} \left[ \left( \frac{itt}{itmax} \cdot t_{max} < \frac{t_{s_i}}{sec} \right) \cdot (ptryd_{i,it} > 0), c_{ry_{i,it}}, 0 \right]$$

Combined pulse shape

$$p_{front} := e_{ry} + f_{ry}$$

The pressure load experienced by the front face is shown below for 100mbar peak incident overpressure



## Pressure on Rear Face

The way in which the pressure on the rear face of the building is calculated is described in more detail in Section 2.3.3.

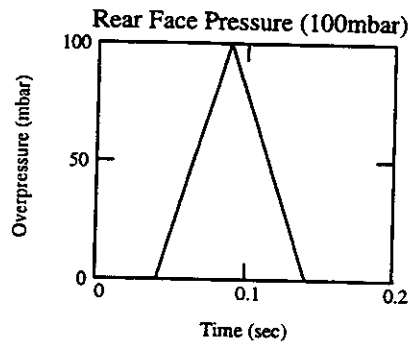
Rise of rear face pressure

$$Drtry_{i,itt} := \frac{pb_i}{mbar} \cdot \left[ \frac{\frac{itt}{itmax} \cdot t_{max} - t_{back_i} \cdot \frac{1}{sec}}{t_{maxp_i} \cdot \frac{1}{sec}} \right]$$

Fall of rear face pressure

$$Crtry_{i,itt} := \frac{pb_i}{mbar} \cdot \left[ \frac{\left( t_p + t_{back_i} \cdot \frac{1}{sec} \right) - \frac{itt}{itmax} \cdot t_{max}}{t_p - t_{maxp_i} \cdot \frac{1}{sec}} \right]$$

"prear", the variable plotted below is the pressure force which acts on the rear face of the building. It is the sum of "Drtry" and "Crtry", which make up the rise and fall in the pulse, respectively, assuming the time taken to reach the peak is less than the time taken for the pulse to pass the rear face. However, if the time taken to reach the peak of the pulse is greater than the time taken for the pulse to pass the rear face, then the pulse is assumed not to reach its maximum value and drop straight to zero.



## Internal pressure due to glazing/cladding failure

If the front face glazing and/or cladding fail, the pressure inside the building will start to increase. The calculation of internal pressure is based on the method presented in [7], and leads to the average pressure increase inside a void equal in volume to that of the building.

*Glazing failure pressure*

$$G_f := build_{s,1} \cdot mbar$$

$$G_f = 55 \cdot mbar$$

This needs to be increased to take into account the fact that the pulse duration is shorter than 1sec

$$G_f := gfactor \cdot G_f$$

$$G_f = 68.149 \cdot mbar$$

*Cladding Failure Pressure*

$$C_f := READPRN(Pfail)_1 \cdot mbar$$

$$C_f = 175 \cdot mbar$$

This is an incident pressure - the cladding actually fails at the reflected pressure corresponding to this incident value:

**Calculation variables**

The method in [7] is outlined in psi - hence the units need to be converted for use here.

$$C_f := \frac{C_f}{\text{psi}} \quad C_f = 2.538$$

Time division

$$\Delta\text{time} := T1 \cdot \text{sec}$$

$$\Delta\text{time} = 5 \cdot 10^{-4} \cdot \text{sec}$$

$$it := 0..itmax$$

$$tps_{it} := \frac{\Delta\text{time}}{\text{sec}} \cdot it$$

External pressure pulse: the unreflected pulse shape is used as the glazing breaks and is assumed not to reflect

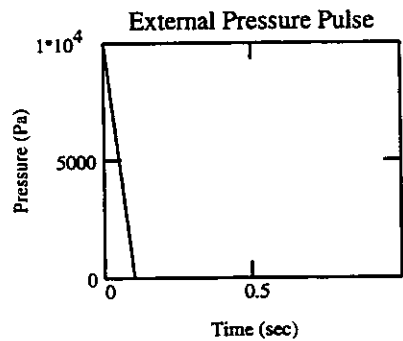
$$\Delta p_{i,it} := P_{s_i} \cdot \left( 1 - \frac{tps_{it}}{t_p} \right)$$

$$\Delta p_{i,it} := \text{if}(\Delta p_{i,it} \geq 0, \Delta p_{i,it}, 0)$$

Convert units

$$\Delta\text{tps} := \frac{\Delta p}{\text{psi}}$$

$$\Delta\text{tps}_{i,it} := \text{if}(\Delta p_{i,it} > \text{zero}, \frac{\Delta p_{i,it}}{\text{psi}}, 0)$$



Building volume

$$V_o := B \cdot L \cdot H$$

$$V_o = 983.84 \cdot \text{m}^3$$

Maximum dimension for vent area is whole wall facing blast

$$A_o := \text{if}(A_f > B \cdot H, B \cdot H, A_f)$$

$$A_o = 3.188 \cdot \text{m}^2$$

A / V ratio

$$AV := \frac{A_o}{V_o}$$

$$AV = 3.24 \cdot 10^{-3} \cdot \text{m}^{-1}$$

Initial internal overpressure

$$\Delta P_{i,0} := 0 \cdot \text{Pa}$$

Initial pressure difference outside/inside

$$P_{diff_{i,1}} := (\Delta p_{i,0} - \Delta P_{i,0})$$

$$P_{diff_{i,1}} = 50 \cdot \text{mbar}$$

### Calculate Internal Pressure

Constant for glazing:  $\text{constg} := AV \cdot \Delta\text{time} \cdot \left( \frac{\text{ft}}{0.001 \cdot \text{sec}} \right)$   $\text{constg} = 4.938 \cdot 10^{-4}$

Constant for cladding  
NB Arbitrary factor of 0.8  $\text{constc} := \frac{0.8 \cdot B \cdot H}{V_o} \cdot \Delta\text{time} \cdot \left( \frac{\text{ft}}{0.001 \cdot \text{sec}} \right)$   $\text{constc} = 8.526 \cdot 10^{-3}$

If the cladding fails, this constant is assumed to be equal to that for cladding, otherwise the constant for glazing is used.

$$\text{const}_i := \text{if} \left[ \left( \frac{P_{s_i}}{\text{mbar}} \geq \frac{C_f}{\text{mbar}} \right), \text{constc}, \text{constg} \right]$$

The internal pressure is now calculated for each of the peak incident overpressures considered and at each time step used in the iterations. Above, the constants to be applied in the internal pressure equation have been calculated, "const", depending on whether the glazing or cladding have failed at the overpressure considered. (On failure of the glazing the open area is calculated the area of the windows, whereas if the cladding fails then the open area is considered to be 80 % of the total facing area of the building.) The internal pressure is calculated by application of:

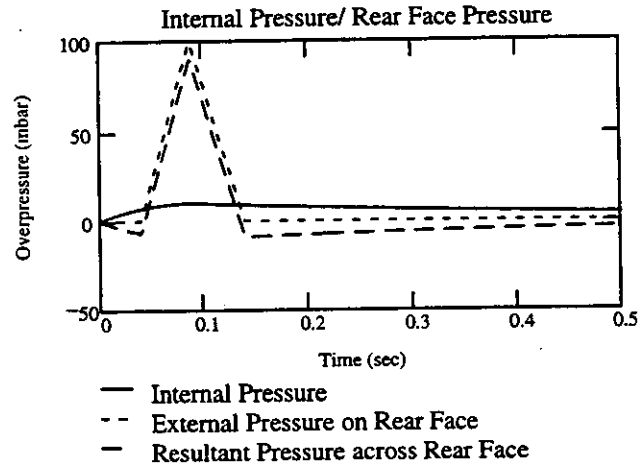
$$\Delta P = C_L \times \text{const} \times \Delta t$$

where  $C_L$  is the leakage pressure coefficient (Figure 2.10), a function of the pressure difference at the opening.

This is an iterative calculation, iterating over  $\Delta t$ .

**Resultant Pressure on Rear Face**

The internal pressure is shown on the graph below, for 100mbar peak incident overpressure. Also shown is the rear face pressure and the difference between the rear face pressure and the internal pressure. This represents the resultant pressure across the rear face.



It is necessary to determine the maximum and minimum pressures across the rear face. An iterative calculation is performed which loops through all the rear face pressure profiles and extracts the maximum and minimum values. These values are used subsequently to determine the maximum pressures which the glazing/cladding experience at the rear face.

Maximum and Minimum Rear Face Pressures:  
 (A negative value indicates a direction out of the building)

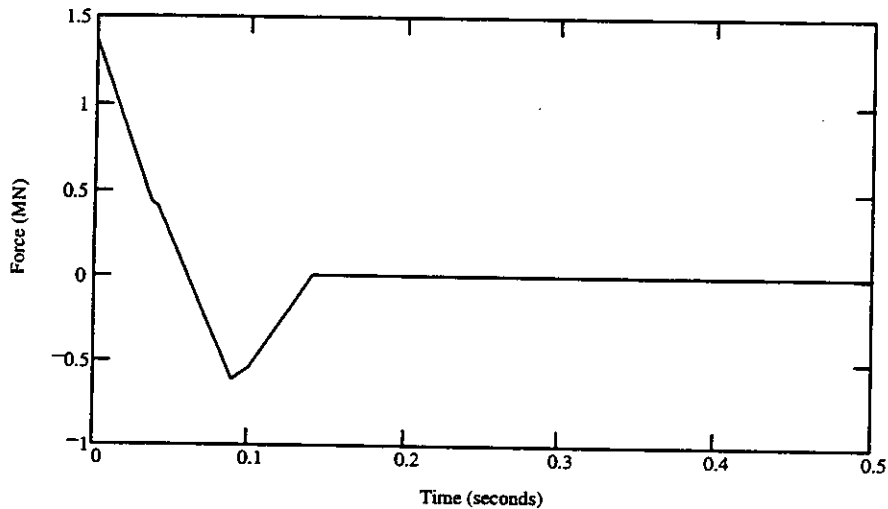
hop =	Max	Min
0	0	0
1	44.97	-4.435
2	89.76	-8.776
3	135.016	-13.04
4	129.772	-117.799
5	159.71	-146.447
6	189.047	-174.633
7	216.187	-202.503
8	244.547	-229.924
9	270.526	-256.861
10	295.998	-283.275
11	322.69	-309.128
12	348.431	-334.383
13	373.026	-359.001
14	396.373	-382.945

## Resultant Force Variation on Building

The resultant force variation experienced by the building is calculated from the front face pressure, the rear face pressure and the internal pressure as described in Section 2.3.5 (Equation 12):

Force on Building: Shock Pulse  $F_s := [p_{\text{front}} \cdot (H \cdot B - A_f) - p_{\text{rear}} \cdot H \cdot B + p_{\text{internal}} \cdot A_f] \cdot 100 \cdot \text{Pa}$

### Force acting on building



## Structural Response

Having calculated the force on the building, it is now necessary to calculate the resultant building displacement:

### **Mass of building:**

Assume for now (arbitrarily) that the mass of the whole building is 50% higher than the mass of the exterior and interior walls alone:

Density of brick  $\rho_b := \text{build}_{6,2} \cdot \text{kg} \cdot \text{m}^{-3}$

Mass of building  $\text{Mass} := (B \cdot H \cdot \text{tw} \cdot \rho_b \cdot 3 + L \cdot H \cdot \text{tw} \cdot \rho_b \cdot 3) \cdot 1.5$        $\text{Mass} = 3.545 \cdot 10^5 \cdot \text{kg}$

$$M := \frac{\text{Mass}}{\text{kg}}$$

### **Stiffness of building:**

From Lees [8] and Equation 14, an empirical equation for the natural period is:

$$T := \frac{0.05 \cdot \frac{H}{\text{ft}}}{\sqrt{\frac{B}{\text{ft}}}} \cdot \text{sec} \qquad T = 0.247 \cdot \text{sec}$$

Using this and the mass of the building, we can derive a value for the stiffness:

$$\text{Stiffness} := \frac{\text{Mass}}{\left(\frac{T}{2 \cdot \pi}\right)^2}$$

$$\text{Stiffness} = 2.293 \cdot 10^8 \cdot \text{newton} \cdot \text{m}^{-1}$$

Non-dimensional value:  $K := \frac{\text{Stiffness}}{\text{newton} \cdot \text{m}^{-1}}$   $K = 2.293 \cdot 10^8$

### Elastic Limits of SDOF System

For this building type, the brick walls form the load-bearing frame of the structure. Hence the failure pressure of the frame is the same as that of the walls.

If we assume that the capacity of the solid brick wall is 275 mbar

	$\text{Fail}_d := \text{READPRN}(b22)_{5,2} \cdot \text{mbar}$	$\text{Fail}_d = 275 \cdot \text{mbar}$
Positive yield	$\text{Posy} := \text{Fail}_d \cdot B \cdot H$	$R0 := \frac{\text{Posy}}{\text{newton}}$ $R0 = 1.892 \cdot 10^6$
Negative yield	$\text{Negy} := \text{Posy} \cdot -1$	$R1 := \frac{\text{Negy}}{\text{newton}}$ $R1 = -1.892 \cdot 10^6$
Elastic limit	$y_{el} := \frac{R0}{K}$	$y_{el} = 8.252 \cdot 10^{-3}$
% critical damping	$Bc := 0.0$	
Ductility	$\mu := 5$	
Displacement at Failure	$y_{max} := y_{el} \cdot \mu$	$y_{max} = 0.041 \text{ (m)}$

The above calculations have defined the force on the building, its stiffness and mass such that it is possible to find a solution to Equation 5, the equation of motion. The building is assumed to behave as a single degree of freedom elasto-plastic system, with a bi-linear stiffness. Failure, i.e. structural collapse, is assumed to occur if the displacement of the structure exceeds the elastic limit multiplied by the ductility.

The equation of motion is solved using an iterative procedure to give the displacement of the structure in time. This is performed for each increment of peak incident overpressure, and the maximum and minimum (i.e. greatest -ve) displacement at each incident overpressure are extracted. By comparing these displacements with the displacement at failure,  $y_{max}$ , the collapse pressure of the structure can be derived:



## Maximum and minimum displacements of structure

'as' is a matrix containing the calculated maximum and minimum displacements

		Maximum	Minimum		
		0	1	0	1
Displacements	as =	0	0	0	0
		$2.82 \cdot 10^{-3}$	$-2.815 \cdot 10^{-3}$	0.068	-0.068
		$5.612 \cdot 10^{-3}$	$-5.602 \cdot 10^{-3}$	0.136	-0.136
		$8.181 \cdot 10^{-3}$	$-8.351 \cdot 10^{-3}$	0.198	-0.202
		$8.108 \cdot 10^{-3}$	-0.012	0.196	-0.283
		0.01	-0.01	0.251	-0.254
		0.013	$-8.154 \cdot 10^{-3}$	0.315	-0.198
		0.016	$-5.204 \cdot 10^{-3}$	0.387	-0.126
		0.019	$-1.761 \cdot 10^{-3}$	0.465	-0.043
		0.023	0	0.55	0
		0.026	0	0.641	0
		0.03	0	0.737	0
		0.035	0	0.838	0
				0.944	0
			1.055	0	

Ratio of displacements to  $y_{\max}$

Failure occurs when the displacement of the structure is greater than  $y_{\max}$  - for this structure it is at about increment 14, which corresponds to 700mbar peak incident overpressure

Increment in which structure collapses:  $\text{colls} = 14$

Corresponding peak incident overpressure  $P_{\text{colls}} = 700$

Ratio of max displacement to displacement at failure in collapse increment  $\frac{\text{as}_{\text{colls},0}}{y_{\max}} = 1.055$

Ratio of max displacement to displacement at failure in increment immediately prior to collapse increment  $\frac{\text{as}_{(\text{colls}-1),0}}{y_{\max}} = 0.944$

Interpolate between these two values to derive an estimate of failure pressure

Variables for interpolation  $V1 := \frac{\text{as}_{\text{colls},0}}{y_{\max}}$   $V2 := \frac{\text{as}_{(\text{colls}-1),0}}{y_{\max}}$

Collapse pressure (peak incident overpressure)  $P_{\text{coll}} := \frac{P_{\text{colls}} - P_{\text{colls}-1}}{V1 - V2} \cdot 1.0 + P_{\text{colls}-1} - \frac{P_{\text{colls}} - P_{\text{colls}-1}}{V1 - V2} \cdot V2$

$P_{\text{coll}} = 675.184$  (mbar)



Increment in which structure collapses:  $\text{collsl} = 10$

Corresponding peak incident overpressure  $P_{\text{collsl}} = 500$

Ratio of max displacement to displacement at failure in collapse increment  $\frac{\text{asl}_{\text{collsl},0}}{y_{\text{max}}} = 1.074$

Ratio of max displacement to displacement at failure in increment immediately prior to collapse increment  $\frac{\text{asl}_{(\text{collsl}-1),0}}{y_{\text{max}}} = 0.909$

Interpolate between these two values to derive an estimate of failure pressure

Variables for interpolation  $V1 := \frac{\text{asl}_{\text{collsl},0}}{y_{\text{max}}}$   $V2 := \frac{\text{asl}_{(\text{collsl}-1),0}}{y_{\text{max}}}$

Collapse pressure (peak incident overpressure)  $P_{\text{coll}} := \frac{P_{\text{collsl}} - P_{\text{collsl}-1}}{V1 - V2} \cdot 1.0 + P_{\text{collsl}-1} - \frac{P_{\text{collsl}} - P_{\text{collsl}-1}}{V1 - V2} \cdot V2$

$$P_{\text{coll}} = 477.609 \text{ (mbar)}$$

$$\text{coll}_1 := P_{\text{coll}}$$

Vector of collapse values  $\text{coll} = \begin{pmatrix} 675.184 \\ 477.609 \end{pmatrix} \text{ (mbar)}$

This vector is written out for use in subsequent calculations

## 6. Calculation of the global structural response of the building (Pressure Pulse)

The overall load on the structure and its response to that load are calculated here. This encompasses the load on the front face, load on the rear face and internal pressure calculations, as described in detail in Section 2.3. The methodology is illustrated in Figure 2.23.

### Definition of units

$$\text{mbar} := 100 \cdot \text{Pa}$$

$$\text{zero} := 0 \cdot \frac{\text{newton}}{\text{m}^2}$$

### Input variables

The characteristics of the building which are required for this set of calculations are read in as a matrix and assigned variable names for use in this sheet only:

$$\text{build} := \text{READPRN}(\text{b22})$$

*Height of building*

$$H := \text{build}_{0,0} \cdot \text{m}$$

$$H = 8 \cdot \text{m}$$

*Breadth of building (width)*

$$B := \text{build}_{1,0} \cdot \text{m}$$

$$B = 8.6 \cdot \text{m}$$

*Length of building (front to back)*

$$L := \text{build}_{2,0} \cdot \text{m}$$

$$L = 14.3 \cdot \text{m}$$

*Wall thickness*

$$\text{tw} := \text{build}_{3,0} \cdot \text{m}$$

$$\text{tw} = 0.215 \cdot \text{m}$$

*Length of Glazing on Short Side*

$$\text{L2f} := \text{build}_{3,1} \cdot \text{m}$$

$$\text{L2f} = 1.275 \cdot \text{m}$$

*Height of Windows*

$$\text{Hwin} := \text{build}_{6,1} \cdot \text{m}$$

$$\text{Hwin} = 1.25 \cdot \text{m}$$

*Length of Glazing on Long Side*

$$\text{L1} := \text{build}_{1,1} \cdot \text{m}$$

$$\text{L2s} := \text{build}_{2,1} \cdot \text{m}$$

$$\text{L4} := \text{build}_{4,1} \cdot \text{m}$$

$$\text{L5} := \text{build}_{5,1} \cdot \text{m}$$

Select the larger glazing area

$$\text{LG} := \text{if}((\text{L1} + \text{L2s}) \geq (\text{L4} + \text{L5}), (\text{L1} + \text{L2s}), (\text{L4} + \text{L5}))$$

$$\text{LG} = 4.05 \cdot \text{m}$$

Area of glazing on short side  
(nominal glazing on side wall)

$$A_f := \text{L2f} \cdot \text{Hwin} \cdot 2$$

$$A_f = 3.188 \cdot \text{m}^2$$

Area of glazing on long face

$$A_1 := \text{LG} \cdot \text{Hwin} \cdot 2 \cdot 2$$

$$A_1 = 20.25 \cdot \text{m}^2$$

NB This assumes identical glazing on lower and upper floors  
 $\gamma$  for air

$$\gamma := 1.4$$

Atmospheric pressure

$$p_o := 1103 \cdot \text{mbar}$$

Coefficient of drag

$$C_D := 1.05$$

Speed of sound in atmosphere

$$C_o := 340 \cdot \frac{\text{m}}{\text{sec}}$$

**Applied pressure wave**

In this sheet, a series of iterative calculations for a range of peak incident overpressures are performed. It is first necessary to define the overpressures of interest:

$$\text{imax} = 20 \quad \text{pit} = 0.. \text{imax} \quad P_{\text{pit}} = \text{pit} \cdot 50$$

Maximum overpressure  $P_s := P \cdot \text{mbar}$  20 values ranging from 0 to 1000mbar in 50mbar increments

Total shock wave duration  $t_p := \text{READPRN}(\text{pdur})_0$   $t_p = 0.1$

Factor on glazing failure calculation  $\text{gfactor} := -0.141 \cdot \ln(t_p) + 0.104 \cdot t_p + 0.904$   
 $\text{gfactor} = 1.239$

Time division for calculations  $T1 := 0.0005$

Total time for calculations  $t_{\text{max}} := 1.0$

Total number of iterations  $\text{itmax} := \frac{t_{\text{max}}}{T1}$   $\text{itmax} = 2 \cdot 10^3$

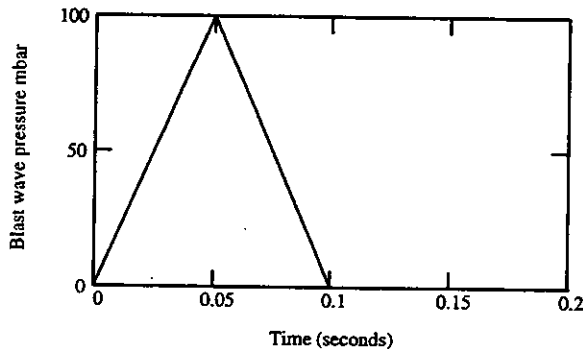
**Pulse shape**  $i := 0.. \text{imax}$   $\text{itt} := 0.. \text{itmax}$

Pressure rise  $\text{up}_{i,\text{itt}} := \text{if} \left[ \left( \frac{\text{itt}}{\text{itmax}} \cdot t_{\text{max}} \leq \frac{t_p}{2} \right), 2 \cdot P_{s_i} \cdot \frac{\text{itt} - t_{\text{max}}}{t_p \cdot \text{itmax}}, 0 \right]$

Pressure drop  $\text{down}_{i,\text{itt}} := \text{if} \left[ \left( \frac{\text{itt}}{\text{itmax}} \cdot t_{\text{max}} > \frac{t_p}{2} \right) \cdot \left( \frac{\text{itt}}{\text{itmax}} \cdot t_{\text{max}} < t_p \right), \left[ P_{s_i} - \left( \frac{P_{s_i}}{t_p} \cdot \frac{\text{itt}}{\text{itmax}} \cdot t_{\text{max}} \right) \right] \cdot 2, 0 \right]$

Combination  $\text{pt} := \text{up} + \text{down}$

**Pressure wave diagram**



**Interaction of Pulse with Front Face**

Initially it is assumed that the short side of the building faces the blast. It is necessary to calculate how the pulse interacts with the building in order to determine the load. This is described further in Section 2.3.2. For an incident pressure pulse, it is assumed that no reflection of the pulse occurs at the front face, and the subsequent load on the wall is calculated from the incident pulse shape plus the dynamic pressure.

### Calculation of building dimension

S is the average distance from any wall section to the wall edge.

$$\text{Wall dimension } S := \text{if} \left( H \leq \frac{B}{2}, H, \frac{B}{2} \right) \quad S = 4.3 \cdot \text{m}$$

### Calculation of pressure Q - Use MEM Curve fit for Pressure Pulse

$$Q_{s_i} := \left[ 4.403 \cdot 10^{-13} \cdot \left( \frac{P_{s_i}}{\text{mbar}} \right)^5 + 0.09 \cdot \frac{P_{s_i}}{\text{mbar}} + 1.868 \cdot 10^{-4} \right] \cdot \text{mbar} \quad Q_{s_5} = 22.93 \cdot \text{mbar}$$

$$Q_{s_0} := 0 \cdot \text{mbar}$$

### Dynamic pressure at front face

$$Q_{D_i} := C_{D_i} \cdot Q_{s_i} \quad Q_{D_5} = 2.408 \cdot 10^3 \cdot \frac{\text{newton}}{\text{m}^2}$$

### Velocity of wave front (Equation 9)

$$U_i := C_o \cdot \sqrt{1 + \frac{6 \cdot P_{s_i}}{7 \cdot p_o}} \quad U_5 = 371.562 \cdot \frac{\text{m}}{\text{sec}}$$

### Time required to reach the back face

$$t_{\text{back}_i} := \frac{L}{U_i} \quad t_{\text{back}_5} = 0.038 \cdot \text{sec}$$

### Time to reach maximum pressure on back face (outside)

$$t_{\text{maxpp}_i} := \frac{4 \cdot S}{U_i} + \frac{t_p \cdot \text{sec}}{2} \quad t_{\text{maxpp}_5} = 0.096 \cdot \text{sec}$$

### Maximum pressure on back face

$$p_{bp} := P_s \quad p_{bp_5} = 250 \cdot \text{mbar}$$

## Pressure on Front Face

$$\text{Peak Stagnation pressure } P_{\text{tot}_i} := P_{s_i} + (C_{D_i} \cdot Q_{s_i})$$

Pressure rise including dynamic pressure

$$\text{upf}_{i,\text{itt}} := \text{if} \left[ \left( \frac{\text{itt}}{\text{itmax}} \cdot t_{\text{max}} \leq \frac{t_p}{2} \right), 2 \cdot \frac{P_{\text{tot}_i}}{\text{mbar}} \cdot \frac{\text{itt} \cdot t_{\text{max}}}{t_p \cdot \text{itmax}}, 0 \right]$$

Pressure drop including dynamic pressure

$$\text{downf}_{i,\text{itt}} := \text{if} \left[ \left( \frac{\text{itt}}{\text{itmax}} \cdot t_{\text{max}} > \frac{t_p}{2} \right) \cdot \left( \frac{\text{itt}}{\text{itmax}} \cdot t_{\text{max}} < t_p \right), \left[ \frac{P_{\text{tot}_i}}{\text{mbar}} - \left[ \frac{P_{\text{tot}_i}}{\text{mbar}} \cdot \frac{\text{itt}}{t_p} \cdot \frac{t_{\text{max}}}{\text{itmax}} \right] \right] \cdot 2, 0 \right]$$

Combination - resultant pulse shape at front face

$$p_{\text{front}} := \text{upf} + \text{downf}$$

## Pressure on Rear Face

The way in which the pressure on the rear face of the building is calculated is described in more detail in Section 2.3.3.

Time to reach maximum pressure at rear face  $t_{bp} := t_{back} + t_{maxpp}$

Time to reach rear face plus rise time of pulse  $t_{try} := t_{back} + t_p \cdot sec$

Select the shorter of the above two times,  $T$ : this takes into account whether or not the pressure has time to reach its maximum value before the blast pulse has passed the building

$$T_i := \text{if} \left( t_{bp_i} \leq t_{try_i}, \frac{t_{bp_i}}{\text{sec}}, \frac{t_{try_i}}{\text{sec}} \right)$$

Rise of pressure on rear face:

$$a_{try_{i,itt}} := \text{if} \left[ \left( \frac{itt}{itmax} \cdot t_{max} > \frac{t_{back_i}}{\text{sec}} \right) \cdot \left( \frac{itt}{itmax} \cdot t_{max} < T_i \right), \frac{pbp_i}{\text{mbar}} \cdot \left[ \frac{\frac{itt}{itmax} \cdot t_{max} - \frac{t_{back_i}}{\text{sec}}}{\left( \frac{t_{maxpp_i}}{\text{sec}} \right)} \right], 0 \right]$$

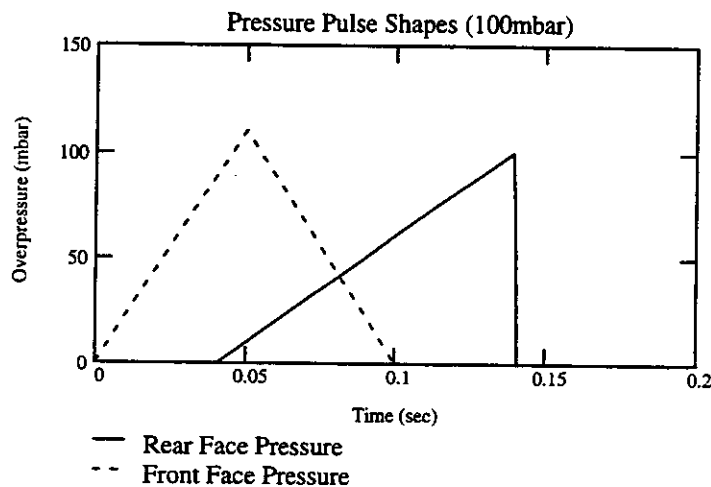
Fall of pressure at rear face

$$b_{try_{i,itt}} := \text{if} \left[ \left( \frac{itt}{itmax} \cdot t_{max} > T_i \right) \cdot \left( \frac{itt}{itmax} \cdot t_{max} < \frac{t_{try_i}}{\text{sec}} \right), \frac{pbp_i}{\text{mbar}} \cdot \left[ \frac{\left( t_p + \frac{L}{U_i} \cdot \frac{1}{\text{sec}} \right) - \frac{itt}{itmax} \cdot t_{max}}{\frac{t_p}{2} - 4 \cdot \frac{S}{U_i} \cdot \frac{1}{\text{sec}}} \right], 0 \right]$$

Combination - resultant pulse shape at rear face

$$prear := a_{try} + b_{try}$$

The resultant pulse shapes at the front and rear of the building are shown below for a 100mbar peak incident overpressure



## Internal pressure due to glazing/cladding failure

If the front face glazing and/or cladding fail, the pressure inside the building will start to increase. The calculation of internal pressure is based on the method presented in [7], and leads to the average pressure increase inside a void equal in volume to that of the building.

The calculation for an incident pressure pulse is slightly more complicated than for an incident shock pulse as the pressure rise is gradual and hence failure of the front face glazing will cause the internal pressure to rise and will affect the differential pressure across the front face cladding. This in turn will affect whether or not the front face cladding fails.

The calculation is performed in 2 stages: first the internal pressure due to glazing failure alone is calculated. The differential pressure across the front wall is then calculated and if the pressure is high enough to fail the front wall, the internal pressure rise due to failure of the cladding is calculated.

*Glazing failure pressure*  $G_f := \text{build}_{g,1} \cdot \text{mbar}$   $G_f = 55 \cdot \text{mbar}$

This needs to be increased to take into account the fact that the pulse duration is shorter than 1sec

$G_f := \text{gfactor} \cdot G_f$   $G_f = 68.149 \cdot \text{mbar}$

*Cladding Failure Pressure*  $C_{failp} := \text{READPRN}(\text{Pfail})_2 \cdot \text{mbar}$   $C_{failp} = 325 \cdot \text{mbar}$

This is an effective pressure, i.e. the differential pressure across the cladding.

### Calculation variables

The method in [7] is outlined in psi - hence the units need to be converted for use here.

$C_f := \frac{C_{failp}}{\text{psi}}$   $C_f = 4.714$

Time division  $\Delta \text{timep} := T1 \cdot \text{sec}$   $\Delta \text{timep} = 5 \cdot 10^{-4} \cdot \text{sec}$

$it2 := 0 \dots itmax$   $itmax = 2 \cdot 10^3$

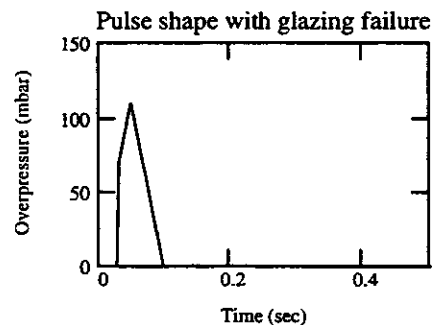
$t_{pp_{it2}} := it2 \cdot T1$

External pressure pulse: failure of the glazing does not occur until the pressure has increased to a value equal to the failure pressure of the glazing

Pressure rise after glazing failure  $\Delta p_{u_{1,it2}} := \text{if} \left[ \left( p_{\text{front}_{1,it2}} > \frac{G_f}{\text{mbar}} \right) \cdot \left( \frac{it2}{itmax} \leq \frac{t_p}{2} \right), p_{\text{front}_{1,it2}}, 0 \right]$

Pressure drop  $\Delta p_{d_{1,it2}} := \text{if} \left[ \left( \frac{it2}{itmax} > \frac{t_p}{2} \right), p_{\text{front}_{1,it2}}, 0 \right]$

Combination - pulse shape  $\Delta p_t := (\Delta p_u + \Delta p_d) \cdot \text{mbar}$





Convert units

$$\Delta t_{pp} := \frac{\Delta p_t}{\text{psi}}$$

$$\Delta t_{pp_{i,i2}} := \text{if} \left[ \left( \Delta p_{t_{i,i2}} > \text{zero} \right), \frac{\Delta p_{t_{i,i2}}}{\text{psi}}, 0 \right]$$

Building volume

$$V_o := B \cdot L \cdot H$$

$$V_o = 983.84 \cdot \text{m}^3$$

Maximum dimension for vent area is whole wall facing blast

$$A_o := \text{if} \left[ \left( A_f > B \cdot H \right), B \cdot H, A_f \right]$$

$$A_o = 3.188 \cdot \text{m}^2$$

A / V ratio

$$AV := \frac{A_o}{V_o}$$

$$AV = 3.24 \cdot 10^{-3} \cdot \text{m}^{-1}$$

Initial internal overpressure

$$\Delta P_{pi_{i,0}} := 0 \cdot \text{Pa}$$

Initial pressure difference

$$P_{p \text{ diff}_{i,1}} := \left( \Delta p_{t_{i,0}} - \Delta P_{pi_{i,0}} \right)$$

$$P_{p \text{ diff}_{2,1}} = 0 \cdot \text{Pa}$$

### Calculate Internal Pressure

Constant for glazing:

$$\text{constpg} := AV \cdot \Delta t_{imep} \cdot \left( \frac{\text{ft}}{0.001 \cdot \text{sec}} \right)$$

$$\text{constpg} = 4.938 \cdot 10^{-4}$$

Constant for cladding  
NB Arbitrary factor of 0.8

$$\text{constpc} := \frac{0.8 \cdot B \cdot H}{V_o} \cdot \Delta t_{imep} \cdot \left( \frac{\text{ft}}{0.001 \cdot \text{sec}} \right)$$

$$\text{constpc} = 8.526 \cdot 10^{-3}$$

The internal pressure is now calculated for each of the peak incident overpressures considered and at each time step used in the iterations. Above, the constants to be applied in the internal pressure equation have been calculated, "const", depending on whether the glazing or cladding have failed at the overpressure considered. (On failure of the glazing the open area is calculated the area of the windows, whereas if the cladding fails then the open area is considered to be 80 % of the total facing area of the building.) The internal pressure is calculated by application of:

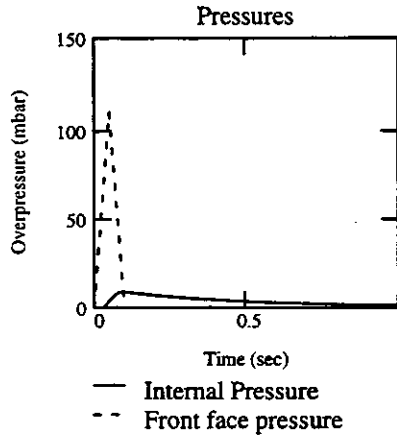
$$\Delta P = C_L \times \text{const} \times \Delta t$$

where  $C_L$  is the leakage pressure coefficient (Figure 2.10), a function of the pressure difference at the opening.

This is an iterative calculation, iterating over  $\Delta t$ . In the first calculation, it is assumed that only the glazing fails.

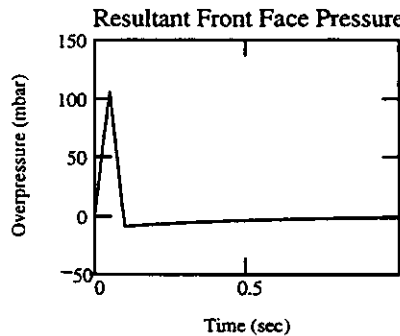
**Internal Pressure due to front face glazing failure only**

The following figure shows the internal pressure and the front face pressure for a 100mbar peak incident overpressure



The resultant pressure across the front face is calculated by subtracting the internal pressure from the external pressure:

$$ppresf := pfront - pptry$$



The maximum differential pressure across the front face is extracted for each increment of peak incident overpressure. This is written out for use in subsequent calculations

Maximum differential pressure

hopp = (mbar)

If this value is greater than the failure pressure of the front wall, Cfailp, the wall is assumed to fail

$$\text{Check for front wall failure } \text{Checkf}_i := \text{if} \left( \text{hopp}_i \geq \frac{\text{Cfailp}}{\text{mbar}}, 1, 0 \right)$$

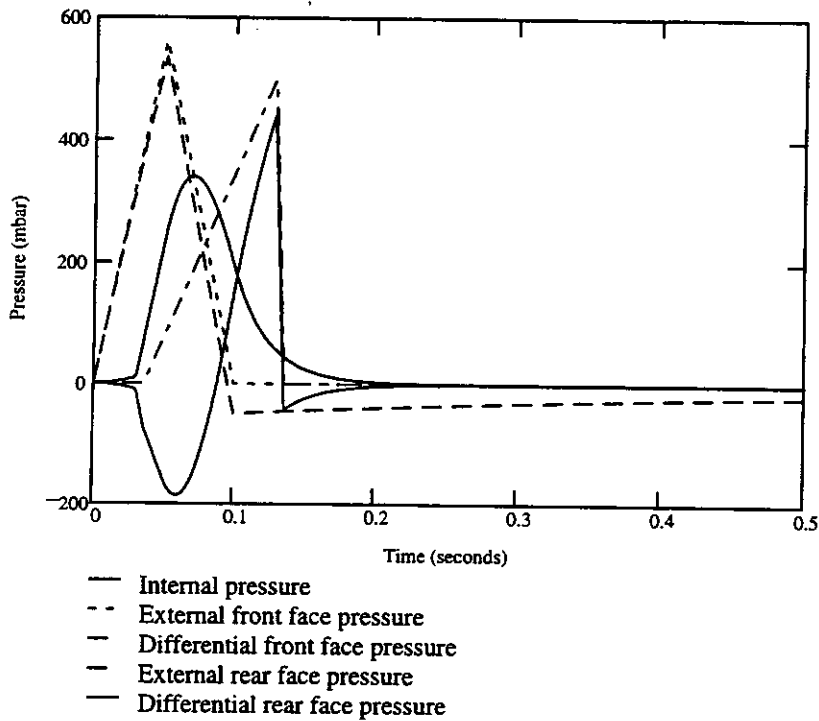
0
1 0
2 54.725
3 105.914
4 157.111
5 208.899
6 261.014
7 313.694
8 367.08
9 421.54
10 477.482
11 535.588
12 596.479
13 661.226
14 730.879
15 806.833

Having calculated whether or not the front wall fails, the internal pressure can be re-calculated, taking this into account. The iterative calculation is similar to that used previously except that at each pressure value it checks whether the front wall has failed or not. If it has, the open area at the front face is effectively increased, and 'constc' is used instead of 'constg'.

The resultant pressure across the rear face can then be calculated from the external rear face pressure and the internal rear face pressure.

The resultant pressure contributions and their combination are illustrated below, for a 500mbar peak incident overpressure:

**Individual pressure contributions**



The maximum and minimum rear face pressures are extracted from the differential pressure curve

Maximum and Minimum Rear Face Pressures:  
(A negative value indicates a direction out of the building)

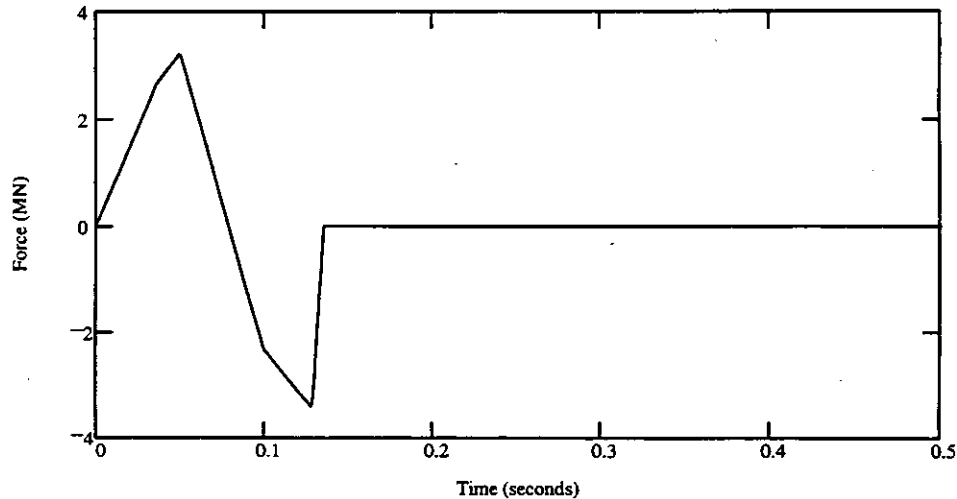
0	0
1	47.221
2	91.647
3	136.154
4	181.003
5	225.775
6	270.414
7	316.387
8	356.297
9	398.663
10	440.463

## Resultant Force Variation on Building

The resultant force variation experienced by the building is calculated from the front face pressure, the rear face pressure and the internal pressure as described in Section 2.3.5 (Equation 12):

$$\text{Force on Building: Pressure Pulse} \quad F_p := [p_{\text{front}} \cdot (H \cdot B - A_f) - p_{\text{rear}} \cdot H \cdot B + p_{\text{pgt}} \cdot A_f] \cdot 100 \cdot \text{Pa}$$

**Force acting on building (500mbar peak incident overpressure)**



## Structural Response

Having calculated the force on the building, it is now necessary to calculate the resultant building displacement:

### **Mass of building:**

Assume for now (arbitrarily) that the mass of the whole building is 50% higher than the mass of the exterior and interior walls alone:

*Density of brick*

$$\rho_b := \text{build}_{6,2} \cdot \text{kg} \cdot \text{m}^{-3}$$

Mass of building

$$\text{Mass} := (B \cdot H \cdot \text{tw} \cdot \rho_b \cdot 3 + L \cdot H \cdot \text{tw} \cdot \rho_b \cdot 3) \cdot 1.5$$

$$\text{Mass} = 3.545 \cdot 10^5 \cdot \text{kg}$$

$$M := \frac{\text{Mass}}{\text{kg}}$$

### **Stiffness of building:**

From Lees [8] and Equation 14, an empirical equation for the natural period is:

$$T := \frac{0.05 \cdot \frac{H}{\text{ft}}}{\sqrt{\frac{B}{\text{ft}}}} \cdot \text{sec} \quad T = 0.247 \cdot \text{sec}$$

Using this and the mass of the building, we can derive a value for the stiffness:

$$\text{Stiffness} := \frac{\text{Mass}}{\left(\frac{T}{2 \cdot \pi}\right)^2}$$

$$\text{Stiffness} = 2.293 \cdot 10^8 \text{ newton} \cdot \text{m}^{-1}$$

Non-dimensional value:

$$K := \frac{\text{Stiffness}}{\text{newton} \cdot \text{m}^{-1}}$$

$$K = 2.293 \cdot 10^8$$

### Elastic Limits of SDOF System

For this building type, the brick walls form the load-bearing frame of the structure. Hence the failure pressure of the frame is the same as that of the walls.

If we assume that the capacity of the solid brick wall is 275 mbar

$$\text{Fail}_d := \text{READPRN}(\text{b22})_{5,2} \cdot \text{mbar} \quad \text{Fail}_d = 275 \cdot \text{mbar}$$

Positive yield

$$\text{Posy} := \text{Fail}_d \cdot B \cdot H \quad R0 := \frac{\text{Posy}}{\text{newton}} \quad R0 = 1.892 \cdot 10^6$$

Negative yield

$$\text{Negy} := \text{Posy} \cdot -1 \quad R1 := \frac{\text{Negy}}{\text{newton}} \quad R1 = -1.892 \cdot 10^6$$

Elastic limit

$$y_{el} := \frac{R0}{K} \quad y_{el} = 8.252 \cdot 10^{-3}$$

% critical damping

$$Bc := 0.0$$

Ductility

$$\mu := 5$$

Displacement at Yield

$$y_{max} := y_{el} \cdot \mu \quad y_{max} = 0.041$$

The above calculations have defined the force on the building, its stiffness and mass such that it is possible to find a solution to Equation 5, the equation of motion. The building is assumed to behave as a single degree of freedom elasto-plastic system, with a bi-linear stiffness. Failure, i.e. structural collapse, is assumed to occur if the displacement of the structure exceeds the elastic limit multiplied by the ductility.

The equation of motion is solved using an iterative procedure to give the displacement of the structure in time. This is performed for each increment of peak incident overpressure, and the maximum and minimum (i.e. greatest -ve) displacement at each incident overpressure are extracted. By comparing these displacements with the displacement at failure,  $y_{max}$ , the collapse pressure of the structure can be derived:

**Maximum and minimum displacements of structure**

'ap' is a matrix containing the calculated maximum and minimum displacements

		Maximum	Minimum			
		0	1	0		
Displacements	ap =	7	9.33 · 10 <sup>-3</sup>	-0.014	7	0.226
		8	0.011	-0.013	8	0.263
		9	0.013	-0.012	9	0.303
		10	0.014	-0.011	10	0.347
		11	0.016	-8.905 · 10 <sup>-3</sup>	11	0.396
		12	0.019	-6.455 · 10 <sup>-3</sup>	12	0.451
		13	0.021	-3.395 · 10 <sup>-3</sup>	13	0.514
		14	0.024	0	14	0.586
		15	0.028	0	15	0.67
		16	0.032	0	16	0.769
		17	0.037	0	17	0.888
		18	0.043	0	18	1.032
		19	0.05	0		
		20	0.059	0		

Ratio of displacements to y<sub>max</sub>

$$\frac{ap}{y_{max}}$$

Failure occurs when the displacement of the structure is greater than y<sub>max</sub> - for this structure it is at about increment 18, which corresponds to 900mbar peak incident overpressure

Increment in which structure collapses: collp = 18

Corresponding peak incident overpressure P<sub>collp</sub> = 900

Ratio of max displacement to displacement at failure in collapse increment  $\frac{ap_{collp,0}}{y_{max}} = 1.032$

Ratio of max displacement to displacement at failure in increment immediately prior to collapse increment  $\frac{ap_{(collp-1),0}}{y_{max}} = 0.888$

Interpolate between these two values to derive an estimate of failure pressure

Variables for interpolation  $V1 := \frac{ap_{collp,0}}{y_{max}}$   $V2 := \frac{ap_{(collp-1),0}}{y_{max}}$

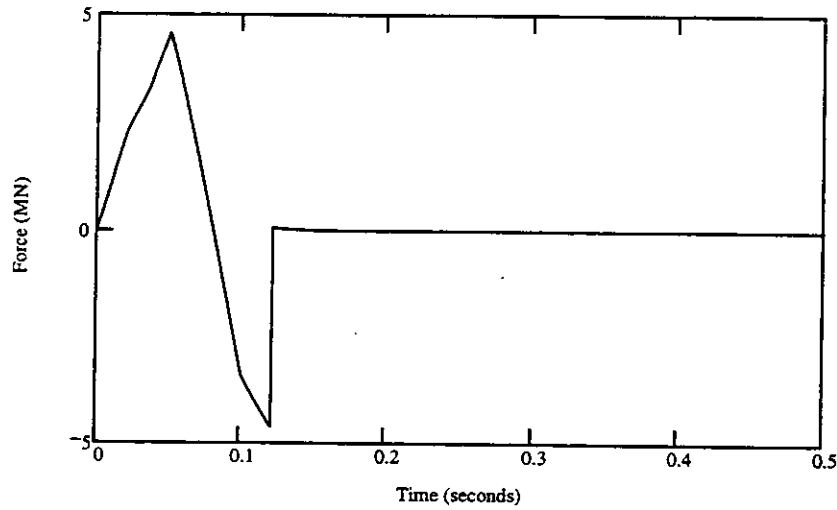
Collapse pressure (peak incident overpressure)  $P_{coll} := \frac{P_{collp} - P_{collp-1}}{V1 - V2} \cdot 1.0 + P_{collp-1} - \frac{P_{collp} - P_{collp-1}}{V1 - V2} \cdot V2$

P<sub>coll</sub> = 888.959 (mbar)

## Opposite Orientation of Building

The calculations are repeated assuming that the long side of the building faces the blast. In this case, the load on the structure changes, due to changes in the front face pressure, the rear face pressure and the internal pressure. The load on the building is as follows:

**Force acting on building (500mbar peak incident overpressure)**



Applying this load to the structure using a similar approach gives rise to the following results:

		Maximum	Minimum			
		0	1			
Displacements	apl =	0	0	Ratio of displacements to $y_{max}$	apl =	
		$2.047 \cdot 10^{-3}$	$-2.047 \cdot 10^{-3}$			0
		$3.953 \cdot 10^{-3}$	$-3.94 \cdot 10^{-3}$			0.05
		$5.924 \cdot 10^{-3}$	$-5.903 \cdot 10^{-3}$			0.096
		$7.944 \cdot 10^{-3}$	$-7.916 \cdot 10^{-3}$			0.144
		$6.85 \cdot 10^{-3}$	$-9.83 \cdot 10^{-3}$			0.166
		$7.93 \cdot 10^{-3}$	-0.012			0.192
		$9.26 \cdot 10^{-3}$	-0.012			0.224
		0.011	-0.012			0.27
		0.013	-0.01			0.322
		0.016	$-7.716 \cdot 10^{-3}$			0.381
		0.018	$-4.97 \cdot 10^{-3}$			0.448
				0.525		
				0.613		
				0.716		
				0		

Failure occurs when the displacement of the structure is greater than  $y_{max}$  - for this structure it is at about 500mbar:

Increment in which structure collapses:  $\text{collpl} = 17$

Corresponding peak incident overpressure  $P_{\text{collpl}} = 850$

Ratio of max displacement to displacement at failure in collapse increment  $\frac{\text{apl}_{\text{collpl},0}}{y_{\text{max}}} = 1.164$

Ratio of max displacement to displacement at failure in increment immediately prior to collapse increment  $\frac{\text{apl}_{(\text{collpl}-1),0}}{y_{\text{max}}} = 0.986$

Interpolate between these two values to derive an estimate of failure pressure

Variables for interpolation  $V_1 := \frac{\text{apl}_{\text{collpl},0}}{y_{\text{max}}}$   $V_2 := \frac{\text{apl}_{(\text{collpl}-1),0}}{y_{\text{max}}}$

Collapse pressure (peak incident overpressure)  $P_{\text{coll}} := \frac{P_{\text{collpl}} - P_{\text{collpl}-1}}{V_1 - V_2} \cdot 1.0 + P_{\text{collpl}-1} - \frac{P_{\text{collpl}} - P_{\text{collpl}-1}}{V_1 - V_2} \cdot V_2$

$P_{\text{coll}} = 803.99$  (mbar)

$\text{coll}_1 := P_{\text{coll}}$

Vector of collapse values  $\text{coll} = \begin{pmatrix} 888.959 \\ 803.99 \end{pmatrix}$  (mbar)

This vector is written out for use in subsequent calculations



## 7. Calculation of fatality probability of building occupants (Shock Pulse)

The results of the previous calculations are brought together here to calculate the overall probability of fatality of the building occupants. The calculations performed here are described in Section 2.5, in particular Section 2.5.4., and are illustrated in Figure 2.25.

### Definition of units

$$\text{mbar} := 100 \cdot \text{Pa}$$

$$\text{zero} := 0 \cdot \frac{\text{newton}}{\text{m}^2}$$

### Input variables

The characteristics of the building which are required for this set of calculations are read in as a matrix and assigned variable names for use in this sheet only. Initially it is assumed that the short side of the building faces the blast

	$\text{build} := \text{READPRN}(\text{b22})$	
<i>Height of building</i>	$H := \text{build}_{0,0} \cdot \text{m}$	$H = 8 \cdot \text{m}$
<i>Breadth of building (width)</i>	$B := \text{build}_{1,0} \cdot \text{m}$	$B = 8.6 \cdot \text{m}$
<i>Length of building (front to back)</i>	$L := \text{build}_{2,0} \cdot \text{m}$	$L = 14.3 \cdot \text{m}$
<i>Wall thickness</i>	$\text{tw} := \text{build}_{3,0} \cdot \text{m}$	$\text{tw} = 0.215 \cdot \text{m}$
<i>Wall height</i>	$\text{Hwall} := \text{build}_{0,2} \cdot \text{m}$	$\text{Hwall} = 2.6 \cdot \text{m}$
<i>Length of Glazing on Short Side</i>	$\text{L2f} := \text{build}_{3,1} \cdot \text{m}$	$\text{L2f} = 1.275 \cdot \text{m}$
<i>Height of Windows</i>	$\text{Hwin} := \text{build}_{6,1} \cdot \text{m}$	$\text{Hwin} = 1.25 \cdot \text{m}$
<i>Length of Glazing on Long Side</i>	$\text{L1} := \text{build}_{1,1} \cdot \text{m}$	
	$\text{L2s} := \text{build}_{2,1} \cdot \text{m}$	
	$\text{L4} := \text{build}_{4,1} \cdot \text{m}$	
	$\text{L5} := \text{build}_{5,1} \cdot \text{m}$	
Select the larger glazing area	$\text{LG} := \text{if}((\text{L1} + \text{L2s}) \geq (\text{L4} + \text{L5}), (\text{L1} + \text{L2s}), (\text{L4} + \text{L5}))$	$\text{LG} = 4.05 \cdot \text{m}$
$\gamma$ for air	$\gamma := 1.4$	
Atmospheric pressure	$\text{po} := 1103 \cdot \text{mbar}$	
<i>Pulse Duration</i>	$\text{t}_p := \text{READPRN}(\text{pdur})_0$	$\text{t}_p = 0.1$
Factor on glazing failure calculation	$\text{gfactor} := -0.141 \cdot \ln(\text{t}_p) + 0.104 \cdot \text{t}_p + 0.904$	
	$\text{gfactor} = 1.239$	(Mainstone)
<i>Glazing failure pressure</i>	$\text{G}_f := \text{build}_{8,1} \cdot \text{mbar}$	$\text{G}_f = 55 \cdot \text{mbar}$
This needs to be increased to take into account the fact that the pulse duration is shorter than 1sec		
	$\text{G}_f := \text{gfactor} \cdot \text{G}_f$	$\text{G}_f = 68.149 \cdot \text{mbar}$
<i>Cladding Failure Pressure</i>	$\text{C}_f := \text{READPRN}(\text{Pfail})_1 \cdot \text{mbar}$	$\text{C}_f = 175 \cdot \text{mbar}$

**Applied shock wave shape**

In this sheet, a series of calculations for a range of peak incident overpressures are performed. It is first necessary to define the overpressures of interest:

imax = 20      pit = 0..imax      P<sub>pit</sub> = pit·50

Maximum overpressure      P<sub>s</sub> := P·mbar      20 values ranging from 0 to 1000mbar in 50mbar increments

Total time for calculations      t<sub>max</sub> := 1.0

**Maximum and Minimum Pressures**

Front Face: the maximum pressures are equal to the reflected pressure

Calculation of perpendicularly reflected overpressure due to shock wave

$$Pr_i := 2 \cdot P_{s_i} + \frac{(\gamma + 1) \cdot (P_{s_i})^2}{[(\gamma - 1) \cdot P_{s_i}] + 2 \cdot \gamma \cdot p_0}$$

i := 0..imax  
Pr<sub>s</sub> = 5.47·10<sup>4</sup>  $\frac{\text{newton}}{\text{m}^2}$

Rear Face/Sides: the maximum and minimum pressures have been calculated previously:

hop := READPRN(mxmns)

Short      Long

*Maximum and minimum pressures for both short side facing blast and long side facing blast*

	0	1	2	3
0	0	0	0	0
1	44.97	-4.435	36.54	-12.98
2	89.76	-8.776	72.52	-25.32
3	135	-13.04	108.6	-37.08
4	129.8	-117.8	172.3	-133.1
5	159.7	-146.4	212.4	-164.8
6	189	-174.6	250.9	-196
7	216.2	-202.5	287.7	-226.9
8	244.5	-229.9	322.8	-256.7
9	270.5	-256.9	356	-285.9
10	296	-283.3	389.4	-314.9
11	322.7	-309.1	422.7	-342.2
12	348.4	-334.4	453.3	-369.9
13	373	-359	483.1	-395.8
14	396.4	-382.9	515	-422.1

Extract the relevant maximum and minimum values for the short side of the building facing the blast.

Max. Internal      Pr<sub>int<sub>i</sub></sub> := |hop<sub>i,1</sub>|      Pr<sub>int<sub>1</sub></sub> = 4.435

Max External      Pr<sub>ext<sub>i</sub></sub> := hop<sub>i,0</sub>      Pr<sub>ext<sub>1</sub></sub> = 44.97

Max Value      Pr<sub>max<sub>i</sub></sub> := if(Pr<sub>ext<sub>i</sub></sub> ≥ Pr<sub>int<sub>i</sub></sub>, Pr<sub>ext<sub>i</sub></sub>, Pr<sub>int<sub>i</sub></sub>)      Pr<sub>max<sub>1</sub></sub> = 44.97

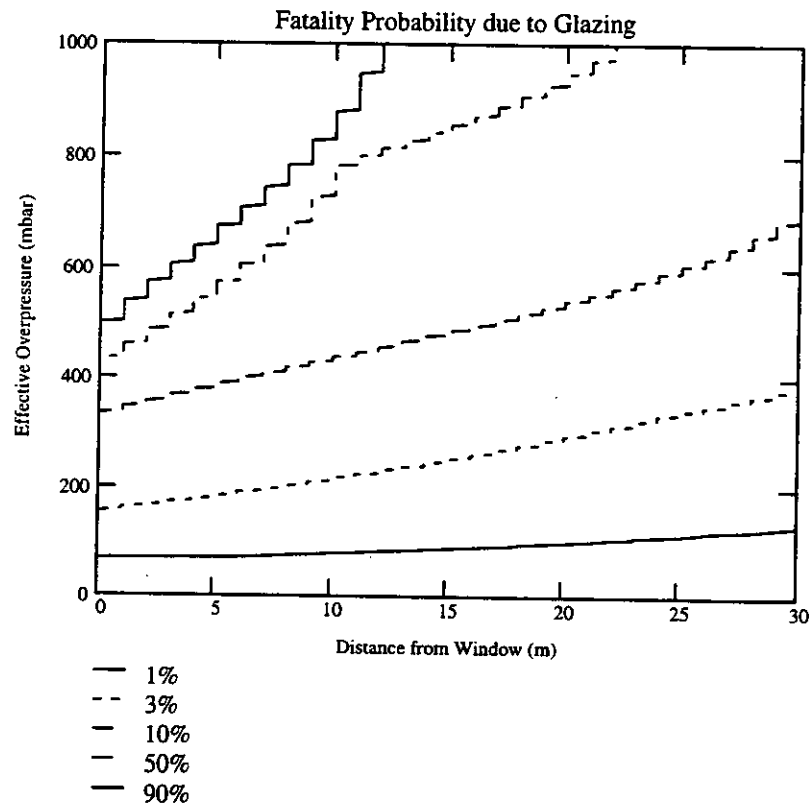
## Glazing Fatality Probability

The ranges for different levels of fatality probability due to glazing impact have been calculated previously (Calculation Set 2)

```
gvul := READPRN(gv22r)
```

```
i := 0.. 500
```

```
Peff(Ix) := Ix·2·mbar
```



This building is divided into 10 rooms, as illustrated in Figure A.4, but as it is semi-detached and symmetrical about its mid-point, this can be simplified to 5.

For each room in the building, the effective pressure across the windows is calculated and compared against the above graph. The corresponding fatality ranges are extracted from the graph, taking into account the fact that the glazing cannot travel any further than the internal walls. The internal walls are thus assumed to present an effective barrier to glazing travel.

If the minimum pressure is sufficient to fail the glazing, it is assumed that the glazing is blown out of the building. This assumption is made because the peak minimum pressure occurs before the peak maximum pressure, and hence even if the peak maximum pressure is greater than the peak minimum (absolute) value, the pressure will have already failed outwards before the peak maximum pressure hits the window.

**Front Glazing - Rooms 2 and 3**

At the front face, the pressure of interest is the peak reflected pressure, Pr

Maximum range in rooms 2 and 3

$$\text{maxr} = 3.72 \cdot m$$

$$\text{rab} := \text{rab1}(\text{int}, \text{maxr})$$

2% 6.5% 30% 70% 95%

Distribution of fatality probabilities extracted from graph:

	0	1	2	3	4
0	0	0	0	0	0
1	3.72	0	0	0	0
2	0	3.72	0	0	0
3	0	3.72	0	0	0
4	0	0	3.72	0	0
5	0	0	0	1.72	2
6	0	0	0	0	3.72
7	0	0	0	0	3.72
8	0	0	0	0	3.72
9	0	0	0	0	3.72
10	0	0	0	0	3.72
11	0	0	0	0	3.72
12	0	0	0	0	3.72
13	0	0	0	0	3.72
14	0	0	0	0	3.72

$$\text{bit}(\text{rab}) =$$

	0
0	0
1	101.93
2	207.672
3	317.152
4	430.299
5	547.046
6	667.323
7	791.067
8	918.212
9	$1.049 \cdot 10^3$
10	$1.182 \cdot 10^3$
11	$1.319 \cdot 10^3$
12	$1.46 \cdot 10^3$

$$\text{Pr} =$$

mbar

Fatality Probabilities

$$\text{FG} := \text{bit}(\text{rab}) \cdot m$$

**Rear Glazing - Rooms 2 and 3**

At the rear face and sides, the pressures of interest are the maximum differential pressures calculated previously and given above in Pmax

Maximum range in rooms 2 and 3

$maxr = 3.72 \cdot m$

$rab := rab1(int, maxr)$

2% 6.5% 30% 70% 95%

NB int is now different as the differential pressure is different

Distribution of fatality probabilities extracted from graph:

	0%	6.5%	30%	70%	95%
0	0	0	0	0	0
1	0	0	0	0	0
2	3.72	0	0	0	0
3	3.72	0	0	0	0
4	3.72	0	0	0	0
5	2.72	1	0	0	0
6	0	3.72	0	0	0
7	0	3.72	0	0	0
8	0	3.72	0	0	0
9	0	3.72	0	0	0
10	0	3.72	0	0	0
11	0	3.72	0	0	0

$bit(rab) =$

	0%
0	0
1	44.97
2	89.76
3	135
4	129.8
5	159.7
6	189
7	216.2
8	244.5
9	270.5
10	296
11	322.7

$Pr_{max} =$

Fatality Probabilities

$RG := bit(rab) \cdot m$

Sides:

**Room 1**

Maximum range

$maxr1 := build_{5,0} \cdot m$

$maxr1 = 4.95 \cdot m$

$rab := rab1(int, maxr1)$

Fatality Probabilities

$SG1 := bit(rab) \cdot m$

**Room 2**

Maximum range

$maxr2 := build_{6,0} \cdot m$

$maxr2 = 3.85 \cdot m$

$rab := rab1(int, maxr2)$

Fatality Probabilities

$SG2 := bit(rab) \cdot m$

**Room 4**

Maximum range

$maxr4 := build_{7,0} \cdot m$

$maxr4 = 2.93 \cdot m$

$rab := rab1(int, maxr4)$

Fatality Probabilities

$SG4 := bit(rab) \cdot m$

**Room 5**

Maximum range

$maxr5 := build_{8,0} \cdot m$

$maxr5 = 3.65 \cdot m$

$rab := rab1(int, maxr5)$

Fatality Probabilities

$SG5 := bit(rab) \cdot m$

**Fatality Probability due to glazing**  $i := 0..imax$

Having calculated the fatality probability distribution within the room, it remains to sum the affected areas multiplied by the relevant probability and divide by the room area to derive the room's contribution to the glazing fatality probability

**Room 1**

*Length of glazing*  $Lwin1 := build_{1,1} \cdot m$   $Lwin1 = 2.025 \cdot m$

$$Vg1_i := \frac{SG1_{i,0} \cdot Lwin1}{B \cdot L} \cdot 0.02 + \frac{SG1_{i,1} \cdot Lwin1}{L \cdot B} \cdot 0.065 + \frac{SG1_{i,2} \cdot Lwin1}{L \cdot B} \cdot 0.3 + \frac{SG1_{i,3} \cdot Lwin1}{L \cdot B} \cdot 0.7 + \frac{SG1_{i,4} \cdot Lwin1}{L \cdot B} \cdot 0.95$$

**Room 2 - front**

*Room dimensions*  $L_F := build_{6,0} \cdot m$   $L_F = 3.85 \cdot m$

$L_S := build_{4,0} \cdot m$   $L_S = 3.72 \cdot m$

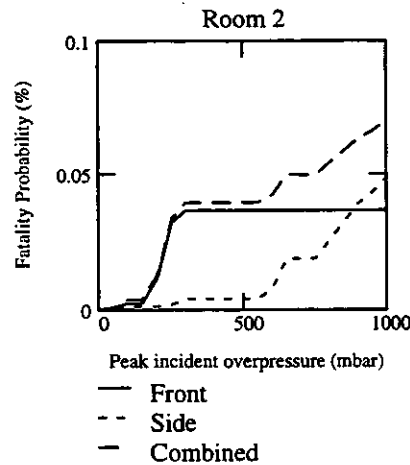
*Length of glazing*  $Lwins2 := build_{2,1} \cdot m$   $Lwins2 = 2.025 \cdot m$

$Lwinf2 := build_{3,1} \cdot m$   $Lwinf2 = 1.275 \cdot m$

$$Vgf2_i := \frac{FG_{i,0} \cdot Lwinf2}{B \cdot L} \cdot 0.02 + \frac{FG_{i,1} \cdot Lwinf2}{L \cdot B} \cdot 0.065 + \frac{FG_{i,2} \cdot Lwinf2}{L \cdot B} \cdot 0.3 + \frac{FG_{i,3} \cdot Lwinf2}{L \cdot B} \cdot 0.7 + \frac{FG_{i,4} \cdot Lwinf2}{L \cdot B} \cdot 0.95$$

$$Vgs2_i := \frac{SG2_{i,0} \cdot Lwins2}{B \cdot L} \cdot 0.02 + \frac{SG2_{i,1} \cdot Lwins2}{L \cdot B} \cdot 0.065 + \frac{SG2_{i,2} \cdot Lwins2}{L \cdot B} \cdot 0.3 + \frac{SG2_{i,3} \cdot Lwins2}{L \cdot B} \cdot 0.7 + \frac{SG2_{i,4} \cdot Lwins2}{L \cdot B} \cdot 0.95$$

Overlap calculation  $Vg2f_i := (Vgf2_i + Vgs2_i) - Vgf2_i \cdot Vgs2_i \cdot \left( \frac{B \cdot L}{L_F \cdot L_S} \right)$



**Room 3 - front**

*Length of glazing*  $Lwin3 := 0.0 \cdot m$

$$Vg3f_i := \frac{FG_{i,0} \cdot Lwin3}{B \cdot L} \cdot 0.02 + \frac{FG_{i,1} \cdot Lwin3}{L \cdot B} \cdot 0.065 + \frac{FG_{i,2} \cdot Lwin3}{L \cdot B} \cdot 0.3 + \frac{FG_{i,3} \cdot Lwin3}{L \cdot B} \cdot 0.7 + \frac{FG_{i,4} \cdot Lwin3}{L \cdot B} \cdot 0.95$$

Room 4

Length of glazing

$$Lwin4 := build_{4,1} \cdot m$$

$$Lwin4 = 2.025 \cdot m$$

$$Vg4_i := \frac{SG4_{i,0} \cdot Lwin4}{B \cdot L} \cdot 0.02 + \frac{SG4_{i,1} \cdot Lwin4}{L \cdot B} \cdot 0.065 + \frac{SG4_{i,2} \cdot Lwin4}{L \cdot B} \cdot 0.3 + \frac{SG4_{i,3} \cdot Lwin4}{L \cdot B} \cdot 0.7 + \frac{SG4_{i,4} \cdot Lwin4}{L \cdot B} \cdot 0.95$$

Room 5

Length of glazing

$$Lwin5 := build_{5,1} \cdot m$$

$$Lwin5 = 2.025 \cdot m$$

$$Vg5_i := \frac{SG5_{i,0} \cdot Lwin5}{B \cdot L} \cdot 0.02 + \frac{SG5_{i,1} \cdot Lwin5}{L \cdot B} \cdot 0.065 + \frac{SG5_{i,2} \cdot Lwin5}{L \cdot B} \cdot 0.3 + \frac{SG5_{i,3} \cdot Lwin5}{L \cdot B} \cdot 0.7 + \frac{SG5_{i,4} \cdot Lwin5}{L \cdot B} \cdot 0.95$$

Room 2 - rear

$$Vgr2_i := \frac{RG_{i,0} \cdot Lwinf2}{B \cdot L} \cdot 0.02 + \frac{RG_{i,1} \cdot Lwinf2}{L \cdot B} \cdot 0.065 + \frac{RG_{i,2} \cdot Lwinf2}{L \cdot B} \cdot 0.3 + \frac{RG_{i,3} \cdot Lwinf2}{L \cdot B} \cdot 0.7 + \frac{RG_{i,4} \cdot Lwinf2}{L \cdot B} \cdot 0.95$$

$$Vgs2_i := \frac{SG2_{i,0} \cdot Lwins2}{B \cdot L} \cdot 0.02 + \frac{SG2_{i,1} \cdot Lwins2}{L \cdot B} \cdot 0.065 + \frac{SG2_{i,2} \cdot Lwins2}{L \cdot B} \cdot 0.3 + \frac{SG2_{i,3} \cdot Lwins2}{L \cdot B} \cdot 0.7 + \frac{SG2_{i,4} \cdot Lwins2}{L \cdot B} \cdot 0.95$$

$$Vg2r_i := Vgr2_i + Vgs2_i - Vgr2_i \cdot Vgs2_i \cdot \left( \frac{B \cdot L}{L_F L_S} \right)$$

Room 3 - rear

$$Lwin3 = 0 \cdot m$$

$$Vg3r_i := \frac{RG_{i,0} \cdot Lwin3}{B \cdot L} \cdot 0.02 + \frac{RG_{i,1} \cdot Lwin3}{L \cdot B} \cdot 0.065 + \frac{RG_{i,2} \cdot Lwin3}{L \cdot B} \cdot 0.3 + \frac{RG_{i,3} \cdot Lwin3}{L \cdot B} \cdot 0.7 + \frac{RG_{i,4} \cdot Lwin3}{L \cdot B} \cdot 0.95$$

The total glazing fatality probability is obtained from the combination of these values

$$Vgtot_i := (Vg1_i + Vg4_i + Vg5_i) \cdot 2 + Vg2f_i + Vg3f_i + Vg2r_i + Vg3r_i$$

If  $Indg = 1$ , it signifies that the side and rear glazing is blown out of the building. Hence the vulnerability is from front rooms alone:

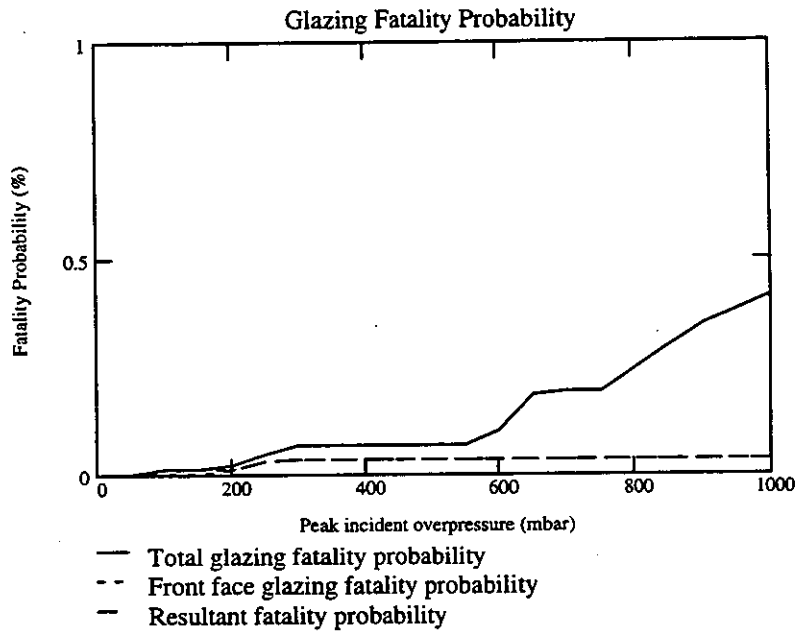
Front face glazing contribution

$$Vfront_i := Vgf2_i + Vg3f_i$$

Resultant fatality probability, taking glazing blowing out into account

$$Vg_i := \text{if}(Indg = 1, Vfront_i, Vgtot_i)$$

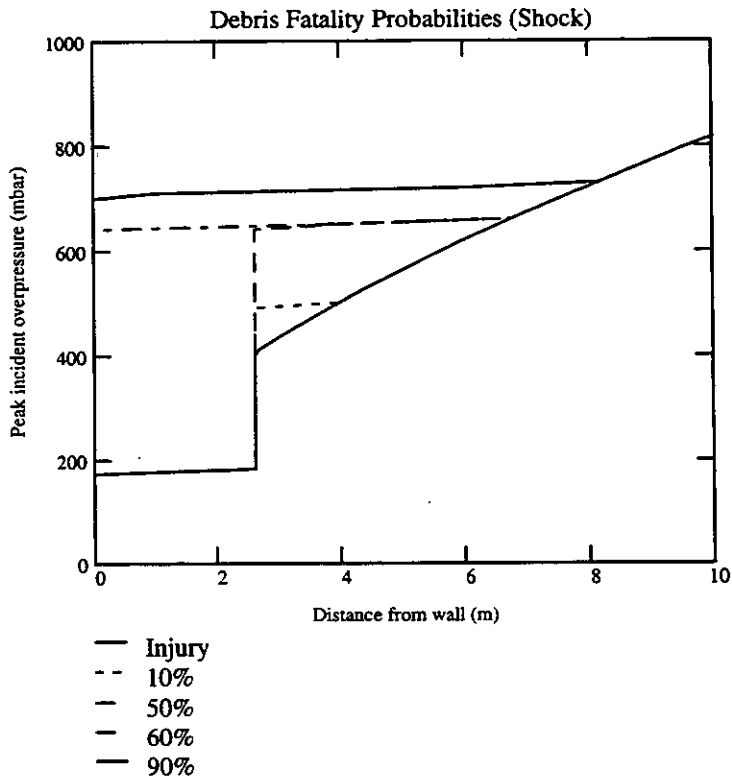
The contribution of the glazing to the overall fatality probability is shown below.



### Debris Fatality Probability

The ranges for different levels of fatality probability due to cladding impact have been calculated previously (Calculation Set 4). The pressure used here incorporates the reflection effects at the front face. This set of fatality probability ranges is used for the front face only.

$$i := 0..100 \quad \text{bvuls} := \text{READPRN}(\text{bvuls}) \quad P_{\text{incident}}(I_x) := I_x \cdot 10 \cdot \text{mbar}$$





A similar calculation is performed here as for the glazing above. The peak incident overpressures are compared against the above graph, and the fatality ranges extracted.

**Front Face Debris**

Assuming the maximum range is the same for debris as for glazing:

Maximum range       $maxr = 3.72 \cdot m$   
 $rabd := rabdeb(int, maxr)$

5.5% 30% 60% 70% 95%

	0	1	2	3
0	0	0	0	0
1	0	0	0	0
2	0	0	0	0
3	0	0	0	0
4	0	0	2.6	0
5	0	0	2.6	0
6	0	0	2.6	0
7	0	0	2.6	0
8	0	0	2.6	0
9	0.626	0	2.6	0
10	0	1.12	2.6	0
11	0	1.12	2.6	0

bitd(rabd) =

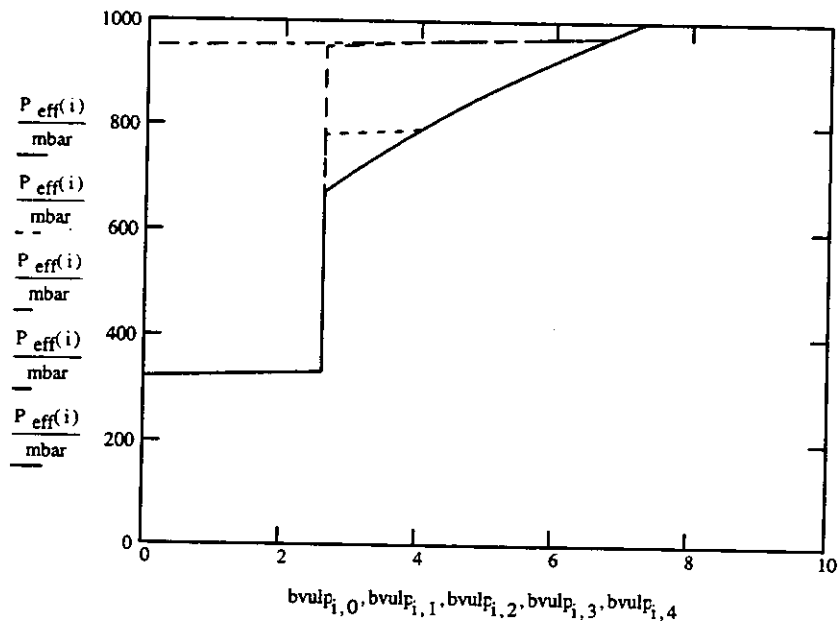
Fatality Probabilities       $DF := bitd(rabd) \cdot m$

**Rear face/side pressures**

For the rear face and sides, the ranges for fatality probability are assumed to be similar to those for an incident pressure pulse:

Rear Face     $i := 0..100$      $bvulp := READPRN(bvulp)$

$P_{eff}(lx) := lx \cdot 10 \cdot mbar$



**Rear Face**

Assuming the maximum range is the same for debris as for glazing:

Maximum range       $\text{maxr} = 3.72 \cdot \text{m}$   
 $\text{rabdp} := \text{rabdbp}(\text{int1}, \text{maxr})$

5.5% 30% 60% 70% 95%

	0	1	2	3	4
0	0	0	0	0	0
1	0	0	0	0	0
2	0	0	0	0	0
3	0	0	0	0	0
4	0	0	0	0	0
5	0	0	0	0	0
6	0	0	0	0	0
7	0	0	0	0	0
8	0	0	0	0	0
9	0	0	0	0	0
10	0	0	0	0	0
11	0	0	0	0	0
12	0	0	2.6	0	0
13	0	0	2.6	0	0
14	0	0	2.6	0	0

$\text{bitd}(\text{rabdp}) =$

Fatality Probabilities       $\text{DR} := \text{bitd}(\text{rabdp}) \cdot \text{m}$

**Sides:**

The ranges are different in rooms 1,2,4 and 5. Plus we need to check for overlap in rooms 2 and 4, front and rear.

**Room 1**

Maximum range       $\text{maxr1} = 4.95 \cdot \text{m}$   
 $\text{rabdp} := \text{rabdbp}(\text{int1}, \text{maxr1})$

Fatality Probabilities       $\text{SD1} := \text{bitd}(\text{rabdp}) \cdot \text{m}$

**Room 2**

Maximum range       $\text{maxr2} = 3.85 \cdot \text{m}$   
 $\text{rabdp} := \text{rabdbp}(\text{int1}, \text{maxr2})$

Fatality Probabilities       $\text{SD2} := \text{bitd}(\text{rabdp}) \cdot \text{m}$

**Room 4**

Maximum range       $\text{maxr4} = 2.93 \cdot \text{m}$   
 $\text{rabdp} := \text{rabdbp}(\text{int1}, \text{maxr4})$

Fatality Probabilities       $\text{SD4} := \text{bitd}(\text{rabdp}) \cdot \text{m}$

**Room 5**

Maximum range       $\text{maxr5} = 3.65 \cdot \text{m}$   
 $\text{rabdp} := \text{rabdbp}(\text{int1}, \text{maxr5})$

Fatality Probabilities       $\text{SD5} := \text{bitd}(\text{rabdp}) \cdot \text{m}$

### Fatality Probability due to debris

Having calculated the fatality probability distribution within the room, it remains to sum the affected areas multiplied by the relevant probability and divide by the room area to derive the room's contribution to the debris fatality probability

Room 1

Room length  $L_d := \text{build}_{9,0} \cdot \text{m}$   $L_d = 3.43 \cdot \text{m}$

$$V1_i := \frac{SD1_{i,0} \cdot L_d}{B \cdot L} \cdot 0.055 + \frac{SD1_{i,1} \cdot L_d}{B \cdot L} \cdot 0.3 + \frac{SD1_{i,2} \cdot L_d}{L \cdot B} \cdot 0.6 + \frac{SD1_{i,3} \cdot L_d}{L \cdot B} \cdot 0.7 + \frac{SD1_{i,4} \cdot L_d}{L \cdot B} \cdot 0.95$$

Room 2

Room length  $L_F := \text{build}_{6,0} \cdot \text{m}$   $L_F = 3.85 \cdot \text{m}$

$L_S := \text{build}_{4,0} \cdot \text{m}$   $L_S = 3.72 \cdot \text{m}$

$$Vd2F_i := \frac{DF_{i,0} \cdot L_F}{B \cdot L} \cdot 0.055 + \frac{DF_{i,1} \cdot L_F}{B \cdot L} \cdot 0.3 + \frac{DF_{i,2} \cdot L_F}{L \cdot B} \cdot 0.6 + \frac{DF_{i,3} \cdot L_F}{L \cdot B} \cdot 0.7 + \frac{DF_{i,4} \cdot L_F}{L \cdot B} \cdot 0.95$$

$$Vd2S_i := \frac{SD2_{i,0} \cdot L_S}{B \cdot L} \cdot 0.055 + \frac{SD2_{i,1} \cdot L_S}{B \cdot L} \cdot 0.3 + \frac{SD2_{i,2} \cdot L_S}{L \cdot B} \cdot 0.6 + \frac{SD2_{i,3} \cdot L_S}{L \cdot B} \cdot 0.7 + \frac{SD2_{i,4} \cdot L_S}{L \cdot B} \cdot 0.95$$

$$Vd2R_i := \frac{DR_{i,0} \cdot L_F}{B \cdot L} \cdot 0.055 + \frac{DR_{i,1} \cdot L_F}{B \cdot L} \cdot 0.3 + \frac{DR_{i,2} \cdot L_F}{L \cdot B} \cdot 0.6 + \frac{DR_{i,3} \cdot L_F}{L \cdot B} \cdot 0.7 + \frac{DR_{i,4} \cdot L_F}{L \cdot B} \cdot 0.95$$

Combined - front  $V2F_i := Vd2F_i + Vd2S_i - Vd2F_i \cdot Vd2S_i \cdot \left( \frac{B \cdot L}{L_F \cdot L_S} \right)$

Combined - rear  $V2R_i := Vd2R_i + Vd2S_i - Vd2R_i \cdot Vd2S_i \cdot \left( \frac{B \cdot L}{L_F \cdot L_S} \right)$

Room 3

Room length  $L_d := \text{build}_{10,0} \cdot \text{m}$   $L_d = 1.82 \cdot \text{m}$

Front  $V3F_i := \frac{DF_{i,0} \cdot L_d}{B \cdot L} \cdot 0.055 + \frac{DF_{i,1} \cdot L_d}{B \cdot L} \cdot 0.3 + \frac{DF_{i,2} \cdot L_d}{L \cdot B} \cdot 0.6 + \frac{DF_{i,3} \cdot L_d}{L \cdot B} \cdot 0.7 + \frac{DF_{i,4} \cdot L_d}{L \cdot B} \cdot 0.95$

Rear  $V3R_i := \frac{DR_{i,0} \cdot L_d}{B \cdot L} \cdot 0.055 + \frac{DR_{i,1} \cdot L_d}{B \cdot L} \cdot 0.3 + \frac{DR_{i,2} \cdot L_d}{L \cdot B} \cdot 0.6 + \frac{DR_{i,3} \cdot L_d}{L \cdot B} \cdot 0.7 + \frac{DR_{i,4} \cdot L_d}{L \cdot B} \cdot 0.95$

Room 4

Room length  $L_F := \text{build}_{7,0} \cdot \text{m}$   $L_F = 2.93 \cdot \text{m}$

$L_S := \text{build}_{4,0} \cdot \text{m}$   $L_S = 3.72 \cdot \text{m}$

$$Vd4F_i := \frac{DF_{i,0} \cdot L_F}{B \cdot L} \cdot 0.055 + \frac{DF_{i,1} \cdot L_F}{B \cdot L} \cdot 0.3 + \frac{DF_{i,2} \cdot L_F}{L \cdot B} \cdot 0.6 + \frac{DF_{i,3} \cdot L_F}{L \cdot B} \cdot 0.7 + \frac{DF_{i,4} \cdot L_F}{L \cdot B} \cdot 0.95$$

$$Vd4S_i := \frac{SD4_{i,0} \cdot L_S}{B \cdot L} \cdot 0.055 + \frac{SD4_{i,1} \cdot L_S}{B \cdot L} \cdot 0.3 + \frac{SD4_{i,2} \cdot L_S}{L \cdot B} \cdot 0.6 + \frac{SD4_{i,3} \cdot L_S}{L \cdot B} \cdot 0.7 + \frac{SD4_{i,4} \cdot L_S}{L \cdot B} \cdot 0.95$$

$$Vd4R_i := \frac{DR_{i,0} \cdot L_F}{B \cdot L} \cdot 0.055 + \frac{DR_{i,1} \cdot L_F}{B \cdot L} \cdot 0.3 + \frac{DR_{i,2} \cdot L_F}{L \cdot B} \cdot 0.6 + \frac{DR_{i,3} \cdot L_F}{L \cdot B} \cdot 0.7 + \frac{DR_{i,4} \cdot L_F}{L \cdot B} \cdot 0.95$$

Combined - front  $V4F_i := Vd4F_i + Vd4S_i - Vd4F_i \cdot Vd4S_i \cdot \left( \frac{B \cdot L}{L_F \cdot L_S} \right)$

Combined - rear  $V4R_i := Vd4R_i + Vd4S_i - Vd4R_i \cdot Vd4S_i \cdot \left( \frac{B \cdot L}{L_F \cdot L_S} \right)$

Room 5

Room length

$Ld := \text{build}_{11,0} \cdot m$

$Ld = 3.43 \cdot m$

$$V5_i := \frac{SD5_{i,0} \cdot Ld}{B \cdot L} \cdot 0.055 + \frac{SD5_{i,1} \cdot Ld}{B \cdot L} \cdot 0.3 + \frac{SD5_{i,2} \cdot Ld}{L \cdot B} \cdot 0.6 + \frac{SD5_{i,3} \cdot Ld}{L \cdot B} \cdot 0.7 + \frac{SD5_{i,4} \cdot Ld}{L \cdot B} \cdot 0.95$$

**Overall Debris Fatality Probability**

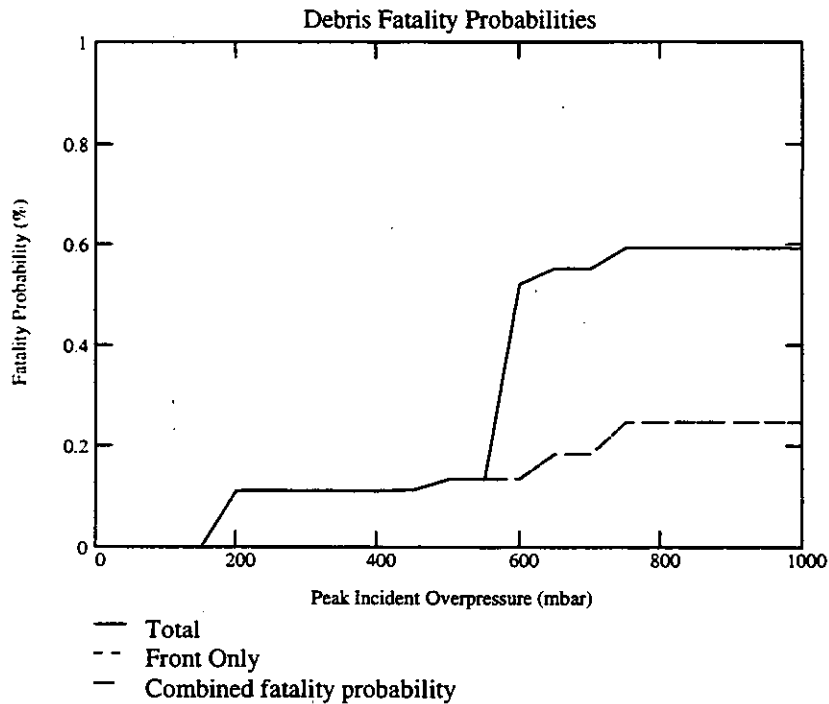
The total debris fatality probability is obtained from the combination of these values

$$Vdtot_i := (V1_i + V5_i) \cdot 2 + V2F_i + V2R_i + V3F_i + V3R_i + V4F_i + V4R_i$$

If Indc = 1, it signifies that the side and rear walls are blown out of the building. Hence the vulnerability is from front rooms alone:

Front only  $Vdfront_i := Vd2F_i + V3F_i + Vd4F_i$

Combined Value  $Vd_i := \text{if}(\text{Indc}_i = 1, Vdfront_i, Vdtot_i)$



### Fatality Probability due to Building Collapse:

For a shock wave duration of 0.1s, the collapse pressure for this particular building has been calculated previously as:

$$\begin{aligned} \text{Collapse pressure (incident)} \quad P_{\text{coll}} &:= \text{READPRN}(\text{collas})_0 \cdot \text{mbar} \\ P_{\text{coll}} &= 675.2 \cdot \text{mbar} \end{aligned}$$

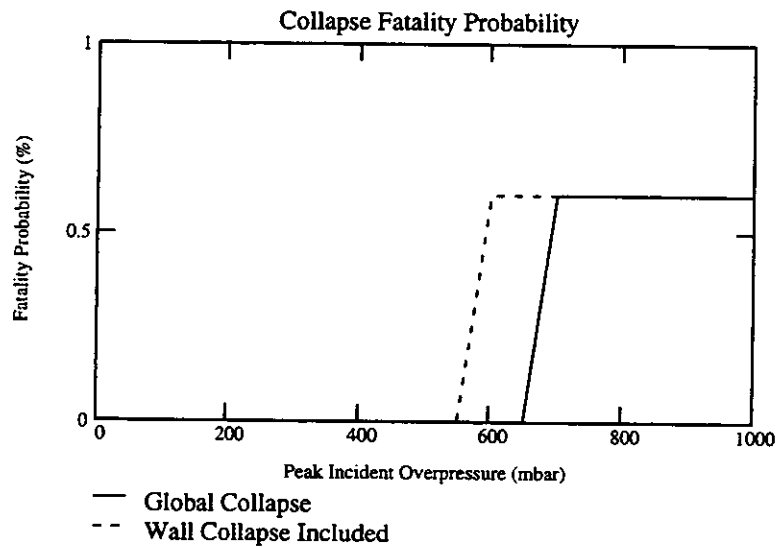
If the incident pressure exceeds this value, the building will collapse and 60% fatality probability is assumed

$$V_{\text{ctot}_i} := \text{if} \left[ \left( P_{s_i} \geq P_{\text{coll}} \right), 0.6, 0 \right]$$

If the internal pressure exceeds the dynamic failure pressure of the walls, the walls will collapse and vulnerability will be that due to building collapse i.e.60%:

$$b_{\text{coll}_i} := \text{if} \left[ \left( V_{5_i} > 0 \right) \cdot \left( V_{2F_i} > 0 \right), 1, 0 \right]$$

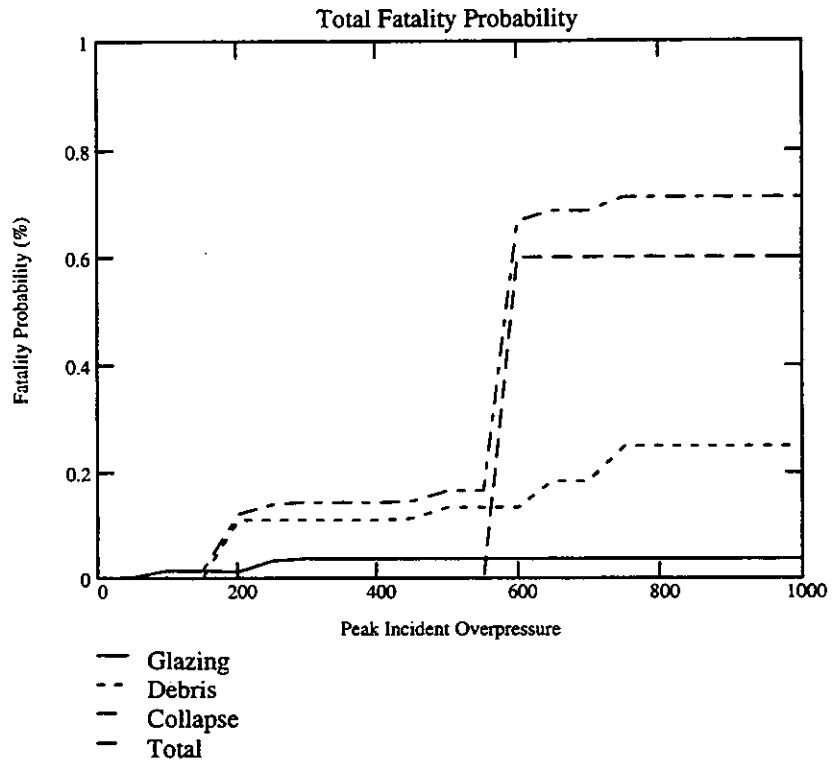
$$\text{Combined value} \quad V_{c_i} := \text{if} \left( b_{\text{coll}_i} > 0, 0.6, V_{\text{ctot}_i} \right)$$



## Overall Fatality Probability

The total fatality probability, taking into account that it is not possible for people to be killed twice is:

$$V_i := V_{g_i} + V_{d_i} + V_{c_i} - (V_{g_i} \cdot V_{d_i}) - (V_{g_i} \cdot V_{c_i}) - (V_{d_i} \cdot V_{c_i}) + (V_{g_i} \cdot V_{d_i} \cdot V_{c_i})$$

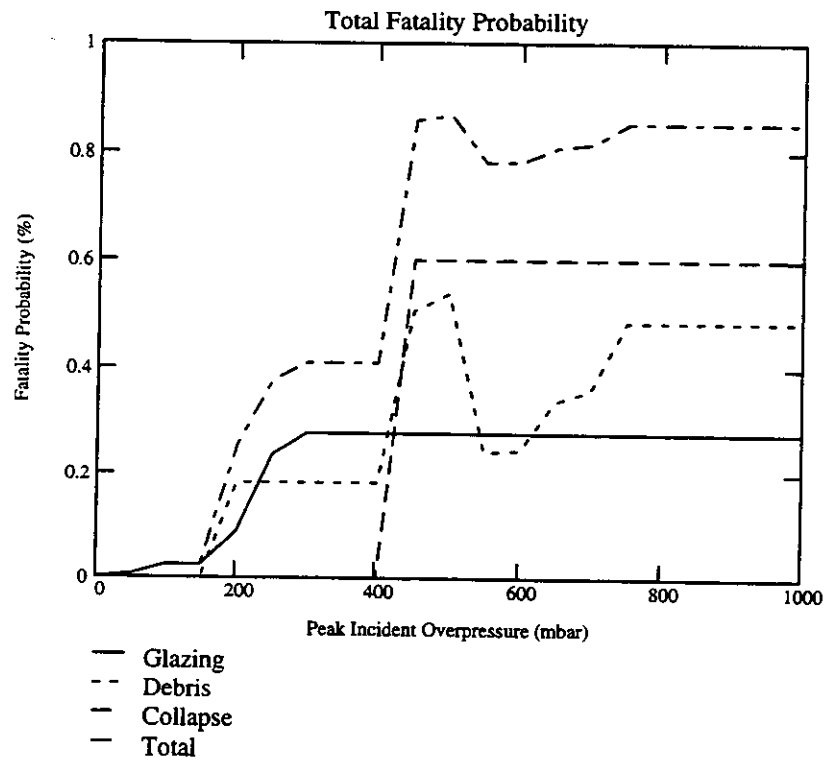


## Alternative Orientation

The calculations are repeated for the alternative orientation of the building, i.e. with the long side of the building facing the blast

The total vulnerability, taking into account that it is not possible for people to be killed twice is:

$$V_i := Vg_i + Vd_i + Vc_i - (Vg_i \cdot Vd_i) - (Vg_i \cdot Vc_i) - (Vd_i \cdot Vc_i) + (Vg_i \cdot Vd_i \cdot Vc_i)$$



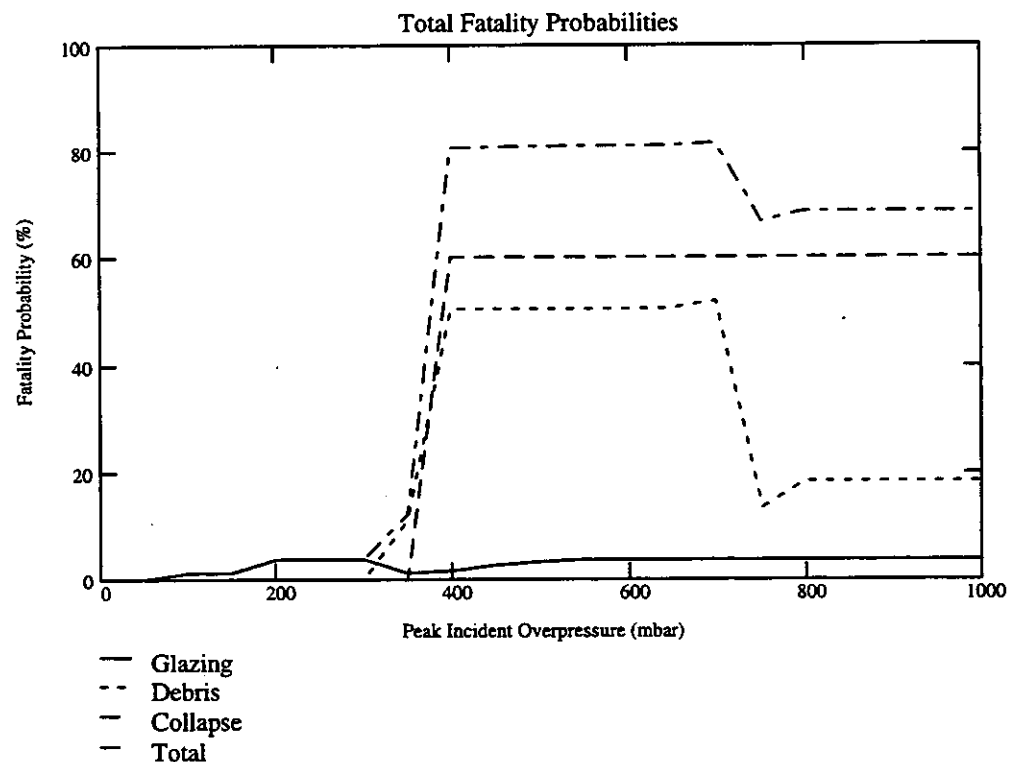
## **8. Calculation of fatality probability of building occupants (Pressure Pulse)**

The results of the previous calculations are brought together here to calculate the overall probability of fatality of the building occupants. The calculations performed here are described in Section 2.5, in particular Section 2.5.4., and are illustrated in Figure 2.25.

The calculations for the incident pressure pulse are very similar to those for the incident shock pulse, except that care must be taken to use the correct pressure across each structural component. For example, differential pressures across the front wall, taking into account the internal pressure due to glazing failure, have been calculated, and these should be used to calculate the fatality probability due to debris from the front face. For the front face glazing, the sum of the peak incident overpressure and the dynamic pressure should be used. For the rear face and the sides, differential pressures have been calculated as for the incident shock pulse.

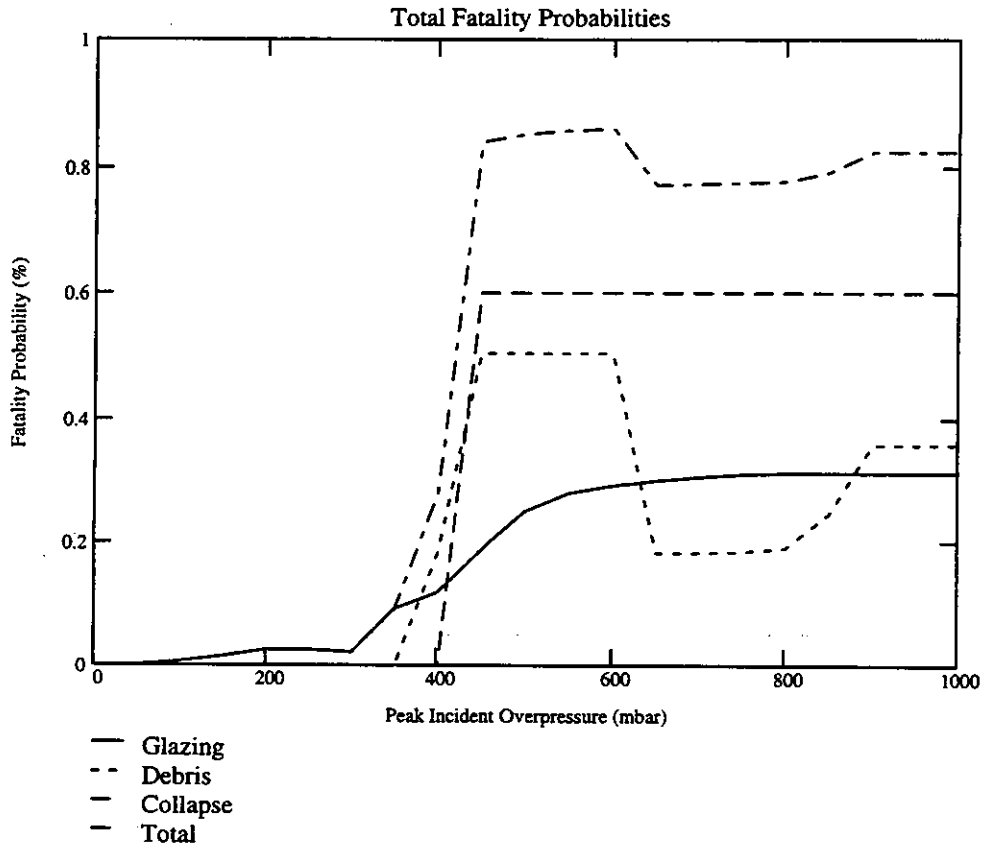
The results of the calculations are given below:

### **Short Side Facing Blast**





**Long Side Facing Blast**





**MAIL ORDER**

HSE priced and free  
publications are  
available from:  
HSE Books  
PO Box 1999  
Sudbury  
Suffolk CO10 6FS  
Tel: 01787 881165  
Fax: 01787 313995

**RETAIL**

HSE priced publications  
are available from  
good booksellers

**HEALTH AND SAFETY ENQUIRIES**

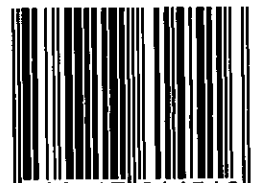
HSE InfoLine  
Tel: 0541 545500  
or write to:  
HSE Information Centre  
Broad Lane  
Sheffield S3 7HQ

HSE home page on the World Wide Web:  
<http://www.open.gov.uk/hse/hsehome.htm>

**CRR 151**

**£89.50 net**

ISBN 0-7176-1451-4



9 780717 614516